THE UNIVERSITY
of EDINBURGH

This thesis has been submitted in fulfilment of the requirements for a postgraduate degree (e.g. PhD, MPhil, DClinPsychol) at the University of Edinburgh. Please note the following terms and conditions of use:

This work is protected by copyright and other intellectual property rights, which are retained by the thesis author, unless otherwise stated.
A copy can be downloaded for personal non-commercial research or study, without prior permission or charge.
This thesis cannot be reproduced or quoted extensively from without first obtaining permission in writing from the author.
The content must not be changed in any way or sold commercially in any format or medium without the formal permission of the author.
When referring to this work, full bibliographic details including the author, title, awarding institution and date of the thesis must be given.

Development of Low-Oxidation State Nitrogen, Carbon, and Silicon Catalysts

Alexandros Papafilippou

Doctor of Philosophy

University of Edinburgh

EastCHEM School of Chemistry

College of Science and Engineering

December 2016

Author’s Declaration

I declare that the work in this thesis was carried out with the regulations of the University of Edinburgh. This work is original, except where indicated by reference in the text, and no part has been submitted for any academic award. Any views expressed in the dissertation are those to author.

Signed:

Date:

Acknowledgements

First of all, I would like to thank my family for their continuous support during my PhD. I would like to thank my friends Andreas, Nicos, Harris, Peter and Jonathan.

I would like to thank my supervisor, Uwe Schneider for giving me the opportunity to carry out research in his group and for his supervision during my PhD. I would like also to thank the Schneider group (past and present) for their support and ideas. It was fun the last four years.

I would like to thank the State Scholarships Foundation, Greece (I.K.Y) and School of Chemistry for the financial support. I would like to thank the School of Chemistry and ScotChem for providing the facilities for the research as well as funding.

Summary

In this project, the introduction of new catalysts to the synthetic community was investigated. Catalysts are chemical compounds that either facilitate or accelerate the reactions between two or more chemical species. Catalysts do not participate in the formation of the new chemical products and are regenerated in their initial shape at the end of the process. We focused on organocatalysis; a field of catalysis that develops organic compounds as catalysts and does not include use of metals; indeed, we were driven to develop sustainable chemistry. The direction of our research was to create methodologies of industrial interest within the range of 'green chemistry'. The industrial domains we targeted for, are chemicals, pharmaceuticals and agrochemicals. Our aim was to employ under-explored organic species with carbon, silicon and nitrogen atoms as active centres in the field of base catalysis. Carbon and silicon atom form normally four bonds with other atoms within organic compounds, while nitrogen connects to three different atoms in nature. In this publication though, carbon, silicon and nitrogen atoms connected with two different atoms were investigated in a structure of peculiar chemical species. Indeed, during this investigation we took advantage of 'state-of-the-art' equipment and lately developed knowledge and techniques in the field of chemistry in order to prepare and secure the high quality of our products.

Abstract

This PhD thesis is focused on the development of novel low-oxidation state main group catalysis for organic synthesis. More specifically, the major objective has been to explore and design non-toxic and effective catalysts based on the following isoelectronic species: nitreones [nitrogen(I)], carbones [carbon(0)], and silylones [silicon(0)]; the corresponding central non-metal atom in these molecules is in the formal low-oxidation state '+I' and '0', respectively. These species have been calculated to be strong Lewis and Brønsted bases. In addition, compared with established base catalysts such as *N*-heterocyclic carbenes (NHCs), nitreones, carbones, and silylones formally possess an additional lone pair of electrons at the central atom. In turn, these species may be used in base catalysis or as ligands in metal catalysis, and in the context of frustrated Lewis pair (FLP) or dual catalysis. The Lewis basicity of these N(I), C(0), and Si(0) compounds has been assessed with ^{11}B NMR analysis using a variety of boron Lewis acids. These boron binding data have been compared with results obtained using NHCs as a Lewis base. Nitreones –more specifically cyclopropen-imines– have been explored in base catalysis. These N(I) Lewis bases have been uncovered to catalytically activate a variety of silicon-based pro-nucleophiles for subsequent bond formation with carbonyl and imine derivatives as well as aziridines. Successfully used pro-nucleophiles include TMS–CN, TMS–CF_3, TMS–N_3, and TMS–Cl. The characteristic features of this unprecedented cyclopropenimine Lewis base catalysis include low catalyst loading, mild reaction conditions, and broad substrate scopes. Various "normal" imines have proved to be catalytically inactive under the same conditions. In a similar context, carbones and silylones have been used to develop novel catalytic *umpolung* reactions, which turned out to be too challenging at this stage. Importantly though, silylones have been shown to activate the B–H bond of suitable pro-nucleophiles. Finally, several carbone–metal complexes have been synthesized and characterized. These novel species may be used in Lewis acid or dual catalysis after appropriate activation of the corresponding metal site.

1 Abbreviations

Ac	Acetyl
Ar	Aryl
BAC	Bis(dialkylamino)cyclopropenylidene
BBN	9-borabicyclo[3.3.1]nonane
Bn	Benzyl
bp	Boiling point
CAAC	Cyclic alkyl amino carbene
Cat	Catalyst
Cy	Cyclohexyl
d	doublet
DBE	Dibenzyl ether
DCE	Dichloroethane
DCM	Dichloromethane
DFT	Density functional theory
DME	Dimethoxy ether
DMF	Dimethyl formamide
DMSO	Dimethyl sulfoxide
DIPP	Diisopropyl phenyl
EA	Ethyl acetate
EE	Diethyl ether
EI	Electron ionisation
equiv	equivalent
Et	Ethyl
G	grams
HOMO	Highest occupied molecular orbital
H	hour
HMDS	Hexamethyldisilazane
IR	Infrared
MeCN	Acetonitrile
Mes	Mesityl
Mg	milligram
MHz	Megahertz
MS	Mass spectroscopy
Mp	Melting point
m/z	Mass per charge number
NHC	*N*-heterocyclic carbene
NMR	Nuclear Magnetic Resonance
PE	Petroleum ether
Pin	pinacolyl
PG	Protecting group
Ph	Phenyl
PhH	Benzene
PhMe	Toluene
ppm	Parts per million
PTLC	Preparative thin liquid chromatography
Quant	quantitative
Q	quartet
Rf	Retardation factor
rt	Room temperature
S	singlet
S_N	Nucleophilic substitution
TBAB	Tetra-n-butylammonium bromide
TBAF	Tetra-n-butylammonium fluoride
TBME	*tert*-Butyl methyl ether
^{t}Bu	*tert*-butyl
TMS	trimethylsilyl

^{i}Pr	Isopropyl	THF	tetrahydrofuran
LA	Lewis acid	Ts	Tosyl
LB	Lewis base	TTMPP	Tris(2,4,6-trimethoxyphenyl) phosphine
M	Metal	T	triplet
Me	Methyl	UV	Ultraviolet

2 General Introduction

Catalysis is a phenomenon by which catalytic reactions are accelerated in presence of foreign compounds that are called catalysts (Scheme 2.1).[1] In contrast to the other participants **A** and **B** in the reaction, the catalyst **E** is regenerated at the end of the process.[2] Catalyst **E** is a part of the intermediate **F** formed during the reaction progress and is regenerated simultaneously with the formation of the final products **C** and **D**.[3]

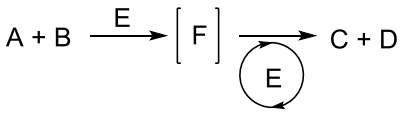

Scheme 2.1: A, B = reagents, E = catalyst, F = intermediate, C, D = products.

The catalyst increases the rate of a thermodynamically feasible reaction, however, it does not modify the position of the thermodynamic equilibrium (Figure 2.1).[1] The rate is enhanced by reducing the energy barrier required to transform the reagents **A** and **B** into the products **C** and **D**.[1,3] Furthermore, it provides control of conversion towards the desired product instead of forming unwanted side-products.[1] The vast majority of catalysts reported so far are in solid or liquid phase, however, there are a few examples of catalysts in the gas phase.[1] Indeed, depending on the reaction conditions and the nature of the other chemicals in the reaction mixture, the catalyst may decompose and lead to side-products; thus, its life is not indefinite.[1]

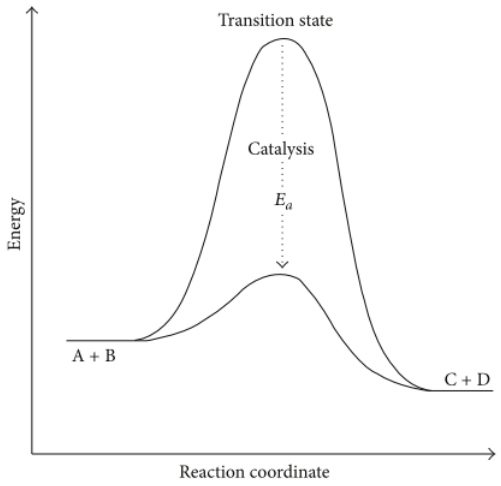

Figure 2.1: Effect of the catalyst in the progress of a reaction.

Catalysis consists of two main categories; homogeneous and heterogeneous catalysis. In homogeneous catalysis, the reaction mixture, including reagents, catalyst and potentially a solvent, forms a common physical phase.[1] For example, organometallic complexes are common homogeneous catalysts. In contrast, in heterogeneous catalysis the reagents and the catalyst form separate physical phases. Inorganic salts are widely used as heterogeneous catalysts.[1]

Recently, 'green chemistry' has drawn the global attention, since environmental-friendly technologies had to be urgently developed.[3] The fundamental principles of green chemistry are high reaction yield and selectivities combined with high atom economy and energy efficiency. Indeed, catalysis is a key technology for green chemistry and especially in the fields of chemical, petrochemical, biochemical and pharmaceutical industries.

Organocatalysis is a special case of homogeneous catalysis.[4] An organocatalyst accelerates a chemical reaction through addition of a substoichiometric quantity of a chemical compound which does not contain a metal atom. The advantages of organocatalysis are identified as:[4]

1. Large scale production in industry.
2. Unique organic reactions are catalysed; other forms of catalyst are not able to accelerate these reaction processes.
3. Low cost (precious metals are not included in the catalyst structure).
4. Organocatalysed reactions proceed under mild conditions.
5. Final products are not contaminated by toxic materials. In heterogeneous catalysis, traces of toxic metals are located in the product. This is a major concern for pharmaceutical and food industries.

Since we were keen to contribute in the field of organocatalysis, the recent developments in the low-oxidation group 14 and 15 species drawn our attention. The last 20 years, carbon(II)

species, the so-called ‘carbenes’, demonstrated excellent catalytic activity towards challenging organic reactions.[5–8] Recently, electron-rich nitrogen(I), carbon(0) and silicon(0) species have been reported to provide a new perspective regarding the valency and coordination chemistry of the group 14 and 15 species.[9–11] The catalytic potential of the nitrogen(I) species have been underexplored and our research focused on the development of new C–C, C–N and C–Cl bond formation methodologies based on activation of silicon pro-nucleophiles to react with various electrophiles. Indeed, mechanistic investigations using ^{29}Si NMR were conducted to suggest a plausible mechanistic pathway. Furthermore, the σ donor ability of the carbon(0) species towards various Lewis acids has been studied. Indeed, ^{11}B NMR, ^{31}P NMR, ^{11}Ga NMR proved to be powerful tools to investigate the interaction between these reaction partners. Finally, silicon(0) species have been explored to provide evidence regarding their ability to bind to various Lewis acids and catalyse a C–C bond formation.

3 Nitrogen(I) or Nitreones

3.1 Introduction

3.1.1 Chemistry of Cyclopropenimines – Example of a Nitrogen(I) Compound

3.1.1.1 Concept – Nitrogen(I) vs. Carbon(0)

Carbon belongs to main group fourteen and has therefore four valence electrons to form four covalent bonds. In 1991, Arduengo *et al.* isolated for the first time an *N*-heterocyclic carbene (NHC), which is a neutral molecule with a central divalent sp^2-hybridized carbon atom bearing a lone pair and a vacant p orbital (carbon in the formal '+II' oxidation state).[5,8,12] Recent studies have shown that there are 'non-classical' allenes and heterocumulenes, which may go beyond carbenes in terms of both properties and catalyst potential [Scheme 3.1 a)].[9,13–16] 'Classical' allenes and heterocumulenes have an sp-hybridized central carbon atom and hence a linear structure (X=C=X). However, if X is a strong σ donor and weak π acceptor, certain of these neutral compounds were shown to display a bent structure with an sp^2-type hybridized central carbon atom formally bearing two lone pairs. Indeed, several computational and experimental studies suggest the existence of: (i) C–X bonds with only partial double bond character;[9,13,15,16] (ii) two lone pairs at the central carbon atom, which is in a formal '0' oxidation state.[9,17] The X groups have been considered to act as ligands to the 'metal-like' carbon centre, and these so-called *carbones* have thus been described as zerovalent species.[9,17] If the carbon atom in these compounds is replaced by its neighbour in main group 15, nitrogen, an isoelectronic molecule with a similar structure and a nitrogen atom in the formal '+I' oxidation state may be postulated [Scheme 3.1 b)]. This hypothesis was studied both computationally and experimentally suggesting similar electronic and structural properties compared to carbones.[18–20] These so-called *nitreones* or N(I) compounds would be cationic, and may be described as zerovalent with a central 'metal-like' nitrogen cation coordinated by two neutral 'ligand-like' substituents X. Later on, neutral N(I) compounds were synthesized by replacing one of the neutral ligands X by an anionic substituent R.[10] R had to be a strong σ donor and weak π acceptor to minimize back donation from the nitrogen to the carbene moiety.[10] The nucleophilicity of such a neutral N(I) species proved to be significantly higher compared to its cationic analogue [Scheme 3.1 c)].[10]

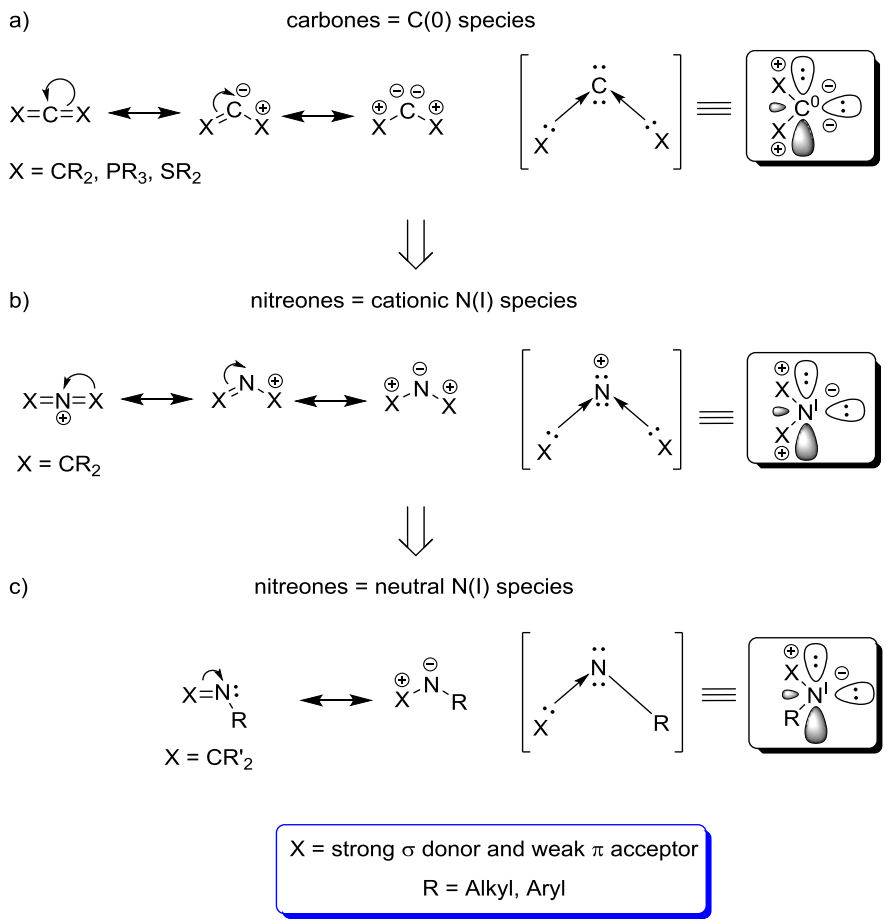

Scheme 3.1: Comparison of electronic properties between C(0) and N(I) compounds.[9,10,18–20]

Next, an overview of literature-known nitreones or nitrogen(I) compounds are displayed with a focus on structural and electronic properties as a result of experimental and computational studies.

3.1.1.2 History of Nitreones – Recognition of Cyclopropenimine Properties

In 2009, Bharatam *et al.* reported the first computational study of a cationic nitrogen(I) species [Figure 3.1 a)].[21] An electronic structure analysis was conducted proposing for compound **1** a formal charge of '+I', two lone pairs at the central nitrogen atom, with an overall bent C–N–C arrangement (C–N–C bond angle = 123.9°).[21] This outcome was ascribed to the 'NR' substituents within the NHC ligands, which bind –as a strong σ donor and a weak π acceptor– to the central nitrogen atom. Later on, Alcarazo *et al.* provided an experimental proof of such a cationic nitrogen(I) molecule through the synthesis of **2** bearing a bis(dialkylamino) cyclopropenylidene (BAC) as a ligand.[20] An X-ray diffraction analysis of **2** displayed a trigonal planar environment around the nitrogen atom. DFT calculations suggested that the HOMO and HOMO–1 orbitals corresponded to π and σ orbitals, respectively.

Meanwhile, Bharatam *et al.* undertook a quantum chemical analysis of specific cationic nitreones to provide structural details, description of molecular orbitals, and charge localization trends. These species displayed low proton affinities and low nucleophilicity resulting in an inability to bind to metal centres.[18] However, due to the medicinal importance of thiazol-based guanidines, the potential divalent N(I) character of 2-thiazol-2-yl guanidine **3** was thoroughly investigated using electronic structure analysis, which suggested that these species may have a 'hidden' neutral N(I) character [Figure 3.1 b)].[19] Earlier on, based on the assumption that the overall positive charge of a cationic nitreone might be a limiting factor for chemical reactivity, Alcarazo *et al.* synthesized a variety of neutral N(I) compounds of type **4**. In this study, a neutral ligand was simply replaced by an anionic substituent.[10] An extensive study to examine both bonding situation and coordination behavior has been reported leading to the conclusion that those nitreones or cyclopropenimines were particularly electron-rich. Indeed, the central nitrogen atom has formally two lone pairs in the HOMO and HOMO–1 orbitals, respectively.

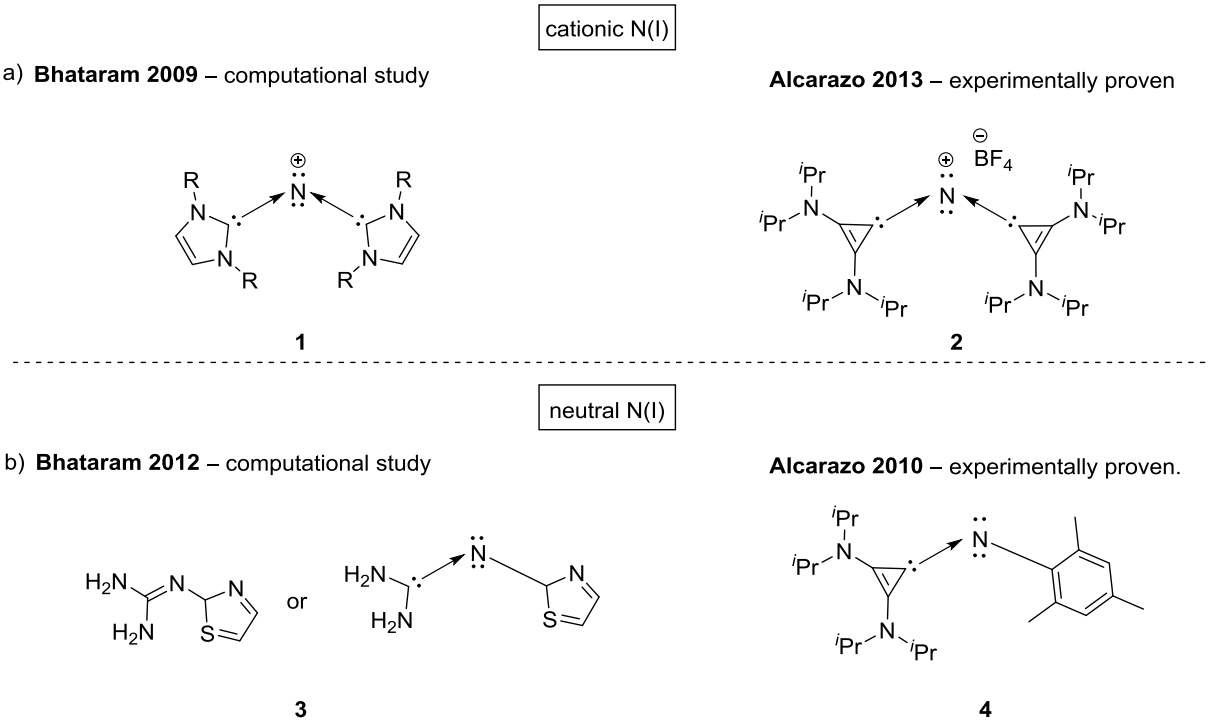

Figure 3.1: Computational studies and experimental reports of both neutral and cationic N(I) compounds.

The comparison of the proton affinities (PAs) of cationic and neutral N(I) species with NHCs [C(II)] and C(0) compounds provided an insight into the basicity of these species (Figure 3.2). As expected, NHCs **5** displayed a high proton affinity (250–251 Kcal • mol^{-1}),[22] while carbone **6** exhibited even higher basicity in the gas phase (292 Kcal • mol^{-1}).[23] The proton affinity of

cationic N(I) compound **1** was significantly lower (121 Kcal • mol^{-1}), which confirmed the already reported computational findings.[23] Interestingly, neutral N(I) species **3** demonstrated a similar proton affinity compared to NHCs (254 Kcal • mol^{-1}), which strongly suggests that this class of compounds may be potentially used in metal complex formation and Lewis or Brønsted base catalysis.[19]

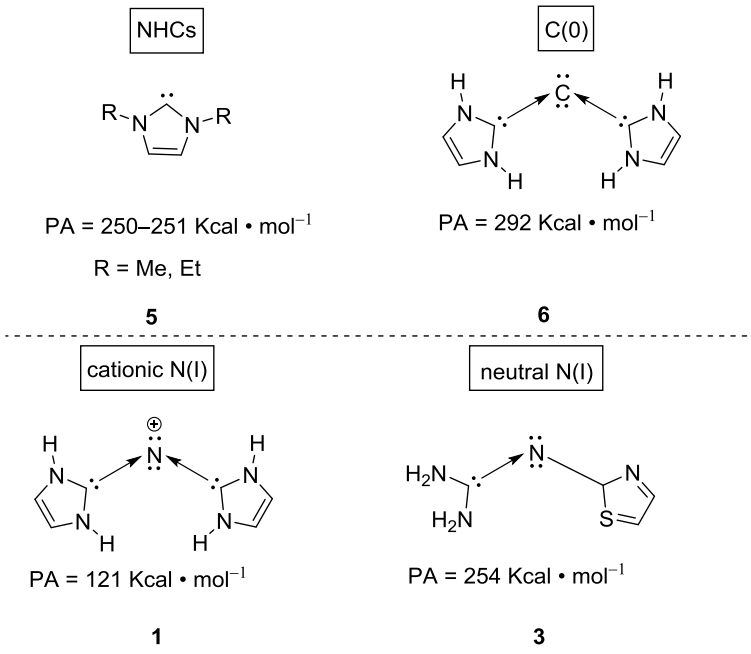

Figure 3.2: Proton affinities of cationic and neutral N(I) compounds compared to C(II) and C(0) species.[19,22,23]

In the same study, various ligand candidates were examined (Scheme 3.2).[10] As it has been already stated, the ligand has to be both a strong σ donor and poor π acceptor for a 'formal localization' of two lone pairs at the central nitrogen atom. Carbenes are ideal candidates for this purpose: two 6- and 5-membered ring NHCs and one BAC were selected for the synthesis of N(I) compounds **7**–**9**. The mesityl group was selected as an 'anionic' substituent (Ar^{-}), since it hardly affects the donor ability of the molecule. In all cases, the corresponding rhodium–N(I) complexes were prepared and their stretching CO frequencies were studied using IR spectroscopy. The donor ability of the carbene ligands was remarkable in all three complexes, however, the BAC ligand proved to be the best option (**9**).

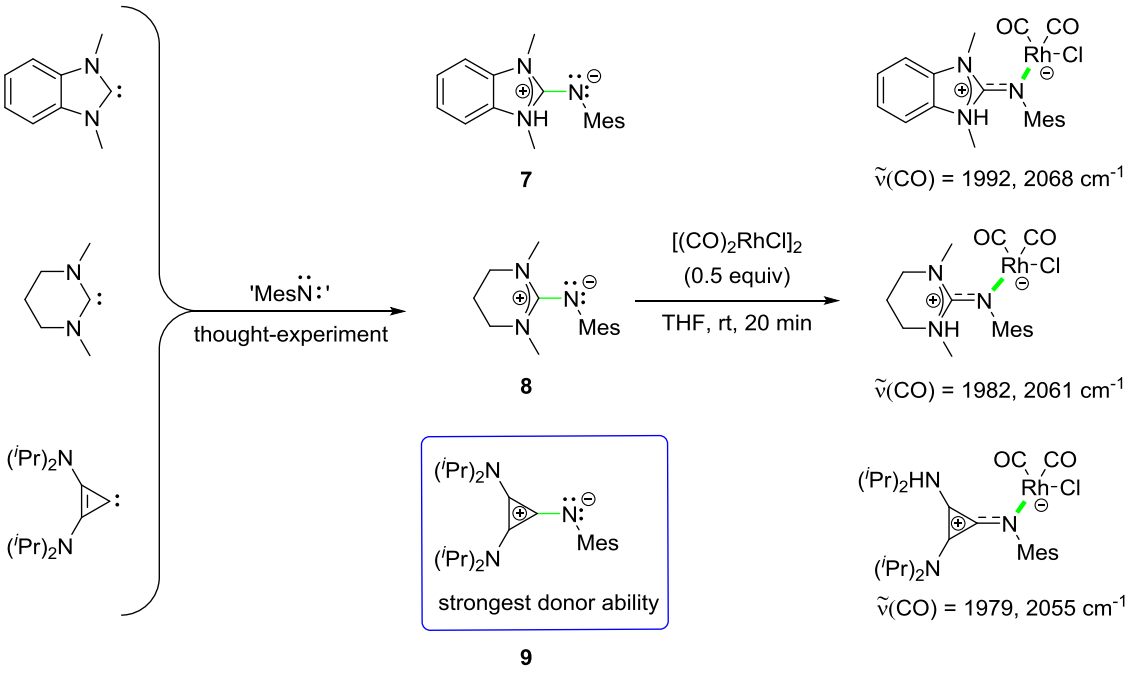

Scheme 3.2: Direct comparison of NHCs and BACs as σ donors using the same Ar substituent.[10]

The investigations in the field of nitreones were expanded to bidentate N(I) species (Scheme 3.3). As early as 1979, Appel *et al.* reported the synthesis of compound **10**,[24] which was described as a molecule bearing two P=N double bonds and an N–N single bond. More recently however, Frenking *et al.* reported a computational study, which indicated rather a nitrogen(I) bonding environment for both nitrogen atoms with two lone pairs at each nitrogen atom and a phosphine ligand being coordinated to each nitrogen center.[25] It is noted that in compound **10** there is no linker between the two nitrogen atoms and the two phosphine ligands. Based on X-ray crystallography studies, the two ligands are in an *anti*-periplanar arrangement.[25] More recently, Alcarazo *et al.* have synthesized N(I) compound **11**.[20] In contrast to Appel's molecule, a two-carbon unit was chosen as a linker between the two electron-rich nitrogen atoms; moreover, a cyclopropenylidene ligand was selected to replace the phosphine. Interestingly, X-ray crystallographic studies confirmed that **11** should be represented as a '*cis*-like' geometric isomer.[20]

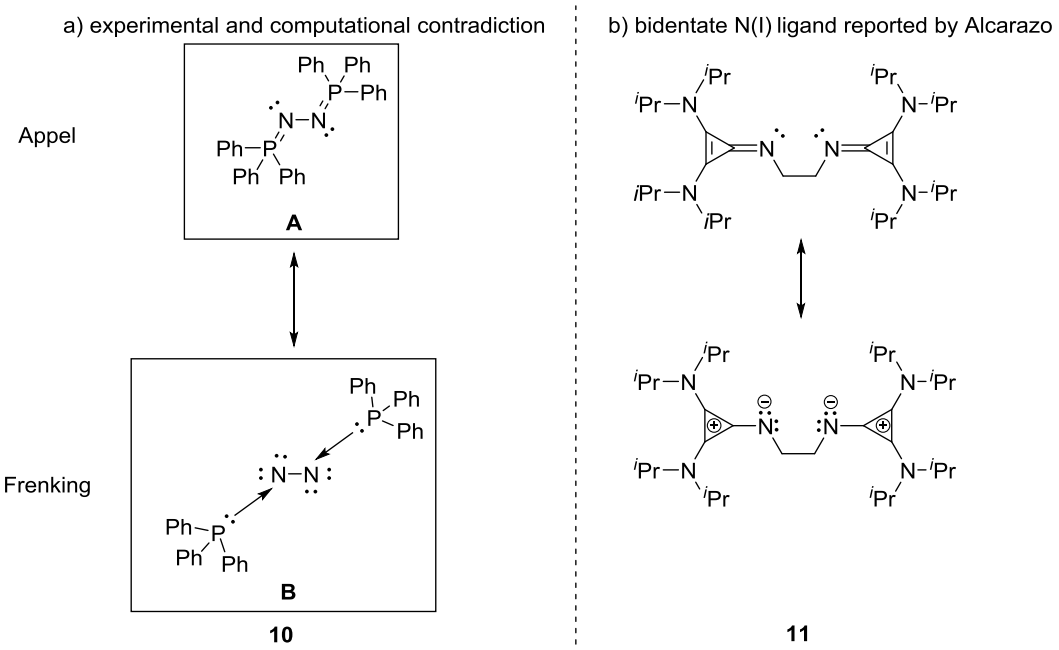

Scheme 3.3: Bidentate N(I) species reported by Appel and Alcarazo.[10,24,25]

3.1.1.3 Synthetic Routes to Cyclopropenimines

In 1984, Kreb *et al.* reported the first synthesis of a cyclopropenimine using a [2+1] cycloaddition between diamino-substituted alkynes and aryl isocyanides (Scheme 3.4).[26] It is notable that a high reaction temperature was required to afford the corresponding cyclopropenimines in low to moderate yields in most cases. Furthermore, free carbenes as side-products were shown to be formed *in situ* followed by the decomposition in the presence of oxygen or water traces. Indeed, this side-reaction increased the level of difficulty in the purification process.

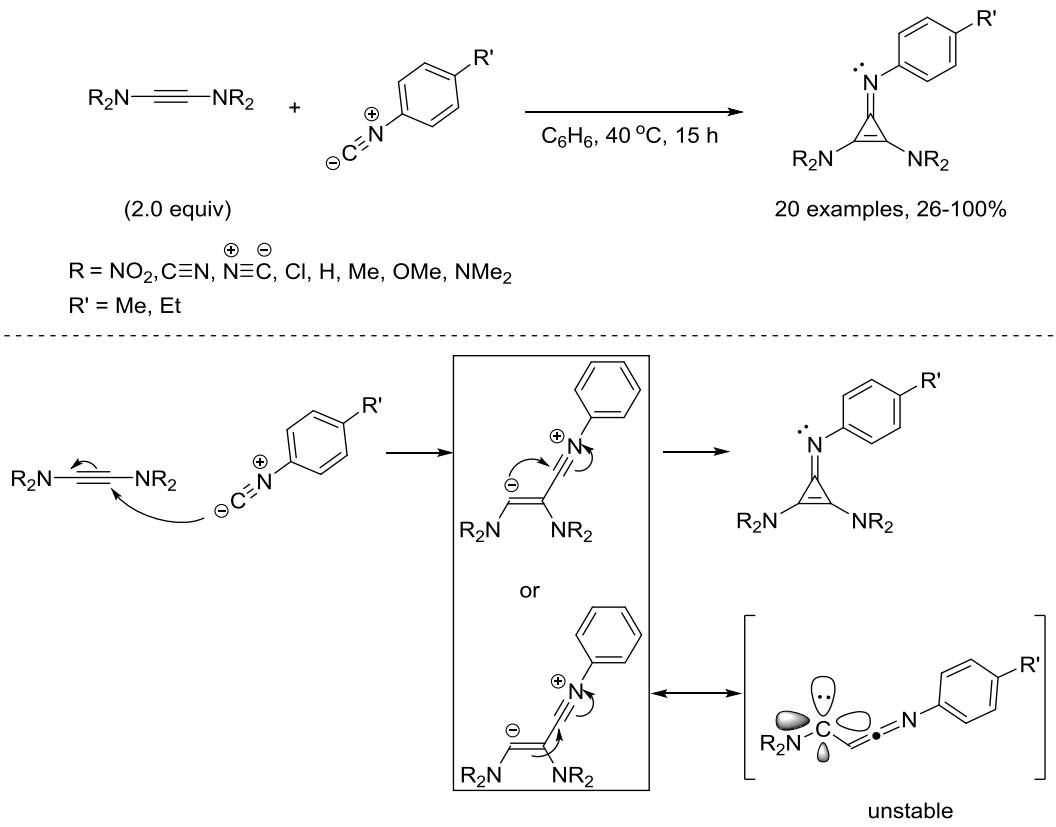

Scheme 3.4: One-step synthesis of N(I) compounds reported by Kreb.[26]

In 1987, Eicher *et al.* reported a two-step process for the synthesis of cyclopropenimines (Scheme 3.5).[27,28] The condensation of commercially available cyclopropenones with primary amines mediated by Meervein's reagent gave a range of the corresponding cyclopropeniminium tetrafluoroborate salts. The latter were deprotonated by Hünig's base at low temperature to form the 'free' cyclopropenimines. The work-up including recrystallization required the use of dry solvents. Typically, the isolated cyclopropenimines were reported to be not particularly stable even under an inert atmosphere. As storage at –30 °C was not ideal, and such issues may render the target compounds less attractive as potential novel catalyst systems.

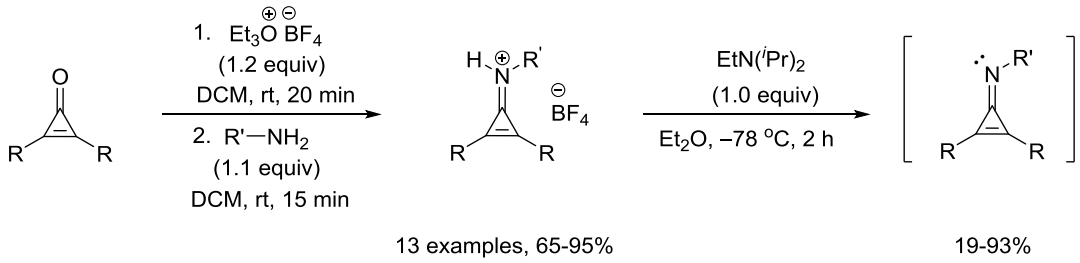

R = cyclopentyl, Me, Ph, 4–Me–Ph, Mes.

R' = Ph, 4–Me–Ph, 4–MeO–Ph, 4–CF_3–Ph, 4–CN–Ph, 4–NO_2–Ph, 2–pyrimidyl.

Scheme 3.5: Two-step process for the synthesis of cyclopropenimines reported by Eicher.[27,28]

In 2010, Alcarazo *et al.* reported a straightforward, high-yielding three-step synthesis of cyclopropenimines (Scheme 3.6).[10] The commercially available tetrachlorocyclopropene underwent double nucleophilic substitution by an excess of a secondary amine. Two equivalents of the amine were required for one chloride leaving group: the nucleophilic substitution of the latter and quenching of the released HCl. After an anion exchange between the chloride anion and tetrafluoroborate, the 3-chlorocyclopropeniminium tetrafluoroborate salt was formed. In the next step, two equivalents of a primary amine were used for the condensation with the chlorocyclopropeniminium salt and the quenching of the released HCl. Finally, the corresponding precursor was deprotonated using potassium hydride to afford the corresponding cyclopropenimines in 80–97% yield. The products proved to be stable under an inert atmosphere for more than two years. It is notable that a variety of *N*-substituted cyclopropenimines were prepared as well.

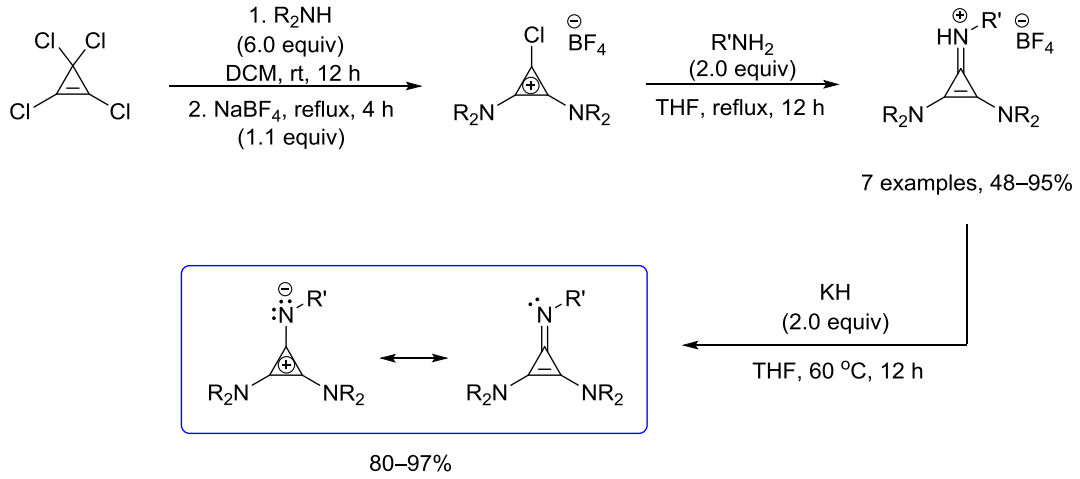

Scheme 3.6: Three-step process for the preparation of N(I) compounds reported by Alcarazo.[10]

3.1.2 Reactions of Cyclopropenimines

3.1.2.1 Stoichiometric Applications

In the course of metal coordination studies, Alcarazo *et al.* synthesized mono-aurated complexes of neutral nitrogen(I) compounds (R = 1-pyrrolidine or mesitylene).[10] The N(I) compounds were treated with one equivalent of a gold(I) salt in THF at room temperature for two minutes to form the intended metal complexes in 76% and 84%, respectively (Scheme 3.7).

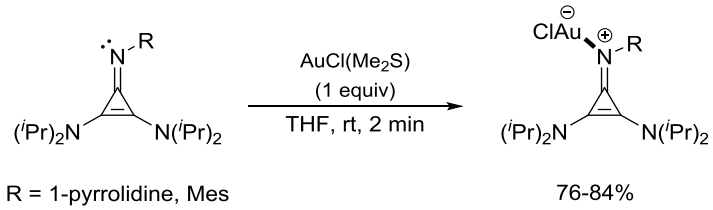

Scheme 3.7: Synthesis of gold complexes using monodentate N(I) ligands.[10]

The donor ability of cyclopropenimines was further studied with Rh(I) species. In the solid state, the various bond lengths of structures **12**, **13**, and **14** were measured and compared (in color; Scheme 3.8).[10] Regarding cyclopropeniminium tetrafluoroborate **12**, the bond lengths of the cyclopropene unit were shown to be similar, which suggested that the positive charge was delocalized; in turn, resonance form **12** seemed more likely than resonance form **12'**. After deprotonation, the C=N double bond was shown to be substantially shorter, while the three-membered ring lost its 2π aromaticity; indeed, two longer and one shorter C–C bonds were observed (1.420 Å, 1.411 Å, and 1.371 Å, respectively). The resonance forms of the 'normal' imine (**13'**) and the 'zwitterionic neutral' amide (**13**) can be drawn. In structure **13**, the nitrogen atom contains two lone pairs and is thus negatively charged, while the cyclopropene ring is positively charged. After the formation of the corresponding rhodium(I) complex, the cyclopropenimine unit proved to regain its aromaticity and the C–N bond was shown to be elongated, which strongly indicated that resonance form **14 s**hould be more 'populated' than **14'**.[10] The cyclopropene ring may be considered as an electron sink upon coordination to a Lewis acid; the imine species counterbalances the electron density delivered to the Lewis acid by regaining aromaticity and pushing electrons to the nitrogen atom (structure **14**).[10] This effect nicely explains the fact that in the course of calculations the central nitrogen remains negatively charged, and this charge is increased after the metal complexation.

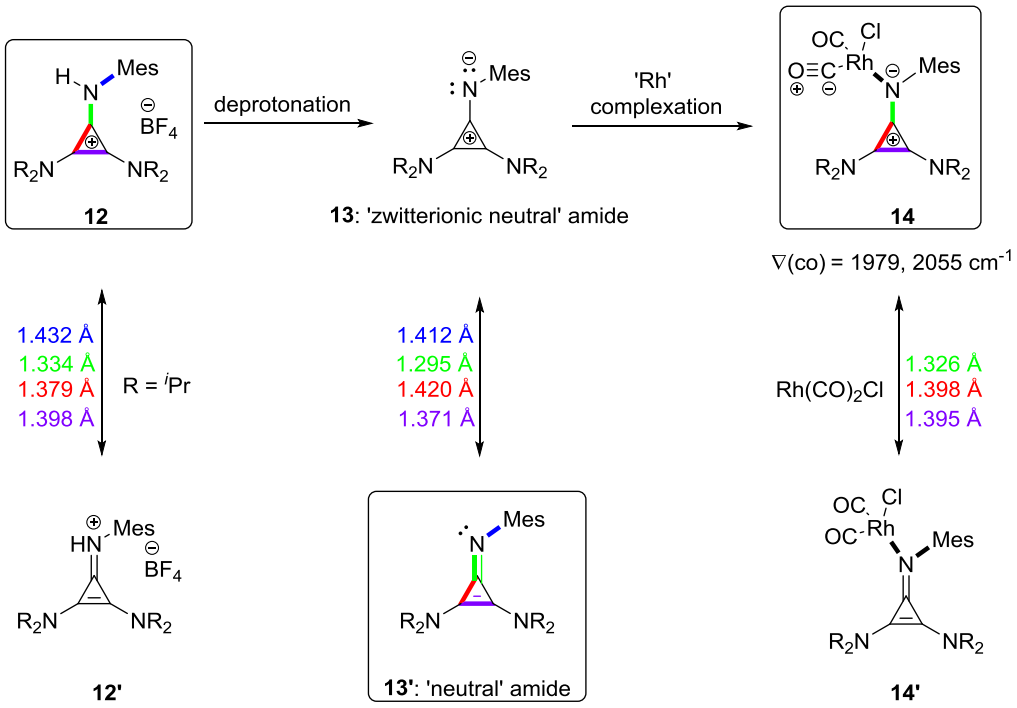

Scheme 3.8: Bond lengths of pre-N(I), N(I), and N(I)–metal complex species.[10]

Further studies with bidentate cyclopropenimine ligand **11** provided further insight into the electronic properties of these cyclopropenimines and confirmed their outstanding σ donor ability (Scheme 3.9).[10] **11** was exposed to two equivalents of $PdCl_2(MeCN)_2$ to form dipalladated complex **15**. X-ray crystallographic studies confirmed that each nitrogen atom coordinated to both palladium centers.[10] However, in the final structure, there was overall an equal number of nitrogen and palladium atoms. To the best of our knowledge, dimetallation of a monodentate nitrogen(I) species has not been reported to date.

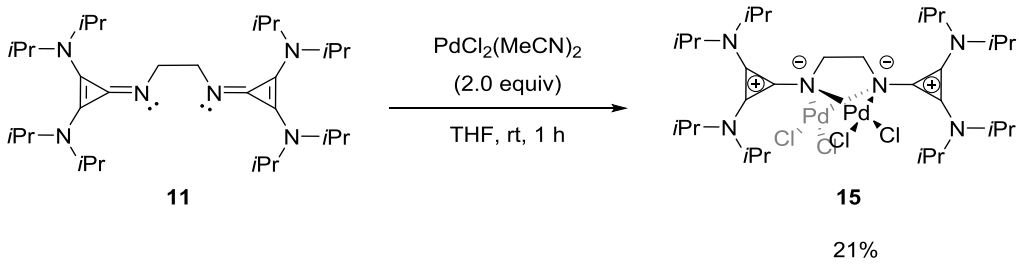

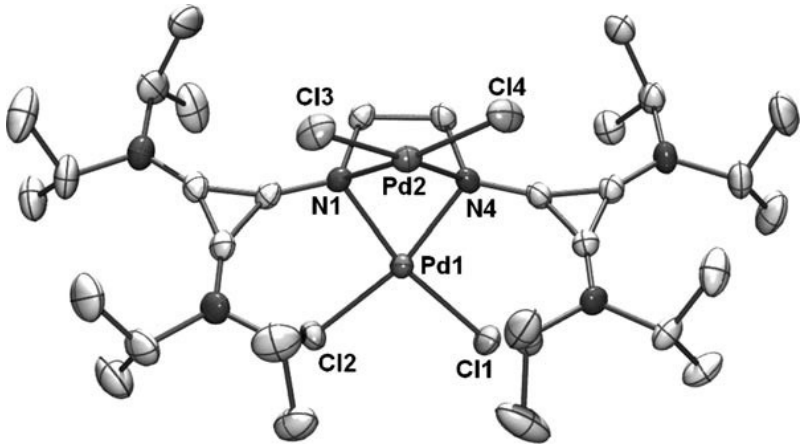

Scheme 3.9: Synthesis and X-rays of the dipalladated complex **15**.[10]

The availability of two lone pairs at the central nitrogen atom of these neutral nitreones, or cyclopropenimines, for chemical reactivity was further investigated (Scheme 3.10). Cyclopropenimine **16** was submitted to *N*-methylation using two equivalents of Meerwein's reagent, and dimethylated salt **18** was obtained.[10] The reaction was carried out step-wise; initially, **16** was exposed to one equivalent of Meerwein's reagent at 0 °C to form **17** in 84% yield. Next, **17** was treated with an extra equivalent of Meervein's reagent and refluxed in DCM to give **18**. These slightly harsher conditions seem to be required for the activation of the second lone pair. The dimethylation of the cyclopropenimine represented a formal proof of principle for the central dibasic nitrogen atom.

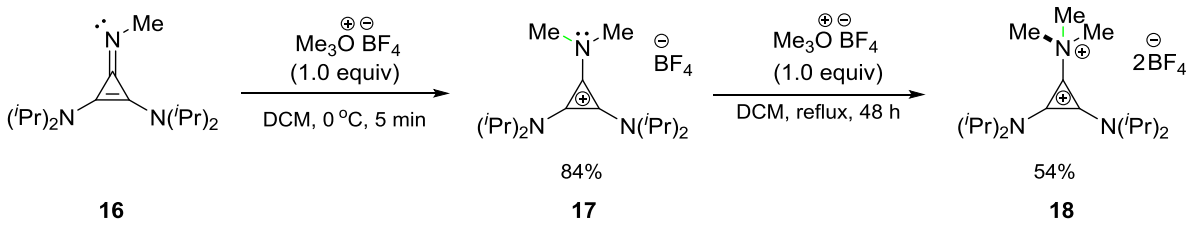

16 **17** **18**

Scheme 3.10: Dimethylation of N(I) compound **16**, illustrating the two lone-pair character at the central N atom.[10]

Overview

Due to the higher σ donor ability of bis(dialkylamino) cyclopropenylidenes (BACs) compared with *N*-heterocyclic carbenes (NHCs), the former were preferred as ligands for the central nitrogen atom in the proposed catalyst structure (Figure 3.3).[10] Similarly to **13**, Appel's compound **10** displayed outstanding proton affinity (245 Kcal • mol^{-1}; reported by Frenking *et al.*); however, it proved to be extremely air– and moisture–sensitive thereby raising issues for its use as a potential catalyst.[29] The information reported by Alcarazo *et al.* for bidentate ligand **11** was limited, therefore it was decided to study the catalyst potential of cyclopropenimines of type **13**, as these have been used in metal complexation studies by Alcarazo *et al*.[10]

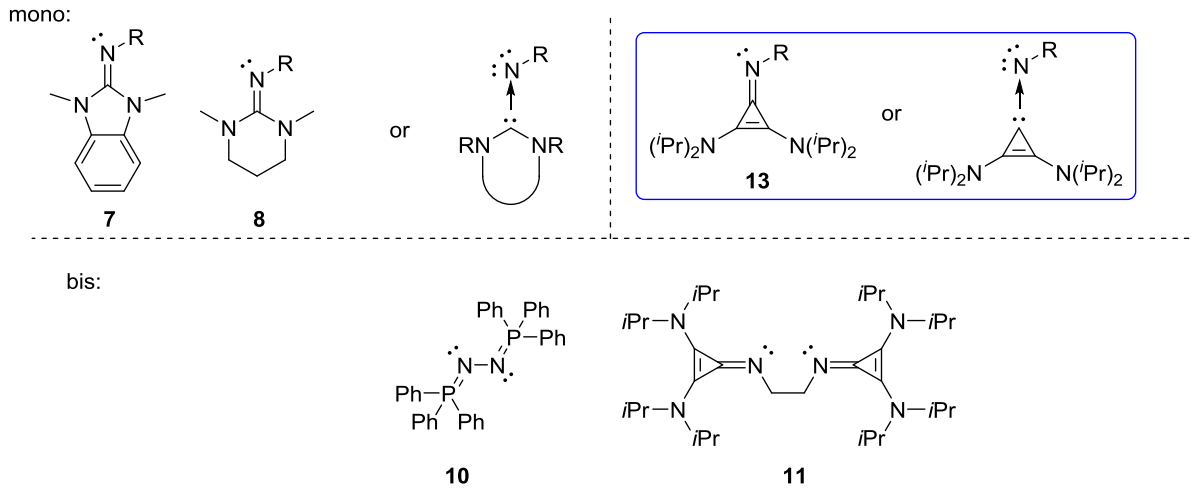

Figure 3.3: Overview.

At the outset of our project a single literature report on asymmetric Brønsted base catalysis using enantiopure cyclopropenimine **19** had been published by Lambert *et al.* (Scheme 3.11).[30] The pK_a value of the corresponding cyclopropeniminium ion (25–30; MeCN)[30] was reported to be higher than the one of the conjugate acid of guanidinium ions (22–24; MeCN),[31] i.e., a cyclopropenimine should be a stronger base than a guanidine. This tendency may be ascribed to the donor ability of the dialkyl amino groups and the aromatic character of the 'neutral zwitterionic' amide form of the cyclopropenimine core. Considering that the pK_a of the glycine imine-derived Schiff base is significantly lower (15–20; DMSO) the complete deprotonation of this pro-nucleophile is facilitated.

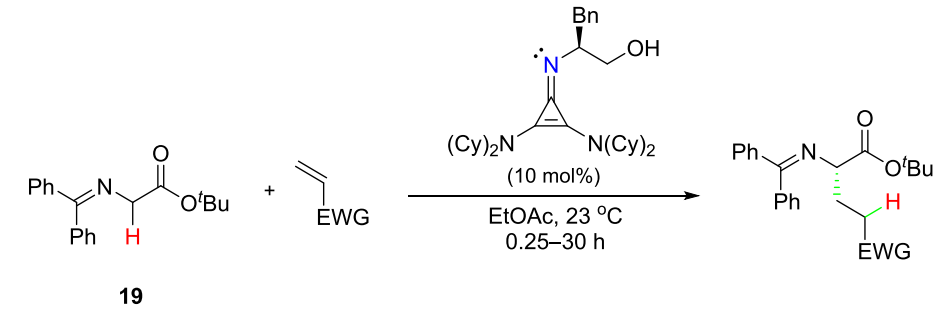

Scheme 3.11: First asymmetric catalysis with an enantiopure cyclopropenimine.[30]

3.2 Aims

Imines of type **I** are widely established as either electrophilic reagents[32,33] or σ donors (e.g. as part of salen ligands).[34–36] In contrast, the aforementioned 'unusual' imines –nitreones or cyclopropenimines of type **II**– may be drawn as two resonance forms $\mathbf{II_a}$ and $\mathbf{II_b}$ (Scheme 3.12).[10] In addition to the common imine form, experimental and theoretical studies strongly indicated that the 'zwitterionic neutral' amide form was also reasonable. Therefore, cyclopropenimines may be described with two lone pairs at the central nitrogen atom, which renders them more electron-rich compared to 'normal' imines. On the other hand, anionic metal amides such as LDA are established stoichiometric Brønsted basic reagents with only few catalysis examples reported.[37–40] The presence and identity of the metal cation proved to be critical for the outcome of several reactions.[39,40]

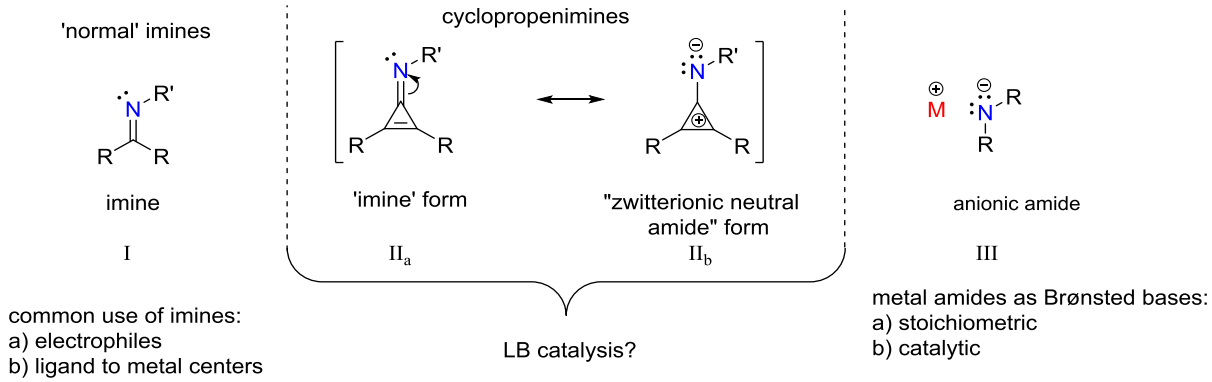

Scheme 3.12: Comparison of cyclopropenimines with 'normal' imines and anionic amides.

Based on the outstanding donor ability of cyclopropenimines, our aim was to investigate their potential in Lewis base catalysis [Scheme 3.13 a)]. This concept included activation of Lewis acidic pro-nucleophiles and subsequent addition to a suitable electrophile. In addition, dual catalysis was one of our goals considering that metal complexes of N(I) compounds provide a Lewis acidic centre (metal) and potentially a Lewis basic centre [a second lone pair at the nitrogen atom; Scheme 3.13 b)]. The metal centre may activate a basic electrophile, while the Lewis basic nitrogen may activate a Lewis acidic pro-nucleophile for subsequent bond formation. Furthermore, a potential frustrated Lewis pair (FLP) catalysis using an N(I) compound was anticipated [Scheme 3.13 c)].[41–43] The state, that an interaction between a Lewis base and a Lewis acid is *not* observed due to steric congestion of one or both reaction

partners, is called ‘frustration’; it has been reported that such a frustrated Lewis pair can potentially cause heterolytic cleavage of strong σ bonds X–Y to form two more active species available for follow-up chemistry.[44,45] This concept has been rapidly expanding due to its great potential in the activation of small molecules, including catalysis.

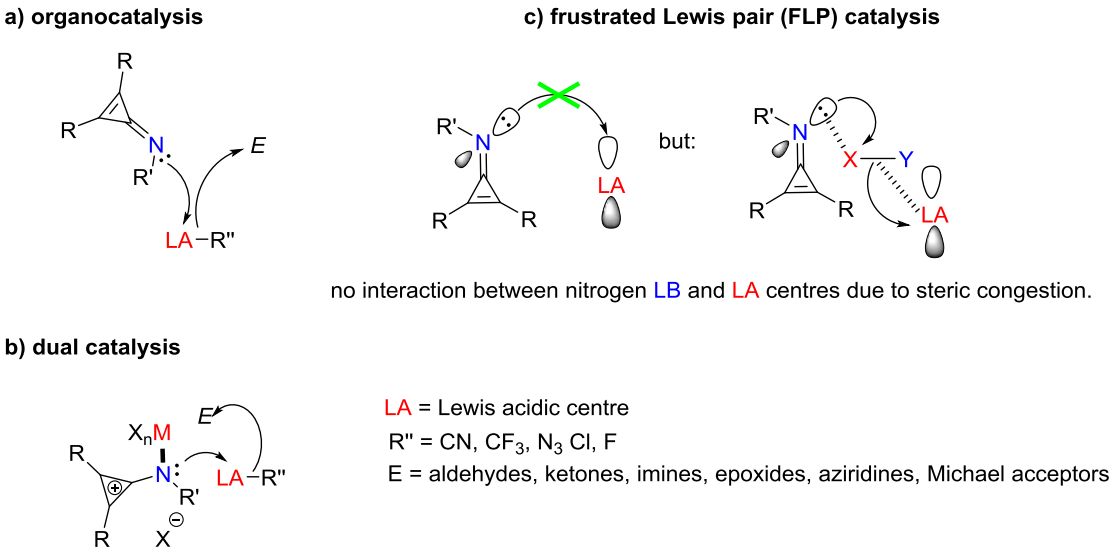

Scheme 3.13: Aims.

3.3 Results and Discussion

In this sub-chapter, new methodologies in the field of organocatalysis, especially Lewis base catalysis, will be presented (Scheme 3.14). Cyclopropenimines were used as a Lewis base catalyst for the activation of silylated pro-nucleophiles, such as trimethylsilyl cyanide, Ruppert's reagent, trimethylsilyl azide, and trimethylsilyl chloride. According to our concept, the cyclopropenimine (LB) would add to the Lewis acidic silicon atom (LA–R) to release the corresponding R^- group; the latter would subsequently add a neutral electrophile (E) to form a C–C, C–N, or C–Cl bond with catalyst turnover. The selected electrophiles (E) were aldehydes, ketones, imines, and aziridines.

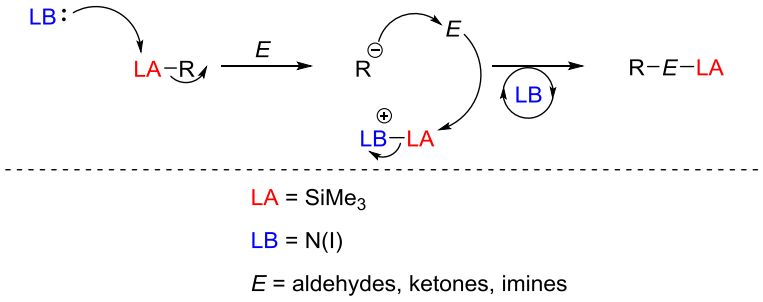

Scheme 3.14: Proposed Lewis base catalysis with a cyclopropenimine.

3.3.1 Preparation of Cyclopropenimines

Initially, cyclopropenimine **22** was prepared in a two-step process in our lab (Scheme 3.15).[27] First, the condensation of commercially available ketone **20** with aniline was carried out in the presence of Meerwein's reagent. The purified and dried cyclopropeniminium salt **21** was isolated in 75% yield. The deprotonation of **21** occurred under an inert atmosphere with KHMDS (0.95 equiv) in acetonitrile at room temperature. The N(I) compound **22** was used *in situ* for catalysis due to instability issues.[27] The full consumption of KHMDS was confirmed by ^{1}H NMR spectroscopy.

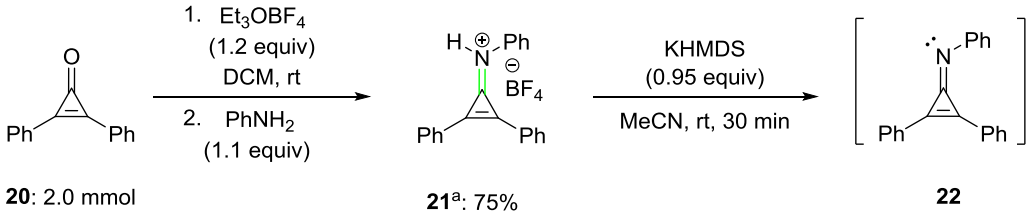

[a] Reaction performed by Jonathan Richards

Scheme 3.15: Two-step process for the preparation of Eicher's compound.[27]

A library of additional N(I) precursors was prepared following Alcarazo's methodology (Figure 3.4).[10] In contrast to **22**, the deprotonation of the Alcarazo-type N(I) precursors would form cyclopropenimines that could be isolated and stored under an inert atmosphere for long-term use. First, our aim was to modify the R groups attached to the nitrogen atoms in the backbone of the catalyst. For this purpose, catalysts were prepared bearing isopropyl and cyclohexyl groups. Lambert *et al.* reported that the use of cyclopropenimines with the sterically demanding dicyclohexyl amino substituent led to higher yields and asymmetric induction compared to a diisopropyl amino group.[30,46] However, the steric bulk provided by dicyclohexyl groups may inhibit the activation of a sterically bulky pro-nucleophile. Second, we were interested in modifying the R' groups directly attached to the central nitrogen atom. In turn, a wide range of catalyst precursors with aliphatic and aromatic groups attached to the Lewis basic nitrogen atom have been synthesized. The steric bulk placed in vicinity to the nitrogen atom may be critical for the activation of a pro-nucleophile.

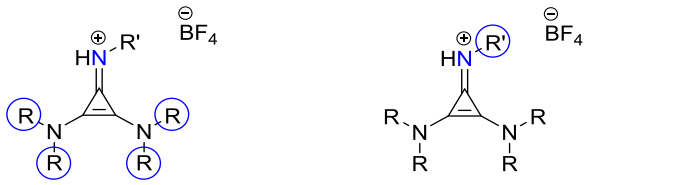

Figure 3.4: Synthesis of several N(I) precursors varied at R and R' groups.

The preparation of cyclopropenimines was achieved in a fairly starightforward process.[47] In the first step, the commercially available tetrachlorocyclopropene (**23**) underwent double nucleophilic substitution with an excess of a dialkyl amine (R = isopropyl or cyclohexyl; Scheme 3.16). The excess was required in order to trap the hydrogen chloride released during the course of the reaction. When the reaction reached completion, sodium tetrafluoroborate was added for an anion exchange with chloride; initially, the mixture was stirred for 12 h at room temperature and then was refluxed for 4 h. Large-scale batches were prepared by this

method, and isolated in 80% and 87% yields, respectively. After filtration at ambient pressure (removal of the excess of sodium tetrafluoroborate and dialkyl ammonium chloride), the solution was dried *in vacuo*. The yellow residue was washed extensively with diethyl ether to result in a colorless solid, which was recrystallized from diethyl ether. The product was stored in open air for two years without decomposition.

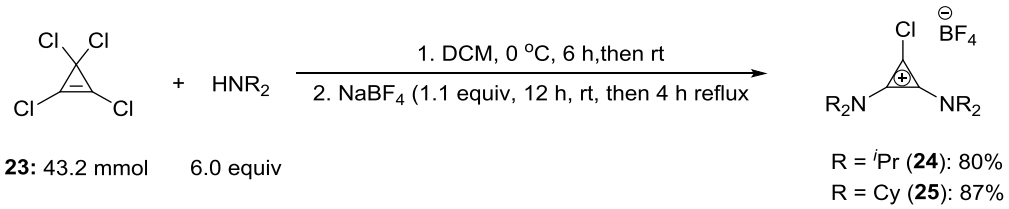

Scheme 3.16: Nucleophilic amination of tetrachlorocyclopropene.

Reflux of the chlorocyclopropenium salts **24** or **25** with a range of primary amines was carried out overnight to form the corresponding cyclopropeniminium salts **26**–**34** and **35**–**45** (Scheme 3.17 and Scheme 3.18, respectively). Again, an excess of the primary amine was used in order to quench hydrogen chloride released during the reaction. The resulting iminium salts were purified with ether, grounded using a mortar, dried under vacuum and stored in open air (67–96%).

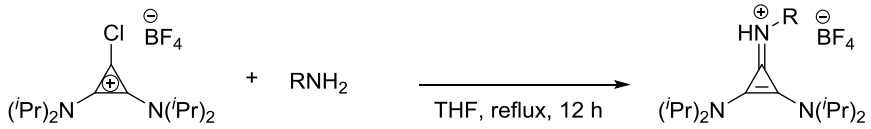

24: 11.4 mmol 2.8 equiv

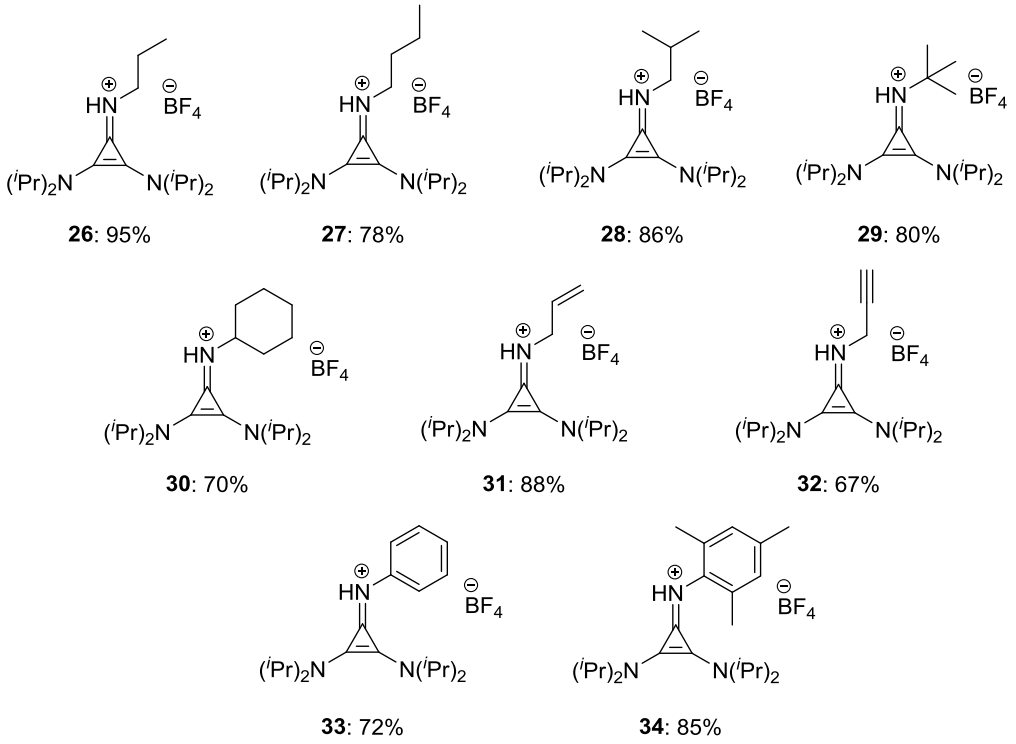

26: 95% **27**: 78% **28**: 86% **29**: 80%

30: 70% **31**: 88% **32**: 67%

33: 72% **34**: 85%

*Preparation of **26–34** was shared with Jonathan Richards

Scheme 3.17: Condensation of the cyclopropenium salt **24** with the corresponding amines.

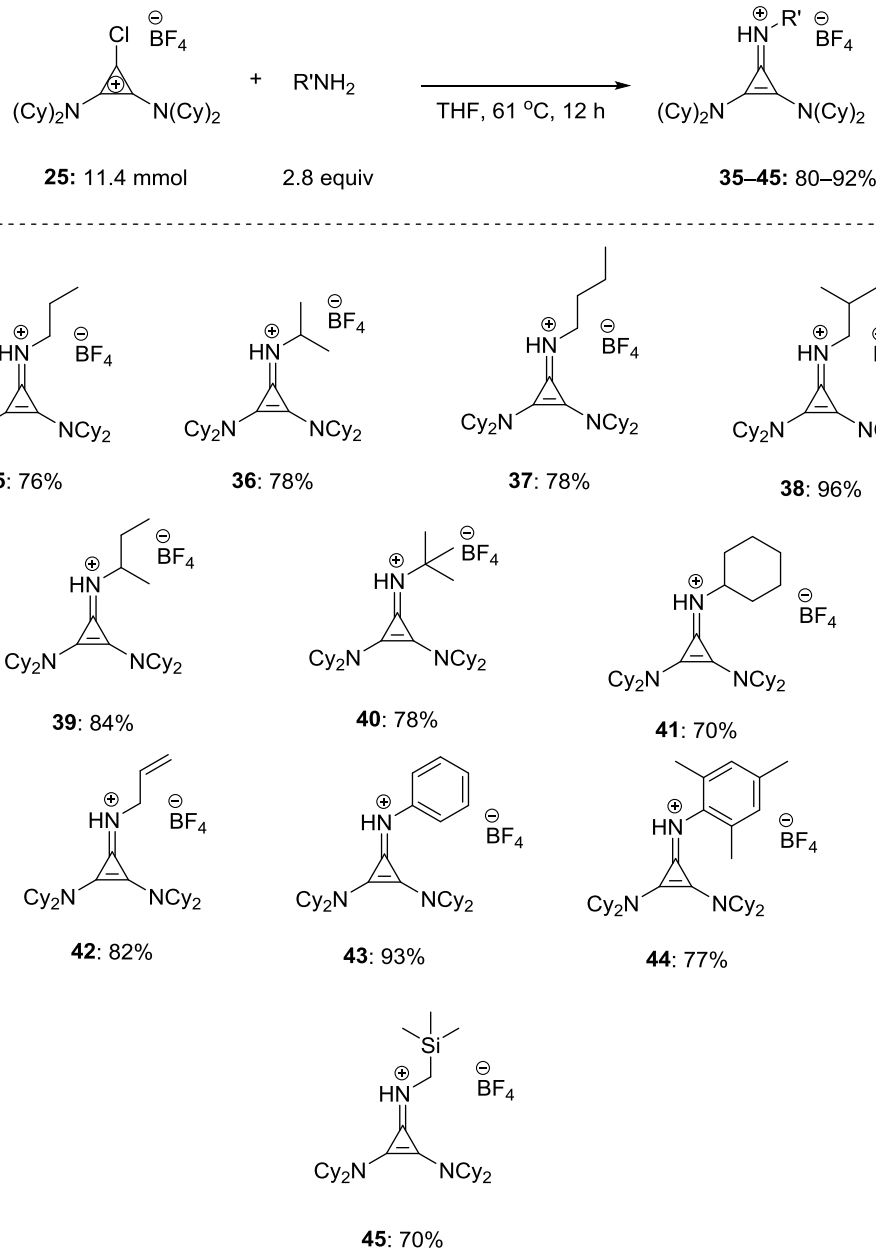

*Preparation of **35–45** was shared with Jonathan Richards

Scheme 3.18: Condensation of the cyclopropenium salt **25** with the corresponding amines.

The deprotonation of the cyclopropeniminium tetrafluoroborates was carried out using KHMDS (0.9 equiv) in THF at –78 °C for 15 min and left stirring at room temperature for one hour (Scheme 3.19). The formed by-product, potassium tetrafluoroborate, was removed by filtration through a Celite layer on a sintered frit and the volatiles were removed *in vacuo* under an inert atmosphere to give cyclopropenimines **46**–**51** in 86–97% yields. The resulting cyclopropenimines were stored under an inert atmosphere for more than two years without decomposition.

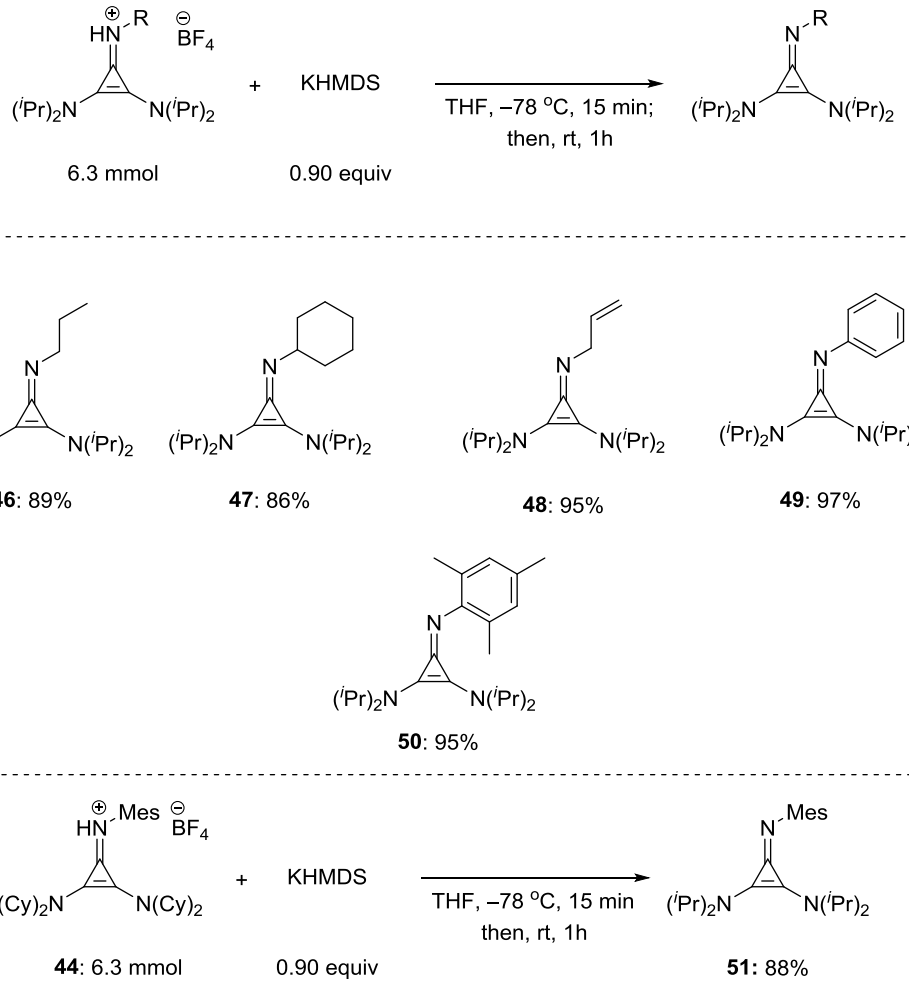

*Preparation of **46–51** was shared with Jonathan Richards and Peter Neate

Scheme 3.19: Deprotonation of the iminium salt using KHMDS.

With these cyclopropenimines in hand, we aimed to explore these as a Lewis base catalyst (Scheme 3.20). Indeed, cyclopropenimines may add to the Lewis acidic silicon atom of the pro-nucleophiles to trigger the release of the cyanide ion. The latter may add to an electrophile (aldehydes, ketones, imines) to generate a nucleophilic species, such as the corresponding alkoxide or amide, which may be trapped by the *in situ* generated silylium species to provide the silylated product with simultaneous regeneration of the cyclopropenimine catalyst.

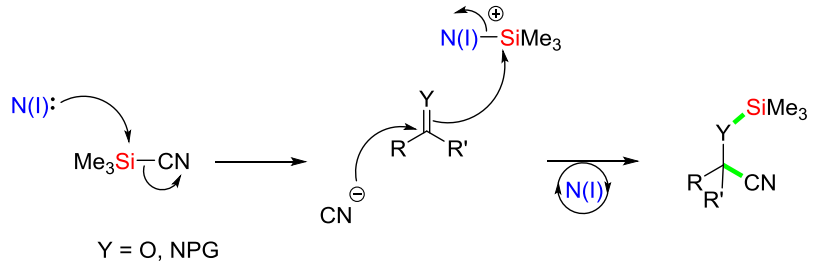

Scheme 3.20: Potential catalytic cycle to generate the intended silylated product in cyanation.

3.3.2 Cyclopropenimine-Catalysed Cyanation of C=O and C=N Electrophiles

3.3.2.1 Literature-Reported Metal- and Lewis Base-Catalysed Cyanation Methods

Several examples of metal-catalyzed cyanation of carbonyl electrophiles and imines have been reported. Indeed, metal salts based on Li,[48] Ti(IV),[49–51], Ru(II),[52] Al(III),[53,54] and La(III)[55] combined with chiral ligands have been used to induce asymmetry within the cyanohydrin products. For example, Feng *et al*. reported the cyanation of aldehydes, ketones, and imines using a Ti(IV) catalysts combined with chiral ligands **52** or **53** to give protected cyanohydrins or α-amino nitriles in good yields with high asymmetric induction (Scheme 3.21).[51] Isopropanol was critical as an additive, since the 'real' cyanide source proved to be HCN and *not* trimethylsilyl cyanide.

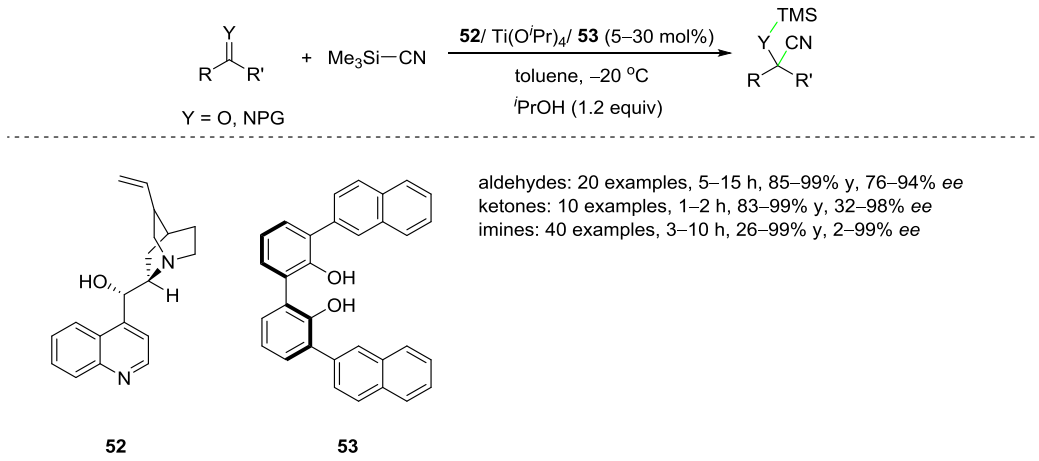

Scheme 3.21: Lewis acid-catalyzed cyanation of carbonyl compounds and imines developed by Feng.[51]

In contrast to metal catalysis, Lewis base-catalyzed cyanation was shown to be limited to the use of Verkade's bases (**54**) and an NHC (**55**; Scheme 3.22).[56–58] In the first case, the carbonyl electrophiles were treated with trimethylsilyl cyanide (1.2 equiv) and 5–10 mol% of a Verkade base at 0–25 °C to give the corresponding product in 83–98% yields. Since Verkade bases are very strong bases, cooling to 0 °C was required. In addition, long reaction times were

necessary in several cases. In the second case, the NHC-catalyzed cyanation of carbonyl compounds and imines under mild conditions provided the products in 33–99% yields. Here again, long reaction times were required in several cases. It is noted that in both publications a limited scope with poor functional group (FG) tolerance and *no asymmetric versions* have been reported.

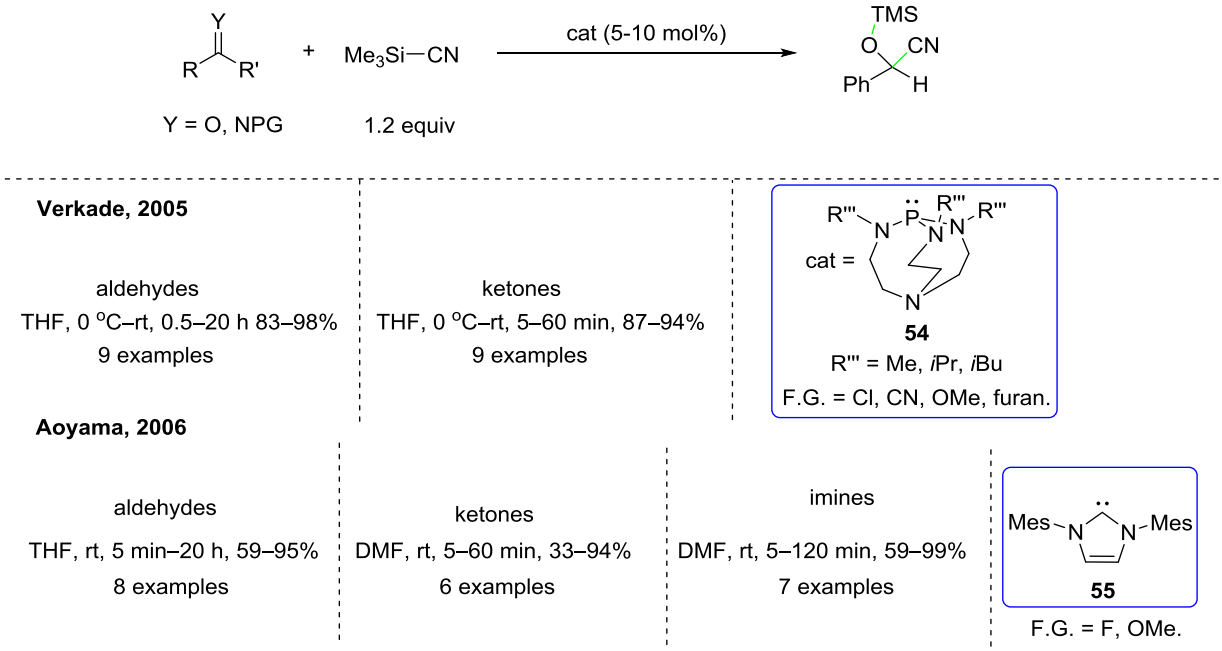

Scheme 3.22: Lewis base-catalysed cyanation of carbonyl compounds and imines.

In contrast to the literature reports, we aimed to develop a metal-free methodology for the catalytic cyanation of a broad variety of electrophiles with a considerably improved functional group tolerance.

3.3.2.2 Initial Lead – Metal-Free Cyanation of Benzaldehyde

First, the cyclopropenimine-catalyzed cyanation of benzaldehyde using trimethylsilyl cyanide as a pro-nucleophile in acetonitrile at 25 °C was investigated [Scheme 3.23 a)]. The *in situ* preparation of cyclopropenimine catalyst **22** was carried out using precursor **21** and KHMDS (0.95 equiv). The catalytic cyanation proceeded smoothly to give cyanation product **56** in 99% NMR yield after 1 h. The NMR yield was calculated using a dibenzyl ether (DBE) in mesitylene (25 mol%) as an internal standard [Scheme 3.23 b)]. The molarity was selected in view of convenience for the integration of the ^{1}H NMR signals, since dibenzyl ether has 4 equivalent benzylic hydrogen atoms with a chemical shift at 4.6 ppm, while the benzylic hydrogen atom of the product displayed a signal at 5.0 ppm. Despite the excellent result using **22** as a catalyst, we decided to further optimise the catalyst structure; cyclopropenimine **22** is less stable than other potential candidates and cannot be stored for long-term use. Thus, we

turned our attention to the use of isolated cyclopropenimine **49**, which may be considered as a vinylogous guanidine analogue. Under identical conditions, the use of **49** gave the product also in 99% NMR yield.

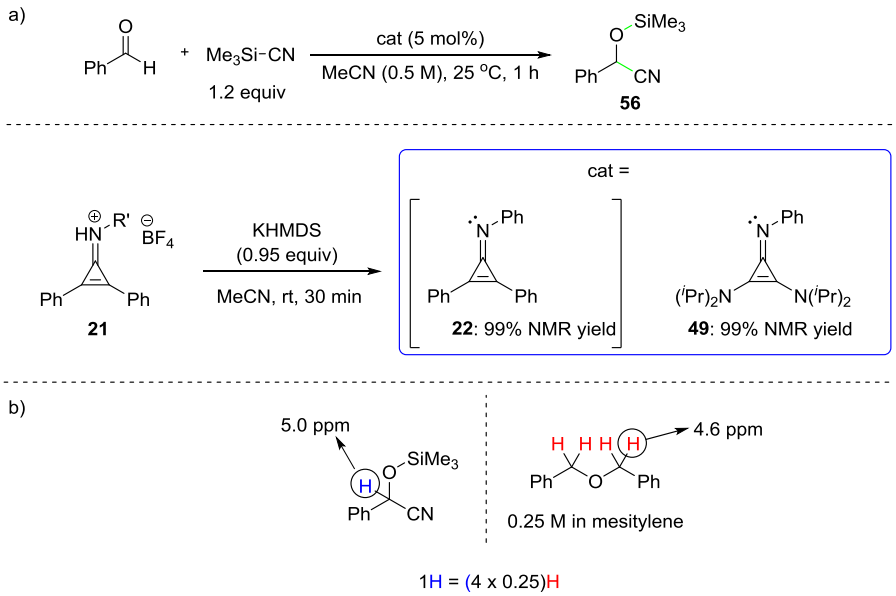

Scheme 3.23: Cyclopropenimine-catalysed cyanation of benzaldehyde.

3.3.2.3 Optimisation and Control Experiments

In order to confirm the catalyst potential of these 2π electron cyclopropenimines, control experiments were conducted with a variety of other imines as potential catalysts (Table 3.1). A library of imines **57**–**64** was prepared, including: classical aldimines and ketimines (**57**–**62),** as well as acyclic and cyclic 4π electron imines **63** and **64**. Gratifyingly, imines **57**–**64** failed to give any catalytic activity except compound **59** (*traces* of the product were detected in ^{1}H NMR spectroscopy). Due to potential instability issues encountered with catalyst **22**, we decided to continue further optimisation with the more stable cyclopropenimine **49**.

Table 3.1: Screening of various imines as catalysts.

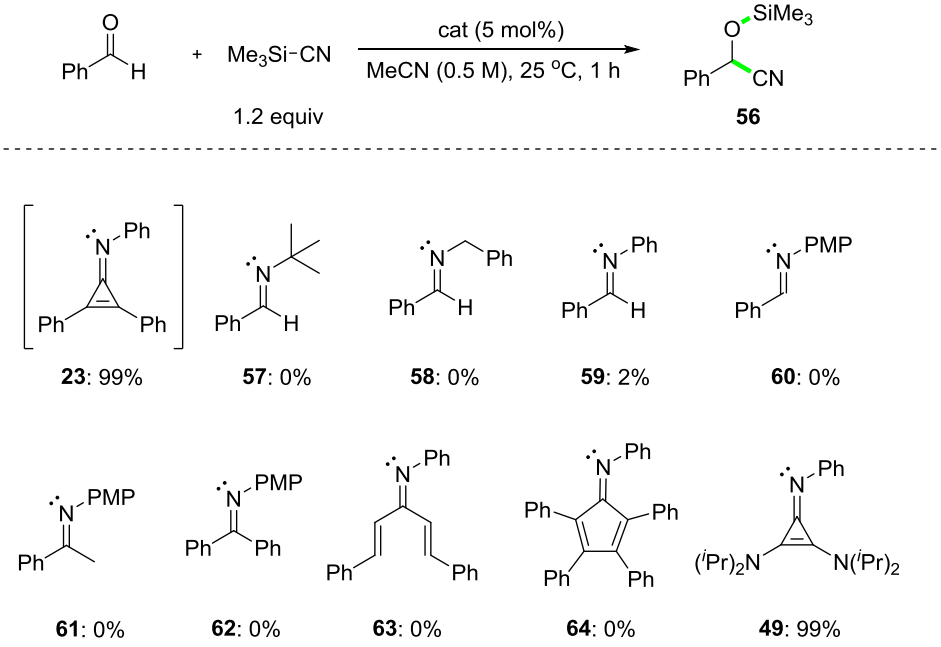

The yield was determined by ^{1}H NMR spectroscopy of the reaction mixture; internal standard: dibenzyl ether (25 mol% in mesitylene).

A solvent screening clearly indicated that various polar and apolar solvents were tolerated by the catalyst system to provide the cyanation product in >95% conversion after 1 h (Scheme 3.24). The screening included dioxane, toluene, diethyl ether, ethyl acetate, tetrahydrofuran, dichloromethane, and acetonitrile. In view of convenience and future investigations into asymmetric catalysis, dioxane was selected as the solvent of choice.

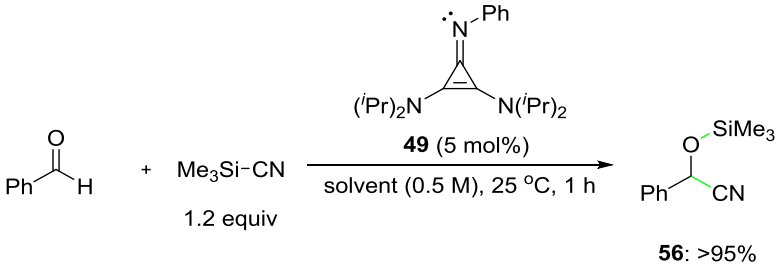

Scheme 3.24: Solvent screening for cyanation of benzaldehyde.

Catalyst **49** (R = Ph) was also directly compared with two other synthesized cyclopropenimines, **47** (R = cyclohexyl) and **50** (R = mesityl; Table 3.2). While the yields proved to be identical at 25 °C (99% NMR yield of product **65** after 5 min reaction time), analogues **47** and **50** have exhibited an increased steric demand. Therefore, in view of the

substrate scope and due to the lower price of the corresponding amine precursor, catalyst **49** was used for further studies.

Table 3.2: Screening of various cyclopropenimines as catalysts for cyanation.

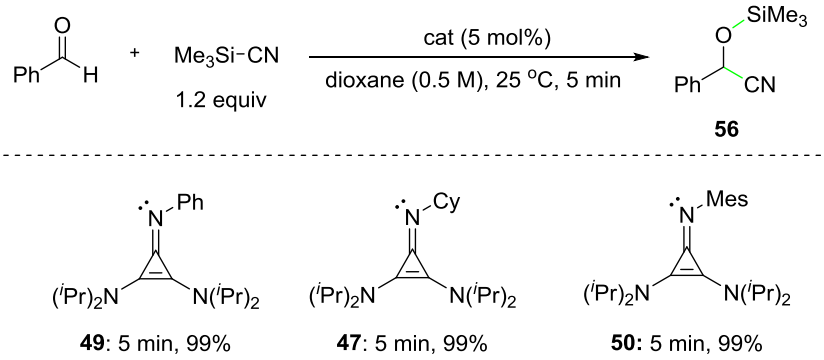

The yield was determined by ^{1}H NMR analysis of the reaction mixture; internal standard: dibenzyl ether (25 mol%).

Thus, the chosen optimized conditions required the treatment of the electrophile with trimethylsilyl cyanide (1.2 equiv) and cyclopropenimine catalyst **49** (5 mol%) at 25 °C (1 h).

3.3.2.4 Substrate Scope for Cyanation of Aldehydes and Aldimines

The optimized conditions were applied to the use of a wide variety of aldehydes to give the corresponding aromatic (**56**, **65–69**), heteroaromatic (**70–72**), and aliphatic (**73–75**) products in high ^{1}H NMR yields (Table 3.3). The novel methodology displayed excellent functional group tolerance; hydroxy, trifluoromethyl, cyano, pyridyl, furyl, and thienyl groups were tolerated by the catalytic system to give the cyanation products in ≥92% isolated yield. Products **56**, **66–69**, and **71–73** have been isolated in their *O*-acetylated form. It should be noted that all the products were *not* isolated.

Table 3.3: Cyclopropenimine-catalysed cyanation of aldehydes.

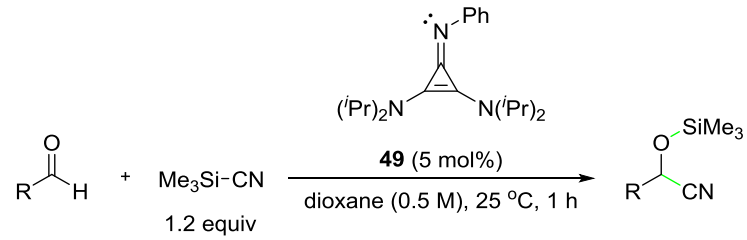

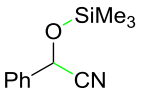

56: 99% (96%)

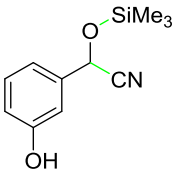

65: 99%

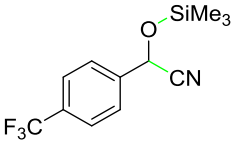

66: 99% (95%)

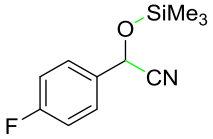

67: 99% (96%)

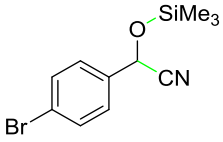

68: 99% (93%)

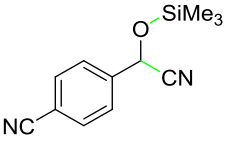

69: 99% (93%)

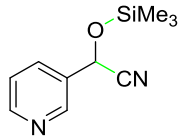

70: 93%

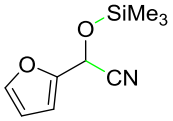

71: 94% (93%)

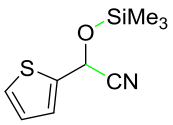

72: 99% (96%)

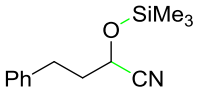

73: 95% (92%)

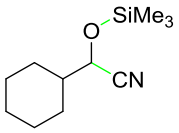

74: 96%

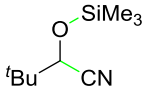

75: 99%

NMR yields were determined by ^{1}H NMR spectroscopy with DBE (0.25 M in mesitylene) as internal standard. Isolated yields of acetylated products in parenthesis.

Attempts to isolate both the silyl ethers and the corresponding 'free' alcohols –according to literature methods– failed due to decomposition of the intended products in contact with both silica gel and neutral alumina.[48,51,59,60] In turn, the silyl ethers were deprotected to the corresponding alcohols and *in situ* acetylated according to a one-pot literature report (Scheme 3.25).[49] The deprotection was carried out using a large excess of hydrogen chloride in diethyl ether at room temperature. The acetylation was conducted using acetic anhydride (2.0 equiv) and pyridine (2.0 equiv) at room temperature. The high NMR yields (≥93%) determined by ^{1}H NMR spectroscopy were reflected by high isolated yields (≥92%). The isolations of *O*-acetylated products were carried out using preparative thin-layer chromatography (PTLC) on silica gel.

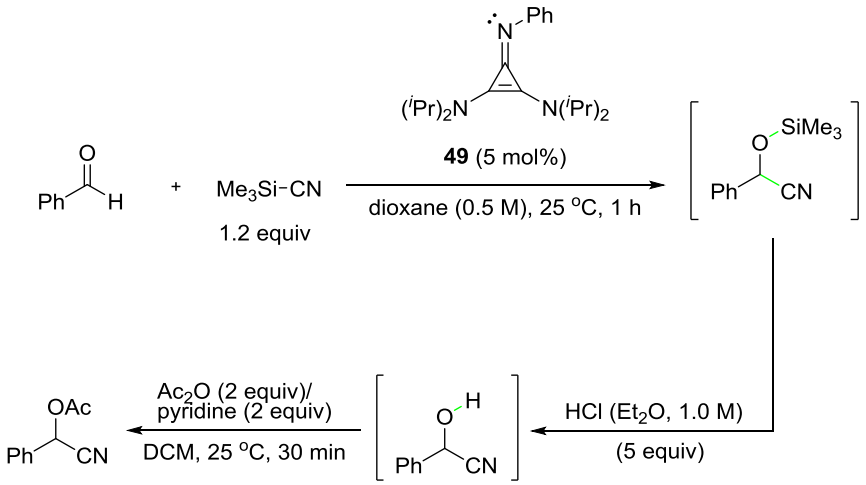

Scheme 3.25: Deprotection of silyl ethers and *O*-acetylation of the *in situ*-generated alcohols.

Encouraged by the efficiency of catalyst **49** for the catalytic cyanation of aldehydes, the use of an aldimine as electrophile was probed using *N*-tosyl aldimine **76** (Table 3.4). Under otherwise identical conditions, we initially conducted a solvent screening with various apolar and polar solvents. Here again, the use of dioxane demonstrated the highest conversion to the intended α-aminonitrile **77** (99%, entry 1), which was confirmed by a high NMR yield (96%). The use of ethyl acetate, tetrahydrofuran, and dichloromethane provided good conversions (entries 2–4), while the use of DMF and acetonitrile led to no reaction and low conversion, respectively (entries 5 and 6). It should be noted that α-aminonitriles represent an important class of precursors to *N*-protected amino acids, which displayed significant pharmaceutical activity.[61,62]

Table 3.4: Cyclopropenimine-catalysed cyanation of *N*-tosyl aldimine **76**.

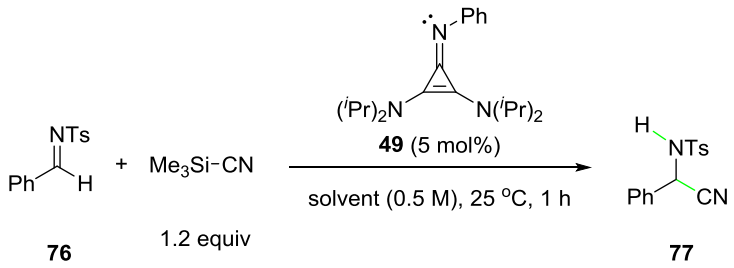

76 **77**

Entry	Solvent (ε)	Conv (%)[a]
1	Dioxane (2.3)	99[b]
2	EtOAc (6.2)	87
3	THF (7.6)	83
4	DCM (8.9)	71
5	DMF (36.7)	NR
6	MeCN (37.5)	17

[a] The conversion was determined by ^{1}H NMR spectroscopy based on the molar ratio **76**:**75**. [b] NMR yield = 96% [determined by ^{1}H NMR spectroscopy with DBE (0.25 M in mesitylene) as internal standards]

Next, we applied the optimized conditions to less reactive aldimines **78** and **79** (Scheme 3.26). At 30–40 °C, both substrates did not display any reactivity to form α-aminonitriles **80** and **81**. After heating at 60 °C for 15 hours, 14% conversion of **78** to **80** was detected by ^{1}H NMR spectroscopy. Under identical conditions, **79** remained unreacted.

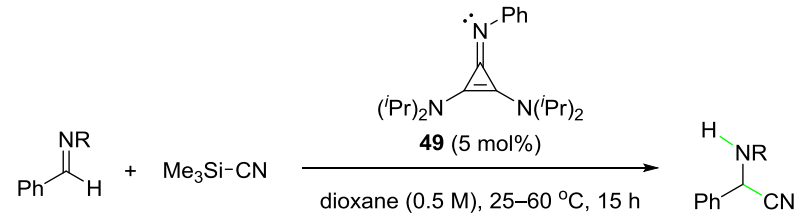

78: R = Ph
79: R = PMP
1.2 equiv

80: 14%
81: NR

Scheme 3.26: Trials to increase the aldimine scope of cyanation. PMP = para-methoxyphenyl.

3.3.2.5 Cyclopropenimine-Catalysed Cyanation of Acetophenone

Next, we investigated the reactivity of ketones using the same catalytic system and acetophenone as model substrate (Table 3.5). The initial solvent screening revealed an interesting dependence on the solvent polarity, i.e., the dielectric constant (ε) proved to be of critical importance. The use of dioxane and ethyl acetate did not lead to any detectable C–C bond formation (entries 1 and 2), while the use of THF gave a poor conversion of acetophenone (4%; entry 3). The more polar DCM provided a moderate conversion (44%;

entry 4). Gratifyingly, the use of solvents with a higher dielectric constant, such as DMF and acetonitrile led to 70% and 97% conversion, respectively (entries 5 and 6). The excellent result using acetonitrile as a solvent to generate **82** was confirmed by the highest NMR yield (97%). This outcome may be ascribed to the fact that a more polar solvent should stabilize the ionized form of the pro-nucleophile better than an apolar solvent. Thus, instead of a potential silicon–ate complex, the more reactive silylium cyanide may be formed. Control experiments in the absence of the catalyst in DMF and acetonitrile did not lead to formation of the intended product; i.e., DMF and acetonitrile did not act as Lewis bases.

Table 3.5: Cyclopropenimine-catalysed cyanation of acetophenone.

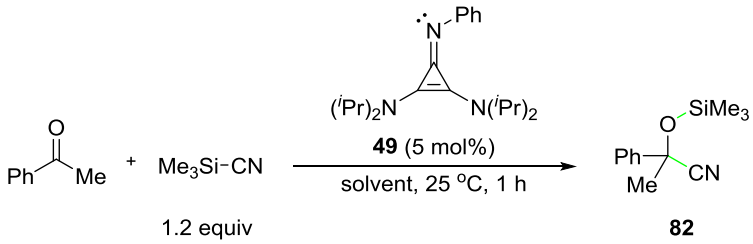

Entry	Solvent (ε)	Conv (%)[a]
1	dioxane (2.3)	0
2	EtOAc (6.2)	0
3	THF (7.6)	4
4	DCM (8.9)	44
5	DMF (36.7)	70
6	MeCN (37.5)	97

[a] The conversion is determined by ^{1}H NMR spectroscopy based on the product-to-substrate ratio.

3.3.2.6 Substrate Scope for Cyanation of Ketones

Next, the optimized conditions were applied to a variety of ketones (Table 3.6). A wide range of ketones were used and provided the aromatic (**82–86**), heteroaromatic (**87**), and aliphatic (**88**) cyanation products in excellent NMR yields in all cases (99%). The cyclopropenimine catalysis proved to tolerate various functional groups, such as trifluoromethyl, bromine, thienyl, and ester groups. Regarding the product isolation, silyl ethers were *in situ* converted to the corresponding alcohols and *O*-acetylated following the same one-pot protocol mentioned above.[49] The isolation of **82** was accomplished with only a moderate yield (40%); furthermore, aliphatic impurities have been observed repeatedly in the ^{1}H NMR spectra of this experiment/product. Despite the fact that in all reported methodologies silica gel was used for chromatographic purification, attempts to isolate products **84** and **86** on silica gel led to

complete decomposition. Likewise, in case of substrates **85** and **87**, the isolated yields were substantially lower compared to the detected NMR yields. The decomposition in all cases (**84**–**87**) led to the corresponding ketone (verified by R_f analysis and ^{1}H NMR spectroscopy). Efforts to modify the solvent system used for PTLC through addition of a few drops of triethylamine gave disappointing results. Moreover, the use of neutral and basic alumina was also attempted, albeit unsuccessful. Gratifyingly, the ethyl pyruvate-derived product **88** displayed a high stability and was isolated in 92% yield.

Table 3.6: Cyclopropenimine-catalysed cyanation of ketones

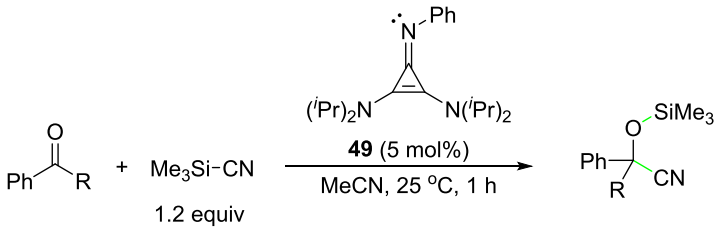

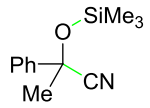

82: 99% (40%)

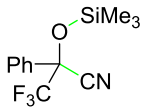

83: 99%

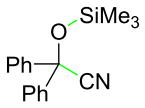

84: 99%

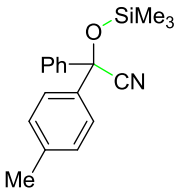

85: 99% (73%)

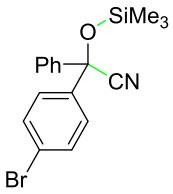

86: 99%

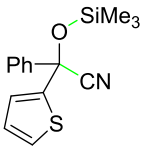

87: 99% (77%)

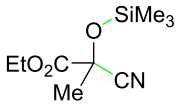

88: 99% (92%)

NMR yield was determined by ^{1}H NMR analysis. Isolated yields of acetylated products in parenthesis.

Finally, we also attempted to apply this novel *nucleophilic* imine catalysis to the use of ketimines as *electrophilic* substrates (Scheme 3.27). Under the optimized conditions, the use of ketimines **89**–**91** did not give the corresponding products **92**–**94** at 30–60 °C. Ketimines are substantially less reactive compared to aldimines, which may explain the non-reactivity of **89** compared to aldimine **76**.

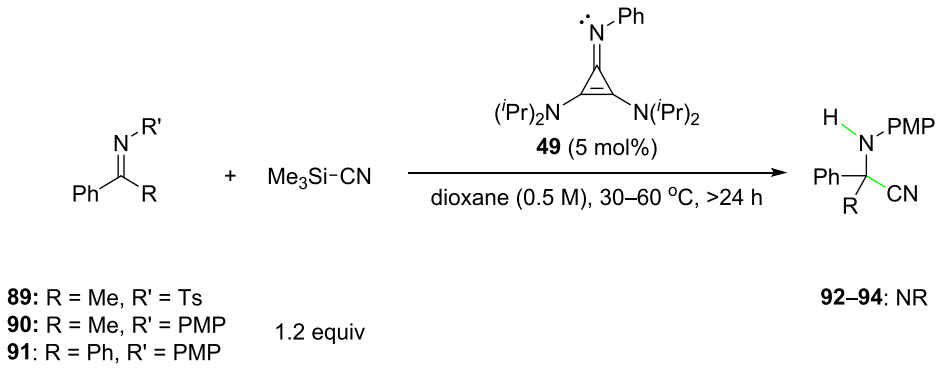

Scheme 3.27: Efforts to increase the aldimine scope of cyanation.

To conclude, the experiments with aldimines **80**–**81** and ketimines **92**–**94** should be tested in acetonitrile since this solvent proved to be critical for the chemical reactivity of ketones.

3.3.2.7 Mechanistic Studies for Cyanation

Due to the outstanding catalyst potential of cyclopropenimines vs. other imines, we were keen to investigate the potential mechanistic pathway of the cyanation (Scheme 3.28). In the first scenario, the reaction may proceed step-wise through nucleophilic addition–elimination. The electron-rich nitrogen of the cyclopropenimine may add to the silicon pro-nucleophile to generate a penta-coordinate silicon species. X^- may be released and added to the electrophilic carbonyl group to form an alkoxide, which may add to the silicon of the *in situ* generated silylium ion to form the corresponding silyl ether product with concomitant catalyst regeneration. The second scenario is a concerted mechanism; cyclopropenimine may add to the silicon pro-nucleophile to directly eliminate X^-; the latter may add to the electrophilic carbonyl group. The third scenario is that the cyclopropenimine may act as an initiator to activate the silylated pro-nucleophile, which may add to the electrophile to generate an alkoxide. The latter Lewis base may provide turnover of the catalytically active species.

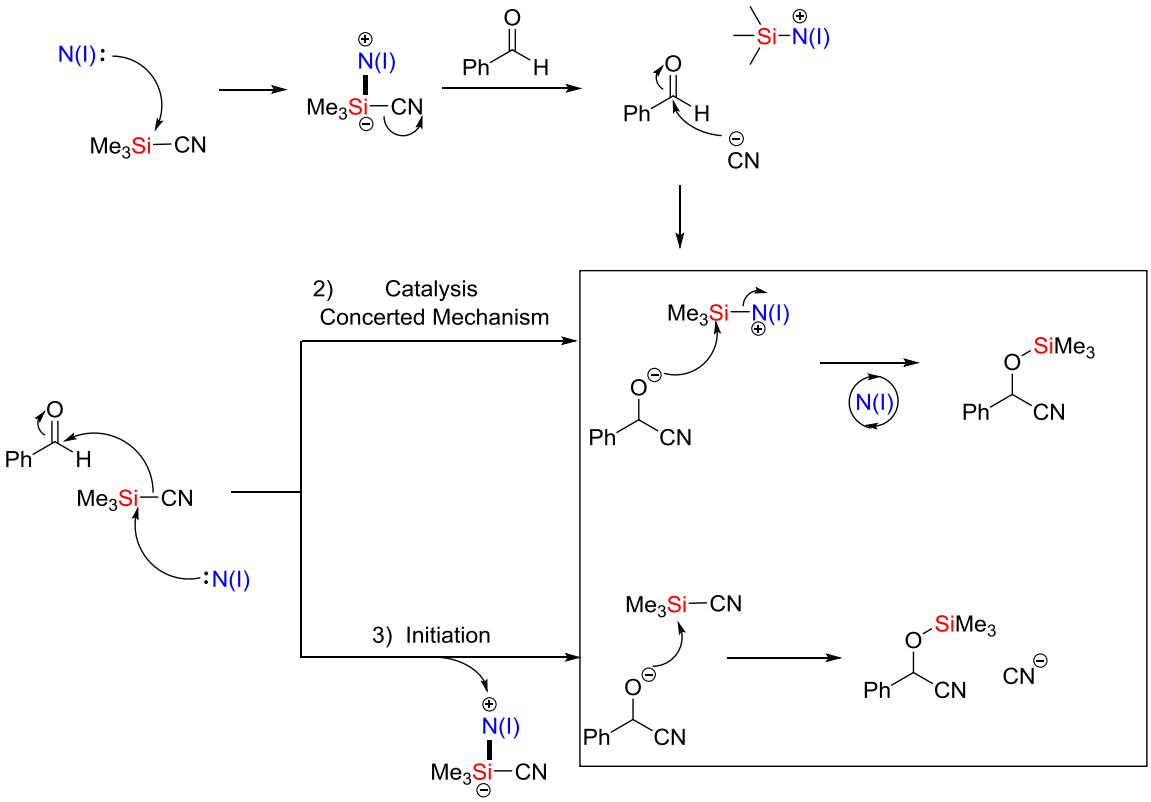

Scheme 3.28: Potential mechanistic pathways for cyanation of benzaldehyde.

A well-known methodology for studies of Lewis base–Lewis acid interactions is Gutmann's empirical analysis.[63] The latter proved to be reliable for the study of Lewis acid–base adducts. After adduct formation, the electron density in the acceptor fragment is increased and the overall redistribution of the electron density may lead to a considerable rearrangement of the bond lengths. Gutmann's analysis consists of four major principles:[63]

1. 'The smaller the intramolecular distance between the donor (D) and the acceptor (A), the greater the induced lengthening of the peripheral bonds (A–X)'. [64,65]
2. 'The longer the bond between D and A, the greater the degree of polarisation of electron density across that bond.'[64,65]
3. 'As the coordination number of an atom increases, so do the lengths of all the bonds originating from that coordination center'.[64,65]
4. The lengths of the bonds adjacent to D and A will either decrease or increase as a result of the redistribution in electron density of donors and acceptors.[64,65] For example, an interaction between antimony chloride ($SbCl_5$; a Lewis acid) and tetrachloroethylene carbonate (a Lewis base) was studied by X-ray crystallography (Scheme 3.29).[64,66] The metal complexation led to modifications of bond lengths of

both substrates, i.e., the bonds were lengthened or shortened as an outcome of a redistribution of the electron density after binding of the carbonyl oxygen atom to the antimony (V) centre.

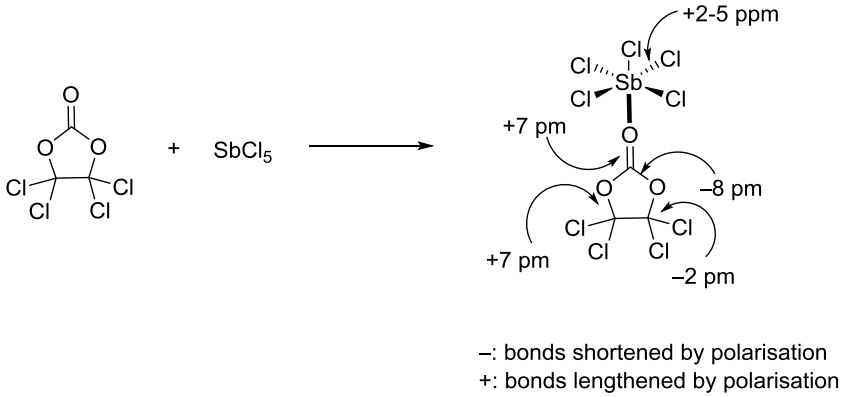

Scheme 3.29: Bond length study by X-rays of $SbCl_5$ and its metal complex with tetrachloroethylene carbonate.[64,66]

X-ray crystallographic analysis is the most reliable tool to provide all the necessary information regarding the structural modification of acid–base complexes [e.g. binding study of various Lewis bases with antimony chloride ($SbCl_5$)].[63] Notably, electronic consequences such as the fractional charges of donor and acceptor can be studied only by computational analysis.[63] Indeed, Mulliken charges for SiX_4, SiX_5, SiX_6 (X = halogen) were strikingly increased by additional base–acid interactions between the silicon and the newly bound halogen atoms.

We conducted this mechanistic investigation using NMR spectroscopy. Since trimethylsilyl cyanide was the pro-nucleophile of our choice, we relied on ^{29}Si NMR spectrocopy; basic principles of silicon chemistry and the range of ^{29}Si NMR signals that can be obtained alongside with their potential rationalisation will be presented below.

Silicon is located in main group 14 and is the higher homologue of carbon (Scheme 3.30). Hypervalent silicon species proved to be crucial intermediates for C–C bond formation.[67] The silicon atom may form higher coordination complexes than carbon due to different bonding characteristics. The silicon valency is the key for reactivity of organosilicon compounds as it may expand its coordination sphere to five or even six.[67] The 'so-called' extra-coordination or hypervalency may be ascribed to vacant d orbitals of silicon or accessible σ* (Si–L) orbitals.[67] Formally, the silicon species are tetravalent having a tetrahedral geometry with sp^3 hybridization (structure **A**). Expansion to a penta-coordinate silicon complex may decrease the electron density at the silicon atom to result in an increase of its Lewis acidity.[67] However, the penta-coordinate silicon species may be simultaneously Lewis acid and Lewis base, since the ligands coordinated to the silicon are particularly electron-rich. The penta-coordinate

silicon species may be able to expand to hexa-coordinate species to considerably increase the Lewis acidity of the central silicon atom. In this case, the Lewis acidity of the silicon atom would reach its highest level and the hexa-coordinate silicon complex would act as a nucleophile, since the electron density of the ligands would be vastly increased. Considering the metalloid character of silicon, structures **B** and **C** could be described as electropositive metal cations with very strong carbon nucleophiles or hydrides as ligands coordinated to the silicon.[67] Structures **B** and **C** proved to be valuable candidates for C–X bond formation (X = C or heteroatom).

Denmark, Beutner and co-workers reported a different explanation regarding the ability of the tetravalent silicon species to expand their valency to penta- and hexa-coordinate silicon species (Scheme 3.30).[63] The availability of 3d orbitals of silicon for coordination leads to an analogy with transition metal complexation.[68] However, silicon is not a metal and nowadays, it is accepted that the 3d orbitals on silicon are too diffuse to engage in a hypervalent bonding.[63] As it has been already mentioned, silicon conventionally forms tetravalent species with tetrahedral geometry and sp^3 hybridization. In order to expand in a hypervalent species, it is required to engage in hypervalent three-center four-electron bonding, which may result in sp^2 hybridization and therefore a trigonal-bipyramidal structure.[63] Further expansion to hexa-coordinate silicon species will require a second p orbital combined with sp-hybridized silicon atom. Formation of p symmetry orbitals lowers the energy of the hybrid orbitals by increasing the proportion of 's' character.[63]

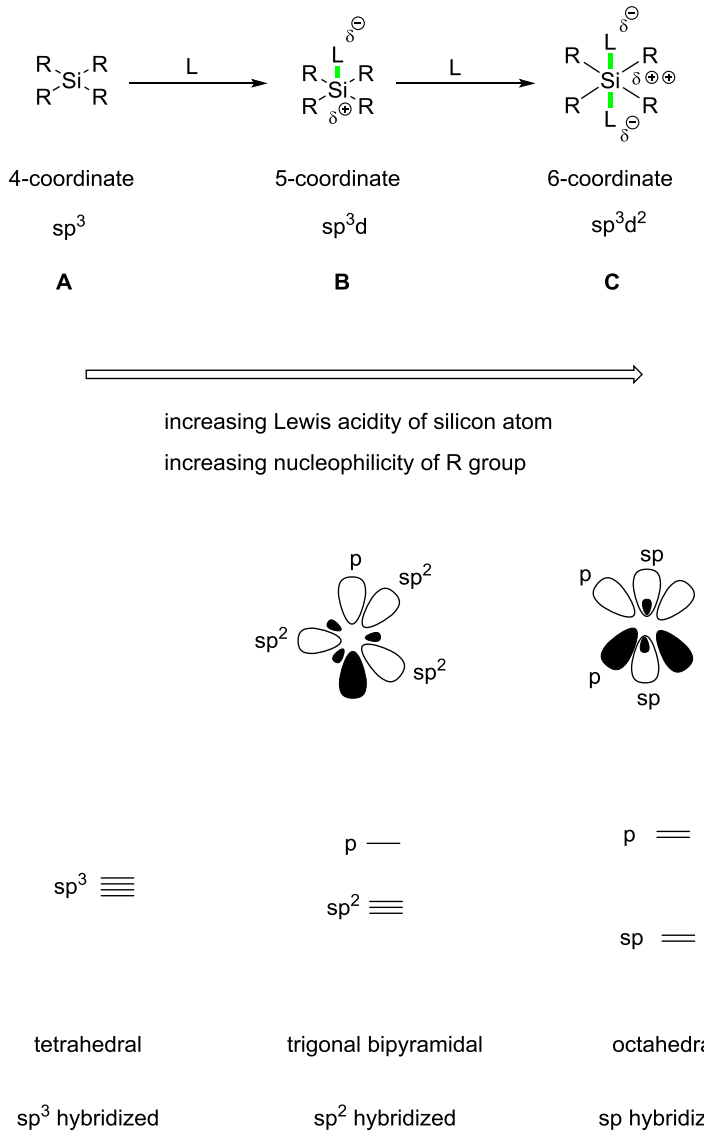

Scheme 3.30: Study of penta- and hexa-coordinate silicon species reported by Oestreich[67] and Denmark.[68]

The ^{29}Si NMR signals that have been reported suggest that the boundaries between the different electronic environments are not definitive in the ^{29}Si NMR scale [Scheme 3.31 a)]. As it may be expected, the silylium ion is a particularly strong electrophile (from 200 to 50 ppm).[69–71] In contrast to tertiary carbocations (R_3C^+), the C–Si bonds are longer and the orbital overlapping is less effective, and therefore less efficient for π conjugation and hyperconjugation.[69] Thus, the silylium ion is more reactive towards σ and π electron donors.[69] Silicon normally engages in bonding with only other 4 atoms to complete the electronic requirement for an outer-shell octet. Therefore, it is expected that silicon tetravalent species will be less Lewis acidic (50 to –80 ppm). The penta- and hexa-coordinate silicon species are indeed more electron-rich, which nicely explains why the signals at ^{29}Si NMR are normally displayed up-field (from 0 to –120 and from –100 to –200 ppm, respectively). ^{29}Si NMR

signals of penta-coordinate species have been notoriously challenging to be obtained at room temperature. West *et al.* reported that the intramolecular N:→Si coordination may be captured at low temperatures [down to –60 °C; Scheme 3.31 b)].[72] Signals of aromatic non-substituted silanes and aromatic silanes substituted at ortho-position have been compared to lead to the conclusion that due to intramolecular interaction the signals move up-field compared with the non-substituted aromatic silanes. Later on, Holmes *et al.* reported intermolecular interaction between tetravalent silicon species and a Lewis base [Scheme 3.31 c)].[73] Again, the signals of the penta-coordinated species in the ^{29}Si NMR were captured at low temperatures. Treatment of (tetraethoxy)silane with potassium ethoxide (1.0 equiv) and [18]crown–6 (1.0 equiv) at 40 °C led to no signal exhibition. Cooling slightly to 30 °C provided a signal of penta-coordinate species at –131 ppm. Further cooling to –10 °C led to the exhibition of two signals at –77.3 and –82.6 ppm, which may be two new tetra-coordinate species. However, the signal of the penta-coordinate species is still dominant. Cooling down to –65 °C resulted in the disappearance of the signal at –77.3 ppm. Finally, excess of potassium methoxide did not lead to the appearance of new signals up-field, which strongly suggests the absence of hexa-coordinate species

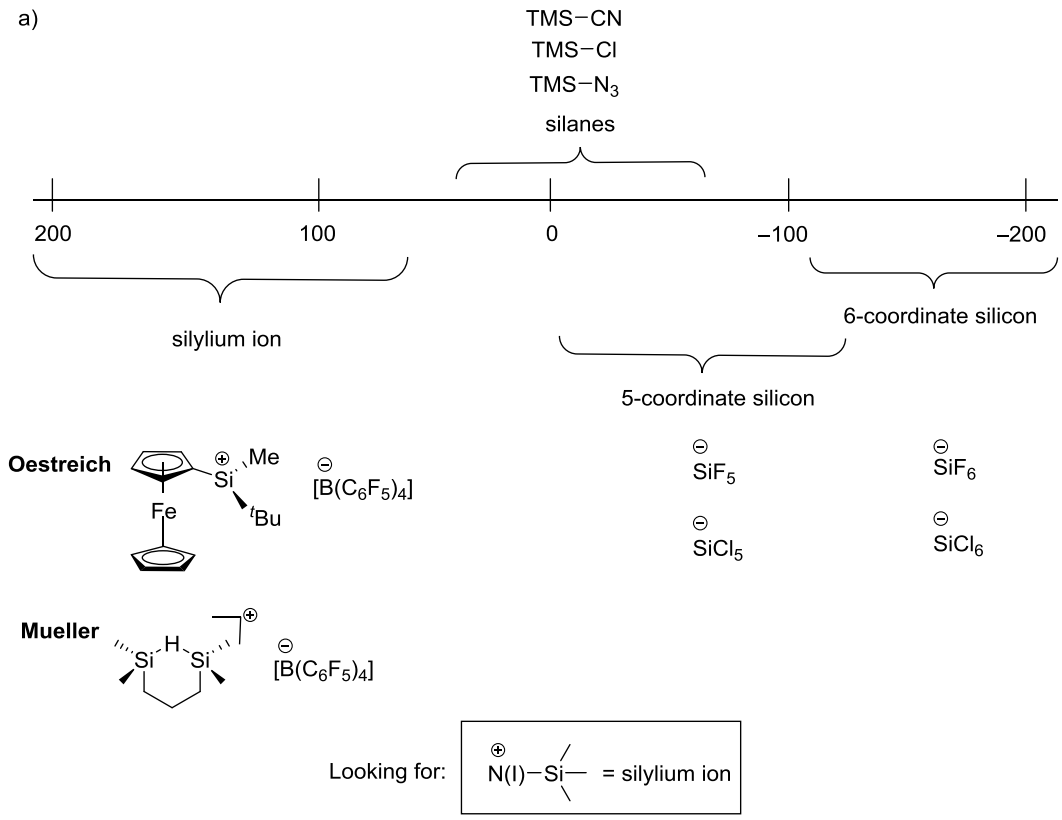

b) **West**, 1983

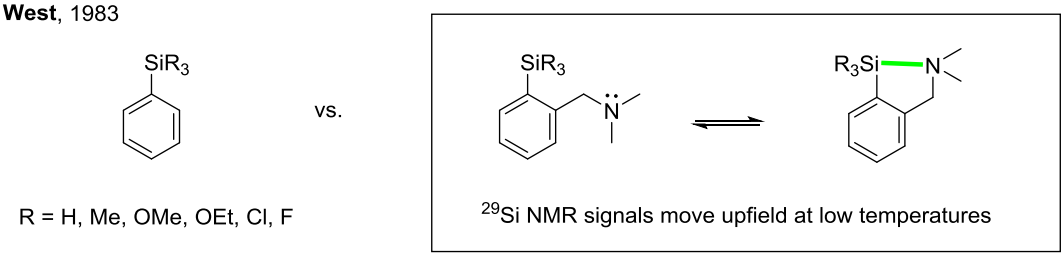

c) **Holmes**, 1990

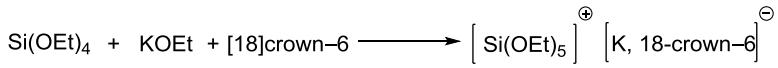

+ 40 °C: no signal
+ 30 °C: –131 ppm (pentacoordinate)
– 10 °C: –77 and –82.6 ppm (tetracoordinate), –131 ppm (pentacoordinate)
– 65 °C: –77 (tetracoordinate), –131 ppm (pentacoordinate)

Scheme 3.31: a) Rationalisation of ^{29}Si NMR signals[69–71] b) ^{29}Si NMR of pentacoordinated silicon species developed by West *et al.*[72] c) ^{29}Si NMR of pentacoordinate silicon species developed by Holmes *et al.*[73]

In ^{29}Si NMR spectropcopy, we anticipated to detect a distinct N:→Si signal [Scheme 3.32]. Following the principles of Gutmann's analysis, this interaction would trigger electronic redistribution to lead to considerable modifications in the electronic environment of the silicon atom. As a result, the ^{29}Si NMR shifts of the new silylium cation or penta-coordinate species would be distinguished. The signal of the substrate, trimethylsilyl cyanide (TMS–CN), was

shown to be a singlet at –12 ppm in dioxane. The tiny signal at 7 ppm was confirmed to correspond to hexamethyldisiloxane (TMSOTMS); it might be either an impurity in the commercially available bottle of trimethylsilyl cyanide, or it is an outcome of a side-reaction between trimethylsilyl cyanide and traces of moisture in dioxane. Addition of cyclopropenimine **49** (1.0 equiv) did not lead to any detectable new signals at room temperature. Unfortunately, the melting point of the dioxane is at 10 °C, therefore we were not able to cool down to a lower temperature. Inspired by Holmes *et al.*,[73] we decided to heat instead. Heating up to 50 °C did not lead to the disappearance of the initial signals or the appearance of new peaks [a) ~ e)].

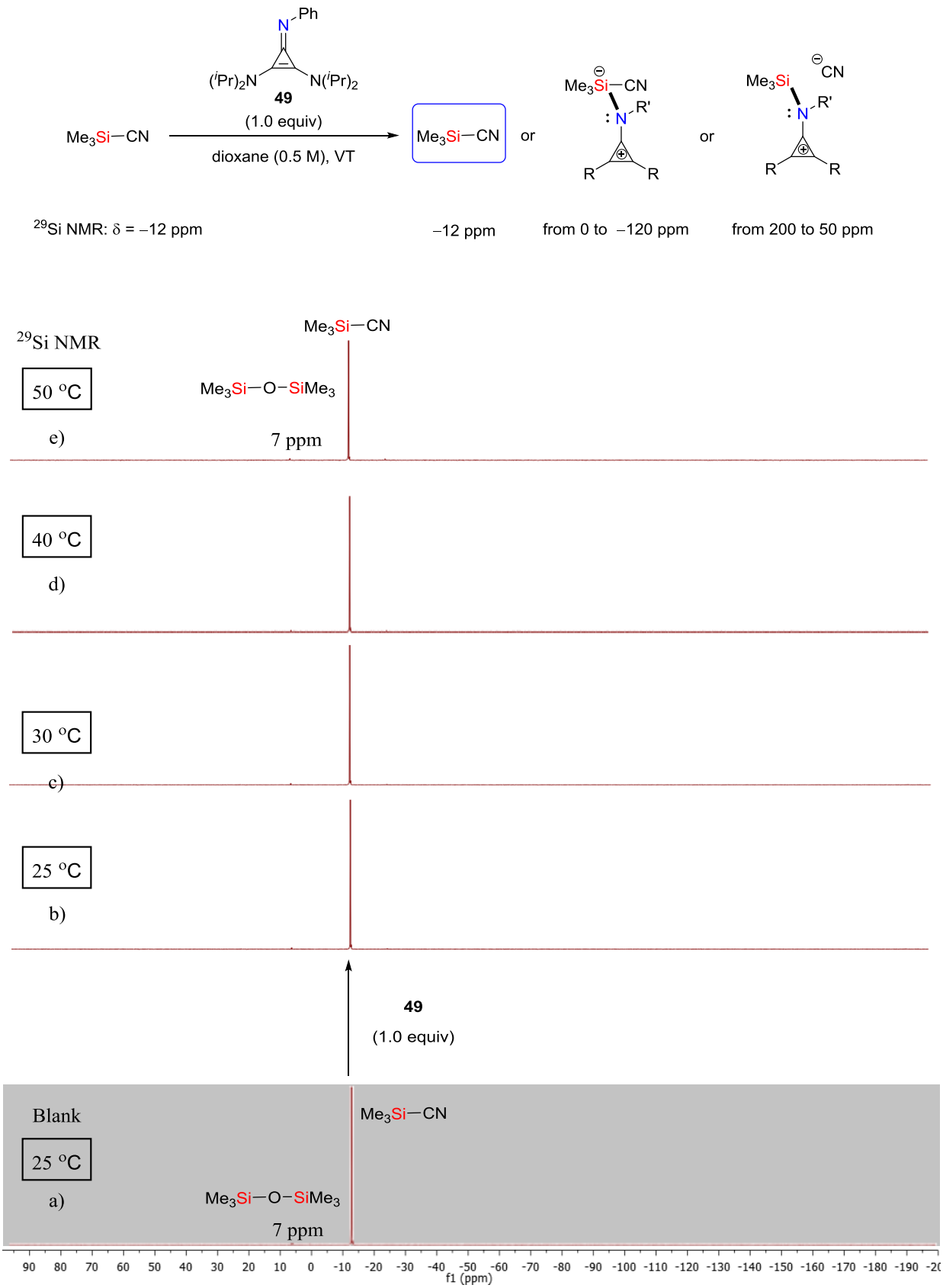

Scheme 3.32: ^{29}Si NMR studies of interaction between TMS–CN and cyclopropenimine at variable temperatures in dioxane.

Due to the high melting point of dioxane and the better catalytic results in acetonitrile, we next used acetonitrile as a solvent (melting point = –44 °C; Scheme 3.33). However, the melting point of trimethylsilyl cyanide is at 8 °C, therefore cooling further (below 8 °C) was prohibited. Considering that 0.5 mmol of trimethylsilyl cyanide were added, freezing of the latter may lead to the breaking of NMR tube inside the NMR machine, which would generate high repair costs. As it has been already mentioned, the signal of the starting material in ^{29}Si NMR spectroscopy was displayed at –12 ppm. Addition of cyclopropenimine **49** did not give any new signals at 25 °C. Heating up to 50 °C led to the exhibition of a new signal at –22 ppm. This signal may either be a formed side-product or penta-coordinate silicon species, since it is displayed both up-field relative to the substrate and within the range suggested for penta-coordinated silicon species [Scheme 3.31 a)].

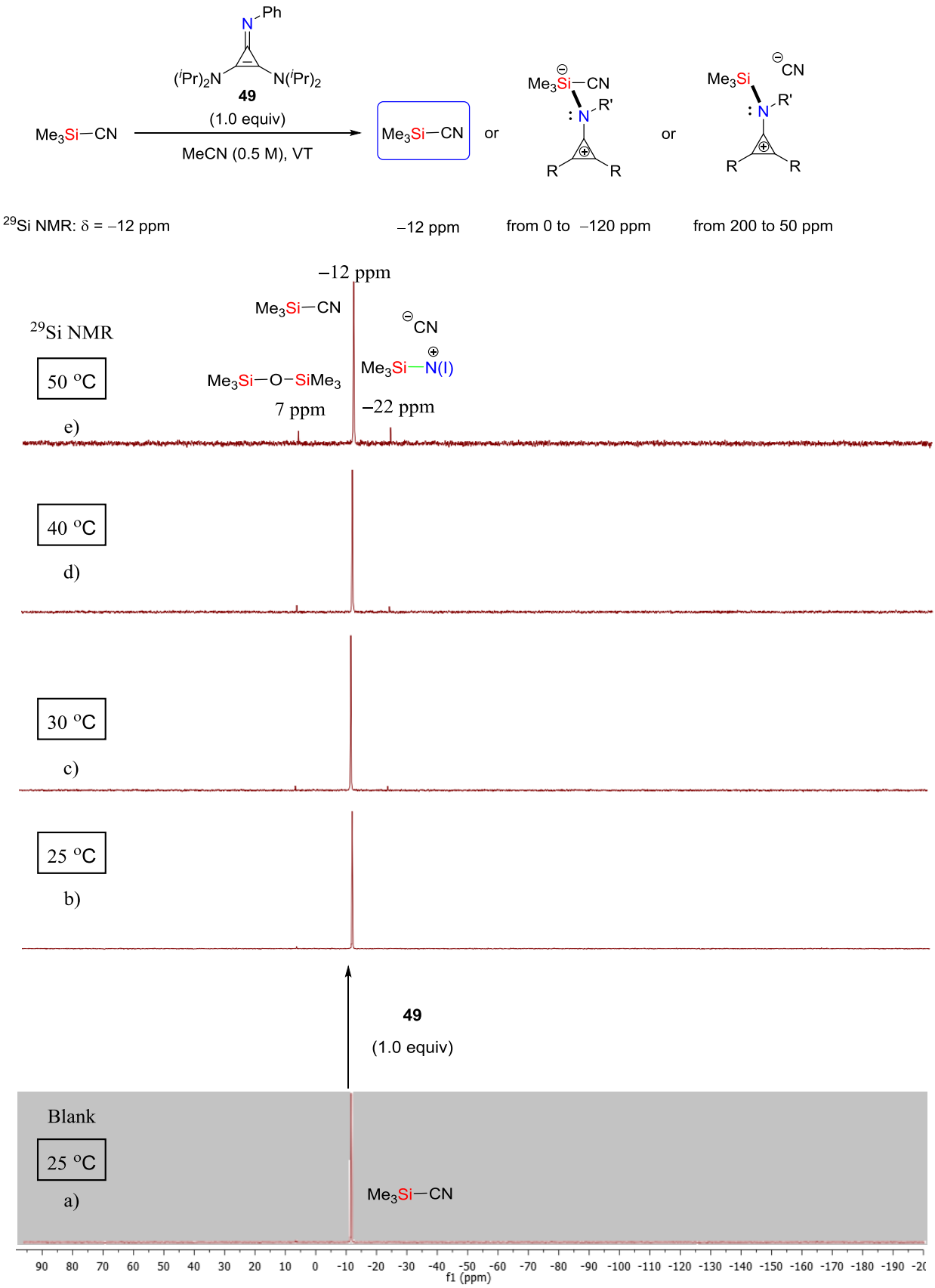

Scheme 3.33: ^{29}Si NMR studies of interaction between TMS–CN and cyclopropenimine at VT in MeCN.

To conclude, we have been unable to suggest a specific mechanistic pathway; we would be able to get a better insight into a potential step-wise mechanism as long as we were allowed to cool down to a lower temperature (below 0 °C) and capture ^{29}Si NMR signals of potentially formed penta-coordinate silicon species. Therefore, we cannot eliminate this possibility. Concerted mechanism and initiation seem to be possible scenarios considering that ^{29}Si NMR spectroscopic analysis at 25 °C did not display any interaction between cyclopropenimine **49** and the silylated pro-nucleophile; both scenarios require the presence of an electrophile to provide new signals in ^{29}Si NMR spectrocopy. Indeed, when benzaldehyde (0.8 equiv) was added at room temperature to a mixture of trimethylsilyl cyanide and cyclopropenimine **49** the formation of the product within 1 h was confirmed by ^{1}H, ^{19}F, and ^{29}Si NMR spectroscopy (Scheme 3.34). The formed silyl ether displayed a signal at 25 ppm, which is a considerable shift downfield compared with the starting material (–12 ppm).

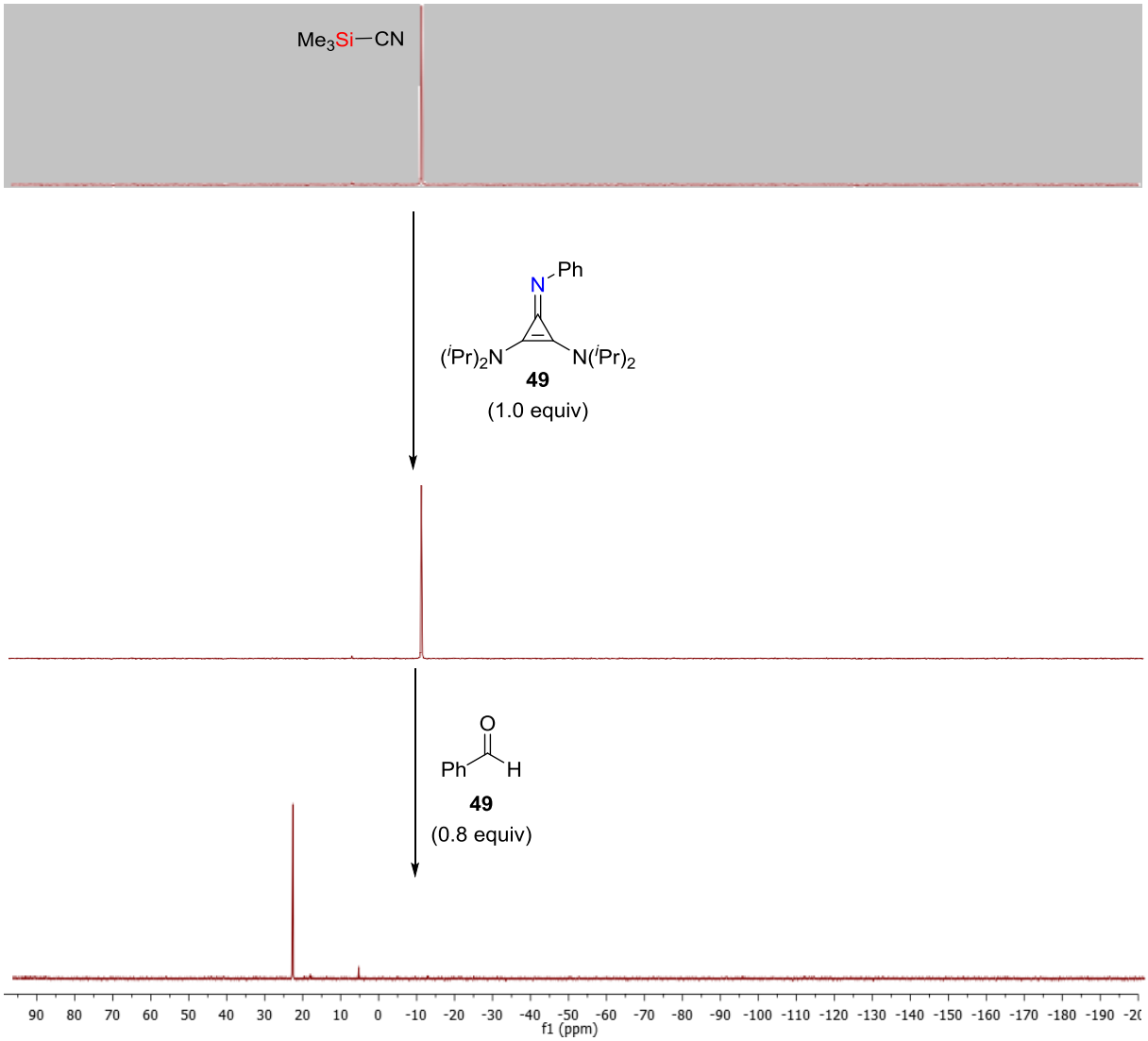

Scheme 3.34: ^{29}Si NMR studies of interaction between TMS–CN, cyclopropenimine **49** and benzaldehyde in MeCN.

3.3.3 Trifluoromethylation of C=O Electrophiles

In this sub-chapter, nucleophilic trifluoromethylation of various carbonyl compounds was developed using cyclopropenimines as Lewis base catalysts (Scheme 3.35). Cyclopropenimines may activate the silicon pro-nucleophile to release the trifluoromethyl group, which may add to a suitable electrophile (aldehydes, ketones) to generate the corresponding alkoxide. The latter would add to the silylium ion to form the intended silylated product with catalyst turnover.

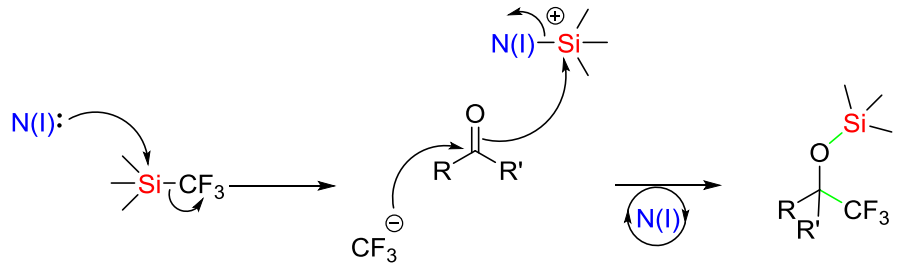

Scheme 3.35: Potential catalytic cycle of trifluoromethylation to give C–C bond formation with carbonyl compounds.

3.3.3.1 The Trifluoromethyl Group in Drug Molecules

Various methodologies have been applied for the synthesis of drugs containing a CF_3 group, such as nucleophilic trifluoromethylation,[74–76] electrophilic trifluoromethylation,[77] free radical trifluoro-methylation,[78] and transition metal-catalyzed strategies.[79–81] A trifluoromethyl group provides a series of properties to a drug candidate, which may render it more effective.[82] A trifluoromethyl group contributes to the metabolic stability of the drug due to its chemical stability to amplify the overall xenobiotic nature.[82] Furthermore, it increases the electrophilicity of the neighbouring functions (e.g. carbonyl groups), while it decreases the basicity of proximal amino groups.[82] It also displays poor hydrogen bond acceptor ability combined with local hydrophobicity.[82] Last but not least, peptide mimics may include a trifluoromethyl group in their structure, which may facilitate their binding to an acceptor site of an enzyme of the targeted organism.[82] Fluoxetine (**95**; Prozac) and befloxatone (**96**) are antidepressants; Efavirenz (**97**) is used for the treatment of human immunodeficiency virus (HIV; Figure 3.5).[83–85] The common attribute of the industrial synthesis of **96** and **97** is that asymmetric nucleophilic trifluoromethylation of carbonyl groups was required for the synthesis of optically active trifluoromethylated alcohols.

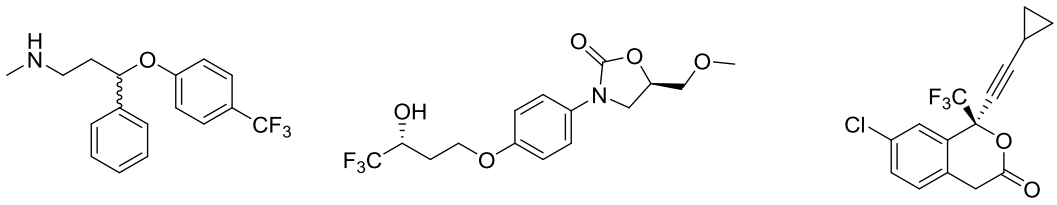

Fluoxetine (Prozac) Befloxatone Efavirenz (Sustiva)

95 **96** **97**

Figure 3.5: Trifluoromethyl group incorporated into blockbuster drugs.

3.3.3.2 Literature-Reported Trifluoromethylation Methods

The first methodology reported for nucleophilic trifluoromethylation was based on the concept of initiation using organic and inorganic salts (Scheme 3.36).[75,83,86–88] In 1991, Prakash *et al.* reported trifluoromethylation of carbonyl compounds using TBAF (2 mol%) in THF at 0 °C to give the corresponding products in 60–92% yields.[86,88] Later on, Kobayashi *et al*. accomplished asymmetric trifluoromethylation by using quaternary enantiopure ammonium fluorides (1–20 mol%) in toluene at –78 °C to generate the products in 87–99% yield with 15–51% *ee*.[75] In 1999, Shreeve *et al.* reported trifluoromethylation of carbonyl compounds with CsF under solvent-free conditions or in glyme at room temperature to give the corresponding products in 85–95% yields.[87] In 2007, Mizuta *et al.* reported trifluoromethylation of carbonyl compounds using KF/TBAB (2 mol%) in toluene at –78 °C to give the corresponding products in 15–99% yields.[83] It should be noted that all these methodologies displayed either no or poor functional group (FG) tolerance. Furthermore, several methodologies required a low reaction temperature, which renders these processes less practical. In general, TBAF and metal salts (KF or CsF) were used as fluoride sources. Fluoride add to the silicon to form the notoriously strong Si–F bond. Next, the trifluoromethyl group was released to add to a carbonyl compound and form an alkoxide. The latter is a strong Lewis base, which can catalyse the reaction.

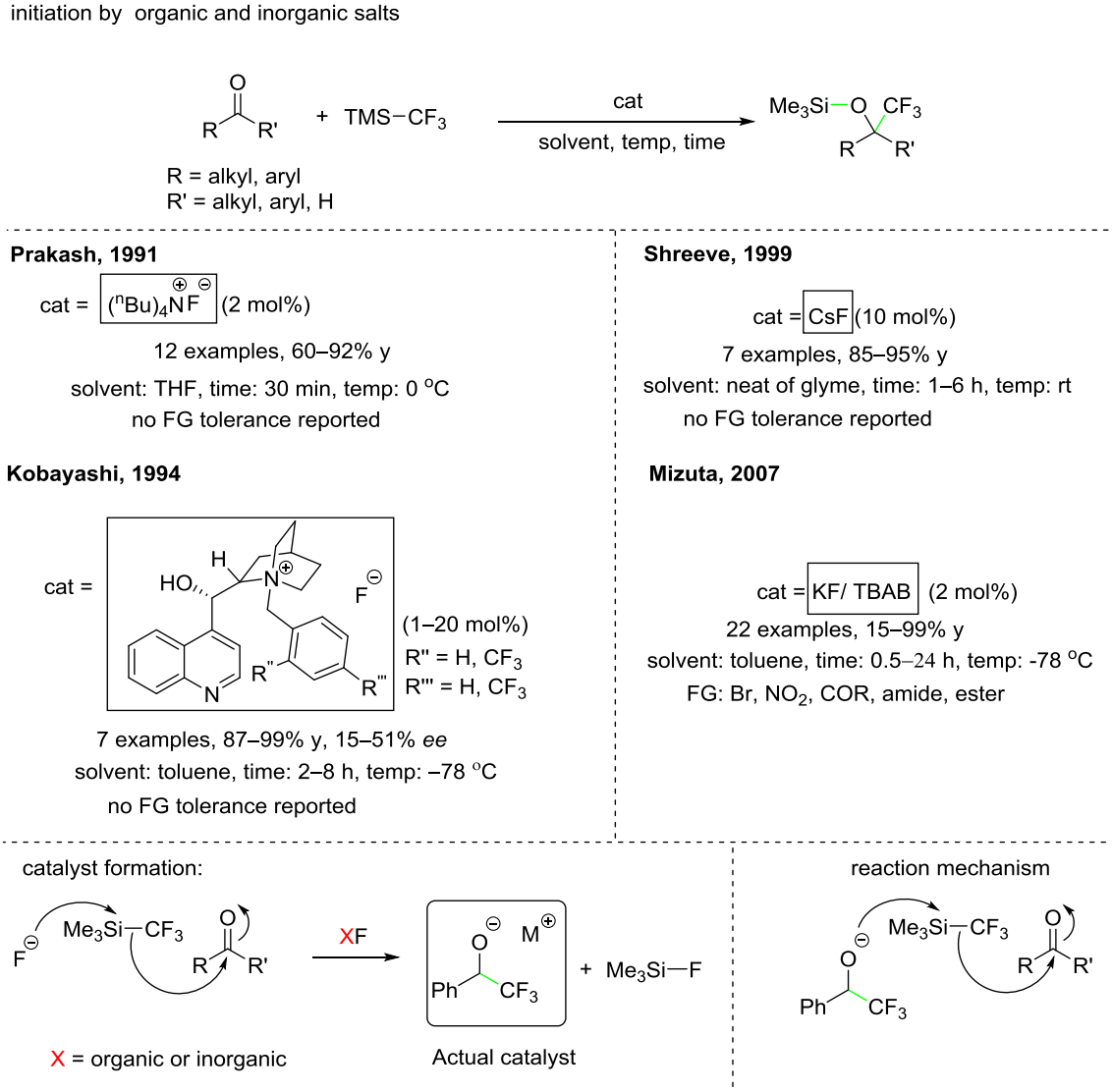

Scheme 3.36. Organic and inorganic salts initiate cyanation of carbonyl compounds and imines.

Song *et al.* reported another methodology using an NHC catalyst (0.5–1 mol%; Scheme 3.37).[89] Facile Lewis base-catalysed trifluoromethylation of aldehydes was accomplished under mild conditions using Ruppert's reagent (3.0 equiv) to display good functional group tolerance. Nevertheless, this methodology was applied only to aldehydes and required a large excess of the substrate; NHC-catalyzed trifluoromethylation of ketones has not been reported.

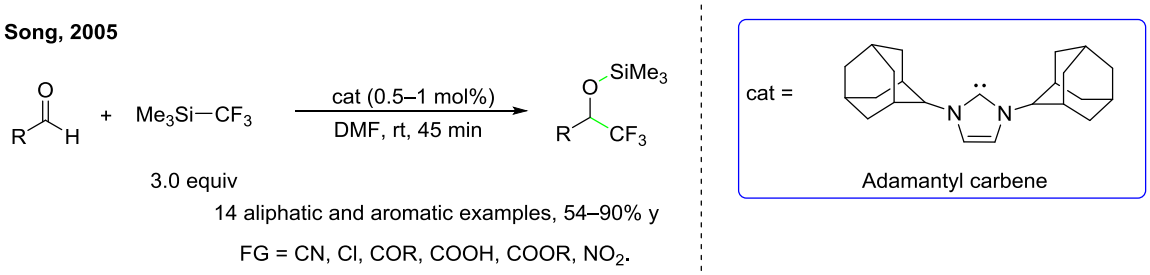

Scheme 3.37: Trifluoromethylation of aldehydes using carbenes.

Matsukawa *et al.* reported catalytic trifluoromethylation of aldehydes, ketones, and imines (Scheme 3.38);[90] the electrophile was treated with Ruppert's reagent (2.0 equiv) and a phosphine (TTMPP; 5–20 mol%) at room temperature to afford the corresponding products in 48–92% yields. However, a long reaction time was required in several cases and a high catalyst loading for the trifluoromethylation of imines (20 mol%). Finally, a poor functional group tolerance was observed as well.

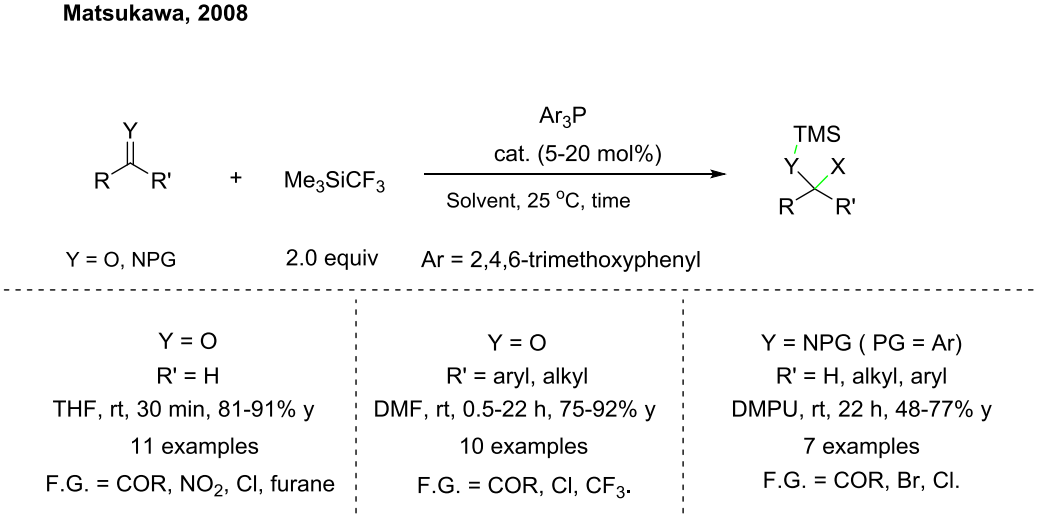

Scheme 3.38: Trifluoromethylation of carbonyl compounds and imines using TTMPP.

To conclude, the reported methods do not represent an efficient, environmentally friendly process with a broad scope and excellent group tolerance. Thus, we aimed at using cyclopropenimine catalysis to provide a methodology that may fulfil the aforementioned requirements.

3.3.3.3 Cyclopropenimine-Catalysed Trifluoromethylation of Benzaldehyde

In analogy to cyanation, we investigated initially the cyclopropenimine-catalyzed trifluoromethylation of benzaldehyde using trimethyl(trifluoromethyl)silane (Ruppert's reagent) as a pro-nucleophile in acetonitrile at 25 °C (Scheme 3.39). Cyclopropenimine **22**

was prepared *in situ* (following the process described in 3.3.2.2) and triggered C–C bond formation to give product **98** in 99% NMR yield (1 h). As it has been already mentioned, due to instability issues of catalyst **22**, we modified the catalyst structure; the vinylogous guanidine analogue **49** was used due to its electronic properties, straightforward synthesis, and excellent stability under inert atmosphere. The use of **49** under otherwise identical conditions led to the formation of product **98** in 99% NMR yield as well.

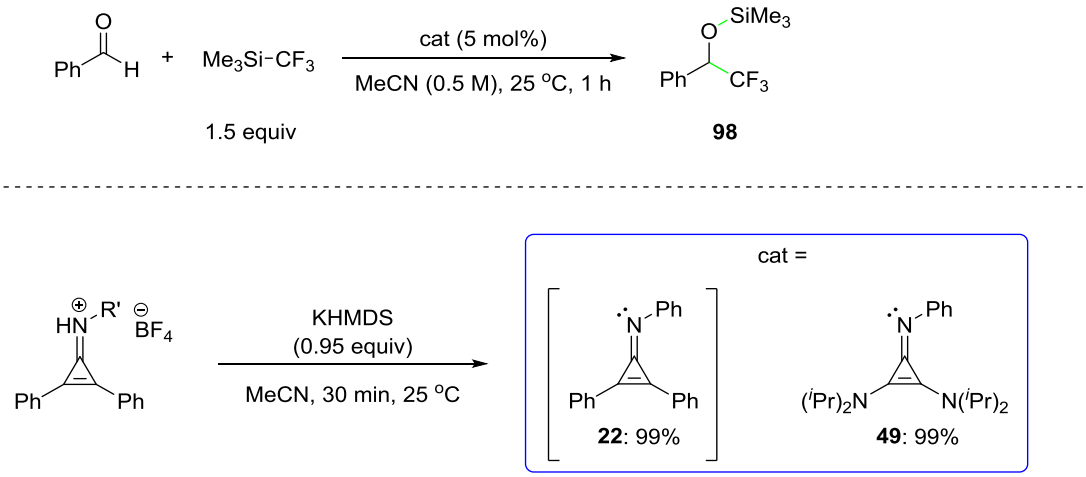

Scheme 3.39: Trifluoromethylation of benzaldehyde catalysed by the cyclopropenimines **23** and **49**.

3.3.3.4 Optimisation and Control Experiments

The 2π electron cyclopropenimines were compared directly with a broad range of imines regarding their catalyst potential for catalytic trifluoromethylation (Table 3.7). The library of imines **57–64** was examined, including: classical aldimines and ketimines (**57–62**), as well as acyclic and cyclic 4π electron imines (**63** and **64**, respectively). However, as anticipated the use of imines **56–62** in these control experiments did not lead to any conversion, while catalysts **22** and **49** gave excellent yields.

Table 3.7: Screening of various imines as catalysts

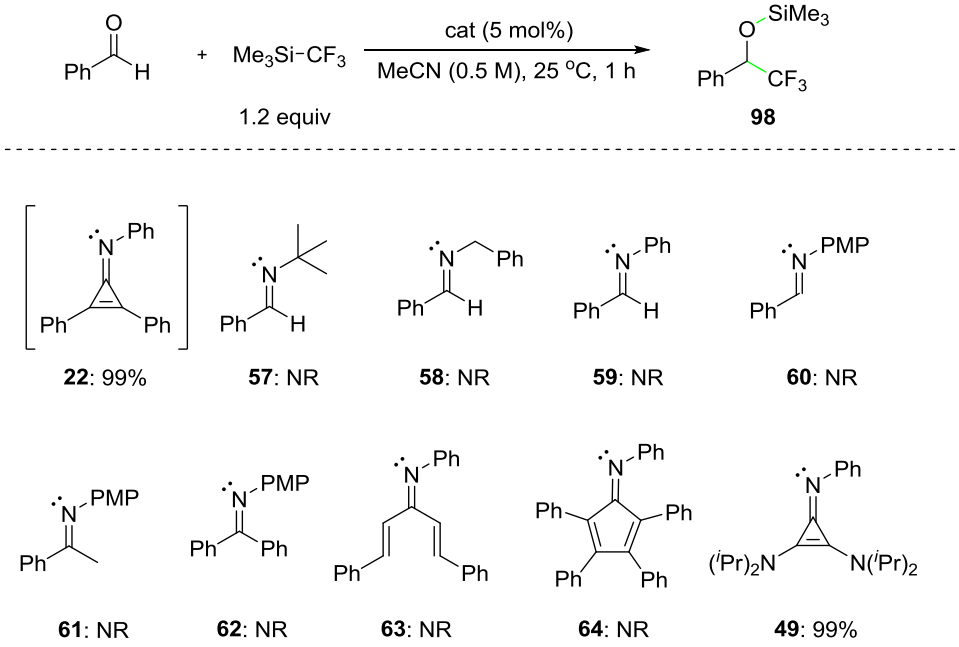

Yield determined by ^{1}H NMR analysis of an aliquot of the reaction mixture; internal standard: dibenzyl ether (25 mol%).

In contrast to cyanation, the trifluoromethylation of benzaldehyde does not proceed at all in common solvents such as dioxane, toluene, ethers, ethyl acetate, and chlorinated solvents (Table 3.8; Scheme 3.40); only starting materials were recovered. Likewise, the use of a more polar and *protic* solvent, methanol, did not give the intended product, but led to the decomposition of trimethyl(trifluoromethyl)silane (Scheme 3.40). Based on ^{1}H NMR spectroscopy, fluoroform and methoxytrimethylsilane were formed. The pK_a value of the conjugate acid of cyclopropenimines (25–30; MeCN) is reported to be similar to the one of the methanol (29; DMSO). However, the pK_a values cannot be directly compared, since they have been measured in different solvents. Nevertheless, cyclopropenimine **49** may deprotonate methanol to form the the corresponding cyclopropeniminium methoxide.[30] The alkoxide should then add to the silylated pro-nucleophile to release the trifluoromethyl anion. The latter may either deprotonate the cyclopropeniminium species or another molecule of methanol to generate fluoroform (pK_a = 27; H_2O). Dimethylformamide and acetonitrile are both *aprotic* solvents and have the minimum polarity seem to be required to stabilize the critical ionized intermediate(s); side-products were not observed in this case. Although acetonitrile is an aprotic solvent (pK_a = 31; DMSO), its deprotonation by **49**

should also considered. However, in the absence of the silylated pro-nucleophile, the formation of the corresponding anion and its addition to benzaldehyde were not observed in ^{1}H NMR spectroscopy. To conclude, acetonitrile was selected for the investigation of the substrate scope because it is easier to handle in the work-up compared to dimethylformamide (boiling point = 152 °C). It should be noted that DMF can act as a Lewis base (10–30% NMR yield) in the absence of **49**. In contrast, control experiments with acetonitrile did not lead to formation of the intended product **98**.

Table 3.8: Solvent screening of trifluoromethylation of benzaldehyde

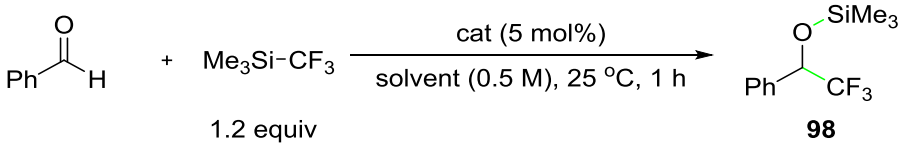

98

Entry	Solvent (ε)	Conv (%)[a]
1	dioxane (2.3)	0
2	toluene (2.38)	0
3	EE (4.3)	0
4	EtOAc (6.2)	0
5	THF (7.6)	0
6	DCM (8.9)	0
7	DCE(10.4)	0
8	DMF (36.7)	99[b]
9	MeCN (37.5)	99

[a] The conversion was determined by ^{1}H NMR spectroscopy based on the molar ratio **98**:PhCHO. [b] Control experiments with DMF led to formation

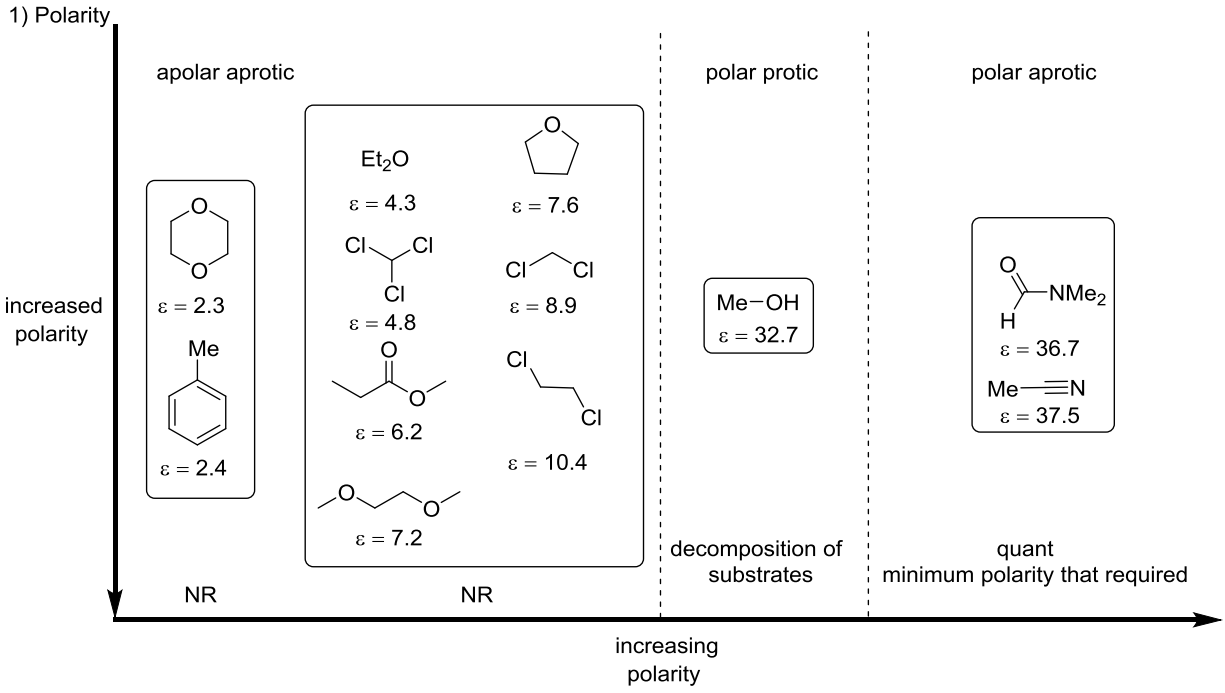

2) Mechanism of decomposition in methanol:

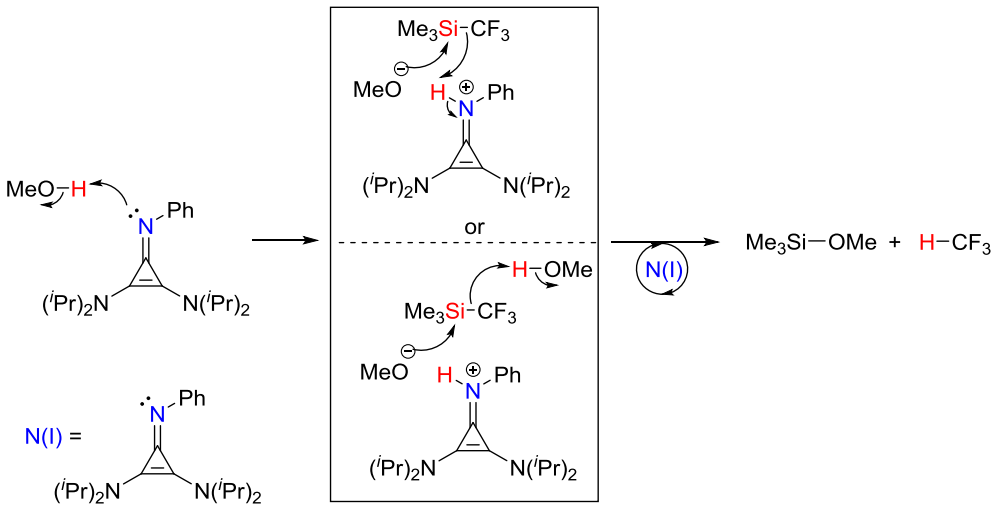

Scheme 3.40: Solvent screening in the course of the optimisation process for trifluoromethylation of aldehydes.

Finally, we were interested in comparing different vinylogous cyclic guanidines varied at the *N*-protecting group (Table 3.9). Cyclopropenimines **47**, **49**, and **50** were equally efficient in the trifluoromethylation of benzaldehyde under optimised conditions within 1 h. However, treatment of benzaldehyde with Ruppert's reagent (1.5 equiv) and catalyst **49** (5 mol%) at 25 °C for 5 min led to only 13% NMR yield. On the other hand, catalysts **47** and **50** under identical conditions gave the product in 99% NMR yield. The striking difference in reactivity between the three catalysts is not surprising from an electronic point of view considering that the aliphatic cyclohexyl group applies an inductive donating effect to the Lewis basic nitrogen

atom, while the aromatic mesityl group –due to the three methyl groups attached–is less electron-withdrawing relative to a simple phenyl group.

Table 3.9: Screening of **47, 49** and **50** for the trifluoromethylation of benzaldehyde.

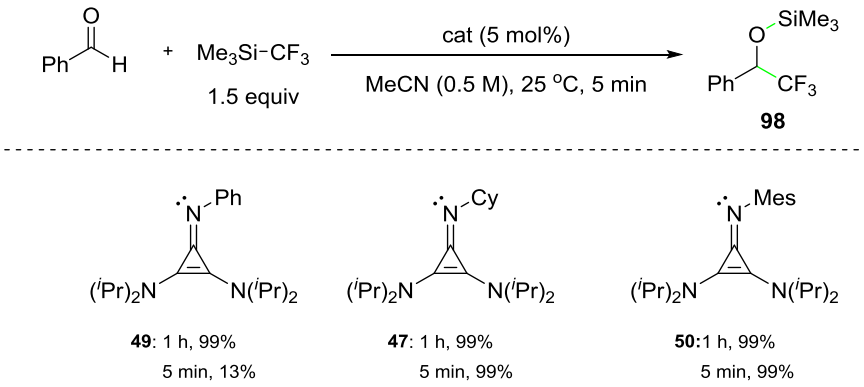

The yield was determined by ^{1}H NMR analysis using internal standards: dibenzyl ether (25 mol%).

3.3.4 Substrate Scope for Trifluoromethylation of Aldehydes

The optimized conditions were applied to the use of a wide variety of aldehydes to give the corresponding aromatic **(98–102**), heteroaromatic (**103–105**), and aliphatic (**106–108**) products (Table 3.10). An excellent functional group tolerance (hydroxy, methoxy, pyridyl, furyl) was displayed and the methodology provided the corresponding product in ≥91% isolated yields under mild conditions. In contrast to cyanation, no further chemical transformation was necessary for the isolation of the formed silyl ethers. Products **98–99** and **103–108** were not isolated due to their high volatility. However, ^{1}H NMR spectroscopy confirmed that complete and clean conversion of the aldehydes to the intended products occurred; side-products were not observed.

Table 3.10: Cyclopropenimine-catalysed trifluoromethylation of aldehydes.

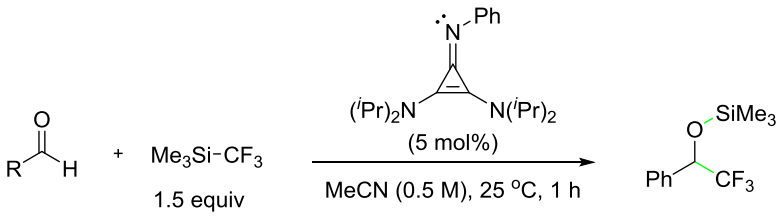

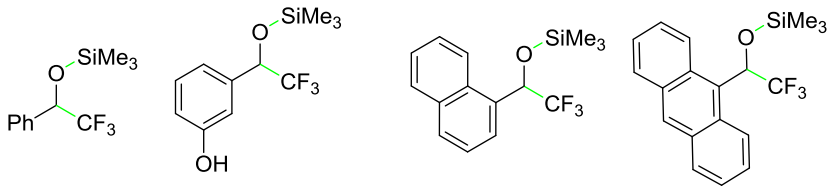

98: 99%

99: 94%

100: 99% (91%)

101: 99% (92%)

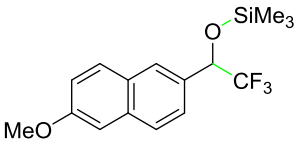

102: 99% (94%)

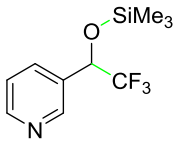

103: 99%

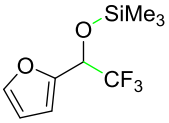

104: 93%

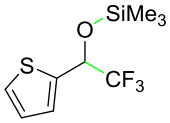

105: 99%

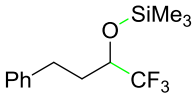

106: 98%

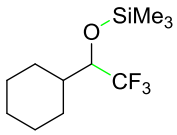

107: 99%

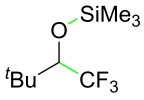

108: 99%

NMR yields were determined by ^{1}H NMR spectroscopy with DBE (0.25 M in mesitylene) as internal standard. Isolated yields of products in parenthesis.

3.3.5 Cyclopropenimine-Catalysed Trifluoromethylation of Ketones

Next, ketones were evaluated as substrates (Table 3.11). When the reaction was carried out in acetonitrile, a conversion of acetophenone was not observed (entry 1). Therefore, we decided to examine dimethylformamide and dimethylsulfoxide, which both led to high conversions (91% and 95%; entries 2 and 3, respectively). The solvent effect of the experiments with MeCN and DMF may not be ascribed to a polarity difference because the values of the dielectric constant (ε) for MeCN (37.5) and DMF (36.5) are very similar. However, DMF may be considered more Lewis basic compared to MeCN; also, DMF does not have an acidic hydrogen atom. Matsukawa *et al.* suggested that DMF may assist the Lewis base catalyst and coordinate to penta-coordinate silicon species to contribute to the activation of silicon pro-nucleophiles.[90] In our catalytic system, this scenario would mean that the release of the critical trifluoromethyl anion may be facilitated. The difference in reactivity between MeCN and DMSO may be explained by the fact that more polar solvents may be able to

stabilize the ionised form of the pro-nucleophile. Thus, instead of a potential silicon–ate complex, the more reactive silylium ion with the trifluoromethyl group as a counter anion may be formed. It should be noted that ^{1}H NMR spectroscopic analysis of blank experiments in DMF and DMSO alone –in the absence of a cyclopropenimine catalyst– did not display the formation of the trifluoromethylation products, i.e., both solvents were not able to trigger the trifluoromethylation of acetophenone. Dimethylformamide was selected as the solvent due to its lower boiling point (152 °C) compared to dimethylsulfoxide (189 °C).

Table 3.11: Solvent screening for the trifluoromethylation of acetophenone.

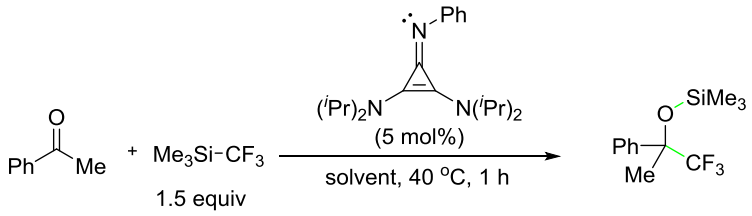

109

*Reaction with DMSO was performed by Peter Neate

Entry	Solvent (ε)	Conv (%)[a]
1	MeCN (37.5)	NR
2	DMF (36.7)	91
3	DMSO (46.7)	95

Solvent: **MeCN**

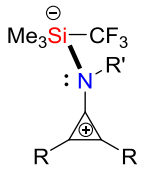

Solvent: **DMF**

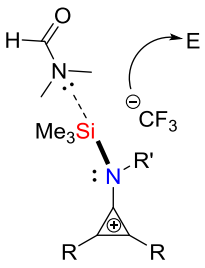

Matsukawa 2009:

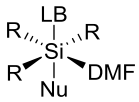

Solvent: **DMSO**

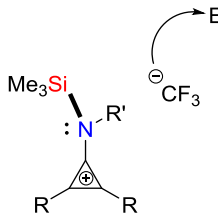

[a] The conversion was determined by ^{1}H NMR spectroscopy based on the molar ratio **109**:acetophenone.

It should be noted that cyanation of ketones was carried out in acetonitrile, whereas the trifluoromethylation of ketones may require the stronger Lewis basic DMF as a 'co-catalyst'. This observation may be ascribed to the leaving group ability of cyanide and trifluoromethyl

group. For this purpose, the basicity of hydrogen cyanide and fluoroform was compared (Scheme 3.41). The pK_a of fluoroform (27) is significantly higher compared to hydrogen cyanide (9.1). Therefore, the cyanide anion is a weaker conjugate base compared to trifluoromethyl group; i.e., the former is a better leaving group and the activation of the corresponding pro-nucleophile is facilitated.

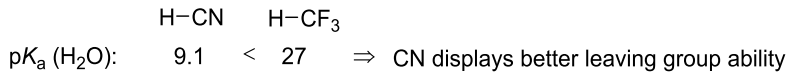

Scheme 3.41: Cyano is better leaving group than trifluoromethyl.

3.3.6 Substrate Scope for Trifluoromethylation of Ketones

The optimised conditions were applied to a wide variety of ketones to give the corresponding aromatic (**109–114**), heteroaromatic (**115**), and aliphatic products (**116**; Table 3.12). The methodology displays excellent functional group tolerance (trifluoromethyl, nitro, thienyl, ester groups and bromine) to provide the intended C–C bond formation in excellent NMR yields (≥90%) and isolated yields (≥91%) under mild conditions. Products **109**, **110** and **116** were not isolated due to their high volatility.

Table 3.12: Cyclopropenimine-catalysed trifluoromethylation of ketones.

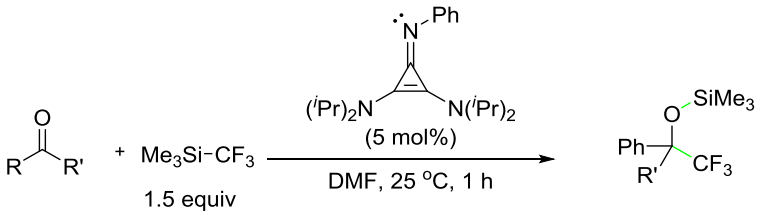

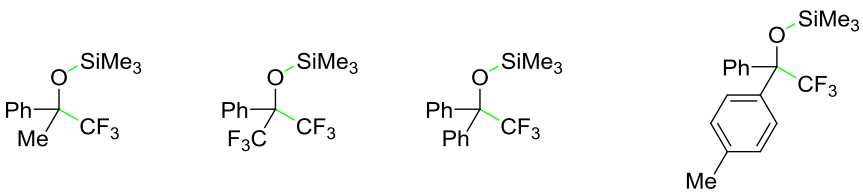

109: 90% **110:** 93% **111:** 99% (94%) **112:** 99% (91%)

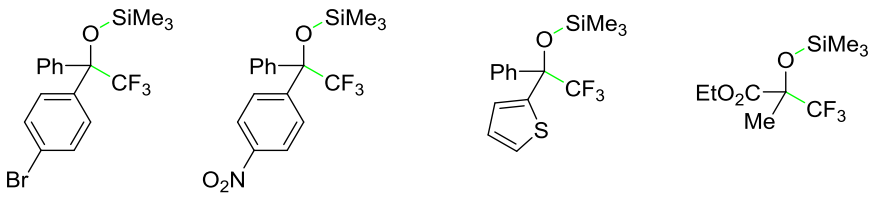

113: 99% (97%) **114:** 99% (95%) **115:** 99% (92%) **116:** 99%

NMR Yields were determined by ^{1}H NMR spectroscopy with DBE (0.25 M in mesitylene) as internal standard. Isolated yields of products in parenthesis.

Next, we set up also a large-scale trifluoromethylation with low catalyst loading (Scheme 3.42). Benzaldehyde (50 mmol) was reacted with an excess of Ruppert's reagent (1.5 equiv) in the presence of cyclopropenimine **49** (0.1 mol%) in acetonitrile. After 3 h reaction time, product **98** was obtained in 94% NMR yield.

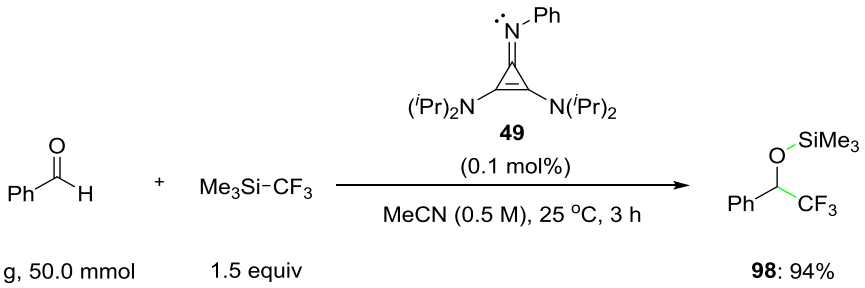

Scheme 3.42: Big-scale cyclopropenimine-catalysed trifluoromethylation of benzaldehyde. NMR yield was determined by ^{1}H NMR spectroscopy with DBE (0.25 M in mesitylene) as internal standard.

3.3.7 Mechanistic Studies for Trifluoromethylation

In analogy to the cyclopropenimine-catalyzed cyanation, several potential mechanistic pathways may be suggested for the trifluoromethylation: 1) stepwise mechanism; 2) 'concerted' mechanism; and 3) initiation (Scheme 3.43). Detailed description of the potential mechanistic pathways has been provided in sub-chapter 3.3.2.7 with the difference that here the nucleophile attached to the silicon atom is a trifluoromethyl group (instead of the cyano group). Potential differences between cyanation and trifluoromethylation may be ascribed to the significantly better leaving group ability of the cyanide group compared to the trifluromethyl group.

1) Catalysis – Stepwise Mechanism

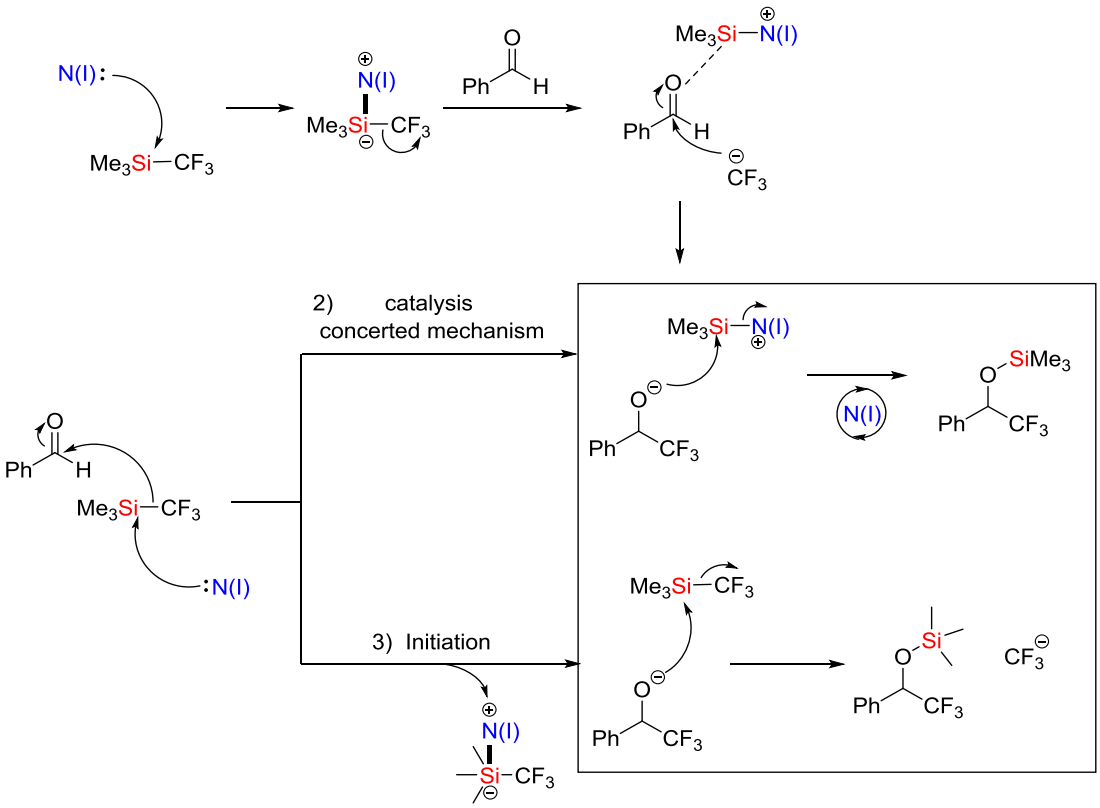

Scheme 3.43: Potential mechanistic pathways for trifluoromethylation of benzaldehyde.

These mechanistic studies were carried out using ^{29}Si NMR spectroscopy between +50 and –20 °C (melting point of Ruppert's reagent = –20 °C). The signal of (trifluoromethyl)trimethylsilane was shown to be at 5 ppm (q, J = 36.5 Hz) in acetonitrile (Scheme 3.44). Addition of cyclopropenimine **49** did not lead to the appearance of any new signals. Heating up to 50 °C did not provide any new signals neither. Therefore, the mixture was gradually cooled to –20 °C, however, only the signal of the remaining (trifluoromethyl)trimethylsilane was detected. In addition, we observed that the used catalyst precipitated at –20 °C, resulting in a poor resolution of the corresponding charts. It is noted that ^{19}F NMR spectroscopy was also used in parallel, however, only the signal of the (trifluoromethyl)trimethylsilane was displayed in the spectra at all variable temperatures.

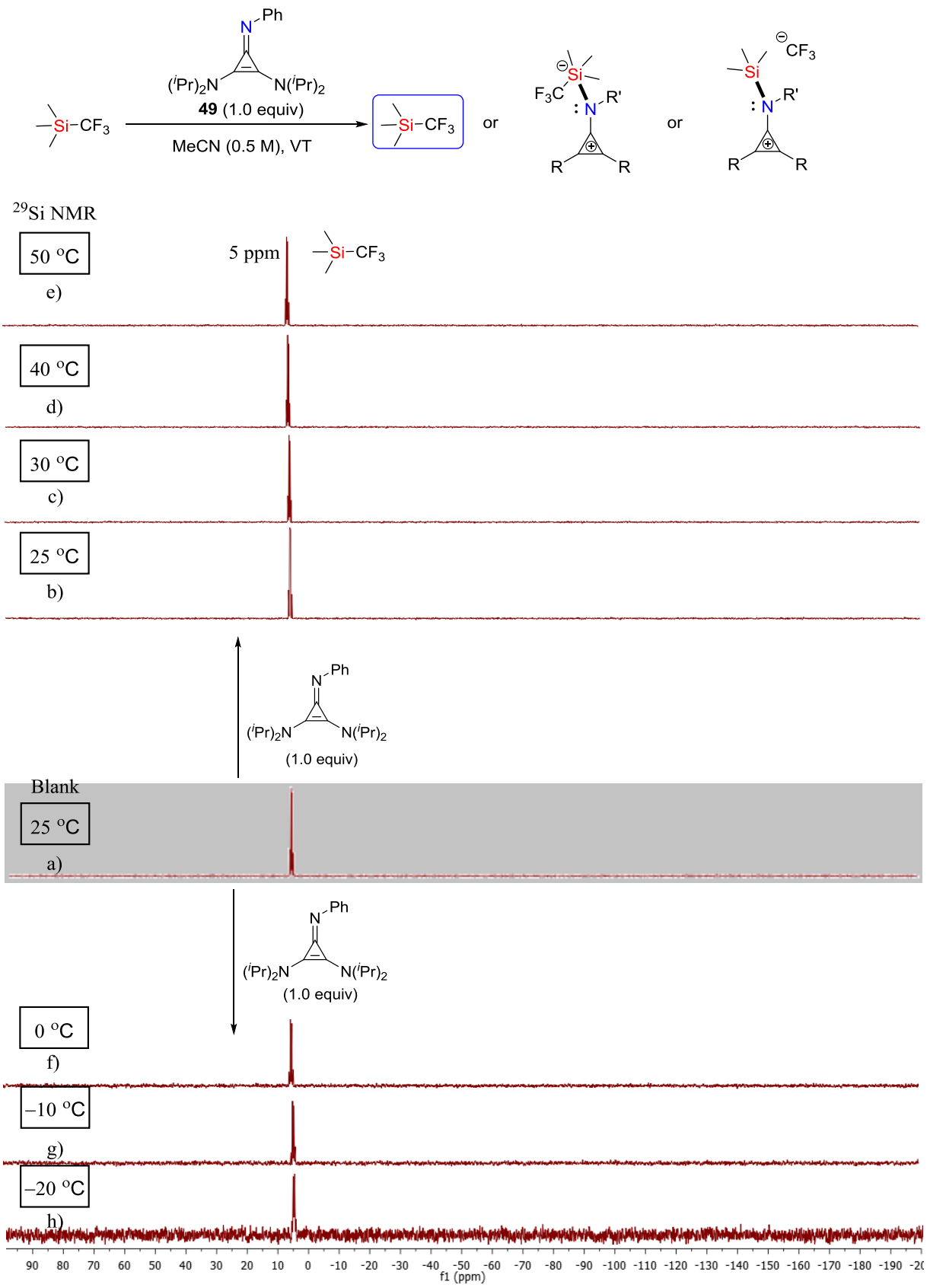

Scheme 3.44: ^{29}Si NMR studies of trimethyl trifluoromethylsilane with cyclopropenimine **49**.

Indeed, benzaldehyde (0.8 equiv) was added at room temperature in a mixture of Ruppert's reagent and cyclopropenimine **49** in acetonitrile and the mixture was stirred for 1 h to form the intended product confirmed by ^{1}H, ^{19}F and ^{29}Si NMR analysis (Scheme 3.45). The formed silyl ether displayed a signal at 24 ppm, which is a considerable shift downfield compared to the starting material (5 ppm).

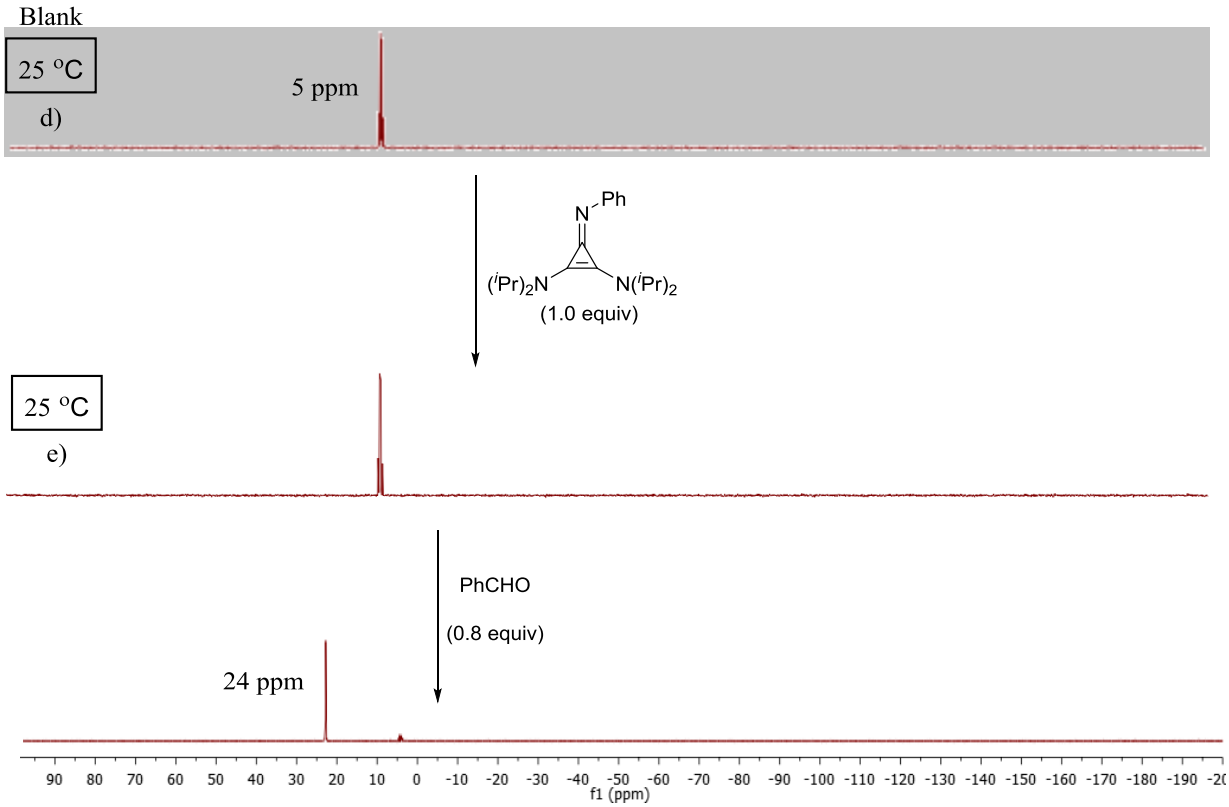

Scheme 3.45: ^{29}Si NMR studies of trimethyl trifluoromethylsilane with the cyclopropenimine **49** and benzaldehyde.

To conclude, we were unable to suggest a specific mechanistic pathway; we would be able to get a better insight into a potential step-wise mechanism as long as we could cool to lower temperatures than –20 °C and capture a potentially formed penta-coordinate silicon species. Therefore, we cannot eliminate this possibility. The concerted mechanism and initiation seem to be possible scenarios considering that ^{29}Si NMR spectroscopy at variable temperature did not display any interaction between cyclopropenimine **49** and the silylated pro-nucleophile before the addition of benzaldehyde; both scenarios require the presence of the electrophile to provide new signals in the ^{29}Si NMR.

Next, the azidation of carbonyl compounds was investigated (Scheme 3.46). Cyclopropenimines were used to activate the Si–N bond of trimethylsilyl azide. The former

may coordinate to the tetra-coordinate silicon to generate a penta-coordinate silicon species, and the azide anion may be released to add to an electrophile and give a C–N bond formation. The resulting alkoxide may add to the silylium cation to generate the intended product with simultaneous catalyst turnover.

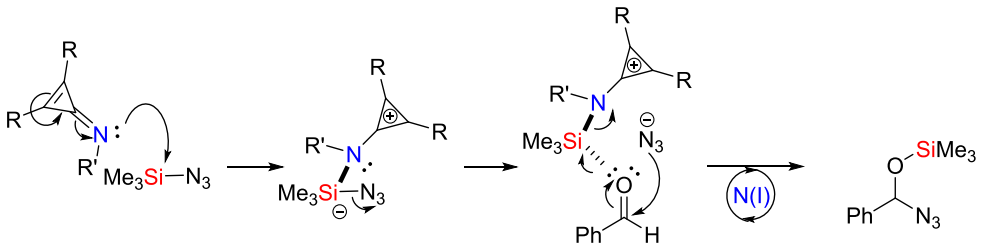

Scheme 3.46: Initial proposal for the catalytic cycle regarding cyclopropenimine-triggered azidation.

3.3.8 Cyclopropenimine-Catalysed Azidation of Benzaldehyde

Lewis base-catalysed azidation of carbonyl compounds has not been reported so far. There are a few examples of metal catalysis in literature (Scheme 3.47). In 1967, the first catalytic example using $ZnCl_2$ was reported; however, the stoichiometry and catalyst loading have not been mentioned.[91] Indeed, the scope was limited to aliphatic aldehydes without functional group tolerance (71–78%). In 1988, Nishiyama *et al.* reported the azidation of carbonyl compounds treated with trimethylsilyl azide (2.0 equiv), sodium azide (10%), and [15]crown-5 (5 mol%) at room temperature to form the corresponding α-siloxy azides in 4–80% yields (Scheme 3.47).[92] The reaction did not proceed in the absence of sodium azide, while there were several examples with poor yields. This method displayed poor functional group tolerance as well.

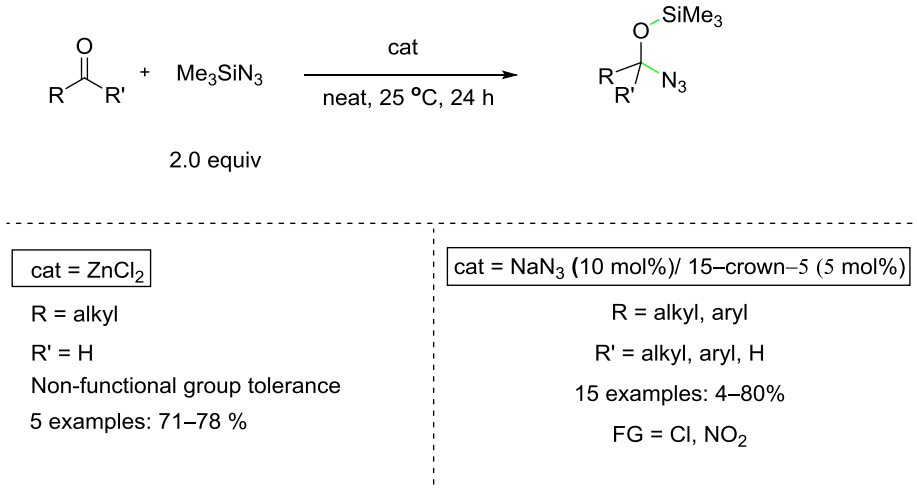

Scheme 3.47: Literature-reported methods for the azidation of carbonyl compounds.

Benzaldehyde was used as an electrophile in our study (Table 3.13). Initially, cyclopropenimines **49**, **50** and **117**–**119** were prepared *in situ* by deprotonation of the precursor (5 mol%) using KHMDS (4.5 mol%) and compared with commercially available Lewis bases and KHMDS. Following literature procedures for the deprotonation of carbene precursors, THF was used for the *in situ* formation of the cyclopropenimines.[7,93,94] Benzaldehyde was treated with trimethylsilyl azide (1.2 equiv) and a series of *in situ* generated cyclopropenimines (4.5 mol%) in a mixture of THF and diethyl ether (added after deprotonation) at 40 °C to lead to a moderate conversion to the azidation product **120** (30–40%; entries 1–5). The use of KHMDS and organic bases led to traces of product formed, or no conversion at all (0–8%; entries 6–10).

Table 3.13: Screening and comparison of cyclopropenimines with commercial available organobases.

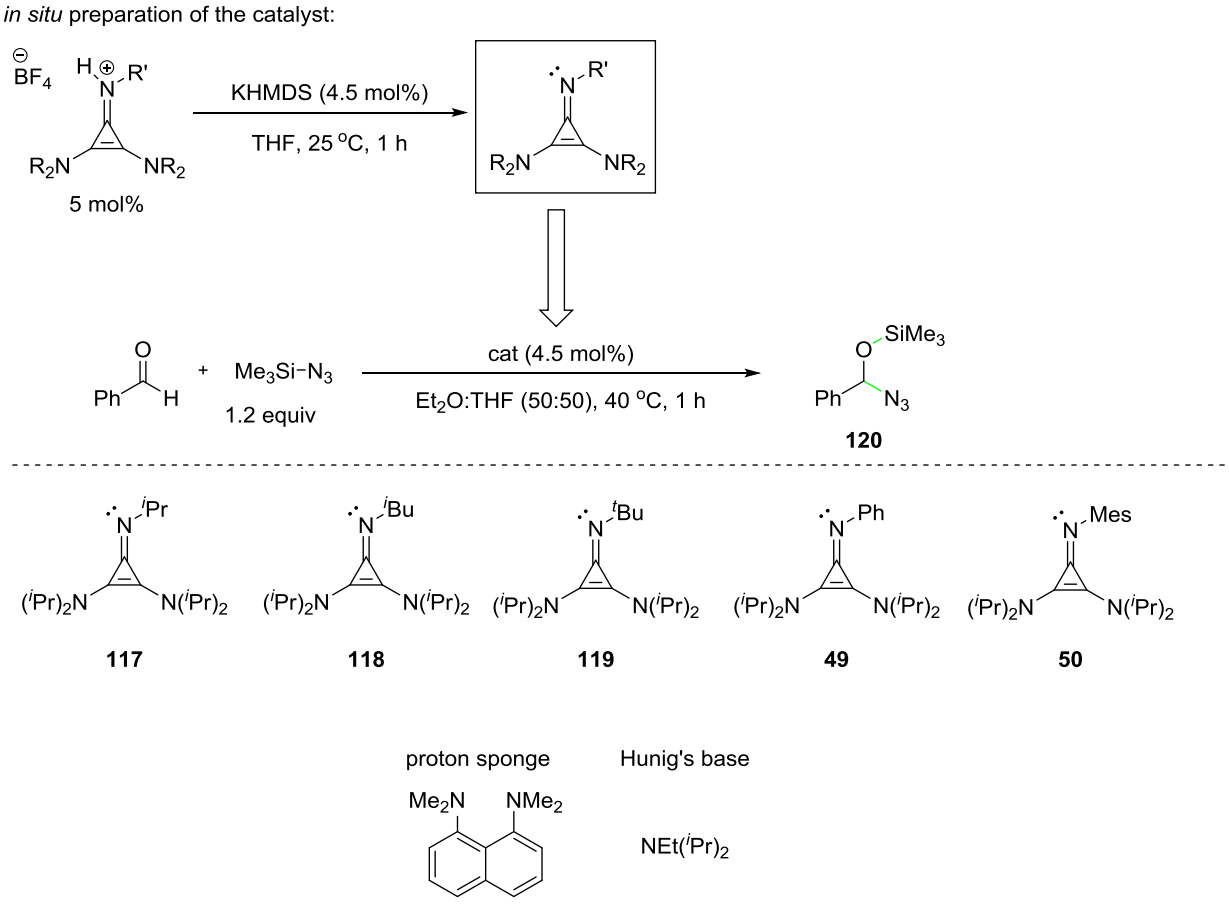

Entry	Organobase	Conv[a] (%)
1	**117**	33
2	**118**	34
3	**119**	34
4	**49**	40
5	**50**	30
6	KHMDS	2
7	proton sponge	NR
8	Hünig's base	NR
9	NEt_3	5
10	PPh_3	8

[a] The conversion is determined based on the **120**:benzaldehyde ratio.

Next, we screened several solvents with the deprotonated form of **49** and doubled catalyst loading at 40 °C for 24 h; i.e., *in situ* formation of the catalyst would not be required (Table 3.14). The use of hexane, toluene, various ethers, ethyl acetate and acetonitrile gave the intended product in 31–60% conversion; diethyl ether gave the highest conversion at 40 °C after 24 h (60%). However, the isolated yield was only 33%, which suggested that the α-siloxy azide partially decomposed on silica gel (verified by R_f analysis and ^1H NMR spectroscopy). In the reported methods, significantly lower isolated yields compared to the conversion prior to work-up have been reported.[91]

Table 3.14: Solvent screening for the cyclopropenimine-catalysed azidation of benzaldehyde.

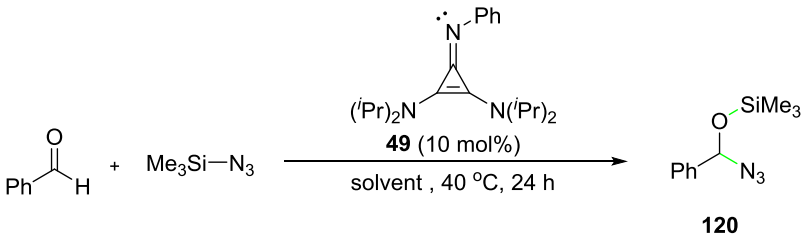

120

Entry	Solvents (ε)	Conv[a] (%)
1	hexane (2.1)	54
2	dioxane (2.25)	31
3	toluene (2.38)	43
4	Et_2O (4.33)	60[b]
5	TBME (4.5)	50
6	EtOAc (6.02)	42
7	Me-THF (6.97)	45
8	DME (7.2)	37
9	THF (7.58)	45
10	MeCN (37.5)	40

[a] The conversion is determined based on molar ratio **120**:benzaldehyde. [b] Isolated yield: 33%.

This outcome of decomposition led us to consider an alternative class of electrophiles in order to develop cyclopropenimine-catalyzed azidation. Thus, we focused on cyclopropenimine-catalyzed ring-opening of *N*-tosyl aziridines using various silylated pro-nucleophiles.

3.3.9 Cyclopropenimine-Catalysed Aziridine Ring-Opening Reactions

At the start, a potential mechanistic pathway was suggested (Scheme 3.48). The cyclopropenimine may add to the silicon atom of the pro-nucleophile to release the

corresponding nucleophile. Then, the latter may add to aziridine to form an amide that may add to the formed silylium cation to give the intended *N*-silylated product with subsequent catalyst turnover.

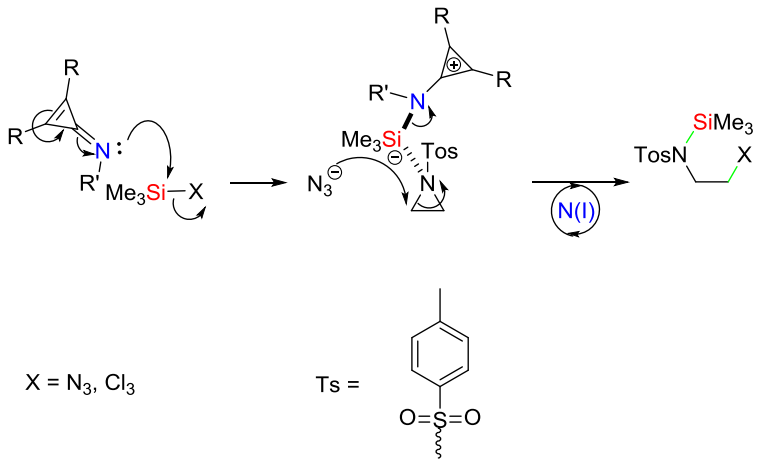

Scheme 3.48: Concept of Lewis base-catalysed aziridine ring opening using cyclopropenimines.

3.3.9.1 Literature-Reported Metal-Free Aziridine Ring-Opening Methods

Ring-opening of *N*-tosyl aziridines has been extensively investigated with Lewis acid catalysts. Rare earth metals, such as lanthanides, used in combination with chiral ligands have proved to induce asymmetry within the nitrogen-containing building blocks useful for the synthesis of biologically active molecules.[95–100]

However, there are limited examples in the field of organocatalysis. In 2005, Komatsu *et al.* reported a metal-free methodology for the ring opening of *N*-tosyl aziridines (Scheme 3.49). The latter were treated with various silylated pro-nucleophiles (1.2 equiv) and tetramethylethylene diamine (TMEDA; 20 mol%), in acetonitrile or dimethylformamide to generate β-functionalised sulfonamides in 57–99% yields.[101] High catalyst loading and harsh conditions in several cases (heating up to 60 °C) were required. Furthermore, the scope was limited to aliphatic aldehydes. Complete regioselectivity for the ring-opening of the *N*-tosylaziridines based on an S_N2 mechanism has been reported with the exception of styrene-derived aziridine **121**. The latter led to the formation of a mixture of products [**122**:**123** = 4:1; addition to benzylic and non-benzylic carbon, respectively). Surprisingly, the former mechanistic pathway provided the major product, which may indicate that a silicon species in the reaction mixture should act as a Lewis acid. Further details of the mechanistic investigation will be discussed at the end of the chapter.

Komatsu 2005

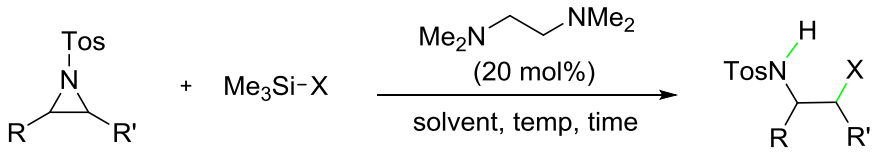

X	Scope (examples)	Solvent	Temp (°C)	Time (h)	Yield (%)
CN	5	MeCN	25–60	24–64	47–93
N_3	4	DMF	25–50	24–48	88–98
I	2	DMF	25	24–48	97–99
Br	1	DMF	25	48	88

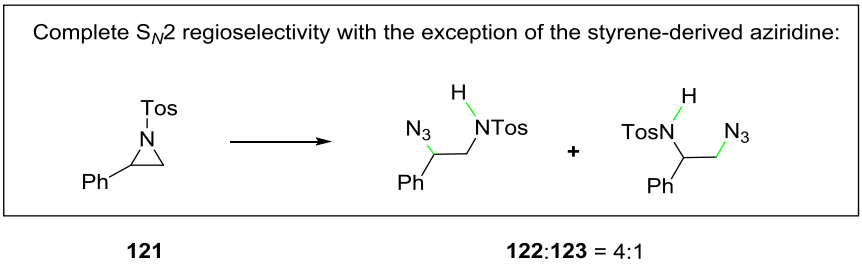

Scheme 3.49: Metal-free ring opening of *N*-tosylaziridines developed by Komatsu *et al.*[101]

In 2009, Matsukawa *et al.* reported another metal-free method for the ring-opening of *N*-tosyl aziridines (Scheme 3.50). The latter were treated with silylated pro-nucleophiles (1.5 equiv) and tris(2,4,6-trimethoxyphenyl)phosphine (TTMPP, 10 mol%) in DMF to generate the reaction product in 50–99% with complete regioselectivity.[102] Again, the only exception was the experiment with styrene-derived *N*-tosylaziridine, which led to the generation of a mixture of products (addition to benzylic and non-benzylic carbon); the ratio of the two regioisomers was similar to the one reported by Komatsu *et al.* [**122**:**123** = 4:1].[101]

Matsukawa 2009

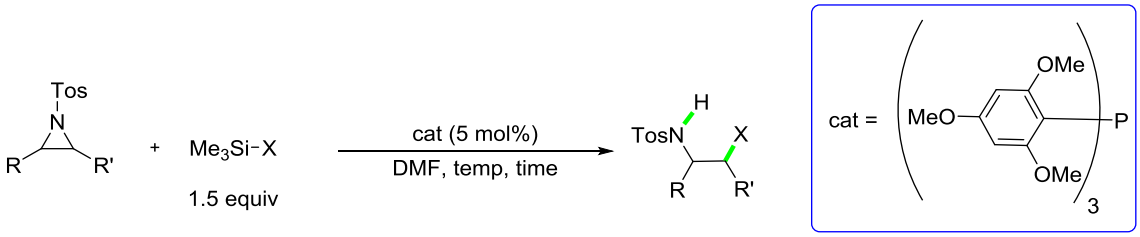

X	**Scope** (examples)	**Temp (°C)**	**Time (h)**	**Yield (%)**
CN	8	50	1–24	68–99
N_3	4	25	1–12	77–98
Cl	3	25	1.5–4	83–96

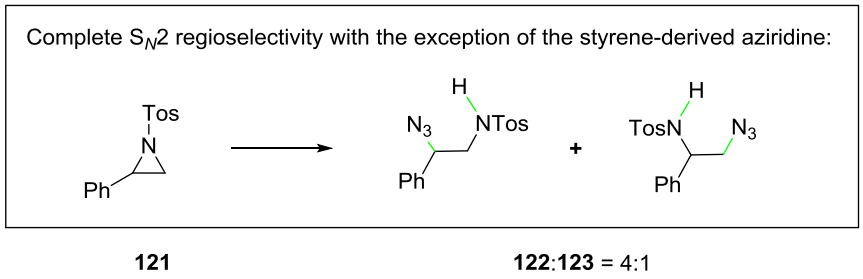

Scheme 3.50: Metal-free ring opening of *N*-tosylaziridines using TTMPP developed by Komatsu *et al.*[102]

In 2012, another Lewis base-catalyzed method for the ring-opening of *N*-tosyl aziridines using a polystyrene-linked superbase catalyst (PS-TBD) was reported (Scheme 3.51).[103] The latter has a highly basic guanidine moiety and was polymer-supported, which provided a simplified work-up procedure with the regeneration of the catalyst. The *N*-tosyl aziridines were treated with various silylated pro-nucleophiles (1.25 equiv) and PS-TBD (5 mol%) in DMF at room temperature to generate a broad scope of nitrogen-containing bioactive compounds. With the exception of trimethylsilyl cyanide (heating up to 80 °C), mild conditions were used to give the products in high yields. Again, the use of the styrene-derived aziridine in the context of azidation led to the formation of a mixture of products [product ratio **122**:**123** = (4:1)].

Matsukawa 2012

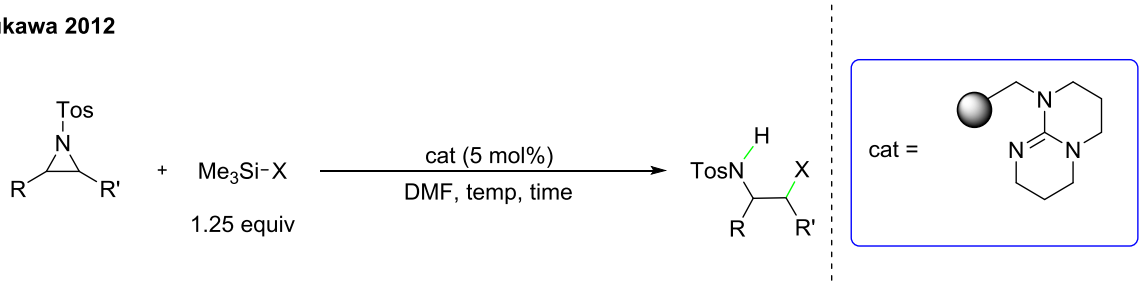

X	Scope (examples)	Temp (°C)	Time (h)	Yield (%)
CN	8	50	4–12	12–95
N_3	4	25	8–12	92–97
Cl	3	25	1–12	90–98
Br	2	25	1–2	97–98

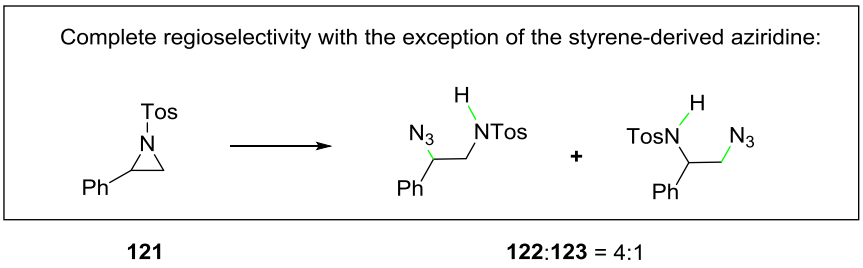

Scheme 3.51: Metal-free ring-opening of *N*-tosylaziridines using PS-TBD developed by Matsukawa *et al.*[103]

3.3.9.2 Preparation of Aziridines

Since the commercial availability of *N*-tosyl aziridines is limited, with the exception of *N*-(p-toluenesulfonyl)aziridine (**124**), further aziridine substrates had to be prepared according to literature methods (Figure 3.6).[104–109] The scope of the synthesized aziridines was fairly broad including acyclic aliphatic (**125**–**126**), aromatic (**121**, **127**), vinyl (**128**) mono-substituted and 1,2-disubstituted (**129**–**130**) aziridines; and cyclic aziridines (**131**–**132**).

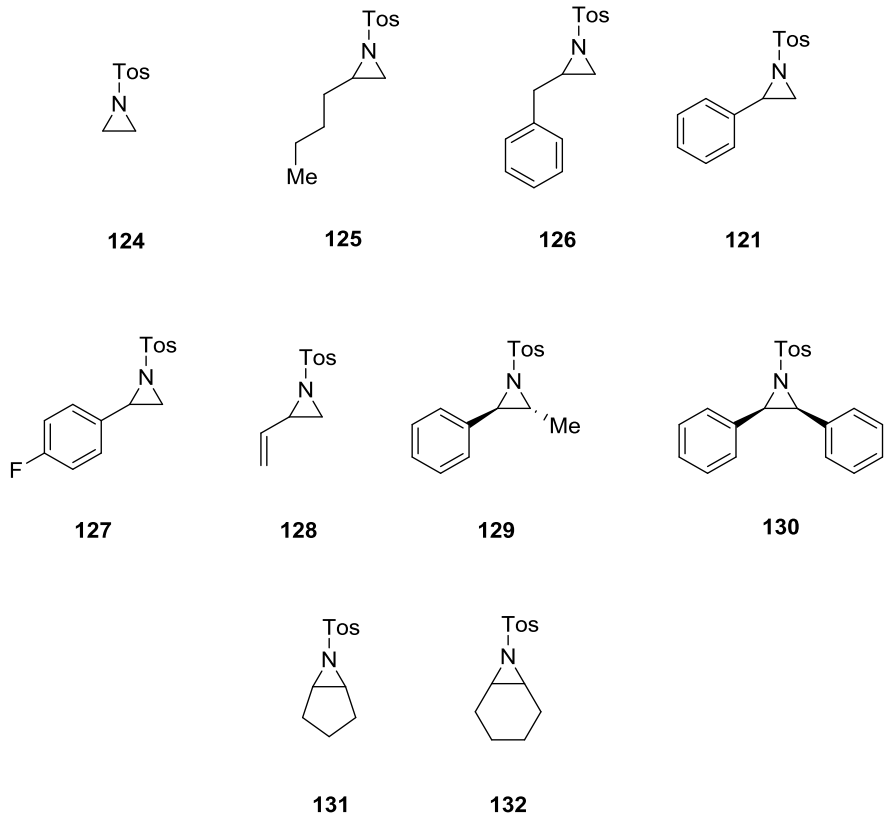

Figure 3.6: Library of aziridines prepared based on literature methods.

The aryl-substituted aziridines **121** and **127** were prepared using chloramine T • 3 H_2O and the corresponding styrene, in the presence of iodine (10 mol%) and benzyl triethyl ammonium chloride ($BnNEt_3Cl$; 10 mol%) as a phase transfer catalyst, to give the *N*-tosyl aziridines in moderate yields [Scheme 3.52 a)]. A plausible mechanism that was suggested is presented below [Scheme 3.52 b)]. [110] Iodine acts as a source of an I^+ species that may react with chloramine T • 3 H_2O to form species **A**. The latter may react with the olefin to form iodonium ion **B**. Anionic chloro-tosyl amide may ring-open the iodonium ion to form the first C–N bond leading to the two potential intermediates **C** and **D**. In both cases, instant intramolecular ring closure should occur to form the second C–N bond thus giving the *N*-tosyl aziridine. Finally, the formed Cl–I species reacts with chloramine T • 3 H_2O to complete the catalytic cycle.

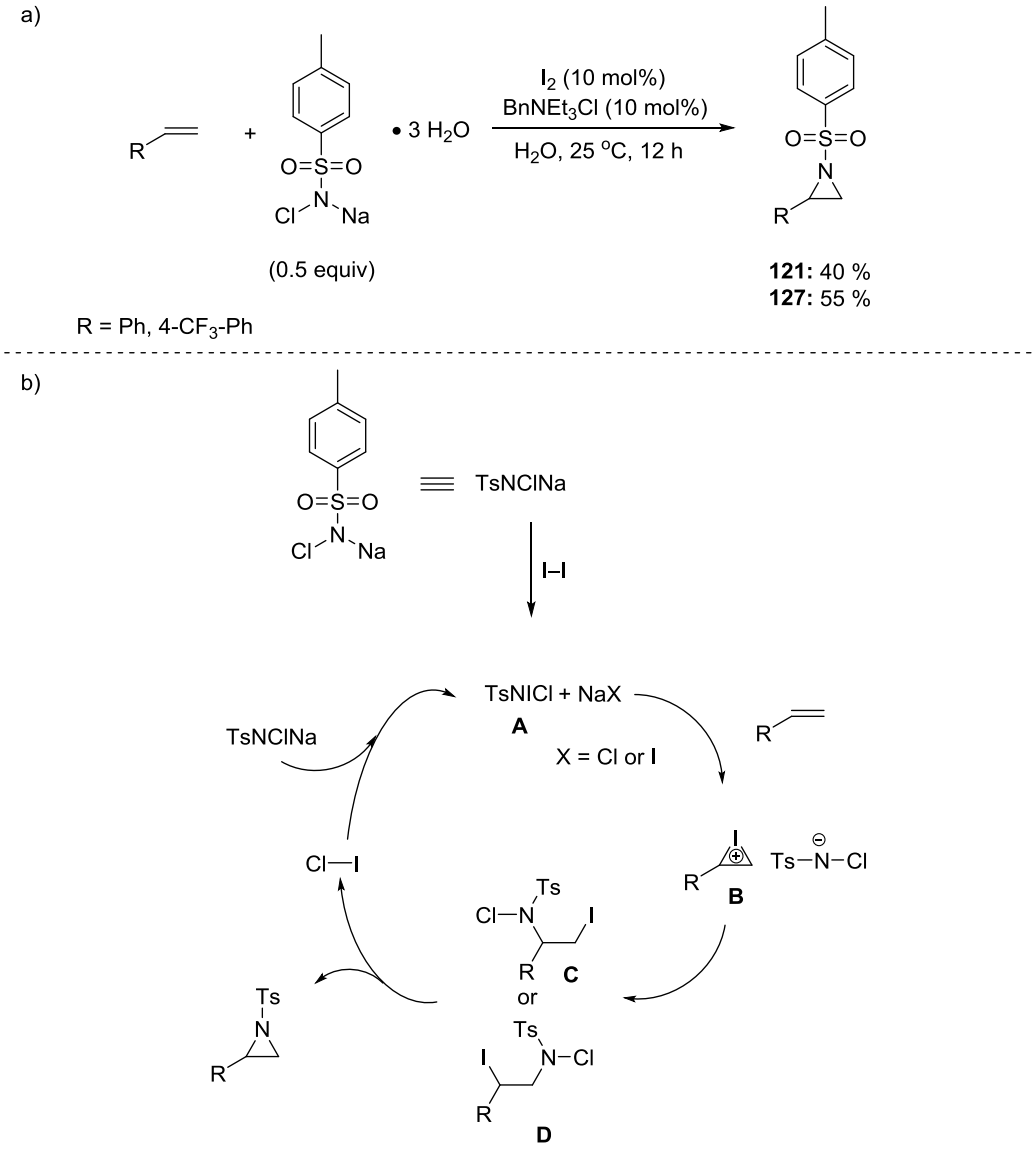

Scheme 3.52: Preparation of aziridines **121** and **127**.

The *N*-tosyl aziridines **125**–**126** and **128**–**132** were prepared following a different protocol (Scheme 3.53).[111] Various *trans*-alkenes were treated with chloramine T • 3 H_2O (1.1 equiv) and phenyl-trimethylammonium tribromide (PTAB; 10 mol%) to give the corresponding aziridines in 32–67% yields.

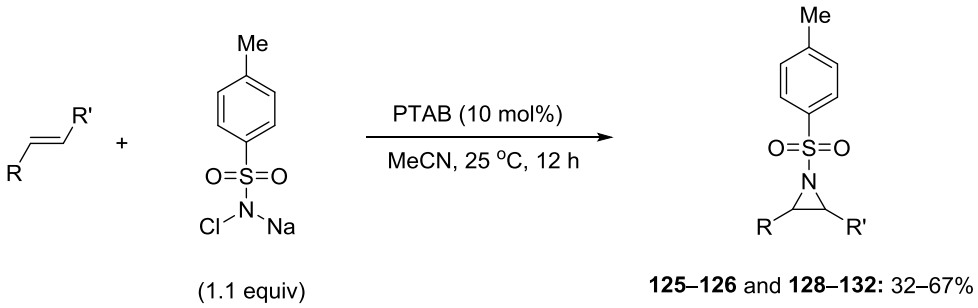

Scheme 3.53: Preparation of aziridines **125**–**126** and **128**–**132**.

3.3.9.3 Initial Result and Optimisation of Reaction Parameters

Our major goal was to develop a catalytic metal-free ring-opening of *N*-tosyl aziridines under mild conditions including a short reaction time, to generate *N*-containing potentially bioactive molecules in high yield with complete regioselectivity. The styrene-derived *N*-tosyl aziridine **121** was selected as a model substrate in the initial study using trimethylsilyl azide as a pro-nucleophile at 30 °C. First, a solvent screening was conducted using cyclopropenimine **49** as a catalyst (Table 3.15); apolar solvents, such as petroleum ether and dioxane did not lead to any reaction (entries 1 and 2). The use of toluene led to the detection of traces of product in the ^{1}H NMR spectroscopy of a reaction aliquot (entry 3). The use of solvents with a slightly higher polarity –such as chloroform, ethyl acetate, and dimethoxyethane– did not lead to any reaction neither (entries 4–6). Gratifyingly, the use of chlorinated solvents, such as dichloromethane and dichloroethane, resulted in a conversion of 37% and 24%, respectively (entries 7 and 8). Finally, acetonitrile and propionitrile were used as polar solvents to give a conversion of 87% and 62%, respectively (entries 9 and 10). Although the use of these solvents led to an increase of the reaction rate, the regioselectivity was moderate (4.6:1 and 6.5:1, respectively).

Table 3.15: Solvent screening for aziridine ring-opening by trimethylsilyl azide.

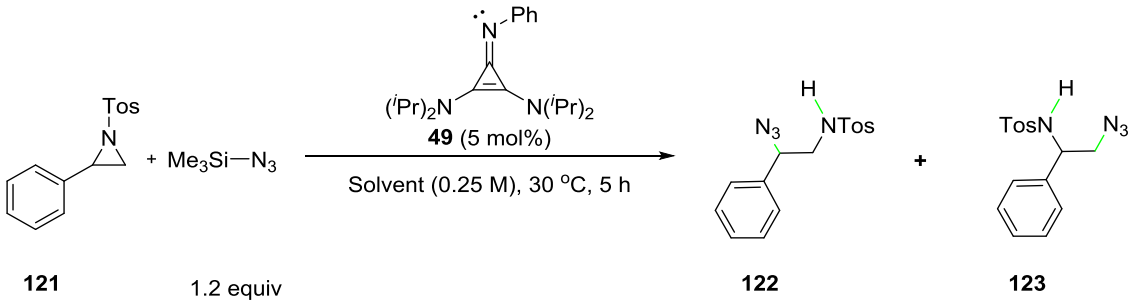

*Reactions of entries 1–6 have been performed by Jonathan Richards

Entry	Solvents (ε)	Conv[a] (%)	Ratio 122:123
1	P. E. 40/60 (2.0)	NR	–
2	dioxane (2.3)	NR	–
3	PhMe (2.4)	3	1:1
4	$CHCl_3$ (4.8)	NR	–
5	EtOAc (6.2)	NR	–
6	DME (7.2)	NR	–
7	DCM (8.9)	37	7:1
8	DCE (10.4)	24	1:1
9	EtCN (28.0)	62	4.6:1
10	MeCN (38.0)	87	6.5:1

[a] The conversion is determined based on the product-to-substrate ratio.

To conclude, acetonitrile proved to be most suitable for our methodology considering both reaction rate and regioselectivity. In dichloromethane, the use of catalyst **49** led to a similar regioselectivity, however, the conversion was significantly lower compared to acetonitrile in the same amount of time. Next, the catalyst structure was examined to see its influence on the regioselectivity (Table 3.16). Treatment of **121** with trimethylsiyl azide (1.2 equiv) and cyclopropenimines **47**, **49**, **50** (5 mol%) at 30 °C for 24 h gave the intended products **122** and **123** at 99% conversion for all cases. The use of **47** and **49** led to a higher regioselectivity compared to **50** (6.5:1 and 5:1, respectively). Therefore, **49** was used in further experiments.

Table 3.16: Catalyst screening for aziridine ring-opening by trimethylsilyl azide.

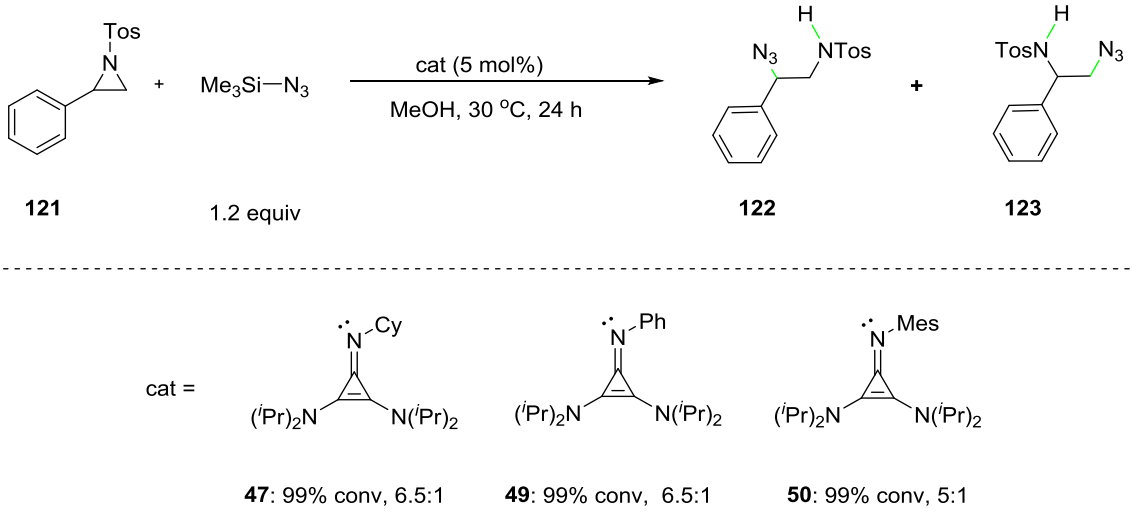

The conversion is determined based on the ratio (**122**+**123**):**121**.

Considering the challenges faced in our attempts to develop a highly regioselective methodology for the aziridine ring-opening, styrene-derived aziridine **121** was used to optimize the procedure. The ring-opening of *N*-tosyl aziridines may proceed either through addition to the benzylic or non-benzylic carbon (Scheme 3.54). The addition to the benzylic carbon is a two-step process and requires the presence of either a Lewis or a Brønsted acid (silylium cation or MeOH, respectively), which may accomplish initially the ring-opening and contribute to the stabilization of the secondary carbocation. The phenyl group attached to the positively charged carbon plays an important role as the filled p orbitals of the aromatic system stabilize the empty p orbital of the positively charged carbon. In an alternative scenario, the *N*-tosylaziridine may undergo a nucleophilic attack by cyclopropenimine **49** to the non-benzylic carbon following the S_N2-type reaction pathway. However, nucleophilic addition to benzylic carbon through an S_N2-type reaction mechanism should not be ruled out, since the steric congestion due to the phenyl ring is not significant. Our best results suggested that both reaction pathways could take place and further optimisation was required to develop a synthetically useful catalytic method.

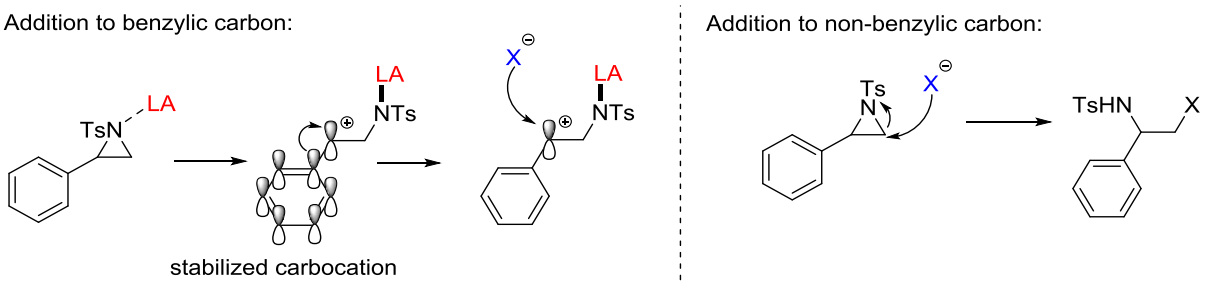

Scheme 3.54: Mechanisms for addition to benzylic and non-benzylic carbons.

3.3.9.4 Scope for Aziridine Ring-Opening with various Pronucleophiles

In our efforts to increase the scope, ring-opening of various aziridines was attempted using trimethylsilyl azide and trimethylsilyl chloride. It should be mentioned that we also used trimethylsilyl chloride as a silicon pro-nucleophile. Styrene-derived aziridine **121** was treated with trimethylsilyl azide (1.2 equiv) and cyclopropenimine **49** (5 mol%) in acetonitrile at 30 ^{o}C for 24 h to generate **122** and **123** in excellent yield (98%) and moderate regioselectivity (6.5:1 ratio; entry 1). Not surprisingly, the use of 4-fluoro-styrene-derived aziridine **125** treated under the identical conditions led to the formation of **133** and **134** (97% y, 6.5:1 regioselectivity; entry 2). Cis-stibene-derived aziridine **130** proved to be more challenging substrate, since heating at 80 ^{o}C for 24 h was required to provide 86% conversion to the intended product **135** with *trans* configuration (entry 3). ^{1}H NMR spectroscopy confirmed that the 14% of the starting material remained unreactive, while no side-products were formed. The reason for this outcome may be steric congestion due to the aromatic rings attached at the 2- and 3-carbons of the aziridine ring. Cyclopentene-derived aziridine **131** proved to be also a challenging substrate, since heating at 60 ^{o}C was required to generate the corresponding β-functionalised sulfonamide **136** at 60% conversion (entry 4). Indeed, the 40% of **131** remained unreacted and no formation of side-product was confirmed by ^{1}H NMR spectroscopy. In contrast, treatment of cyclohexene-derived aziridine **132** under identical conditions led to full conversion to **137** that was obtained in 95% isolated yield (entry 5). The striking difference between the outcome of the reactions with **131** and **132** may be their different ring conformation. Cyclopentane ring of **131** displays an "envelope" conformation, which provides a significant steric bulk. In contrast, cyclohexane ring of **132** exhibits a "chair" conformation, which is less sterically hindered. Control experiment was conducted as well; a mixture of aziridine **121** with trimethylsilyl azide in the absence of cyclopropenimine **49** led to no product formation based on ^{1}H NMR spectroscopy.

Table 3.17: Aziridine ring-opening using trimethylsilyl azide in acetonitrile.

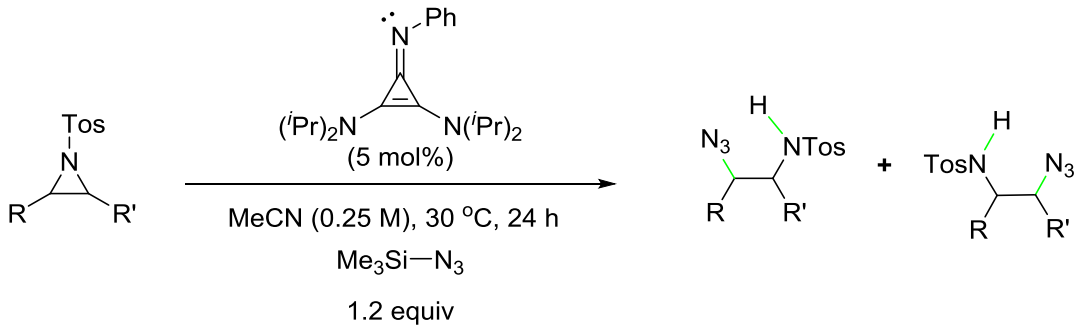

Entry	Aziridines	Temp (°C)	Conv[a] (%)	Products	Yield (%)
1	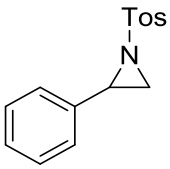	30	quant	**122:123**	98/ (6.5:1.0)
2	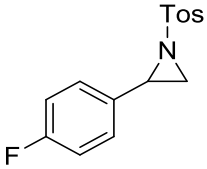	30	quant	**133:134**	97/ (6.5:1.0)
3	[b] 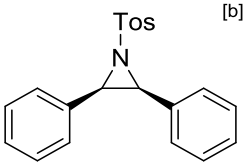	80	86	[b] 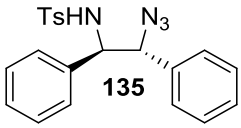	--
4		60	60	**136**	--
5	[b] 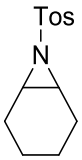	60	quant	**137**	95

[a] The conversion is determined based on the major product-to-substrate ratio. [b] The reaction was carried out in DMF.

The formation of the *trans* isomer **135** suggests that the reaction may proceed through an S_N2 mechanistic pathway (Scheme 3.55). This conclusion can be drawn because the starting

material is *cis*-stilbene and inversion is usually observed in an S_N2 reaction mechanism. However, an S_N1 mechanistic pathway may not be ruled out. Indeed, coordination of the cyclopropenimine **49** to the trimethylsilyl azide will lead to formation of silicon–ate complex, which is a good Lewis acid and good nucleophile.[67] Therefore, the Lewis acidic silicon may ring-open the aziridine **130** following the principles of S_N1 mechanism. The ring-opening may be accomplished with two phenyl groups in *trans* configuration due to the steric repulsion (*cis* configuration is thermodynamically unfavourable). The *cis* and *trans* configurations of the carbocation may be in equilibrium, which lies on the right side (*trans* configuration). Although the intermediate should be planar and a mixture of *cis*/*trans* products should be obtained, the positively charged carbon is attached to a stereogenic centre. Therefore, formation of only one diastereomer may be favoured. To conclude, both mechanistic scenarios may be suggested.

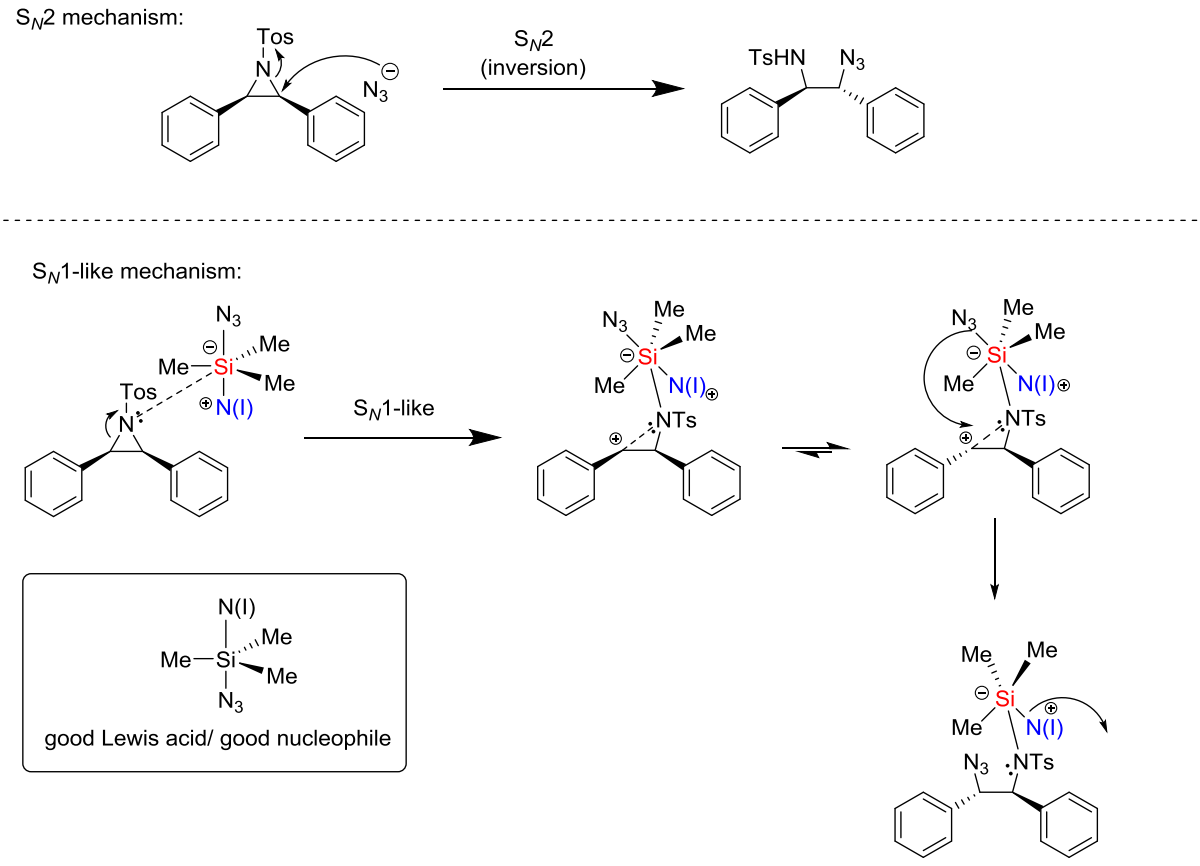

Scheme 3.55: Potential mechanistic pathways for ring-opening of *cis*-stilbene using trimethylsiyl azide.

Chlorination of *N*-tosyl aziridines to form the corresponding β-chloro sulfonamides displayed absolute S_N1-type regioselectivity (Table 3.18). This finding provided further evidence about the significant role of interaction with a Lewis or Brønsted acid in the reaction mechanism as it will be presented later (subschapter 3.3.12). Styrene-derived aziridine **121** was treated with trimethylsilyl chloride (1.2 equiv) in the presence of cyclopropenimine **49** (5 mol%) in acetonitrile at 25 °C to generate **138** in 95% isolated yield (entry 1). Following the exact trend with azidation, **129** and **131** were heated at 60 °C for 24 h to display 66% and 50% conversion to **139** and **140**, respectively (entries 2 and 3). It should be noted, that **139** was obtained with *cis* configuration. Again, **132** proved to react with a higher reaction rate and under milder conditions to generate **141** analytically pure and in 97% isolated yield (entry 4). Again, a mixture of aziridine **121** with trimethylsilyl chloride in the absence of cyclopropenimine **49** led to no product formation based on ^{1}H NMR spectroscopy, which rules out a potential catalytic activity of acetonitrile.

Table 3.18: Aziridine ring-opening using trimethylsilyl chloride in acetonitrile.

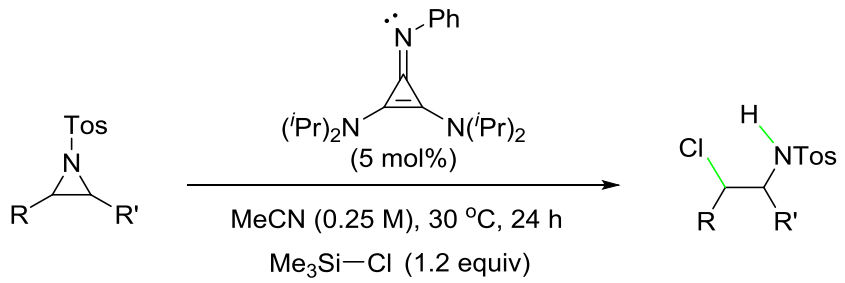

Entry	Aziridines	Temp (°C)	Convers. (%)	Products	Yield (%)/
1	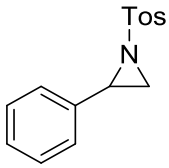	30	quant	**138**	95
2	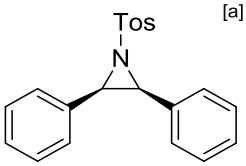 [a]	60	66	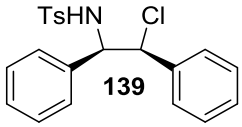 [a]	--
3		60	50	**140**	--
4	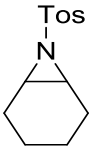	30	quant	**141**	97

[a] The reaction in those solvents was carried out in DMF.

Interestingly, ring-opening of *cis*-stilbene-derived aziridine **130** gives product **139** with retention of stereoselectivity (Scheme 3.56). Therefore, single S_N2 mechanism was ruled out. In contrast, double S_N2 mechanism was considered. Cyclopropenimine **49** may act as a Lewis base to ring-open aziridine **130** with inversion; indeed, the positively charged **49** is a good leaving group and chloride anion may add to the benzylic carbon with simultaneous withdrawal of the regenerated **49** and second inversion. After two successive inversions, the overall stereochemistry of the product is retained. Finally, S_N1-like mechanism was not ruled out. The pentavalent silicon species formed after the coordination of **49** with the silicon atom

of trimethylsilyl azide may act as a Lewis acid to ring-open aziridine **130** to form the corresponding carbocation. Although the intermediate should be planar and a mixture of *cis*/*trans* products should be obtained, the positively charged carbon is attached to a stereogenic centre. Therefore, formation of only the *cis* stereoisomer may be favoured.

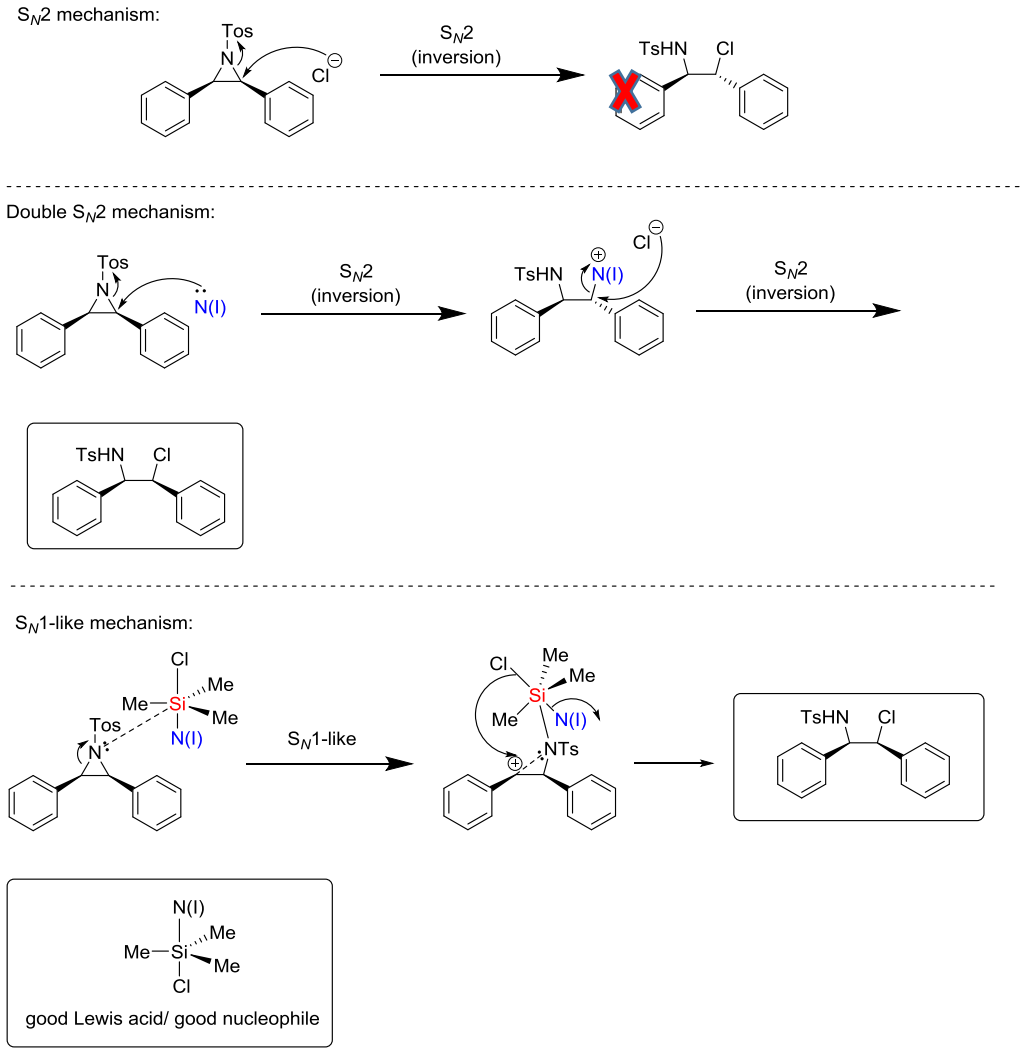

Scheme 3.56: Potential mechanistic pathway for ring-opening of *cis*-stilbene using trimethylsiyl chloride.

To conclude, the ring-opening of **130** has been accomplished with both *cis* and *trans* regioselectivity depending on the use of the appropriate silicon pro-nucleophile. The use of trimethylsilyl azide and trimethylsilyl chloride led to formation of the *trans* and *cis* geometric isomer, respectively (Scheme 3.57). An explanation of this difference in stereochemistry could be relied on the leaving group ability of azide and chloride. The pK_a of hydrogen chloride is –6.1 (H_2O) and HN_3 is 4.5 (H_2O). Thus, chloride is a better leaving group and the negative charge on the atom can be adequately stabilized. In contrast, the azide is not equally stable as negatively charged and needs to carry out a faster nucleophilic addition. This

hypothesis nicely explains the S_N2 mechanistic pathway for both silicon pro-nucleophiles. Nucleophilic addition of the azide (coordination of the cyclopropenimine and consequent release of the nucleophile) may have higher reaction rate compared to ring-opening by cyclopropenimine itself to result in the inverted product [pathway a)]. However, the most stable chloride anion may add after the cyclopropenimine (which has already ring-opened the aziridine) to lead to a second inversion in a row [pathway b); overall retention].

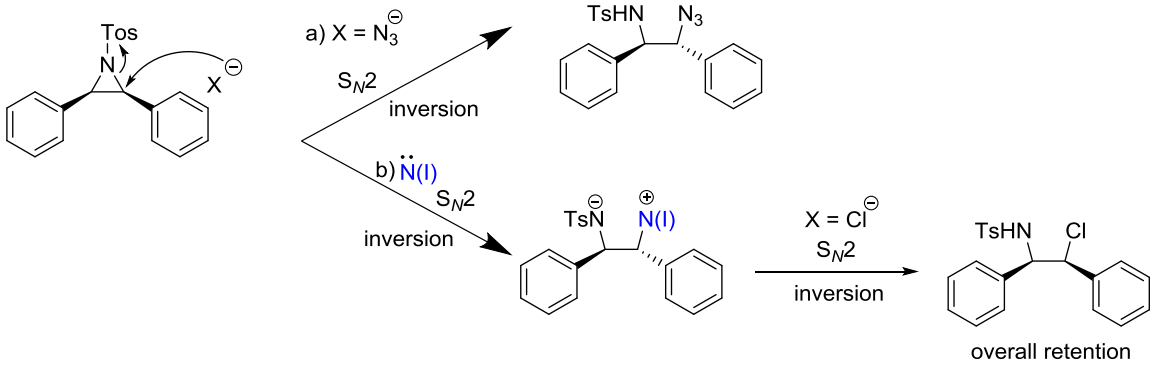

Scheme 3.57: Comparison of leaving group ability of azide and chloride.

Work published by Lambert during the course of our studies

As it has been already mentioned in the introduction, at the outset of our project Lambert *et al.* had reported an enantioselective Brønsted base-catalysed Michael addition. [30] During our studies, Lambert *et al.* reported as well a cyclopropenimine-catalysed enantioselective Mannich reaction between Schiff-base ester and various aldimines using cyclopropenimine **19** (Scheme 3.58).[112] This Mannich-type reaction proceeded smoothly to give the Mannich alcohols in 63–99% yields with excellent diastereoselectivity and 38–98% *ee*.

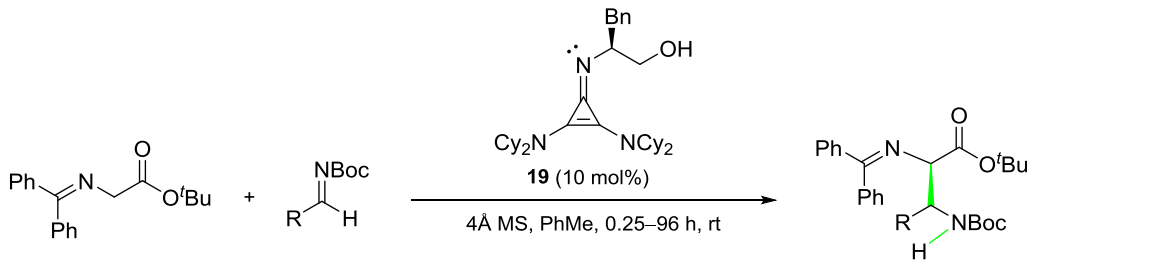

R = Ar, 11 examples, 84–99% y, 91:9–99:1 dr, 38–97% *ee*
R = Alk, 6 examples, 63–99% y, 93:7–99:1 dr, 44–98% *ee*

Scheme 3.58: Enantioselective Mannich reaction reported by Lambert *et al.*[112]

In both Michael and Mannich reactions, it was suggested that the presence of a hydroxyl group in the catalyst structure may be crucial for its reactivity and selectivity. Later on, Lambert *et al.* investigated the significance of this hydroxyl group for the asymmetric Michael addition (Scheme 3.59).[113] The performance of the benchmark cyclopropenimine **19** was compared directly with several analogues lacking an OH group. The reaction using cyclopropenimine **142** was completed within 1 h resulting in quantitative conversion and 98% *ee*. On the other hand, the use of cyclopropenimines **143** or **144**, which lack an H-bond donor ability, resulted in only 11% conversion and 0% *ee* or no reaction, respectively. Cyclopropenimine **144** displayed 13% conversion and 89% *ee*, despite the fact that the primary amide group may allow for H-bond donation. To conclude, phenyl, ester and amide groups proved to be poor candidates for the replacement of the CH_2OH group, which highlighted the critical role of a free OH group.

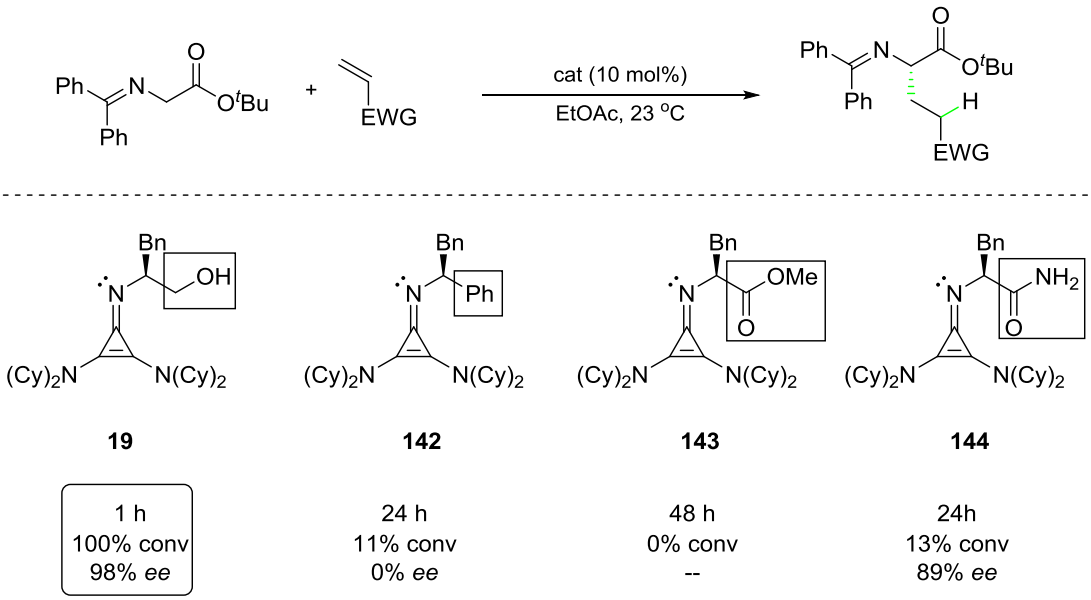

Scheme 3.59: Significance of H–bonding functionality for higher reactivity and enantioselectivity.[113]

The importance of the cyclohexyl group within the backbone of the catalyst structure was also investigated (Scheme 3.60).[113] Cyclopropenimine **19** with the cyclohexyl groups was compared with **145** and **146** (the isopropyl and pyrolidinyl analogues, respectively). It provided significantly higher conversion and better enantioselectivity after a shorter reaction time than the two other candidates.

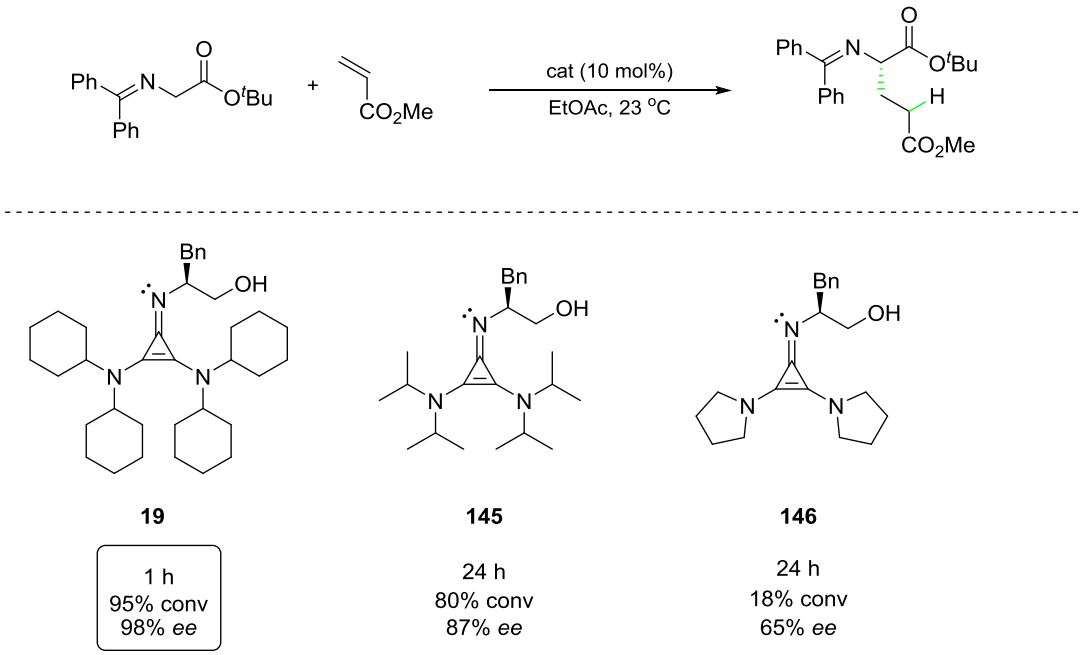

Scheme 3.60: Importance of steric bulk of the 2,3-amino substituents in the backbone of the catalyst structure.[113]

The pK_a value of a cyclopropenimine's conjugated acid (25–30; MeCN) is significantly higher than the one of the glycinate substrate (9–11).[113,114] Thus, the catalyst may deprotonate the glycinate to form the corresponding cyclopropenium enolate complex (Scheme 3.61). Despite the fact that experimental proof could not be obtained, computational studies suggested that the *E* diastereomer of the cyclopropenium enolate complex is favoured due to the dual hydrogen bonding that can be offered by both the N–H of the protonated cyclopropenimine and the hydroxyl group (**I**). [113] Next, it was suggested that the N–H may interact with the carbonyl group of the Michael acceptor, while the hydroxyl group may interact with the negatively charged oxygen of the enolate.[113] Overall, the hydroxyl group in the catalyst may contribute to lower the energy barrier.[113] Furthermore, this transition state encourages a secondary orbital interaction between the α-carbon of the Michael acceptor and the C=N carbon of the glycinate.[113] The formation of the enolate **II** is the rate-limiting step, because the latter will be protonated immediately after its formation to generate the major enantiomeric product.

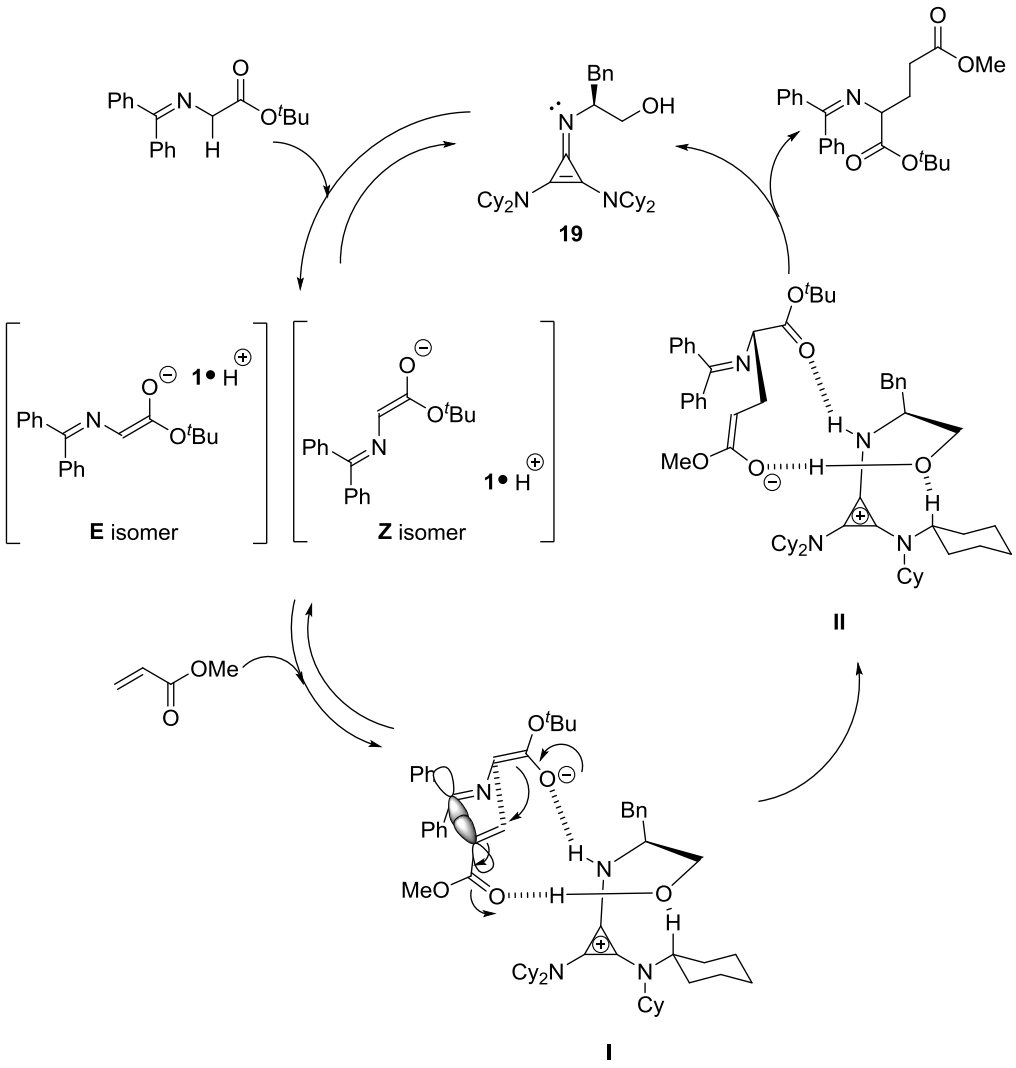

Scheme 3.61: Catalytic cycle of the enantioselective Michael addition.[113]

Inspired by Lambert's work, we decided that the effect of potential hydrogen bonding on the regioselectivity of the aziridine ring-opening should be investigated. For this purpose, various protic solvents were used; in the preliminary screening the effect of the polarity (ε) and the Brønsted acidity (pK_a) were investigated (Table 3.19). Aziridine **121** was treated with trimethylsilyl azide (1.2 equiv) in the presence of catalyst **49** (5 mol%) in an alcohol at 25 °C for 5 h. Among the alcohols tested, *tert*-butanol was the least polar and least Brønsted acidic (pK_a = 16.5 in H_2O), resulting in a very poor conversion and moderate regioselectivity (entry 1). The use of ethanol led to 32% conversion and excellent regioselectivity, however, the generation of a side-product was observed (31:1:1, entry 2). The use of methanol led to similar conversion, lower regioselectivity, and increased formation of the side-product **147** (15:1:6, entry 3). Ethylene glycol proved to be a poor solvent; its use led to low conversion and poor reverse regioselectivity (entry 4). An important reason for this disappointing result may be

the bad solubility of both aziridine **121** and catalyst **49**. Experiments with ethanol and methanol demonstrated considerably higher conversion than *tert*-butanol and ethylene glycol and excellent regioselectivity (31:1 and 15:1, respectively); however, side-products **147** and **148** were generated, respectively. In order to optimise this transformation and increase the ratio of major:minor in favour of the major product, and suppress the formation of side-product, the effect of a longer reaction time and an increased temperature were investigated.

Table 3.19: The effect of protic solvents on the conversion and regioselectivity.

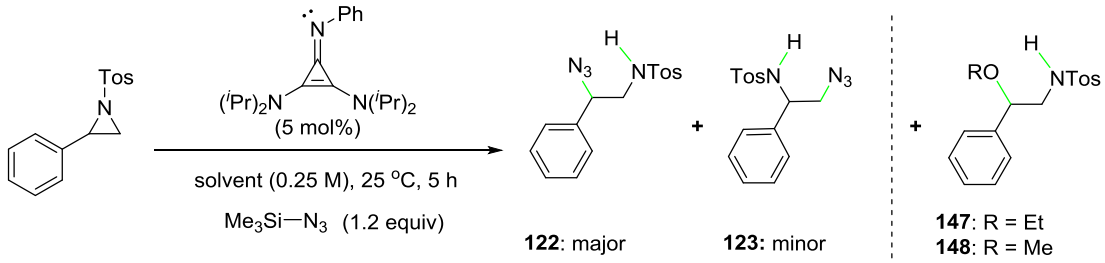

*Work shared with Jonathan Richards

Entry	Solvents (ε)	Conv[a] (%)	122:123:147/148
1	^{t}BuOH (10.7)	6	9:1: –
2	EtOH (24.5)	32	31:1:0.3
3	MeOH (32.7)	35	15:1:6
4	$HOCH_2CH_2OH$ (37.0)	10	0.5:1: –

[a] The conversion is determined based on the major product-to-substrate ratio.

49 may deprotonate an alcohol to form the corresponding cyclopropeniminium alkoxide (Scheme 3.62).[115] H–bonding interaction between the proton of the cyclopropeniminium and the nitrogen of the *N*-tosyl aziridine may lead to a facilitated ring-opening, and the alkoxide may act as a nucleophile to add to the secondary carbocation. Alternatively, the deprotonation of another molecule of alcohol was considered as well. To conclude, based on ^{1}H NMR spectroscopy, structure **147** was suggested as a side product, which is in agreement with literature.[115]

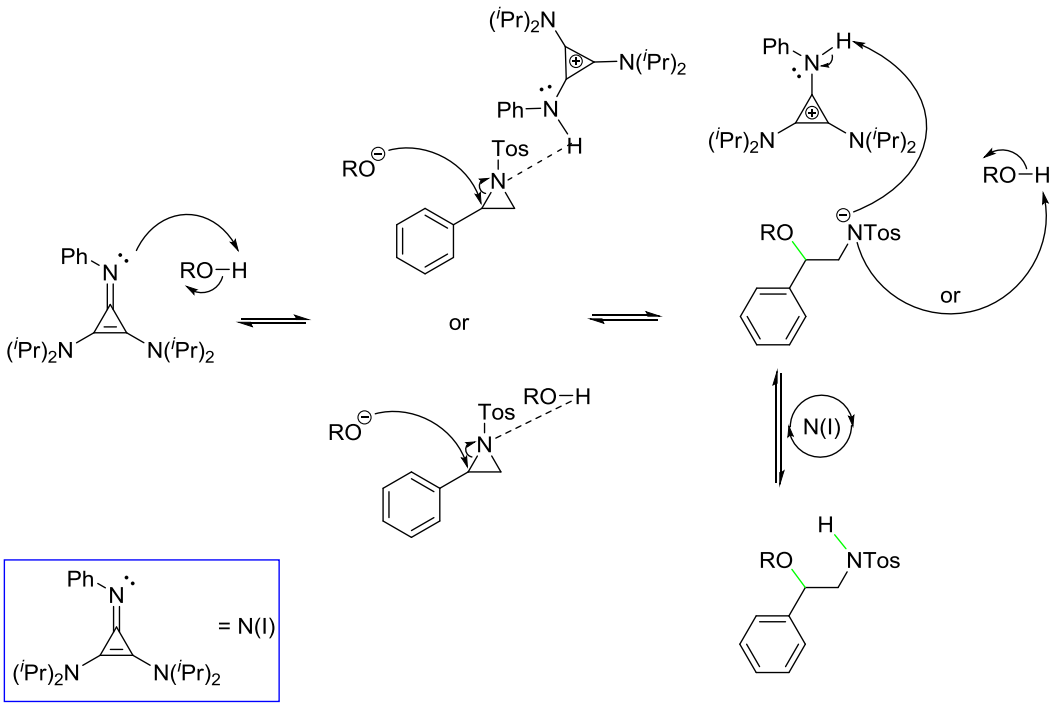

Scheme 3.62: Alkoxy groups act as nucleophiles to form side-products **147**.

Styrene-derived aziridine **121** was treated with trimethylsilyl azide (1.2 equiv) in the presence of cyclopropenimine **49** (5 mol%) in both protic solvents at 25 °C and 40 °C for 15 h (Table 3.20). At 25 °C, the use of ethanol led to 77% conversion of the starting material to **122**, **123**, and **147** in 14:1:0.4 ratio, respectively (entry 1). Under identical conditions, methanol gave 65% conversion and a higher regioselectivity compared to ethanol, but also increased the ratio in favour of side-product **148** (17:1:3; entry 2). At 40 °C, a considerably higher conversion was observed (99%, entries 3 and 4). However, the use of ethanol at 40 °C led to an increase of minor product and **147** compared to the corresponding experiment at 25 °C (11:1:0.5; entry 3). The use of methanol at 40 °C proved to influence slightly positively the outcome of the reaction as the ratio was increased in favor of the major product compared to the experiment at 25 °C (18:1:3; entry 4). To conclude, there was a temperature effect on reaction rate, regioselectivity, and the formation of side-products **147** and **148**.

Table 3.20: Effect of temperature in the reaction rate, regioselectivity and side-product formation.

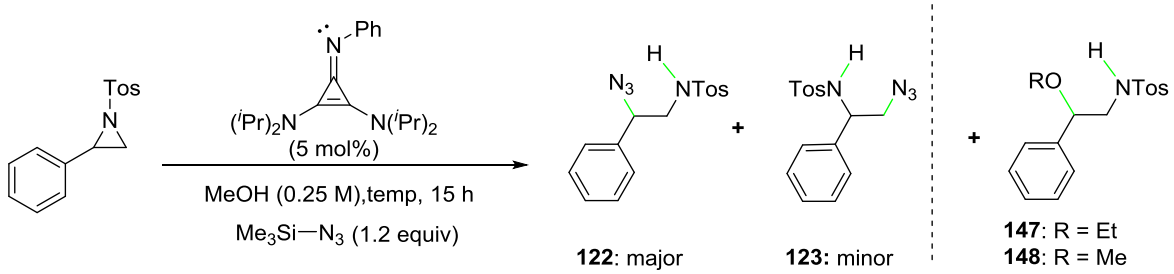

*Work shared with Jonathan Richards

Entry	Solvents (ε)	Temp (°C)	Conv[a] (%)	122:123:147/148
1	EtOH (24.5)	25	77	14:1:0.4
2	MeOH (32.7)		65	17:1:3
3	EtOH (24.5)	40	99	12:1:0.5
4	MeOH (32.7)		99	18:1:3

[a] The conversion is determined based on the major product-to-substrate ratio.

The isolation of **122** and **123** was attempted using methanol and ethanol as solvents (Table 3.21). The goal of those experiments was to compare the solvent effect on the regioselectivity of this reaction. **121** was treated with trimethylsilyl azide (1.2 equiv) in the presence of **49 (**5 mol%) in methanol and ethanol to give the product mixture in excellent yield with high regioselectivity after isolation using PTLC on silica gel (18:1:1 and 26:1:1, respectively; entries 1 and 2). Unfortunately, the side-product could not be separated from the intended products **122** and **123**. However, after isolation of the mixture of products, it was apparent that methanol was a more suitable solvent.

Table 3.21: Aziridine ring-opening using trimethylsilyl azide in protic solvents.

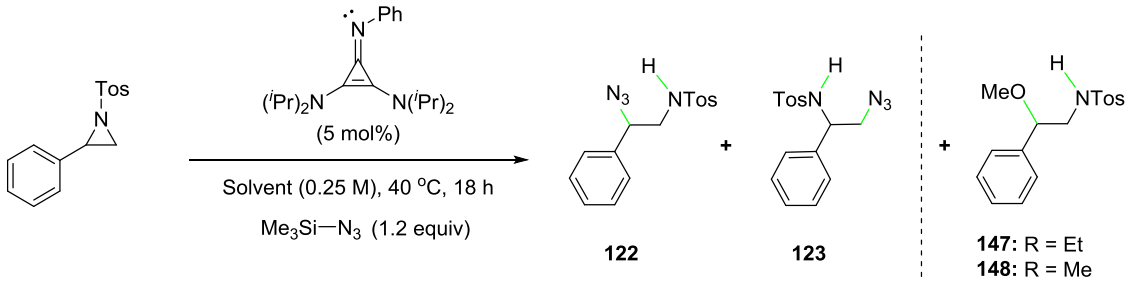

Entry	Solvents (ε)	Yield (%)[a]	122:123:147
1	EtOH (24.5)	96	18:1:1
2	MeOH (32.5)	97	26:1:1

[a] Isolated yields.

Methanol was chosen to study the influence of water on the reaction outcome (Table 3.22). Water can also provide hydrogen bonding, while it is considered a 'green' solvent. In the absence of water, there was full conversion with high regioselectivity and formation of side-product **148** in 18:1:2 ratio (entry 1). One equivalent of water proved to maintain high conversion (95%) with an increased regioselectivity and decreased ratio of the side-product (20:1:2.4; entry 2). Overall though, the combined ratio of the minor product and the side-product was slightly decreased compared to the experiment in the absence of water. Addition of five equivalents of water led to a significant decrease of the reaction rate (75%), and an increase of regioselectivity and the formation of **148** (20:1:4; entry 3).

Table 3.22: Effect of water in the reaction rate, regioselectivity and side-product formation.

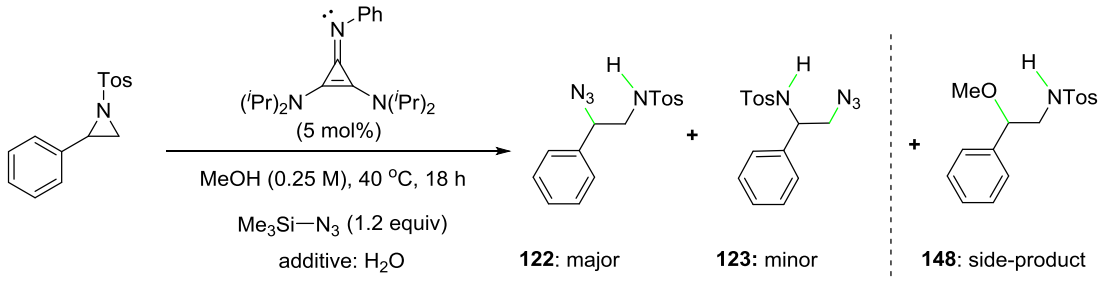

*Work shared with Jonathan Richards

Entry	H_2O (equiv)	Conv [a] (%)	121:122:148
1	0	>99	18:1:3
2	1	95	20:1:2.4
3	5	75	20:1:4

[a] The conversion is determined based on the major product-to-substrate ratio.

The use of ethanol and methanol as solvents led to considerably higher regioselectivity compared to the non-protic solvents. However, both protic solvents led to formation of the side-products **147** and **148**, respectively. Therefore, we decided to expand the scope of the protic solvents (Table 3.23). Phenol was included in our solvent choices, despite the fact that it is a solid (mp = 40 °C), since it is more acidic and less nucleophilic than alcohols. Aziridine **121** was treated with trimethylsilyl azide (1.2 equiv) in the presence of cyclopropenimine **49** (5 mol%) in the corresponding protic solvent at 40 °C for 18 h to give the intended product in excellent conversions (97–99%; Table 3.23). Regioselectivity and side-product formation were measured and compared between the different alcohols using ^{1}H NMR spectroscopy. The use of trifluoroethanol resulted in a regioselectivity of 7:1; a side-product was not formed (entry 1). Neopentyl alcohol displayed identical product ratios with *t*butanol (9:1:0; entries 2 and 4, respectively). The use of phenol as a solvent led to 99% conversion with complete regioselectivity and no formation of side-product (entry 3). When isopropanol was used as a solvent, similar regioselectivity without generation of the side-product was displayed (17:1:0; entry 5). This may be an outcome of the significantly decreased polarity and Brønsted acidity of isopropanol (pKa = 16.5; H_2O) compared to methanol and ethanol. Use of ethanol and methanol led to high regioselectivities combined with formation of the side-products **147** and **148**, respectively (20:1:2 and 17:1:1, respectively; entries 6–7).

Table 3.23: Screening of protic solvents and their effect on the conversion and regioselectivity.

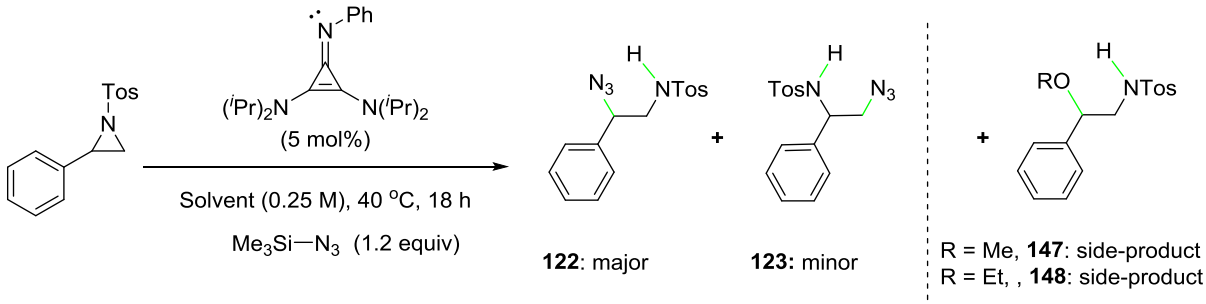

*Work shared with Jonathan Richards

Entry	Solvents (ε)	Conv (%)[a]	122:123:147/148
1	CF_3CH_2OH (8.55)	99	7:1
2	^{t}BuOH (~9.0)	97	9:1
3	PhOH (10.0)	99	>99:1: –
4	^{t}BuOH (10.9)	97	9:1: –
5	^{i}PrOH (17.9)	99	17:1: –
6	EtOH (24.5)	99	17:1:1
7	MeOH (32.7)	99	20:1:2

[a] The conversion is determined based on the major product-to-substrate ratio.

To conclude, isopropanol and phenol provided excellent conversions combined with impressively high regioselectivity and no formation of the side-product. Considering that phenol did not act as a nucleophile and only one product was identified in the reaction mixture, we decided to opt for this solvent. Phenol is a solid and subject of the optimisation was to minimize the amount of phenol required to provide such an excellent regioselectivity in order to facilitate the isolation of the intended product using chromatographic techniques. Thus, phenol was paired with dichloromethane, and the ideal ratio between these two solvents was investigated (Table 3.24). Aziridine **121** was treated with trimethylsilyl azide (1.2 equiv) in the presence of cyclopropenimine **49** (5 mol%) and with a variable amount of phenol in DCM at 25 °C for 18 h to display excellent conversion (entries 1–6). In the absence of phenol, a complete conversion of the starting material was observed and the ratio **122**:**123** was 7:1 (entry 1). 1% of phenol in the reaction mixture did not influence the regioselectivity (entry 2). By increasing the ratio of the phenol in the solvent system (14:86 and 25:75, respectively; entries 3 and 4), an excellent regioselectivity was observed (40:1 and 60:1, respectively; entries 3 and 4). A further increase of the solvent ratio to 50:50 led to an even higher level of

regioselectivity (68:1; entry 5). Finally, phenol in the absence of DCM led to complete regioselectivity (>99:1).

Table 3.24: Investigation of phenol:DCM ratio.

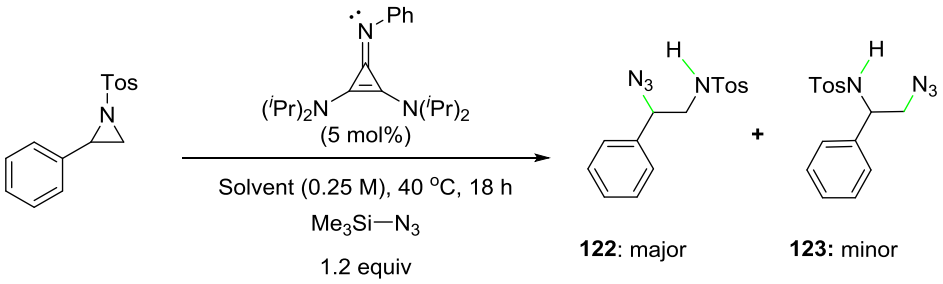

*Work shared with Jonathan Richards

Entry	Solvents	Conv (%)[a]	122:123
1	DCM (100)	99	7:1
2	Phenol: DCM (1:99)	99	9:1
3	Phenol: DCM (14:86)	99	48:1
4	Phenol: DCM (25:75)	99	60:1
5	Phenol: DCM (50:50)	99	68:1
6	Phenol (100)	99	>99:1

[a] The conversion is determined based on the major product-to-substrate ratio.

Participation of phenol in the mechanistic pathway was investigated as well. A plausible scenario would be that cyclopropenimine **49** deprotonates phenol to form the corresponding cyclopropeniminium phenoxide (Scheme 3.63). The pK_a of the cyclopropenimine's conjugate acid (25–30; MeCN)[30] is similar with the one reported for phenol (29; MeCN).[117] While it is conceivable that deprotonation of phenol by **49** occurred, the phenoxide is not a strong nucleophile. In turn, the side-product (ring-opening by phenoxide) was not observed.

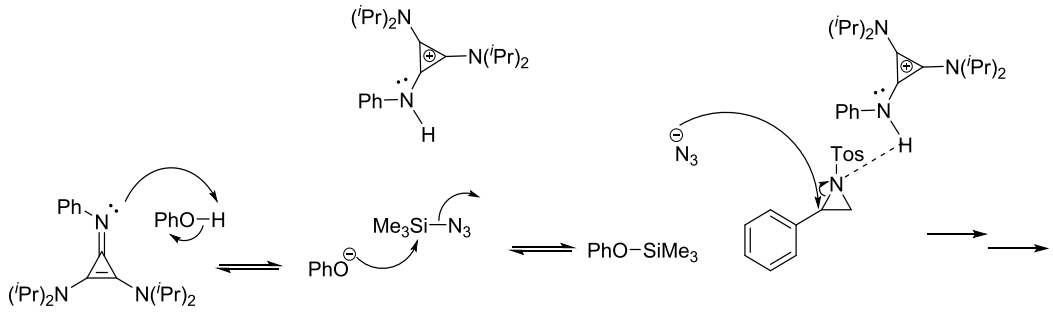

3.63: Plausible mechanistic pathway in reactions that phenol is used as a solvent.

3.3.9.5 Mechanistic Studies For Catalytic Aziridine Ring-Opening

The principles and the interpretation of ^{29}Si NMR spectroscopy in order to rationalise the appearance or disappearance of ^{29}Si NMR signals, related to the structure of intermediate (environment of silicon) has been already described (subchapter 3.3.2.7). Herein, initially three conceivable mechanistic pathways are proposed, followed by ^{1}H and ^{29}Si NMR studies alongside with a conclusion. In the first scenario, the reaction may proceed through addition/elimination in a step-wise mechanism (Scheme 3.64). The electron-rich nitrogen atom of the cyclopropenimine may add to the silicon pro-nucleophile to form a penta-coordinate silicon species. Then, the leaving group X^- may go off and the silylium cation may activate the aziridine; next, X^- may attack to accomplish aziridine ring-opening. This scenario would explain the S_N1-type regioselectivity that the reaction displayed. The anionic sulfonamide formed to add to the Lewis acidic silylium ion to generate the final product and regenerate catalyst **49**. The second scenario is the concerted mechanism (Scheme 3.61). Cyclopropenimine **49** may add to the silicon pro-nucleophile to directly release X^-, which may immediately add to the less sterically hindered carbon. The final scenario is that the catalyst may act as an initiatior; i.e., it may activate the silylated pro-nucleophile and X^- may add to the least sterically hindered carbon of the styrene-derived aziridine to generate an anionic sulfonamide, which is a good enough Lewis base to catalyse further the reaction (Scheme 3.61).

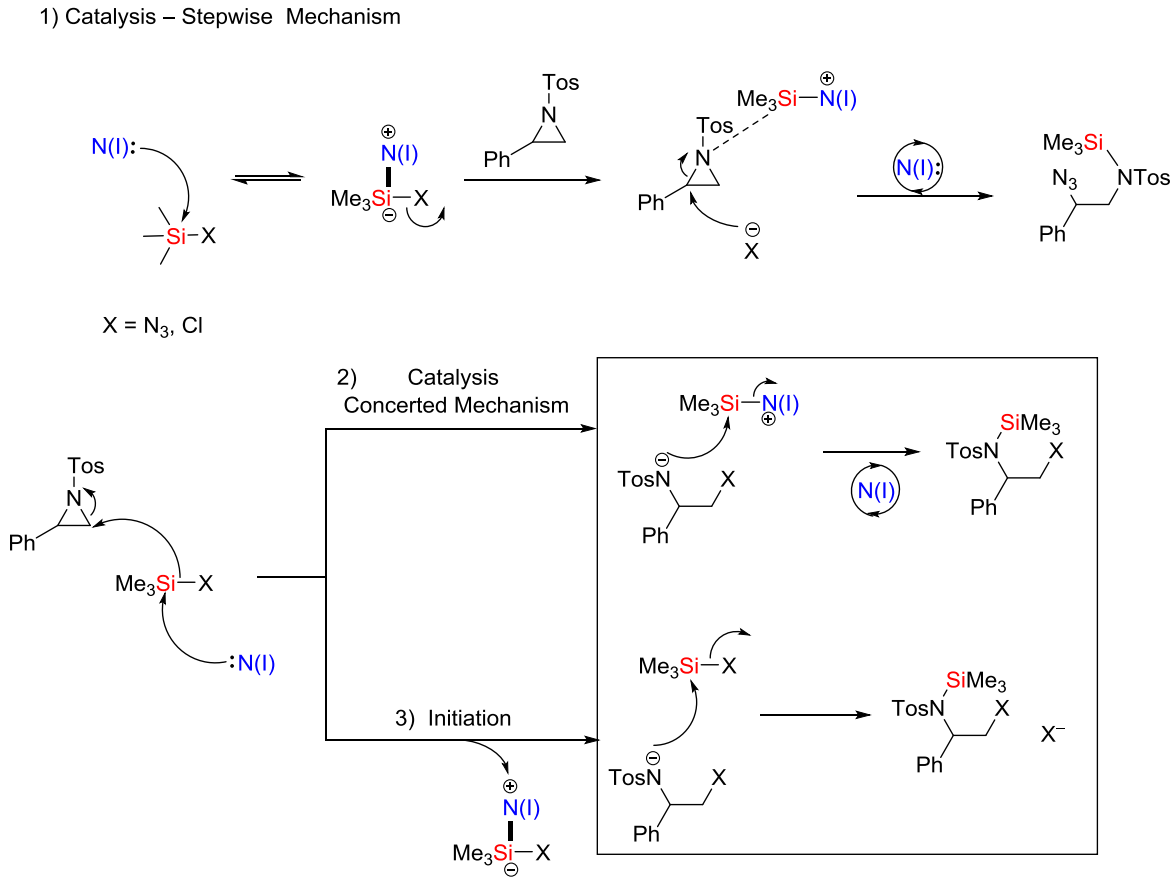

Scheme 3.64: Potential mechanistic pathways of ring opening of *N*-tosyl aziridines with silicon pro-nucleophiles.

Initially, the interaction of trimethylsilyl azide with cyclopropenimine **49** (1.0 equiv) was investigated in dichloromethane (Scheme 3.62). In the absence of **49**, the silylated pronucleophile displayed a signal at 17 ppm in ^{29}Si NMR spectroscopy. There was tiny signal at 7 ppm as well, which was suspected that it may correspond to hexamethyldisiloxane (TMSOTMS) or trimethylsilylanol. Control ^{29}Si NMR experiments led us to the conclusion that the signal at 7 ppm corresponds to TMSOTMS. The latter may be an impurity in the commercially available bottle of trimethylsilyl azide or it may be formed because of a reaction between trimethylsilyl azide and the moisture traces from dichloromethane. Addition of **49** to the solution did not lead to the appearance of any new signals in ^{29}Si NMR spectroscopy. Cooling gradually to –50 °C in order to detect potential penta-coordinate silicon species failed to give evidence in accordance to this hypothesis.

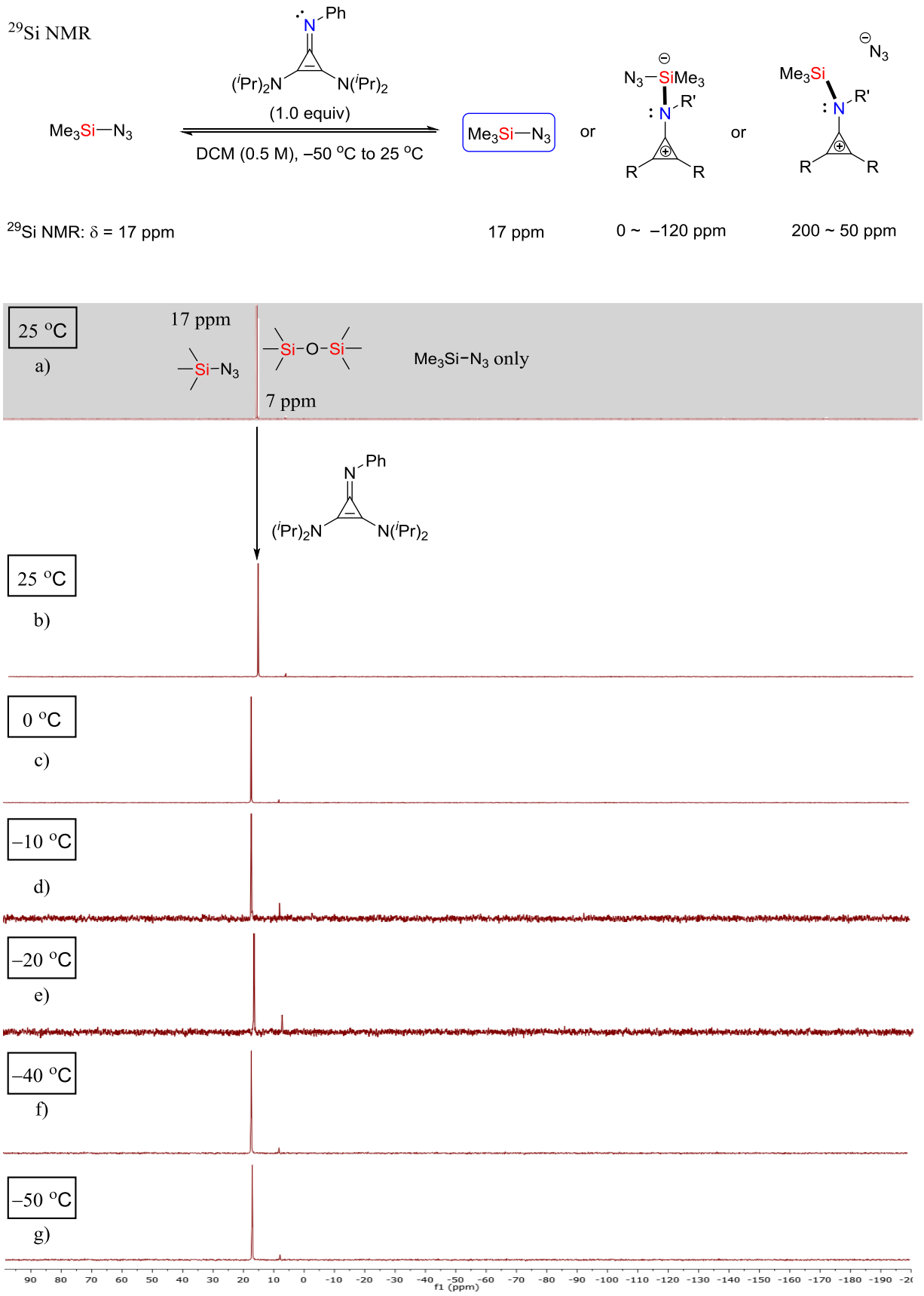

Scheme 3.62: ^{29}Si NMR studies of interaction between TMS–N_3 and cyclopropenimine at variable temperatures.

Next, any potential interaction between trimethylsilyl chloride and cyclopropenimine **49** was investigated (Scheme 3.63). In control experiments, the former displayed a signal at 31 ppm in ^{29}Si NMR spectroscopy, while the latter exhibited a signal at 3.68 ppm in ^{1}H NMR spectroscopy. **49** was added at 25 ^{o}C to the solution of trimethyl chloride in dichloromethane to generate two singlets at 26 ppm and 13 ppm, respectively. In ^{1}H NMR spectroscopy, there are two signals at 3.52 and 3.78 ppm, which represent two different species. However, both correspond to the proton of the tertiary carbon in an isopropyl group. Cooling progressively to –30 ^{o}C increased the ratio of the signal at 13 ppm in ^{29}Si NMR spectroscopy. This observation was in accordance to the increase of ratio for the signal at 3.78 ppm compared to the signal at 3.52 ppm in ^{1}H NMR spectroscopy, i.e., these two signals (13 ppm in^{29}Si NMR and 3.78 in ^{1}H NMR) correspond to the same species. The signal at 3.52 ppm corresponds to free cyclopropenimine **49**. Unfortunately, there are no evidence reported regarding trimethylsilylium cations in ^{29}Si NMR spectroscopy in literature and therefore, we were not able to compare our rationalised data with other groups' work. However, Alcarazo *et al.* reported that the signal of a proton of the isopropyl group in the pre-N(I) structure was shifted downfield compared to the free cyclopropenimine.[10] Considering that in the precursor the proton attached to the central nitrogen is a Brønsted acid, it may be compared with the silicon atom of the trimethylsilylium cation. Thus, the shifts in the signals of a proton of the isopropyl group before and after the deprotonation in the ^{1}H NMR spectroscopy [pre-N(I) and free cyclopropenimine, respectively] are in analogy with the shifts of the corresponding proton between the trimethylsilylium cation and free **49**, respectively.

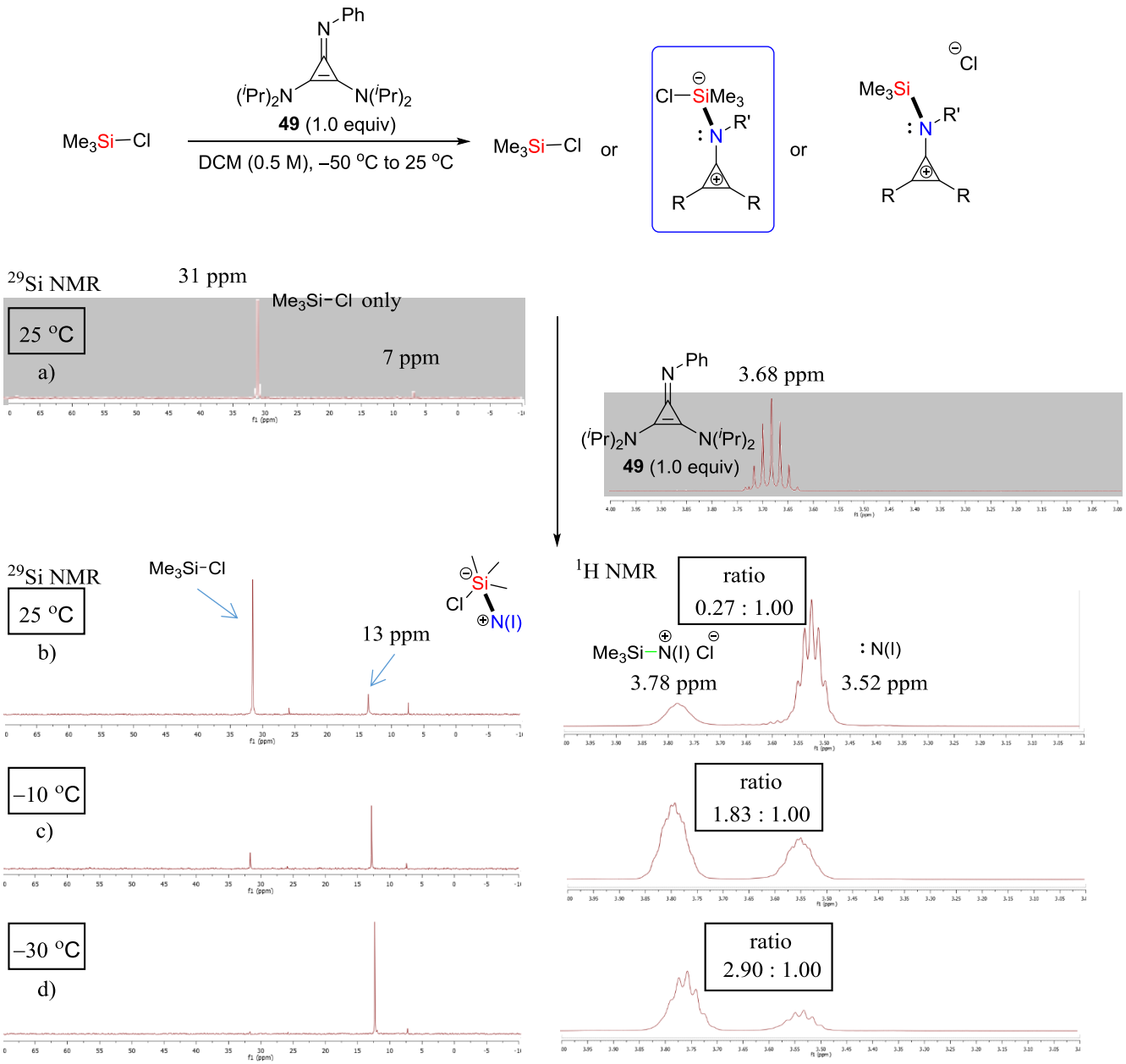

Scheme 3.63: ^{29}Si and ^{1}H NMR studies of interaction between TMS–Cl and cyclopropenimine at variable temperatures.

In our effort to rationalise these NMR data, we have suggested the following pathway (Scheme 3.64). Cyclopropenimine **49** may coordinate initially to the silylated pro-nucleophile to form the penta-coordinate silicon species (**149**); subsequently, the chloride anion may be released to generate silylium ion **150**. At 25 °C, this equilibrium lies on the side of the starting materials; cooling progressively to –30 °C may lead to the formation of the silylium ion. However, considering that the new shift was displayed up-field compared to the signal of the starting material, it may be suggested that it corresponds to the penta-coordinate species (**149**).

Indeed, the possibility of this peak to correspond to **150** should not be eliminated. This would be explained by a potential rapid equilibrium. Efforts to isolate the species that corresponds to the signal at 13 ppm in the ^{29}Si NMR failed.

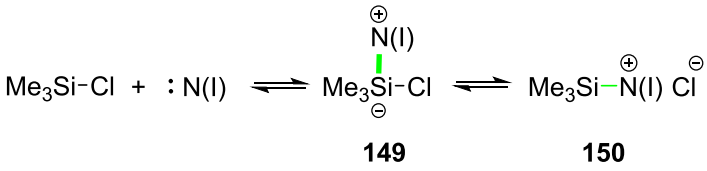

Scheme 3.64: Suggested equilibrium between the different silicon species at ^{29}Si NMR.

3.4 Summary

In this chapter, we successfully synthesized a library of cyclopropeniminium tetrafluoroborate salts and their corresponding cyclopropepimines, which were examined in catalysis. Both varied at the R groups attached to the nitrogen atoms in the backbone of the catalyst and the R' group attached to the central nitrogen atom (Scheme 3.65). The free cyclopropenimines were obtained after deprotonation in >90% yields. Initially, cyclopropenimine-catalysed cyanation and trifluoromethylation of carbonyl compounds and imines was explored resulting in a fairly broad scope with excellent functional group tolerance under mild conditions (Scheme 3.65; 40 examples with 73–96% yield). The cyclopropenimine-catalysed ring-opening of a library of *N*-tosyl aziridines using trimethyisilyl azide and chloride as pro-nucleophiles was also investigated. The intended products were generated in 50–99% (Scheme 3.65). We also developed an optimised system that provides the corresponding β-functionalised sulfonamide with complete regioselectivity. NMR studies using ^{29}Si NMR, ^{1}H NMR and ^{19}F NMR (*for trifluoromethyation only*) were carried out in order to provide a greater insight into the potential mechanistic pathways.

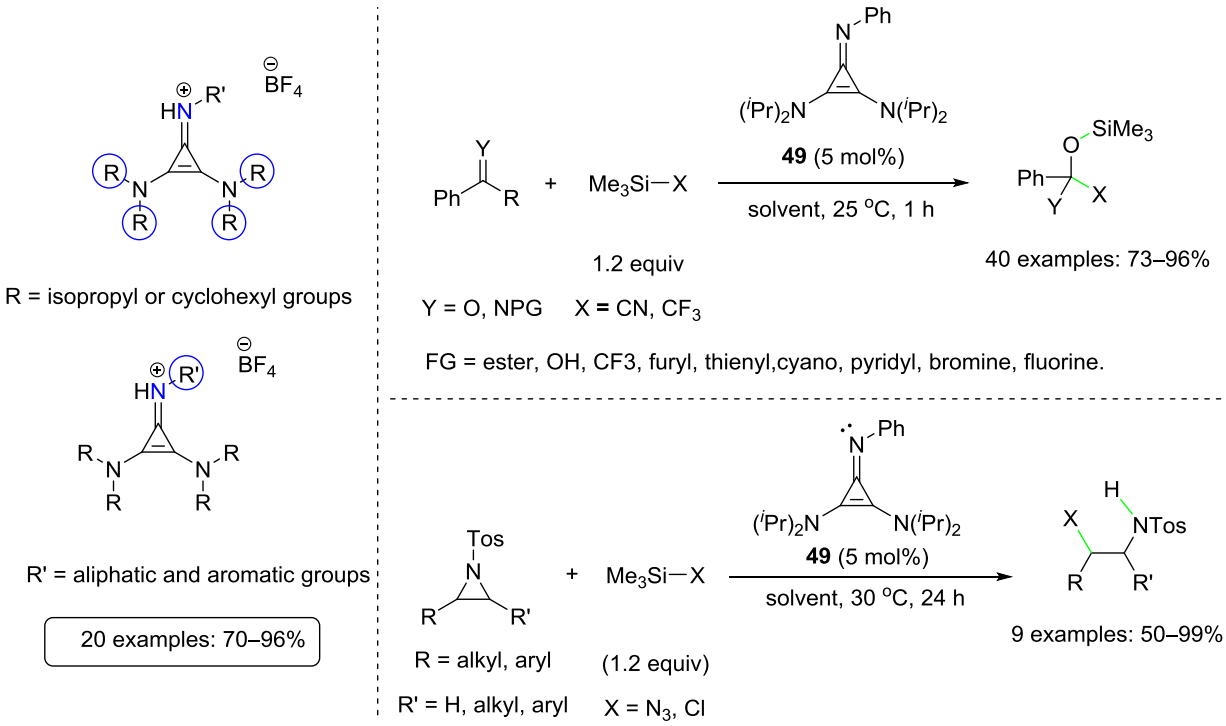

Scheme 3.65: Overview.

4 Carbones [C(0) Compounds]

4.1 Introduction

4.1.1 Chemistry of Carbones [C(0) Compounds]

4.1.1.1 Concept and Comparison to Carbenes [C(II) Compounds]

One of the basic principles in chemistry is the difference between a coordinative and a covalent bond.[14] In the first case, the central atom of a complex is bound to the surrounding ligands through an acceptor–donor interaction. In the (ideal) second case, the atoms contribute their required valence electrons equally to covalent bond formation. Typically, the majority of carbon-containing compounds do have tetravalent carbon atoms (forming four covalent bonds to their substituents). As an example, classic allenes have a linear structure with an sp-hydridized central carbon [Scheme 4.1 a)]. However, in recent studies a group of non-classic allenes and heterocumulenes with modified hybridization has emerged.[9,13] The first long-row elements, and thus carbon, tend to form hybrids from s and p orbitals that lead to the familiar linear (sp), trigonal (sp^2), and tetragonal (sp^3) bonding geometries of the carbon compounds.[116] However, second or higher long-row elements tend to avoid hybridization, suggesting that these elements tend to not form multiple bonds; in turn, π bonds between these heavier elements are rather weak.[116] Consequently, it was envisioned that weakening the π bonds of both allenes and heterocumulenes would lead to a more flexible structure [Scheme 4.1 b)].[116] This weakening may be due to a polarization of the two double bonds as a result of a push–push pattern.[116] Indeed, when the substituent X is a strong σ donor *and* a weak π acceptor, certain of these compounds display a bent structure with an sp^2-type hybridized central carbon atom.[15,17,116,117] The electronic distribution at the central carbon atom can be described as a hybrid between the structure of two C=X double bonds *and* a central carbon with two lone pairs and two neutral X substituents attached.[9,13]

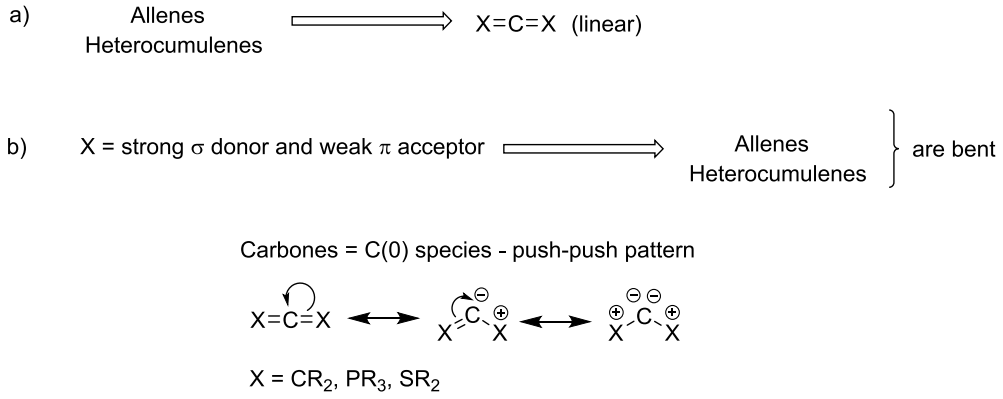

Scheme 4.1: Classic and non-classic allenes and heterocumulenes.

The latter can be also displayed as a carbon-based complex, i.e., the central carbon atom may be considered as 'metal-like' coordinated by two 'ligand-like' neutral groups (Figure 4.1).[9,13,14] These 'bent' allenes and heterocumulenes have been termed *carbones*.

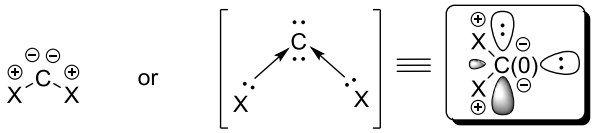

Figure 4.1: Representation of carbones by two distinct resonance structures.

In this context, a brief introduction to the properties and applications of *carbenes* is required. In 1991, Arduengo *et al.*[8] isolated for the first time an *N*-heterocyclic carbene (NHC), which is a neutral carbon-containing molecule with a central divalent carbon atom (forming two single bonds to the substituents; Figure 4.2).[5,12] The central carbon atom is considered to be in the formal '+II' oxidation state, which means that carbenes are classified as carbon(II) compounds [C(II)]. NHCs have proved to be excellent Lewis base catalysts,[7,93,94] and ligands for metal catalysis.[118,119] The central carbon atom is substituted by two nitrogen (or other hetero) atoms, and has both an occupied σ orbital (sp^2) and a vacant π orbital (p). NHCs are stabilized: (1) by π electron donation from nitrogen into the vacant p orbital of the sp^2 hybridized carbon, and (2) by electron withdrawal from the filled σ orbital to the electronegative nitrogen atom.[12] Overall, NHCs are electron-rich and thus nucleophilic species, while other carbenes are considered as electrophilic (e.g. **:**CCl_2). This strong σ donor ability of NHCs has made these powerful tools in the field of organic synthesis and organometallic chemistry, including catalysis.[5,7,12,94,118,119]

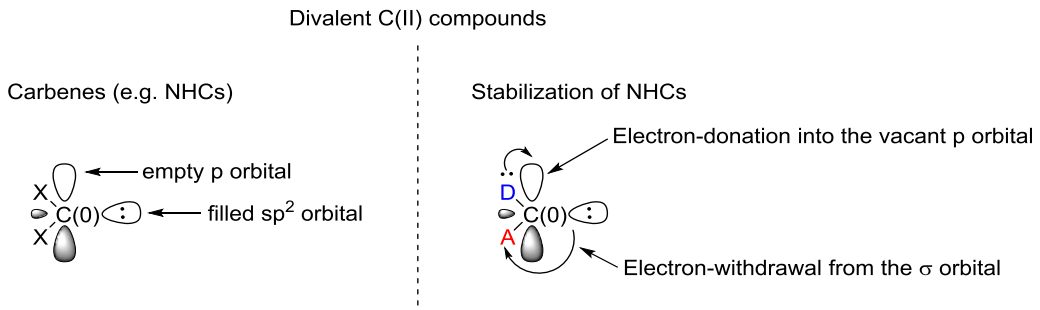

Figure 4.2: Electronics of *N*-heterocyclic carbenes (NHCs).

In contrast to *carbenes*, the central carbon atom of the so-called *carbones*, is considered to be in the '0' oxidation state, which means that carbones are classified as carbon(0) compounds [C(0); Figure 4.3]. The central carbon atom is formally divalent like in carbenes, but it has potentially two lone pairs available for chemical reactivity. The first lone pair is located in the σ orbital, while the second one is in the π orbital of the central carbon atom. This electronic situation nicely explains why carbones have been calculated to be more basic than carbenes,[17] which is also supported by experimental findings confirming the availability of both lone pairs.[9,13,14] In contrast to carbenes that can provide only one lone pair to coordinate to a Lewis acidic centre, carbones have proved to exploit both lone pairs to form dimetallated complexes (Figure 4.3).[9] These experimental findings were in accordance with computational studies, in which carbenes –despite a high 1st proton affinity– displayed a poor 2nd proton affinity (e.g. carbene **151** with a 1st PA = 273.4 kcal • mol^{-1} and a 2nd PA = 13.8 kcal • $mol^{-}1$; Figure 4.3).[17] In contrast, carbones displayed very high first *and* second proton affinities (e.g. carbodiphosphorane **152** with a 1st PA = 280.0 kcal • mol^{-1} and a 2nd PA = 185.0 kcal • mol^{-1}; Figure 4.3).[17]

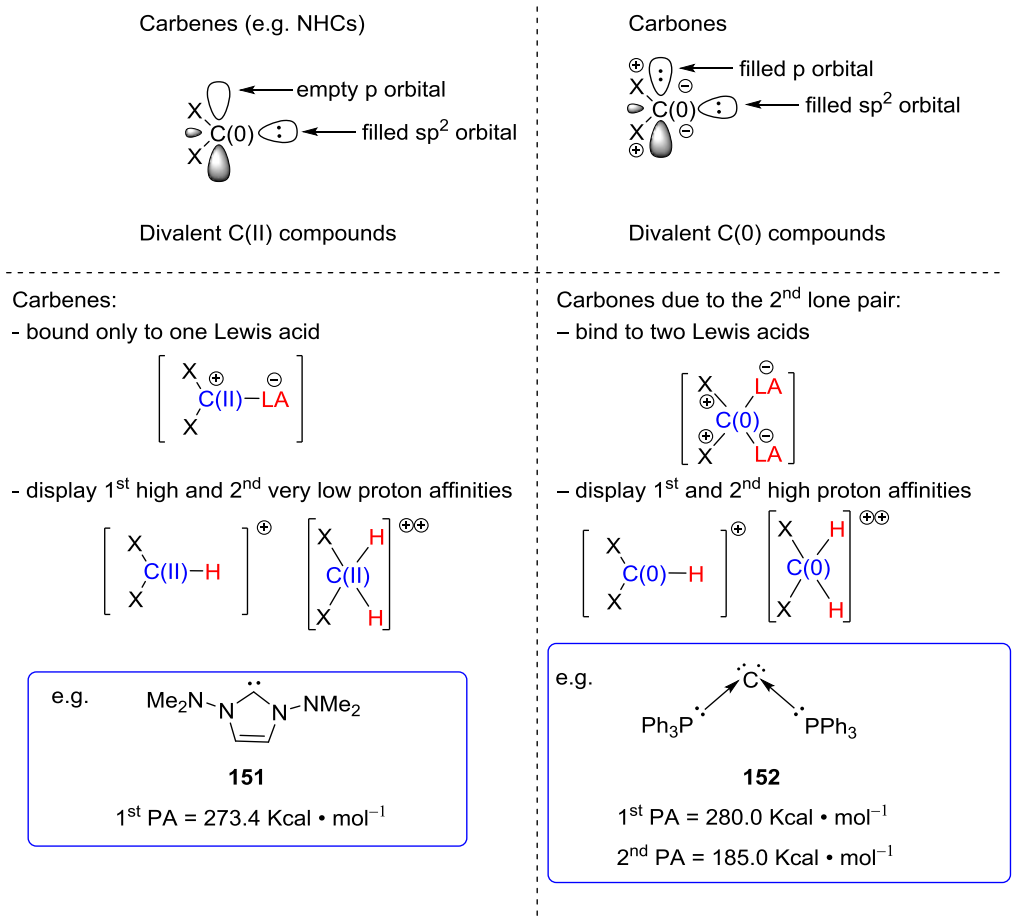

Figure 4.3: Comparison of electronic properties and basicity between carbenes and carbones.

4.1.1.2 Literature-Known C(0) Compounds

The first compound that has been confirmed as a carbon(0) species was carbodiphosphorane **152** [Scheme 4.2 a)].[120] This compound was initially synthesized by Ramirez *et al.*[121,122] Later on, Vincent *et al.* calculated –based on crystallographic studies– that the P–C–P bond angle was approximately 140º, which means that the molecule is strongly bent.[122] Kaska *et al.* recognized this 'unusual' cumulene as a 'prime example of a bis(phosphine)–carbon complex', with the central carbon atom in its formal '0' oxidation state.[123] Thus, it was proposed that this divalent carbon atom bearing two lone pairs –available for reaction with Brønsted or Lewis acids– was coordinated by two phosphine ligands. This molecule was shown to be dimetallated at the carbon centre with tungsten and gold Lewis acids.[122] These data were also in agreement with a computational analysis, in which the molecular orbitals HOMO and HOMO–1 were characterized as lone pair-MOs of π and σ symmetry, respectively, but not as bonding orbitals [Scheme 4.2 b)].[17]

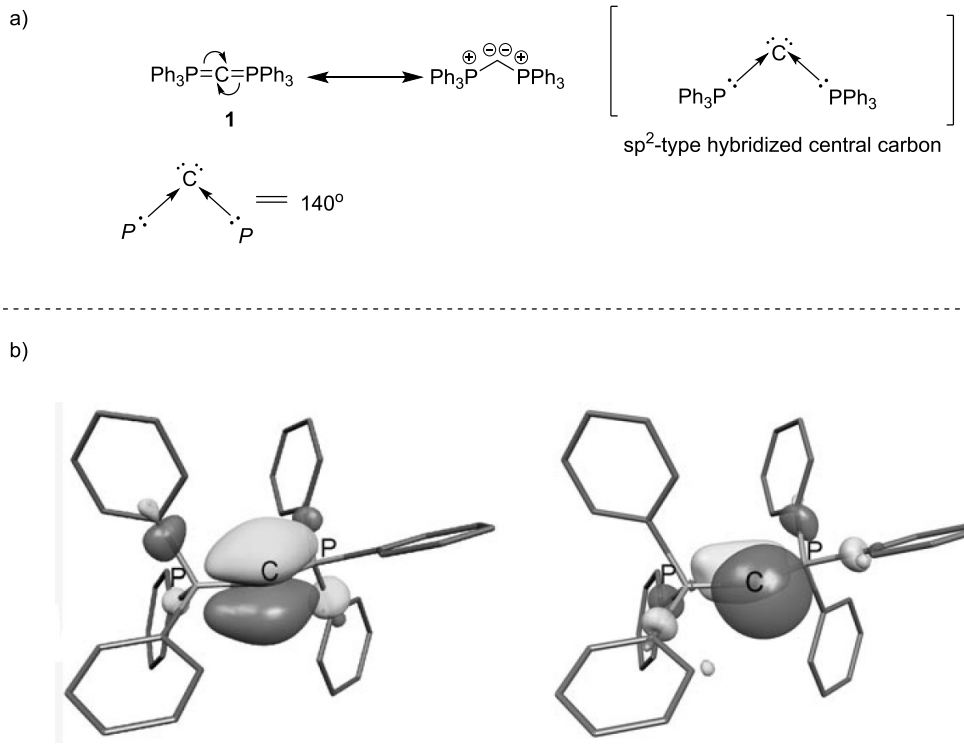

Scheme 4.2: a) The first reported example of a C(0) compound. b) HOMO (left) and HOMO–1 (right).

The displacement of one of the two phosphine 'ligands' in **152** by a carbon-based substituent led to the synthesis of the so-called Bestmann's ylide (**153**) and its isocyanide analogue **154** (Figure 4.4).[9,124,125] Subsequent displacement of the carbon 'ligands' by a formal "bis(oxo)carbene" substituent gave carbone **155**, in which the [**:**C(OEt)$_2$] group has proved to be a weaker π acceptor than (**:**C=O) or (**:**C=NR).[9,124] Further studies led to another interesting species, compound **156**, with strong σ donor ability through the combination of a phosphine and a fluorenyl unit;[9,126] this molecule may be considered as a classic ylide or a non-classic carbone. The same research group also reported molecule **157**, which can be considered as a mono-nitrogen analogue of **155**. All these molecules have been classified as potential (*P,C*)-C(0) species. Furthermore, different 'mixed' C(0) compounds –without carbon-based ligands– were synthesized and examined in the same context. (*P,S*)-C(0) species **158** was reported as a fairly stable ylide or carbone.[127] Finally, (*C,C*)-C(0) compounds –so-called carbodicarbenes (CDCs)– were synthesized. Species **159** can be described as an extremely bent acyclic allene with outstanding σ donor ability.[116] Nevertheless, species **160** does not belong to the electron-rich molecules typically discussed here. Rather, **160** was shown to act as a carbon-based Lewis acid.[14,122] Investigations have demonstrated that it can be paired with sterically hindered NHCs to act as a frustrated Lewis pair (FLP).[42]

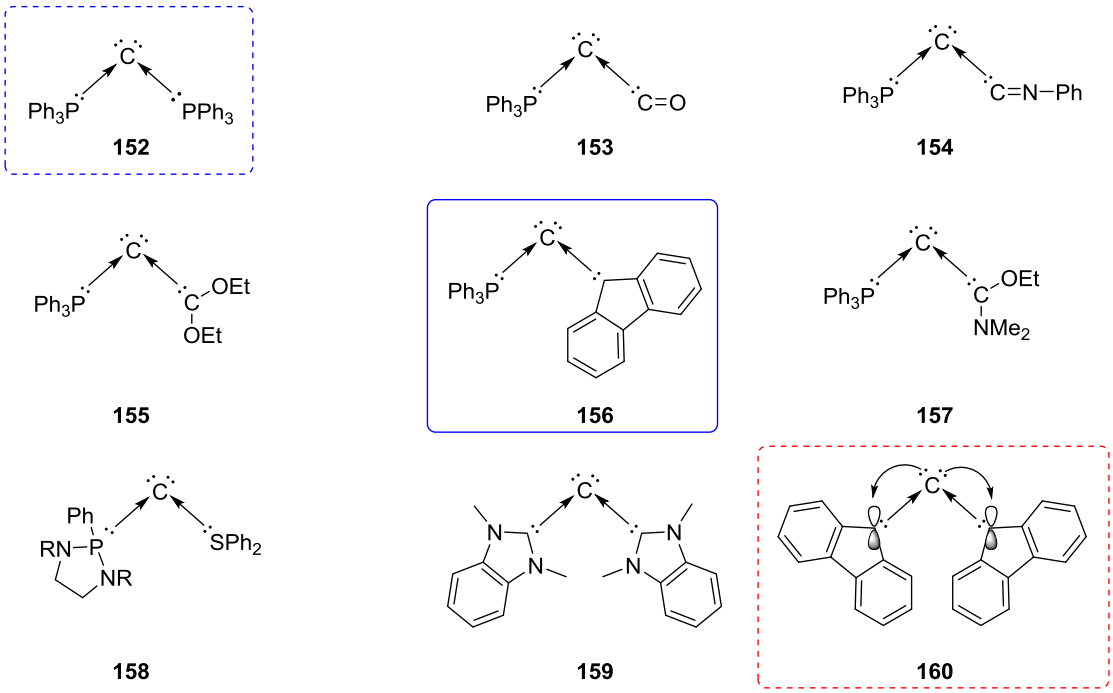

Figure 4.4: Overview of potential C(0) species.

For simplicity, these (potential) C(0) compounds are drawn as linear structures in the rest of the thesis manuscript (Figure 4.5).

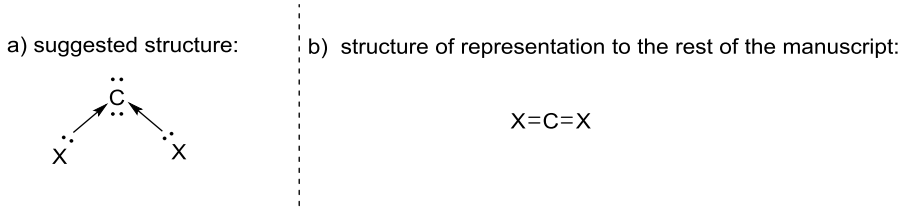

Figure 4.5: a) suggested structure based on literature reports[9,13] b) representation to the rest of the manuscript.

4.1.1.3 Synthetic Routes

Preparation of a CDP (Carbodisphosphorane)

The first method reported for the preparation of carbodiphosporane **152** was a two-step process (Scheme 4.3).[121] Initially, methylene dibromide was reacted with triphenyl phosphine (2.0 equiv) in molten triphenylphosphate to form the corresponding methylenebis(triphenylphosphonium) dibromide (**161**). Next, **161** was refluxed with potassium metal (2.0 equiv) in diglyme to give **152** in 60% yield.[121] Alternatively, Matthew *et al.* reported a two-step deprotonation of precursor **161** (Scheme 4.2); first, BuLi (1.0 equiv) was used in ether at room temperature to form **162**; second, NaH (1.0 equiv) was added to a solution of **162** in refluxing diglyme to generate **152** (27% yield overall).[128]

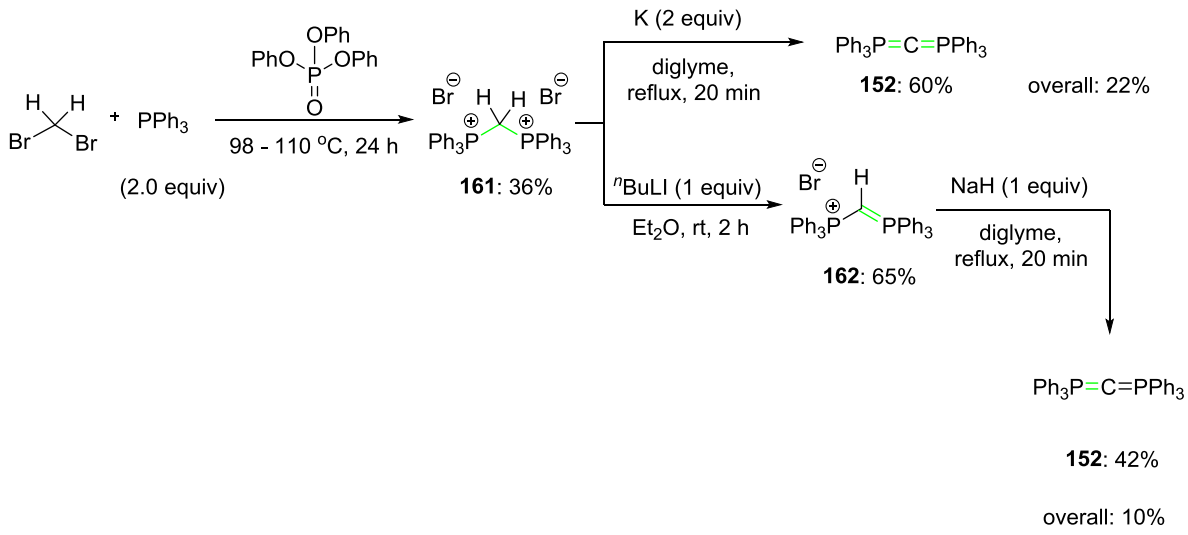

Scheme 4.3: Initial methods reported for the CDP synthesis.

A 3rd approach was reported by Appel *et al.* (Scheme 4.4).[129] Here, tetrachloromethane was treated with triphenylphosphine (3.0 equiv) to form methylenebis(triphenylphosphonium) dichloride (**163**) in 74% yield. In the next step, a chlorine cation was abstracted by hexamethylphosphorus triamide at room temperature to give **152** in 61% yield.

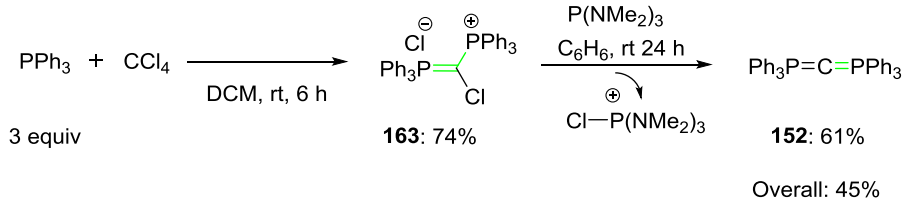

Scheme 4.4: Recent method reported for the CDP synthesis.

Preparation of Mixed C(0) Compounds

In 1978, Bestmann *et al.* reported probably the most commonly known mixed 'carbone', the so-called Bestmann's 'ketene' (**153**).[130,131] It was prepared in a fairly easy one-step process (Scheme 4.5). Ylide **164** was heated with NaHMDS (1.0 equiv) in benzene at 60 °C to generate Bestmann's ketene (**153**) in 75% yield.

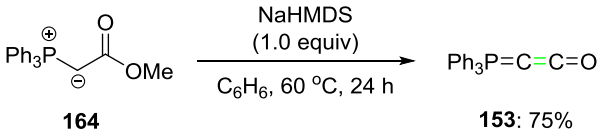

Scheme 4.5: Preparation of Bestmann's ketene.[130]

In addition, the imine analogue of Bestmann's ketene was synthesized in another one-step process (Scheme 4.6).[122,132] Isocyanide dichloride **165**, a nitrogen analogue of phosgene, was treated with an excess of methylenetriphenylphosphorane **166** in benzene and THF under mild conditions to give carbone 1**54**. The reaction proceeded smoothly through nucleophilic addition of the phosphorane to the electrophilic carbon of the carbon–nitrogen double bond with subsequent elimination of hydrogen chloride to form the middle double bond of carbone **154**.

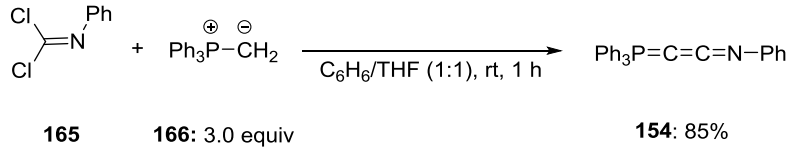

Scheme 4.6: Preparation of Bestmann ketene-type isocyanide analogue.[122,132]

Furthermore, an acetal analogue of Bestmann's ketene was synthesized in two steps. Ylide **167** (3.0 equiv) was treated with Meerwein's reagent in DCM at 0 ºC to give **168** in 68% yield through nucleophilic addition/elimination (Scheme 4.7). Next, sodium amide was used to deprotonate at the vinylic position in benzene under reflux to afford **155** in 48% yield.[133]

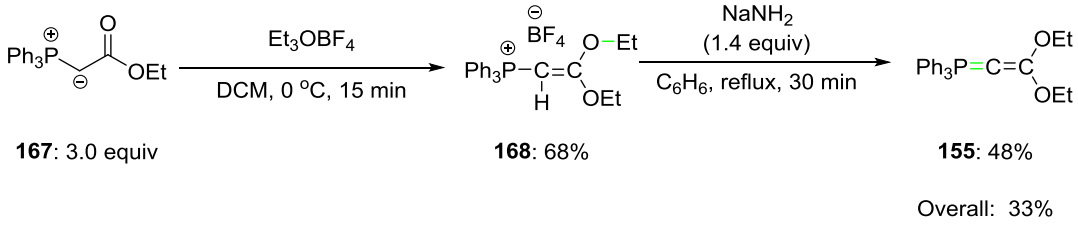

Scheme 4.7: Preparation of an acetal analogue of Bestmann's ketene.[133]

The synthesis of (*P*,*C*)-C(0) compound **156** is a fairly easy four-step process (Scheme 4.8).[9,126] In the first step, **169** was deprotonated using NaHMDS to afford Wittig reagent **170**. Next, a solution of fluorenone was added at low temperature to generate alkenyl bromide **171** through a Wittig reaction in 82% yield. Use of triphenylphosphine (nucleophilic substitution) and sodium tetrafluoroborate (anion exchange) led to the generation of C(0) precursor **172** in 55% yield. The latter underwent deprotonation using KHMDS at low temperature to form carbone **156**. It should be noted that this compound has proved to be unstable at room temperature, therefore it was *not* isolated. Triphenylphosphine is a strong σ donor and weak π acceptor, while the fluorenyl ring is a π acceptor. In turn, structure **156** may foster back-donation of electron density from the central carbon atom to the adjacent carbene 'ligand' by virtue of the

14 π electron aromaticity of the incipient fluorenyl unit. It seems that only one lone pair may be available for chemical reactivity, but treatment under harsh conditions may render the second lone pair 'available'.

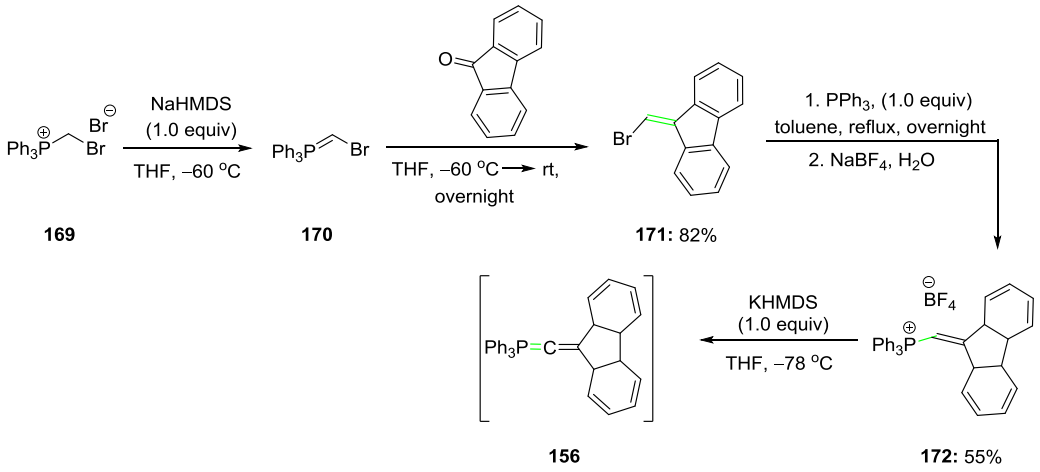

Scheme 4.8. Synthesis of mixed carbone **156**.[9,126]

Following an identical process for the preparation of **155**, Fürstner *et al.* reported the two-step preparation of **157** (replacement of an ethoxy by a dimethylamino group; Scheme 4.9). Initially, ylide precursor **173** was treated with Meerwein's reagent in DCM at 0 °C to provide C(0) precursor **174** in 79% yield through nucleophilic addition/elimination. Next, sodium amide in liquid ammonia was used to deprotonate **174** at the vinylic position resulting in the formation of **157** in 84% yield.[9]

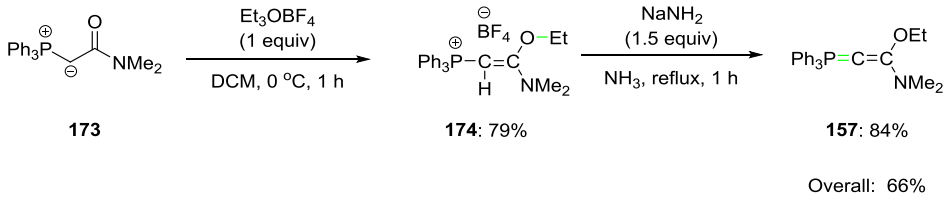

Scheme 4.9: Synthesis of mixed carbone **157**.[9]

Mixed (*P*,*S*)-C(0) compound **158** was prepared in a three-step process (Scheme 4.10).[127] Diazophospholidine **175** was treated with hexachloroethane (1.0 equiv) in DCM to form phosphonium salt **176** in 76% yield. Methyldiphenylsulfonium triflate (**177**) was deprotonated at the terminal methyl group by BuLi in THF at –80 °C to form the corresponding ylide; the latter was treated with **176** in THF at –80 °C to give (*P*,*S*)-C(0) precursor **178**. KHMDS was used at low temperature to deprotonate **178** for the formation of (*P*,*S*)-C(0) compound **158**.

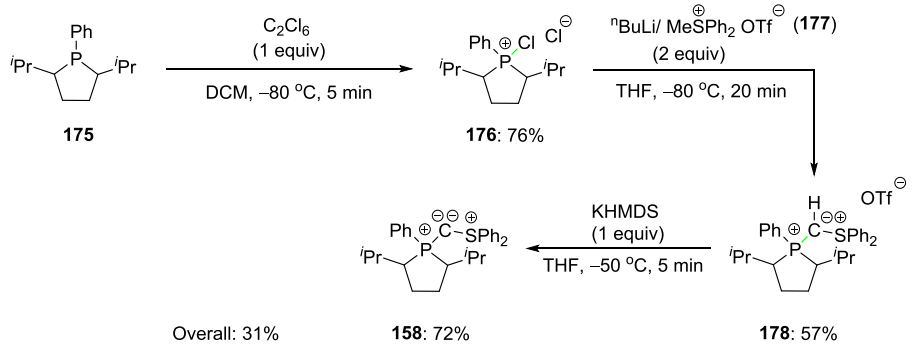

Scheme 4.10: Synthesis of CDC **159**.[127]

Preparation of a Carbodicarbene (CDC)

Finally, CDC **159** was synthesized in a two-step process (Scheme 4.11).[116] **179** was treated with methyl triflate (2.0 equiv) in acetonitrile under mild conditions to give double salt **180** [(bis)alkylation]. Next, KHMDS (2.0 equiv) was used to deprotonate **180** twice, initially at room temperature and then at reflux, to give **159** in 32% yield.

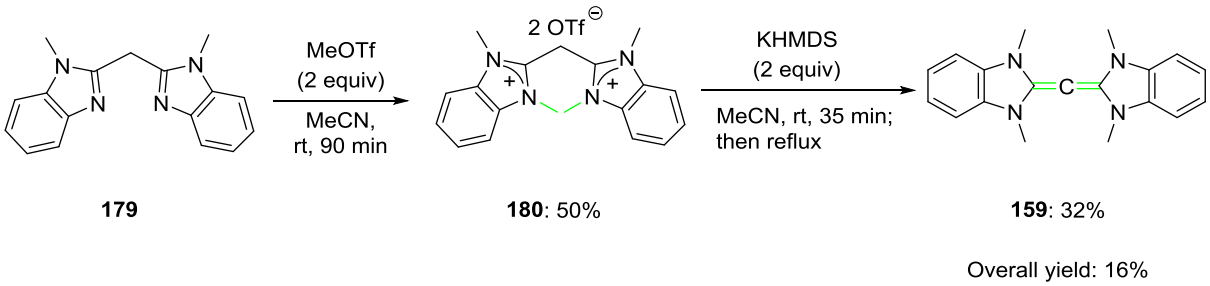

Scheme 4.11: Synthesis of CDC **159**.[116]

4.1.2 Reactions of C(0) Compounds

4.1.2.1 Stoichiometric Applications

Frustrated Lewis Pair (FLP) Chemistry Using CDPs

Alcarazo *et al.*[45] reported the first *stoichiometric* application of CDPs in the context of frustrated Lewis pair chemistry (FLP; Scheme 4.12). Indeed, CDP **152** was shown to act as a Lewis base and was paired with tris(perfluorophenyl) borane [$B(C_6F_5)$], a particularly strong Lewis acid. Despite the fact that the electronics of such a Lewis pair would suggest a strong interaction between the Lewis basic carbon atom and the Lewis acidic boron atom, due to significant steric hindrance the formation of a C→B dative bond was precluded. Instead, *at room temperature* CDP **152** replaced a fluoride anion through nucleophilic addition/elimination at the *para* position of the perfluorinated ring; the free fluoride added subsequently to the vacant p orbital of the boron atom resulting in the formation of the corresponding boron–ate complex [Scheme 4.12 a)]. However, *at –78 °C* there was no interaction between the two molecules, and this state may be called 'frustration'; in turn, the two reactants form a so-called 'frustrated Lewis pair' (FLP). The interaction of this FLP with a terminal alkyne has led to a mixture of products [Scheme 4.12 b)]. **152** deprotonated the alkyne at the terminal position to form an acetylide anion that subsequently bound to the boron atom to generate **181**, which was the major product (78%). In addition, the FLP reacted with the acetylene through Markovnikov addition leading to the formation of a C=C double bond to form **182**, which was the minor product (12%).

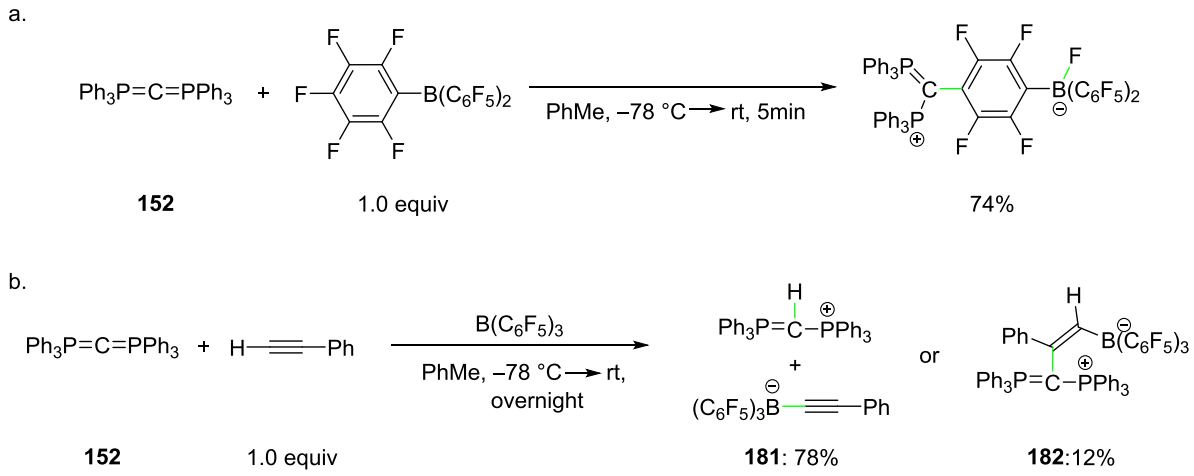

Scheme 4.12: a. C–F bond activation b. Small molecule activation.[45]

Furthermore, it was reported that the same FLP was explored in *stoichiometric* B–H, Si–H and H–H bond activation.[45,134]

Ylide Chemistry of CDPs and Mixed Carbones

Classic Wittig chemistry using carbones bearing a P–C–P or a P–C–C pattern has been already reported[124,135] C(0) compounds may be described as ylides, which have been well-known as Wittig reagents. The nuclophilic addition of an ylide to an electrophilic carbonyl group took place thereby forming the corresponding zwitterionic acyclic betaine, which closed to a four-membered cyclic intermediate, an oxaphosphetane. The P=O bond formation of the triphenylphosphine oxide acts as a driving force towards the formed allene product. CDP **152** accomplished a Wittig reaction with *α,β*-unsaturated *β*-keto-lactone **183** under mild conditions to give ring-closed product **184** in 70% yield (Scheme 4.13).[135] However, **183** is a particularly reactive ketone and Wittig reaction between **154** and a 'regular' ketone has not been reported yet.

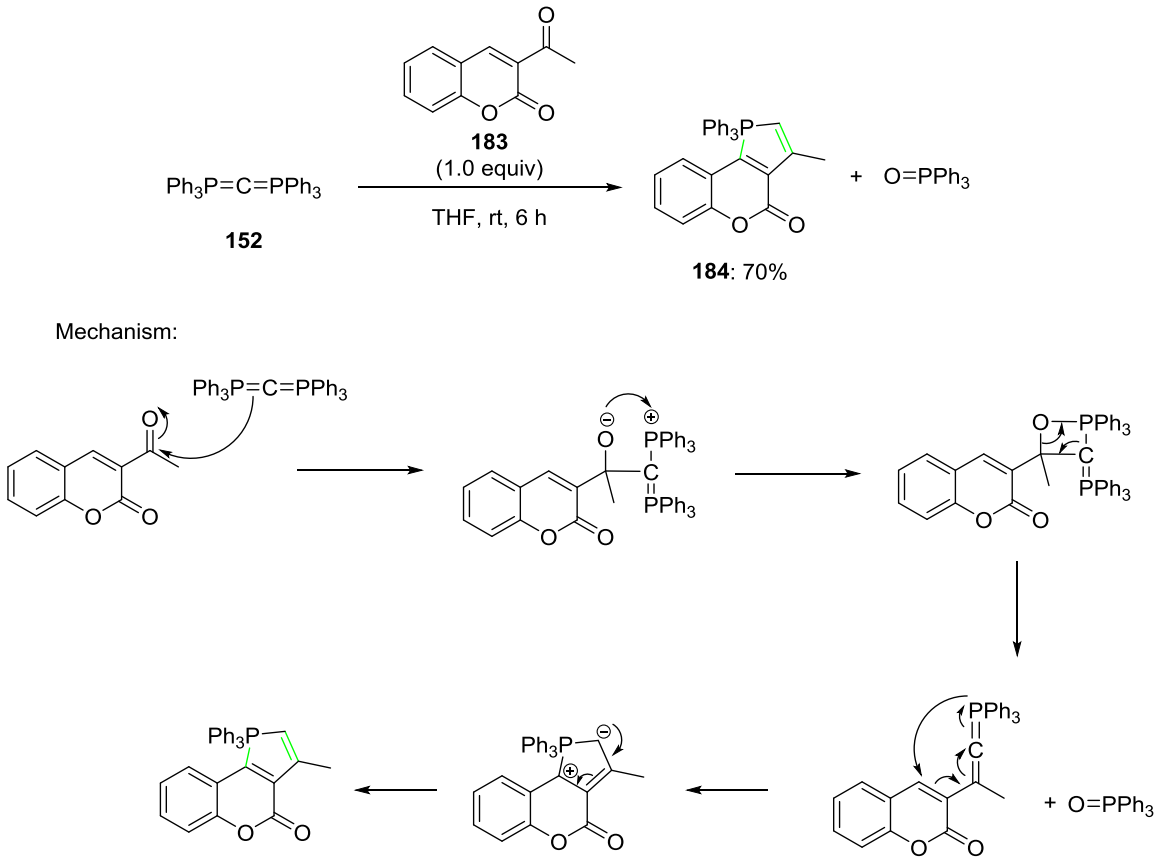

Scheme 4.13: Proof of the 'ylidic' nature of CDP **152**.[135]

In the context of mixed carbones, Bestmann's ketene (**153**) reacted with salicylaldehyde (**185**) to form lactone **186** in 73% yield (Scheme 4.14).[124] This reaction has been the first application of Bestmann's ketene in organic synthesis.

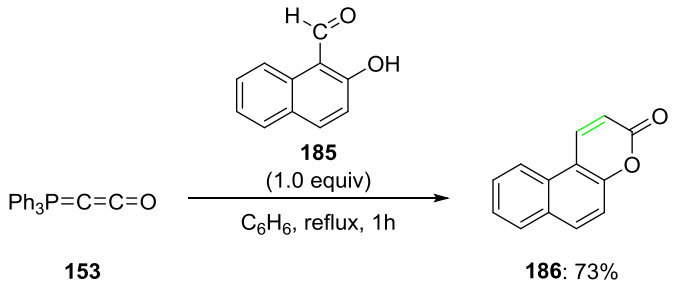

Scheme 4.14: Bestmann's ketene used as a Wittig reagent.[124]

Carbone **155** also proved to react with a cyclic ketone at room temperature in a classic Wittig reaction to form allene **187**, which subsequently dimerized quickly (Scheme 4.15).[124]

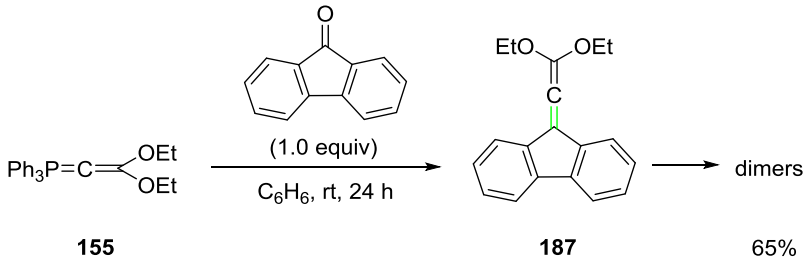

Scheme 4.15: An example for the 'ylidic' nature of carbone **155**[124]

4.1.2.2 Monometal Complexes with C(0) Ligands

The binding ability of CDPs to metals has been widely explored and led to a wide range of metal complexes. Transition metal salts of group 11 (Cu, Ag, Au) have been used for the formation of monometallated species (Figure 4.6, left).[136–138] In addition, Zn(II),[139] Cd(II),[139] Al(III)[140] and In(III)[140] were coordinated by CDPs. Furthermore, two equivalents of a CDP were reacted with one equivalent of a metal salt to generate a linear complex (Figure 4.6, right).[141] Namely, Cu, Ag, and Hg complexes have been prepared and isolated as overall neutral complexes.

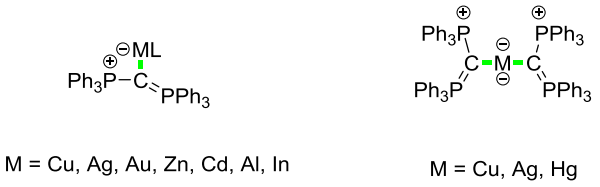

Figure 4.6: Transition metal and main group metal complexes with the CDP **154**.[136–142]

In another subgroup of monometallated complexes, the interaction of CDPs with carbonyl complexes resulted in the loss of one carbonyl group (Scheme 4.16). Specifically, W, Re, and Ni complexes were shown to undergo this process.[123,143,144] In addition, the reaction with $BeCl_2$ displays particular interest because the beryllium(II) centre proved to act as a double Lewis acid. Indeed, two chloride anions have been displaced by two CDP ligands.[142]

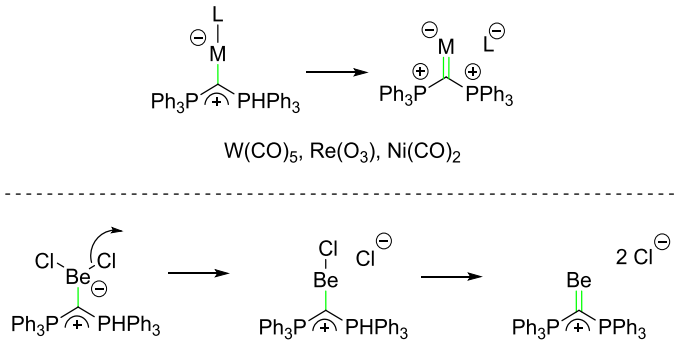

Scheme 4.16: Transition metal complexes with loss of one CO group.[123,142–144]

In case of carbone **153**, only a single metal complex has been reported so far (Scheme 4.17). Here, **153** was metallated by a gold(I) species in THF at room temperature. The formation of the complex was confirmed by IR spectroscopy based on the wavenumber of the 'CO' subunit, which was shown to shift from $\tilde{\nu}$ = 2,096 cm^{-1} to $\tilde{\nu}$ = 2,079 cm^{-1} after metal complexation. The mono-aurated metal complex was isolated, but it was not specified whether it is water- or oxygen-sensitive.[9] In this context, it should be mentioned that Bestmann's ketene (**153**) was the first example of a mixed (*P*,*C*)-carbone species to be described as a 'mixed ligand–carbon complex' (Scheme 4.17).[122]

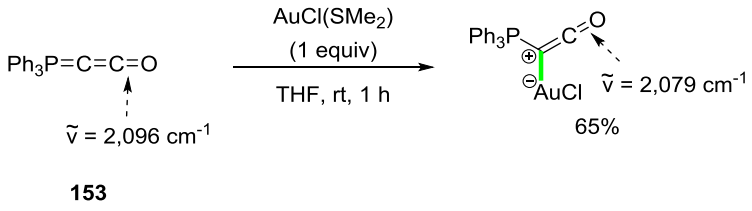

Scheme 4.17: Gold complex of Bestmann's ketene.[9]

Use of (P,C)-C(0) Compounds ***155*** *and* ***157***

Carbone ***155*** *is the only compound in this 'non-classic heterocumulene' context that was reported to be both mono- and dimetallated.* In terms of gallium complexes, both **155** and its aza-analogue **157** demonstrated significant σ donor ability. Gallium complexes **188** and **189** have been synthesized under mild conditions in 91% and 62% isolated yields, respectively (Scheme 4.18); their crystal structures were resolved as well (Figure 4.7).[9,14]

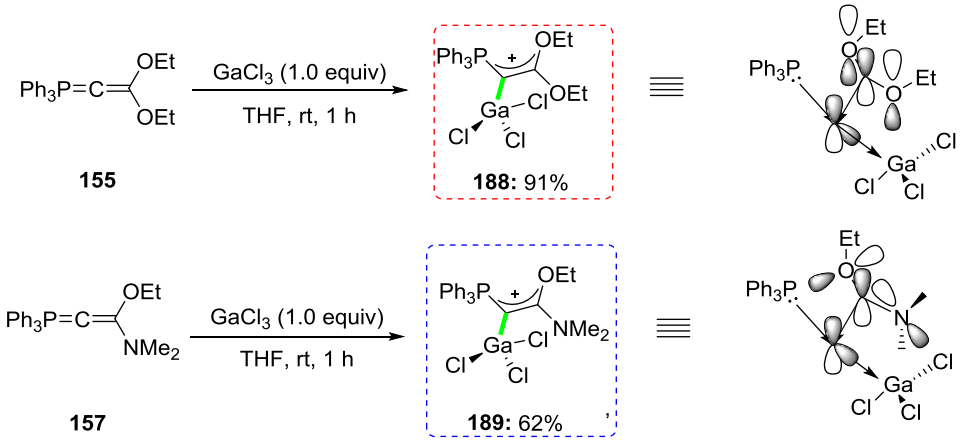

Scheme 4.18: Preparation of gallium(III) complexes of carbones **155** and **157**.[9]

In case of species **155**, the conformation adopted by the ethoxy groups is almost planar allowing the lone pairs of the oxygen atoms to interact ideally with the empty p orbital of the carbon centre to stabilize it. Concerning compound **157**, the replacement of one ethoxy group by a dimethylamino group led to a twisting of both substituents (dimethylamino and ethoxy groups). This means that there is no overlap *between* the lone pairs of the heteroatoms *and* the vacant p orbital at the carbon centre; therefore, an electron flow towards the central carbon atom is not expected, which means that electron back-donation of the second lone pair of electrons is required for stabilization of the internal ligand. Hence, the potential carbon(0) nature of the central carbon atom in **157** has not been confirmed yet (Figure 4.7).

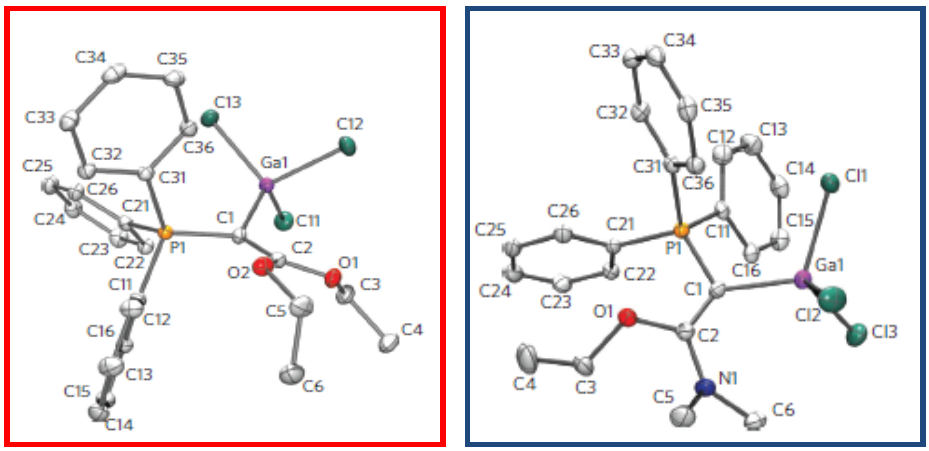

Ga–C(0) complex **188** Ga–C(0) complex **189**

Figure 4.7: Crystal structures of **188** and **189** complexes.[9]

Use of (P,C)-C(0) Compound ***156***

Fürstner *et al.* examined compound **156** as a potential carbone and considered both obvious resonance forms; a linear (heterocumulene) and a carbene structure (Scheme 4.19).[9,14,126]

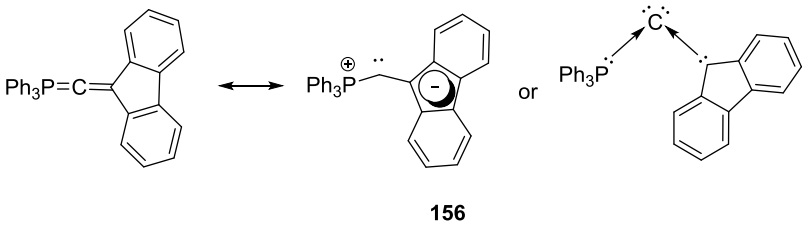

156

Scheme 4.19: Potential resonance forms of **156.**[9,14,126]

In their first screening, a gold(I) species was reacted with *in situ*-generated compound **156** resulting in the formation of complex **190** (Scheme 4.20).[9]

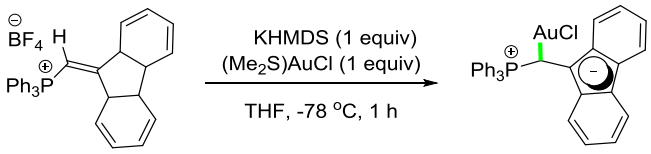

172 **190:** 41%

Scheme 4.20: The first reported metal complex of **156.**[9]

Compound **156** proved to form as well rhodium complex through reaction with $[Rh(CO)_2Cl]_2$. **172** was added to a solution of KHMDS (1.0 equiv) at –78 °C prior to the addition of $[Rh(CO)_2Cl]_2$ to form **191**. Accordingly, **156** and its pyridine derivative were treated with $[Rh(cod)Cl]_2$ (1.0 equiv) to give the corresponding complexes **192** and **193**, respectively

(Figure 4.8). All the aforementioned complexes have been reported to be air- and/or moisture-stable, thus demonstrating potential for applications in catalysis.[14,126]

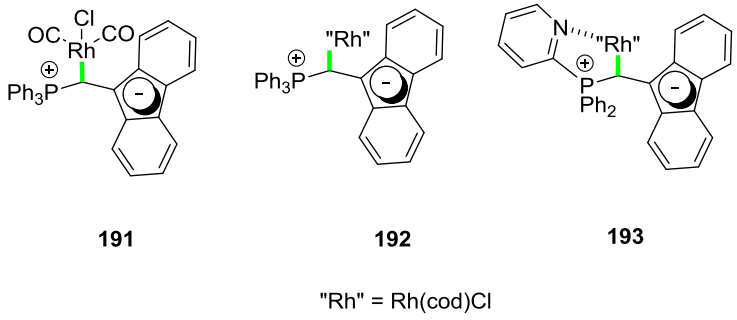

Figure 4.8: Rh complexes of **156** and its pyridine derivative.[14,126]

Bertrand *et al.* prepared carbodicarbene (CDC) **159** and tested its potential as a ligand (Scheme 4.21).[116] Based on ^{13}C NMR spectroscopic data, the π system of this molecule was shown to be strongly polarized. X-ray crystallography exhibited evidence that the four amino groups have a significant effect on the geometry of this allene-type molecule. The C=C bonds of the C=C=C unit are slightly longer than a typical C=C bond and the N–C–N bonds are twisted by 69°. Furthermore, the C=C=C unit is severely bent (134.8°).

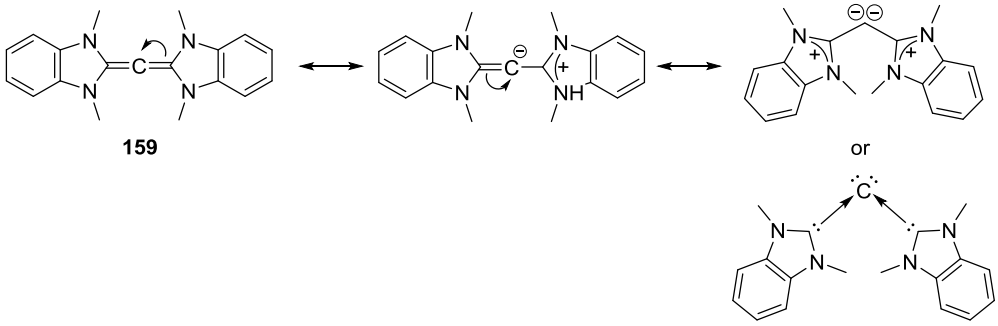

Scheme 4.21: Conceivable resonance forms of CDC **159**.

CDC **159** demonstrated its outstanding σ donor ability (Scheme 4.22).[116] It reacted with a rhodium(I) species under mild conditions to form rhodium–CDC complex **194** in 56% yield. The wavenumber of *cis*-[$RhCl(CO)_2(L)$] were used as a measure of the electronic properties of ligand L.[116] The average value of the wavenumber for the complex bearing CDC **159** as a ligand are considerably lower than the corresponding wavenumber of the complex with a comparable NHC ligand ($\tilde{\nu}$ = 2014 cm^{-1} vs. $\tilde{\nu}$ = 2036–2058 cm^{-1}). In turn, it can be concluded that CDC **159** is substantially more nucleophilic than typical NHCs. This finding is very

important because NHCs are established strong σ donors and commonly used in both organocatalysis and metal catalysis.

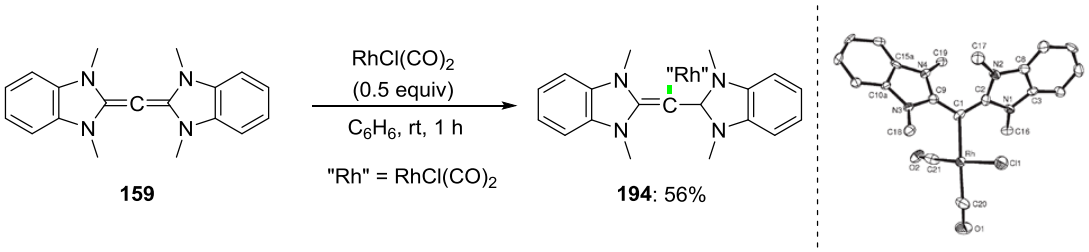

Scheme 4.22: Rh–CDC **194** complex and its crystal structure.

4.1.2.3 Dimetal Complexes with C(0) Ligands

The dimetallation of CDP **152** was reported in 1976 by Schmidbaur *et al.* (Scheme 4.23).[145] Methyl(triphenylphosphine)gold(I) (2.0 equiv) was quantitatively coordinated to the central carbon atom of **152** in THF at low temperature to give complex **195**. This experiment represents the first experimental proof-of-principle that two lone pairs at the central carbon are available for chemical reactivity.

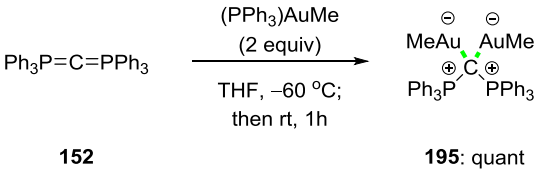

Scheme 4.23: Diauration of CDP.[145]

Fürstner and Alcarazo *et al.* reported the formation of heterobimetallic CDP complex **198** (Scheme 4.24).[146] Pentaphenyl pyridyl carbodiphosphorane **196** was used as a CDP ligand and exposed to $(Ph_3P)AuCl$ (1.0 equiv) in THF at low temperature to afford complex **197** in 97% yield. Next, **197** was treated with copper(I) chloride (1.0 equiv) in DCM at low temperature to give **198** in 95% yield. The ability of the CDP to coordinate to two different metal centres emphasizes its potential as a dual catalyst.

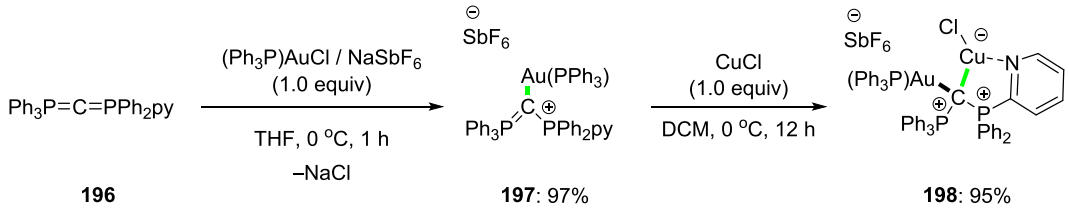

196 **197**: 97% **198**: 95%

Scheme 4.24: Formation of the heterobimetallic complex.[146]

CDP **152** demonstrated its two-fold Lewis basicity when treated with diborane in toluene at room temperature (Scheme 4.25). This is the first example of CDP, which binds to two Lewis acids larger than protons.[147] Initially, complex **199** was expected; however, the final structure proved to be a complex with two boron atoms bridged by one hydride (3-center 2-electron bond).[147]

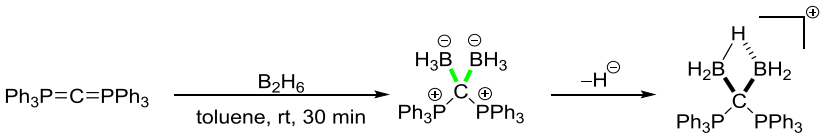

152 **199** **200**

Scheme 4.25: Diboration of the CDP **152**.[147]

In a similar context, Fürstner *et al.* [9] attempted the dimetallation of mixed carbone **155**. It was proposed that **155** could be represented with the following resonance structures (Scheme 4.26).

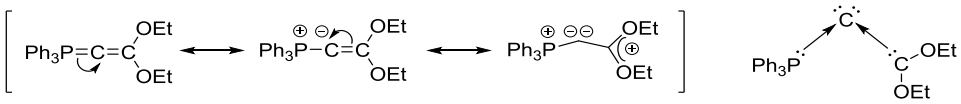

155

Scheme 4.26: Resonance structures of **155.**

In turn, species **155** was reacted with a gold(I) complex (1.0 equiv) in THF at room temperature leading to the formation of the expected mono-aurated complex **201** in 87% yield (Scheme 4.27). Importantly, when the process was repeated with two equivalents, di-aurated complex **202** was generated in 89% yield. The latter displays an ideal tetrahedral coordination sphere, which was confirmed by crystal structure analysis; thus, the central carbon atom can be considered as a pro-chiral carbon centre.[9,14]

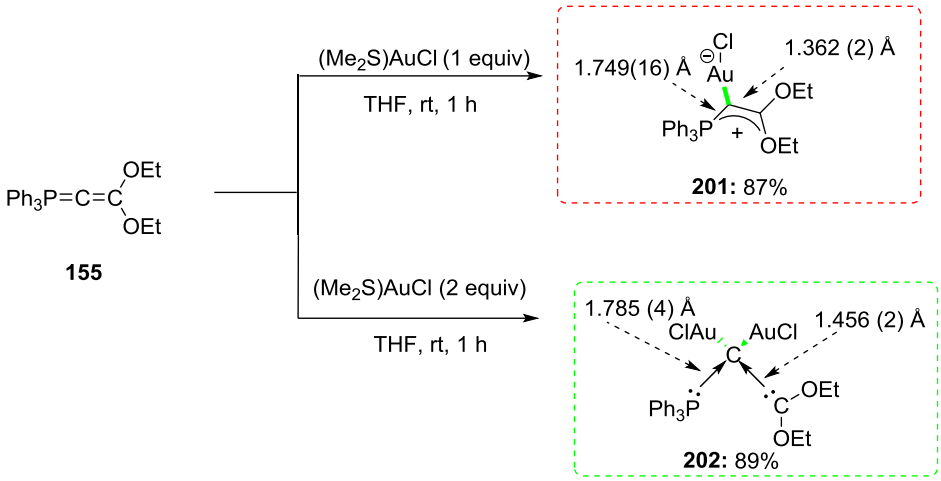

Scheme 4.27: Mono- and di-aurated complexes of C(0) compound **155**.

It is noteworthy that the mono-aza-analogue of **155**, potential C(0) species **157**, was also examined in the same set of experiments (Scheme 4.28).[9] Nitrogen being less electronegative than oxygen, it was expected that the corresponding carbene ligand would be a stronger σ donor and weaker π acceptor; thus, a similar result, i.e., a dimetallation should be observed. Nonetheless, following exactly the same process, only mono-aurated complex **203** was detected, while efforts to prepare di-metallated complex **204** have failed (Scheme 4.28).[9]

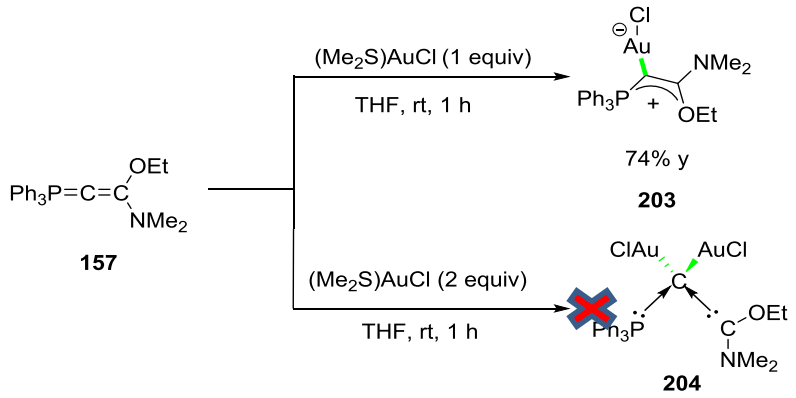

Scheme 4.28: Mono-auration and unsuccessful di-auration of C(0) compound **157**.[9]

4.2 Aims

Carbones [C(0)] have been calculated to be stronger Lewis and Brønsted bases than carbon(II) species, i.e., NHCs. The greater basicity can be explained by the fact that the central carbon atom of C(0) molecules may have one extra lone pair available for chemical reactivity compared to NHCs. Thus, the catalysis potential of carbones may go far beyond classic NHC catalysis. In turn, the aim of this study was to test and compare the basicity/nucleophilicity of both carbenes and carbones across a range of boron electrophiles in terms of binding ability [Scheme 4.29 a)]. In cases where a Lewis acid–base adduct was detected, *direct* organocatalysis may be developed, in which a C(0) Lewis base may activate a Lewis acidic pro-nucleophile, i.e., boron or silicon reagents with a transferable organic rest [Scheme 4.29 b)]. However, if there is *no* interaction due to the steric congestion of the reaction partners ('frustration'), frustrated Lewis pair (FLP) chemistry may be the alternative pathway [Scheme 4.29 c)].

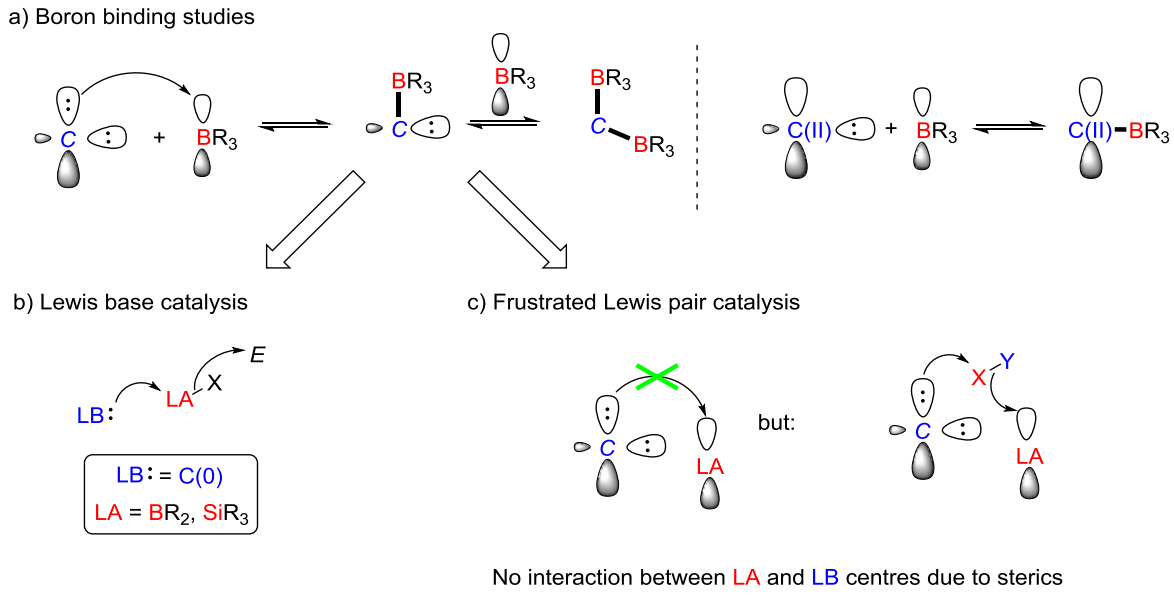

Scheme 4.29: Boron binding activity and potential catalysis pathways.

Another worthwhile goal was the selective preparation of mono-metal complexes (Scheme 4.30). We have been interested in the preparation of novel metal–C(0) complexes utilizing 'green' main group metals (groups I, II and XIII) and first-row transition metals (from manganese to zinc). These new metal complexes may display unique catalytic properties due to the specific electronic and steric properties of carbon(0) ligands. Coordination of the Lewis acid to the central carbon atom will render the former more electron-rich. This newly formed

metal complex may still be utilized in catalysis. However, X^- may go off to form a salt with a cationic centre. While the latter is stronger Lewis acid, its Lewis acidity may be enhanced with anion metathesis [e.g. using silver(III)triflate]. As an example, such a metal Lewis acid may efficiently coordinate to an alkyne to create an electrophilic carbon centre in vicinal position. Thus, appropriate nucleophiles may add to this electrophilic site to form new C–C or C–X bonds.

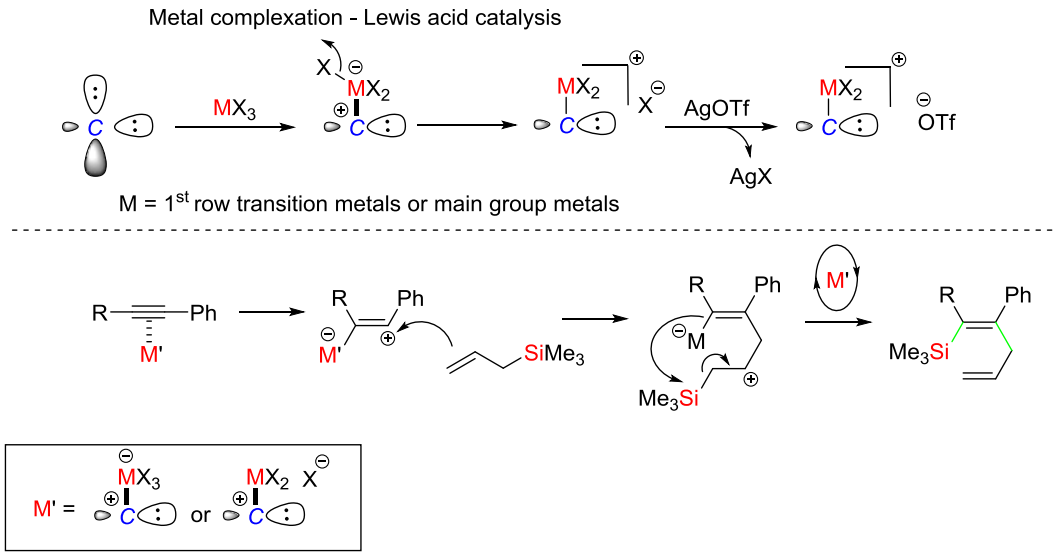

Scheme 4.30: Metal complexes and application in Lewis acid catalysis.

Finally, we were also interested in dual catalysis taking into consideration that mono-metal complexes of C(0) compounds provide a Lewis acidic centre (metal), while a second lone pair at the carbon atom may be available for Lewis base activity (Scheme 4.31). The former may activate a basic electrophile, while the Lewis basic carbon may activate a Lewis acidic pro-nucleophile for subsequent bond formation.

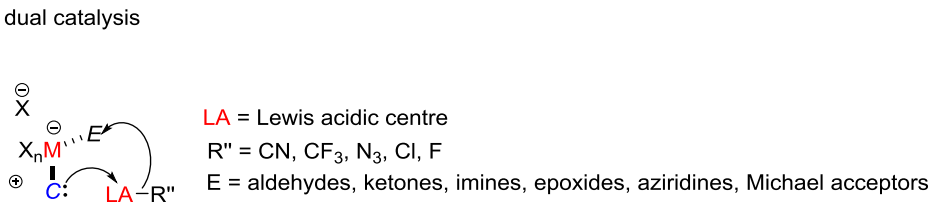

Scheme 4.31: Dual catalysis using C(0)–metal complexes.

4.3 Results and Discussion

A library of C(II) (e.g. NHCs) and C(0) compounds have been used to investigate the 'coordination at carbon'(Scheme 4.32). While the precursors of the *in situ* formed NHCs and actual NHCs have been purchased, the C(0) compounds had to be prepared in the lab. The next step was the investigation of the binding activity of these Lewis bases towards various boron Lewis acids. Unless otherwise stated, the mixed C(0) compounds were prepared and investigated by myself, while CDP **152** and CDC **159** have been prepared and investigated by Hanno Kossen and Xun Lu, respectively.

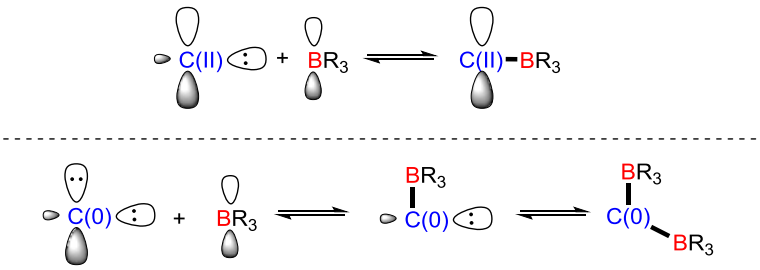

Scheme 4.32: Boron binding study of various Lewis bases.

4.3.1 Preparation of C(0) Compounds

4.3.1.1 Preparation of Bestmann Ketene (153)

Following the thorough study of the electronic and structural properties of **152**, the ketene-type molecules became part of the investigation.[122] The preparation of the Bestmann ketene (**153**) has been reported in an one-step process (Scheme 4.33). Commercially available ylide **164** was treated with NaHMDS in benzene at 60 °C for 24 hours to generate Bestmann ketene in 75% yield.[130,131] The reaction was monitored by ^{31}P NMR spectroscopy. When it reached completion, the mixture was filtered over celite, while it was hot, dried *in vacuo* and recrystallized from hot toluene.

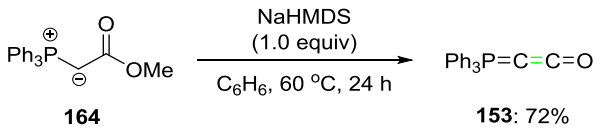

Scheme 4.33: Preparation of the Bestmann ketene.[130,131]

4.3.1.2 Preparation of C(0) Compound 155

Next, C(0) **155** was synthesized in two steps. The replacement of the carbon monoxide ligand with an acetal-type carbene ligand would provide a greater insight, since the latter is

significantly weaker acceptor. The preparation of **155** is a two-step process. Ylide **167** was treated with Meervein's reagent (1.0 equiv) at 0 °C in DCM to form **168** in 40% yield (Scheme 4.34).[122] After the reaction reached completion, DCM was removed *in vacuo*, and the residue was dissolved in benzene. After aqueous work-up, the crude compound was recrystallized from THF.

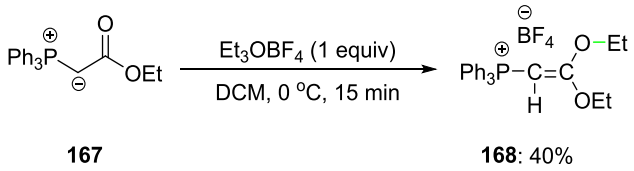

167 **168**: 40%

Scheme 4.34: Preparation of the C(0)-prec **168**.[122]

In the reported method, the Brønsted base used for deprotonation of the vinylic proton of **168** was sodium amide in liquid ammonia.[148] However, the use of ammonia in the lab may pose risks; indeed, it is highly corrosive in contact with skin, while it is an irritating gas on air for eyes, nose and throat to lead to potential respiratory issues or death. Thus, we decided to investigate an alternative deprotonation method using sodium or potassium hydride (1.2 equiv), respectively. Initially, acetonitrile was the solvent of our choice, since inorganic hydrides display poor solubility in apolar solvents. The reactions were set at 30 °C for 15 hours and monitored by ^{31}P NMR spectroscopy (Scheme 4.35). The signal of **168** and **155** was displayed in 17.2 and 3 ppm, respectively.[133] Unfortunately, no conversion to the intended product was observed, while use of these bases led to formation of side-products (several signals between 14–18 ppm). Notably, the use of potassium hydride led to significantly greater conversion to side-products (55%; entry 1) compared to sodium hydride (26%; entry 2); this could be explained by the fact that potassium hydride is a considerably stronger Brønsted base (sodium ions are smaller than potassium ions). Unfortunately, we were not able to identify the structured of the side-products based on ^{31}P NMR spectroscopy.

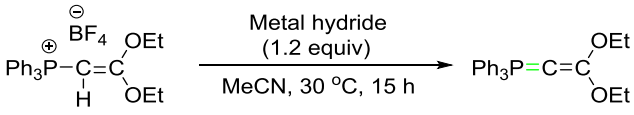

168 **155**

Scheme 4.35: Preparation of the C(0)-prec **145**.[122]

However, we suspected that the choice of acetonitrile as a solvent was the main cause for the formation of side-products; thus, we decided to replace it with THF (Table 4.1). Compound **168** was treated with lithium and sodium hydride (1.2 equiv), under otherwise identical

conditions to give intended product **155**. Again, the progress of the reactions was monitored by ^{31}P NMR spectroscopy. Lithium hydride exhibited no reactivity, since only the signal of the starting material was displayed in the ^{31}P NMR chart (17.2 ppm; entry 1). Gratifyingly, the use of sodium hydride led to a significantly increased selectivity to provide **155** in 65% conversion to the intended product (3 ppm) and 7% formation of side-products (13–18 ppm; entry 2). Indeed, 27% of the starting material remained unreacted, which reflects to a low reaction-rate. Thus, we conducted further investigation to shorten the reaction time. Next, NaHMDS (1.0 equiv) and KHMDS (1.0 equiv) were examined. In both cases, the addition of the Brønsted base was accomplished dropwise to a solution of **168** in THF at low temperature for 15 minutes and then, the reaction mixture was warmed to room temperature within one hour. At this point, both reactions reached to completion. Use of NaHMDS led to 46% conversion to the intended product based on ^{31}P NMR spectroscopy (3 ppm), while the rest of the starting material reacted towards unintended pathways to generate side-products with signals at 14 and 19 ppm (entry 3). Use of KHMDS led to formation of side-products only (signals at 16.9 and 18 ppm; entry 4), which can be explained by the fact that the former is considerably stronger Brønsted base compared to NaHMDS. Finally, we decided to optimise the reaction conditions using sodium hydride as a Brønsted base.

Table 4.1: Deprotonation of **168** using metal hydrides in THF.

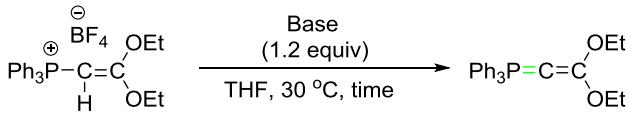

168 **155**

Entry	Metal Hydride	Time (h)	Conv (Pr:SP:SM) (%)[a][b]
1	LiH	24	0:0:100
2	NaH	24	66:07:27
3	NaHMDS[c]	1	46:54:0
4	KHMDS[c]	1	0:100:0

[a] Conversion was monitored by ^{31}P NMR. [b] Pr = product; SP = side-product; SM = starting material [c] 1.0 equiv of NaHMDS and KHMDS were added.

For this purpose, we conducted solvent screening for deprotonation of **168** using sodium hydride at 30 °C for 24 h (Table 4.2). The use of dioxane led to 55% conversion to the intended product based on ^{31}P NMR spectroscopy (3 ppm), while 9% was transformed into side-products (–54 and 13 ppm; entry 1) and, 36% of the starting material remained unreacted (17.2

ppm). The choice of TBME as a solvent proved to be inappropriate, since the solubility of both **168** and sodium hydride was poor (entry 2). Furthermore, formation of **155** was not observed in the ^{31}P NMR chart, while side-product (28%; 13 ppm) was formed and a significant amount of the starting material remained unreacted (72%; 17.2 ppm). Indeed, the experiment with THF as a solvent displayed the highest reaction rate towards the formation of the intended product (71%; 3.0 ppm), although the generation of the side-product was 14% based on ^{31}P NMR spectroscopy (13–18 ppm; entry 3); slightly higher compared to the experiment that dioxane was used. Although DCM gave the solubility of both **168** and NaH, in the ^{31}P NMR, only the signal of the starting material was displayed (entry 4).

Table 4.2: Deprotonation of **168** using NaH in various solvents.

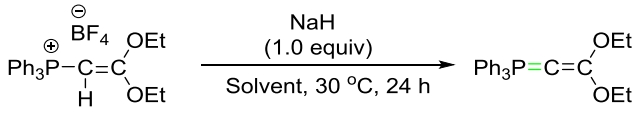

168 **155**

Entry	Solvent	Conv (Pr:SP: SM) (%)[a]
1	Dioxane (2.3)	55:9:36
2	TBME (4.5)	0:28:72
3	THF (7.6)	71:14:15
4	DCM (8.9)	0:0:100

[a] Conversion was monitored by ^{31}P NMR. [b] Pr = product; SP = side-product; SM = starting material.

To conclude, further investigation was required in order to identify the optimised conditions. However, time limitations impinged the ability to carry out any further optimisation. We could suggest that the most appropriate candidate as a Brønsted base is the sodium hydride and the solvent of our choice would be between dioxane or THF.

4.3.1.3 Preparation of C(0) Compound 158

The synthesis of carbone **158** was reported as a four-step process.[127] In the first step, diazophospholidine **175** was treated with hexachloroethane (1.0 equiv) in DCM at –80 °C temperature to generate phosphonium salt **176** in 78% yield, which was isolated by precipitation as a grey solid (Appel-type reaction; Scheme 4.36).

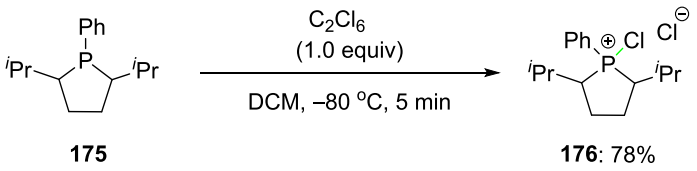

175 176: 78%

Scheme 4.36: Synthesis of the diazophospholidine **152**.[127]

Methyldiphenylsulfonium triflate was prepared in the lab, following a literature process (Scheme 4.37).[149] Diphenyl sulfide was treated with methyl triflate (1.0 equiv) in DCM at 25 °C for 2 days to give the intended product in 96% yield. The reaction was monitored by ^{19}F NMR spectroscopy and methyldiphenylsulfonium triflate **177** was obtained by a fairly easy process using extraction and filtration as the main purification methods.

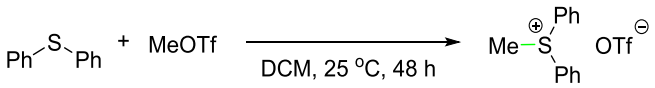

(1.0 equiv) **177**: 96%

Scheme 4.37: Synthesis of methyldiphenyl sulfonium triflate (**177**).[149]

Next, ″butyl lithium was used to deprotonate the methyl group of the methyldiphenylsulfonium triflate **177** in THF at –80 °C for 1 h to form diphenylsulfonium ylide (Scheme 4.38).[127] Then, addition of phosphonium chloride **176** at –80 °C for 5 min led to the generation of C(0)-precursor **178** in 65% yield through an addition/elimination process. The work-up for the isolation of **178** proved to be fairly straightforward as well. The mixture was warmed-up progressively to room temperature. The volatiles were removed *in vacuo* and the resulting white solid was dissolved in DCM and the diphenylsulphonium ylide was precipitated after the addition of diethyl ether.

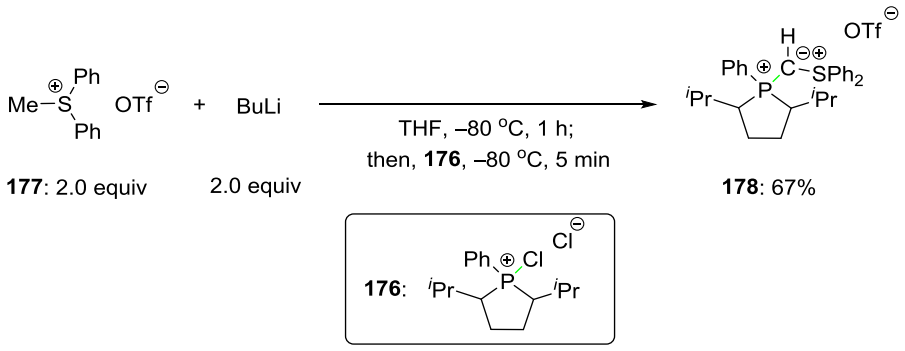

177: 2.0 equiv 2.0 equiv **178**: 67%

Scheme 4.38: Synthesis of the C(0) prec **178**.[127]

The final step for the preparation of **160** was the deprotonation of diphenylsulphonium ylide **180** by KHMDS in THF at –50 °C in 30 minutes; the reaction mixture was warmed-up

progressively to room temperature within 6 h (Scheme 4.39).[127] The reaction was monitored by ^{31}P NMR spectroscopy to confirm that the starting material was converted into the intended product (39 ppm; 50%), side-products (–48, 34 and 47 ppm; 30%), while 20% of the starting material remained unreacted (49 ppm). Indeed, the large percentage of side-products within the resulting reaction mixture was a discouraging factor for our further investigations.

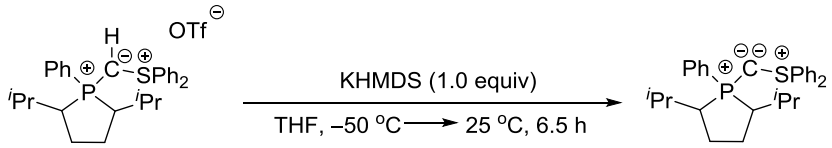

178 **158**

Scheme 4.39: Synthesis of mixed carbone **158**.[127]

4.3.1.4 Preparation of Mixed C(0) Compound 156

The direct precursor of C(0) species **156** was synthesized in three steps (Scheme 4.40).[9] **169** was deprotonated using sodium amide in THF at –60 °C to give ylide **170**. A following Wittig reaction between **170** and fluorenone led to the formation of alkenyl bromide **171** in 40% yield. **171** was then refluxed in toluene in the presence of triphenylphosphine (addition/elimination), followed by an anion exchange with sodium tetrafluoroborate. The precursor of C(0) species **156** was obtained on a gram-scale; it is air- and moisture-stable. The intended final product, (*P*,*C*)-C(0) **156**, was not isolated due to decreased stability at room temperature, but it was synthesized several times *in situ* through deprotonation with KHMDS; its formation was confirmed in the ^{11}B NMR and ^{31}P NMR spectroscopy (*vide infra*).

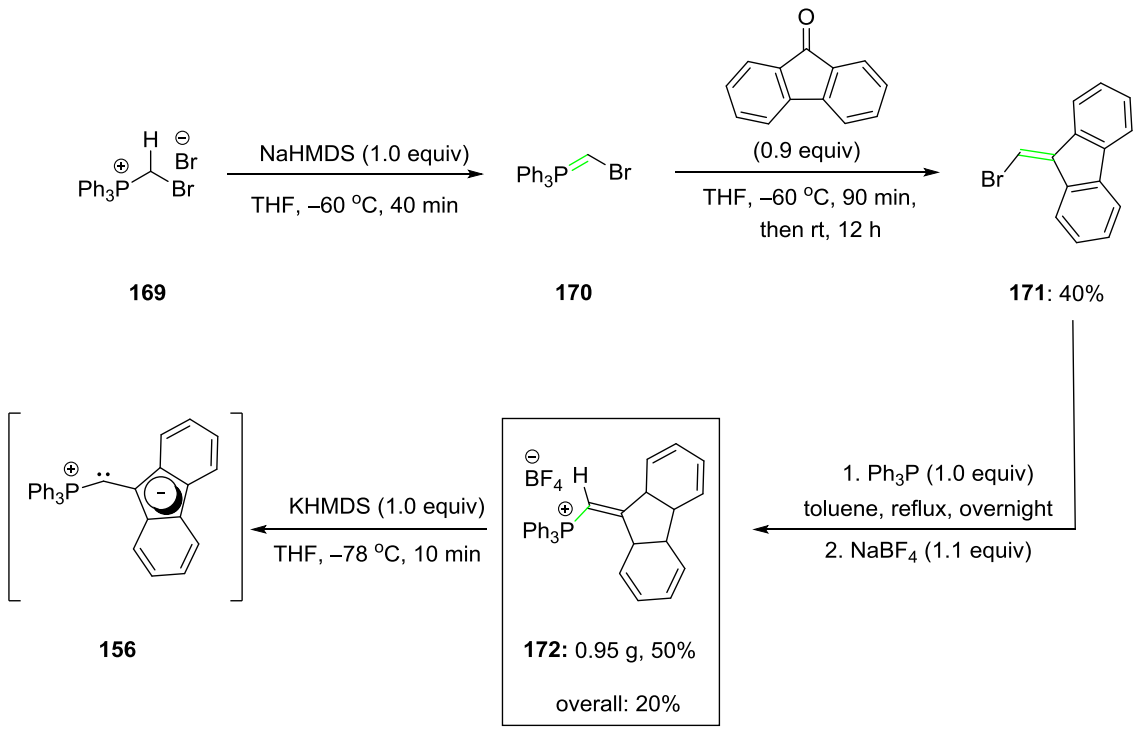

Scheme 4.40: Synthesis of mixed carbone.[9]

4.3.1.5 Preparation of a CDP 152

Parent compound **152** was prepared based on the Appel protocol due to its simplicity and high yields.[129] Indeed, triphenylphosphine (3.0 equiv) was reacted with carbon tetrachloride in DCM at room temperature for 24 hours to form chlorinated precursor **163** (66%; Scheme 4.41). The next step was a dechlorination of **163** using an hexamethyl phosphoramide following the principles of Appel reaction (61%). C(0) species **152** proved to be stable at room temperature under an inert atmosphere.

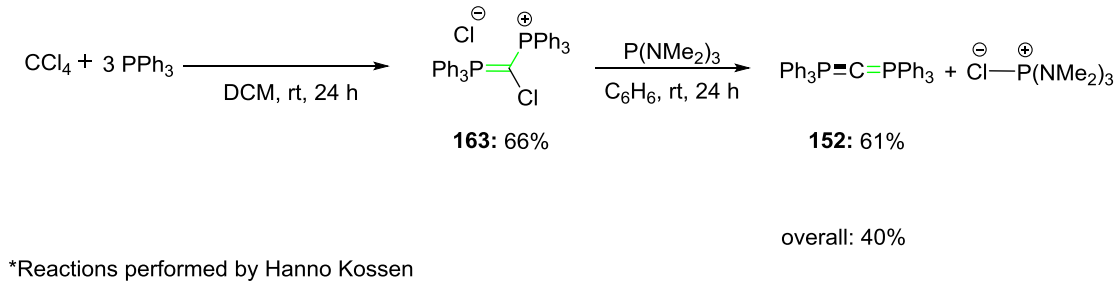

Scheme 4.41: Synthetic route of the CDP **152**.[129]

4.3.1.6 Preparation of CDC 159

CDC **159** was prepared in four-step process (Scheme 4.42).[116] *N*-methyl-1,2-phenylenediamine was heated with diethyl malonate in 2,6-dichlorotoluene at 170 °C for two hours to generate **179**. The latter was treated with methyl triflate (2.0 equiv) in acetonitrile to provide **180** [(bis)alkylation]. Next, KHMDS (1.0 equiv) was used to deprotonate **180** in acetonitrile at 25 °C to form **205**. The latter was deprotonated by KHMDS (1.0 equiv) in dichloroethane to afford CDC **159** in 80% yield.

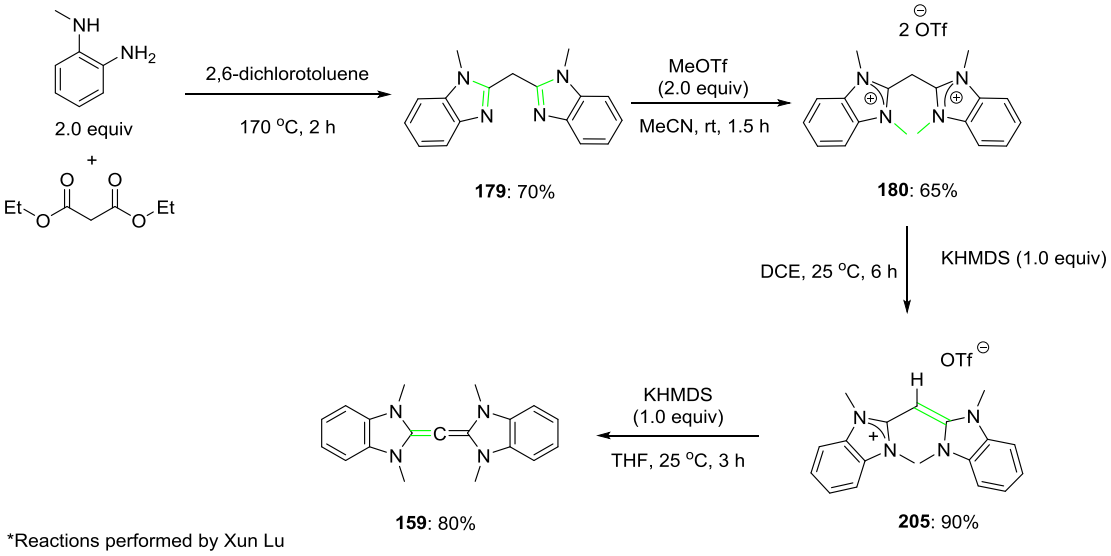

Scheme 4.42: Synthetic route of CDC **159**.[116]

4.3.2 Experimental Comparison between C(II) and C(0) Compounds

4.3.2.1 ^{11}B NMR Analysis – Assessment of Lewis Basicity

Background for ^{11}B NMR Spectroscopic Analysis

In our project, the starting materials to be used and the product before hydrolysis are boron-based compounds; thus, it is possible to monitor our experiments using ^{11}B NMR spectroscopy. ^{11}B NMR analysis can be considered as a kind of Lewis acidity scale for boron compounds. Indeed, the more electron-withdrawing the environment of a boron atom, the more Lewis acidic is the boron atom, i.e., a strong down-field shift can be observed (Figure 4.9). Boron-based pro-nucleophiles with three carbon atoms connected to the boron atom are considered particularly electrophilic and their ^{11}B NMR chemical shifts are around 80 ppm. Subsequently, replacement of one carbon atom with an oxygen atom renders the boron-based compounds less electrophilic and their ^{11}B NMR chemical shifts are around 50–60 ppm. Boron-based pro-nucleophiles (e.g. boronic esters) are frequently used in organic synthesis;

these reagents contain one B–C and two B–O bonds and their relative Lewis acidity is represented by a chemical shift of around 30 ppm in ^{11}B NMR chart. A boron atom connected to three oxygen atoms, the so-called borate is less Lewis acidic and therefore its chemical shift in ^{11}B NMR is around 20 ppm (relative up-field shift). Such a phenomenon can be rationalized by considering that, in contrast to carbon atoms, oxygen atoms do have lone pairs of electrons, which can be partially donated to the bound boron atom, thereby decreasing its Lewis acidity. The Lewis acidic boron has an empty p orbital, and therefore σ donors may offer a lone pair to coordinate forming a boron–ate complex. The ^{11}B NMR shifts of the boron–ate complexes are from 10 to –40 ppm and by definition $Et_2O{\bullet}BF_3$ with a signal at 0 ppm has a perfectly tetrahedral geometry.

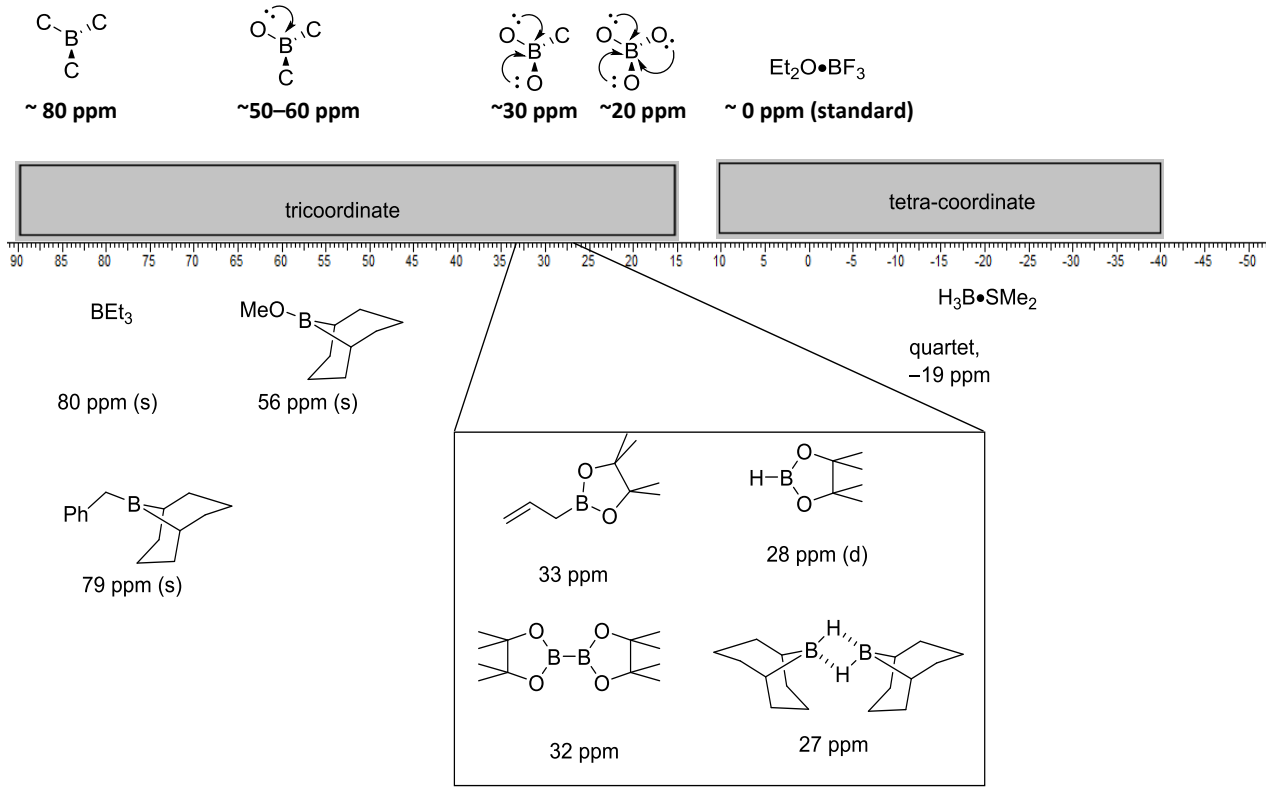

Figure 4.9: ^{11}B NMR spectroscopy as a Lewis acidity scale for boron compounds.

Information from ^{11}B NMR Analysis for Our Purpose

The goal of this boron study was to react the Lewis basic carbones of interest – and a few carbenes for comparison – with a variety of boron Lewis acids in order to detect by ^{11}B NMR spectroscopy whether a boron–ate complex was formed or not. If a boron–ate complex was detected, the corresponding Lewis acidic boron compound may be used directly as a pro-nucleophilic reagent in catalysis; if no boron–ate complex is generated with a certain boron Lewis acid, the latter may be still used – together with the carbone – in the context of

"frustrated" Lewis pair (FLP) catalysis. The boron Lewis acids used in this manuscript and the corresponding values in ^{11}B NMR spectroscopy are presented below (Scheme 4.43). In terms of carbenes, we used three NHCs (**206**–**208**) alongside with four carbones; Bestmann's ketene **153**, mixed carbone **156,** parent CDP compound **152**, and CDC species **159** (Scheme 4.43). The formation of boron–ate complexes can be monitored with ^{11}B NMR spectroscopy, which is an easy way in order to confirm the *in situ* formation of less stable Lewis bases that cannot be isolated. In the case of carbones, two molecules of the corresponding boron Lewis acid may be bound to the reactive central carbon atom, which should also be detectable in the ^{11}B NMR spectroscopy [Scheme 4.43]. *It is noted that for boron binding studies, deuterated benzene (C_6D_6) was the solvent of choice. However, in several cases, it was not possible to isolate successfully the in situ formed Lewis base. Thus, the solvent for the in situ deprotonation of the corresponding precursor, THF, was also part of the reaction mixture in (THF/C_6D_6 = 3:1). Specifically, experiments with **206**, **156**, and control experiments with KHMDS and HMDS have been conducted using THF/C_6D_6 = 3:1. Experiments with **207**, **208**, **153**, **152**, and **159** have been conducted using C_6D_6.*

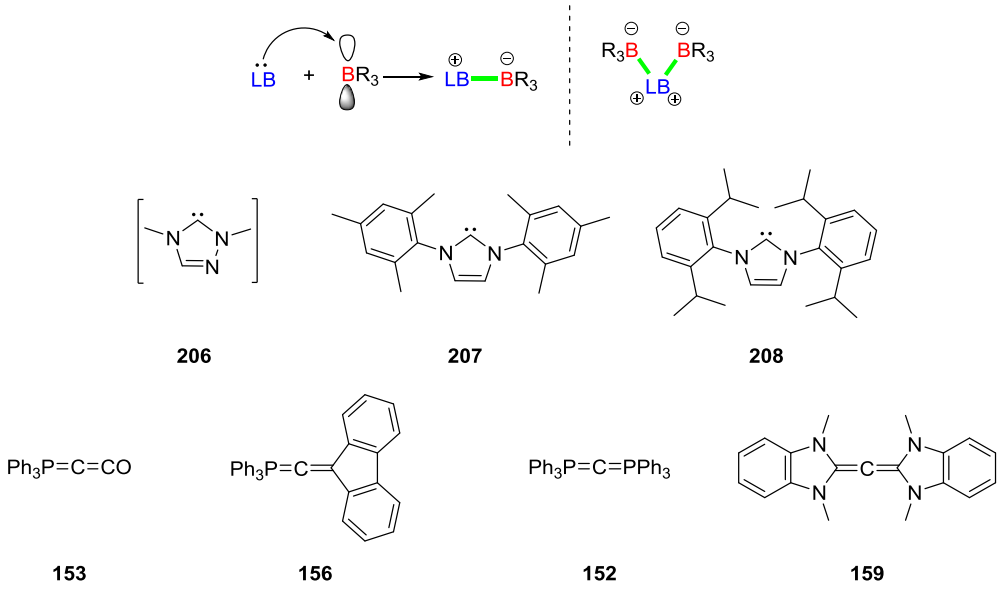

Scheme 4.43: a) Interaction of carbenes and carbones with boron Lewis acids.

4.3.2.2 Lewis Basicity Study with Carbenes [C(II)] and Carbones [C(0)]

Triethyl borane (BEt_3) is a particularly strong Lewis acid that displays a signal at 86 ppm in ^{11}B NMR spectroscopy [Scheme 4.44 a)]. The binding potential of several carbon-based Lewis bases were examined with this boron Lewis acid (1.2 equiv) using a solvent system THF/C_6D_6 (3:1) or sole C_6D_6.

Triazolium-based NHC **206**, generated *in situ* through deprotonation of the imidazolium precursor using KHMDS, proved to coordinate to the boron centre thereby leading to the clean formation of a boron–ate complex (**209**) as evidenced by the appearance of a new distinct signal at –13 ppm in ^{11}B NMR spectroscopy [Scheme 4.44 b)]. In the same line, the use of the two commercially available NHCs, **207** and **208,** resulted in the smooth formation of the corresponding boron–ate complexes (**210** and **211**, respectively) as indicated with signals at –12 ppm in ^{11}B NMR spectroscopy [Scheme 4.44 c) and d), respectively]. There was an additional minor signal at 54 ppm in both cases, but we were unable to assign a structure.

The use of the Bestmann's ketene (**153**) did not lead to the formation of a boron–ate complex; only the signal of BEt_3 was detected [Scheme 4.44 e)]. Carbon monoxide as a ligand may display a strong π acceptor effect resulting in a decreased nucleophilic character of the central carbon. Interestingly, the use of mixed carbone **156** led to a single signal at 54 ppm in ^{11}B NMR spectroscopy, which may be the result of a weak interaction between BEt_3 and **156** [Scheme 4.44 f)]. Indeed, the signal at 54 ppm could be ascribed to a rapid equilibrium between unreacted BEt_3 and the formed boron–ate complex **212**. If so, an averaged signal between the tri- and tetra-coordinate boron species would be expected. The fact that the chemical shift (54 ppm) is closer to the value of BEt_3 would correspond to a C–B interaction, i.e, the equilibrium lies on the left side. In contrast, the use of CDP species **152** did not lead to any detectable interaction with BEt_3, likely due to the significant steric demand around the carbon centre [Scheme 4.44 g)]. This result might also be partially ascribed to the fact that **152** was not fully soluble in C_6D_6, which would suggest that the potentially formed boron–ate complex would be even less soluble and thus not detectable. Finally, the use of CDC species **161** resulted in the generation of a boron–ate complex (**213**) with a signal at 1 ppm in ^{11}B NMR spectroscopy [Scheme 4.44 h)].

Since the *in situ* formations of NHC **206** and C(0) species **156** were carried out using KHMDS as a Brønsted base, a control experiment with BEt_3 and KHMDS had to be conducted as well [Scheme 4.44 i)]. As expected, the *N–B* adduct was completely formed as evidenced by the detection of a new signal at –4 ppm, which is clearly distinct from the values observed for the use of **206** and **156** (–13 ppm and 54 ppm, respectively). In turn, this meant that KHMDS was fully consumed in the deprotonative generation of the carbon-based species, as it did not interfere with the ^{11}B NMR spectroscopy results. Since HMDS is the stoichiometric by-product of the *in situ* deprotonation, the Lewis basicity of this amine was also examined [Scheme 4.44 j)]. In this experiment, the signal of BEt_3 in ^{11}B NMR spectroscopy was displayed as a sole chemical shift at 80 ppm. Indeed, the latter was observed up-field compared to the blank experiment [Scheme 4.44 a)]. This difference in the chemical shift is

that experiments with HMDS was conducted using THF/C_6D_6 (3:1); THF is formally a Lewis base and is able to apply solvent effect to a strong Lewis acid, such as BEt_3, displaying its chemical shift relatively up-field. This hypothesis was confirmed by a blank ^{11}B NMR experiment with BEt_3 and HMDS in THF/C_6D_6 (3:1) solvent mixture (80 ppm).

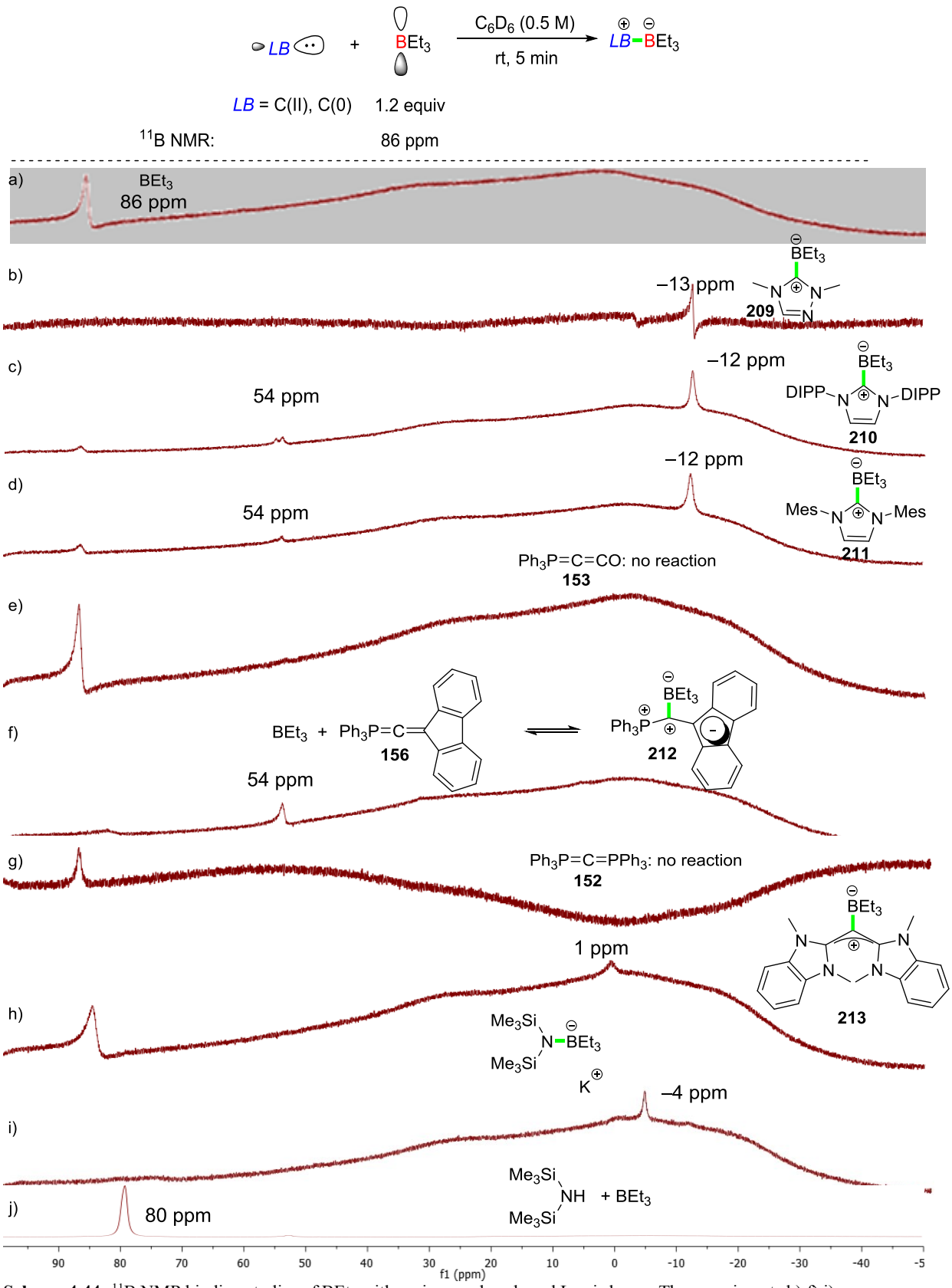

Scheme 4.44: ^{11}B NMR binding studies of BEt_3 with various carbon-based Lewis bases. The experiments b) f) i) j) have been conducted with THF/C_6D_6 (3:1) as a solvent system.

The experiments with phosphorus-containing carbones **153, 156**, and **152** was monitored as well by ^{31}P NMR spectroscopy (Scheme 4.45). In accord with ^{11}B NMR spectroscopy, the ^{31}P NMR spectrum of the experiment with Bestmann's ketene **153** displayed only the signal of the starting material at 3 ppm [Scheme 4.45 a)]. In contrast, **156** has displayed reactivity with BEt_3 (54 ppm) in ^{11}B NMR spectroscopy, which may be a result of equilibrium between BEt_3 and formed boron–ate complex **212**. In ^{31}P NMR spectroscopy, three distinct signals were displayed [Scheme 4.45 b)]. The signal at –5 ppm can be unambiguously ascribed to unreacted **156**; indeed, Alcarazo *et al.* reported this value for *in situ* generated **156** at low temperature (–78 °C).[9] There are two additional signals at 30 ppm (major) and 25 ppm (minor). The signals at 30 ppm and –5 ppm have been ascribed to boron–ate complex **212** *and* free **156** in equilibrium, respectively. As it is already presented, the ^{11}B NMR experiment with CDP **152** and BEt_3 did not display new signals. In accordance, the ^{31}P NMR chart exhibited only the signal of CDP **152** as reaction with BEt_3 did not proceed [Scheme 4.45 c)].

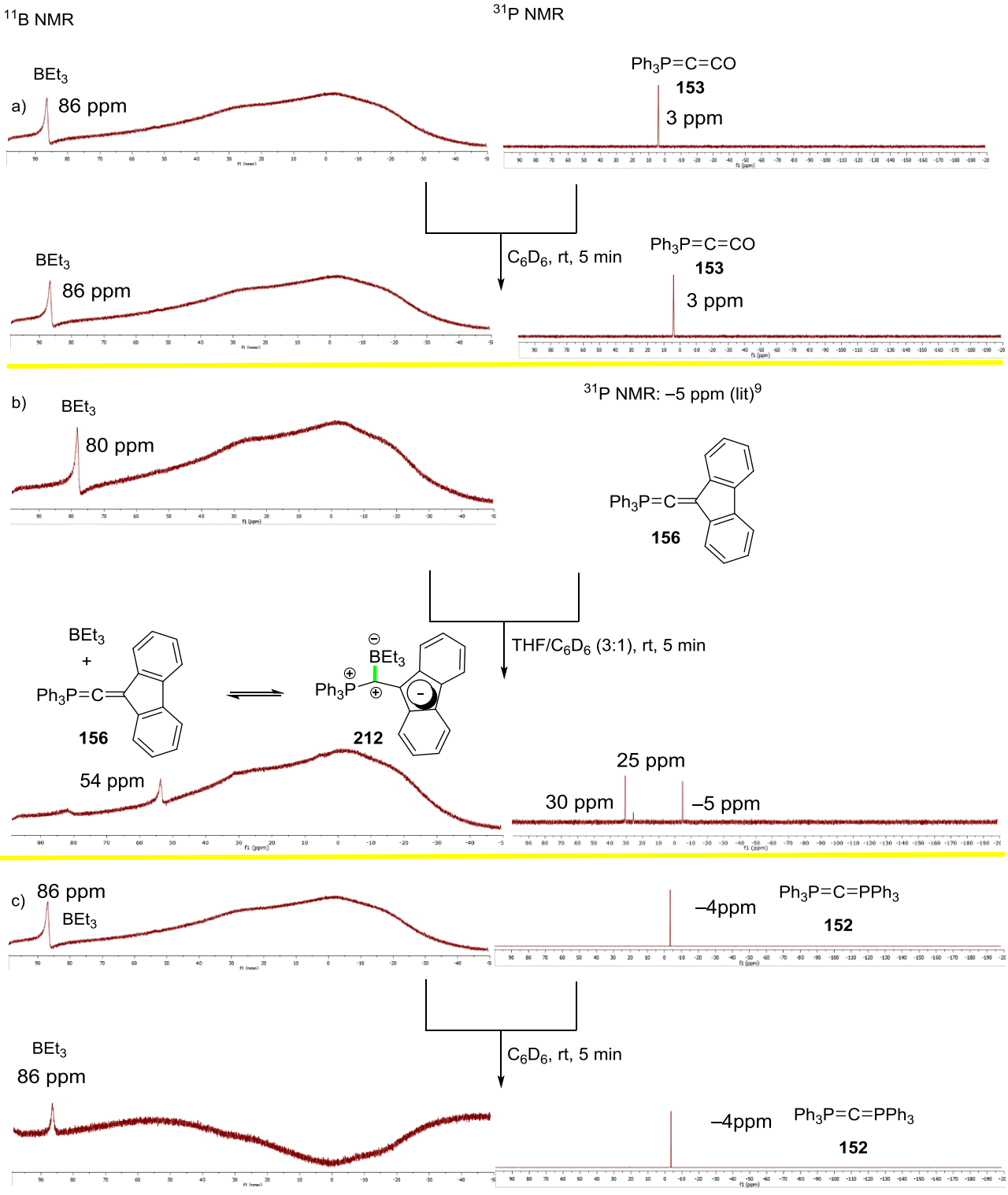

Scheme 4.45: ^{11}B NMR and ^{31}P NMR studies of phosphorus-containing carbones with BEt_3.

The scope of boron Lewis acid species was expanded using also benzyl–B(9-bbn) (80 ppm). The binding potential of various carbon-based Lewis bases onto benzyl–B(9-bbn) (1.2 equiv) in either C_6D_6 or THF/C_6D_6 (3:1) was investigated, as this may imply that a potential benzyl transfer to suitable electrophiles (Table 4.3). At this stage, it should be noted that benzyl–B(9-bbn) was purchased in THF solution; indeed, THF applied solvent effect to the electronic environment of boron to cause a shift up-field. The obtained results were similar but distinct compared with BEt_3.

NHC carbenes **206**–**208** formed in all cases the corresponding boron–ate complexes (**214**, **215**, **216**, respectively; –11 ppm and –12 ppm). The use of the Bestmann's ketene (**153**) did not lead to the generation of a boron–ate complex as evidenced by ^{11}B NMR spectroscopy; only the signal of the starting material was detected. This lack of interaction was confirmed by ^{31}P NMR spectroscopy where only the signal of **153** was displayed at 3 ppm. Likewise, the use of mixed carbone **156** and CDP **152** did not lead to any interaction with the benzyl–B(9-bbn) (^{31}P NMR spectroscopy confirmed decomposition and non-interaction, respectively). Finally, CDC compound **159** formed directly a boron–ate complex (**217**) with benzyl– B(9-bbn) (^{11}B NMR: –9 ppm).

In the blank experiment with KHMDS, a new signal at 1 ppm in the ^{11}B NMR spectroscopy was observed, which proved the formation of the *N–B* adduct; indeed, it is clearly distinct from the values observed in the experiments with **206** and **156** (–12 ppm and no shift at all, respectively). As HMDS is the by-product of the *in situ* deprotonation, the Lewis basicity of HMDS was also examined. New chemical shifts at 48 and 30 ppm were observed in the ^{11}B NMR spectroscopy. The signal at 48 ppm could be rationalized with an initial activation of the benzyl–B(9-bbn) by HMDS and release of the organic rest. The latter may 'attack' to the acidic proton attached to the nitrogen of HMDS to form toluene. Thus, tri-coordinate species with two carbon atoms and one nitrogen atom attached to the boron centre will be formed to display a chemical shift at ~50 ppm. If so, another molecule of HMDS may coordinate to the newly formed boron species to generate another boron–ate complex. The chemical shift at 30 ppm could be ascribed to a rapid equilibrium between the newly formed tri-coordinate boron species and the latest formed boron–ate complex (Table 4.6). Thus, an averaged signal between the tri- and tetra-coordinate boron species would be expected, as the interaction would be weak. Nevertheless, the side-product HMDS did not form an adduct with benzyl–B(9-bbn) based on the ^{11}B NMR spectroscopy of the experiments with **206** and **156**.

Table 4.3: Examination of various carbon Lewis bases using Bn–B(9-bbn).

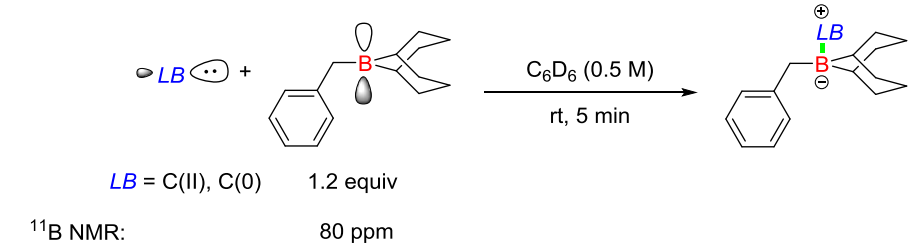

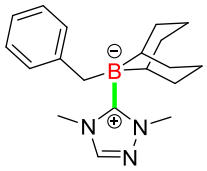

214: –12 ppm[a]

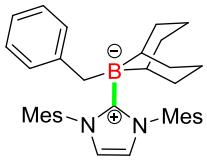

215: –11 ppm

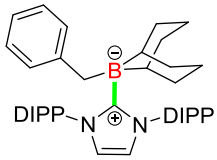

216: –11 ppm

$Ph_3P=C=CO$

153: NR[b]

31P NMR: δ = 3 ppm

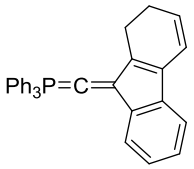

156: NR[a][b]

31P NMR: decomp

$Ph_3P=C=PPh_3$

152: NR[b]

31P NMR: –4 ppm

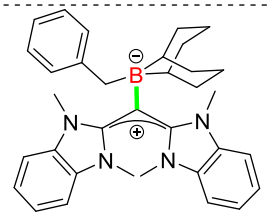

217: –9 ppm

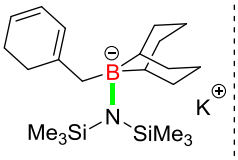

–4 ppm[a]

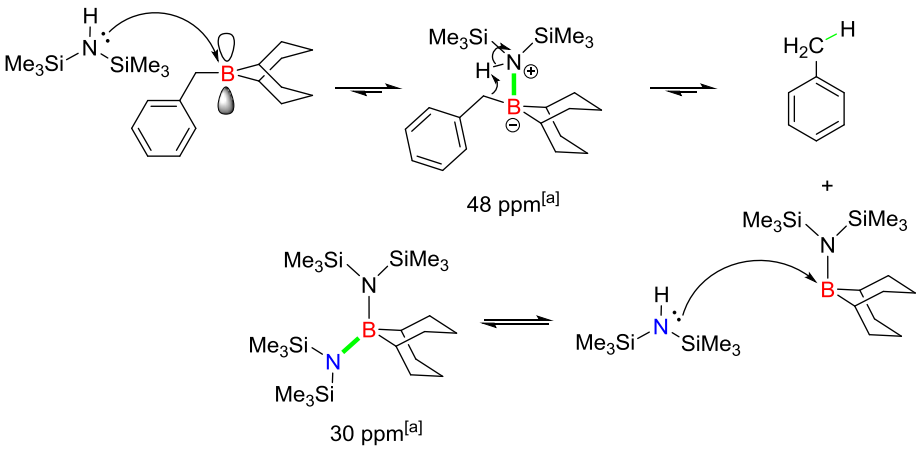

[a] THF/C_6D_6 (3:1) was the solvent system of the reaction. [b] No Δδ observed for MeO–B(9-bbn).

The Lewis basicity of various carbon species was examined using MeO–B(9-bbn) as a Lewis acid (Table 4.4). MeO–B(9-bbn) displays a signal at 57 ppm in ^{11}B NMR spectroscopy using either C_6D_6 as a solvent or THF/C_6D_6 (3:1) as a solvent mixture.

The use of triazolium-based carbene **206** and MeO–B(9-bbn) gave a new signal at –12 ppm, which indicated the formation of boron–ate complex **218**. Carbene **207** proved to coordinate

to the boron atom thereby leading to the formation of boron–ate complex **219** showing a signal at –2 ppm. Interestingly, the use of the bulkier carbene **208** did not lead to any interaction with MeO–B(9-bbn). Likewise, the Bestmann' s ketene (**153**) did not interact with the boron Lewis acid as concluded by both ^{11}B and ^{31}P NMR spectroscopy. Mixed carbone **156** reacted with MeO–B(9-bbn). ^{11}B NMR spectroscopy displayed a signal at 25 ppm, which has been ascribed to a rapid equilibrium between the unreacted MeO–B(9-bbn) and boron–ate complex **220**; thus, an averaged signal for the tri-coordinate and tetra-coordinate boron species is expected. The fact that the chemical shift (25 ppm) is closer to the value of free MeO–B(9-bbn) would mean that the *C–B* interaction is relatively weak, i.e, the equilibrium lies on the left side. In ^{31}P NMR spectroscopy, the detected signals at 25 ppm and –5 ppm have been ascribed to boron–ate complex **220** and unreacted mixed carbone **156** (two species in equilibrium), respectively. CDP **154** did not react with MeO–B(9-bbn) based on both ^{11}B and ^{31}P NMR spectroscopy. On the other hand, CDC **159** formed boron–ate complex **221** with MeO–B(9-bbn) with a signal at –9 ppm. The reaction between MeO–B(9-bbn) and KHMDS formed a boron–ate complex that displayed a signal at 5 ppm, while HMDS did not show any interaction with MeO–B(9-bbn).

Table 4.4: Examination of various carbon Lewis bases using MeO–B(9-bbn).

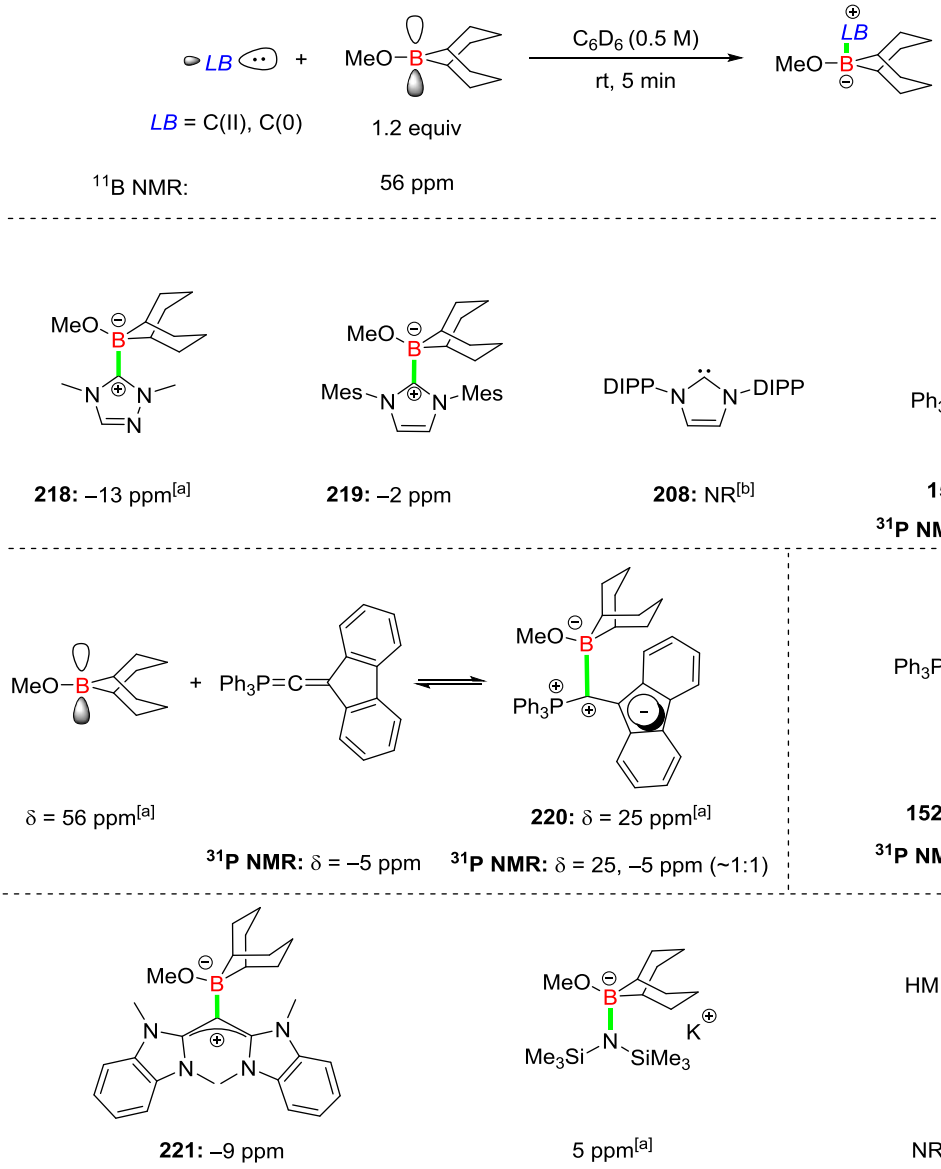

[a] THF/C_6D_6 (3:1) was the solvent system of the reaction. [b] No Δδ observed for MeO–B(9bbn).

Next, another sterically bulky boron Lewis acid, bis(pinacolato)diboron [$B_2(pin)_2$], was used (Table 4.5). $B_2(pin)_2$ displays a signal at 32 ppm in ^{11}B NMR spectroscopy.

NHC **206** reacted with $B_2(pin)_2$ to form boron–ate complex **222** with a signal at –4 ppm. NHCs **207** and **208** are significantly more sterically hindered and were shown to be unreactive towards $B_2(pin)_2$ (unchanged ^{11}B and ^{31}P NMR spectra). Likewise, the four carbones (**153, 156**, **152**, and **159**) did not lead to any interaction with $B_2(pin)_2$. In ^{11}B NMR chart, the signal of the starting material was only exhibited in all four cases. The ^{31}P NMR spectroscopy of

carbones **153** and **152** displayed single signals of the starting material. In contrast, ^{31}P NMR chart of **156** displayed evidence of decomposition. ^{11}B NMR spectroscopic analysis of control experiments between $B_2(pin)_2$ and KHMDS or HMDS did not show any evidence for an interaction with $B_2(pin)_2$. i.e., the signal at –4 ppm of the experiment with NHC **206** was not related with the Brønsted base and the stoichiometric side-product, respectively.

Table 4.5: Examination of various carbon Lewis bases using $B_2(pin)_2$.

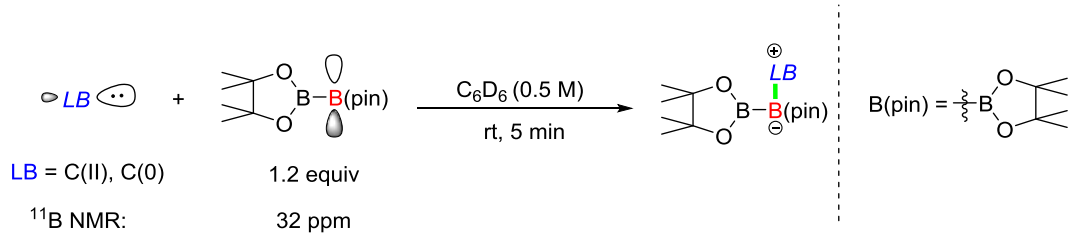

222: –4 ppm[a] **207**: NR[b] **208**: NR[b] **153**: NR[b]
^{31}P NMR: δ = 3 ppm

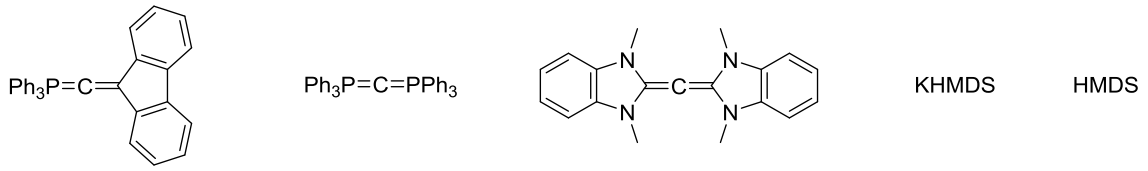

156: NR[a][b] **152**: NR[b] **159**: NR[b] NR[a][b] NR[a][b]
^{31}P NMR: decomp **^{31}P NMR:** δ = –4 ppm

[a] THF/C_6D_6 (3:1) was the solvent system of the reaction. [b] No Δδ observed for MeO–B(9bbn).

The binding potential of several Lewis bases towards allyl boron pinacol [allylB(pin)] was investigated (Table 4.6). In contrast to the experiment with $B_2(pin)_2$, the use of *in situ* generated triazolium-based NHC **206** did not lead to the formation of a boron–ate complex based on ^{11}B NMR spectroscopy. The reaction between CDC **159** and allylB(pin) did not lead to formation of a boron–ate complex.

Table 4.6: Examination of various carbon Lewis bases using allylB(pin).

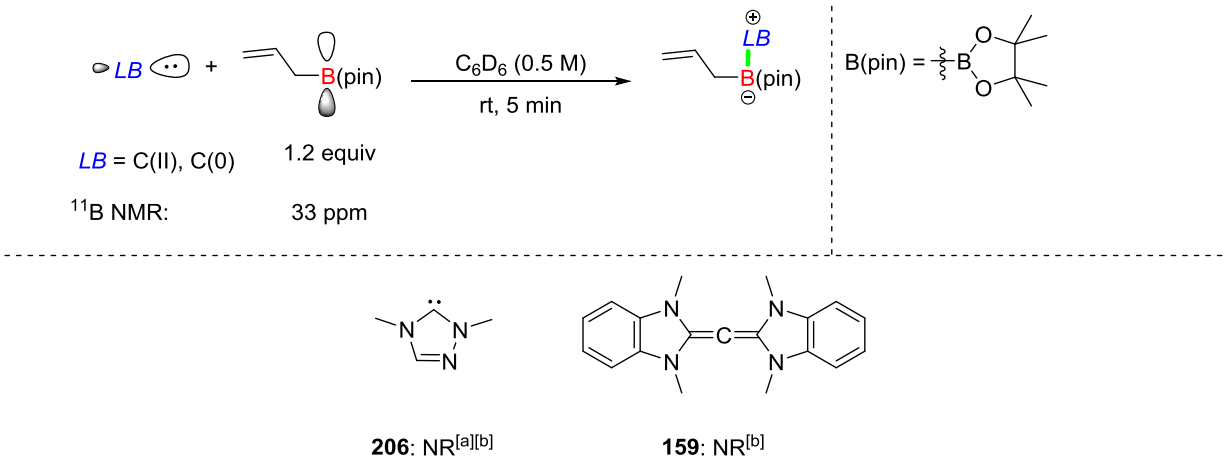

[a] THF/C_6D_6 (3:1) was the solvent system of the reaction. [b] No Δδ observed for MeO–B(9bbn).

Next, various carbon Lewis bases were investigated with the less sterically demanding pinacol borane [HB(pin)] (Scheme 4.46). HB(pin) display a signal at 29 ppm [d, J = 176 Hz; Scheme 4.46 a)] in ^{11}B NMR spectroscopy.

Indeed, the boron centre may be easily accessed by several Lewis base candidates, however, HB(pin) is a well-known hydride source. As expected, the use of NHCs **207** and **208** led to the generation of new signal at 22 ppm in the ^{11}B NMR spectroscopy [Scheme 4.46 b)–c)]. The initially formed boron–ate complexes may undergo an intramolecular boron-to-carbon hydride shift to form 'carbon-ligated B(pin)' species **223** and **224**, respectively. The corresponding B–H bond should be activated for hydride transfer to the proximal electrophilic carbon centre. **223** and **224** species should display a signal at ~ +30 ppm. The observed signal at +22 ppm has been ascribed to a rapid equilibrium between the initially formed boron–ate complex and the corresponding 'carbon-ligated B(pin)' species, which rests on the left side. The signal of the experiment with NHC **208** at 8 ppm was not rationalised. The use of **153** did not lead to interaction with HB(pin) as the single signal of the latter was displayed in ^{11}B NMR spectroscopy [Scheme 4.46 d)]. As with NHCs **207** and **208**, the use of carbone **156** resulted in an equilibrium between the boron–ate complex and the 'carbon-ligated B(pin)' species **225** [Scheme 4.46 e)]. The use of **152** did not lead to any detectable interaction with HB(pin) in ^{11}B NMR spectroscopy [Scheme 4.46 f)]. Finally, CDC **159** displayed identical reactivity with **208**, **209**, and **158** to form initially a boron–ate complex with HB(pin) and then, undergo an intramolecular boron-to-carbon hydride shift and form 'carbon-ligated B(pin)' species **226** to give a signal at 26 ppm [Scheme 4.46 g)]. The boron–ate complex and **226** are in equilibrium.

The control experiment between HB(pin) and KHMDS gave a signal at +25 ppm, which may be ascribed to an equilibrium between the amide boron–ate complex and a "$B(pin)_2$ species" generated through intramolecular hydride transfer from boron-to-silicon [Scheme 4.46 h)]. Last, the HMDS did not react with the HB(pin) according with ^{11}B NMR spectroscopy [Scheme 4.46 i)].

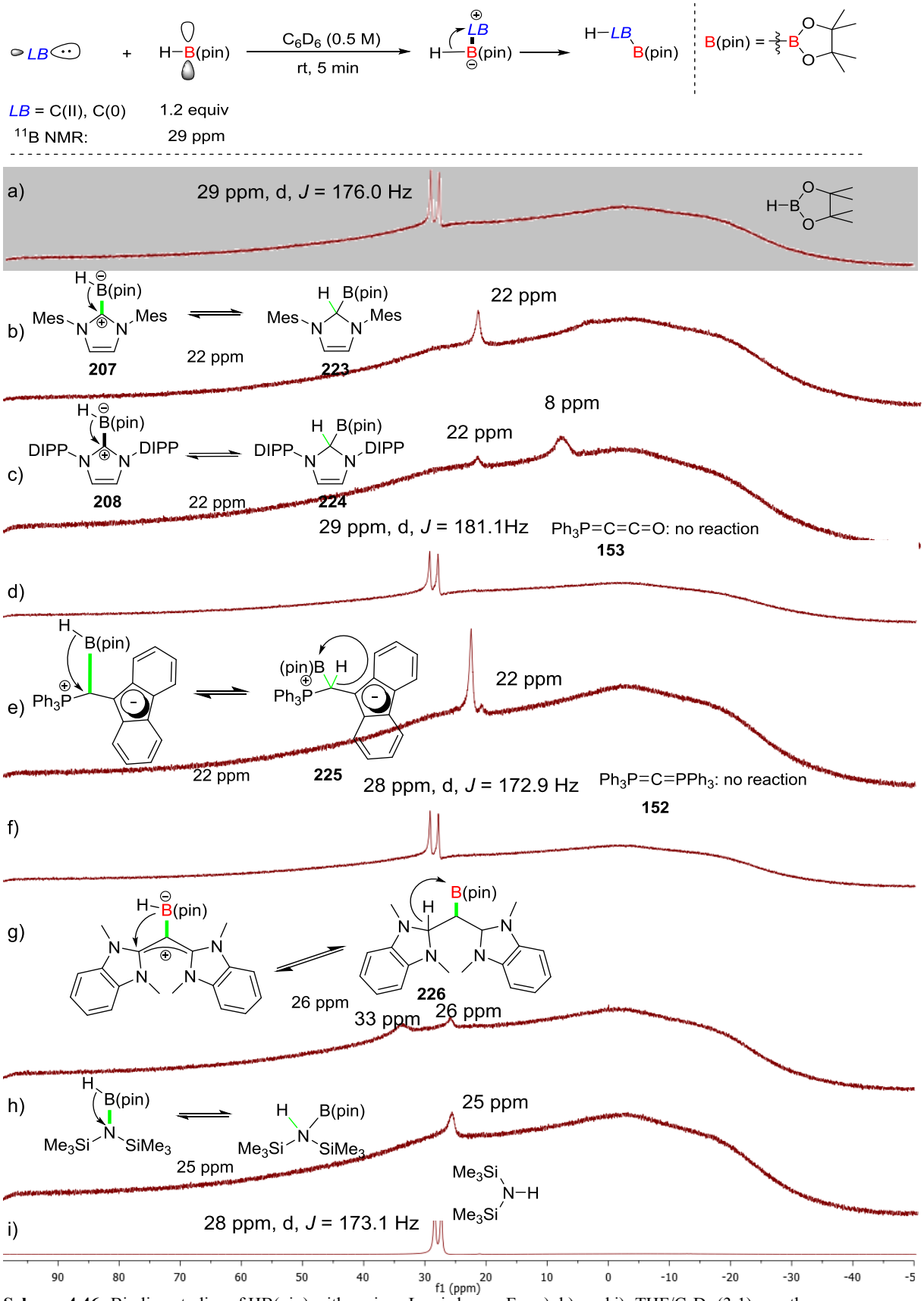

Scheme 4.46: Binding studies of HB(pin) with various Lewis bases. For e), h), and i); THF/C_6D_6 (3:1) was the solvent system of the reaction.

The experiments with carbones **153**, **156** and **152** were monitored by ^{31}P NMR spectroscopy (Scheme 4.47). Concerning **153**, as with ^{11}B NMR chart, only the signal of the starting material was observed in ^{31}P NMR spectroscopy to confirm no interaction with HB(pin) [Scheme 4.47 a)]. In contrast, the use of **156** led to formation of **225** [Scheme 4.47 b)]. In ^{31}P NMR spectroscopy, three distinct signals were displayed at 30, 25 and –5 ppm. The signal at 30 ppm has been ascribed to **225**, while the signal at –5 ppm to the unreacted **156** (reported by Alcarazo *et al*).[126] The ^{11}B NMR experiment with CDP **152** and HB(pin) did not display new signals [Scheme 4.47 c)]. However, ^{31}P NMR chart of CDP **152** displayed several signals, which may be a result of decomposition.

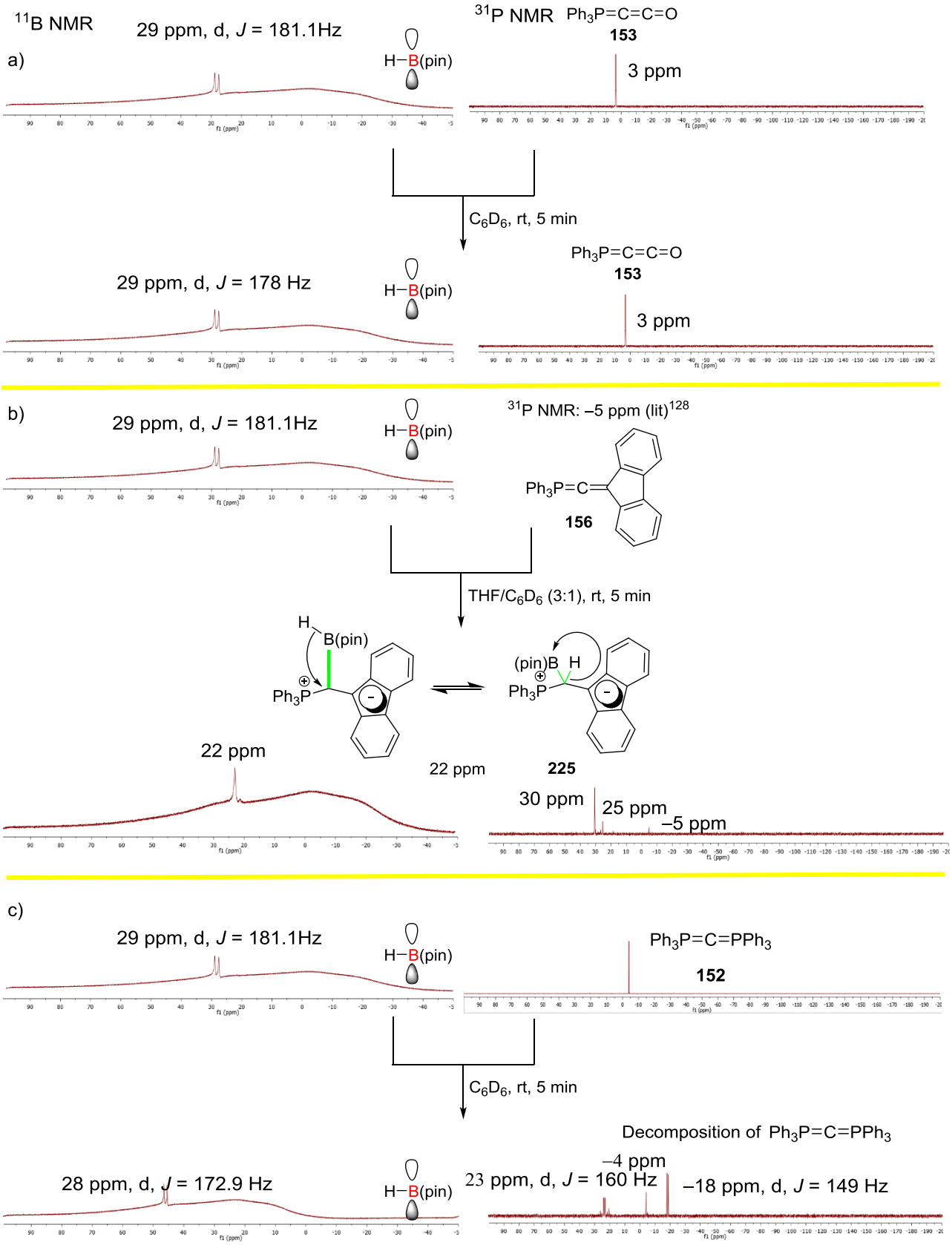

Scheme 4.47: ^{11}B NMR and ^{31}P NMR studies of phosphorus-containing carbones with HB(pin).

9-Borabicyclo[3.3.1]nonane [H–B(9-bbn)] species forms a pseudo boron–ate complex (dimer), therefore its signal is displayed up-field at 28 ppm (doublet, J = 173.1 Hz) in ^{11}B NMR spectroscopy. The Lewis basicity of various carbon Lewis bases was examined using this dimer as a Lewis acid (Table 4.7).

NHCs **207** and **208** proved to coordinate to the boron centre thereby leading to the clean formation of a boron–ate complex as evidenced by the appearance of a new distinct signal at –15 ppm (**227** and **228**, respectively). Interestingly, the use of carbone **156** led to a single signal at 53 ppm, which could be ascribed to a rapid equilibrium between the unreacted H–B(9-bbn) and the formed boron–ate complex. Thus, an averaged signal between the tri-coordinate and tetra-coordinate species would be expected. The fact that the chemical shift (53 ppm) is closer to the value of free H–B(9-bbn) would mean that the *C–B* interaction is weak, i.e, the equilibrium lies on the left side. In ^{31}P NMR spectroscopy, there are two signals at 30 ppm (major) and –5 ppm (minor); the former has been ascribed to **229**, while the latter is the signal of free **156** (reported by Alcarazo).[126] The use of **152** and **153** did not lead to any interaction with H–B(9-bbn) based on both ^{11}B and ^{31}P NMR spectroscopy. Finally, the use of CDC **159** resulted in the generation of a boron–ate complex (**230**) with a signal at –10 ppm in ^{11}B NMR spectroscopy.

The blank experiment with KHMDS displayed a signal at –18 ppm, which is within the boron–ate complex area. Finally, H–B(9-bbn) did not react with HMDS based on ^{11}B NMR spectroscopy.

Table 4.7: Examination of various carbon Lewis bases with H–B(9-bbn).

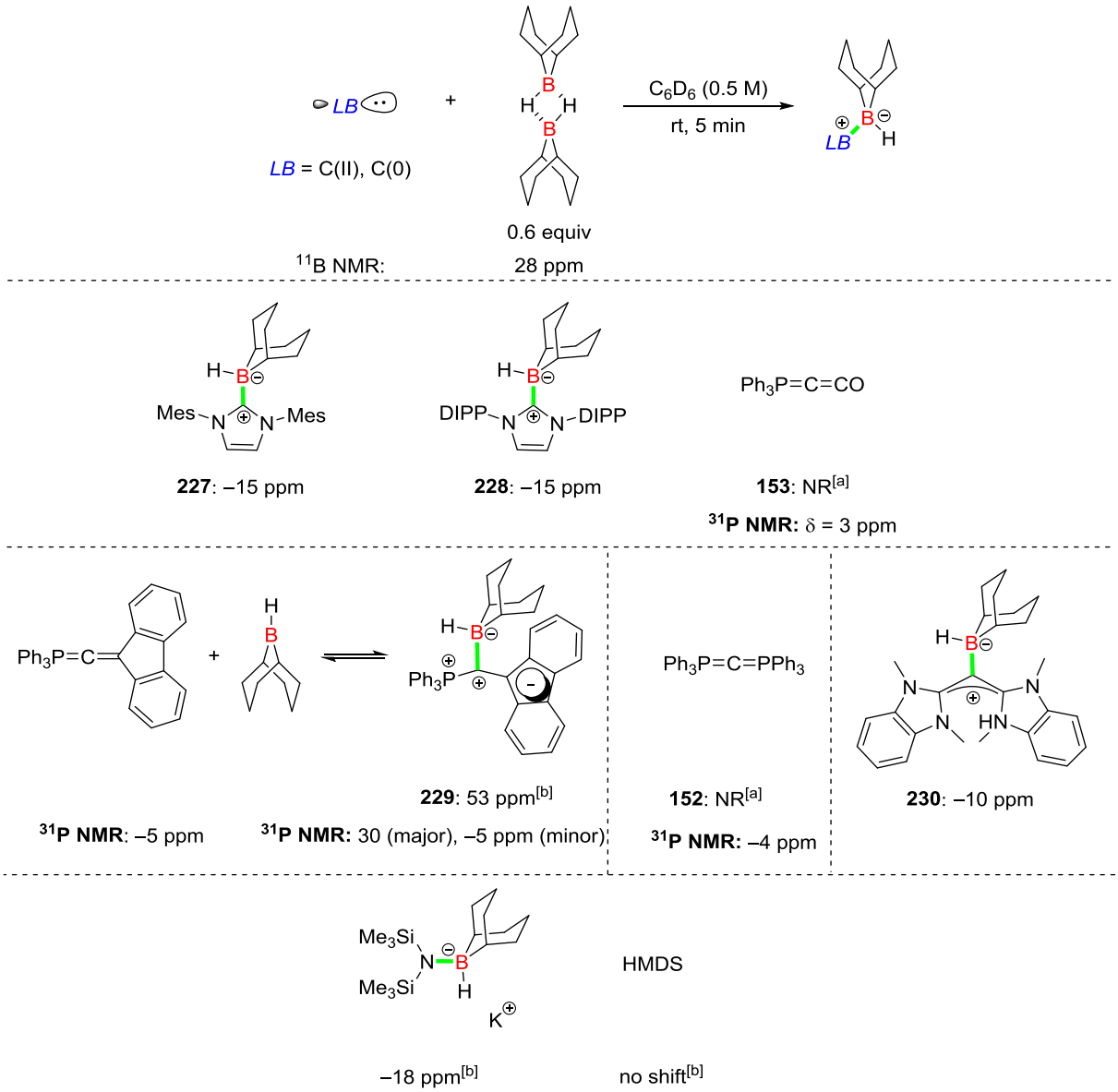

[a] No Δδ observed for MeO–B(9bbn). [b] THF/C_6D_6 (3:1) was the solvent system of the reaction.

Last, borane (BH_3) species was used to expand the scope of boron Lewis acids. BH_3 is a gas and forms a pseudo boron–ate complex (dimer, B_2H_6), therefore its chemical shift is displayed up-field at 18 ppm. However, a solution of the borane–dimethylsulfide complex (BH_3•SMe_2) in toluene was purchased and used for our boron studies, which displays a chemical shift at –19 ppm in ^{11}B NMR spectroscopy [Scheme 4.48 a)].

The use of commercially available NHCs **207** and **208** resulted in a smooth formation of boron–ate complexes **231** and **232**, respectively [Scheme 4.48 b)–c)]. The use of **207** led to partial dissociation of the dimethyl sulfide from the initial complex to replace it and form a

new boron–ate complex with a signal at –35 ppm. However, the chemical shift of BH_3•SMe_2 remained dominant, which suggests that the dissociation is a slow process. In contrast, the use of **208** led to a greater signal at –35 ppm. Again, the Bestmann's ketene (**153**) did not react with BH_3•SMe_2 [–19 ppm in ^{11}B NMR spectroscopy; Scheme 4.48 d)]. *In situ* generated mixed carbone **156** proved to coordinate to the boron centre thereby leading to the clean formation of a boron–ate complex as evidenced by the appearance of a new distinct ^{11}B NMR signal at –37 ppm [**233**; Scheme 4.48 e)]. The reaction between CDP **152** and BH_3 has already been reported.[147] In accordance with literature, CDP **152** was treated with BH_3•SMe_2 (2.0 equiv) to form bis-adduct **200** with a chemical shift at –24 ppm [Scheme 4.48 f)].[147] Finally, the use of CDC **159** resulted in the display of a new chemical shift at 25 ppm [d, J = 156.6 Hz; Scheme 4.48 g)], which could be ascribed to a rapid equilibrium between the unreacted BH_3•SMe_2 and the formed boron–ate complex. However, we are cautious, since most of BH_3•SMe_2 remains unreacted. The control experiment between BH_3•SMe_2 and KHMDS formed a signal at 41 ppm, which may be ascribed to an equilibrium between the amide boron–ate complex and a "BH_2 species" generated through intramolecular hydride transfer from boron-to-silicon [Scheme 4.48 h)]. HMDS proved to partially coordinate to the boron centre to form a boron–ate complex with a signal at –1 ppm [q, J = 104.9 Hz; Scheme 4.48 i)].

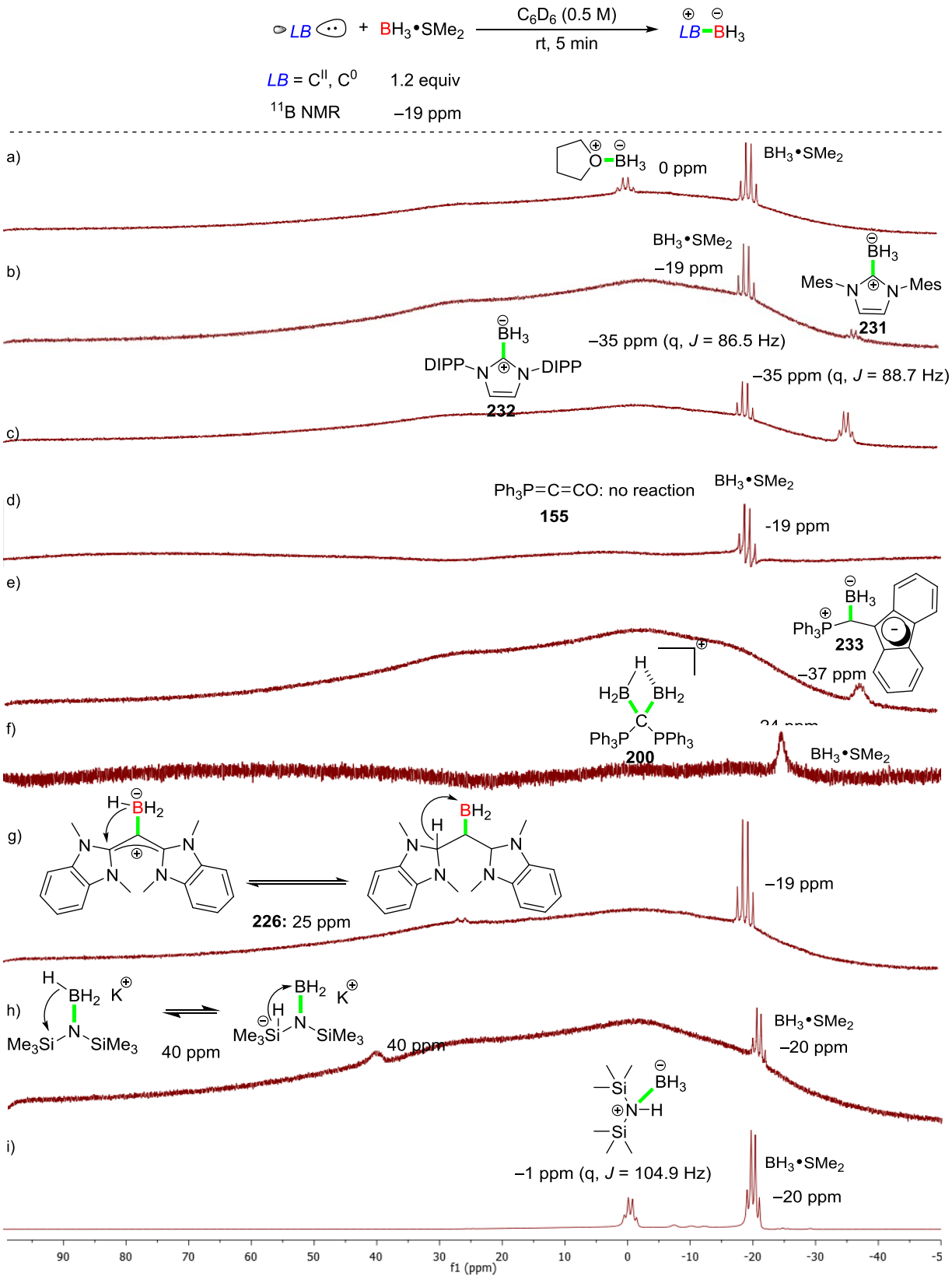

Scheme 4.48: Binding studies of BH_3•SMe_2 with various Lewis bases. For e), h), and i); THF/C_6D_6 (3:1) was the solvent system of the reaction. f) 2.0 equiv of BH_3•SMe_2 were added to the reaction mixture.

The experiments with carbones **153**, **156** and **152** were monitored by ^{31}P NMR spectroscopy (Scheme 4.49). In accordance with ^{11}B NMR spectroscopy, the ^{31}P NMR chart of **153** demonstrated only the chemical shift of the starting material [3 ppm; Scheme 4.49 a)]. In contrast, the use of **156** led to formation of **233**. In ^{31}P NMR spectroscopy, three distinct signals were displayed. The chemical shifts at –5 ppm (free **156**)[126] and 30 ppm (minor) were detected, however, the dominant peak was detected at 21 ppm [Scheme 4.49 b)]. The latter corresponds to boron–ate complex **156**. In ^{11}B NMR spectroscopy, treatment of CDP **152** with BH_3•SMe_2 formed species, which correspond to a chemical shift at –24 ppm. The nature of this species was confirmed to be **200** by ^{31}P NMR spectroscopy in accord with Frenking *et al* [21 ppm; Scheme 4.49 c)].[147]

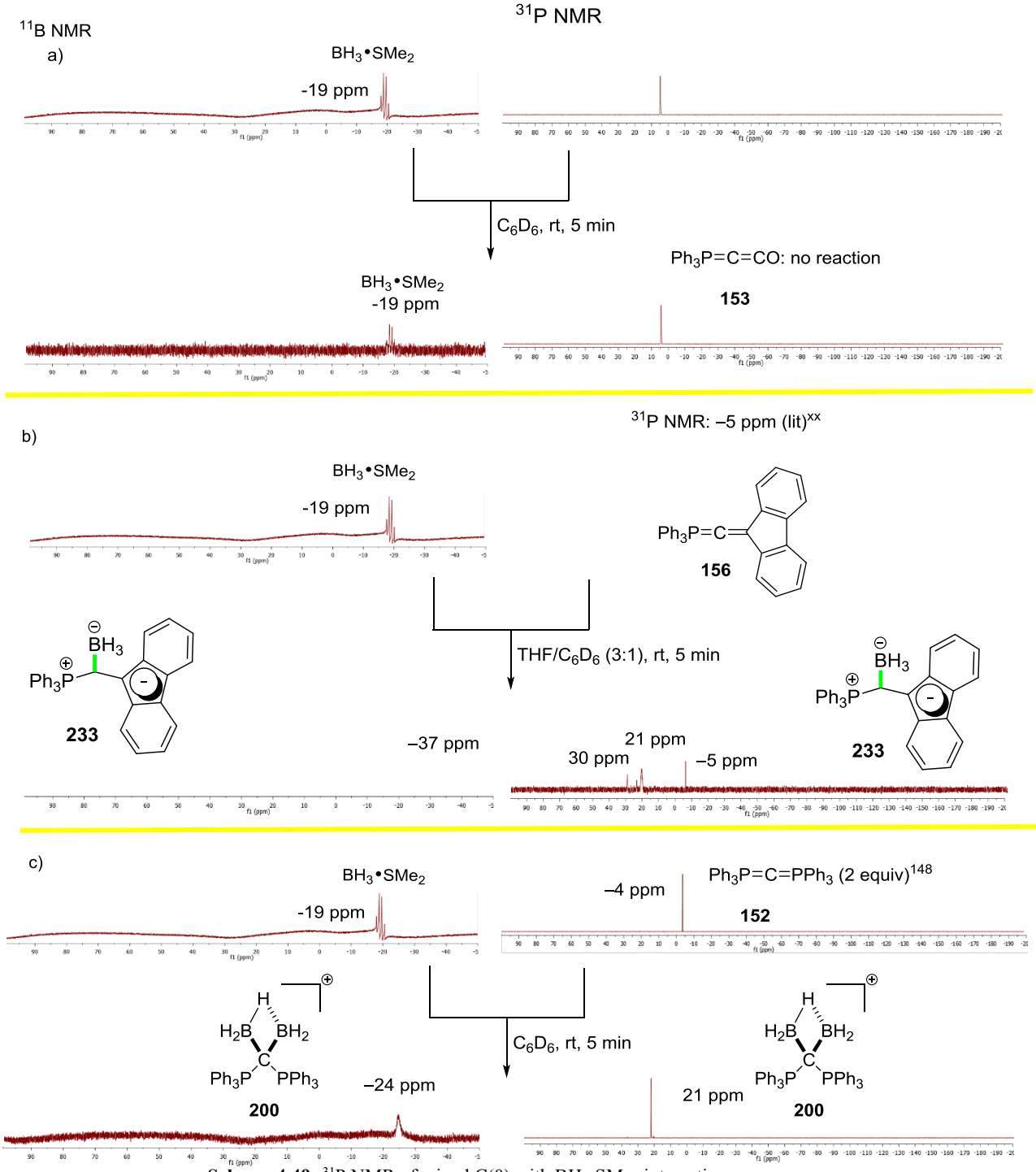

Scheme 4.49: ^{31}P NMR of mixed C(0) with BH_3•SMe_2 interaction.

4.4 Summary and Future Work

4.4.1 Summary

In this chapter, the Lewis basicity of various carbon Lewis bases, including carbenes and carbones, was examined towards binding with a range of boron Lewis acids. This reactivity was investigated with ^{11}B NMR spectroscopy and where applicable, ^{31}P NMR spectroscopy. The most important results were obtained using mixed carbone **156**. Studies of **156** with BEt_3, MeO–B(9-bbn), HB(pin), H–B(9-bbn), BH_3•SMe_2 gave the most interesting results. Based on ^{11}B NMR and ^{31}P NMR chemical shifts, the new species formed either were in equilibrium witht the starting materials or formed clean boron–ate complexes.

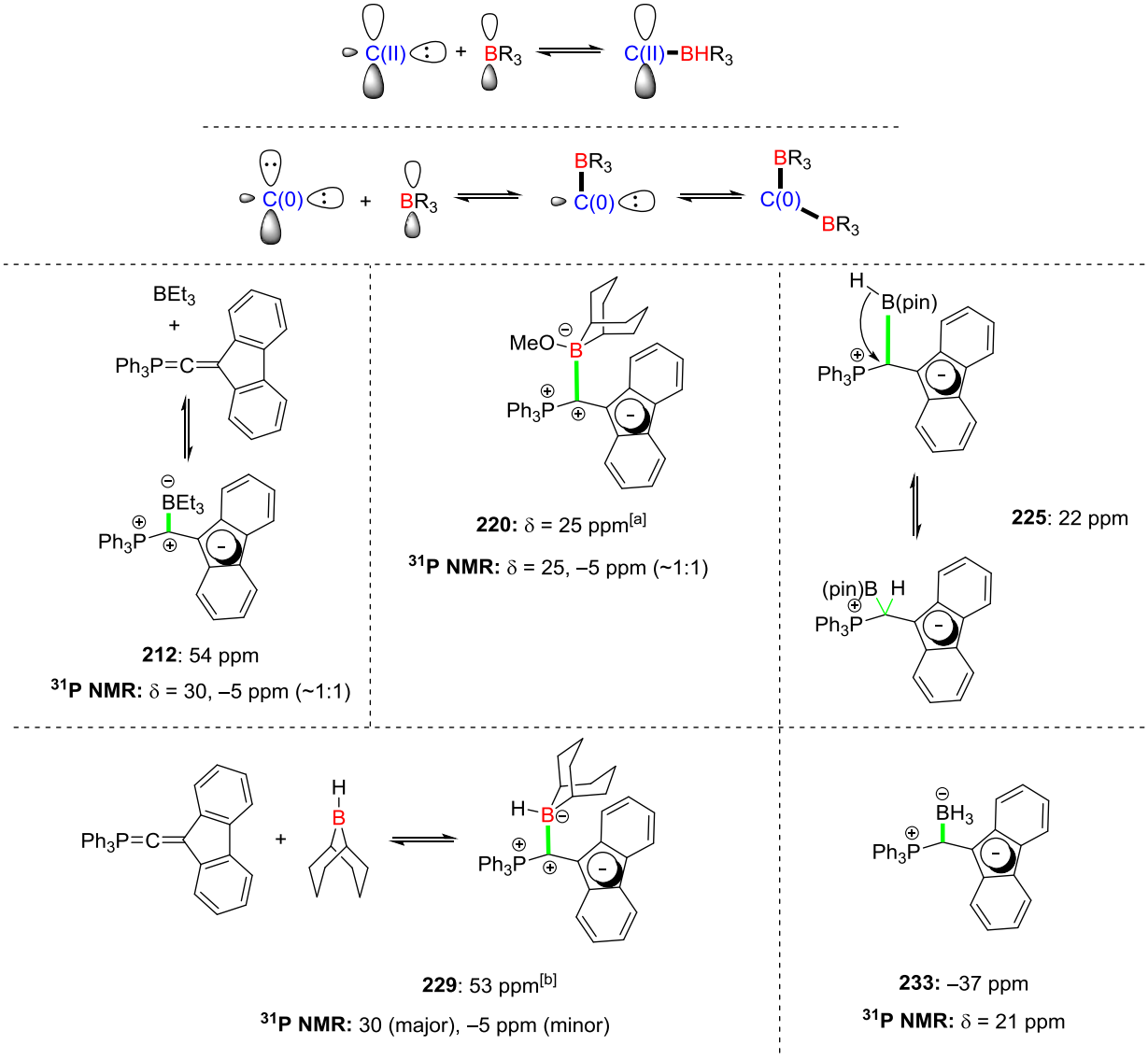

Scheme 4.50: 11B and 31P NMR binding study of C(II) and C(0) species onto various boron Lewis acids.

4.4.2 Metal Complexation and Catalytic Applications of Carbodicarbenes (CDCs)

Lewis acid catalysis using CDC-metal complexes

In the course of our studies, various groups have reported methodologies of Lewis acid catalysis using CDC–metal complexes. Meek *et al.* reported the complexation of CDC-pincer ligand to rhodium(I) chloride to form metal species bearing a tridentate CDC ligand (**234**; Scheme 4.51).[150] This metal complex was used as Lewis acid catalyst for intermolecular hydroamination of a diene; the latter was treated with a secondary amine (1.1 equiv) and catalyst (1–5 mol%) in chloro-benzene and heating (50–80 °C) to generate the intended product in 14–96 % yields. While the metal complex itself displayed poor catalytic activity combined with silver(I) tetrafluoroborate, a highly active catalyst was generated *in situ* (anion metathesis). Indeed, silver(I) chloride precipitated and the rhodium complex with tetrafluoroborate as counter anion proved to be more Lewis acidic; it coordinated to phenyl-1,3-butadiene and activated the terminal C=C bond. In the next step, the nucleophilic secondary amine may attack at the γ-position demonstrating excellent regioselectivity (>98%). This methodology could also tolerate primary amines. The same concept was applied successfully to C–C cross coupling and hydroarylation.[150,151] In addition, Stephan *et al.* reported ruthenium complexes of CDCs as excellent catalysts for the hydrogenation of inert olefins.[152] All these examples represent 'classical' Lewis acid catalysis where the carbone was utilized as a ligand to the metal center.

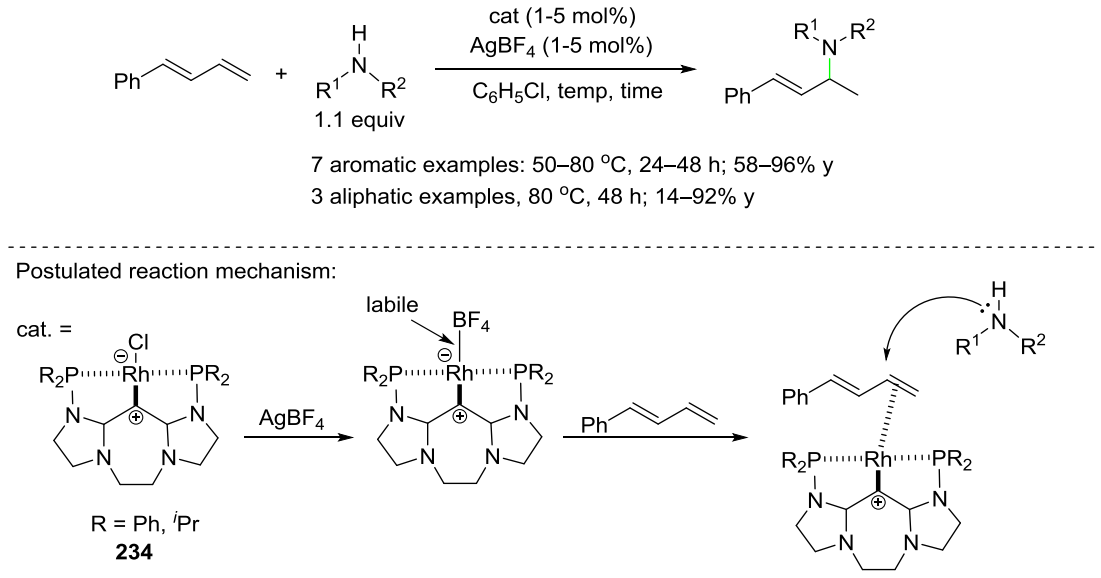

Scheme 4.51: Intermolecular hydroamination of 1,3-Dienes catalysed by CDP-Rh complexes.

Lewis base catalysis using non-symmetric CDCs

In 2015, Ong *et al.*[153] reported a new method for the preparation of carbones and especially a new class of non-symmetric CDCs (Scheme 4.52). Indeed, two different species are required and the reaction proceeds through S_N2 nucleophilic substitution. This method can be applied to the preparation of mixed carbones as well. The non-symmetric carbone was successfully used for the catalytic preparation of methylamines. An excess of H–B(9-bbn) (4.0 equiv) were added; one equivalent was used to reduce carbon dioxide and another equivalent was utilized to react readily with primary and secondary amines to form the corresponding borylated amides. Insights into the mechanism led to the isolation of the intermediate **235**. The Lewis basic centre of the CDC coordinated to the empty p orbital of the boron atom and the hydride was released. The latter carried out nucleophilic attack to the carbon in vicinity (benzoimidazolylidene ligand unit) to undergo formally a hydroboration and give **235**.

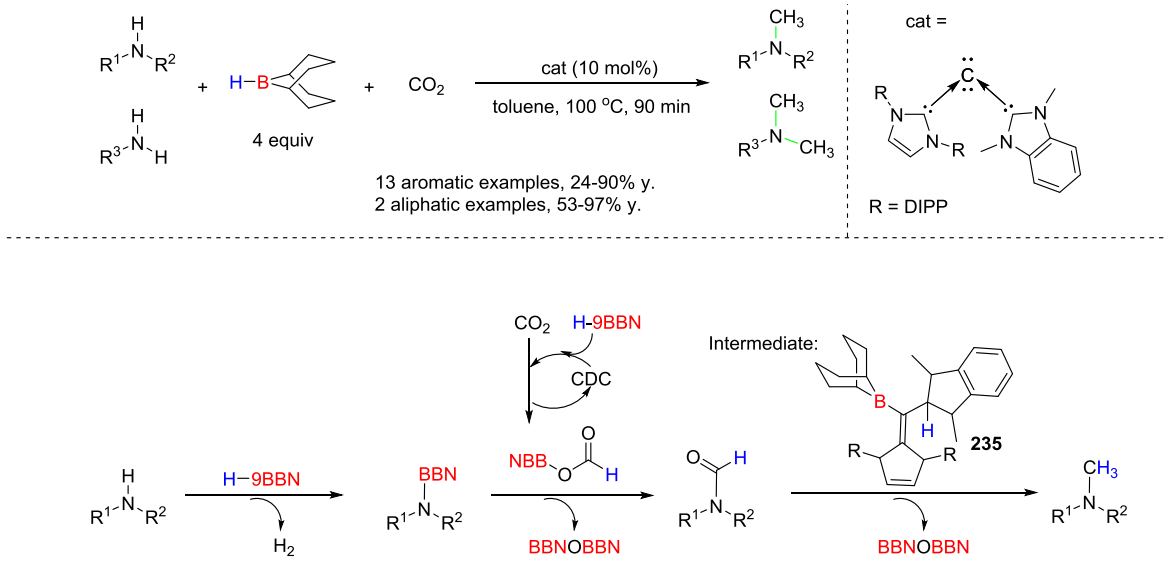

Scheme 4.52: Unsymmetrical CDCs employed into Lewis base catalysis.

Inspired by the progress in the field of Lewis acid catalysis the last few years using CDCs as strong σ donors to the metals, we decided to investigate further the potentials of the mixed carbones as ligands for metal complexation. One of our major goals was to synthesize metal complexes, examine their electronic properties and use them to either dual catalysis or simple Lewis acid catalysis. Mixed carbone **158** exhibited outstanding σ donor ability and the already reported metal complexes of this compound proved to be air- and moisture-stable.[126] We carried out preliminary study and for this purpose, gallium(III), In(III) and Zn(II) metal salts were selected. Herein, we present briefly the proof of principle, the procedures and the preliminary NMR data that was obtained. First of all, the precursor of mixed carbone **158** exhibited a chemical shift at 14 ppm in ^{31}P NMR spectroscopy ([Figure 4.10 a)]. The chemical

shift of the mixed carbone **158** was reported at –5 ppm at –78 °C, however, it decomposes at room temperature.[126] Thus, in all operations, metal salts were added to *in situ*-generated **158** at –78 °C (Figure 4.10 b)].

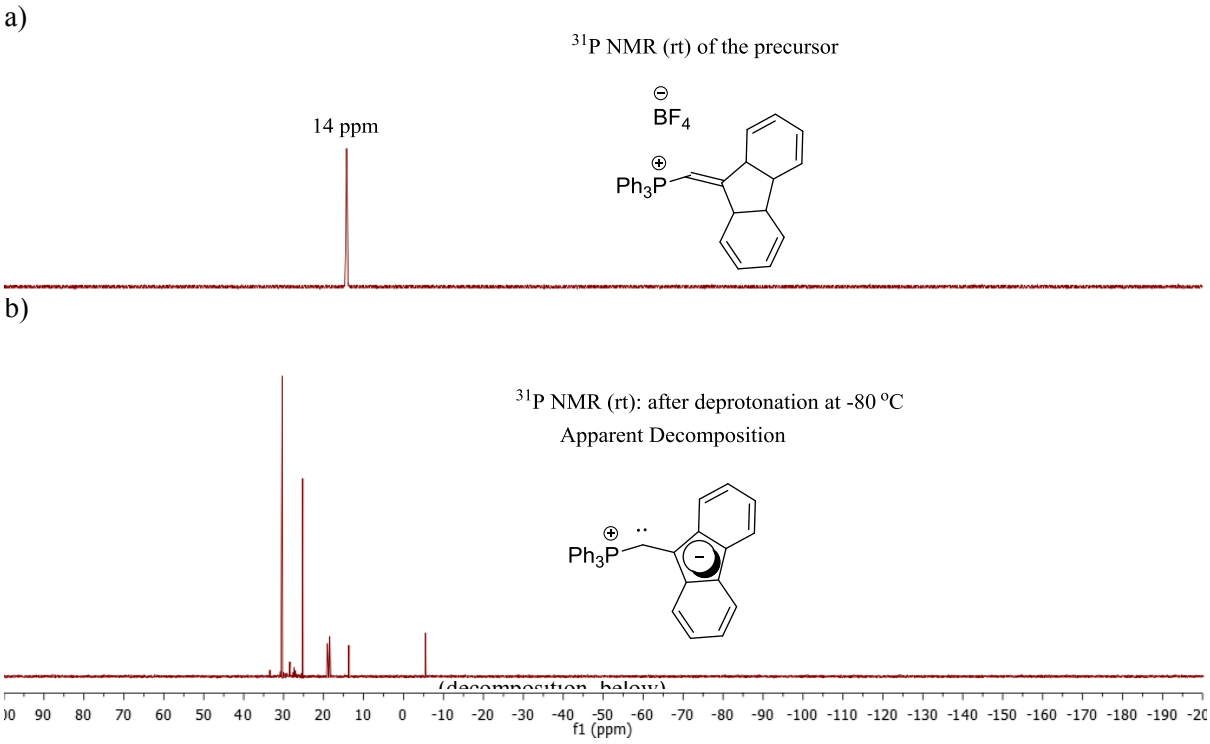

Figure 4.10: a) ^{31}P NMR of **172** b) ^{31}P NMR of decomposed **156** at room temperature

C(0)–Ga(III) **236** complex was prepared in a fairly simple process (Scheme 4.53). The precursor of the mixed carbone **156** was deprotonated *in situ* using KHMDS (1.0 equiv) at low temperature (–78 °C). Gallium(III) chloride (1.0 equiv) was added at the same temperature to provide **236** complex at 20% yield.

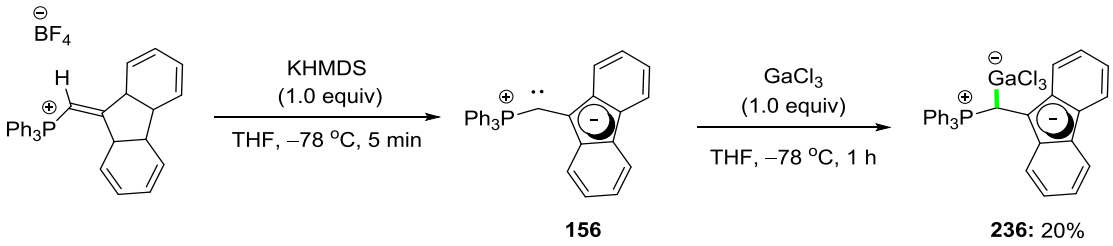

Scheme 4.53: Preparation of Ga–C(0) **236**.

The formation of the metal complex was confirmed by ^{31}P and ^{71}Ga NMR spectroscopy (Figure 4.11). After the work-up, a yellow substance could be isolated and provide a single signal at 14 ppm in ^{31}P NMR spectroscopy. This was identical with the chemical shift of the precursor, however, it has been confirmed that it was fully deprotonated following this

process. Nonetheless, the electronic environment around the phosphorus atom would be similar if the acidic proton of the precursor would be replaced by a metal atom [in this case gallium(III)]. This hypothesis was further supported by ^{71}Ga NMR. The newly formed metal complex coordinates to the gallium(III) chloride exhibiting a ^{71}Ga NMR signal at 250 ppm. As this is in accord with literature findings of Mes and DIPP–Ga(III) complexes, it is a proof that the three atoms of chloride were attached to the gallium(III) atom of the newly formed metal complex.[154]

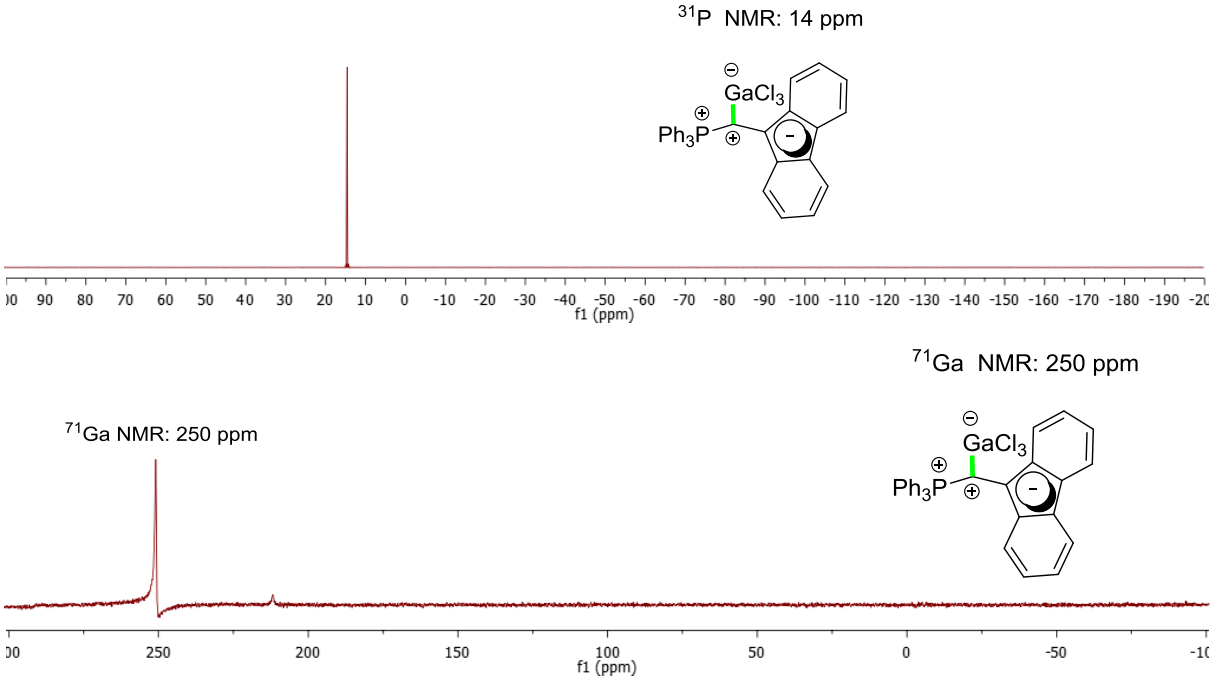

Figure 4.11: ^{31}P NMR and ^{71}Ga spectra of the Ga(III)– C(0) **156** complex or **236**.

Indium(III)

Similarly to **236**, C(0)–In(III) **237** was prepared with *in situ* deprotonation of pre-C(0) **156** at –78 °C using KHMDS (1.0 equiv) and immediate addition of indium(III) chloride (1.0 equiv) to form complex **237** in 70% yield (Scheme 4.54).

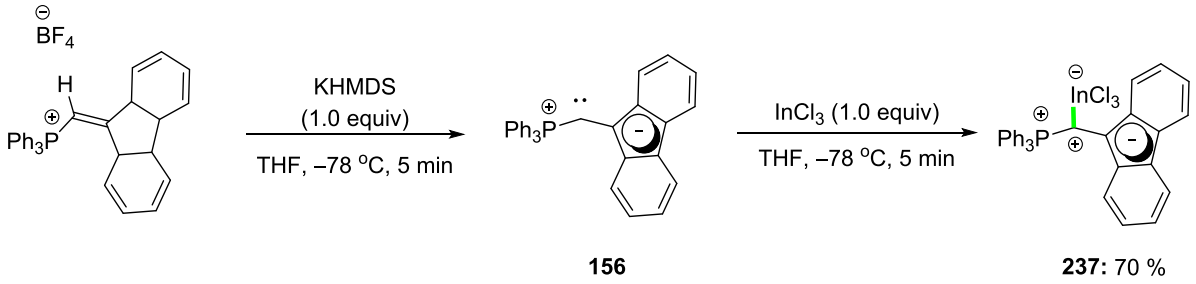

Scheme 4.54: Preparation of the In(III)–C(0) **237.**

The chemical shift of **237** in ^{31}P NMR spectroscopy was also at 14 ppm and was isolated in 70% yield (Figure 4.12).

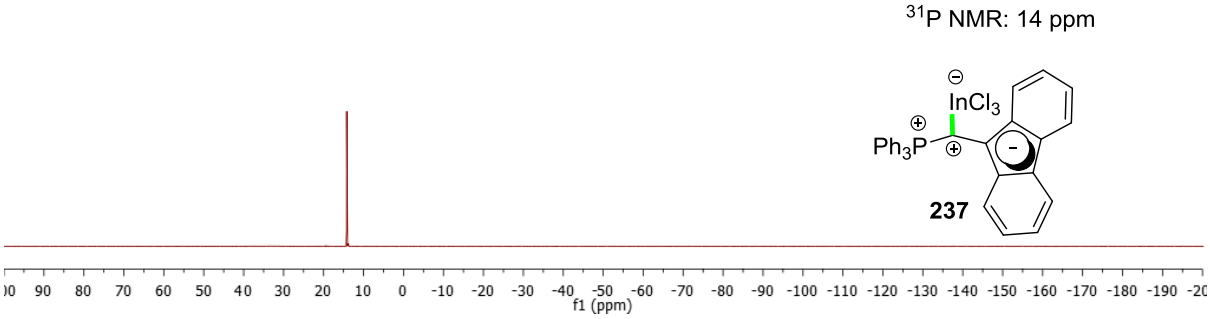

Zinc(II)

C(0)–Zinc(II) **238** was prepared with *in situ* deprotonation of pre-C(0) **172** at low temperature using KHMDS (1.0 equiv) and immediate addition of the zinc(II) chloride to form the intended product in 21% yield (Scheme 4.55).

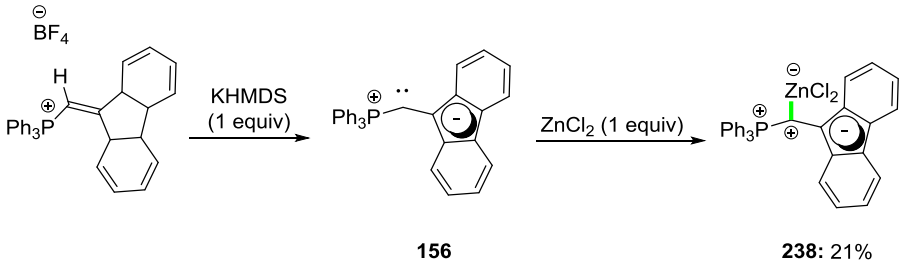

Scheme 4.55: Formation of the C(0)– Zn(II) **238** complex.

The chemical shift of **238** in ^{31}P NMR spectroscopy was identical with gallium(III) and indium(III) metal complexes (Figure 4.13), however, the yield was poor (21%).

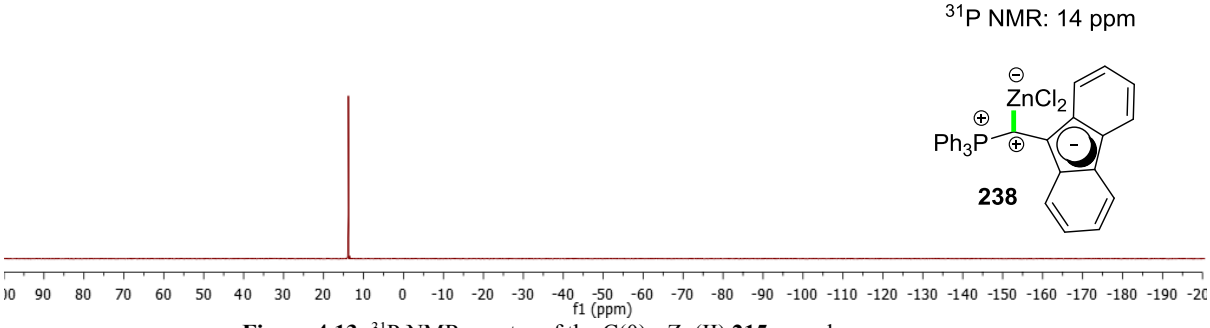

Figure 4.13: ^{31}P NMR spectra of the C(0)– Zn(II) **215** complex.

Next, we intend to isolate these compounds in pure form and obtain crystal structures in order to be able to study the sterics and electronics of the metal complexes. Indeed, we are keen to investigate their potentials in the field of Lewis acid and dual catalysis.

5 Silicon(0) or Silylones

5.1 Introduction

5.1.1 Concept – Silicon(0) vs. Carbon(0) Compounds

Silicon is located in main group 14 and is the higher homologue of carbon. While carbon is considered as a non-metal, silicon displays a metalloid character. Typically, for both elements structures are preferred where carbon and silicon form four bonds with neighboring atoms (*tetravalency*). However, Bertrand[155] and Arduengo[8] gave a new perspective when they reported independently the preparation and characterization of stable carbenes; these represent neutral *divalent* carbon species with a central carbon atom in the formal '+II' oxidation state. Importantly, recent investigations went beyond carbenes and new divalent carbon-based species have been reported where the central carbon atom is in formal '0' oxidation state; these compounds have been termed *carbones* (Scheme 5.1).[9] In these molecules, the central carbon atom was proposed to be *sp^2-type* hybridized with two lone pairs available for chemical reactivity. The first lone pair is located in the sp^2 orbital, while the second one is in the p orbital. C(0) compounds have been calculated to be more basic than carbenes.[17] The silicon-based analogues of carbenes, so called 'silylenes' [Si(II)], have been reported as well (Scheme 5.1).[9,156–160] The latter are neutral divalent species with a lone pair at the central silicon atom. These species are isolable and stable at room temperature under an inert atmosphere. Here again, the central silicon atom has an occupied sp^2 orbital with a lone pair and a vacant p orbital. However, in contrast to carbenes, Si(II) species have displayed limited applications (e.g. radical chemistry). In analogy to low-oxidation state carbon species, silicon-based homologues of C(0) compounds were reported, so-called 'silylones' [Si(0); Scheme 5.1]. In certain of these species, the central silicon atom is divalent with a formal '0' oxidation state with two lone pairs available for chemical reactivity.[11] The first lone pair is located in the sp^2 orbital at silicon; the second one is located in the p orbital with the largest extension at the silicon atom, while it exhibits a significant Si–C π bonding (Scheme 5.1).[11,161–163] Several silylones have demonstrated outstanding stability at room temperature under an inert atmosphere and also high thermal stability (decomposition point >150 °C).[161,164] As it has been reported for C(0) compounds, in an allene-type frame X=Si=X –when X is a strong σ donor and a weak π acceptor– the overall structure is bent.[9,15,16,116,165–167]

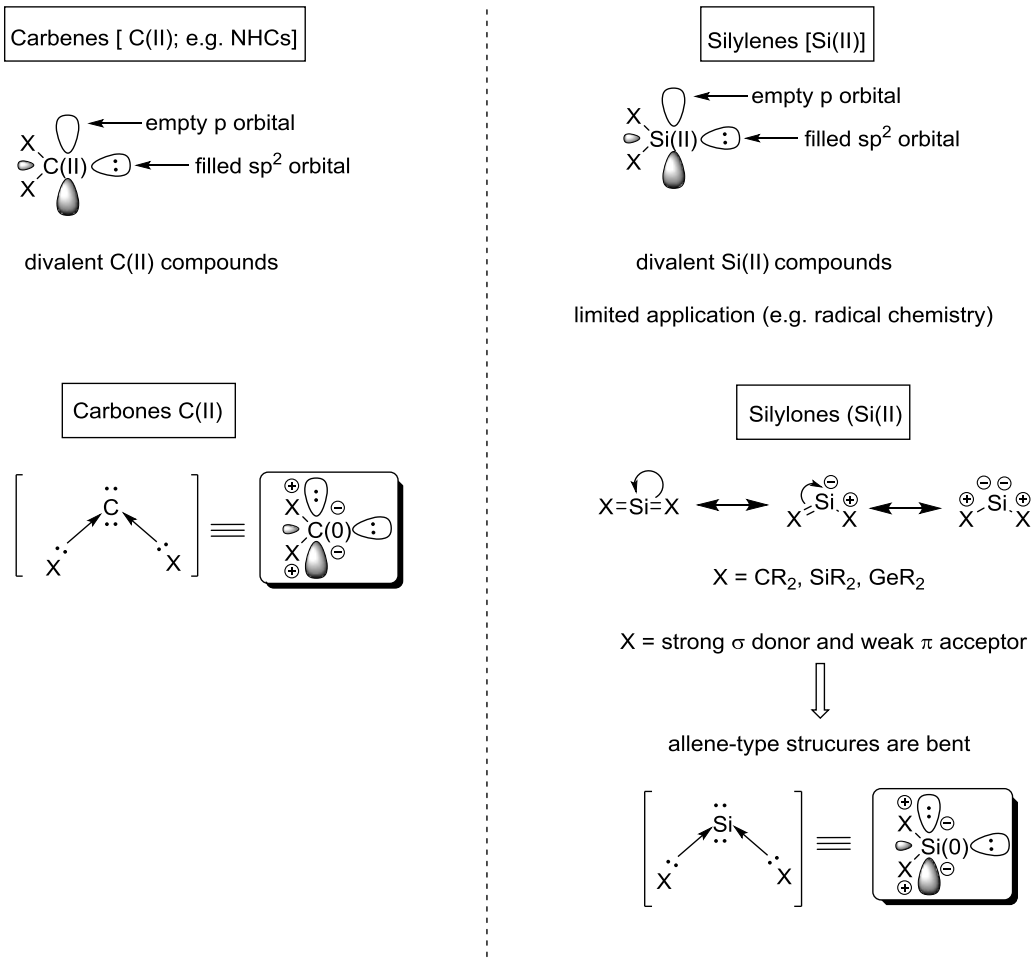

Scheme 5.1: Divalent low-oxidation *carbon* vs. *silicon* species.

In 2009, Fürstner *et al* reported a rationalisation of evidently considerable Lewis basicity of silylenes.[9] Although NHCs are represented with a lone pair of electrons to the central carbon, a resonance form with a diazobutadiene ligand that donates into a C(0) atom was suggested.[9] Indeed, the lone pair in the p orbital will not remain localized, since such a localization would result in reduction of the aromatic character.[9] In the correspondent silylene, a structure with a second lone pair localised at the silicon centre would have greater importance due to the less favourable orbital overlap *between* the two nitrogens *and* the central carbon.[9] Even though these species are known as Si(II) ligands, their tendency to undergo gem-dimetallation may conceal evidence of greater Lewis basicity compared to NHCs.[9] In 2012, Phukan *et al.* reported a computational study that compared directly the effect of NHC ligands coordinated to the carbon and silicon atom in C(0) and Si(0) structures, respectively.[168] Quantum chemical calculations suggested that π donating and σ electron-withdrawing substituents of NHCs, i.e., NR groups affect the basicity of C(0) and Si(0) compounds.[168] Indeed, the strength of the NHC–C(0) bond has proved to depend on the π accepting ability of the NHCs, i.e., the strength of the NHC–C(0) increases with the π accepting ability of the NHCs.[168] Natural bond orbital

analysis (NBO) *and* atoms in molecules analysis evidenced that between C_{NHC}=C=C_{NHC} and L→C←L suggested geometries of $(NHC)_2C(0)$, the former should be preferred.[168] However, 'visual inspection of the frontier orbitals of $(NHC)_2C(0)$ reveal that these compounds have two lone pairs with a higher coefficient at the central carbon atom'.[168] In contrast, both natural bond orbital analysis (NBO) and atoms in molecules analysis strongly indicated that for silylones, the structure with the dative bonds was more favourable compared with the structure with two double bonds (the L→Si←L and C_{NHC}=Si=C_{NHC}, respectively).[168] In addition, although the 1st proton affinity (PA) of C(0) compounds proved to be higher than for Si(0) compounds, the 2nd PA of the latter prevailed over the one of the C(0) species. Considering the great Lewis and Brønsted basicity that silylones displayed in the computational studies, we decided to investigate their catalytic potential.

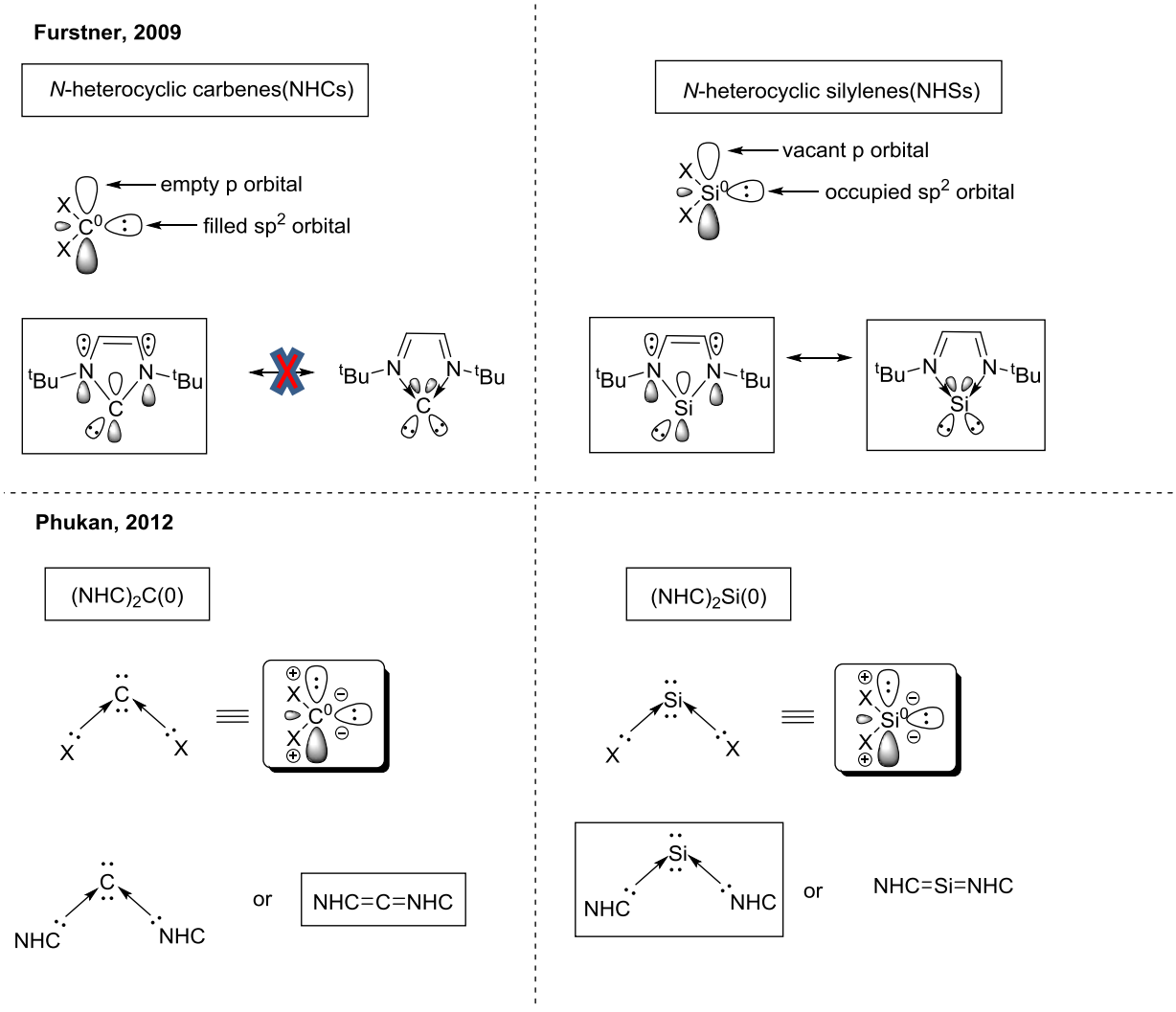

Scheme 5.2: Comparison of electronics and sterics of divalent *carbon* and *silicon* species.

5.1.2 Literature-Known Silicon(0) Compounds

To date, six silylones [Si(0)] have been reported. Kira *et al.* reported silylone **239** in 2003 (Figure 5.1).[164] Initially, this silylone was described as a 'silicon-based allene analogue with a formally sp-hybridized silicon atom'. However, Frenking *et al.*[169] suggested a rather coordinative structure, i.e, a 'divalent species that exhibits two X→Si donor–acceptor bonds and two molecular orbitals of σ and π symmetry'.[9] Indeed, the crystal structure demonstrated a bent geometry with a Si−Si−Si bond angle of 136.5°, very close to a 120° bond angle expected for an ideal sp^2 hybridization.

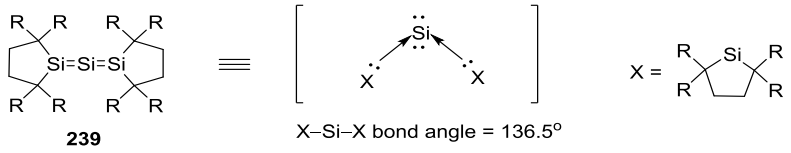

Figure 5.1: The first Si(0) compound reported by Kira *et al.*[164]

The same group reported the synthesis of silylone **240**, an analogue of **239** with modified ligand structure (Figure 5.2).[170] The Lewis basic centre of those ligands is not a silicon atom, but a germanium atom (germylene ligands). The Ge−Si−Ge bond angle of **240** was found to be 125.7°, which is consistent with the theoretical calculations.[170] Sekiguchi *et al.* reported the preparation of silylone **241** (Figure 5.2).[171] In contrast to the earlier Si(0) compounds, no crystal structure was obtained. Thus, *ab initio* calculations were required to determine the Ge−Si−Ge bond angle of 164.4°.[171] This value means that the structure is not as severely bent as the other silylones. More recently, Stalke *et al.* reported the preparation and characterization of carbene-supported silylones **242** and **243** (Figure 5.2).[11] Here, the Si=Si=Si frame has been replaced by a C=Si=C pattern. For this purpose, CAACs were selected as ligands to coordinate to the central silicon atom. Bertrand *et al.* reported a study of increasing nucleophilicity and electrophilicity of carbenes based on sterics and electronics, in which a CAAC proved to be more nucleophilic and more electrophilic than NHCs and thus, stronger σ donor and stronger π acceptor.[172] Bis(carbene)-supported silylone **244** was prepared by Driess *et al.*[163] The differences in structural and electronic properties compared with **242** and **243** were highlighted (Figure 5.2). In the crystal structure of **244**, X-ray crystallographic analysis has confirmed that the C−Si−C bond angle is 89.1°, in contrast to 120° for **242** and **243**. Moreover, the chemical shifts of the central silicon atom in ^{29}Si NMR spectroscopy were shown to be very distinct (−80.1 ppm for **244** and 66.0 ppm for **242**). Driess *et al.* suggested that this striking difference between the two Si(0) compounds may be ascribed to both the stronger σ donor and weaker π acceptor ability of the bis(NHC) ligand

compared to CAACs and the acute C−Si−C bond angle. The outcome of calculations –GIAO (Gauge Independent Atomic Orbitals), NBO (Natural Bond Analysis), and 1st and 2nd proton affinities– was in agreement with this suggestion.

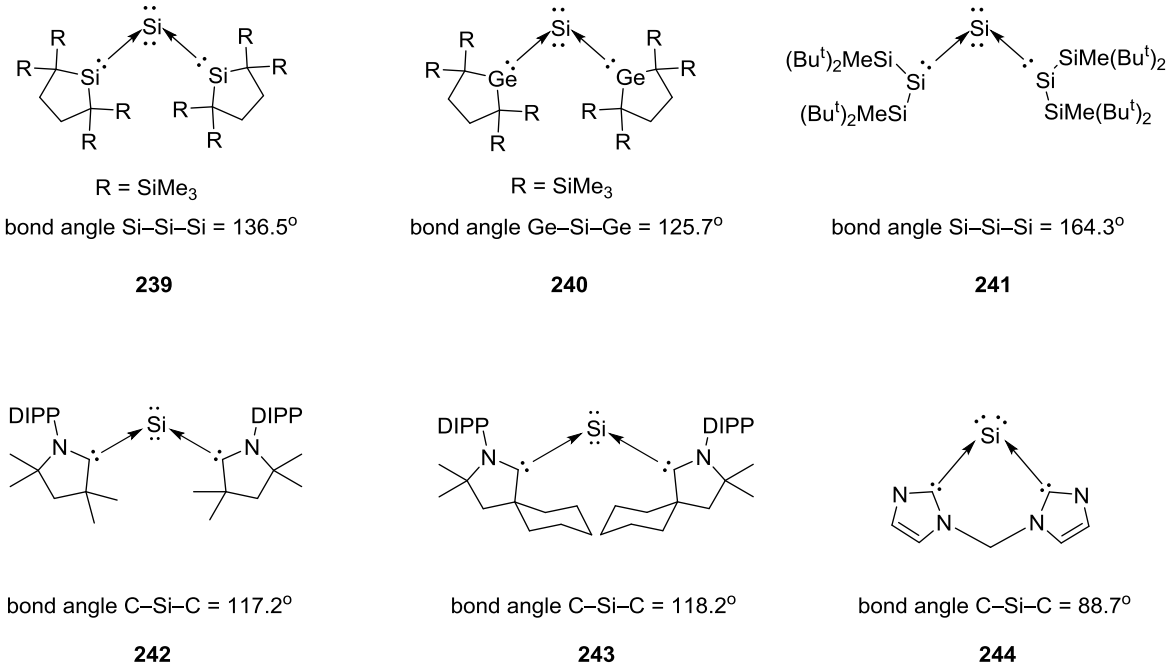

Figure 5.2: Overview of reported silicon(0) compounds.

In order to simplify the synthetic schemes, the linear sila-allene structure has been used in the following paragraphs instead of the structure suggested on literature (Scheme 5.3).

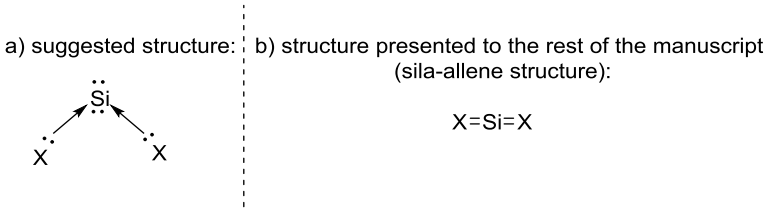

Scheme 5.3: a) suggested structure based on literature.[9,15,16,116,165–167] b) structure used to the rest of the manuscript.

5.1.3 Synthetic Routes to Silicon(0) Compounds

In 2003, Kira *et al.* published the synthesis of the first silylone, compound **239** (Scheme 5.4).[164] Silylene **245**[173] was treated with silicon tetrachloride (9.0 equiv) in THF at room temperature to give the corresponding disilane, tetrachlorodisilane **246**, in 72% yield. Subsequently, potassium graphite (4.0 equiv) was used as a reducing agent at −40 °C to generate trisila-allene **216** in 74% yield. The latter was reported to be stable at room temperature, air- and moisture-sensitive, and thermally stable.

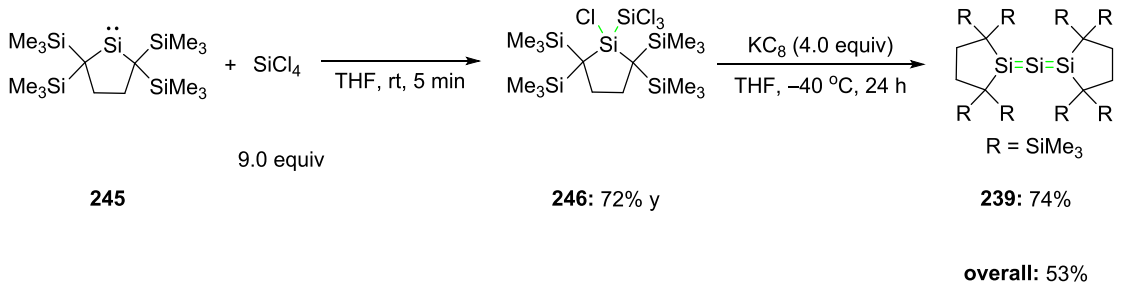

Scheme 5.4: Synthesis of Si(0) compound **239** reported by Kira *et al.*[164]

Silylone **240** was prepared according to the same method, i.e., an initial oxidative insertion of the Ge(II) species **247**[174] into the Si–Cl bond of silicon tetrachloride to form **248** (Scheme 5.5). The latter was reduced by potassium graphite (4.4 equiv). However, **240** was obtained in a considerable lower overall yield compared to the synthesis of **239** (19% and 53%, respectively).[170] Germylene ligands **247** were treated with tetrachlorosilane (5.6 equiv), and the resulting chloro(trichlorosilyl)germane **248** was isolated in 80% yield. **248** was treated with potassium graphite (4.4 equiv) at low temperature to afford **240** in 24% yield.

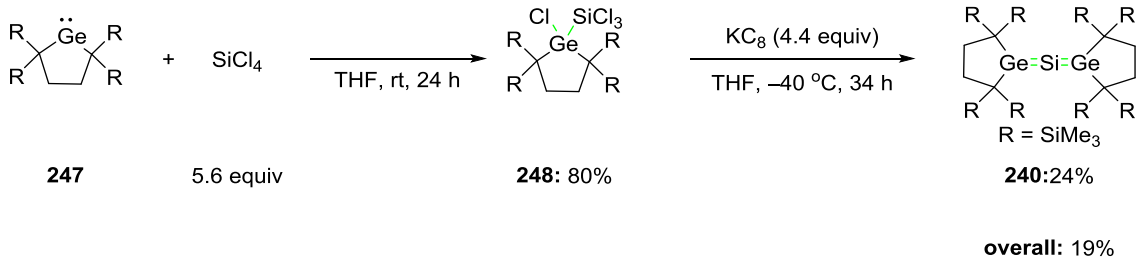

Scheme 5.5: Silylone **240** reported by Kira *et al.*[170]

Treatment of silacyclopropene **249**[175] with lithium (9.0 equiv) in THF at room temperature led to formation of dilithiosilane **250** in 40% yield (Scheme 5.6).[171] **250** was then reacted with NHC-stabilized dichlorosilylene **251** (0.9 equiv) in benzene at room temperature to give Si(0) species **241** in 80% yield.

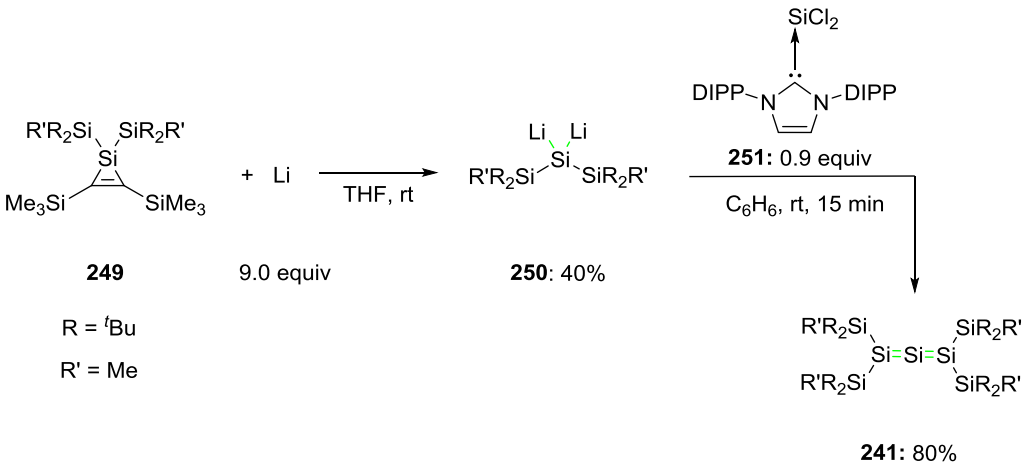

Scheme 5.6: Silylone **241** reported by Sekiguchi *et al*.[171]

Stalke *et al.* reported the synthesis of carbene-supported silylones **242** and **243** (Schemes 5.7 and 5.8). The Si=Si=Si pattern was replaced by a C=Si=C axis.[11] Bertrand *et al.* displayed a study of increasing nucleophilicity and electrophilicity of carbenes.[172] In this investigation, CAACs were found more nucleophilic and more electrophilic than NHCs. This outcome can be rationalised by the fact that NR group of NHC (σ-electron withdrawing, π-donating) was replaced by a quaternary carbon center (σ-electron donating, non π-donating). An exchange between CAAC ligand **252** (3.0 equiv) and the NHC-stabilized dichlorosilylene (**251**; IPr−$SiCl_2$) in THF afforded the CAAC-stabilized biradical **253** in 85% yield (Scheme 5.7). **253** proved to be stable at room temperature under an inert atmosphere. In accord with the preparation of the previously reported silylones, the formed biradical was reduced using potassium graphite (2.0 equiv) to give silylone **242** in 85% yield.

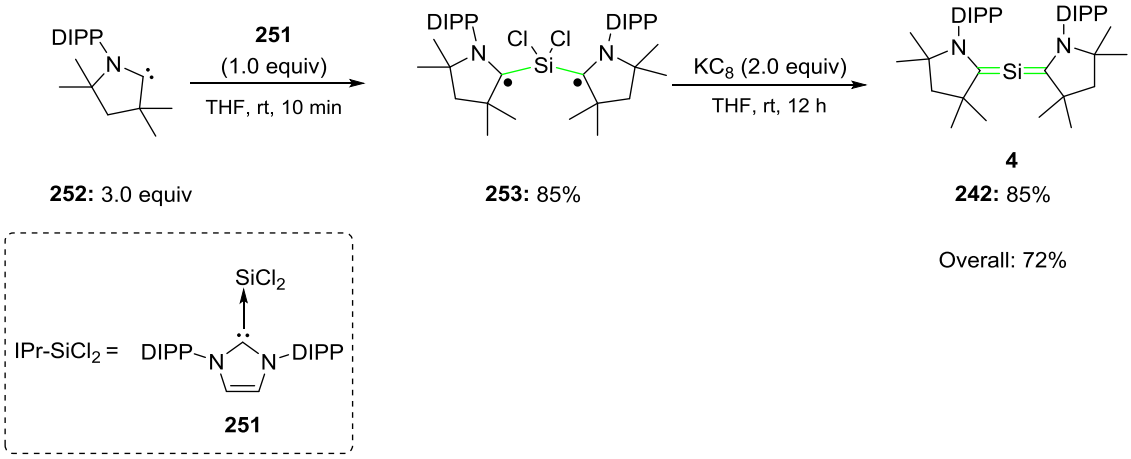

Scheme 5.7: The first reported Si(0) analogue bearing a C=Si=C pattern.

The same methodology was applied to the preparation of silylone **243** (Scheme 5.8).[161] Here, in the CAAC ligand structure, the germinal diethyl group (**253**) was replaced by a cyclohexyl

group (**254**), which has increased the steric demand of the C(II) ligands. In analogy to the earlier syntheses, **254** was treated with **251** (1.0 equiv) in THF at room temperature to give **255** in 80% yield. The latter was treated with KC_8 (2.0 equiv) to afford **243** in 95% yield.

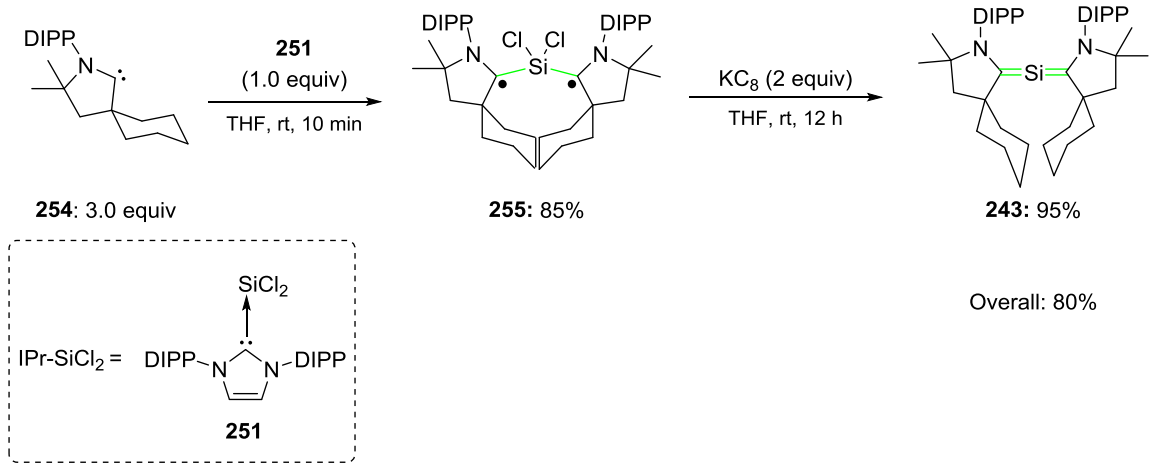

Scheme 5.8: Slightly modified Si(0) analogue bearing a C=Si=C pattern.[161]

Driess *et al.* reported the synthesis of silylone **243**, which contains bis(NHC) **256** as a supporting bidentate ligand (Scheme 5.9).[163] In this species, two carbenes are ligated by a methylene group, which may be the reason for a quite strained structure (C−Si−C = 90°). The bis(NHC) was treated with IPr−$SiCl_2$ (**251**) to form chlorosilyliumylidene **257** in 57% yield. Here, sodium naphthalide was used as a reducing agent to give silylone **243** in 68% yield.

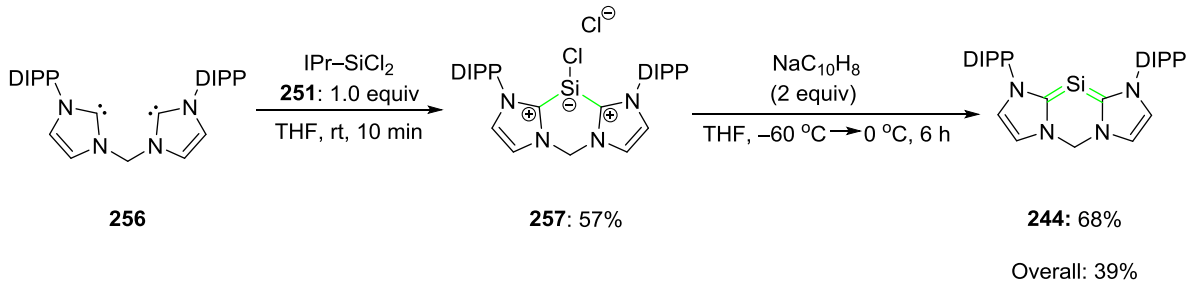

Scheme 5.9: Silylone **243** reported by Driess *et al*.[163]

5.1.4 Stoichiometric Applications of Silicon(0) Compounds

To date, a few stoichiometric applications of silylones have been reported. Silylone **239** was shown to react readily with water at room temperature to form the corresponding 1,3-dioxy-trisilane in 74% yield (Scheme 5.10).[176] Similarly, methanol and ethanol gave the same type of products in 92% and 94% yields, respectively. Less acidic alcohols, such as isopropanol

and *tert*-butanol, proved to be unreactive towards silylone **239**. The latter reacted with an excess of acetone at room temperature to form the strained bicyclic compound **258**, as confirmed by X-ray crystallography.[176]

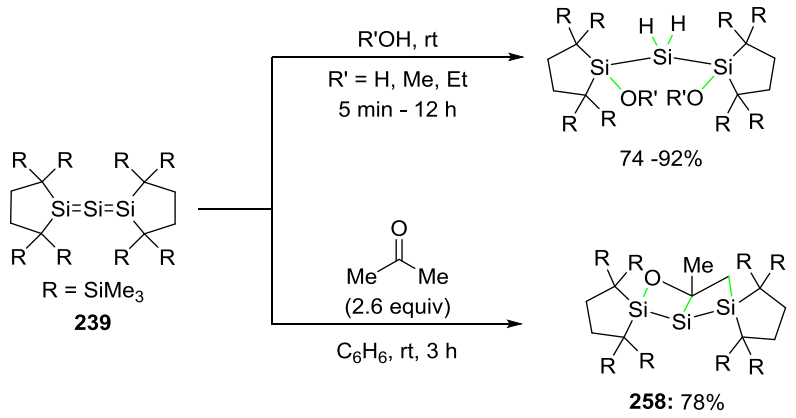

Scheme 5.10: Reaction of silylone **239** with protic solvents and non-protic solvents.

Furthermore, silylone **239** was treated with a large excess of carbon tetrachloride to form **259** in 95% conversion, as confirmed by ^{1}H and ^{29}Si NMR spectroscopy (Scheme 5.11).[176] Silylone **259** also reacted with methyl iodide (2.8 equiv).[176] Interestingly, a silicon–silicon bond cleavage was triggered to give the iodo(methyl)silane **260** in 90% yield through a formal insertion of a silylene ligand into the C−I bond.

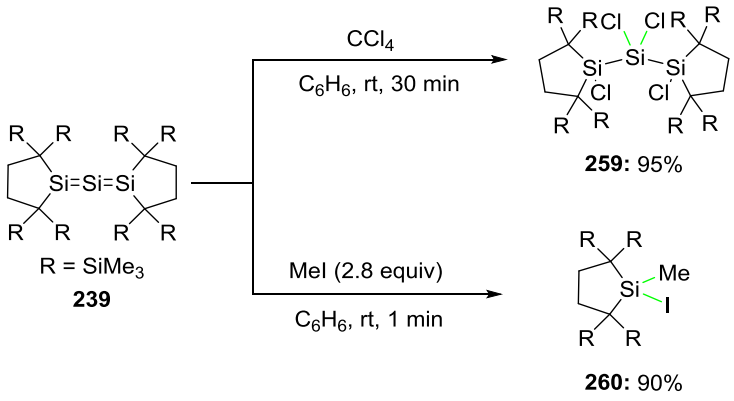

Scheme 5.11: Reaction of silylone **239** with carbon tetrachloride and methyl iodide.

Although silylone **241** was also described as trisila-allene, it displayed different chemical reactivity compared with silylone **239** (Scheme 5.12).[171] Indeed, when **241** was treated with methanol the corresponding 3,3-dimethoxypentasilane **261** was obtained. This result represents a striking difference because the regioselectivity was reversed. Furthermore, silylone **241** exhibited lower thermal stability; in a benzene solution at 120 °C, silylone **241**

underwent a thermal rearrangement to form the more thermodynamically stable cyclotrisilene **262** (Scheme 5.12).[171]

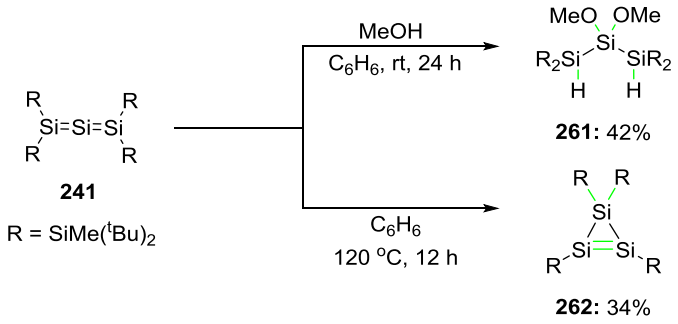

Scheme 5.12: Reported reactions of silylone **241**.

The chemical reactivity of silylone **242** was examined as well (Scheme 5.13).[161] After exposure to air, the central carbon atom of the ligands was oxidized to form the silicon dioxide and corresponding *N*-aryl amide derivative **263** in 93% yield. An alternative access to the same product was shown to be through the reaction between **242** and nitrous oxide (4.0 equiv) in THF at room temperature.

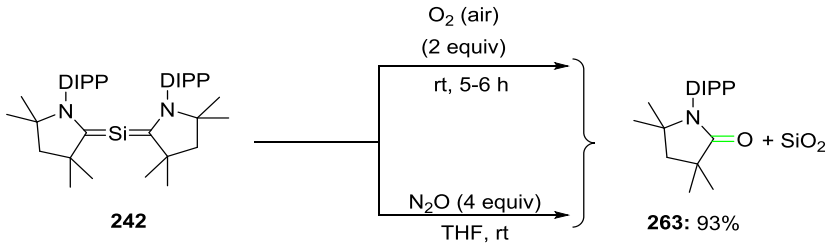

Scheme 5.13: Reported reactions of silylone **242**.

Interestingly, silylone **242** was also activated with a substoichiometric amount of elemental potassium (33%) in THF at room temperature to formally undergo a hydride shift from the tertiary carbon of the isopropyl group to the proximal electrophilic carbon centre (Scheme 5.14).[177] An additional intramolecular C–Si bond was formed to generate a 6-membered cyclic silylene **264**, i.e., the central divalent silicon atom was converted into a three-coordinate silicon atom.

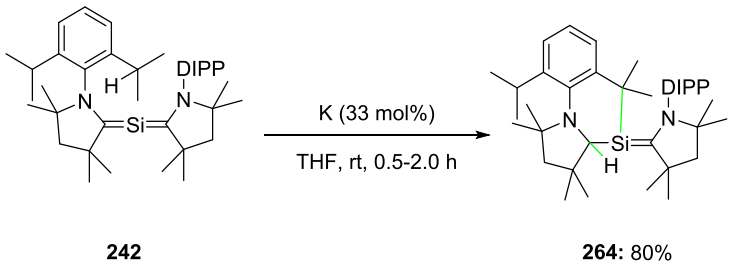

Scheme 5.14: Conversion of silylones **242** to 6-membered cyclic silylene **264** with three-coordinate silicon atom.

5.2 Aims

One of our major goals was the *umpolung* reaction of aldehydes and aldimines using silylones as nucleophilic catalysts. This transformation has already been reported using NHCs. Indeed, one of the most important catalytic applications of NHCs is the *umpolung* of an *aldehyde* (electrophile) to generate the corresponding Breslow intermediate (nucleophile), which may then react with suitable electrophiles to form new C–C bonds. The key to this important reactivity of NHCs was recently shown to be their extremely high *Lewis basicity*.[6] To date however, NHCs were found to be poor *Umpolung* catalysts when *aldimines* were used as substrates. To the best of our knowledge, in this context only one stoichiometric example for C–C bond formation has been reported to date.[178] Thus, the use of potentially more basic silylones may address this issue and new chemistry may be developed [Scheme 5.15 a)]. Another goal was the organocatalytic activation of Lewis acidic pro-nucleophiles [e.g. boron and silicon reagents; Scheme 5.15 b)]. Thereby, an organic rest may be transferred to a suitable electrophile. Furthermore, another potential goal was the development of frustrated Lewis pair chemistry (FLP) by using a suitable Lewis acid as a co-catalyst [Scheme 5.15; c)]. Thus, small molecules may be activated with a pair of sterically demanding silylone and a Lewis acid. Silylone **242** is reasonably bulky, therefore it may not be able to bind to certain Lewis acidic centers to provide a promising FLP. Another worthwhile goal was the use of silylone **242** for preparation of metal complexes with 13th Main group and 1st row transition metals [Scheme 5.15 d)]. Indeed, we were keen to use potentially formed metal complexes in the field of the dual catalysis [Scheme 5.15 e)]. Indeed, one lone pair at the silicon centre would be engaged in metal complexation, while the second lone pair may be available for chemical reactivity. Thus, two catalytic centres may be in vicinity. The metal may act as a Lewis acid to activate an electrophile, while the second lone pair on the silicon may activate a Lewis acidic pro-nucleophile for subsequent bond formation.

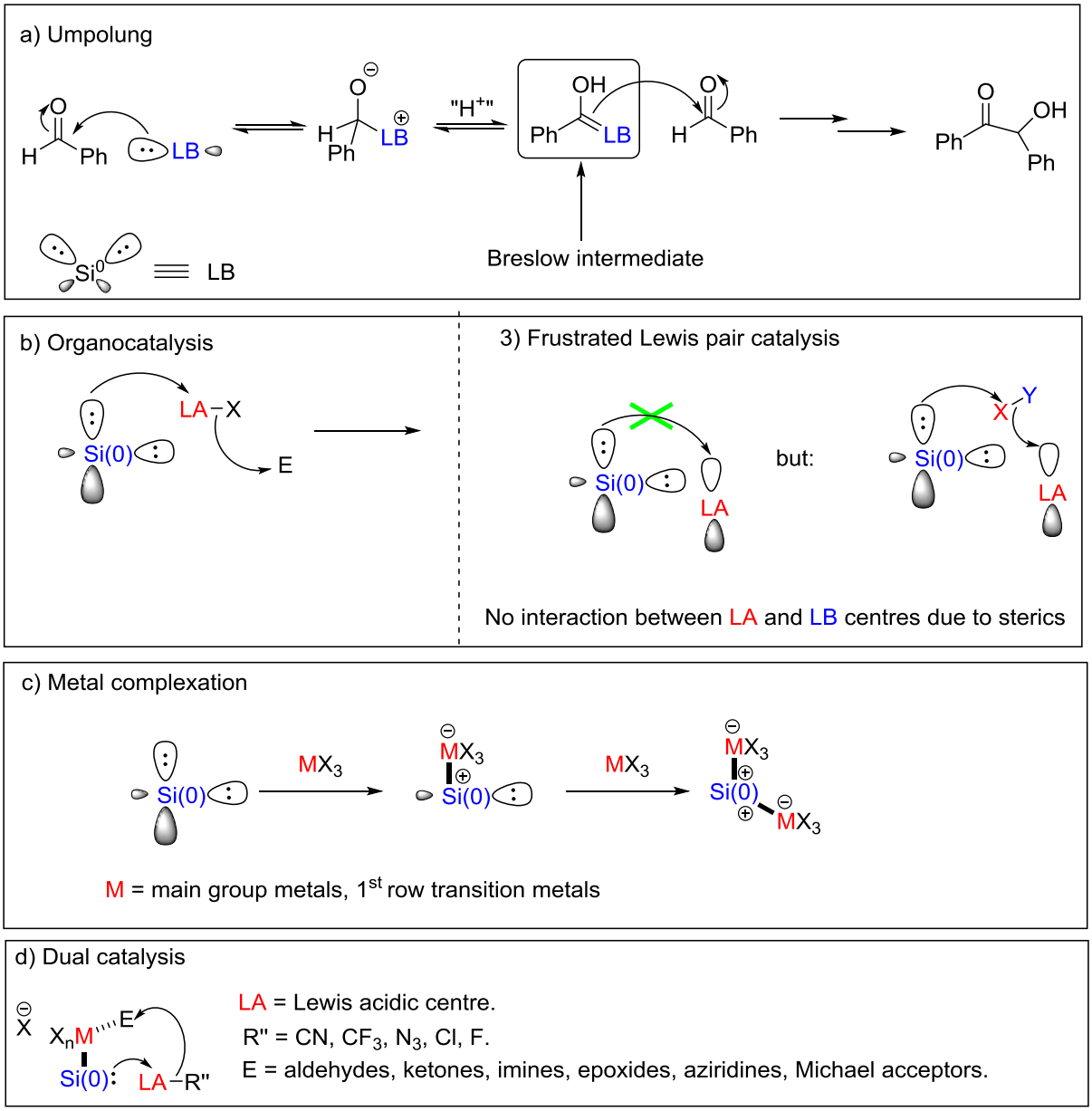

Scheme 5.15: Proposed catalytic scenarios using Si(0) compound **242**.

5.3 Results and Discussion

5.3.1 Preparation of Si(0) Compounds

We decided to prepare the two literature known silylones **243** and **244** (Figure 5.3). Although both siylenes are carbene supported, they are expected to display different chemical reactivity.[161,163] Furthermore, we attempted to synthesize BAC-supported silylone **265**, as it would be interesting to compare CAACs, NHCs and BACs in this context (Figure 5.3). We expected to get a new insight into the significance of the electronic and steric nature of carbenes for the stabilization of the Si(0) center.

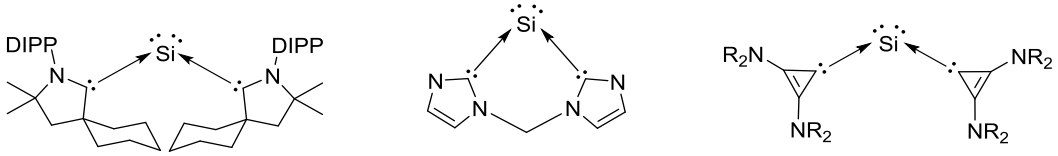

243 **244** **265**

Figure 5.3. a. Silylones **243** and **244** as potential catalytsts. **b.** The less sterically hindered **265**.

5.3.1.1 Synthesis of NHC-Stabilized Dichlorosilylene (IPr–$SiCl_2$)

The synthesis of the DIPP carbene is a 4-step process (Scheme 5.16). Glyoxal (40% in water) was treated with 1,3–diisopropylaniline (2.0 equiv) and a few drops of formic acid in methanol at room temperature for 24 hours to give diazobutadiene **266** in 72% yield. Next, paraformaldehyde (1.1 equiv) and hydrogen chloride in dioxane (4.0 M, 1.5 equiv) were vigorously stirred until paraformaldehyde was fully dissolved. The dissolution of paraformaldehyde to the solution of hydrogen chloride in dioxane is essential for the next step, since the reaction is exothermic and direct contact of solid paraformaldehyde and diazobutadiene **266** will lead to immediate formation of side-product. The resulting solution was treated with **266** in ethyl acetate at room temperature for 16 h to give **267** after filtration and precipitation as a pink solid (92%). Next, the imidazolium chloride (**267**) was treated with HBF_4 (48% in water, 1.1 equiv) in water and stirred for 5 min to generate **268** after extraction and precipitation as a white powder (67%). Then, the well-dried **268** treated with NaH (2.0 equiv) and KO^{t}Bu (using the tip of the spatula) in THF at room temperature under inert atmosphere. The mixture was left stirring overnight at room temperature and after filtration, the volatiles were removed *in vacuo* to afford **208** as a beige solid (97% yield).[179]

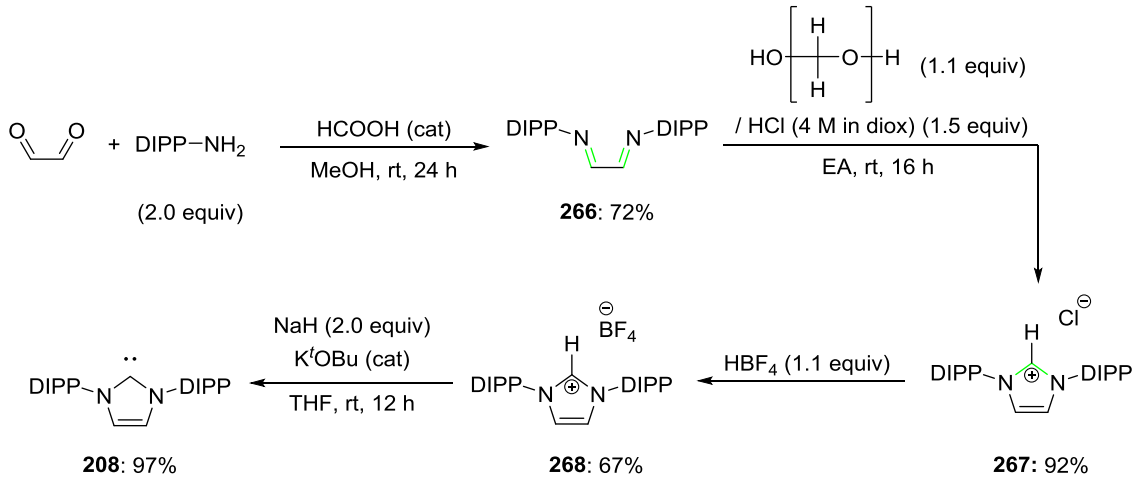

Scheme 5.16: 4-step preparation of the DIPP carbine **208**.[179]

DIPP carbene **208** (2.0 equiv) was treated with trichlorosilane (0.5 equiv) to form the NHC-stabilized dichlorosilylene **251** at room temperature in 79% yield (Scheme 5.17).[179] This product was formed by reductive elimination of hydrogen chloride from the silicon species and subsequent NHC coordination to the Si(II) center. 2.0 equiv of DIPP carbene were used in order to form intended product **251** and neutralize the formed hydrogen chloride. NHC-stabilized dichlorosilylene could be separated by a simple filtration from NHC•HCl salt (**267**). DIPP carbene (**208**) could be regenerated through deprotonation with KO^{t}Bu. The NHC-stabilized dichlorosilylene was obtained in 79% yield and 87% purity as a yellow solid. Based on ^{1}H NMR spectroscopy, DIPP carbene was free in the crude, therefore purification efforts failed due to similar physical properties between IPr−$SiCl_2$ and DIPP carbene.

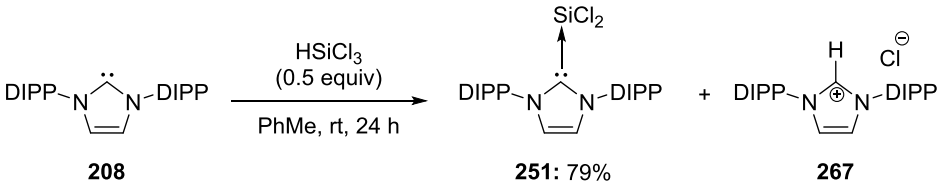

Scheme 5.17: Synthesis of NHC-stabilized dichlorosilylene (IPr−$SiCl_2$, **251**).

5.3.1.2 Attempted Synthesis of Si(0) 244

The bis(carbene) ligand **256** was prepared in a four-step process (Scheme 5.18).[163] The products formed within these steps have not been isolated and characterised with the exception of the imidazole **273** in accordance with the literature-reported method.[180] Initially, a condensation reaction between 2,6-diisopropylaniline (**269**) and thiophosgene was carried out to form the corresponding isothiocyanate **270**. This compound was then reacted through

nucleophilic addition with the aminoacetaldehyde diethyl acetal to generate compound **271** (thiourea). The acetal group was hydrolysed *in situ* using aqueous hydrogen chloride under reflux. The thiol group (–SH) of the formed mercaptoimidazole **272** was cleaved using nitric acid (HNO_3) to form imidazole **273**. Next, **273** reacted with methylene bromide under harsh conditions to form the pre-bis(carbene) species **274**. The precursor was deprotonated with KHMDS (2.1 equiv) at low temperature and the mixture was stirred at room temperature for 4 h. Efforts to isolate and store the bis(carbene) ligand **256** in analytically pure form failed. The THF solution of **232** darkened overtime and the ^{1}H NMR spectroscopy exhibited multiple side-products. Therefore, bis(carbene) ligand **232** was rather prepared *in situ* with satisfactory purity (97% crude yield) and used directly for synthesis.

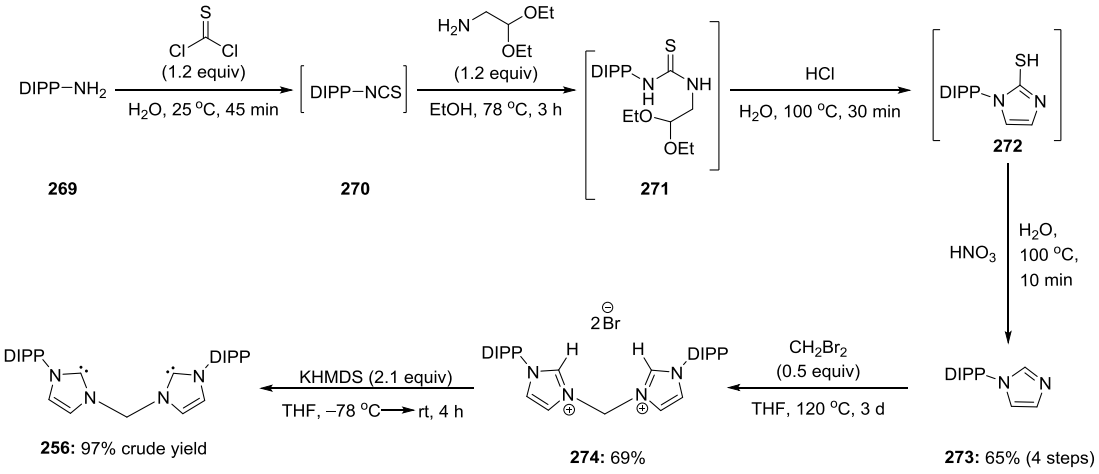

*The reactions performed by Arseni Borisov under my direct supervision

Scheme 5.18: Synthesis of bis(carbene) ligand.

After the *in situ* formation of bis(carbene) ligand **256**, the resulting suspension was filtered over celite, the volume reduced and the solution was used immediately; initially, ligand exchange reaction with IPr–$SiCl_2$ **251** was carried out and then formation of chlorosilyliumylidene precursor **257** (Scheme 5.19). Unfortunately, the pre-Si(0) species **257** was only 75% analytically pure in 52% yield; indeed, it was contaminated with single compound **267** based on ^{1}H NMR spectroscopy. Efforts to purify the yellow solid by washing with several solvents and separate it from the imidazolium species failed, while the chromatography technique could not be applied due to air and moisture sensitivity of the final product. The pre-Si(0) **257** species was used without prior purification and treated with sodium naphthalenide or potassium graphite (2.0 equiv) at low temperature and progressively at room temperature for 6 h. The targeted Si(0) compound **244** was not generated. Although the anticipated red colour was observed in the reaction mixture, during the work-up process

the colour disappeared. The failure of this reaction was also confirmed by ^{1}H NMR spectroscopy. Indeed, the poor analytical purity of the pre-Si(0) **257** species may be the major cause for this outcome.

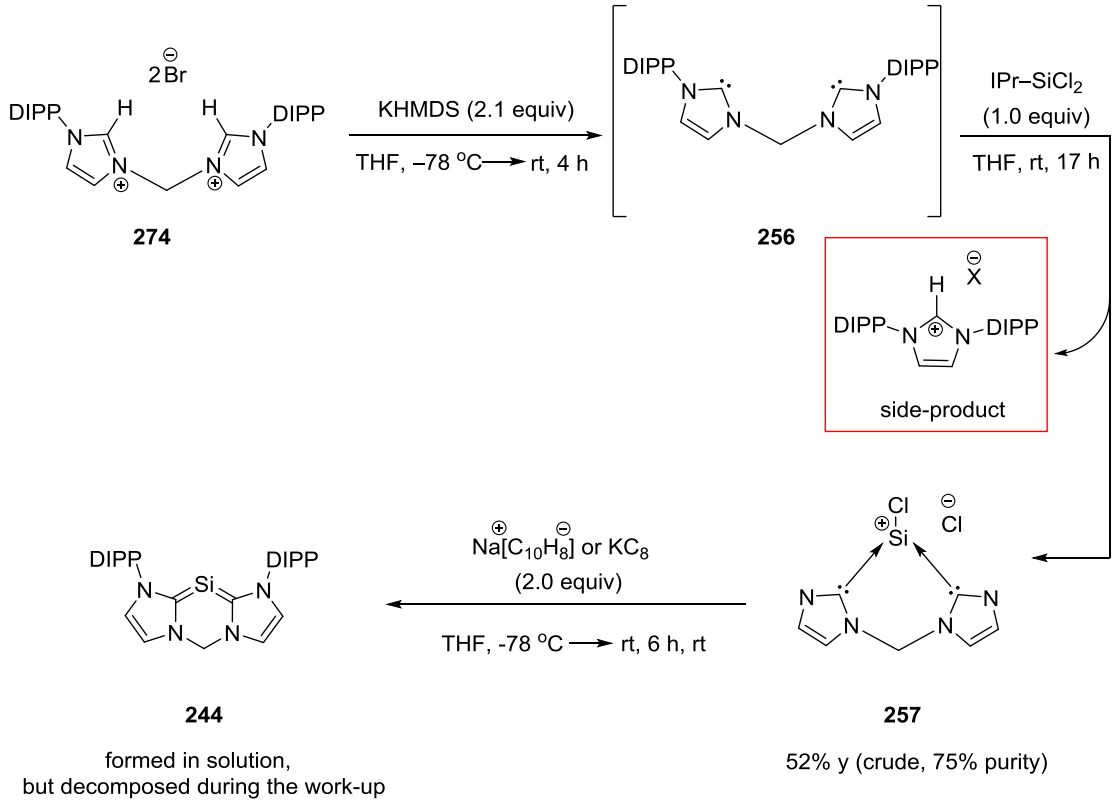

*The reactions performed by Arseni Borisov under my direct supervision

Scheme 5.19: Synthesis of the bis(carbene)-supported silylone **244**.

5.3.1.3 Synthesis of Silylone 243 [(CAAC)$_2$Si(0)]

The preparation of silylone **243** was successfully completed following reported method, although the work-up was modified (Scheme 5.19).[11,161,181] The precursor of the cyclic alkyl amino carbene (CAAC) **275** was recrystallized and carefully dried prior its *in situ* deprotonation to form the CAAC **254**. We used KHMDS as a Brønsted base, filtered over celite the resulting suspension and dried prior to further use. The crude carbene was employed directly in the next step, which was a ligand exchange reaction with IPr−SiCl$_2$ **251**. The reaction end-point was detected by an immediate colour change. Indeed, the royal blue colour represents a key physical property of the formed biradical species **255**. The yield of the ligand exchange reaction proved to be significantly lower in our hands compared to the literature-reported values (55% *vs.* 85%). This difference may be ascribed to the fact that the IPr−SiCl$_2$ **251** was not entirely pure. In the next step, potassium graphite (KC$_8$) was employed as a

reducing agent of the biradical species at low temperature for 1 h. The reaction mixture was then warmed up to room temperature. The resultant reaction mixture was filtered, evaporated to dryness and recrystallized by hexane under an inert atmosphere to afford **243** (82%).

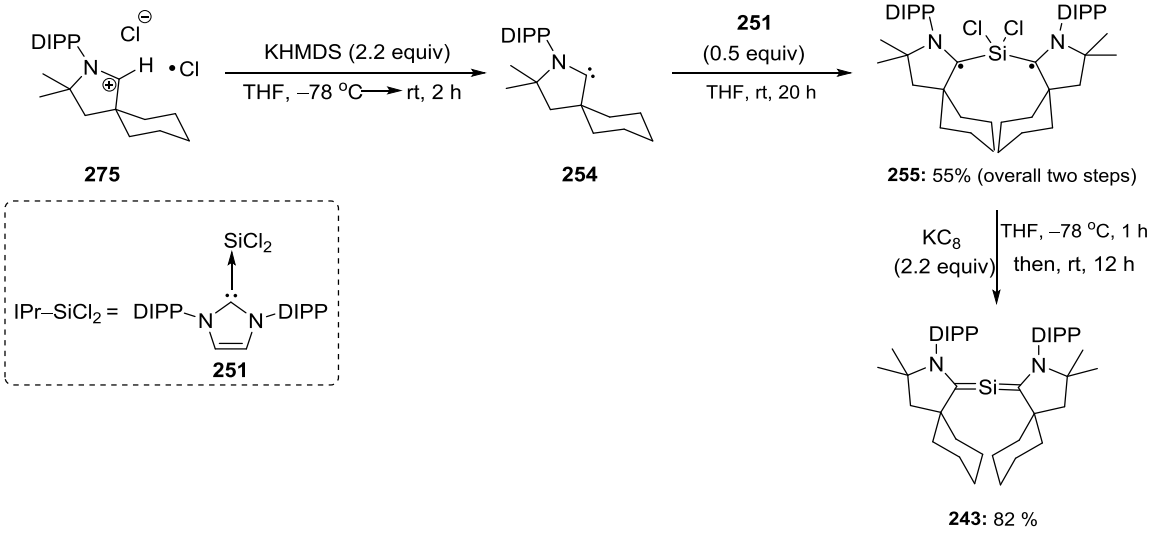

Scheme 5.19 Synthesis of Si(0) **243**.

X-ray crystals were obtained using the vapour diffusion method. Studies of the crystal structure can lead to the conclusion that the Lewis basic centre (silicon) is sterically hindered due to the high steric demand of the diisopropyl group (Figure 5.4).

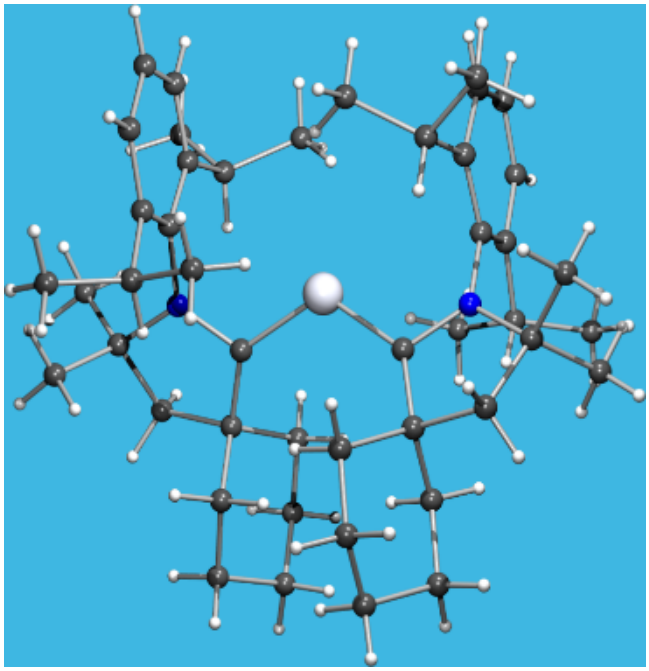

*The crystal structure was obtained by Arseni Borisov under my direct supervision

Figure 5.4: Crystal structure of Si(0) **243.**

5.3.1.4 Attempted Synthesis of Silylone 265 [(BAC)$_2$Si(0)]

Furthermore, the preparation of the BAC-supported silylone **265** was attempted (Scheme 5.20). KHMDS (1.0 equiv) was used as a Brønsted base for the *in situ* deprotonation of the pre-BAC species **276** in THF at –78 °C to form the free BAC carbene **277**. Next, BAC was treated with IPr–$SiCl_2$ (0.5 equiv) in THF at room temperature for 20 h. Immediately after the addition of IPr–$SiCl_2$ in THF solution of the formed BAC carbene, yellow precipitate was observed. The ^{1}H NMR spectroscopy of the reaction mixture indicated the formation of imidazolium species without presence of intended **278**. The latter would be the precursor of **265**. The reaction may not have followed the intended pathway to give **278** due to differences in the electronic and steric properties between the supporting BAC and CAAC ligands.

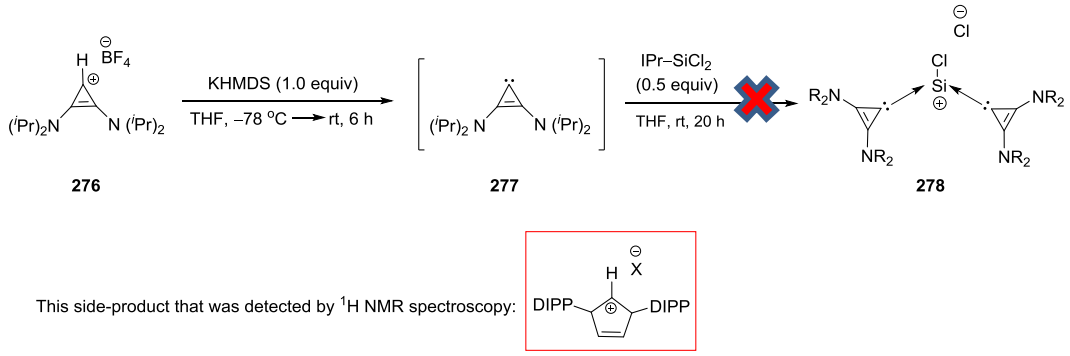

*The reactions performed by Arseni Borisov under my direct supervision

Scheme 5.20: Attempted synthesis of BAC-ligated chlorosilyliumylidenes **278**.

5.3.2 Towards Catalytic Bond Activation by a Si(0) Species

5.3.2.1 Benzoin Condensation and Stetter Reaction

In the context of *umpolung* catalysis, the benzoin condensation and the Stetter reaction were attempted (Scheme 5.21).[182–186] The benzoin condensation is a coupling reaction between two aldehyde molecules or an aldehyde (pro-nucleophile) and a ketone (electrophile). This concept has been reported using cyanide[182,183]or NHCs[184,185]as catalysts. In the generally accepted mechanism, the catalyst adds to the aldehyde to form a resonance-stabilized zwitterionic intermediate. Next, an intermolecular carbon-to-oxygen proton transfer takes place to form the Breslow intermediate, which can be represented either as a zwitterionic carbanion or neutral endiamine. The latter is a nucleophile, which adds to another aldehyde molecule. Next, intermolecular proton transfer takes place followed by elimination of the NHC catalyst to afford the corresponding α-hydroxy ketone. The Stetter reaction is the conjugate addition of an aldehyde to an α,β-unsaturated compound (Scheme 5.18). For

example, Johnson *et al.* reported a Stetter reaction method using ethyl glyoxylate and benzylidene malonate derivatives (a,β-unsaturated compounds; 1.0 equiv) and the Rovis's triazolium carbene catalyst (**279**) to give α-ketoesters in 78–96% yields.[186]

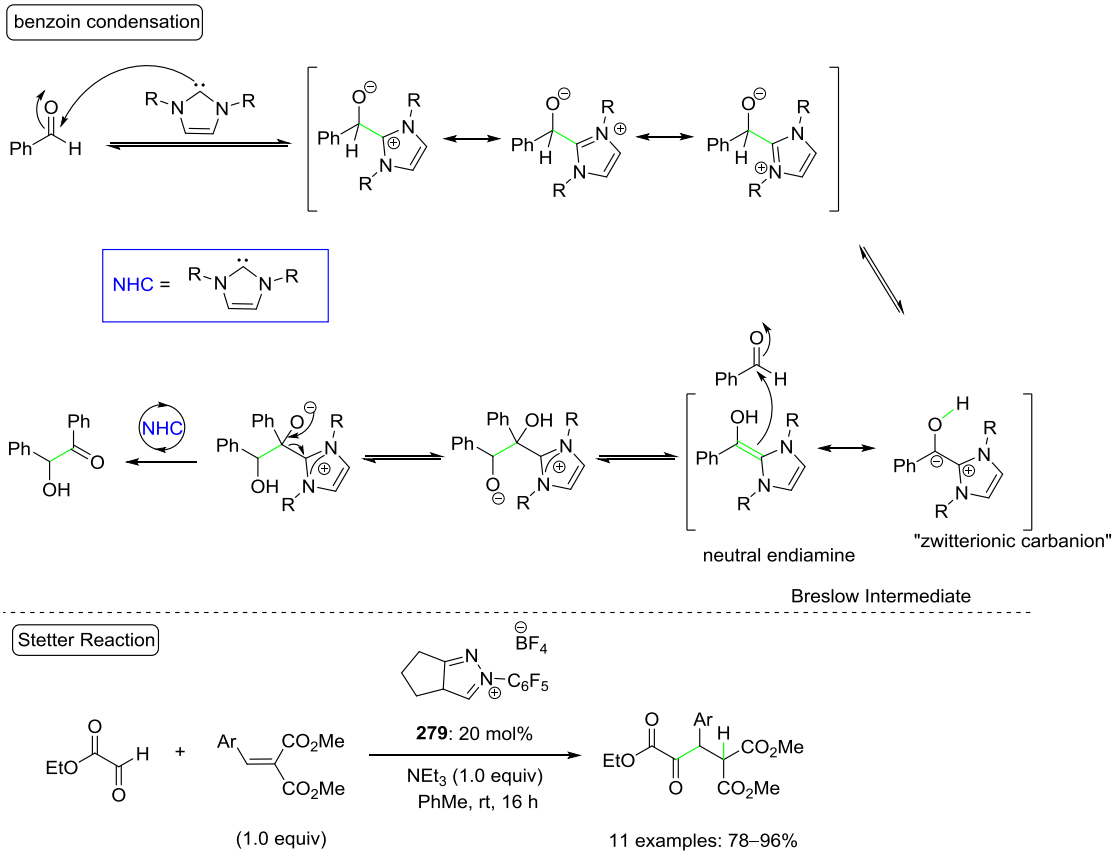

Scheme 5.21: The Benzoin condensation and the Stetter reaction.[184–186]

Umpolung chemistry was attempted using benzaldehyde and Si(0) compound **243** (20 mol%), which was anticipated to form the corresponding Breslow intermediate through nucleophilic addition and carbon-to-oxygen proton transfer (Scheme 5.22). The latter would add to another molecule of benzaldehyde to form ultimately α-hydroxy ketone **280**. In the Stetter reaction, benzaldehyde (1.0 equiv) and Si(0) compound **243** (20 mol%) were treated with methyl vinyl ketone (1.0 equiv) as an electrophile instead of benzaldehyde. Ideally, the formed Breslow intermediate would act as a nucleophile and carry out 1,4-addition to methyl vinyl ketone to give Stetter adduct **281**. Both reactions were tested at 30 °C and 60 °C in C_6D_6, however, the intended products were not detected in ^{1}H NMR spectroscopy. In case of the benzoin

condensation analysis of the ^{1}H NMR spectra revealed partial decomposition of **243**. In case of the Stetter reaction, **243** was shown to fully decompose even at 30 °C.

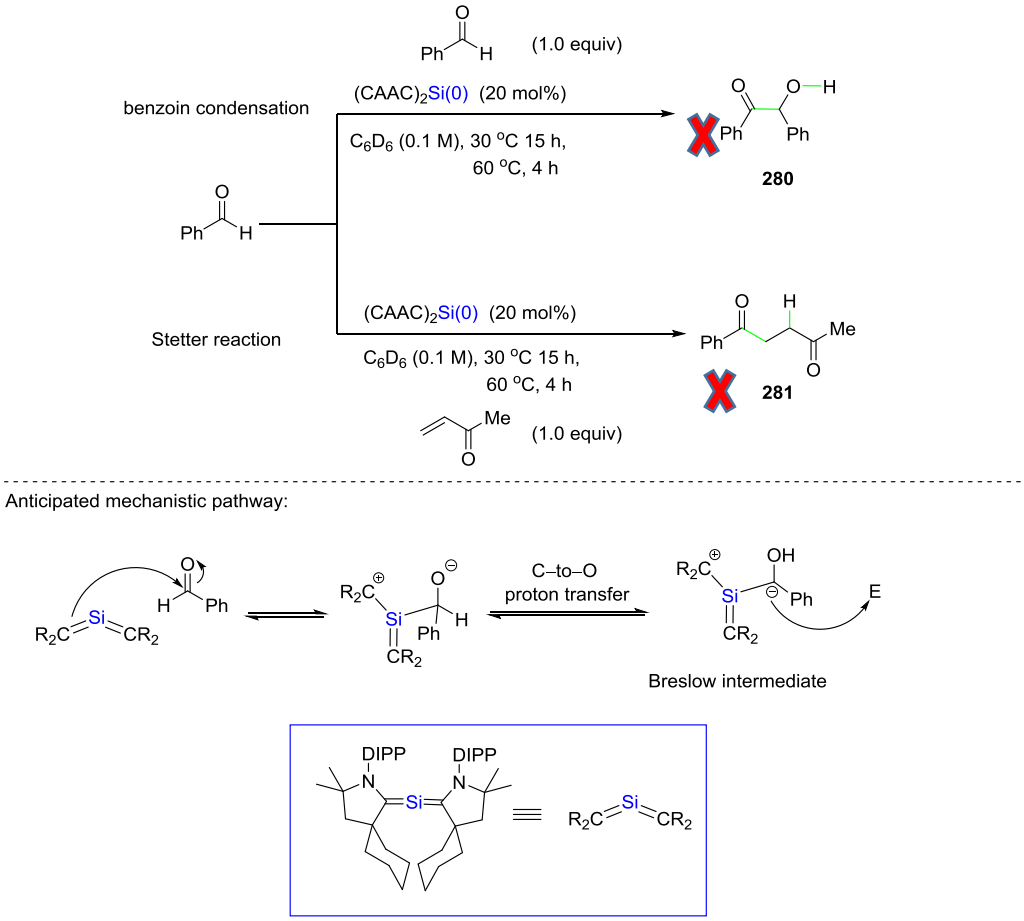

*The reactions performed by Arseni Borisov under my direct supervision

Scheme 5.22: Benzoin condensation and Stetter reaction.

As it has already been mentioned, NHC-catalysed benzoin/Stetter reactions are common.[182–186] The unprecedented use of Si(0) compound **243** as an *umpolung* reagent/catalyst, instead of an NHC, has proved to be challenging (Scheme 5.23). The failure of these C–C bond formations to proceed may be ascribed to unwanted side-reactions of the silylone. A reason for the lack of umpolung chemistry may be the steric demand of silylone **243**, which may inhibit nucleophilic addition to the aldehyde. Indeed, even after initial nucleophilic addition to the aldehyde one of the CAAC ligands may act as a leaving group in the resulting adduct; a sila-epoxide would be formed (ring-closure). This intramolecular reaction may proceed faster than the intermolecular proton transfer. However, evidence for the formation of the sila-epoxide were not detected in the ^{1}H NMR spectroscopy.

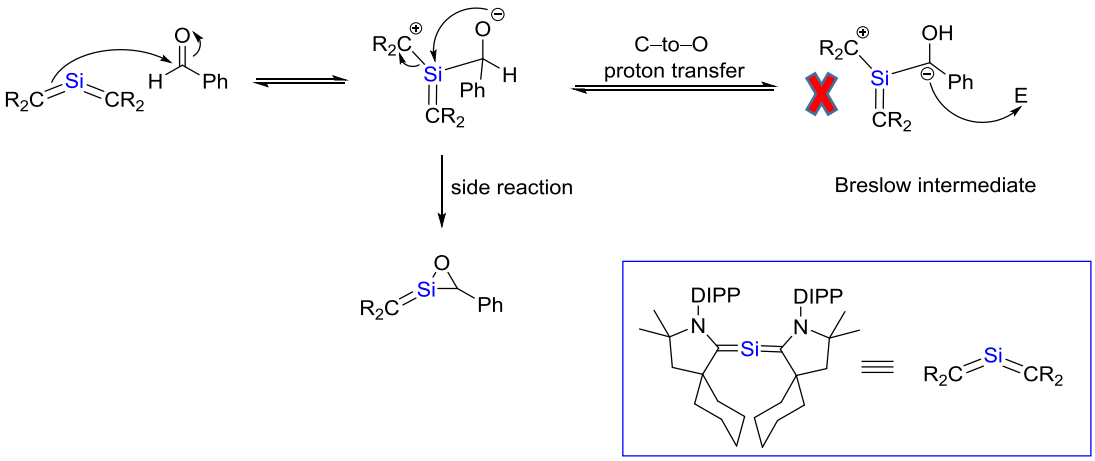

Scheme 5.23: Challenges of *umpolung* chemistry with silylone **243**.

5.3.2.2 Boron Binding Affinity – Oxidative Addition to Boron Pro-Nucleophiles

Boron binding studies were carried out to gain insight into the Lewis basicity of the sterically demanding silylone **243** (Scheme 5.24). **243** was examined to see whether it would react with a broad range of boron pro-nucleophiles to form the corresponding boron–ate complexes. In addition, the ability of silylone **243** to potentially donate all four electrons and bind to two equivalents of a boron Lewis acid was also investigated. However, in cases there was no interaction detected by ^{11}B NMR spectroscopy due to steric congestion of the reaction partners, frustrated Lewis pair (FLP) chemistry could be developed.

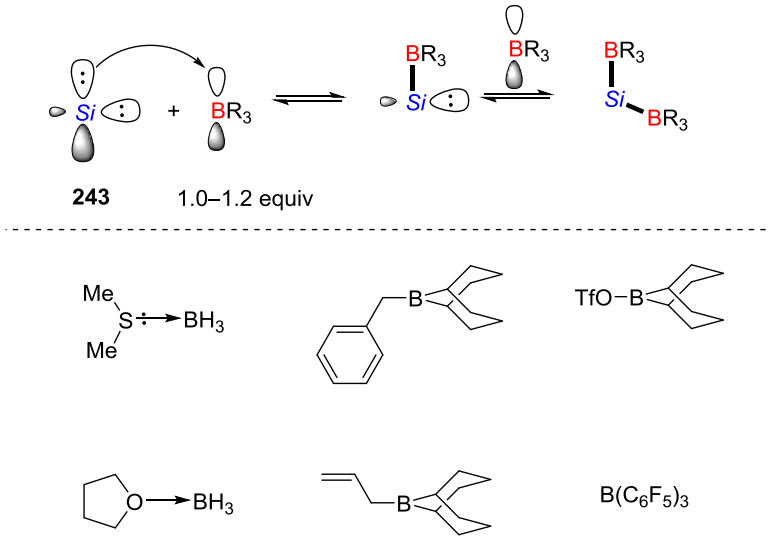

Scheme 5.24: Overview of ^{11}B NMR studies and selected boron compounds.

Interaction between (CAAC)$_2$Si and BH$_3$•SMe$_2$

The reactivity of silylone **243** towards BH$_3$•SMe$_2$ was investigated with ^{1}H and ^{11}B NMR spectroscopy (Scheme 5.25). The corresponding ^{1}H and ^{11}B NMR spectra are displayed in the range from 2.0 ppm to 4.0 ppm and from –18 ppm to 40 ppm, respectively. In the ^{1}H NMR spectrum of silylone **243**, signals *a* and *c* correspond to the C*H* hydrogen atoms of the DIPP isopropyl groups, while signals *b* and *d* correspond to two hydrogen environments of the cyclohexyl groups. In ^{11}B NMR spectroscopy, BH$_3$•SMe$_2$ (1.0 equiv) displays a signal at –19 ppm (q, J = 105 Hz). Silylone **243** was treated with BH$_3$•SMe$_2$ at 40 °C for 72 h. While signals of the starting materials were still visible, several new species were formed as evidenced by the appearance of new signals in both ^{1}H and ^{11}B NMR spectroscopy. The new signals *g* (3.70–3.78 ppm, m), *h* (3.09 ppm, quin, J = 6.8 Hz), *i* (2.91–2.95 ppm, m) and *j* (2.82–2.88, m) were observed and assigned to correspond to the same species with the ^{11}B

NMR signal *k* (t, –29 ppm, *J* = 90.5 Hz). In our effort to identify *k*, considering that it is a triplet, we suggested structures of 'BH_2' species, such as **A**, **B** or **C** (Scheme 5.23). Based on literature data and ^{11}B NMR studies conducted in our group, the signal *l* was unambiguously assigned to the boron–ate complex (**D**; –30 ppm, *J* = 87.5 Hz).[187] Mechanistic proposal is provided in scheme 5.26.

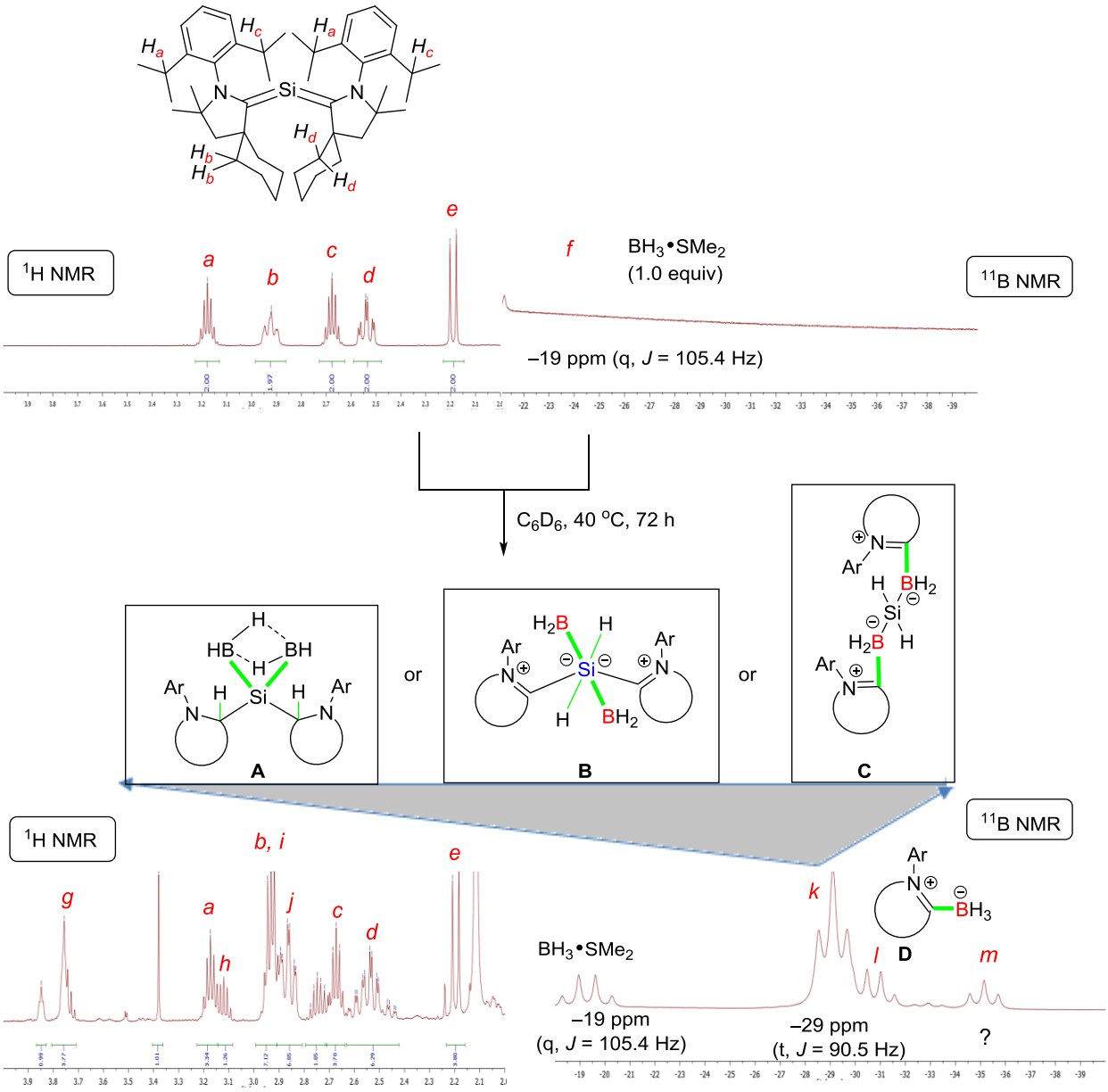

*The reactions performed by Arseni Borisov under my direct supervision

Scheme 5.25: Reaction of Si(0) compound **243** with BH_3•SMe_2 (1.0 equiv).

In this context, the following scenario was anticipated: initially, silylone **243** may displace the sulfide in BH_3•SMe_2 (1.0 equiv) to form the corresponding boron–ate complex (**E**; Scheme 5.26). The ^{11}B NMR chemical shift of **E** should be a quartet in the boron–ate complex area. However, **E** was not detected, therefore it was assumed that it reacted immediately to form new species. Indeed, a signal of triplet (*k*) was observed at –29 ppm (J = 90.5 Hz). Therefore, we suggested that the second lone pair located to the central silicon atom may coordinate to a second molecule of BH_3 to result in structure **F**. In pathway I, **F** may undergo a boron-to-silicon hydride shift because the corresponding Si–B bonds may be activated for nucleophilic hydride transfer to the proximal electrophilic carbon centre to form hexa-coordinated Si(IV) species **B**. The hydrides connected to the boron atoms may coordinate to the other boron atom in vicinity to form a pseudo boron–ate complex, which nicely explains both the multiplicity and the signal *k* (–29 ppm, t, J = 90.5 Hz). Next, CAACs in the structure **B** may migrate from the central silicon atom to the more Lewis acidic boron centres in vicinity to generate the structure **C**. Indeed, the ^{11}B NMR signal of **C** would be expected to be a triplet in the boron–ate complex area, such as *k*. In pathway II, structure **F** may undergo a double oxidative addition of Si(0) **242** into the B–H bond to generate species **A**. The latter would be expected to give a triplet in the boron–ate complex area. So far, structures **A**, **B** and **C** could be suggested as the structures that correspond to the species with signal *k* (–29 ppm, t, J = 90.5 Hz).

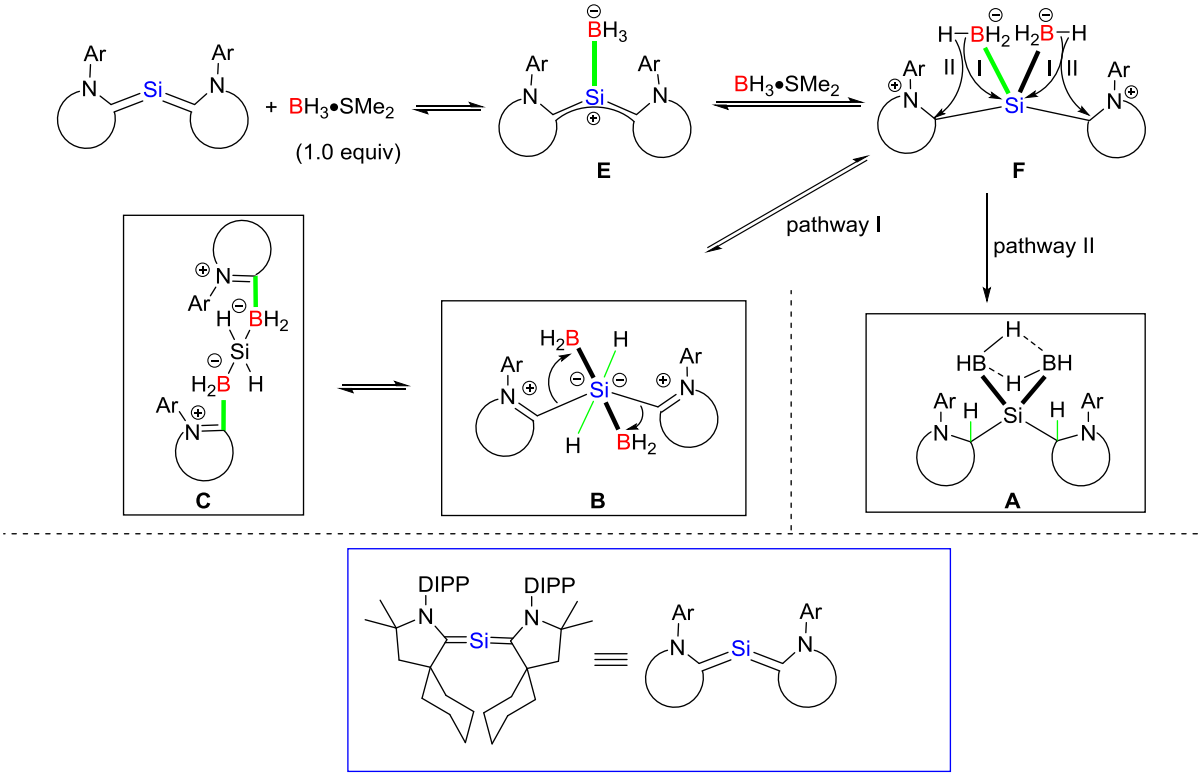

Scheme 5.26: Plausible reaction mechanistic pathways of **243** with BH_3•SMe_2 (1.0 equiv).

Next, we added one extra equivalent of BH_3•SMe_2 and heated the reaction mixture to 60 °C (Scheme 5.27). The signals *g, h, i* and *j* disappeared in ^{1}H NMR spectroscopy after heating at 60 °C, while the signals *o* (3.85–3.88, m), *p* (2.68–2.79, m), *q* (2.56–2.62, m) and *r* (td, J = 13.6, 13.0, 3.8 Hz, 1H) became dominant. This observation is in agreement with the outcome of the ^{11}B NMR spectroscopy; the initially major signal *k* disappeared after heating at 60 °C and the signals *l* and *m* became dominant in ^{11}B NMR spectrum: –30 ppm (q, J = 87.5 Hz) and –35 ppm (t, J = 90 Hz), respectively. In 2010, Lacôte *et al*. reported the formation of a CAAC-based boron–ate complex (**D**; q, –30 ppm).[187] An experiment in our group conducted by Hanno Kossen gave an identical outcome with the additional information of the coupling constant [–30 ppm (q, J = 88.3 Hz)].

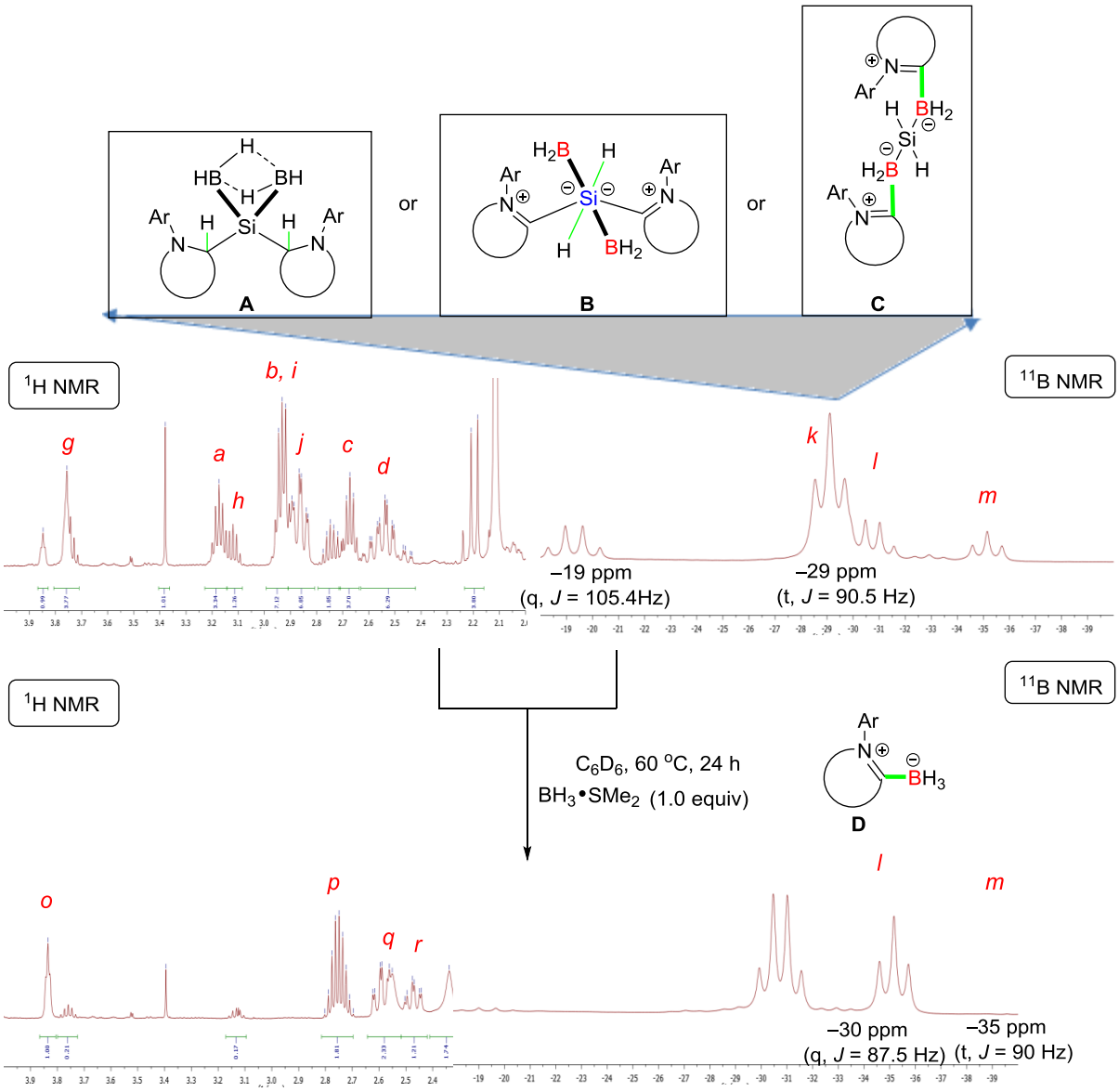

*The reactions performed by Arseni Borisov under my direct supervision

Scheme 5.27: Progress of the reaction with a second equivalent of BH_3•SMe_2 (1.0 equiv).

Therefore, it was assumed that the signal *l* [–30 ppm (q, *J* = 88.3 Hz)] was a result of dissociated CAAC **254** that bound to the one extra equivalent of BH_3•SMe_2 (structure **D**) that was added prior heating at 60 °C (Scheme 5.28). As it has already been mentioned, in structure **E**, migration of hydrides from the boron centres to the central carbons of CAACs to form structure **A** is possible. However, this dissociation suggests that the latter is not the precursor of **D** (pathway II), since the central carbon of the CAAC ligands were converted into tetravalent species. Thus, formation of **D** and **F** species is not possible through this pathway. According to pathway I, if structure **B** is the correct intermediate and the CAAC dissociates

to coordinate to the additional BH_3 (**D**), a signal of penta-coordinate Si(IV) species **G** in the boron–ate complex area would be expected [*m*: –35 (t, *J* = 90 Hz) ppm] but also a signal down-field, since the boron atom previously coordinated by the dissociated CAAC will be tri-coordinate. Unfortunately, a signal down-field was not detected and the formation of **G** was eliminated. In structure **B**, if CAACs migrate to the more Lewis acidic boron atoms (compared to silicon) to form **C**, treatment with one extra BH_3•SMe_2 would lead to generation of species **D** and **H**. In the structure **H**, there would be a tetra-coordinate [*m*: –35 ppm (t, *J* = 90 Hz)] and a tri-coordate boron atom with an ^{11}B NMR signal down-field. Unfortunately, no signal down-field was observed in the ^{11}B NMR spectroscopy. To conclude, while we suggest structure **C** [^{11}B NMR signal *k*: –29 ppm (t, *J* = 90.5 Hz) ppm] as a possible outcome of the reaction after heating at 40 °C and structure **D** after heating at 60 °C [^{11}B NMR signal at –30 (q, *J* = 87.5 Hz) ppm], we are not able to suggest a structure for the boron species that correspond to the ^{11}B NMR signal at –35 ppm (t, *J* = 90 Hz).

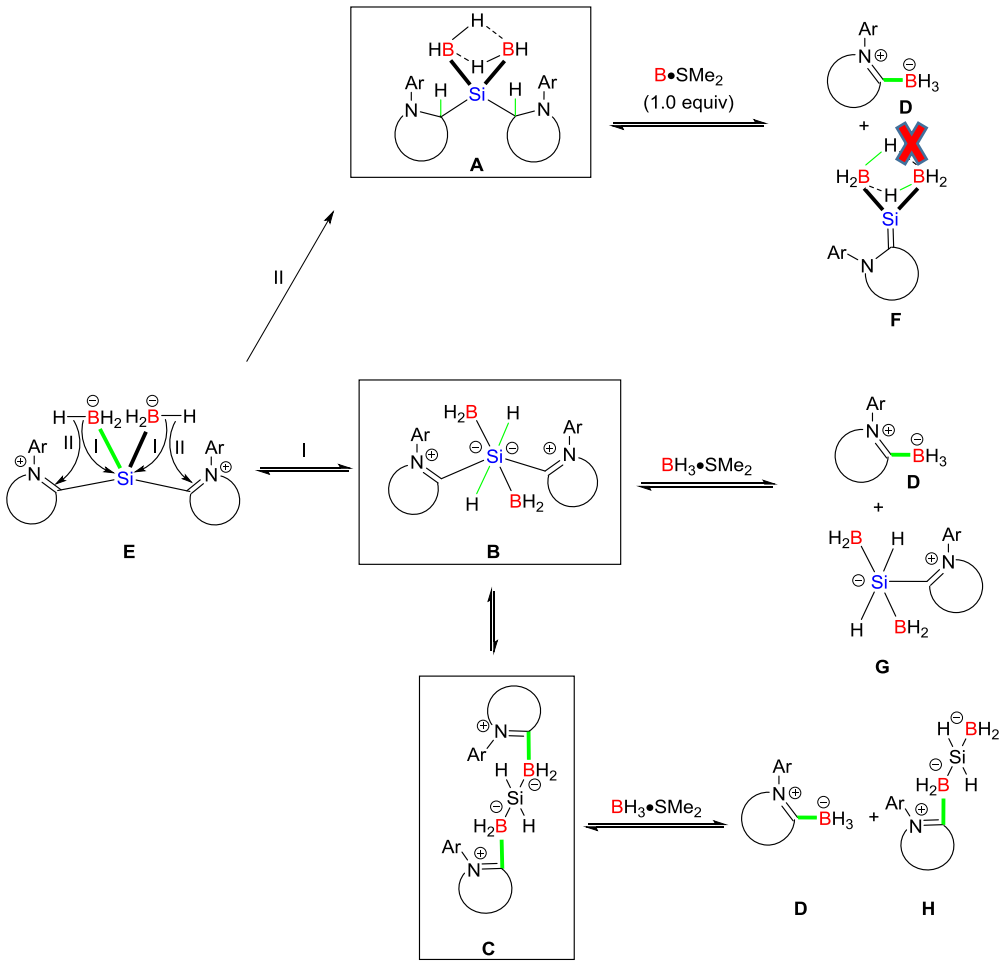

Scheme 5.28: CAAC dissociation after heating at 60 °C and plausible outcomes.

The rationalisation of the ^{1}H and ^{11}B NMR spectroscopy strongly suggests that this is a two-stage reaction. To date, this conclusion is not definitive and additional investigation was required. Efforts to obtain crystals of the species that correspond to the signal *m* suitable for X-ray crystallographic analysis using vapour diffusion method failed. Furthermore, we conducted literature investigation to spot reported compounds with a similar frame; a Lewis basic centre coordinated with boron hydride species (Scheme 5.29). The three-coordinate dicationic borane **256** bearing a hydride ligand has been reported by Ong *et al*.[187] Although, there is not striking similarity between **282** and structures **C** or **E**, considering that we have not fully confirmed that **B** or **C** represent the boron species at –29 ppm (t, J = 90.5 Hz), we decided to explore this hypothesis. IR, ^{11}B NMR and X-ray crystallography techniques have been applied for the characterization of **282**. In ^{11}B NMR spectroscopy, two signals have been displayed; –25.4 ppm that was assigned to the B–H and –38.6 ppm that corresponds to the boron tetrahydride (BH_4^-). The former would be expected to be a doublet and the latter a quintet; however, the ^{11}B NMR spectroscopy that has been conducted was decoupled, therefore no multiplicity was reported to provide a further insight into our efforts to identify structure with signal *k*. Next, we were keen to compare our NMR findings with the spectroscopy of **200** reported by Frenking *et al*.[147] Again, IR, X-ray crystallography with ^{31}P NMR spectroscopy was reported for this cationic compound. Unfortunately, ^{11}B NMR spectroscopy was not provided. The latter would give a valuable insight into our investigation to decide the identity of the boron species with signal *k* [–29 ppm (t, J = 90.5 Hz)].

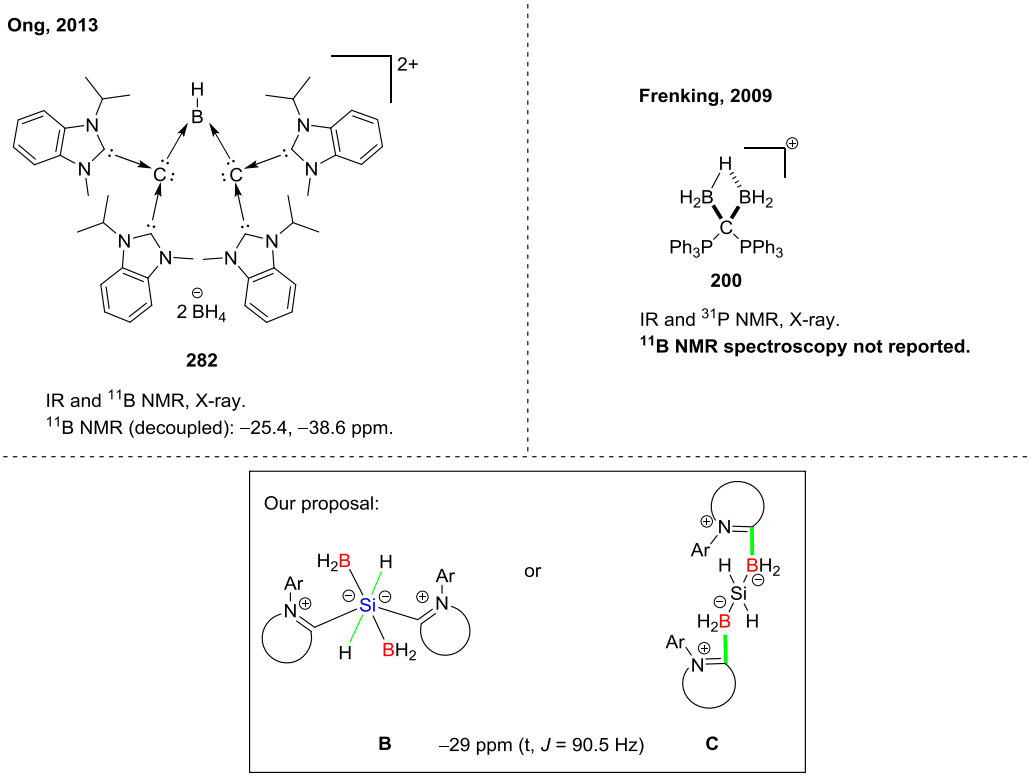

Scheme 5.29: Comparison of structure **B** and **C** with literature.[147,187]

Interaction between (CAAC)$_2$Si(0) and benzyl–B(9-bbn) and benzylation trials.

Limited synthetic applications using benzyl–B(9-bbn) have been reported, since the alkyl boron compounds proved to be reluctant to transfer the alkyl groups.[188] However, Lewis acid catalysis has been successfully applied in the context of Suzuki-Miyaura coupling.[144] To the best of our knowledge, there are no examples reported in the field of the Lewis base catalysis, and one of the reasons may be the significant steric bulk around the Lewis acidic boron centre of benzyl–B(9-bbn).[190] Next, benzyl–B(9-bbn) was treated with silylone **243** (1.2 equiv) to investigate whether the benzylic *B–C* bond could be activated for benzyl transfer to suitable electrophiles (Scheme 5.30). The former displays a signal at 80 ppm in the ^{11}B NMR spectroscopy. Since this compound is commercialized in a THF solution (1.0 M) and THF is formally a Lewis base, it may interact with the boron reagent to provide the signal at 57 ppm. After the addition of silylone **243**, a newly formed signal was observed at 2.9 ppm, which may correspond to the generation of a boron–ate complex. The scenario of dissociation of CAAC from the silylone **243** and subsequent formation of boron–ate complex with the benzyl–B(9-bbn) was also considered, however, data obtained by Hanno Kossen in Scnhneider group did not indicate interaction between CAAC and benzyl–B(9-bbn). To date, we decided to

investigate the activation of the benzyl–B(9-bbn) using **243** in the presence of various electrophiles.

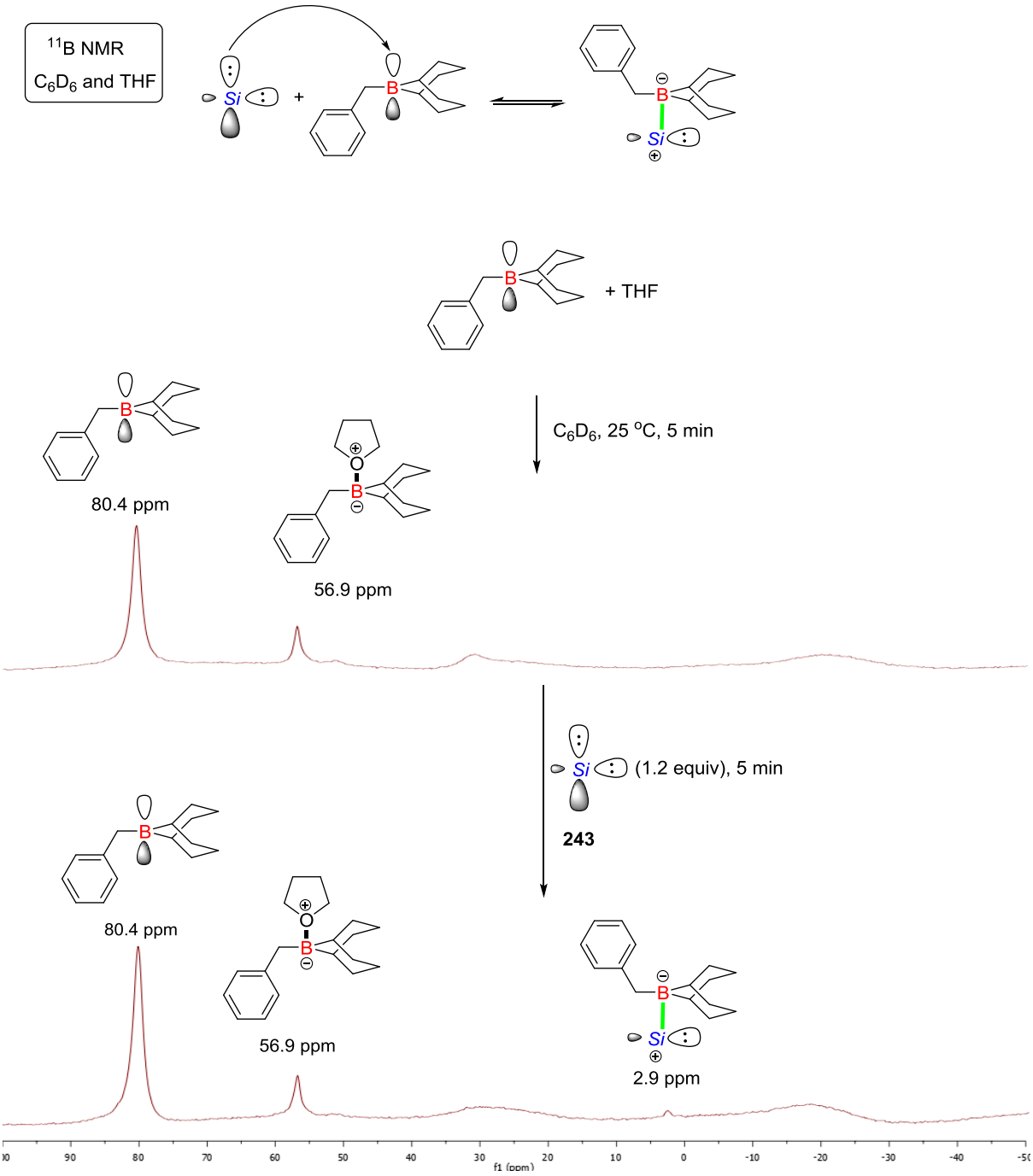

*The reactions performed by Arseni Borisov under my direct supervision

Scheme 5.30: Potential interaction of the silylone **243** with benzyl–9BBN monitored by ^{11}B NMR spectroscopy.

Next, benzaldehyde was treated with benzyl–B(9-bbn) (1.0 equiv) in the presence of silylone **243** (20 mol%) in C_6D_6 at 25 °C and 40 °C for 24 and 5 hours, respectively (Scheme 5.31). ^{11}B NMR spectroscopy of the reaction mixture suggested that the boron reagent remained unreacted. In addition, ^{1}H NMR spectroscopy displayed partial decomposition of the catalyst and no product formation, while aldehyde remained unreacted (25 °C and 40 °C). The fact

that the decomposition of silylone **243** was partial, it was also confirmed by the royal blue color of the reaction mixture that was retained (full decomposition would lead to total loss of the royal blue colour).

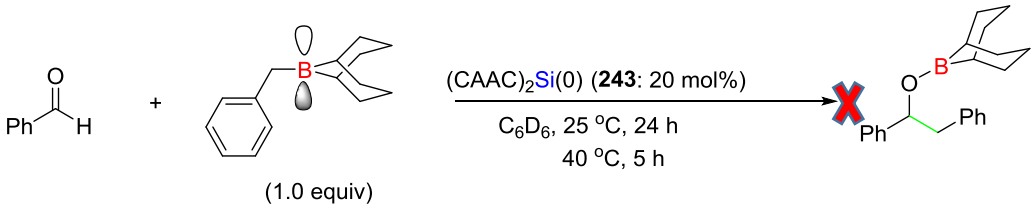

*The reaction performed by Arseni Borisov under my direct supervision

Scheme 5.31: Benzyl group transfer onto benzaldehyde.

Next, silylone-mediated benzyl transfer to an electrophilic halogen source, *N*-chlorosuccinimide, was examined at 25 °C (Scheme 5.32). After the addition of *N*-chlorosuccinimide to a solution of the boron reagent and silylone **243** (1.0 equivalent) in C_6D_6, instant colour change to brown solution occurred indicating decomposition of silylone **243**. Indeed, ^{1}H NMR spectroscopy confirmed decomposition of **243** without generation of the intended product, while the integrity of the boron reagent was confirmed by ^{11}B NMR spectroscopy.

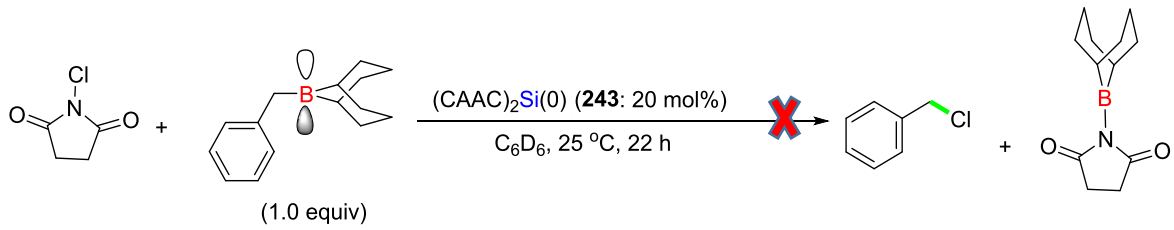

*The reactions performed by Arseni Borisov under my direct supervision

Scheme 5.32: Benzyl group transfer onto *N*-chlorosuccinimide.

Interaction between (CAAC)$_2$Si(0) and Alllyl–B(9BBN) and allylation trials.

We thought that the disappointing results using benzyl–B(9-bbn) as a pro-nucleophile may be ascribed to the significant steric bulk of the Lewis acidic boron centre and also the notorious reluctance of the alkyl boron compounds to transfer their alkyl groups. Thus, we decided to use the significantly less bulky and particularly reactive allyl–B(9-bbn). Initially, interaction between silylone **243** and allyl– B(9-bbn) was examined under our standard conditions (Scheme 5.33). Allyl–B(9-bbn) was prepared in our lab and stored as a solution in hexane (0.3 M) in the glovebox.[191] This boron reagent displayed a singlet at 86 ppm in C_6D_6 in ^{11}B NMR spectroscopy. The addition of silylone **243** did not lead to the generation of a new boron species as only the signal of the starting material was displayed ^{11}B NMR spectroscopy. ^{1}H

NMR chart provided evidence of partial decomposition of the silylone **243** in the reaction mixture, however, the signals of the Si(0) compound remained dominant. Heating of the solution to 40 °C and 60 °C did not lead to any reaction (as confirmed by ^{11}B and ^{1}H NMR spectroscopy). However, the non-interaction between the two species in this experiment does not preclude potential coordination and activation of the B(9-bbn)-derived allylborane to transfer the allyl unit to an appropriate electrophile in a reaction mixture. Therefore, we decided to investigate this possibility using various electrophiles.

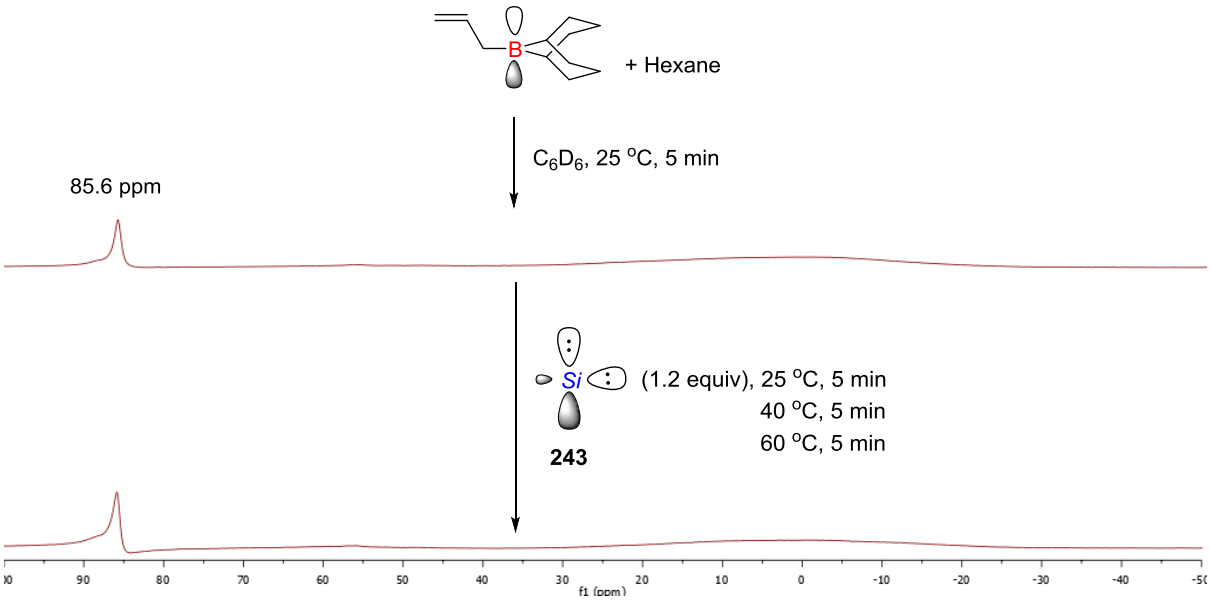

*The reactions performed by Arseni Borisov under my direct supervision

Scheme 5.33: Potential interaction of the silylone **220** with benzyl–9BBN monitored by ^{11}B NMR spectroscopy.

Next, allylation of various ionic electrophiles was investigated using allyl–B(9-bbn) as a pro-nucleophile in the presence of stoichiometric quantity of silylone **243** (1.0 equiv). The 9BBN-derived allylborane was initially treated with tropylium tetrafluoroborate (1.0 equiv) in C_6D_6 (Scheme 5.34). Tropylium ion is a very strong electrophile and even with absence of silylone **243**, the ^{1}H NMR spectroscopy of the reaction mixture shown evidence of reaction between these two species; the new signals proved to be difficult to interpret. Addition of silylone **243** as a mediator in a solution of allyl–B(9-bbn) in C_6D_6 followed by addition of the tropylium tetrafluoroborate led to exhibition of new signals in ^{1}H NMR spectroscopy, however, these signals did not correspond to the intended product **283**; efforts to rationalize them, failed. ^{1}H NMR spectroscopy in combination with the royal blue color of the reaction mixture suggested partial only decomposition of silylone **243**.

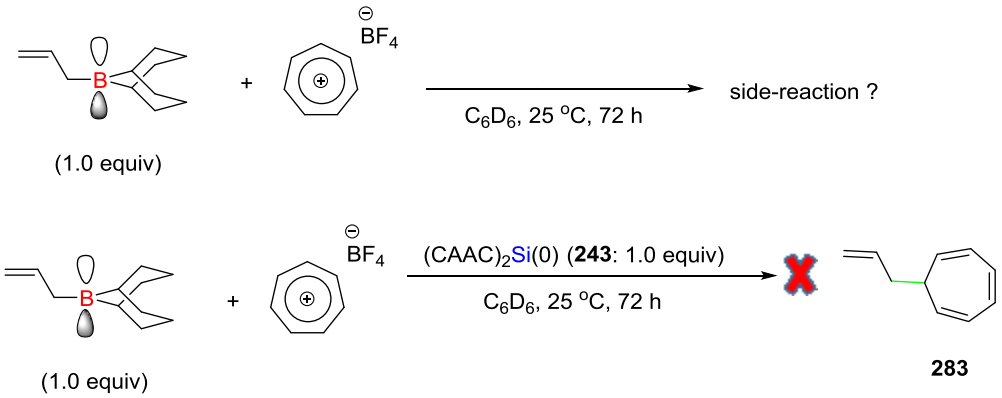

*The reactions performed by Arseni Borisov under my direct supervision

Scheme 5.34: Allyl group transfer onto tropylium tetrafluorobate.

Allylation of iminium substrates was also investigated (Scheme 5.35). Firstly, the allylation of the Eschenmoser's salt (**284**; 1.0 equiv) was attempted. However, allyl–B(9-bbn) seemed to react with **284** with the absence of silylone **243** in C_6D_6. ^{11}B NMR spectroscopy provided evidence of decomposition of allyl– B(9-bbn). Indeed, iodide may act as a Lewis base to coordinate to the boron, which may trigger a cascade of side-reactions. It was proposed that the decomposition of allyl-B(9-bbn) could be avoided simply by switching the order of addition. Unfortunately, the decomposition of silylone **243** (1.0 equiv) in the presence allyl-B(9-bbn) in C_6D_6 was evident by ^1H NMR spectroscopy, prior to the addition of Eschenmoser's salt, and the intended product (**285**) was not observed. Similarly, use of the Vilsmeier reagent **286** (1.0 equiv) under identical conditions did not give the intended product. Based on ^{11}B NMR spectroscopy, Vilsmeier reagent reacted with allyl–B(9-bbn) to generate a boron–ate complex (signal at 1.0 ppm) in C_6D_6; the chloride anion and the chloride attached to the C=N carbon (as it is an outstanding leaving group) may have coordinated to the boron. Notably, the presence of silylone **243** in the reaction mixture prior to the addition of the Vilsmeier reagent influenced the outcome of the reaction. However, ^1H NMR spectroscopy did not evidence the formation of the intended product (**287**), while complete decomposition of **243** was confirmed in accordance to gradual colour changes observed (initially green, and yellow solution overnight).

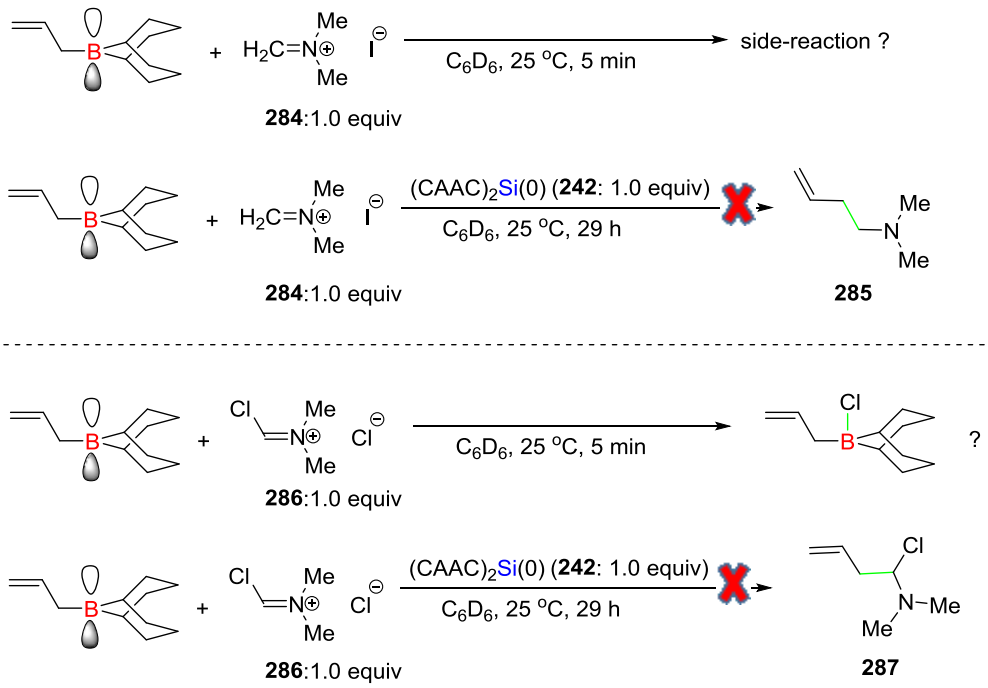

*The reactions performed by Arseni Borisov under my supervision

Scheme 5.35: Allyl group transfer onto iminium substrates.

Finally, the Staudinger reaction was also examined using stoichiometric quantity of silylone **243** (1.0 equiv; Scheme 5.36). Addition of diazonium chloride **288** (1.0 equiv) to a solution of allyl–B(9-bbn) in C_6D_6 led to generation of a boron–ate complex with a signal at 0 ppm in ^{11}B NMR spectroscopy. The chloride may have coordinated to the boron Lewis acid to form the corresponding species. Prior addition of silylone **243** did not influence the final outcome of the reaction, since the signal at 0 ppm was displayed again in ^{11}B NMR spectroscopy. Furthermore, ^{1}H NMR spectroscopy provided evidence of partial only decomposition of silylone **243** in the absence of intended product **289**.

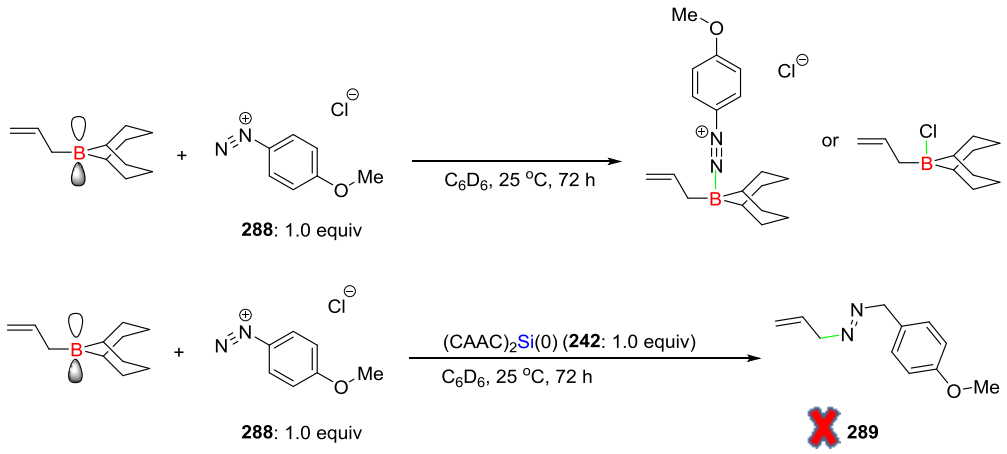

*The reactions performed by Arseni Borisov under my supervision

Scheme 5.36: Staudinger reaction.

Attempts to form borenium ion and Lewis acid catalysis trials

Since our efforts in the field of the Lewis base catalysis were not prosperous, we decided to investigate silylone **243** as a Lewis base candidate to activate weak Lewis acids (Scheme 5.37). Treatment of OTf– B(9-bbn), which is a weak Lewis acid, with a weak Lewis base may not lead to formation of a boron–ate complex.[192] However, a stronger Lewis base may be able to coordinate initially to the boron to generate a boron–ate complex, which would be spontaneously ionised to form a borenium ion.[192] The borenium ion though is a strong Lewis acid and has been used for the activation of electrophiles in the field of Lewis acid catalysis.[192] Indeed, the use of two equilavents of a strong Lewis base may lead to ionisation to form, initially, the borenium ion (1.0 equiv) and then, generate the boronium ion (1.0 equiv).[192] Considering that the silicon atom of silylone **243** may have two lone pairs of electrons available for chemistry, we hypothesized that coordination on the Lewis acidic boron of OTf–9BBN could be feasible.

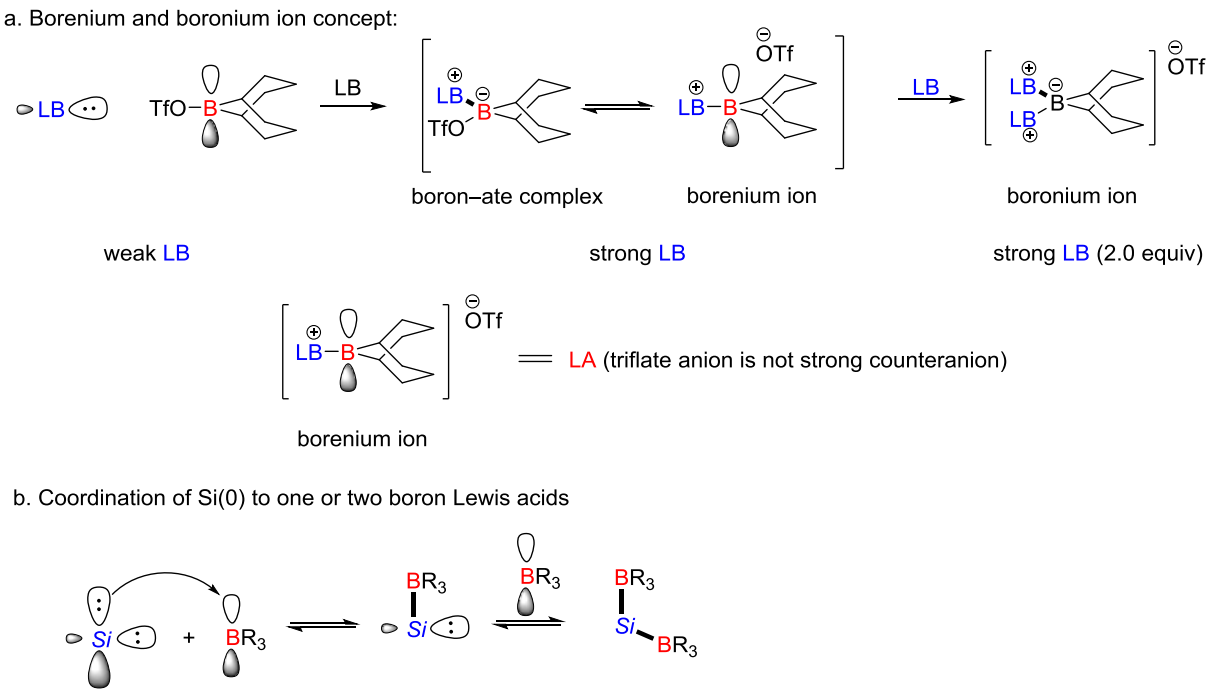

Scheme 5.37: Attempts to form the borenium ion.

OTf–B(9BBN) displays a signal at 63.5 ppm in C_6D_6 in the ^{11}B NMR spectroscopy (Scheme 5.38). Addition of silylone **243** (1.0 equiv) led to the generation of two signals slightly up-field (59 and 53 ppm), while the signal of the starting material at 64 ppm disappeared.

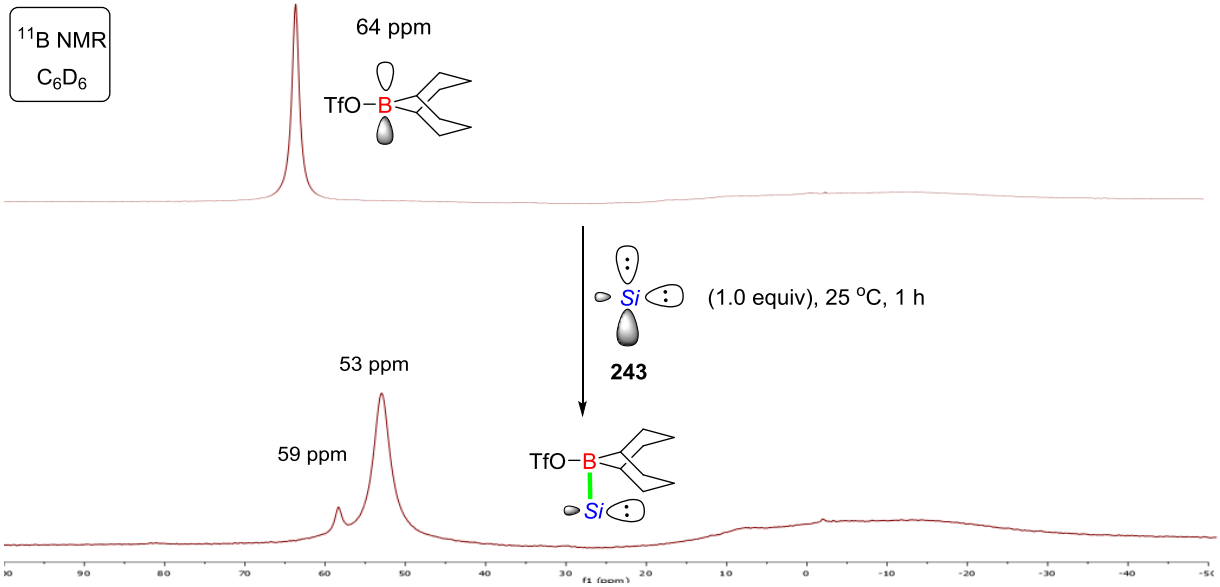

*The reactions performed by Arseni Borisov under my direct supervision

Scheme 5.38: A fast, reversible interaction of silylone **243** with OTf–B(9BBN) to form the borenium ion in C_6D_6.

The same experiment was repeated in toluene–d8 (Scheme 5.39). The signal of the starting material is displayed at 67 ppm (1.2 equiv). Addition of silylone **243** (1.0 equiv) led to a new signal at 58 ppm in ^{11}B NMR spectroscopy. An extra equivalent of OTf–9BBN was added to generate a new signal at 63 ppm in ^{11}B NMR spectroscopy. Denmark *et al.* reported a wide range of ^{11}B NMR signals that correspond to formed borenium ions (56–84 ppm).[192] However, Tf_2N–(B)9BBN was used as a boron Lewis acid instead of OTf–(B)9BBN. Considering that the ^{11}B NMR signals of the reaction mixtures were within the range of a borenium ion (Schemes 5.38 and 5.39) and the royal blue color of the solution was retained, we decided to conduct further investigations in this project.

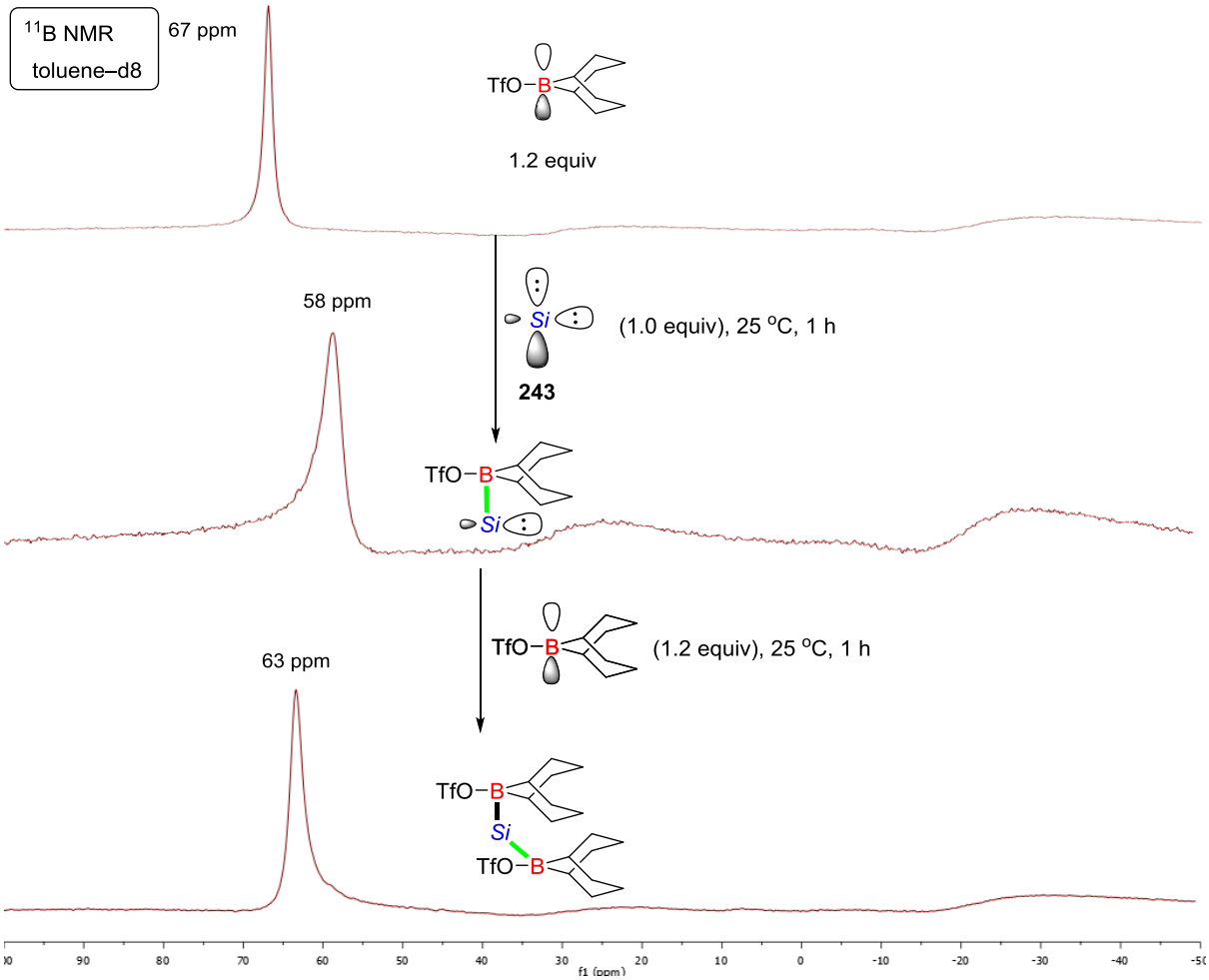

*The reactions performed by Arseni Borisov under my direct supervision

Scheme 5.39: A fast, reversible interaction of silylone **243** with OTf–9BBN to form borenium ion in benzene.

The potential catalytic system was used in the concept of Lewis base-assisted Lewis acid catalysis. Catalytic hydrosilylation of various ketones was attempted using the potentially formed borenium ion (Scheme 5.40). Ketones were treated with triethylsilane (1.0 equiv) and 10 mol% of the potentially formed borenium ion in C_6D_6

at 25 °C. Unfortunately, ^{1}H NMR spectroscopy confirmed that the three ketones with triethylsilane remained unreacted and the catalyst completely decomposed.

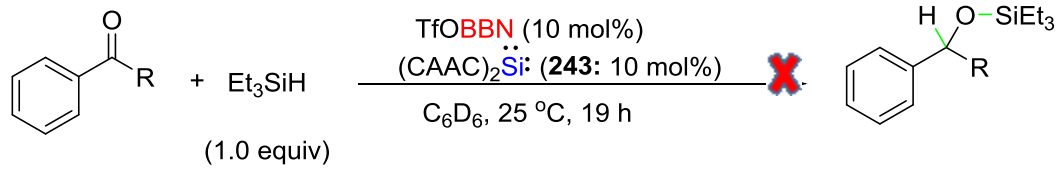

R = Ph,4-tolyl,4-anisyl.

*The reactions performed by Arseni Borisov under my supervision

Scheme 5.40: Hydrosilylations of various ketones.

Identical conditions were applied to the Diels-Alder cycloadditions. Methyl and methoxy vinyl ketones (dienophiles) were treated with 1,3-cyclohexadiene (1.0 equiv; diene) and 10 mol% of the potentially formed borenium ion in C_6D_6 at 25 °C (Scheme 5.41). ^{1}H NMR spectroscopy provided evidence of unreacted starting materials with completely decomposed silylone **243** (instant colour change to purple). A newly formed, single signal, at 33 ppm was confirmed by ^{11}B NMR spectroscopy. However, in the absence of silylone **243**, OTf–(B)9BBN decomposed in contact with 1,3-cyclohexadiene and the Michael acceptors based on the ^{11}B NMR spectroscopy.

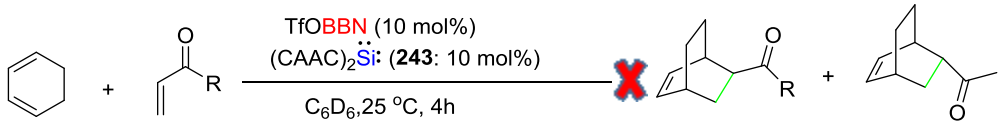

(1.0 equiv)

R = Me, MeO

Scheme 5.41: Diels-Alder cycloaddition.

5.3.2.3 FLP (Frustrated Lewis Pairs) Attempts

Next, a major goal of our project was to investigate **243** in the field of frustrated Lewis pair (FLP) chemistry (Scheme 5.42). The state in which, a pair of a Lewis acid and a Lewis base are not able to form an adduct due to steric congestion, is called frustrated Lewis pair [Sceme 5.42 a)]. The active centres of those species are sterically hindered; an effect that is called 'frustration'. However, applications of FLP chemistry have already been reported.[41,44,141,193–195] Recently, Alcarazo *et al.* reported FLP chemistry between the CDP **152** and the tris(pentafluorophenyl)borane.[45] Similarly, we applied this concept between silylone **243** and tris(pentafluorophenyl)borane [Scheme 5.42 b)]. X-ray crystallographic analysis of silylone **243** provided evidence of significant steric bulk in the surroundings of the electron-rich silicon atom, therefore we decided to apply the FLP concept using the silylone **243** as a Lewis base. Treatment of **243** (1.2 equiv) with tris(pentafluorophenyl)borane in toluene at room temperature led to instant decomposition (brown-red solution) confirmed by ^{1}H NMR spectroscopy. At low temperature (–78 °C), drop-wise addition of a solution of tris-(pentafluorophenyl)borane in toluene, in a toluene solution of silylone **243** did not lead to colour change (royal blue colour was retained), therefore no decomposition was assumed.

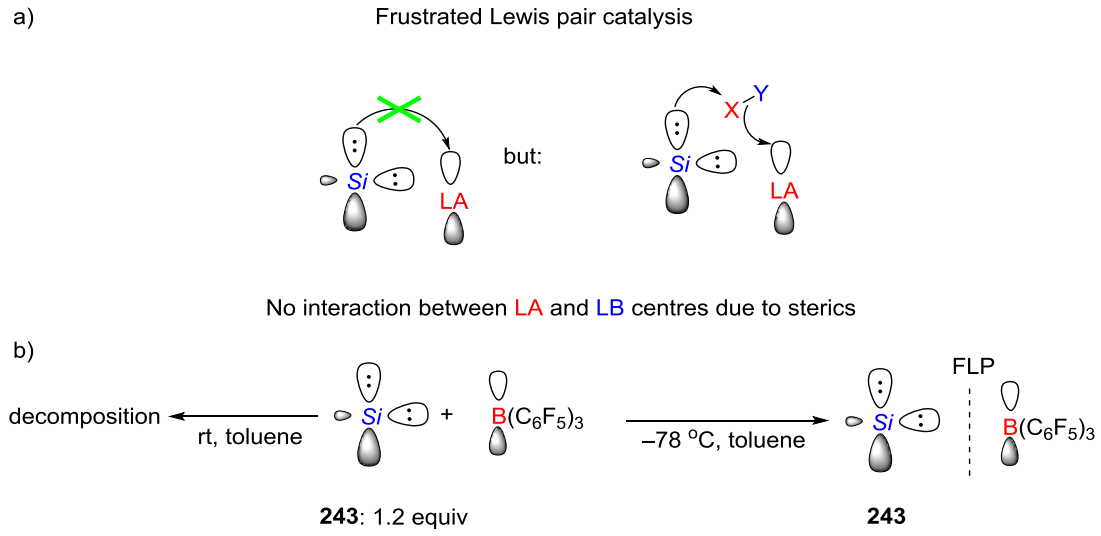

*The reactions performed by Arseni Borisov under my direct supervision

Scheme 5.42: FLP system optimisation.

In the royal blue solution of **243** and tris-(pentafluorophenyl)borane in C_6D_6 at –78 °C in toluene, isobutylene oxide (1.2 equiv) was added aiming to accomplish an FLP-driven bond cleavage of the C–O of the quaternary bond to form **290** (Scheme 5.43). Warm-up of the solution at the room temperature led to decolourisation and ^{1}H NMR spectroscopy evidenced decomposition of isobutylene oxide without formation of the intended product.

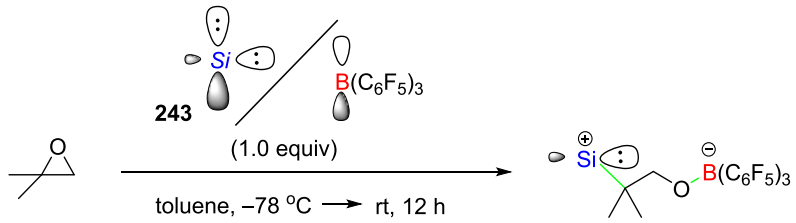

1.2 equiv

290

*The reactions performed by Arseni Borisov under my direct supervision

Scheme 5.43: FLP system applied to the ring-opening of the isobutylene oxide.

Ring opening of tetrahydrofuran was attempted as well (Scheme 5.44). The FLP system (1.6 mol%) was prepared and cooled at –78 °C. THF was added at –78 °C and after the warm-up to the room temperature, colour change was observed (colourless solution). **243** was decomposed and intended product **291** was not formed based on ^{1}H NMR spectroscopy.

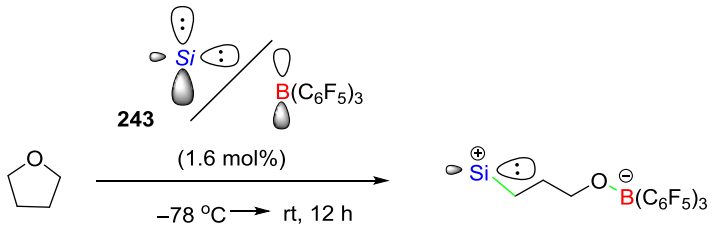

291

*The reactions performed by Arseni Borisov under my direct supervision

Scheme 5.44: FLP system applied to the ring-opening of THF.

Identical FLP system was applied for the heterolytic cleavage of bond of hydrogen, which is the main representative of small molecules (Scheme 5.45). Again, the reaction mixture was warmed-up to room temperature and decolourised. However, the intended product was not detected by ^{1}H NMR spectroscopy.

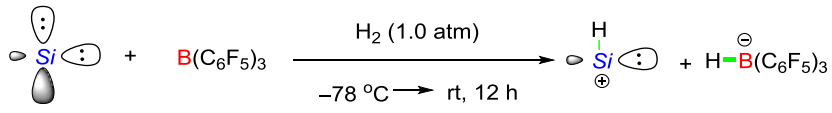

243

*The reactions performed by Arseni Borisov under my supervision

Scheme 5.45: FLP system applied to bond cleavage of H_2.

Overall, the ^{1}H NMR spectroscopy of the aliquots in each case were similar. This outcome strongly suggests interaction between the FLP system at 25 °C, which could not be avoided even reaching this temperature progressively. Investigation of this interaction did not lead to formation of the intended product or boron–ate complex formation (Scheme 5.46).

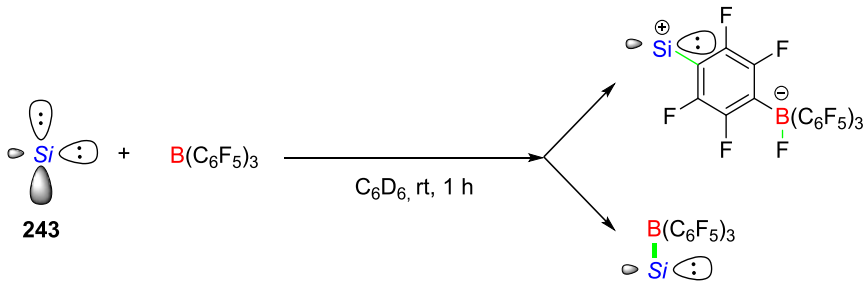

*The reactions performed by Arseni Borisov under my direct supervision

Scheme 5.46: Effort to rationalise the reaction outcome our FLP system.

5.4 Summary and Future work

To conclude, the preparation of silylones **243**, **244** and **265** was attempted (Scheme 5.47). While the preparation of **244** and **265** proved to be challenging, **243** was successfully prepared and used in ^{11}B NMR studies with various boron Lewis acids (Scheme 5.47). ^{11}B NMR studies of **243** with BH_3•SMe_2 drawn our attention, since an interesting reactivity was developed (Scheme 5.47). Indeed, the catalytic potential of **243** was investigated in the field of Lewis base and Lewis acid catalysis, although the formation of the intended products was not detected by ^{1}H NMR and ^{11}B NMR spectroscopy.

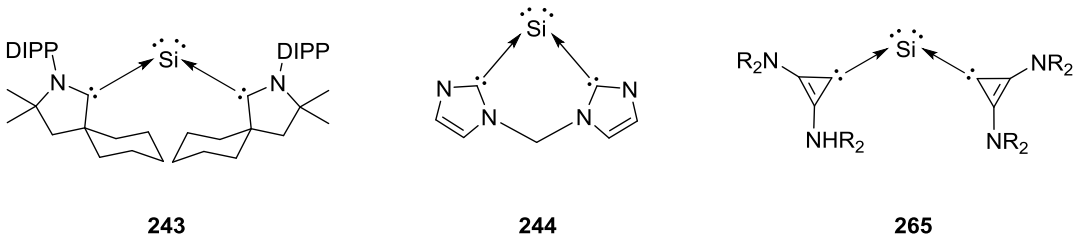

243 **244** **265**

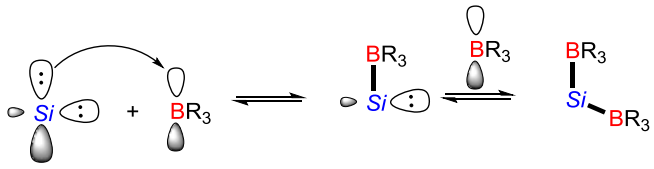

243 1.0–1.2 equiv

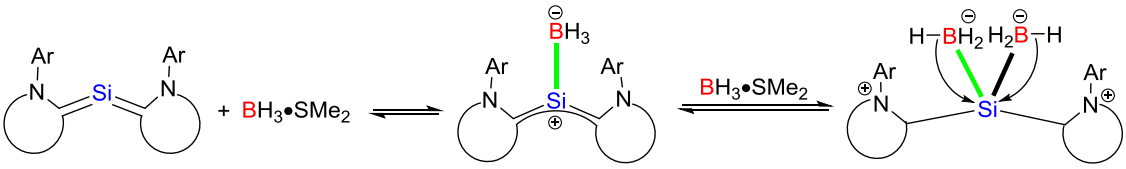

243 (1.0 equiv) **E** **F**

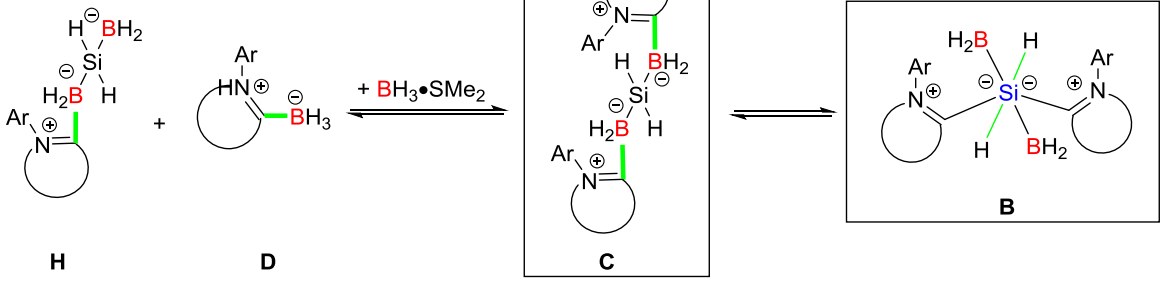

H **D** **C** **B**

Scheme 5.47: Overview.

In our future work, we aim to prepare a library of metal complexes utilizing "green" main group metals (groups I, II and XIII) and first-row transition metals (from manganese to zinc). These new metal complexes may display unique catalytic properties in the field of dual catalysis. In our trials with aluminium(III) chloride and gallium(III) chloride, ^{1}H NMR spectroscopic analysis exhibited decomposition of the Si(0), while there was colour change to a different shade of blue of the reaction mixtures. In contrast, in our experiment with indium(III) chloride, a new set of signals close to the ones of **243** with similar multiplicity have been displayed in ^{1}H NMR spectroscopy to suggest formation of the metal complex **292**. The incomplete reaction of **243** presented challenges in the characterisation of the ^{1}H NMR spectrum due to signal overlap. While metal complexation of Si(0) with $InCl_3$ was suggested, isolation and full characterization of the new species is required alongside further evidence obtained by X-ray crystallographic analysis. This data will provide a valuable insight into the potential of metal complexation of **243** with various metals. The decomposition of **243** in the experiments with Al(III) and Ga(II) may be explained that both metals are more Lewis acidic compared to In(III) to cause the decomposition.

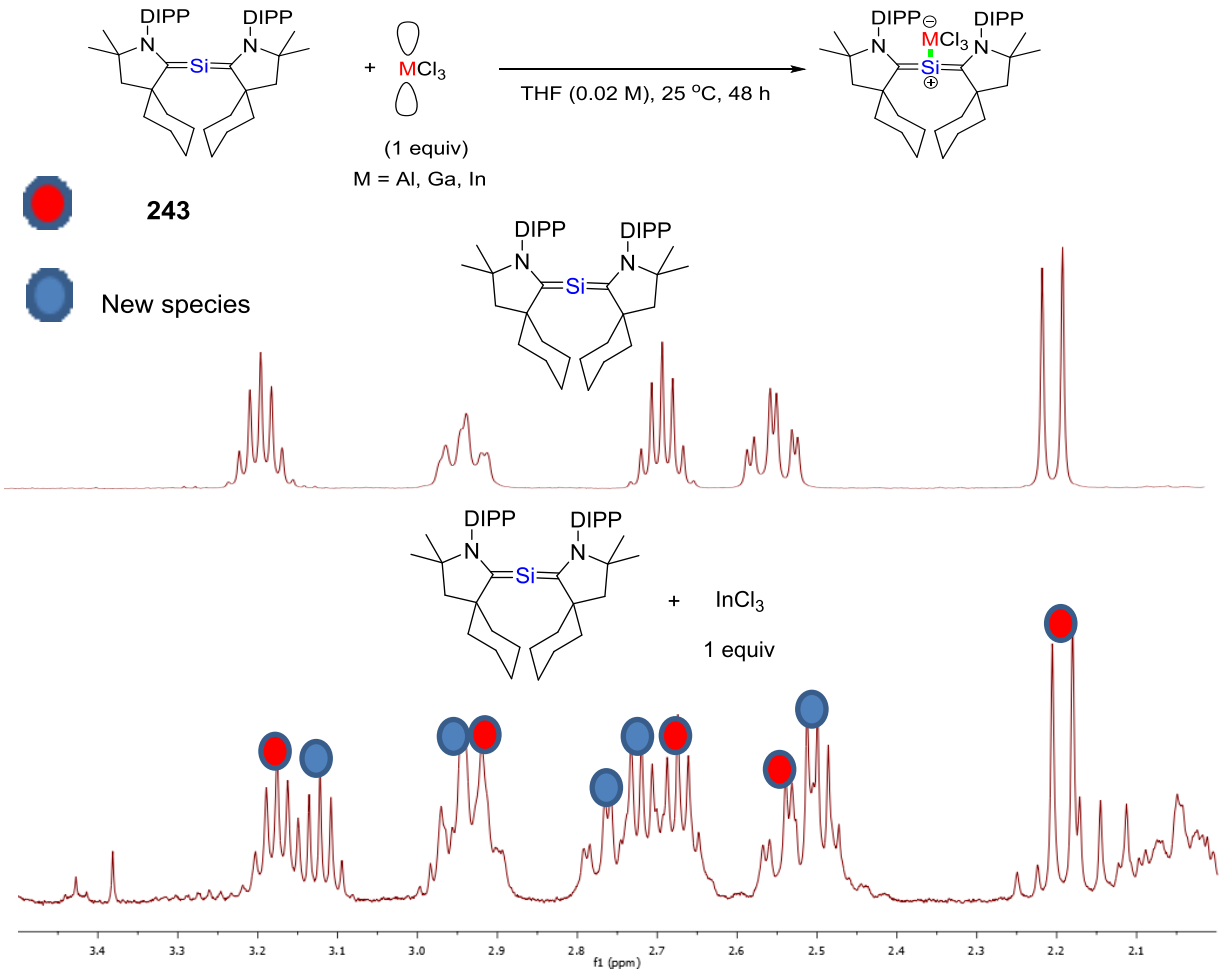

Scheme 5.48: ^{1}H NMR of **243** (above); ^{1}H NMR of **243** and $InCl_3$ reaction mixture .

Then, supposing that we are able to prepare a library of metal complexes with **242** as a ligand, we will investigate the potentials of this compound in the field of dual catalysis. Firstly, we would like to study the σ donor ability of **242** and then, the potentials of activating the second lone pair of electrons. Indeed, the possibility of the metal atom acting as a Lewis acid with a lone pair in vicinity acting as a Lewis base will be the subject of our investigation. The former may activate the electrophile, while the Lewis basic silicon may activate the pro-nucleophile to react with each other.

6 Bibliography

(1) Knözinger, H.; Kochloefl, K. *Ullmann's Encycl. Ind. Chem.* **2009**, *1*, 2–110.

(2) Roberts, M. W. *Catal. Letters* **2000**, *67* (1), 1–4.

(3) Shaikh, I. R. *J. Catal.* **2014**, *2014*, 1–35.

(4) Dalko, P. I.; Moisan, L. *Angew. Chemie - Int. Ed.* **2004**, *43* (39), 5138–5175.

(5) Dröge, T.; Glorius, F. *Angew. Chemie - Int. Ed.* **2010**, *49* (39), 6940–6952.

(6) Maji, B.; Breugst, M.; Mayr, H. *Angew. Chemie - Int. Ed.* **2011**, *50* (30), 6915–6919.

(7) Bugaut, X.; Glorius, F. *Chem. Soc. Rev.* **2012**, *41* (9), 3511.

(8) Arduengo III, A. J.; Harlow, R. L.; Kline, M. *J. Am. Chem. Soc.* **1991**, *113* (7), 2801.

(9) Alcarazo, M.; Lehmann, C. W.; Anoop, A.; Thiel, W.; Fürstner, A. *Nat. Chem.* **2009**, *1* (4), 295–301.

(10) Bruns, H.; Patil, M.; Carreras, J.; Vázquez, A.; Thiel, W.; Goddard, R.; Alcarazo, M. *Angew. Chemie - Int. Ed.* **2010**, *49* (21), 3680–3683.

(11) Mondal, K. C.; Roesky, H. W.; Schwarzer, M. C.; Frenking, G.; Niepötter, B.; Wolf, H.; Herbst-Irmer, R.; Stalke, D. *Angew. Chemie - Int. Ed.* **2013**, *52* (10), 2963–2967.

(12) Kirmse, W. *Angew. Chemie - Int. Ed.* **2004**, *43* (14), 1767–1769.

(13) Bertrand, G. *Nat. Chem.* **2010**, *1* (July), 265.

(14) Alcarazo, M. *Dalton Trans.* **2011**, *40* (9), 1839–1845.

(15) Tonner, R.; Frenking, G. *Chem. - A Eur. J.* **2008**, *14* (11), 3260–3272.

(16) Tonner, R.; Frenking, G. *Chem. - A Eur. J.* **2008**, *14* (11), 3273–3289.

(17) Tonner, R.; Öxler, F.; Neumüller, B.; Petz, W.; Frenking, G. *Angew. Chemie - Int. Ed.* **2006**, *45* (47), 8038–8042.

(18) Patel, D. S.; Bharatam, P. V. *J. Phys. Chem. A* **2011**, *115* (26), 7645–7655.

(19) Bhatia, S.; Bagul, C.; Kasetti, Y.; Patel, D. S.; Bharatam, P. V. *J. Phys. Chem. A* **2012**, *116* (36), 9071–9079.

(20) Kozma, Á.; Gopakumar, G.; Farès, C.; Thiel, W.; Alcarazo, M. *Chem. - A Eur. J.* **2013**, *19* (11), 3542–3546.

(21) Patel, D. S.; Bharatam, P. V. *Chem. Commun. (Camb).* **2009**, No. 9, 1064–1066.

(22) Liu, M.; Yang, I.; Buckley, B.; Lee, J. K. *Org. Lett.* **2010**, *12* (21), 4764–4767.

(23) Patel, D. S.; Bharatam, P. V. *Chem. Commun. (Camb).* **2009**, No. 9, 1064–

1066.

(24) R. Appel, K. Waid. *Angew. Chem. Int. Ed.* **1979**, *375* (2), 833179.

(25) Holzmann, N.; Dange, D.; Jones, C.; Frenking, G. *Angew. Chemie - Int. Ed.* **2013**, *52* (10), 3004–3008.

(26) Adolf Krebs, Andreas Guetner, Sayandro Verstelen, S. S. *Tetrahedron Lett.* **1984**, *25* (22), 2333.

(27) Theophil Eicher, Heinz Erhardt, N. P. *Tetrahedron Lett.* **1973**, *3* (44), 4353–4354.

(28) Theophil Eicher, Richard Grof, Heinz Kunzmann, R. P. *Synthesis (Stuttg).* **1987**, *10*, 887–892.

(29) Paetzold, R.; Rönsch, E. *Angew. Chemie Int. Ed.* **1964**, *3* (12), 805–806.

(30) Bandar, J. S.; Lambert, T. H. *J. Am. Chem. Soc.* **2012**, *134* (12), 5552–5555.

(31) O'Donnell, M. J.; Bennett, W. D.; Bruder, W. a; Jacobsen, W. N.; Knuth, K.; LeClef, B.; Polt, R. L.; Bordwell, F. G.; Mrozack, S. R.; Cripe, T. a. *J. Am. Chem. Soc.* **1988**, *110* (25), 8520–8525.

(32) Akiyama, T.; Itoh, J.; Yokota, K.; Fuchibe, K. *Angew. Chemie Int. Ed.* **2004**, *43* (12), 1566–1568.

(33) Williams, A. L.; Johnston, J. N. *J. Am. Chem. Soc.* **2004**, *126*, 1612–1613.

(34) Garnovskii, A. D.; Nivorozhkin, A. L.; Minkin, V. I. *Coord. Chem. Rev.* **1993**, *126* (1–2), 1–69.

(35) Cozzi, P. G. *Chem. Soc. Rev.* **2004**, *33* (7), 410–421.

(36) E. P. Winpenny, R. *Chem. Soc. Rev.* **1998**, *27* (6), 447.

(37) Phomphrai, K.; Pracha, S.; Phonjanthuek, P.; Pohmakotr, M. *Dalton Trans.* **2008**, 3048–3050.

(38) Rajesh, K.; Berke, H. *Adv. Synth. Catal.* **2013**, *355* (5), 901–906.

(39) Suzuki, H.; Sato, I.; Yamashita, Y.; Kobayashi, S. *J. Am. Chem. Soc.* **2015**, *137* (13), 4336–4339.

(40) Yamashita, Y.; Sato, I.; Suzuki, H.; Kobayashi, S. *Chem. - An Asian J.* **2015**, *10* (10), 2143–2146.

(41) Welch, G. C.; Juan, R. R. S.; Masuda, J. D.; Stephan, D. W. *Science* **2005**, *1883*, 15–18.

(42) Inés, B.; Holle, S.; Goddard, R.; Alcarazo, M. *Angew. Chemie - Int. Ed.* **2010**, *49* (45), 8389–8391.

(43) Nicasio, J. a.; Steinberg, S.; Inés, B.; Alcarazo, M. *Chem. - A Eur. J.* **2013**, *19* (33), 11016–11020.

(44) Stephan, D. W. *Org. Biomol. Chem.* **2008**, *6* (9), 1535–1539.

(45) Alcarazo, M.; Gomez, C.; Holle, S.; Goddard, R. *Angew. Chemie - Int. Ed.*

2010, *49* (33), 5788–5791.

(46) Stukenbroeker, T. S.; Bandar, J. S.; Zhang, X.; Lambert, T. H.; Waymouth, R. M. *ACS Macro Lett.* **2015**, *4* (8), 853–856.

(47) Lavallo, V.; Canac, Y.; Donnadieu, B.; Schoeller, W. W.; Bertrand, G. *Science* **2006**, *312* (5774), 722–724.

(48) Mo, K.; Yang, Y.; Cui, Y. *J. Am. Chem. Soc.* **2013**, *136*, 1746–1749.

(49) Yang, F.; Wei, S.; Chen, C. A.; Xi, P.; Yang, L.; Lan, J.; Gau, H. M.; You, J. *Chem. - A Eur. J.* **2008**, *14* (7), 2223–2231.

(50) Niemeyer, J.; Kehr, G.; Froehlich, R.; Erker, G. *Eur. J. Inorg. Chem.* **2010**, No. 5, 680–684.

(51) Wang, J.; Wang, W.; Li, W.; Hu, X.; Shen, K.; Tan, C.; Liu, X.; Feng, X. *Chem. - A Eur. J.* **2009**, *15* (43), 11642–11659.

(52) Kurono, N.; Yoshikawa, T.; Yamasaki, M.; Ohkuma, T. *Synthesis (Stuttg).* **2011**, *2*, 2009–2012.

(53) Zeng, Z.; Zhao, G.; Zhou, Z.; Tang, C. *European J. Org. Chem.* **2008**, *2008* (9), 1615–1618.

(54) Kim, S. S.; Song, D. H. *European J. Org. Chem.* **2005**, No. 9, 1777–1780.

(55) Hatano, M.; Hattori, Y.; Furuya, Y.; Ishihara, K. *Org. Lett.* **2009**, *11*, 2007–2010.

(56) Fetterly, B. M.; Verkade, J. G. *Tetrahedron Lett.* **2005**, *46* (46), 8061–8066.

(57) Fukuda, Y.; Kondo, K.; Aoyama, T. *Synthesis (Stuttg).* **2006**, *2006* (16), 2649–2652.

(58) Fukuda, Y.; Maeda, Y.; Ishii, S.; Kondo, K.; Aoyama, T. *Synthesis (Stuttg).* **2006**, *2006* (4), 589–590.

(59) Zhang, X.; Luck, R. L.; Fang, S. *Organometallics* **2011**, *30* (9), 2609–2616.

(60) Lv, C.; Cheng, Q.; Xu, D.; Wang, S.; Xia, C.; Sun, W. *European J. Org. Chem.* **2011**, *2011* (19), 3407–3411.

(61) Muccioli, G. G.; Fazio, N.; Scriba, G. K. E.; Poppitz, W.; Cannata, F.; Poupaert, J. H.; Wouters, J.; Lambert, D. M. *J. Med. Chem.* **2006**, *49* (1), 417–425.

(62) Muccioli, G. G.; Wouters, J.; Scriba, G. K. E.; Poppitz, W.; Poupaert, J. H.; Lambert, D. M. *J. Med. Chem.* **2005**, *48*, 7486–7490.

(63) Denmark, S. E.; Beutner, G. L. *Lewis Base Catalysis in Organic Synthesis*; 2008; Vol. 47.

(64) Gutmann, V. *The Donor-Acceptor Approach to Molecular Interactions*; 1978.

(65) Jensen, W. B. *Wiley-Interscience, New York* **1980**, 135–142.

(66) Gutmann, V. *Coord. Chem. Rev.* **1975**, *15* (2–3), 207–237.

(67) Rendler, S.; Oestreich, M. *Synthesis (Stuttg).* **2005**, No. 11, 1727–1747.

(68) Denmark, S. E.; Beutner, G. L. *Angew. Chemie - Int. Ed.* **2008**, *47* (9), 1560–1638.

(69) Klare, H. F. T.; Oestreich, M. *Dalt. Trans.* **2010**, *39* (39), 9176–9184.

(70) Klare, H. F. T.; Bergander, K.; Oestreich, M. *Angew. Chemie - Int. Ed.* **2009**, *48* (48), 9077–9079.

(71) Mueller, T. *Angew. Chemie - Int. Ed.* **2001**, *40*, 3033–3036.

(72) West, R. *J. Organomet. Chem.* **1983**, *251*, 295–298.

(73) Swamy, K. C. K.; Chandrasekhar, V.; Harland, J. J.; Holmes, J. M.; Day, R. O.; Holmes, R. R. *J. Am. Chem. Soc.* **1990**, *112* (6), 2341–2348.

(74) Apperley, D. C.; Mink, J.; Berkesi, O.; A, J. M. C.; Jacobsen, E. N.; Marko, I.; Olah, G. *Configurations* **2001**, *2*, 589–590.

(75) Iseki, K.; Nagai, T.; Kobayashi, Y. *Tetrahedron Lett.* **1994**, *35* (19), 3137–3138.

(76) Mizuta, S.; Shibata, N.; Akiti, S.; Fujimoto, H.; Nakamura, S.; Toru, T. *Org. Lett.* **2007**, *9* (18), 3707–3710.

(77) Umemoto, T. *Chem. Rev.* **1996**, *96* (5), 1757–1778.

(78) Itoh, Y.; Mikami, K. *Org. Lett.* **2005**, *7* (4), 649–651.

(79) Chen, Q.; Wu, S. *J. Chem. Soc.* **1989**, 705–706.

(80) Sato, K.; Omote, M.; Ando, A.; Kumadaki, I. *Org. Lett.* **2004**, *6* (23), 4359–4361.

(81) Reeves, J. T.; Gallou, F.; Song, J. J.; Tan, Z.; Lee, H.; Yee, N. K.; Senanayake, C. H. *Tetrahedron Lett.* **2007**, *48* (2), 189–192.

(82) Gouverneur, Veronique, K. M. *Fluorine in Pharmaceutical and Medicinal Chemistry*, 6th Editio.; 2012.

(83) Mizuta, S.; Shibata, N.; Hibino, M.; Nagano, S.; Nakamura, S.; Toru, T. *Tetrahedron* **2007**, *63* (35), 8521–8528.

(84) Adkins, J. C.; Noble, S. *Drugs* **1998**, *56* (6), 1055–1064.

(85) Rosenzweig, P.; Patat, A.; Curet, O.; Durrieu, G.; Dubruc, C.; Zieleniuk, I.; Legangneux, E. *J. Affect. Disord.* **1998**, *51* (3), 305–312.

(86) Krishnamurti, R.; Bellew, D. R.; Prakash, G. K. S. *J. Org. Chem.* **1991**, *56* (d), 984–989.

(87) Singh, R. P.; Cao, G.; Kirchmeier, R. L.; Shreeve, J. M. *J. Org. Chem.* **1999**, *64* (8), 2873–2876.

(88) Prakash, G. K. S.; Krishnamurti, R.; Olah, G. a. *J. Am. Chem. Soc.* **1989**, *111* (9), 393–395.

(89) Song, J. J.; Tan, Z.; Reeves, J. T.; Gallou, F.; Yee, N. K.; Senanayake, C. H.

Org. Lett. **2005**, *7* (11), 2193–2196.

(90) Matsukawa, S.; Saijo, M. *Tetrahedron Lett.* **2008**, *49* (31), 4655–4657.

(91) Birkofer L., Mueller F., K. W. *Tetrahedron Lett.* **1967**, *29*, 2781–2783.

(92) Kozaburo Nishiyama, T. Y. *Synthesis (Stuttg).* **1988**, *2*, 106–108.

(93) Burstein, C.; Glorius, F. *Angew. Chemie - Int. Ed.* **2004**, *43* (45), 6205–6208.

(94) Fischer, C.; Smith, S. W.; Powell, D. a.; Fu, G. C. *J. Am. Chem. Soc.* **2006**, *128* (5), 1472–1473.

(95) Li, Z.; Fernández, M.; Jacobsen, E. N. *Org. Lett.* **1999**, *1* (10), 1611–1613.

(96) Mita, T.; Fujimori, I.; Wada, R.; Wen, J.; Kanai, M.; Shibasaki, M. *J. Am. Chem. Soc.* **2005**, *127* (32), 11252–11253.

(97) Fukuta, Y.; Mita, T.; Fukuda, N.; Kanai, M.; Shibasaki, M. *J. Am. Chem. Soc.* **2006**, *128* (19), 6312–6313.

(98) Mihara, H.; Xu, Y.; Shepherd, N. E.; Matsunaga, S.; Shibasaki, M. *J. Am. Chem. Soc.* **2009**, 8384–8385.

(99) Schneider, C. *Angew. Chemie - Int. Ed.* **2009**, *48* (12), 2082–2084.

(100) Xu, Y.; Kaneko, K.; Kanai, M.; Shibasaki, M.; Matsunaga, S. *J. Am. Chem. Soc.* **2014**, *136* (25), 9190–9194.

(101) Minakata, S.; Okada, Y.; Oderaotoshi, Y.; Komatsu, M. *Org. Lett.* **2005**, *7* (16), 3509–3512.

(102) Matsukawa, S.; Tsukamoto, K. *Org. Biomol. Chem.* **2009**, *7* (18), 3792–3796.

(103) Matsukawa, S.; Harada, T.; Yasuda, S. *Org. Biomol. Chem.* **2012**, *10* (25), 4886.

(104) Wu, B.; Gallucci, J. C.; Parquette, J. R.; RajanBabu, T. V. *Angew. Chemie* **2009**, *121*, 1146–1149.

(105) Saikia, I.; Kashyap, B.; Phukan, P. *Chem. Commun. (Camb).* **2011**, *47* (10), 2967–2969.

(106) Minakata, S.; Morino, Y.; Oderaotoshi, Y.; Komatsu, M. *Chem. Commun. (Camb).* **2006**, 3337–3339.

(107) Ali, S. I.; Nikalje, M. D.; Sudalai, a. *Org. Lett.* **1999**, *1* (5), 705–707.

(108) Sun, H.; Huang, B.; Lin, R.; Yang, C.; Xia, W. *Beilstein J. Org. Chem.* **2015**, *11*, 524–529.

(109) Jensen, K. L.; Standley, E. A.; Jamison, T. F. *J. Am. Chem. Soc.* **2014**, *136* (31), 11145–11152.

(110) Thakur, V. V.; Sudalai, A. *Tetrahedron Lett.* **2003**, *44* (5), 989–992.

(111) Jeong, J. U.; Tao, B.; Sagasser, I.; Henniges, H.; Sharpless, K. B. *J. Am. Chem. Soc.* **1998**, *120* (27), 6844–6845.

(112) Bandar, J. S.; Lambert, T. H. *J. Am. Chem. Soc.* **2013**, *135* (32), 11799–11802.

(113) Bandar, J. S.; Barthelme, A.; Mazori, A. Y.; Lambert, T. H. *Chem. Sci.* **2015**, *6* (2), 1537–1547.

(114) Bandar, J. S.; Sauer, G. S.; Wulff, W. D.; Lambert, T. H.; Vetticatt, M. J. *J. Am. Chem. Soc.* **2014**, *136* (30), 10700–10707.

(115) Ghosal, N. C.; Santra, S.; Das, S.; Hajra, A.; Zyryanov, G. V; Majee, A. *Green Chem.* **2016**, *18*, 565–574.

(116) Dyker, C. A.; Lavallo, V.; Donnadieu, B.; Bertrand, G. *Angew. Chemie - Int. Ed.* **2008**, *47* (17), 3206–3209.

(117) Klein, S.; Tonner, R.; Frenking, G. *Chem. - A Eur. J.* **2010**, *16*, 10160–10170.

(118) Liu, W.; Gust, R. *Chem. Soc. Rev.* **2013**, *42* (2), 755–773.

(119) Oehninger, L.; Rubbiani, R.; Ott, I. *Dalt. Trans.* **2013**, *42* (10), 3269–3284.

(120) Porter, K. a.; Schier, A.; Schmidbaur, H. *Organometallics* **2003**, *22* (24), 4922–4927.

(121) F. Ramirez, B. Hansen, N. B. Desai, N. M. *J. Am. Chem. Soc.* **1961**, *83*, 3539–3540.

(122) Schmidbaur, H.; Schier, A. *Angew. Chemie - Int. Ed.* **2013**, *52* (1), 176–186.

(123) Kaska, W. C.; Mitchell, D. K.; Reichelderfer, R. F. *J. Organomet. Chem.* **1973**, *47* (2), 391–402.

(124) Bestmann, H. *Angew. Chem. Int. Ed.* **1977**, *16* (19), 349–364.

(125) Zundel, G.; Eds, C. S.; Hydrogen, T.; Hol-, V. N.; Allen, S. F. A.; Taylor, R.; Hans, B.; Bestmann, J.; Schmidt, M. **1987**, 79–81.

(126) Alcarazo, M.; Suárez, R. M.; Goddard, R.; Fürstner, A. *Chem. - A Eur. J.* **2010**, *16* (32), 9746–9749.

(127) Dellus, N.; Kato, T.; Bagán, X.; Saffon-Merceron, N.; Branchadell, V.; Baceiredo, A. *Angew. Chemie - Int. Ed.* **2010**, *49* (38), 6798–6801.

(128) Driscoll, , J. S.; Grisley D. W.; Pustinger J. V.; Harris J. E.; Matthews, C. N. *J. Org. Chem.* **1964**, *29*, 2427–2431.

(129) Appel, R. *Inorg. Synth.* **1986**, *24*, 113–117.

(130) Schobert, R. *Org. Synth.* **2005**, *82* (2005), 140–146.

(131) Boeckman, R. K.; Pero, J. E.; Boehmler, D. J. *J. Am. Chem. Soc.* **2006**, *128* (34), 11032–11033.

(132) Schmid, H. J. B. G.; Jiirgen, H.; Schmid, G. *Chem. Ber.* **1980**, *113*, 3369–3372.

(133) Bestmann, Jurgen and Roth, K. *Synthesis (Stuttg).* **1981**, *12*, 998–999.

(134) Inés, B.; Patil, M.; Carreras, J.; Goddard, R.; Thiel, W.; Alcarazo, M. *Angew. Chemie - Int. Ed.* **2011**, *50* (36), 8400–8403.

(135) Maigali, S. S.; Abd-El-Maksoud, M. a.; Soliman, F. M. *Arch. Pharm.*

(Weinheim). **2011**, *344* (7), 442–450.

(136) Schmidbaur, B. H.; Zybill, C. E.; Miiller, G.; Kriiger, C. *Angew. Chem. Int. Ed.* **1983**, *22*, 729–730.

(137) Moller, B. Y. G.; Kroger, C.; Zybill, C.; Schmidbaur, H. *Acta Crystallogr. Sect. C Cryst. Struct. Commun.* **1986**, *42*, 1141–1144.

(138) Vicente, J.; Singhal, A. R.; Jones, P. G. *Organometallics* **2002**, *21* (26), 5887–5900.

(139) Petz, W.; Neumüller, B. *Eur. J. Inorg. Chem.* **2011**, *3* (31), 4889–4895.

(140) Petz, W.; Kutschera, C.; Tschan, S.; Weller, F.; Neumüller, B. *Zeitschrift für Anorg. und Allg. Chemie* **2003**, *629* (7–8), 1235–1244.

(141) Petz, W.; Öxler, F.; Neumüller, B. *J. Organomet. Chem.* **2009**, *694* (25), 4094–4099.

(142) Petz, W.; Dehnicke, K.; Holzmann, N.; Frenking, G.; Neumüller, B. *Zeitschrift für Anorg. und Allg. Chemie* **2011**, *637* (12), 1702–1710.

(143) W. C. Kaska, D. K. Mitchell, R. F. Reicheld, W. D. K. *J. Am. Chem. Soc.* **1974**, *96*, 2847–2854.

(144) Sundermeyer, J.; Weber, K.; Peters, K.; Schnering, H. G. Von. *Organometallics* **1994**, *13* (8), 2560–2562.

(145) Schmidbaur, B. H.; Gasser, O. *Angew. Chemie - Int. Ed.* **1976**, *15*, 502–503.

(146) Alcarazo, M.; Radkowski, K.; Mehler, G.; Goddard, R.; Fürstner, A. *Chem. Commun.* **2013**, *49* (30), 3140–3142.

(147) Petz, W.; Öxler, F.; Neumüller, B.; Tonner, R.; Frenking, G. *Eur. J. Inorg. Chem.* **2009**, *2009*, 4507–4517.

(148) Bestmann, H.; Saalfvank, R. W. *Chem. Ber.* **1973**, *106*, 2601–2609.

(149) Wyatt, P.; Hudson, A.; Charmant, J.; Orpen, A. G.; Phetmung, H. *Org. Biomol. Chem.* **2006**, *4* (11), 2218–2232.

(150) Roberts, C. C.; Matías, D. M.; Goldfogel, M. J.; Meek, S. J. *J. Am. Chem. Soc.* **2015**, *137*, 6488–6491.

(151) Hsu, Y.-C.; Shen, J.-S.; Lin, B.-C.; Chen, W.-C.; Chan, Y.-T.; Ching, W.-M.; Yap, G. P. a.; Hsu, C.-P.; Ong, T.-G. *Angew. Chemie Int. Ed.* **2015**, *54* (8), 2420–2424.

(152) Pranckevicius, C.; Fan, L.; Stephan, D. W. *J. Am. Chem. Soc.* **2015**, *137* (16), 5582–5589.

(153) Chen, W.; Shen, J.; Jurca, T.; Peng, C.; Lin, Y.; Wang, Y.; Shih, W.; Yap, G. P. a; Ong, T. *Angew. Chemie Int. Ed.* **2015**, 1–7.

(154) Tang, S.; Monot, J.; El-hellani, A.; Michelet, B.; Guillot, R.; Bour, C.; Gandon, V. *Chem. - A Eur. J.* **2012**, *18*, 10239–10243.

(155) Igau, A.; Grutzmacher, H.; Baceiredo, A.; Bertrand, G. *J. Am. Chem. Soc.*

1988, No. 110, 6463–6466.

(156) Hill, N. J.; West, R. *J. Organomet. Chem.* **2004**, *689*, 4165–4183.

(157) Denk, M.; Lennon, R.; Hayashi, R.; West, R.; Belyakov, A. V.; Verne, H. P.; Haaland, A.; Wagner, M.; Metzler, N. *J. Am. Chem. Soc.* **1994**, *116* (6), 2691–2692.

(158) Schmedake, T. a.; Haaf, M.; Apeloig, Y.; Müller, T.; Bukalov, S.; West, R. *J. Am. Chem. Soc.* **1999**, *121* (40), 9479–9480.

(159) Furstner, A.; Krause, H.; Lehmann, C. W. *Chem Commun* **2001**, *80* (22), 2372–2373.

(160) Tuononen, H. M.; Roesler, R.; Dutton, J. L.; Ragogna, P. J. *Inorg. Chem.* **2007**, *46*, 10693–10706.

(161) Mondal, K. C.; Samuel, P. P.; Tretiakov, M.; Singh, A. P.; Roesky, H. W.; Stu, A. C.; Niepo, B.; Carl, E.; Wolf, H.; Herbst-irmer, R.; Stalke, D. *Inorg. Chem.* **2013**, *52*, 4736–4743.

(162) Niepötter, B.; Herbst-Irmer, R.; Kratzert, D.; Samuel, P. P.; Mondal, K. C.; Roesky, H. W.; Jerabek, P.; Frenking, G.; Stalke, D. *Angew. Chemie - Int. Ed.* **2014**, *53* (10), 2766–2770.

(163) Xiong, Y.; Yao, S.; Inoue, S.; Epping, J. D.; Driess, M. *Angew. Chemie - Int. Ed.* **2013**, *52* (28), 7147–7150.

(164) Ishida, S.; Iwamoto, T.; Kabuto, C.; Kira, M. *Nature* **2003**, *421* (6924), 725–727.

(165) Martin, D.; Soleilhavoup, M.; Bertrand, G. *Chem. Sci.* **2011**, *2* (3), 389.

(166) Lavallo, V.; Canac, Y.; Präsang, C.; Donnadieu, B.; Bertrand, G. *Angew. Chemie - Int. Ed.* **2005**, *44* (35), 5705–5709.

(167) Tonner, R.; Frenking, G. *Angew. Chemie - Int. Ed.* **2007**, *46* (45), 8695–8698.

(168) Guha, A. K.; Konwar, B.; Sarmah, S.; Phukan, A. K. *Theor. Chem. Acc.* **2012**, *131* (3), 1–11.

(169) Takagi, N.; Shimizu, T.; Frenking, G. *Chem. - A Eur. J.* **2009**, *15* (14), 3448–3456.

(170) Iwamoto, T.; Masuda, H.; Kabuto, C.; Kira, M. *Organometallics* **2005**, *24* (2), 197–199.

(171) Tanaka, H.; Inoue, S.; Ichinohe, M.; Driess, M.; Sekiguchi, A. *Organometallics* **2011**, *30* (13), 3475–3478.

(172) Martin, D.; Canac, Y.; Lavallo, V.; Bertrand, G. *J. Am. Chem. Soc.* **2014**, *136* (13), 5023–5030.

(173) Kira, M.; Ishida, S.; Iwamoto T.; Kabuto, C. *J. Am. Chem. Soc.* **1999**, *121*, 9722–9723.

(174) Iwamoto, T.; Masuda, H.; Ishida, S.; Kabuto, C.; Kira, M. *J. Organomet. Chem.* **2004**, *689* (8), 1337–1341.

(175) Gaspar, P. P.; Beatty, A. M.; Chen, T.; Haile, T.; Lei, D.; Winchester, W. R.; Braddock-wilking, J.; Rath, N. P.; Klooster, W. T.; Koetzle, T. F.; Mason, S. a; Albinati, A. *Organometallics* **1999**, *18*, 3921–3932.

(176) Iwamoto, T.; Abe, T.; Ishida, S.; Kabuto, C.; Kira, M. *J. Organomet. Chem.* **2007**, *692*, 263–270.

(177) Roy, S.; Mondal, K. C.; Krause, L.; Stollberg, P.; Herbst-irmer, R.; Stalke, D.; Meyer, J.; Stu, A. C.; Maity, B.; Koley, D.; Vasa, S. K.; Xiang, S. Q.; Linser, R.; Roesky, H. W. *J. Am. Chem. Soc. Chem. Soc.* **2014**, *136*, 16776–16779.

(178) Dirocco, D. A.; Rovis, T. *Angew. Chemie - Int. Ed.* **2012**, *51* (24), 5904–5906.

(179) Ghadwal, R. S.; Roesky, H. W.; Merkel, S.; Henn, J.; Stalke, D. *Angew. Chemie - Int. Ed.* **2009**, *48* (31), 5683–5686.

(180) Kumar, M. R.; Park, K.; Lee, S. *Adv. Synth. Catal.* **2010**, *352* (18), 3255–3266.

(181) Mondal, K. C.; Roesky, H. W.; Schwarzer, M. C.; Frenking, G.; Tkach, I.; Wolf, H.; Kratzert, D.; Herbst-Irmer, R.; Niepötter, B.; Stalke, D. *Angew. Chemie - Int. Ed.* **2013**, *52* (6), 1801–1805.

(182) Tarr, J. C.; Johnson, J. S. *Org. Lett.* **2009**, *11* (17), 3870–3873.

(183) Linghu, X.; Johnson, J. S. *Angew. Chemie - Int. Ed.* **2003**, *42* (22), 2534–2536.

(184) Baragwanath, L.; Rose, C. A.; Zeitler, K.; Connon, S. J. *J. Org. Chem.* **2009**, *74* (23), 9214–9217.

(185) Zhang, J.; Xing, C.; Tiwari, B.; Chi, Y. R. *J. Am. Chem. Soc.* **2013**, *135* (22), 8113–8116.

(186) Steward, K. M.; Gentry, E. C.; Johnson, J. S. *J. Am. Chem. Soc.* **2012**, *134* (17), 7329–7332.

(187) Chen, W. C.; Lee, C. Y.; Lin, B. C.; Hsu, Y. C.; Shen, J. S.; Hsu, C. P.; Yap, G. P. A.; Ong, T. G. *J. Am. Chem. Soc.* **2014**, *136* (3), 914–917.

(188) Tatamidani, H.; Kakiuchi, F.; Chatani, N. *Org. Lett.* **2004**, *6* (20), 3597–3599.

(189) Flaherty, A.; Trunkfield, A.; Barton, W. *Org. Lett.* **2005**, *7* (22), 4975–4978.

(190) Fang, G. Y.; Wallner, O. A.; Di Blasio, N.; Ginesta, X.; Harvey, J. N.; Aggarwal, V. K. *J. Am. Chem. Soc.* **2007**, *129* (47), 14632–14639.

(191) Bailey, C. L.; Joh, A. Y.; Hurley, Z. Q.; Anderson, C. L.; Singaram, B. *J. Org. Chem.* **2016**, *81*, 3619–3628.

(192) Denmark, S. E.; Ueki, Y. *Organometallics* **2013**, *32*, 8–11.

(193) Ménard, G.; Stephan, D. W. *Dalt. Trans.* **2013**, *42* (15), 5447–5453.

(194) Dobrovetsky, R.; Stephan, D. W. *Angew. Chemie - Int. Ed.* **2013**, *52* (9), 2516–2519.

(195) Otten, E.; Neu, R. C.; Stephan, D. W. *J. Am. Chem. Soc.* **2009**, *131*, 9918–

9919.

Development of Low-Oxidation State Nitrogen, Carbon, and Silicon Catalysts

Alexandros Papafilippou

Supporting Information

Doctor of Philosphophy

University of Edinburgh

EastCHEM School of Chemistry

College of Science and Engineering

December 2016

1. General Experimental Section

Reaction solvents: Acetonitrile (MeCN), dichloromethane (DCM) and tetrahydrofuran (THF) were dried by Grubb's method (solvent purification system was purchased from the Innovative Technology). Dioxane (anhydrous) was purchased from Merck. Dimethylformamide (DMF; anhydrous) was purchased by Acros. All the solvents were dried over 4 Å molecular sieves for 24 h. THF, toluene and Et_2O were dried over sodium using benzophenone as an indicator. Unless otherwise stated, chemicals were purchased from Sigma, Alfa, Acros or Fischer and used without further purification. Thin-liquid chromatography (TLC) was carried out using Merck DF-Alufoilien 60F254 0.2 mm precoated plates and spots visualised using 254 nm UV-light. Preparative thin liquid chromatography (PTLC) was performed using silica gel (200-300 mesh). Petroleum ether (VWR), diethyl ether (Aldrich), hexane (Aldrich) dichloromethane (Fischer) and ethyl acetate (VWR) were used for thin liquid chromatography and preparative thin liquid chromatography as received. Melting points were recorded on a Gallenkamp melting point apparatus and are uncorrected. NMR analysis was carried out on a Bruker Avance 400 equipped with a $BBFO^+$ room temperature probe (400 MHz, ^1H; 100.6 MHz, ^{13}C; 376 MHz, ^{19}F; 161.9 MHz, ^{31}P NMR) spectrometers, Avance 500 equipped with a DCH cryo-probe (500 MHz, ^1H; 125.7 MHz, ^{13}C), or Bruker Prodigy Cryoprobe 500 (500 MHz, ^1H; 125.7 MHz, ^{13}C; 470 MHz, ^{19}F; 160 MHz,^{11} B; 202 MHz, ^{31}P NMR) MHz, or Bruker Avance 600 equipped with a TCI cryoprobe (600 MHz, ^1H; 150.8 MHz, ^{13}C). Chemical shifts are quoted in parts per million (ppm) downfield of tetramethylsilane (TMS). In $CDCl_3$, TMS was

used as an internal standard set to 0 ppm. In CD_3CN, CD_2Cl_2 and C_6D_6, the solvent residual peak was used as references (1.97, 5.32 and 7.15 ppm, respectively). The following abbreviations were used to explain the multiplicities: s = singlet, d = doublet, t = triplet, q = quartet, quin = quintet, sex = sextet, sept = septet, m = multiplet, b = broad, ddd = doublet of doublets of doublets, qd= quartet of doublets. Coupling constants (*J*) are reported in Hertz (Hz). Infra-red spectra were recorded on a Shimadzu IRAffinity-1 instrument on isolated samples using the attenuated total reflectance sampling technique provided in the School of Chemistry, The Univeristy of Edinburgh. High Resolution Mass Spectrometry (HRMS) was performed by the University of Edinburgh Mass Spectrometry Laboratory on a Thermo Finniga Sector instrument equipped with an electronic ionization source. X-ray diffraction data were collected at 120 K on an Agilent Supernova diffractometer using Mo Kα radiation at 0.71 Å and refined in SHELXTL. All reactions were carried out in oven-dried glassware (100 ^oC) and under an atmosphere of argon, unless otherwise stated. Catalytic reactions were run at either 25, 30, 40, 60 or 80 ^oC in constant temperature sand baths with a stirring rate of 400 rpm. 7 cm screw seal vials were used as catalytic reaction vessels and were further sealed with Teflon and parafilm. All reactions were stirred magnetically. Where stated that a reaction was carried out in a nitrogen-filled glovebox, this refers to an MBraun UNIlab MB-20-G with TP170b / mono.

2. Nitrogen(I) or Nitreones

2.1 Preparation of the N(I) catalysts

*Representative procedure for the preparation of the cyclopropenylium tetrafluoroborates **24** and **25***

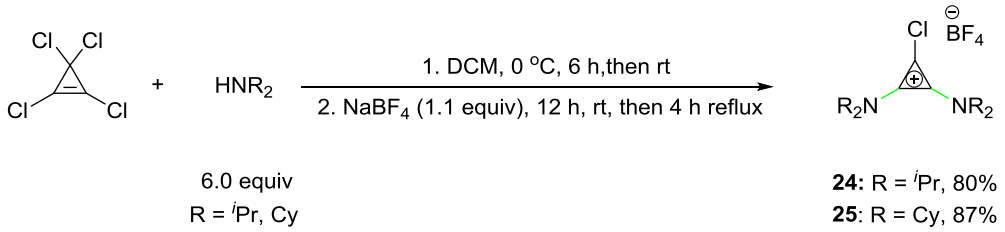

6.0 equiv
R = ^{i}Pr, Cy

24: R = ^{i}Pr, 80%
25: R = Cy, 87%

The corresponding amine (218 mmol, 6.00 equiv) was added dropwise at 0 °C to a solution of tetrachlorocyclopropene (7.70 g, 43.2 mmol) in DCM (300 mL). After 6 hours at 0 °C, the solution was warmed to room temperature. $NaBF_4$ (4.74 g, 51.9 mmol, 1.20 equiv) was added and the suspension was kept stirring overnight (12 h). The mixture was refluxed for 4 h and cooled down to room temperature. After filtration, the mixture was washed with water (3 x 50 mL), the organic phase was dried over $MgSO_4$, filtered and the volatiles were removed *in vacuo*. The residue was washed with diethyl ether (3 x 50 mL) and recrystallized [DCM (50 mL): diethyl ether (10 mL)] at 5 °C to afford product **24** as colorless crystals.

1,2-bis[bis(1-methylethyl)amino]-3-chloro-cyclopropenylium tetrafluoroborate[1]

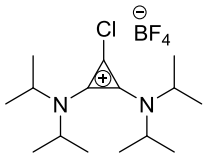

24

Colorless solid.

Yield: 54%.

^{1}H NMR ($CDCl_3$, 500 MHz): δ = 1.40 (d, *J* = 6.8 Hz, 12H), 1.41 (d, *J* = 6.8 Hz, 12H), 3.81 (sept, *J* = 6.8 Hz, 2H), 4.11 (sept, *J* = 6.8 Hz, 2H) ppm.

^{13}C NMR ($CDCl_3$, 100 MHz): δ = 20.7 (4C), 22.5 (4C), 48.3 (2C), 58.0 (2C), 93.3, 132.3 (2C) ppm.

^{11}B NMR ($CDCl_3$, 160 MHz): δ = –1.1 (s) ppm.

^{19}F NMR ($CDCl_3$, 470 MHz): δ = –153.5 ~ –153.7 (m) ppm.

1-chloro-2,3-bis(dicyclohexylamino)-cyclopropenylium tetrafluoroborate[2]

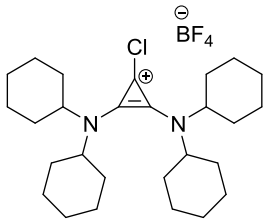

25

Colourless solid.

Yield: 87%.

^{1}H NMR ($CDCl_3$, 500 MHz): δ = 1.14–1.25 (m, 4H), 1.31–1.41 (m, 8C), 1.53–1.62 (m, 8H), 1.72–1.75 (m, 4H), 1.92–1.97 (m, 12H), 2.08–2.11 (m, 4H), 3.34–3.40 (m, 2H), 3.64–3.67 (m, 2H).

^{13}C NMR ($CDCl_3$, 125 MHz): δ = 24.9 (2C), 25.0 (2C), 25.7 (4C), 25.8 (4C), 30.9 (4C), 32.7 (4C), 56.9 (2C), 65.8 (2C), 93.6, 132.6 (2C).

^{11}B NMR ($CDCl_3$, 160 MHz): δ = –1.0 (s) ppm.

^{19}F NMR ($CDCl_3$, 470 MHz): δ = –152.0 ~ –152.1 (m) ppm.

*Representative procedure for the preparation of the iminium salts **26**–**34**:*

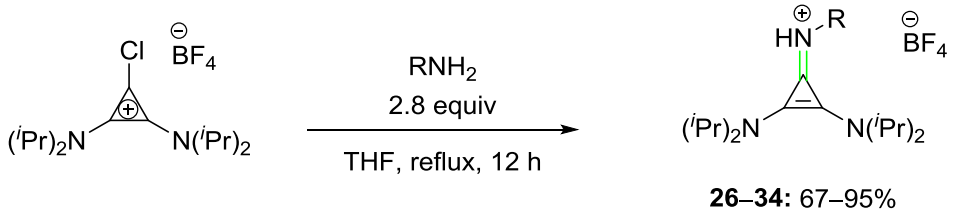

26–**34:** 67–95%

The corresponding amine (2.80 mmol, 2.80 equiv) was added to a suspension of **24** (361 mg, 1.00 mmol) in THF (12 mL) and the mixture was stirred at 60 °C for 24 h. After warming to room temperature volatiles were removed *in vacuo*. The residue was dissolved in DCM (2 mL) and extracted with water (3 x 2 mL). The organic phase was dried over $MgSO_4$, filtered at ambient pressure, and volatiles were removed *in vacuo*. The residue was suspended in EE (5 mL), sonicated for 5 min and filtered at ambient pressure. After evaporation *in vacuo* the residue was washed with EE (3 x 2 mL) and dried *in vacuo* to afford the corresponding cyclopropenium salt.

***N*[1],*N*[1],*N*[2],*N*[2]-tetrakis(1-methylethyl)-3-(propyliminium)-1-Cyclopropene-1,2-dia-mine tetrafluoroborate**

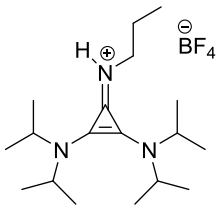

26

Colorless solid.

Yield: 95%.

Mp: 104–106 °C.

^{1}H NMR ($CDCl_3$, 500 MHz): δ = 0.98 (t, *J* = 7.4 Hz, 3H), 1.35 (d, *J* = 6.8 Hz, 24H), 1.74 (sex, *J* = 7.4 Hz, 2H), 3.38–3.47 (m, 2H), 3.83 (sept, *J* = 6.8 Hz, 4H), 6.57 (s, 1H) ppm.

^{13}C NMR ($CDCl_3$, 125 MHz): δ = 10.9, 22.0 (8C), 24.0, 48.4, 50.6 (4C), 113.6 (2C), 116.7 ppm.

^{11}B NMR ($CDCl_3$, 160 MHz): δ = –1.0 (s) ppm.

^{19}F NMR ($CDCl_3$, 470 MHz): δ = –152.3 ~ –152.4 (m) ppm.

IR (neat): ν = 3341, 2976, 2938, 2876, 1520, 1447, 1342, 1213, 1155, 1111, 1058, 1030, 1003, 934, 606 cm^{-1}.

HRMS (EI): calculated for $C_{18}H_{35}N_3^+$: *m*/*z* = 293.2826, found: *m*/*z* = 293.2821.

***N*¹,*N*¹,*N*²,*N*²-tetrakis(1-methylethyl)-3-(butyliminium)-1-Cyclopropene-1,2-dia-mine tetrafluoroborate**[3]

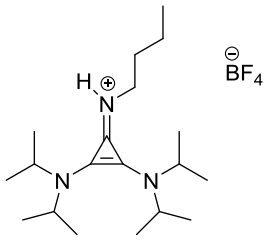

27

Colorless solid.

Yield: 78%.

Mp: 104–106 °C.

^{1}H NMR ($CDCl_3$, 500 MHz): δ = 0.94 (t, *J* = 7.6 Hz, 3H), 1.33 (d, *J* = 6.8 Hz, 24H), 1.36–1.42 (m, 2H), 1.68 (sex, *J* = 7.6 Hz, 2H), 3.43 (quin, *J* = 7.6 Hz, 2H), 3.82 (sept, *J* = 6.8 Hz, 4H), 6.57 (s, 1H) ppm.

^{13}C NMR ($CDCl_3$, 125 MHz): δ = 13.7, 19.7, 22.0 (8C), 32.9, 46.6, 50.6 (4C), 113.6 (2C), 116.4 ppm.

^{11}B NMR ($CDCl_3$, 160 MHz): δ = –1.0 (s) ppm.

^{19}F NMR ($CDCl_3$, 470 MHz): δ = –152.1 ~ –152.2 (m) ppm.

***N*¹,*N*¹,*N*²,*N*²-tetrakis(1-methylethyl)-3-(isobutyliminium)-1-Cyclopropene-1,2-dia-mine tetrafluoroborate**

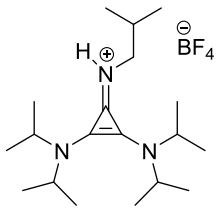

28

Colorless solid.

Yield: 86%.

Mp: 108–109 °C.

^{1}H NMR ($CDCl_3$, 500 MHz): δ = 0.98 (d, *J* = 6.8 Hz, 6H), 1.34 (d, *J* = 6.8 Hz, 24H), 1.91 (sept, *J* = 6.8 Hz, 1H), 3.18–3.32 (m, 2H), 3.83 (hept, *J* = 6.8 Hz, 4H), 6.52 (s, 1H) ppm.

^{13}C NMR ($CDCl_3$, 125 MHz): δ = 19.6 (2C), 22.0 (8C), 29.6, 50.7 (4C), 54.0, 113.6 (2C), 116.5 ppm.

^{11}B NMR ($CDCl_3$, 160 MHz): δ = –1.0 (s) ppm.

^{19}F NMR ($CDCl_3$, 470 MHz): δ = –152.8 ~ –152.9 (m) ppm.

IR (neat): ν = 3340, 2968, 2927, 1512, 1468, 1342, 1213, 1053, 1012, 625 cm^{-1}.

HRMS (EI): calculated for $C_{19}H_{38}N_3^+$: *m*/*z* = 308.3060, found: *m*/*z* = 308.3069.

***N*^{1},*N*^{1},*N*^{2},*N*^{2}-tetrakis(1-methylethyl)-3-(*tert*-butyliminium)-1-Cyclopropene-1,2-dia-mine tetrafluoroborate**[2]

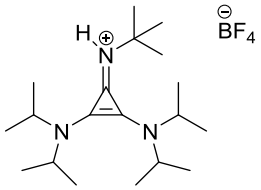

29

Colorless solid.

Yield: 80%.

^{1}H NMR ($CDCl_3$, 500 MHz): δ = 1.35 (d, *J* = 6.9 Hz, 24H), 1.46 (s, 9H), 4.01 (sept, *J* = 6.9 Hz, 4H), 5.84 (s, 1H) ppm.

^{13}C NMR ($CDCl_3$, 125 MHz): δ = 22.2 (8C), 30.1 (3C), 50.5 (4C), 53.1, 114.2, 115.3 (2C) ppm.

^{11}B NMR ($CDCl_3$, 160 MHz): δ = –1.0 (s) ppm.

^{19}F NMR ($CDCl_3$, 470 MHz): δ = –151.5 ~ –151.6 (m) ppm.

***N*¹,*N*¹,*N*²,*N*²-tetrakis(1-methylethyl)-3-(cyclohexyliminium)-1-Cyclopropene-1,2-dia-mine tetrafluoroborate**

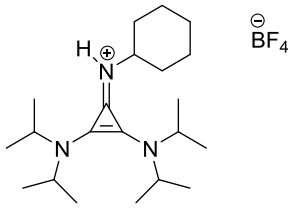

30

Colorless solid.

Yield: 70%.

Mp: 176–178 °C.

¹H NMR ($CDCl_3$, 500 MHz): δ = 1.20–1.26 (m, 3H), 1.33 (d, *J* = 7.0 Hz, 24H), 1.59–1.68 (m, 3H), 1.82-1.85 (m, 2H), 1.91–1.93 (m, 2H), 3.30–3.36 (m, 1H), 3.77–3.85 (sept, *J* = 7.0 Hz, 4H), 6.29 (s, 1H) ppm.

¹³C NMR ($CDCl_3$, 125 MHz): δ = 22.0 (8C), 24.7, 25.3 (2C), 33.6 (2C), 50.7 (4C), 51.2, 113.8 (2C), 115.7 ppm.

¹¹B NMR ($CDCl_3$, 160 MHz): δ = –1.0 (s) ppm.

¹⁹F NMR ($CDCl_3$, 470 MHz): δ = –151.1 ~ –151.2 (m) ppm.

IR (neat): ν = 3319, 2932, 1514, 1474, 1368, 1346, 1293, 115.7, 1115, 1083, 993, 621

cm^{-1}.

HRMS (EI): calculated for $C_{21}H_{39}N_3^+$: *m*/*z* = 333.3139, found: *m*/*z* = 333.3153.

***N*¹,*N*¹,*N*²,*N*²-tetrakis(1-methylethyl)-3-(allyliminium)-1-Cyclopropene-1,2-dia-mine tetrafluoroborate.**

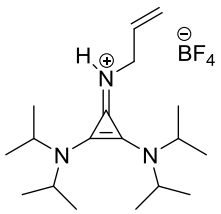

31

Colorless solid.

Yield: 88%.

Mp: 97–98 °C.

^{1}H NMR ($CDCl_3$, 500 MHz): δ = 1.34 (d, *J* = 6.8 Hz, 24H), 3.84 (sept, *J* = 6.8 Hz, 4H), 4.11–4.13 (m, 2H), 5.18–5.29 (m, 2H), 5.93–5.60 (m, 1H), 6.68 (s, 1H) ppm.

^{13}C NMR ($CDCl_3$, 125 MHz): δ = 22.0 (8C), 48.1, 50.6 (4C), 113.8 (2C), 116.2, 116.6, 134.4 ppm.

^{11}B NMR ($CDCl_3$, 160 MHz): δ = –1.0 (s) ppm.

^{19}F NMR ($CDCl_3$, 470 MHz): δ = –152.5 ~ –152.6 (m) ppm.

IR (neat): ν = 3356, 2980, 2935, 1616, 1520, 1452, 1373, 1348, 1213, 1136, 1061, 1020, 918, 752 cm^{-1}.

HRMS (EI): calculated for $C_{18}H_{33}N_3^+$: *m*/*z* = 291.2669, found: *m*/*z* = 291.2656.

N^{1},*N*^{1},*N*^{2},*N*^{2}-tetrakis(1-methylethyl)-3-(propargyliminium)-1-Cyclopropene-1,2-dia-mine tetrafluoroborate

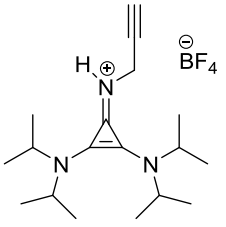

32

Colorless solid.

Yield: 67%.

Mp: 132–134 ^{o}C.

^{1}H NMR ($CDCl_3$, 500 MHz): δ = 1.35 (d, *J* = 6.8 Hz, 24H), 2.41 (s, 1H), 3.92 (sept, *J* = 6.8 Hz, 4H), 4.19–4.29 (m, 2H), 6.91 (s, 1H) ppm.

^{13}C NMR ($CDCl_3$, 125 MHz): δ = 21.9 (8C), 35.4, 50.8 (4C), 73.5, 80.0, 115.0 (2C), 115.1 ppm.

^{11}B NMR ($CDCl_3$, 160 MHz): δ = –1.0 (s) ppm.

^{19}F NMR ($CDCl_3$, 470 MHz): δ = –152.5 ~ –152.6 (m) ppm.

IR (neat): ν = 3343, 3252, 2984, 2938, 1523, 1450, 1371, 1342, 1209, 1138, 1057, 1026, 750, 691 cm^{-1}.

HRMS (EI): calculated for $C_{18}H_{31}N_3^+$: *m*/*z* = 289.2513, found: *m*/*z* = 289.2501.

***N*¹,*N*¹,*N*²,*N*²-tetrakis(1-methylethyl)-3-(phenyliminium)-1-Cyclopropene-1,2-dia-mine tetrafluoroborate**[4]

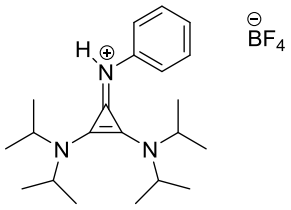

33

Colorless solid.

Yield: 72%.

^{1}H NMR ($CDCl_3$, 500 MHz): δ = 1.28 (d, *J* = 6.8 Hz, 24H), 3.71 (sept, *J* = 6.8 Hz, 4H),

7.15–7.17 (m, 1H), 7.25–7.27 (m, 2H), 7.33–7.36 (m, 2H), 8.27 (s, 1H) ppm.

^{13}C NMR ($CDCl_3$, 150 MHz): δ = 22.0 (8C), 51.2 (4C), 113.0, 116.9 (2C), 122.7 (2C), 125.8, 129.4 (2C), 139.1 ppm.

^{11}B NMR ($CDCl_3$, 160 MHz): δ = –1.0 (s) ppm.

^{19}F NMR ($CDCl_3$, 470 MHz): δ = –151.3 ~ –151.4 (m) ppm.

***N*¹,*N*¹,*N*²,*N*²-tetrakis(1-methylethyl)-3-(mesityliminium)-1-Cyclopropene-1,2-dia-mine tetrafluoroborate**[1]

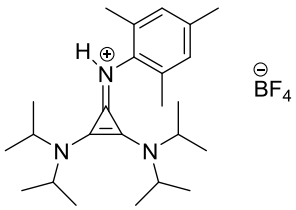

34

Beige solid.

Yield: 85%.

^{1}H NMR ($CDCl_3$, 500 MHz): δ = 1.23 (d, *J* = 6.8 Hz, 24H), 2.25 (s, 6H), 2.28 (s, 3H), 3.57 (sept, *J* = 6.8 Hz, 4H), 6.91 (s, 2H), 7.81 (s, 1H) ppm.

^{13}C NMR ($CDCl_3$, 125 MHz): δ = 18.2 (2C), 20.9, 21.8 (8C), 50.7 (4C), 114.2 (2C), 115.4, 129.3(2C), 133.4, 136.4(2C), 138.2 ppm.

^{11}B NMR ($CDCl_3$, 160 MHz): δ = –1.0 (s) ppm.

^{19}F NMR ($CDCl_3$, 470 MHz): δ = –151.1 ~ –151.2 (m) ppm.

*Representative procedure for the preparation of the iminium salts **35**–**45**:*

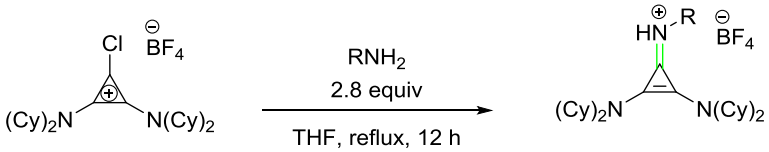

25 **35–45:** 70–96%

The corresponding amine (2.80 mmol, 2.80 equiv) was added to a suspension of **25** (521 mg, 1.00 mmol) in THF (12 mL) and the mixture was stirred at 60 °C for 24 h. After warming to room temperature volatiles were removed *in vacuo*. The residue was dissolved in DCM (2 mL) and extracted with water (3 x 2 mL). The organic phase was dried over $MgSO_4$, filtered at ambient pressure, and volatiles were removed *in vacuo*. The residue was suspended in EE (5 mL), sonicated for 5 min and filtered at ambient pressure. After evaporation *in vacuo* the residue was washed with EE (3 x 2 mL) and dried *in vacuo* to afford the corresponding cyclopropenium salt.

N^1,N^1,N^2,N^2-tetracyclohexyl-3-[propyliminium]-1-cyclopropene-1,2-diamine tetrafluoroborate

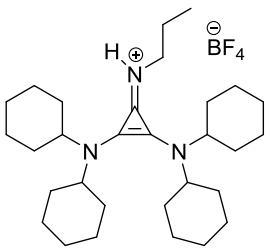

35

Colorless solid.
Yield: 76%.
Mp: 172–174 °C.

^{1}H NMR ($CDCl_3$, 500 MHz): δ = 0.99 (t, *J* = 7.4 Hz, 3H), 1.28–1.39 (m, 11H), 1.48–1.63 (m, 9H), 1.74 (m, 6H), 1.81–1.84 (m, 8H), 1.95–1.97 (m, 8H), 3.32 (tt, *J* = 12.2, 3.8 Hz, 4H), 3.47–3.55 (m, 2H), 6.32 (s, 1H) ppm.

^{13}C NMR ($CDCl_3$, 125 MHz): δ = 10.8, 24.3, 24.6 (4C), 25.8 (8C), 32.4 (8C), 48.2, 59.5 (4C), 114.3 (2C), 116.5 ppm.

^{11}B NMR ($CDCl_3$, 160 MHz): δ = –1.0 (s) ppm.

^{19}F NMR ($CDCl_3$, 470 MHz): δ = –152.8 ~ –152.9 (m) ppm.

IR (neat): ν = 3361, 2932, 2855, 1514, 1450, 1373, 1346, 1180, 1124, 1094, 1055, 1039, 897 cm^{-1}.

HRMS (EI): calculated for $C_{30}H_{51}N_3^+$: *m*/*z* = 453.4078, found: *m*/*z* = 453.4058.

N^{1},*N*^{1},*N*^{2},*N*^{2}-tetracyclohexyl-3-[(isopropyl)iminium]-1-cyclopropene-1,2-diamine tetrafluoroborate

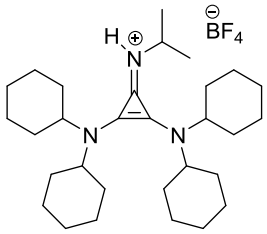

36

Colorless solid.

Yield: 78%.

Mp: 187–189 °C.

^{1}H NMR ($CDCl_3$, 500 MHz): δ = 1.23–1.39 (m, 12H), 1.43 (d, *J* = 6.5 Hz, 6H), 1.48–1.59 (m, 8H), 1.72–1.75 (m, 4H), 1.83–1.85 (m, 8H), 1.94–1.97 (m, 8H), 3.34 (tt, *J* = 12.4, 3.9 Hz, 4H), 3.84–3.92 (m, 1H), 5.92 (s, 1H) ppm.

^{13}C NMR ($CDCl_3$, 150 MHz): δ = 23.4 (2C), 24.6 (4C), 25.7 (8C), 32.4 (8C), 50.0, 59.7 (4C), 114.7 (2C), 115.5 ppm.

^{11}B NMR ($CDCl_3$, 160 MHz): δ = –1.0 (s) ppm.

^{19}F NMR ($CDCl_3$, 470 MHz): δ = –151.3 ~ –151.4 (m) ppm.

IR (neat): ν = 3321, 2930, 2857, 1501, 1449, 1371, 1346, 1317, 1273, 1180, 1056, 897 cm^{-1}.

HRMS (EI): calculated for $C_{30}H_{51}N_3^+$: *m*/*z* = 453.4078, found: *m*/*z* = 453.4083.

***N*^{1},*N*^{1},*N*^{2},*N*^{2}-tetracyclohexyl-3-[butyliminium]-1-cyclopropene-1,2-diamine tetrafluoroborate**[5]

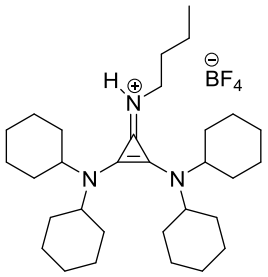

37

Colorless solid.

Yield: 78%.

Mp: 152–154 °C.

^{1}H NMR ($CDCl_3$, 500 MHz): δ = 0.98 (t, *J* = 7.0 Hz, 3H), 1.27–1.45 (m, 13H), 1.50–1.58 (m, 8H), 1.61–1.76 (m, 7H), 1.81–1.84 (m, 8H), 1.94–1.96 (m, 8H), 3.32 (tt, *J* = 12.2, 3.8 Hz, 4H), 3.48–3.59 (m, 2H), 6.28 (s, 1H) ppm.

^{13}C NMR ($CDCl_3$, 125 MHz): δ = 13.8, 19.8, 24.5 (4C), 25.7 (8C), 32.4 (8C), 33.2, 46.5, 59.5 (4C), 114.3 (2C), 116.4 ppm.

^{11}B NMR ($CDCl_3$, 160 MHz): δ = –1.0 (s) ppm.

^{19}F NMR ($CDCl_3$, 470 MHz): δ = –152.8 ~ –152.9 (m) ppm.

IR (neat): ν = 3361, 2932, 2855, 1512, 1450, 1373, 1346, 1052, 991, 895 cm^{-1}.

HRMS (EI): calculated for $C_{31}H_{53}N_3^+$: *m*/*z* = 467.4234, found: *m*/*z* = 467.4219.

***N*^{1},*N*^{1},*N*^{2},*N*^{2}-tetracyclohexyl-3-[*iso*-butyliminium]-1-cyclopropene-1,2-diamine tetrafluoroborate**

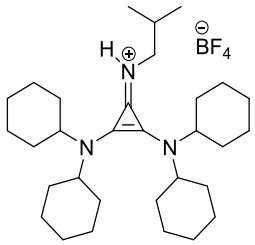

38

Colorless solid.

Yield: 96%.

Mp: 205–208 °C.

^{1}H NMR ($CDCl_3$, 500 MHz): δ = 1.00 (d, *J* = 6.7 Hz, 6H), 1.27–1.39 (m, 12H), 1.49–1.60 (m, 8H), 1.73 (d, *J* = 11.2 Hz, 4H), 1.82–1.84 (m, 8H), 1.94–1.97 (m, 9H), 3.32 (tt, *J* =12.2, 3.8 Hz, 4H), 3.36–3.39 (m, 2H), 6.24 (s, 1H) ppm.

^{13}C NMR ($CDCl_3$, 150 MHz): δ = 19.6 (2C), 24.6 (4C), 25.7 (8C), 29.6, 32.4 (8C), 53.6, 59.5 (4C), 114.4 (2C), 116.7 ppm.

^{11}B NMR ($CDCl_3$, 160 MHz): δ = –1.0 (s) ppm.

^{19}F NMR ($CDCl_3$, 470 MHz): δ = –152.8 ~ –152.9 (m) ppm.

IR (neat): ν = 3358, 2930, 2859, 1512, 1449, 1431, 1373, 1346, 1247, 1180, 1052, 897 cm^{-1}.

HRMS (EI): calculated for $C_{31}H_{53}N_3^+$: *m*/*z* = 467.4234, found: *m*/*z* = 467.4214.

***N*^{1},*N*^{1},*N*^{2},*N*^{2}-tetracyclohexyl-3-[*sec*-butyliminium]-1-cyclopropene-1,2-diamine tetrafluoroborate**

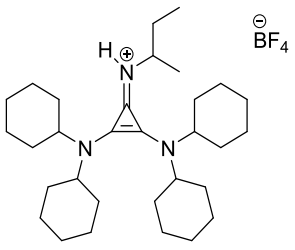

39

Colorless solid.

Yield: 84%.

Mp: 204–207 °C.

^{1}H NMR ($CDCl_3$, 500 MHz): δ = 0.98 (t, *J* = 7.4 Hz, 3H), 1.20–1.43 (m, 16H), 1.46–1.62 (m, 8H), 1.67–1.77 (m, 5H), 1.82–1.87 (m, 8H), 1.94–1.96 (m, 8H), 3.30–3.36 (m, 4H), 3.60–3.67 (m, 1H), 5.83 (s, 1H) ppm.

^{13}C NMR ($CDCl_3$, 125 MHz): δ = 10.9, 21.0 (4C), 24.6 (8C), 25.7 (8C), 30.0, 32.4, 55.6, 59.6 (4C), 114.7 (2C), 115.9 ppm.

^{11}B NMR ($CDCl_3$, 160 MHz): δ = –1.0 (s) ppm.

^{19}F NMR ($CDCl_3$, 470 MHz): δ = –151.5 ~ –151.6 (m) ppm.

IR (neat): ν = 3332, 2930, 2859, 1501, 1449, 1373, 1319, 1263, 1248, 1180, 1054, 1003, 991, 897, 831, 623 cm^{-1}.

HRMS (EI): calculated for $C_{31}H_{53}N_3^+$: *m*/*z* = 467.4234, found: *m*/*z* = 467.4237.

N^1,*N*^{1},*N*^{2},*N*^{2}-tetracyclohexyl-3-[*tert*-butyliminium]-1-cyclopropene-1,2-diamine tetrafluoroborate[5]

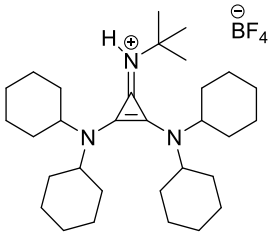

40

Colorless solid.

Yield: 78%.

Mp: 230–233 °C.

^{1}H NMR ($CDCl_3$, 500 MHz): δ = 1.17–1.30 (m, 4H), 1.33–1.41 (m, 8H), 1.49 (s, 9H), 1.53–1.63 (m, 8H), 1.74–1.76 (m, 4H), 1.88–1.96 (m, 16H), 3.55 (tt, J = 12.2, 3.8 Hz, 4H), 5.43 (s, 1H) ppm.

^{13}C NMR ($CDCl_3$, 125 MHz): δ = 24.9 (4C), 25.5 (8C), 30.1 (3C), 32.6 (8C), 53.3, 59.2 (4C), 114.4, 116.5 (2C) ppm.

^{11}B NMR ($CDCl_3$, 160 MHz): δ = –1.0 (s) ppm.

^{19}F NMR ($CDCl_3$, 470 MHz): δ = –151.5 ~ –151.6 (m) ppm.

IR (neat): ν = 3362, 2930, 2860, 2847, 1500, 1449, 1373, 1323, 1244, 1210, 1117, 1058, 1013, 895 cm^{-1}.

HRMS (EI): calculated for $C_{31}H_{53}N_3^+$: *m*/*z* = 467.4234, found: *m*/*z* = 467.4220.

***N*^{1},*N*^{1},*N*^{2},*N*^{2}-tetracyclohexyl-3-[cyclohexyliminium]-1-cyclopropene-1,2-diamine tetrafluoroborate**

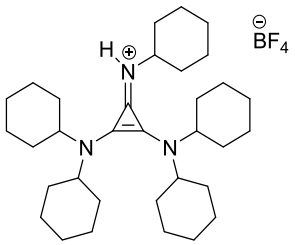

41

Colorless solid.

Yield: 70%.

Mp: 214–216 °C.

^{1}H NMR ($CDCl_3$, 500 MHz): δ = 1.25–1.45 (m, 14H), 1.47–1.59 (m, 8H), 1.62–1.75 (m, 8H), 1.83–1.85 (m, 10H), 1.94–1.97 (m, 10H), 3.33 (tt, J = 12.2, 3.9 Hz, 4H), 3.42–3.54 (m, 1H), 5.75 (s, 1H) ppm.

^{13}C NMR ($CDCl_3$, 125 MHz): δ = 15.3, 24.7 (4C), 25.3 (2C), 25.7 (8C), 32.3 (8C), 33.6 (2C), 56.6, 59.5 (4C), 114.8 (2C), 115.3 ppm.

^{11}B NMR ($CDCl_3$, 160 MHz): δ = –1.0 (s) ppm.

^{19}F NMR ($CDCl_3$, 470 MHz): δ = –152.4 ~ –152.5 (m) ppm.

IR (neat): ν = 3318, 2930, 2907, 2853, 1520, 1493, 1369, 1119, 1077, 988, 895, 849, 762 cm^{-1}.

HRMS (EI): calculated for $C_{33}H_{55}N_3^+$: *m*/*z* = 493.4391, found: *m*/*z* = 493.4402.

***N*^{1},*N*^{1},*N*^{2},*N*^{2}-tetracyclohexyl-3-[allyliminium]-1-cyclopropene-1,2-diamine tetrafluoroborate**

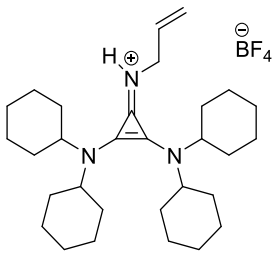

42

Beige solid.

Yield: 82%.

Mp: 155–157 °C.

^{1}H NMR ($CDCl_3$, 500 MHz): δ = 1.22–1.42 (m, 12H), 1.50–1.57 (m, 8H), 1.71–1.73 (m, 4H), 1.80–1.82 (m, 8H), 1.93–1.95 (m, 8H), 3.34 (tt, *J* = 12.2, 3.3 Hz, 4H), 4.19–4.21 (m, 2H), 5.25–5.27 (m, 2H), 5.93–5.60 (m, 1H), 6.39 (s, 1H) ppm.

^{13}C NMR ($CDCl_3$, 125 MHz): δ = 24.5 (4C), 25.7 (8C), 32.3 (8C), 47.7, 59.4 (4C), 114.4 (2C), 116.0, 116.3, 134.3 ppm.

^{11}B NMR ($CDCl_3$, 160 MHz): δ = –1.0 (s) ppm.

^{19}F NMR ($CDCl_3$, 470 MHz): δ = –152.8 ~ –152.9 (m) ppm.

IR (neat): ν = 3358, 2931, 2858, 1508, 1450, 1373, 1346, 1250, 1180, 1053, 997, 897, 786 cm^{-1}.

HRMS (EI): calculated for $C_{30}H_{49}N_3^+$: *m*/*z* = 451.3921, found: *m*/*z* = 451.3909.

N^{1},*N*^{1},*N*^{2},*N*^{2}-tetracyclohexyl-3-[phenyliminium]-1-cyclopropene-1,2-diamine tetrafluoroborate

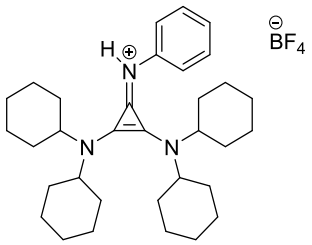

43

Colorless solid.

Yield: 93%.

Mp: 223–225 °C.

^{1}H NMR ($CDCl_3$, 500 MHz): δ = 1.10–1.28 (m, 12H), 1.54 (qd, *J* = 12.0, 3.0 Hz, 8H), 1.64 (d, *J* = 12.0 Hz, 4H), 1.84 (dd, *J* = 28.2, 12.0 Hz, 16H), 3.28 (tt, *J* = 12.0, 3.0 Hz, 4H), 7.15–7.23 (m, 1H), 7.30–7.34 (m, 2H), 7.36–7.38 (m, 2H), 8.15 (s, 1H) ppm.

^{13}C NMR ($CDCl_3$, 125 MHz): δ = 24.5 (4C), 25.7 (8C), 32.3 (8C), 60.0 (4C), 113.0 (2C), 115.1, 123.0 (2C), 125.6, 129.5 (2C), 138.4 ppm.

^{11}B NMR ($CDCl_3$, 160 MHz): δ = –1.0 (s) ppm.

^{19}F NMR ($CDCl_3$, 470 MHz): δ = –152 ppm.

IR (neat): ν = 3273, 2932, 2855, 1601, 1518, 1460, 1369, 1072, 988, 893, 746 cm^{-1}.

HRMS (EI): calculated for $C_{33}H_{49}N_3^+$: *m*/*z* = 487.3921, found: *m*/*z* = 487.3935.

N^1,N^1,N^2,N^2-tetracyclohexyl-3-[mesityliminium]-1-cyclopropene-1,2-diamine tetrafluoroborate

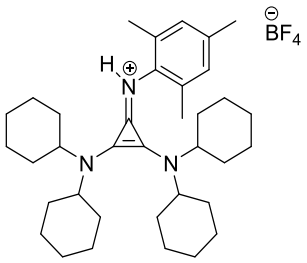

44

Colorless solid.

Yield: 77%.

Mp: 226–228 °C.

^{1}H NMR ($CDCl_3$, 500 MHz): δ = 1.12–1.24 (m, 12 H), 1.44 (q, *J* = 11.2 Hz, 8H), 1.63 (d, *J* = 11.2 Hz, 4H), 1.74–1.76 (m, 8H), 1.83–1.86 (m, 8H), 2.27 (s, 6H), 2.28 (s, 3H), 3.05–3.25 (m, 4H), 6.93 (s, 2H), 7.37 (s, 1H) ppm.

^{13}C NMR ($CDCl_3$, 125 MHz): δ = 18.3 (2C), 20.9, 24.4 (4C), 25.5 (8C), 32.3 (8C), 59.6 (4C), 114.7, 115.5 (2C), 129.6 (2C), 133.3, 136.4 (2C), 138.2 ppm.

^{11}B NMR ($CDCl_3$, 160 MHz): δ = –1.0 (s) ppm.

^{19}F NMR ($CDCl_3$, 470 MHz): δ = –152.4 ~ –152.5 ppm.

IR (neat): ν = 3316, 2928, 2855, 1510, 1050, 1449, 1373, 1346, 1323, 1246, 1090, 1049, 895 cm^{-1}.

HRMS (EI): calculated for $C_{36}H_{55}N_3^+$: *m*/*z* = 529.4391, found: *m*/*z* = 529.4377.

N^1,N^1,N^2,N^2-tetracyclohexyl-3-[trimethylsilylmethyliminium]-1-cyclopropene-1,2-diamine tetrafluoroborate

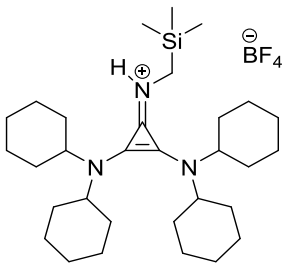

45

Colorless solid.

Yield: 70%.

Mp: 230–233 °C.

^{1}H NMR ($CDCl_3$, 500 MHz): δ = 0.17 (s, 9H), 1.22–1.27 (m, 4H), 1.31–1.39 (m, 8H), 1.51–1.59 (m, 8H), 1.73–1.75 (m, 4H), 1.85–1.87 (m, 8H), 1.94–1.96 (m, 8H), 3.14 (d, *J* = 6.0 Hz, 2H), 3.33 (tt, *J* = 12.2, 3.9 Hz, 4H), 5.66 (s, 1H) ppm.

^{13}C NMR ($CDCl_3$, 150 MHz): δ = –2.9 (3C), 24.8 (4C), 25.8 (8C), 32.3 (8C), 37.2, 59.4 (4C), 114.6 (2C), 117.7 ppm.

^{11}B NMR ($CDCl_3$, 160 MHz): δ = –1.0 (s) ppm.

^{19}F NMR ($CDCl_3$, 470 MHz): δ = –153.0 ~ –153.1 (m) ppm.

IR (neat): ν = 3331, 2932, 2857, 1526, 1508, 1449, 1373, 1346, 1250, 1094, 1050, 856, 841, 696 cm^{-1}.

HRMS (EI): calculated for $C_{31}H_{55}N_3Si^+$: *m*/*z* = 497.4160, found: *m*/*z* = 497.4136.

*Representative procedure for the preparation of cyclopropenimines **46**–**51**:*

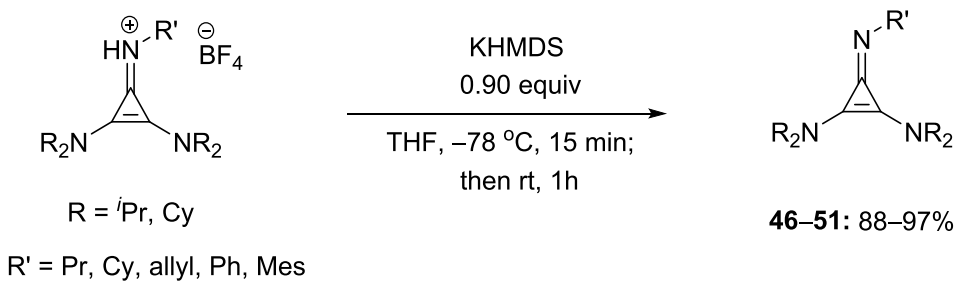

R = ^{i}Pr, Cy

R' = Pr, Cy, allyl, Ph, Mes

46–**51:** 88–97%

KHMDS in THF (1.0 M, 5.67 mL, 0.90 equiv) was added dropwise at –78 °C in a stirred suspension of the corresponding cyclopropenium salt (6.30 mmol, 1.00 equiv) in THF (63 mL). After 15 min at –78 °C, the reaction mixture was warmed to room temperature for 1 h. The solvent was removed *in vacuo* and the residue was dissolved in toluene (8 mL). In a nitrogen-filled glovebox, the suspension was filtered over celite and the volatiles were removed *in vacuo* to afford the corresponding cyclopropenimine.

***N*¹,*N*¹,*N*²,*N*²-tetracyclohexyl-3-[*iso*-butylimino]-1-cyclopropene-1,2-diamine**

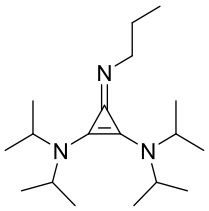

46

Orange liquid.

Yield: 89%.

^{1}H NMR ($CDCl_3$, 500 MHz): δ = 0.91 (t, *J* = 7.4 Hz, 3H), 1.27 (d, *J* = 6.8 Hz, 24H), 1.56 (sex, *J* = 7.4 Hz, 2H), 3.27–3.34 (m, 2H), 3.68 (sept, *J* = 6.8 Hz, 4H) ppm.

^{13}C NMR ($CDCl_3$, 125 MHz): δ = 11.0, 22.1 (8C), 24.4, 47.8, 50.5 (4C), 113.0 (2C), 117.4 ppm.

IR (neat): ν = 2968, 1560, 1427, 1369, 1305, 1223, 1204, 1153, 1038, 903, 692 cm^{-1}.

HRMS (EI): calculated for $C_{18}H_{35}N_3^+$: *m*/*z* = 293.2826, found: *m*/*z* = 293.2816.

***N*¹, *N*¹, *N*², *N*²-tetrakis(1-methylethyl)-3-(cyclohexylimino)-1-Cyclopropene-1,2-diamine**

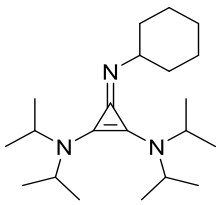

47

Colorless solid.

Mp: 31–33 °C.

^{1}H NMR (C_6D_6, 600 MHz): δ = 1.05 (d, *J* = 6.8 Hz, 12H), 1.22 (d, *J* = 6.8 Hz, 12H), 1.30–1.43 (m, 1H), 1.43–1.56 (m, 1H), 1.66–1.67 (m, 2H), 1.78–1.86 (m, 2H), 1.94–1.98 (m, 2H), 2.15–2.18 (m, 2H), 3.44 (sept, *J* = 6.8 Hz, 4H), 3.56–3.61 (m, 1H) ppm.

^{13}C NMR ($CDCl_3$, 150 MHz): δ = 21.5 (4C), 22.5 (4C), 25.6 (2C), 26.6, 37.6 (2C), 48.8 (2C), 49.3 (2C), 61.3, 110.6, 116.4, 127.0 ppm.

IR (neat): ν = 2968, 2926, 1543, 1425, 1366, 1301, 1223, 1155, 1128, 1039, 885 cm^{-1}.

HRMS (EI): calculated for $C_{21}H_{39}N_3^+$: *m*/*z* = 333.3138, found: *m*/*z* = 333.3138.

***N*¹,*N*¹,*N*²,*N*²-tetrakis(1-methylethyl)-3-(allylimino)-1-Cyclopropene-1,2-diamine.**

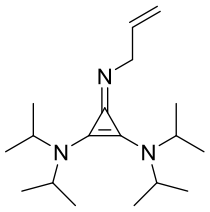

48

Brown liquid.

Yield: 95%.

^{1}H NMR ($CDCl_3$, 500 MHz): δ = 1.26 (d, *J* = 6.8 Hz, 24H), 3.67 (sept, *J* = 6.8 Hz, 4H), 4.07–4.13 (m, 2H), 5.14–5.22 (m, 2H), 5.92–6.03 (m, 1H) ppm.

^{13}C NMR ($CDCl_3$, 125 MHz): δ = 22.1 (8C), 47.8, 50.6 (4C), 113.2 (2C), 115.7, 117.6, 135.6 ppm.

IR (neat): ν = 2968, 2931, 1543, 1427, 1368, 1312, 1219, 1203, 1128, 1009, 903, 766 cm^{-1}.

HRMS (EI): calculated for $C_{18}H_{33}N_3^+$: *m*/*z* = 291.2669, found: *m*/*z* = 291.2678.

***N*¹,*N*¹,*N*²,*N*²-tetrakis(1-methylethyl)-3-(phenylimino)-1-Cyclopropene-1,2-dia-mine.**[4]

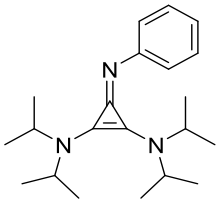

49

Yellow solid.

Yield: 97%.

^{1}H NMR ($CDCl_3$, 600 MHz): δ = 1.22 (d, *J* = 6.8 Hz, 24H), 3.62 (sept, *J* = 6.8 Hz, 4H), 6.73–6.76 (m, 1H), 6.92–6.94 (m, 2H), 7.12–7.16 (m, 2H) ppm.

^{13}C NMR ($CDCl_3$, 150 MHz): δ = 22.4 (8C), 49.4 (4C), 114.4 (2C), 118.9, 122.9 (2C), 125.3 128.2 (2C), 156 ppm.

***N*^{1},*N*^{1},*N*^{2},*N*^{2}-tetrakis(1-methylethyl)-3-(mesitylimino)-1-Cyclopropene-1,2-diamine.**[1]

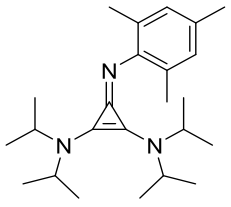

50

Beige solid.

Yield: 95%.

^{1}H NMR ($CDCl_3$, 600 MHz): δ = 1.03 (d, *J* = 6.6 Hz, 24H), 2.00 (s, 6H), 2.06 (s, 3H), 3.35–3.55 (m, 4H), 6.59 (s, 2H) ppm.

^{13}C NMR ($CDCl_3$, 150 MHz): δ = 18.8 (2C), 20.8, 22.1 (8C), 49.1 (4C), 112.2 (2C), 124.4, 127.7 (2C), 129.0, 131.3 (2C), 150.6 ppm.

***N*^{1},*N*^{1},*N*^{2},*N*^{2}-tetrakis(cyclohexyl)-3-(mesitylimino)-1-Cyclopropene-1,2-diamine.**

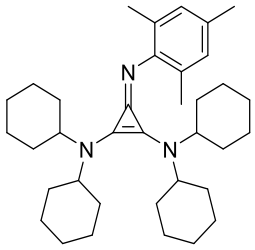

51

Colorless solid.

Yield: 77%.

Mp: 185–187 ^{o}C.

^{1}H NMR ($CDCl_3$, 500 MHz): δ = 1.00–1.25 (m, 12H), 1.49–1.70 (m, 20H), 1.74–1.76 (m, 8H), 2.13 (s, 6H), 2.20 (s, 3H), 2.93–3.07 (m, 4H), 6.75 (s, 2H) ppm.

^{13}C NMR ($CDCl_3$, 125 MHz): δ = 18.9 (2C), 20.6, 25.0 (8C), 26.1 (8C), 32.7 (4C), 58.2 (4C), 112.5 (2C), 124.1, 128.2 (2C), 128.6, 129.0 (2C), 151.0 ppm.

IR (neat): ν = 2926, 2854, 1536, 1435, 1366, 1304, 1256, 1246, 1080, 1029, 893, 799 cm^{-1}.

HRMS (EI): calculated for $C_{36}H_{55}N_3^+$: *m*/*z* = 529.4391, found: *m*/*z* = 529.4393.

***N*-(2,3-diphenyl-2-cyclopropen-1-ylidene)-Benzenamine tetrafluoroborate**[6]

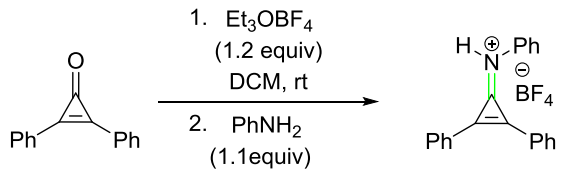

20: 2.0 mmol

21: 75%

To an oven-dried flask with a magnetic stirring bar was added diphenylcyclopropenone **20** (413 mg, 2.00 mmol), triethyloxonium tetrafluoroborate (455 mg, 2.40 mmol, 1.20 equiv), and DCM (4 mL). The mixture was stirred at 16 ºC for 30 min whereupon the solid intermediate precipitated. Aniline (0.20 mL, 2.20 mmol, 1.10 equiv) was added whereupon the solid re-dissolved. After 2 h the precipitate formed was filtered and washed with DCM (3 x 5 ml). Drying *in vacuo* afforded product **21** as a colourless powder (560 mg, 75%).

^{1}H NMR (CD_3CN, 500 MHz): δ = 7.47–7.49 (m, 2H), 7.52–7.55 (m, 1H), 7.62–7.64 (m, 2H), 7.69–7.72 (m, 2H), 7.81–7.84 (m, 3H), 7.89–7.94 (m, 3H), 8.33–8.34 (m, 2H), 10.65 (s, 1H) ppm.

^{13}C NMR (CD_3CN, 125 MHz): δ = 121, 121.6, 123.3 (2C), 129.3, 131.0 (2C), 131.2 (2C), 131.3 (2C), 135.0 (2C), 135.1 (2C), 135.4, 136.5, 137.3, 137.5, 138.6, 143.4 ppm.

^{11}B NMR (CD_3CN, 160 MHz): δ = –1.00 (s) ppm

^{19}F NMR (CD_3CN, 470 MHz): δ = –151.5 ~ –151.6 ppm.

IR (neat): ν = 3250, 1900, 1597, 1547, 1506, 1476, 1445, 1400, 1180, 1070, 995, 759, 680 cm^{-1}.

HRMS (EI): calculated for $C_{21}H_{16}NBF_4^+$: *m*/*z* = 369.1306, found: *m*/*z* = 369.1302.

***N*-[(2*E*)-3-phenyl-1-[(1*E*)-2-phenylethenyl]-2-propen-1-ylidene]-Benzenamine.**[7]

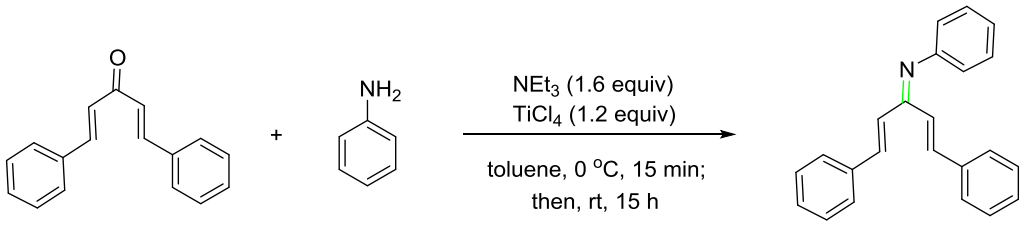

(1.4 equiv)

63: 47%

Aniline (128 µL, 1.40 mmol, 1.40 equiv) and triethylamine (307 µL, 2.20 mmol, 2.20 equiv) were added to a solution of 1,5-diphenyl-1,4-pentadien-3-one (243.3 mg, 1.00 mmol, 1.00 equiv) in toluene (3 mL). The mixture was cooled down to 0 °C and $TiCl_4$ in DCM (1.20 mL, 1.0 M, 1.20 mmol, 1.20 equiv) was added dropwise. The mixture was stirred at 0 °C for 15 min and at 25 °C for 12 h. The mixture was filtered over celite and the volatiles were removed *in vacuo*. The residue was purified by preparative thin-layer chromatography [PTLC; eluant: hexane/diethyl ether = 9:1] to afford product **63** as a yellow solid (145 mg, 47%).

Yellow solid.

^{1}H NMR ($CDCl_3$, 600 MHz): δ = 6.75–6.78 (m, 1H), 6.91–6.93 (m, 2H), 7.10–7.13 (m, 1H), 7.18–7.21 (m, 1H), 7.24–7.25 (m, 1H), 7.27–7.37 (m, 8H), 7.38–7.41 (m, 2H), 7.53–7.56 (m, 1H), 7.60–7.61 (m, 2H) ppm.

^{13}C NMR ($CDCl_3$, 150 MHz): δ = 121.0, 122.4, 123.9, 126.1, 127.4 (2C), 127.6 (2C), 128.8 (2C), 128.9 (2C), 129.1, 129.3, 135.8, 136.3, 138.1 138.4, 150.8, 162.9 ppm.

***N*-(2,3,4,5-tetraphenyl-2,4-cyclopentadien-1-ylidene)benzenamine**

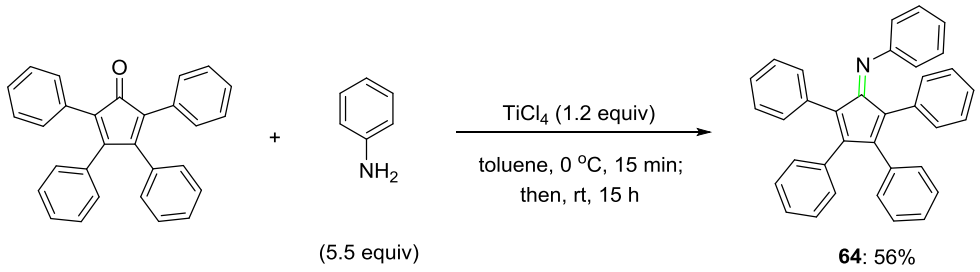

Aniline (501 µL, 5.50 mmol) was added to a solution of tetraphenyl cyclopentanone (385 mg, 1.00 mmol) in DCM (10 mL). The mixture was cooled down to 0 °C and $TiCl_4$ in DCM (5.5 mL, 1.0 M, 5.50 mmol) was added dropwise. The mixture was initially stirred at 0 °C for 15 min and at 25 °C for 15 h. It was filtered over celite and the volatiles were removed *in vacuo*. The residue was purified by column chromatography [eluant: hexane / diethyl ether = 19:1] to afford product **64** as a red solid (257 mg, 56%).

Mp: 233–234 °C.

^{1}H NMR (CD_3CN, 500 MHz): δ = 6.64–6.94 (m, 13H), 7.05–7.35 (m, 12H) ppm.

^{13}C NMR (CD_3CN, 150 MHz): δ = 120.2 (2C), 123.7, 125.6, 126.8, 127.1 (2C), 127.2 (2C), 127.3 (2C), 127.5 (2C), 127.7 (2C), 128.0, 128.1, 128.5, 129.3 (2C), 129.9 (2C), 130.2 (2C), 131.4 (2C), 132.9, 133.1, 133.7, 134.2, 134.5, 147.9, 149.6, 153.5, 167.8 ppm.

IR: ν = 1589, 1483, 1440, 1329, 1260, 1157, 1098, 1072, 1026, 918, 899, 833, 779, 765, 677, 583 cm^{-1}.

HRMS (EI): calculated for $C_{35}H_{25}N^+$: *m*/*z* = 459.1982, found: *m*/*z* = 459.1987.

2-methyl-*N*-(phenylmethylene)-2-propanamine[8]

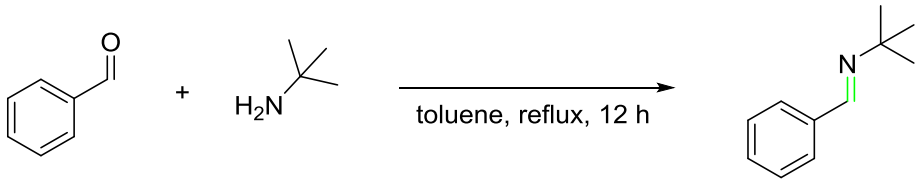

*Imine **57** was prepared from Uwe Schneider lab

Benzaldehyde (1.70 g, 16.1 mmol, 1.00 equiv) was added to a solution of *t*butyl amine (1.69 g, 16.1 mmol, 1.00 equiv) in toluene (60 mL) and the resulting solution was refluxed for 12 hours. In the course of the reaction water was removed under reflux and the completion of the reaction was monitored by ^{1}H NMR. The solution was cooled and the volatiles were removed *in vacuo* to afford product **57** as a colourless liquid (2.30 g, 88% yield).

^{1}H NMR ($CDCl_3$, 500 MHz): δ = 1.35 (s, 9H), 7.43–7.46 (m, 3H), 7.79–7.81 (m, 2H), 8.32 (s, 1H) ppm.

^{13}C NMR ($CDCl_3$, 150 MHz): δ = 29.8 (3C), 57.2, 127.9 (2C), 128.5 (2C), 130.2, 137.2, 155.1 ppm.

***N*-(phenylmethylene)-benzenamine**[9]

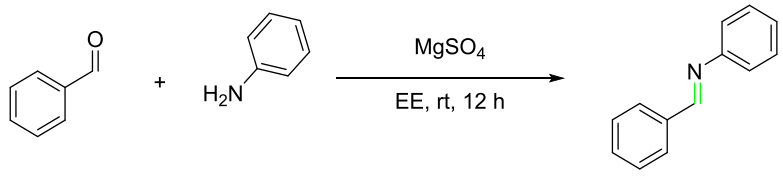

0.9 equiv

59: 90%

*Imine **59** was prepared from Uwe Schneider lab

A mixture of aniline (5.12 g, 55.0 mmol, 1.00 equiv) and benzaldehyde (6.42 g, 60.5 mmol, 1.10 equiv) was stirred for 1 h at room temperature. Next, EE (75 mL) and dried $MgSO_4$ were added to the reaction mixture and it was stirred at room temperature for 24 h. The suspension was filtered at ambient pressure and the volatiles were removed *in vacuo*. The crude was recrystallized from ethanol to afford the product **59** as colourless crystals (9.00 g, 90% yield).

^{1}H NMR ($CDCl_3$, 500 MHz): δ = 7.21–7.32 (m, 3H), 7.42–7.45 (m, 2H), 7.49–7.55 (m, 3H), 7.94–7.96 (m, 2H), 8.5 (s, 1H) ppm.

^{13}C NMR ($CDCl_3$, 125 MHz): δ = 120.9 (2C), 126.0, 128.8 (2C), 128.9 (2C), 129.2 (2C), 131.4, 136.3, 152.1, 160.4 ppm.

4-methoxy-*N*-(phenylmethylene)-benzenamine[10]

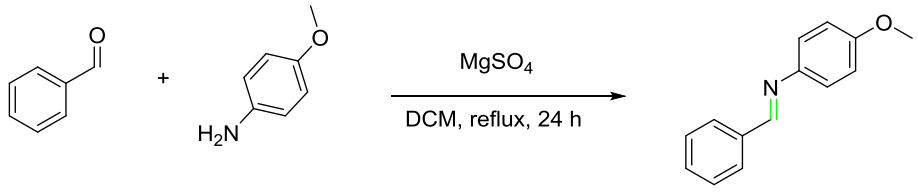

0.95 equiv

60: 72%

*Imine **60** was prepared from Uwe Schneider lab

Benzaldehyde (6.42 g, 60.5 mmol, 1.10 equiv) was added to a solution of *p*-methoxy-phenyl aniline (6.77 g, 55.0 mmol, 1.00 equiv) in DCM (100 mL). Next, dried $MgSO_4$ (10.0 g) was added to the reaction mixture and it was stirred at room temperature for 24 h. The suspension was filtered at ambient pressure and the volatiles were removed *in vacuo*. The crude was recrystallized in ethanol to afford the product **60** as yellow crystals (8.34 g, 72% yield).

^{1}H NMR ($CDCl_3$, 500 MHz): δ = 3.86 (s, 3H), 6.97 (d, *J* = 9.0 Hz, 2H), 7.28 (d, *J* = 9.0 Hz, 2H), 7.44–7.55 (m, 3H), 7.89–7.98 (m, 2H) ppm.
^{13}C NMR ($CDCl_3$, 150 MHz): δ = 55.5, 114.4 (2C), 122.2 (2C), 128.6 (2C), 128.7 (2C), 131.0, 136.5, 145.0, 158.3, 158.4 ppm.

4-methoxy-*N*-(1-phenylethylidene)-benzenamine[10]

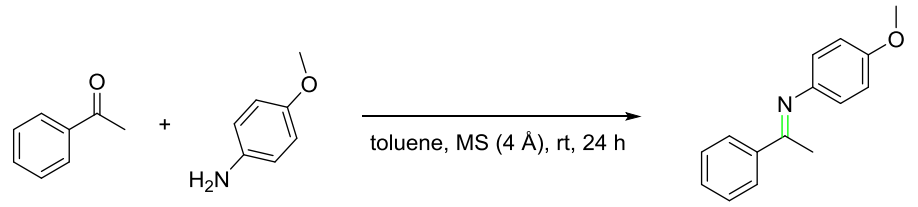

1.0 equiv

61: 94%

*Imine **61** was prepared from Uwe Schneider lab

Acetophenone (4.81 g, 40.0 mmol, 1.00 equiv) was added to a solution of *p*-methoxy-phenyl aniline (4.93 g, 40.0 mmol, 1.00 equiv) in toluene (100 mL). Activated molecular sieves (4 Å) were added to the reaction mixture and it was stirred at room temperature for 24 h. The suspension was filtered at ambient pressure and the volatiles were removed *in vacuo*. The orange crude was

recrystallized from ethanol to afford the product **61** as colourless crystals (9.0 g, 94% yield).

^{1}H NMR ($CDCl_3$, 500 MHz): δ = 2.29 (s, 3H), 3.85 (s, 3H), 6.79 (d, *J* = 7.6 Hz, 2H), 6.95 (d, *J* = 7.6 Hz, 2H), 7.43–7.54 (m, 3H), 7.99–7.81 (m, 2H) ppm.

^{13}C NMR ($CDCl_3$, 150 MHz): δ = 17.3, 55.5, 114.3 (2C), 120.8 (2C), 127.1 (2C), 128.4 (2C), 130.3, 139.8, 144.9, 156.0, 165.7 ppm.

N-(diphenylmethylene)-4-methoxy-benzenamine[10]

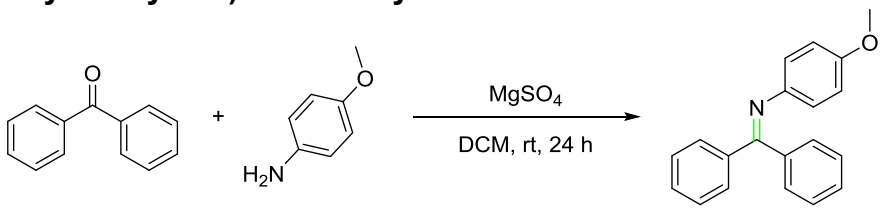

0.95 equiv

62: 91%

*Imine **62** was prepared from Uwe Schneider lab

Benzophenone (1.90 g, 10.5 mmol, 1.00 equiv) was added to a solution of *p*-methoxy-phenyl aniline (1.40 g, 11.1 mmol, 1.05 equiv) in DCM. Next, dried $MgSO_4$ was added to the reaction mixture and it was stirred at room temperature for 12 h. The suspension was filtered at ambient pressure and the volatiles were removed *in vacuo* to afford the product **62** as an orange solid (2.70 g, 85% yield).

^{1}H NMR ($CDCl_3$, 500 MHz): δ = 3.75 (s, 3H), 6.72 (s, 4H), 7.15–7.17 (m, 2H), 7.29–7.33 (m, 3H), 7.40–7.43 (m, 2H), 7.46–7.50 (m, 1H), 7.75–7.77 (m, 2H) ppm.

^{13}C NMR ($CDCl_3$, 150 MHz): δ = 55.3, 113.8 (2C), 122.6 (2C), 128.1 (2C), 128.2 (2C), 128.5, 129.2 (2C), 129.6 (2C), 130.5, 136.7, 140.1, 144.4, 155.9, 167.8 ppm.

N-(phenylmethylene)-benzenemethanamine[11]

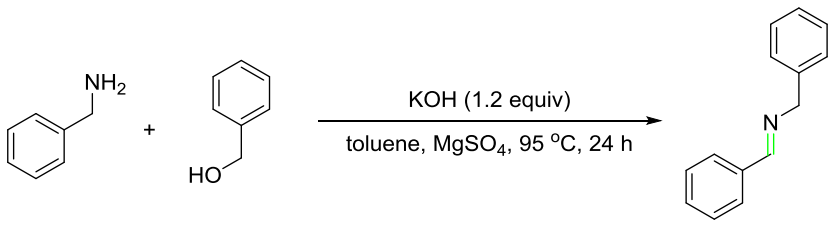

1.2 equiv

58: 80%

In a suspension of KOH (3.70 g, 65.8 mmol, 1.20 equiv) and dried $MgSO_4$ (2.0 g) in toluene (140 mL), benzyl alcohol (7.10 g, 65.8 mmol, 1.20 equiv) was added and the reaction mixture was refluxed for 90 min. Benzyl amine (5.90 g, 54.9 mmol, 1.00 equiv) was added and the resulting suspension was stirred and heated at 95 °C for 24 h. The volatiles were removed *in vacuo* to afford product **58** as an orange oil (6.50 g, 80% yield).

^{1}H NMR ($CDCl_3$, 500 MHz): δ = 4.89 (s, 2H), 7.28–7.36 (m, 1H), 7.40–7.41 (m, 3H), 7.45–7.50 (m, 3H), 7.83–7.87 (m, 2H), 8.45 (s, 1H) ppm.

^{13}C NMR ($CDCl_3$, 150 MHz): δ = 65.1, 127.0, 128.0 (2C), 128.3 (2C), 128.5 (2C), 128.6 (2C), 130.8, 136.2, 139.4, 162.0 ppm.

2.2 Cyanation

Catalytic Cyanation of Aldehydes with ***22****.*

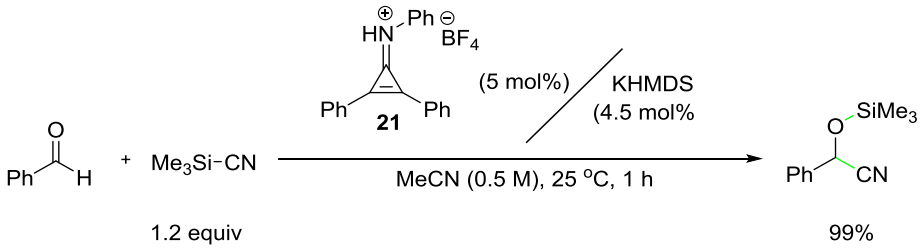

To an oven-dried reaction vessel with a magnetic stirring bar in a nitrogen glovebox were added **21** (3.7 mg, 10.5 μmol, 5.0 mol%), MeCN (100 μL) and KHMDS (2.0 mg, 10.0 μmol, 4.5 mol%) in MeCN (300 μL) dropwise and the resulting mixture was stirred at 25 °C for 30 min to provide **22**. Benzaldehyde (0.20 mmol, 1.00 equiv) and TMSCN (23.8 mg, 0.24 mmol, 1.20 equiv) were added and the mixture was stirred at 25 °C for 1 h. Benzyl ether in mesitylene (200 μL, 0.25 M) was added to afford the NMR yield in ^{1}H NMR (99%).

Catalytic Cyanation of Aldehydes with ***49****.*

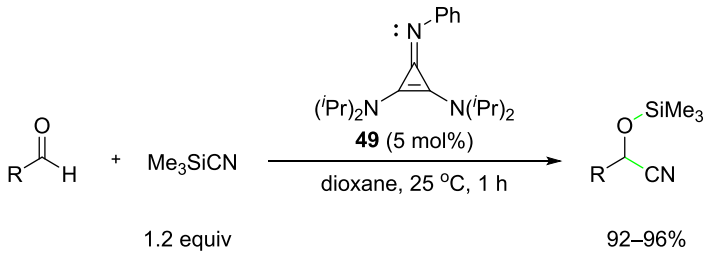

To an oven-dried reaction vessel with a magnetic stirring bar in a nitrogen glovebox were added **49** (3.2 mg, 10.0 μmol, 5.0 mol%), dioxane (400 μL), the corresponding aldehyde (0.20 mmol, 1.00 equiv) and TMSCN (23.8 mg, 0.24 mmol, 1.20 equiv). This mixture was stirred at 25 °C for 1 h. A solution of HCl in ether (1.0 M, 1.00 mL, 5.00 equiv) was added and the reaction mixture was stirred at room temperature for 30 min and concentrated *in vacuo*. DCM (2 mL) was added and the organic phase was washed with brine, dried over $MgSO_4$, and filtered. The filtrate was concentrated *in vacuo*. The residue was dissolved in DCM (400 μL), and acetic anhydride (37.7 μL, 0.40 mmol, 2.00 equiv) and pyridine (32.2 μL, 0.40 mmol, 2.00 equiv) were added. The reaction mixture was stirred for 30 min. The solvent was removed *in vacuo*. The residue was purified by preparative thin-layer chromatography [PTLC; eluant: hexane / ethyl acetate = 9:1] to afford the corresponding acetylated cyanohydrins.

*Catalytic Cyanation of Ketones with **49**.*

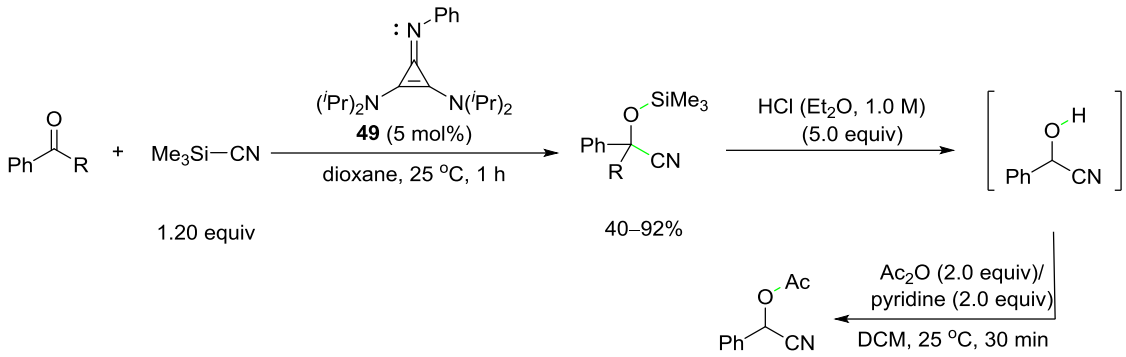

To a flame-dried autoclave reaction vessel with a magnetic stirring bar in a nitrogen glovebox were added **49** (3.2 mg, 10.0 μmol, 5.0 mol%), acetonitrile (400 μL), the corresponding ketone (0.20 mmol, 1.00 equiv) and TMSCN (23.8 mg, 0.24 mmol, 1.20 equiv). This mixture was stirred at room temperature for 1 h. A solution of HCl in ether (1.0 M, 1.0 mL, 5.00 equiv) was added and the reaction mixture was stirred for 30 min. DCM (2 mL) was added and the organic phase was washed with brine (1 mL), dried over $MgSO_4$, and filtered. The filtrate was concentrated *in vacuo*. The residue was dissolved in DCM (400 μL). Acetic anhydride (37.7 μL, 0.40 mmol, 2.00 equiv) and pyridine (32.2 μL, 0.40 mmol, 2.00 equiv) were added. The reaction mixture was stirred for 30 min. The solvent was removed *in vacuo*. The residue was purified by preparative thin-layer chromatography [PTLC; eluant: hexane / ethyl acetate = 9:1] to afford the corresponding acetylated cyanohydrins.

Cyano(phenyl)methyl acetate[12]

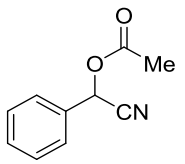

56

Yellow oil.

Yield: 96%.

^{1}H NMR ($CDCl_3$, 500 MHz): δ = 2.17 (s, 3H), 6.42 (s, 1H), 7.43–7.48 (m, 3H), 7.50-7.54 (m, 2H) ppm.

^{13}C NMR ($CDCl_3$, 125 MHz,): δ = 20.3, 63.1, 116.1, 127.9 (2C), 129.3 (2C), 130.4, 131.8, 169.2 ppm.

IR (neat): ν = 2922, 2358, 1751, 1456, 1371, 1210, 1020, 958, 756, 694 cm^{-1}.

HRMS (EI): calculated for $C_{10}H_9NO_2^+$: *m*/*z* = 175.0628, found: *m*/*z* = 175.0627.

Cyano[4-trifluoromethyl)(phenyl)]methyl acetate[13]

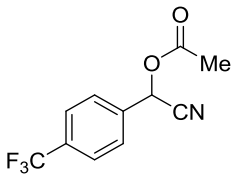

66

Beige solid.

Yield: 95%.

^{1}H NMR ($CDCl_3$, 600 MHz): δ = 2.20 (s, 3H), 6.47 (s, 1H), 7.66 (d, *J* = 8.2 Hz, 2H), 7.73 (d, *J* = 8.2 Hz, 2H) ppm.

^{13}C NMR ($CDCl_3$, 150 MHz,): δ = 20.4, 62.2, 115.5, 123.6 (q, *J* = 272.5 Hz), 126.4 (q, *J* = 3.8 Hz, 2C), 128.3 (2C), 132.6 (q, *J* = 32.9 Hz), 135.6, 168.7 ppm.

^{19}F NMR ($CDCl_3$, 470 MHz): δ = –63.0 (s) ppm.

Cyano(4-fluorophenyl)methyl acetate[14]

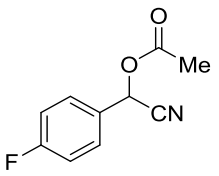

67

Orange liquid.

Yield: 96%.

^{1}H NMR ($CDCl_3$, 600 MHz): δ = 2.16 (s, 3H), 6.39 (s, 1H), 7.13–7.16 (m, 2H), 7.50–7.55 (m, 2H) ppm.

^{13}C NMR ($CDCl_3$, 150 MHz,): δ = 20.5, 62.2, 116.0, 116.4 (d, *J* = 22.2 Hz, 2C), 127.9 (d, *J* = 3.4 Hz), 130.1 (d, *J* = 8.8 Hz, 2C), 163.8 (d, *J* = 251 Hz), 168.9 ppm.

^{19}F NMR ($CDCl_3$, 470 MHz): δ = –109.6 ~ –109.7 (m) ppm.

Cyano(4-bromophenyl)methyl acetate[13]

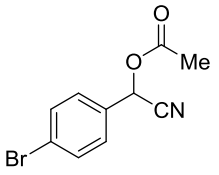

68

Orange liquid.

Yield: 93%.

^{1}H NMR ($CDCl_3$, 600 MHz): δ = 2.14 (s, 3H), 6.35 (s, 1H), 7.37 (d, *J* = 8.4 Hz, 2H), 7.57 (d, *J* = 8.4 Hz, 2H) ppm.

^{13}C NMR ($CDCl_3$, 150 MHz,): δ = 20.4, 62.2, 115.7, 124.9, 129.5 (2C), 130.8, 132.5 (2C), 168.8 ppm.

Cyano(4-cyanophenyl)methyl acetate[12]

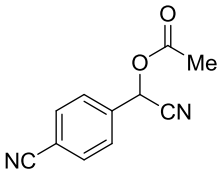

69

Yellow liquid.

Yield: 93%.

^{1}H NMR ($CDCl_3$, 600 MHz): δ = 2.21 (s, 3H), 6.46 (s, 1H), 7.66 (d, *J* = 8.4 Hz, 2H), 7.77 (d, *J* = 8.4 Hz, 2H) ppm.

^{13}C NMR ($CDCl_3$, 150 MHz,): δ = 20.4, 62.0, 114.6, 115.2, 117.7, 128.5 (2C), 133.1 (2C), 136.5, 168.6 ppm.

Cyano(furan-2-yl)methyl acetate[15]

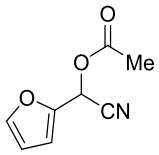

71

Yellow liquid.

Yield: 93%.

^{1}H NMR ($CDCl_3$, 500 MHz): δ = 2.17 (s, 3H), 6.45 (dd, *J* = 3.4, 1.9 Hz, 1H), 6.48 (s, 1H), 6.68 (d, *J* = 3.4 Hz, 1H), 7.51 (dd, *J* = 1.9, 0.8 Hz, 1H) ppm.

^{13}C NMR ($CDCl_3$, 125 MHz): δ = 20.4, 56.0, 111.1, 112.3, 114.1, 144.2, 145.0, 168.8 ppm.

IR (neat): ν = 2922, 2358, 1749, 1499, 1371, 1202, 1011, 916, 881, 748 cm^{-1}.

HRMS (EI): calculated for $C_8H_7NO_3^+$: *m*/*z* = 165.0420, found: *m*/*z* = 165.0439.

Cyano(thiophen-2-yl)methyl acetate[15]

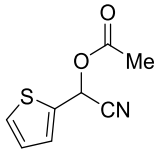

72

Yellow liquid.

Yield: 96%.

^{1}H NMR ($CDCl_3$, 500 MHz): δ = 2.17 (s, 3H), 6.64 (d, *J* = 0.7 Hz, 1H), 7.05 (dd, *J* = 5.1, 3.6 MHz, 1H), 7.35 (ddd, *J* = 3.6, 1.2, 0.7 Hz, 1H), 7.46 (dd, *J* = 5.1, 1.2 MHz, 1H) ppm.

^{13}C NMR ($CDCl_3$, 125 MHz): δ = 20.4, 58.1, 115.4, 127.2, 129.0, 129.6, 133.5, 168.8 ppm.

IR (neat): ν = 2939, 2358, 1749, 1431, 1369, 1200, 1016, 941, 839, 710 cm^{-1}.

HRMS (EI): calculated for $C_8H_7NO_2S^+$: *m*/*z* = 181.0192, found: *m*/*z* = 181.0197.

Cyano(phenylpropyl) methyl acetate[14]

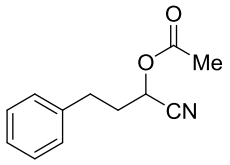

73

Yellow liquid.

Yield: 93%.

^{1}H NMR ($CDCl_3$, 500 MHz): δ = 2.12 (s, 3H), 2.21–2.26 (m, 2H), 2.78–2.88 (m, 2H), 5.27 (t, *J* = 6.8 Hz, 1H), 7.19–7.22 (m, 2H), 7.22–7.25 (m, 1H), 7.29–7.33 (m, 2H) ppm.

^{13}C NMR ($CDCl_3$, 125 MHz): δ = 20.3, 30.3, 33.8, 60.6, 116.8, 126.8, 128.3 (2C), 128.8 (2C), 139.0, 169.1 ppm.

IR (neat): ν = 2936, 2359, 1749, 1497, 1454, 1371, 1229, 1034, 962, 746, 700 cm^{-1}.

HRMS (EI): calculated for $C_{12}H_{13}NO_2^+$: *m*/*z* = 203.0941, found: *m*/*z* = 203.094.

α-(acetyloxy)-α-methyl-benzeneacetonitrile[16]

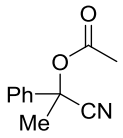

82

Yellow liquid.

Yield: 40%.

^{1}H NMR ($CDCl_3$, 500 MHz): δ = 2.03 (s, 3H), 2.92 (s, 3H), 7.39–7.46 (m, 3H), 7.54–7.57 (m, 4H) ppm.

^{13}C NMR ($CDCl_3$, 125 MHz): δ = 21.0, 29.8, 73.3, 118.1, 124.5 (2C), 129.0 (2C), 138.2, 168.3 ppm.

Cyano(4-methyl-Benzophenoyl)methyl acetate

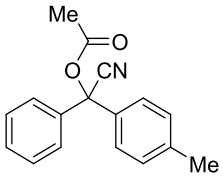

85

Pale yellow oil.

Yield: 73%.

^{1}H NMR ($CDCl_3$, 500 MHz): δ = 2.20 (s, 3H), 2.34 (s, 3H), 7.18–7.19 (m, 2H), 7.42–7.32 (m, 5H), 7.5 (m, 2H) ppm.

^{13}C NMR ($CDCl_3$, 125 MHz): δ = 21.1, 21.2, 77.4, 117.6, 126 (2C), 126.1 (2C), 128.8 (2C), 129.2, 129.5 (2C), 135, 138.1, 139.4, 168.0 ppm.

IR (neat): ν = 2949, 2367, 1760, 1512, 1450, 1368, 1237, 1000, 812, 758, 694 cm^{-1}.

HRMS (EI): calculated for $C_{17}H_{15}NO_2^+$: *m/z* = 265.1097, found: *m/z* = 265.1098.

Cyano(Benzoylthiophenoyl)methyl acetate

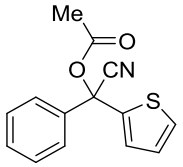

87

Purple solid.

Yield: 77%.

Mp: 32–34 ^{o}C.

^{1}H NMR ($CDCl_3$, 500 MHz): δ = 2.21 (s, 3H), 6.97 (dd, *J* = 3.7, 5.1 Hz, 1H), 7.14 (dd, *J* = 1.3, 3.7 Hz, 1H), 7.37 (dd, *J* = 1.3, 5.1 Hz, 1H), 7.42–7.45 (m, 3H), 7.58–7.60 (m, 2H) ppm.

^{13}C NMR ($CDCl_3$, 125 MHz): δ = 21.1, 74.6, 116.8, 125.6 (2C), 126.9, 128.1, 128.5, 128.9 (2C) 129.7, 137.5, 141.3, 167.1 ppm.

IR (neat): ν = 2928, 2359, 1761, 1450, 1369, 1206, 1115, 1022, 843, 698 cm^{-1}.

HRMS (EI): calculated for $C_{14}H_{11}NO_2S^+$: *m/z* = 257.0505, found: *m/z* = 257.0510.

2-(acetyloxy)-2-cyano-ethyl ester

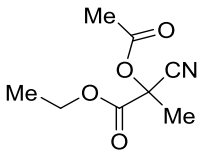

88

Orange liquid.

Yield: 92%.

^{1}H NMR ($CDCl_3$, 500 MHz): δ = 1.35 (t, *J* = 7.1 Hz, 3H), 1.88 (s, 3H), 2.19 (s, 3H), 4.41 –4.27 (m, 2H) ppm.

^{13}C NMR ($CDCl_3$, 125 MHz): δ = 13.9, 20.1, 23.7, 63.4, 69.4, 115.8, 166.3, 168.9 ppm.

IR (neat): ν = 2943, 2372, 1754, 1449, 1265, 1223, 1177, 1098, 1015, 966, 878, 756 cm^{-1}.

HRMS (EI): calculated for $C_8H_{12}NO_4^+$: *m*/*z* = 186.0761, found: *m*/*z* = 186.0762.

2.3 Trifluoromethylation

Catalytic Trifluoromethylation of Aldehydes with **22.**

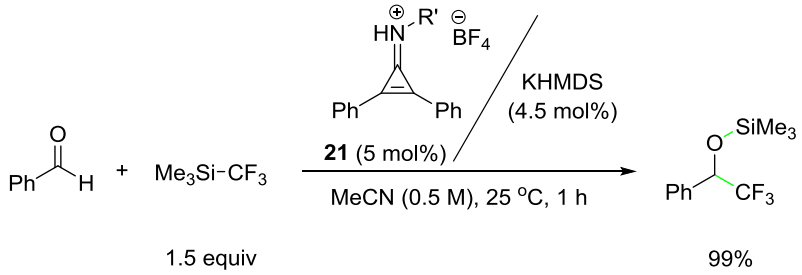

To an oven-dried reaction vessel with a magnetic stirring bar in a nitrogen glovebox were added the catalyst precursor **21** (3.7 mg, 10.5 μmol, 5 mol%), MeCN (100 μL) and KHMDS (2.0 mg, 10.0 μmol, 0.95 equiv) in MeCN (300 μL) dropwise and stirred for 30 min at 25 °C to afford catalyst **22**. The corresponding aldehyde (0.20 mmol) and TMS–CF_3 (0.30 mmol) were added, and the reaction mixture was stirred at 25 °C for 1 h. Benzyl ether in mesitylene (200 μL, 0.25 M) was added to afford the NMR yield in ^{1}H NMR (99%).

Catalytic Trifluoromethylation of Aldehydes with ***49****.*

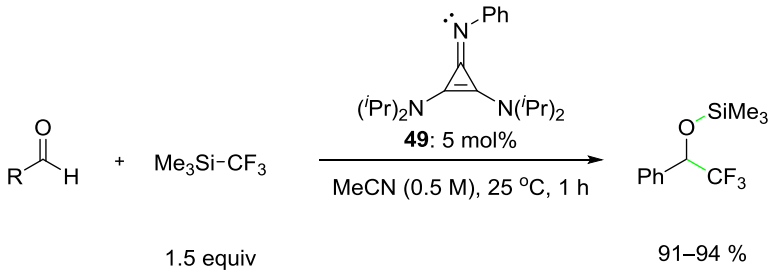

To a flame-dried reaction vessel with a magnetic stirring bar in a nitrogen atmosphere glovebox were added **49** (3.20 mg, 10.0 μmol, 5.0 mol%), acetonitrile (400 μL), corresponding aldehyde (21.2 mg, 0.20 mmol, 1.00 equiv) and TMS–CF_3 (42.7 mg, 0.30 mmol, 1.50 equiv). The reaction mixture was stirred for 30 min before removing the solvent *in vacuo*. The residue was purified by preparative thin-layer chromatography [PTLC; eluant: petroleum

ether (40–60 °C): dichloromethane = 1:1] to afford the trifluoromethylated silyl ethers.

1-(2,2,2-trifluoro-1-naphthylethoxy)-trimethylsilane[17]

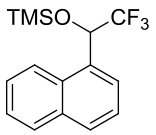

100

Colorless solid.

Yield: 91%.

^{1}H NMR ($CDCl_3$, 500 MHz): δ = 0.10 (s, 9H), 5.76 (q, *J* = 6.3 Hz, 1H), 7.48–7.56 (m, 3H), 7.81–7.83 (m, 1H), 7.86–7.89 (m, 2H), 8.09–8.11 (m, 1H) ppm.

^{13}C NMR ($CDCl_3$, 125 MHz): δ = 0.3 (3C), 69.9–70.7 (q, *J* = 33.1 Hz), 121.6–128.4 (q, *J* = 283.0 Hz), 123.3, 125.5, 125.9, 126.8, 127.3, 129.3, 130.1, 131.4, 131.63, 134.0 ppm.

^{19}F NMR (CDCl3, 470 MHz): δ = –77.2 (d, *J* = 6.3 Hz) ppm.

IR (neat): ν = 2959, 1269, 1165, 1126, 872, 839, 775, 696, 631 cm^{-1}.

HRMS (EI): calculated for $C_{15}H_{17}OF_3Si^+$: *m/z* = 298.0995, found: *m/z* = 298.1003.

(1-Anthracen-9-yl-2,2,2-trifluoro-ethoxy)-trimethylsilane[18]

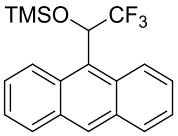

101

Beige solid.

Yield: 92%.

^{1}H NMR ($CDCl_3$, 500 MHz): δ = –0.03 (s, 9H), 6.54 (q, *J* = 7.9 Hz, 1H), 7.45–7.51 (m, 3H), 7.55–7.58 (m, 1H), 7.97 (d, *J* = 8.4 Hz, 1H), 8.02 (d, *J* = 8.4 Hz, 1H), 8.17 (d, *J* = 9.0 Hz, 1H), 8.49 (s, 1H), 9.06 (d, *J* = 9.0 Hz, 1H) ppm.

^{13}C NMR ($CDCl_3$, 125 MHz): δ = –0.52 (3C), 70.5 (q, *J* = 33.6 Hz), 122.3, 124.6, 125.1, 125.4, 125.5 (q, *J* = 281Hz), 126.5, 127.1, 128.0, 128.4, 128.7, 129.7, 130.4, 130.5, 131.2, 132.0 ppm.

^{19}F NMR ($CDCl_3$, 470 MHz): δ = –74.2 (d, *J* = 7.9 Hz) ppm.

Compound 102[18]

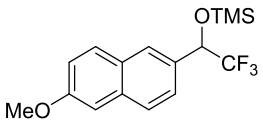

102

Colorless solid.

Yield: 94%.

Mp: 57–59 °C.

^{1}H NMR ($CDCl_3$, 500 MHz): δ = 0.12 (s, 9H), 3.91 (s, 3H), 5.04 (q, *J* = 6.5 Hz, 1H), 7.14–7.18 (m, 2H), 7.52–7.53 (m, 1H), 7.73–7.75 (m, 2H), 7.81 (s, 1H) ppm.

^{13}C NMR ($CDCl_3$, 125 MHz): δ = –0.22 (3C), 55.3, 73.5 (q, *J* = 32.1 Hz), 105.7, 119.3, 124.4 (q, *J* = 282.4 Hz), 125.4, 127.0, 127.1, 127.2, 128.4, 129.7, 130.7, 135.0 ppm.

^{19}F NMR (CDCl3, 470 MHz): δ = –78.2 (d, *J* = 6.6 Hz) ppm.

IR (neat): ν = 2945, 1608, 1485, 1468, 1375, 1269, 1157, 1121, 1098, 1034, 876, 848, 760 cm^{-1}.

HRMS (EI): calculated for $C_{16}H_{19}O_2F_3Si^+$: *m/z* = 328.1101, found: *m/z* = 328.1092.

*Catalytic Trifluoromethylation of Ketones with **24**.*

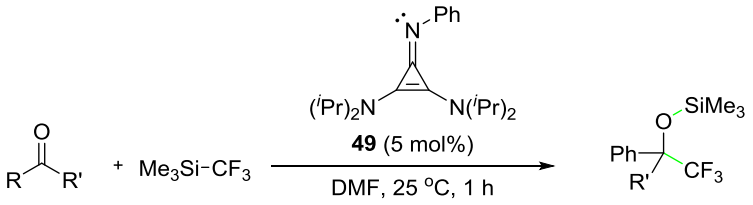

To a flame-dried autoclave reaction vessel with a magnetic stirring bar in a nitrogen atmosphere glovebox were added **52** (3.2 mg, 0.01 mmol, 5.0 mol%), dimethyl formamide (400 µL), corresponding ketone (21.2 mg, 0.2 mmol, 1.00 equiv) and $TMSCF_3$ (42.7 mg, 0.3 mmol, 1.50 equiv). The reaction mixture

was stirred for 30 min before removing the solvent *in vacuo*. The residue was purified by preparative thin-layer chromatography [PTLC; eluant: petroleum ether (40–60 °C): dichloromethane = 1:1] to afford the trifluoromethylated silyl ethers.

Trimethyl-(2,2,2-trifluoro-1,1-diphenyl-ethoxy)-silane[18]

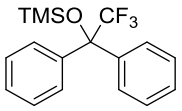

111

Colourless liquid.

Yield: 94%.

^{1}H NMR ($CDCl_3$, 500 MHz): δ = –0.06 (s, 9H), 7.30–7.32 (m, 6H), 7.40–7.41 (m, 4H) ppm.

^{13}C NMR ($CDCl_3$, 125 MHz): δ = 1.3 (3C), 82.0 (q, *J* = 28.4 Hz), 125.2 (q, *J* = 287.4 Hz), 127.8 (4C), 128.2 (4C), 128.3 (2C), 140.9 (2C) ppm.

^{19}F NMR (CDCl3, 470 MHz): δ = –72.7 (s) ppm.

IR (neat): ν = 3063, 1254, 1161, 1123, 1107, 953, 880, 839, 762, 723, 696 cm^{-1}.

HRMS (EI): calculated for $C_{17}H_{19}OF_3Si^+$: *m/z* = 324.1152, found: *m/z* = 324.1150.

Trimethyl-(2,2,2-trifluoro-1-phenyl-1-p-tolyl-ethoxy)-silane[18]

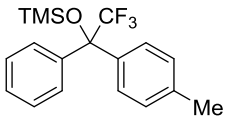

112

Colourless liquid.

Yield: 91%.

^{1}H NMR ($CDCl_3$, 500 MHz): δ = –0.06 (s, 9H), 2.34 (s, 3H), 7.11–7.12 (m, 2H), 7.26–7.31 (m, 5H), 7.39–7.41 (m, 2H) ppm.

^{13}C NMR ($CDCl_3$, 125 MHz): δ = 1.3 (3C), 21.1, 81.9 (q, *J* = 28.5 Hz), 125.2 (q, *J* = 287.5 Hz), 126.4, 127.8 (2C), 128.1 (2C), 128.2 (2C), 128.5 (2C), 138, 138.1, 141.1 ppm.

^{19}F NMR (CDCl3, 470 MHz): δ = –72.7 (s) ppm.

IR (neat): ν = 2959, 1254, 1159, 1107, 932, 841, 758, 723, 696 cm^{-1}.

HRMS (EI): calculated for $C_{18}H_{21}OF_3Si^+$: *m/z* = 338.1308, found: *m/z* = 338.1319.

[1-(4-Bromo-phenyl)-2,2,2-trifluoro-1-phenyl-ethoxy]-trimethylsilane[18]

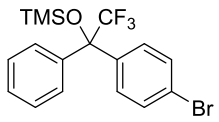

113

Colourless liquid.

Yield: 97%.

^{1}H NMR ($CDCl_3$, 500 MHz): δ = –0.06 (s, 9H), 7.26–7.28 (m, 2H), 7.31–7.33 (m, 3H), 7.36–7.38 (m, 2H), 7.44–7.45 (m, 2H) ppm.

^{13}C NMR ($CDCl_3$, 125 MHz): δ = 1.3 (3C), 81.7 (q, *J* = 28.7 Hz), 122.6, 123.8 (q, *J* = 287.4 Hz), 128.0 (2C), 128.1 (2C), 128.5, 129.9 (2C), 131.0 (2C), 140.2, 140.3 ppm.

^{19}F NMR ($CDCl_3$, 470 MHz): δ = –72.7 (s) ppm.

IR (neat): ν = 2959, 1254, 1156, 1125, 1013, 932, 841, 754, 698, 654 cm^{-1}.

HRMS (EI): calculated for $C_{17}H_{18}OBrF_3Si^+$: *m/z* = 402.0257, found: *m/z* = 402.0267.

[1-(4-Bromo-phenyl)-2,2,2-trifluoro-1-phenyl-ethoxy]-trimethylsilane[18]

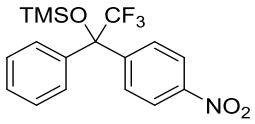

114

Yellow liquid.

Yield: 95%.

^{1}H NMR ($CDCl_3$, 500 MHz): δ = –0.03 (s, 9H), 7.36 (s, 5H), 7.61 (d, *J* = 9.0 Hz, 2H), 8.17 (d, *J* = 9.0 Hz, 2H) ppm.

^{13}C NMR ($CDCl_3$, 125 MHz): δ = 1.3 (3C), 81.8 (q, *J* = 28.9 Hz), 123.0 (2C), 124.7 (q, *J* = 287.7 Hz), 128.0 (2C), 128.4 (2C), 129.0, 129.1 (2C), 139.6, 147.8, 148.2 ppm.

^{19}F NMR (CDCl3, 470 MHz): δ = –72.4 (s) ppm.

Compound 115

115

Colourless liquid.

Yield: 92%.

^{1}H NMR ($CDCl_3$, 500 MHz): δ = –0.01 (s, 9H), 6.97 (dd, *J* = 1.7, 5.1 Hz, 1H), 7.08–7.09 (m, 1H), 7.32 (dd, *J* = 3.2, 5.1 Hz, 1H), 7.34–7.45 (m, 3H), 7.52–7.54 (m, 2H) ppm.

^{13}C NMR ($CDCl_3$, 125 MHz): δ = 1.1 (3C), 79.9 (q, *J* = 29.9 Hz), 124.8 (q, *J* = 287.4 Hz), 126.4, 126.5, 127.7, 127.8 (d, *J* = 1.4 Hz), 128.0, 128.8, 133.2, 139.9, 144.3, 149.0 ppm.

^{19}F NMR (CDCl3, 470 MHz): δ = –72.7 (s) ppm.

IR (neat): ν = 2959, 1275, 1254, 1162, 1105, 1078, 941, 878, 845, 712 cm^{-1}.

MS (EI): calculated for $C_{15}H_{17}OSF_3Si^+$: *m/z* = 330. 0716, found: *m/z* = 330.0719.

2.4 Azidation of benzaldehyde

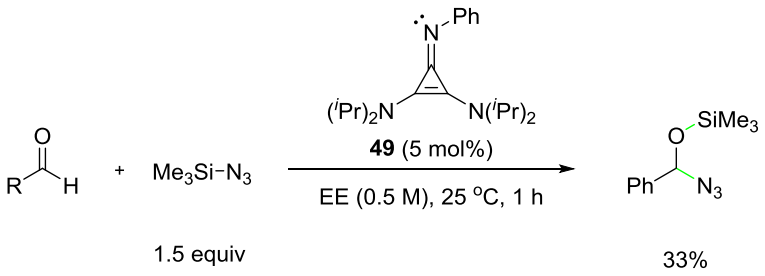

To a flame-dried reaction vessel with a magnetic stirring bar in a nitrogen atmosphere glovebox were added **49** (3.2 mg, 10.0 μmol, 5 mol%), ether (400 μL), benzaldehyde (21.2 mg, 0.20 mmol) and $TMSN_3$ (34.6 mg, 0.30 mmol). The reaction mixture was stirred for 24 h before removing the solvent *in vacuo*. The residue was purified by preparative thin-layer chromatography [PTLC; eluant: petroleum ether (40–60 °C): dichloromethane = 1:1] to afford the azidated silyl ethers.

[azido[(trimethylsilyl)oxy]methyl]benzene[19]

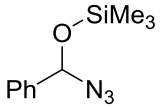

120

Colourless solid.

Yield: 33%.

^{1}H NMR ($CDCl_3$, 500 MHz): δ = 0.26 (s, 9H), 7.46–7.48 (m, 2H), 7.36–7.44 (m, 3H) ppm.

2.5 Aziridine Ring-Opening

2.5.1 Aziridination

Representative procedure for the preparation of aziridines 120 and 125.

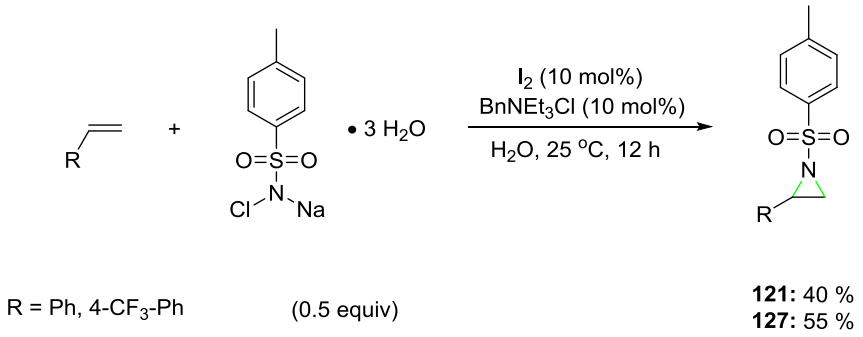

To a mixture of iodine (127 mg, 0.50 mmol, 0.10 equiv), chloramine-T (2.82 g, 10.0 mmol, 0.50 equiv) and benzyltriethylammonium chloride (114 mg, 0.50 mmol, 0.10 equiv) in water (300 mL) was added the corresponding styrene (1.00 equiv). The mixture was stirred at room temperature for 24 hours. The organic phase was extracted with DCM and dried over $MgSO_4$. The suspension was filtered and the volatiles were removed *in vacuo*. The brown oil was recrystallized by methanol to afford the corresponding aziridines.

1-[(4-methylphenyl)sulfonyl]-2-phenylaziridine[20]

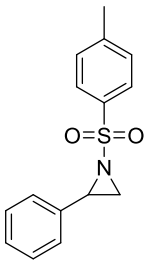

121

Colorless solid.

Yield: 40%.

^{1}H NMR ($CDCl_3$, 500 MHz): δ = 2.38 (d, *J* = 4.5 Hz, 1H), 2.43 (s, 3H), 2.98 (d, *J* = 7.2 Hz, 1H), 3.77 (dd, *J* = 4.5, 7.2 Hz, 1H), 7.20–7.22 (m, 2H), 7.26–7.29 (m, 3H), 7.33 (d, *J* = 8.3 Hz, 2H), 7.87 (d, *J* = 8.3 Hz, 2H) ppm.

^{13}C NMR ($CDCl_3$, 125 MHz): δ = 21.7, 35.9, 41.1, 126.6 (2C), 128.0 (2C), 128.3, 128.6 (2C), 129.8 (2C), 135.0, 135.1, 144.7 ppm.

2-(4-fluorophenyl)-1-[(4-methylphenyl)sulfonyl]aziridine[20]

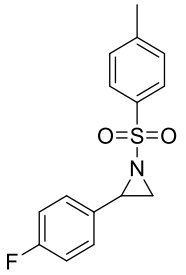

127

Colorless solid.

Yield: 55%.

^{1}H NMR ($CDCl_3$, 500 MHz): δ = 2.35 (d, *J* = 4.4 Hz, 1H), 2.44 (s, 3H), 2.97 (d, *J* = 7.1 Hz, 1H), 3.75 (dd, *J* = 7.1, 4.4 Hz, 1H), 6.98 (t, *J* = 8.6 Hz, 2H), 7.19 (dd, *J* = 8.6 Hz, 5.3 Hz, 2H), 7.34 (d, *J* = 8.4 Hz, 2H), 7.86 (d, *J* = 8.4 Hz, 2H) ppm.

^{13}C NMR ($CDCl_3$, 125 MHz): δ = 21.7, 36.0, 40.3, 115.6 (d, *J* = 21.8 Hz, 2C), 128.0 (2C), 128.3 (d, *J* = 8.3 Hz, 2C), 129.8 (2C), 131 (d, *J* = 3.2 Hz), 134.5, 144.8, 162.7 (d, *J* = 247.2 Hz) ppm.

Representative procedure for the preparation of aziridines 126–132.[21]

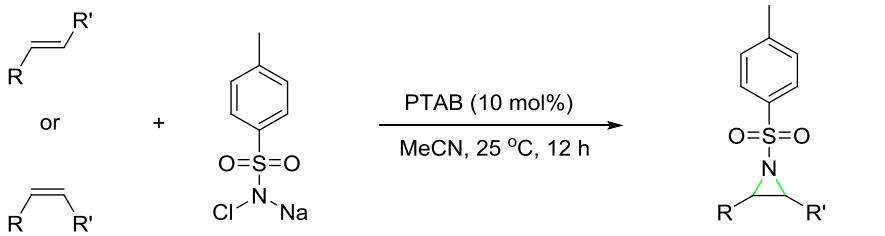

(1.1 equiv)

126–132: 32–67% yield

Phenyl trimethylammonium tribromide (0.22 g, 0.59 mmol, 0.10 equiv) was added to a suspension of chloramine–T • $3H_2O$ (1.83 g, 6.50 mmol, 1.25 equiv) and alkene (5.2 mmol, 1.00 equiv) in acetonitrile (26 mL). After stirring at room temperature for 15 h, the volatiles were removed *in vacuo*. DCM (10 mL) was added and the suspension was filtered quickly over silica. The solvent was removed *in vacuo* and the residue was purified by column chromatography

[PTLC; eluant: petroleum ether / ethyl acetate = 9:1] to afford the corresponding aziridines.

2-butyl-1-[(4-methylphenyl)sulfonyl]aziridine[22]

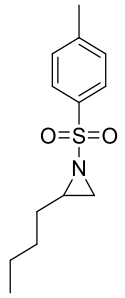

125

Colorless solid.

Yield: 53%.

^{1}H NMR ($CDCl_3$, 500 MHz): δ = 0.81 (t, *J* = 7.0 Hz, 3H), 1.20–1.37 (m, 5H), 1.50–1.59 (m, 1H), 2.07–2.08 (m, 1H), 2.44 (s, 3H), 2.64–2.66 (m, 1H), 2.69–2.75 (m, 1H), 7.34 (d, *J* = 8.1 Hz, 2H), 7.83 (d, *J* = 8.1 Hz, 2H) ppm.

^{13}C NMR ($CDCl_3$, 125 MHz): δ = 13.8, 21.6, 22.1, 28.9, 31.0, 33.8, 40.4, 128.0 (2C), 129.6 (2C), 135.3, 144.4 ppm.

1-[(4-methylphenyl)sulfonyl]-2-(phenylmethyl)aziridine[20]

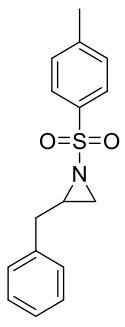

126

Colorless liquid.

Yield: 34%.

^{1}H NMR ($CDCl_3$, 500 MHz): δ = 2.15 (d, *J* = 4.5 Hz, 1H), 2.42 (s, 3H), 2.70–2.74 (m, 2H), 2.81–2.85 (m, 1H), 2.95–3.00 (m, 1H), 7.03–7.05 (m, 2H), 7.14–7.16 (m, 3H), 7.21 (d, *J* = 8.1 Hz, 2H), 7.69 (d, *J* = 8.1 Hz, 2H) ppm.

^{13}C NMR ($CDCl_3$, 125 MHz): δ = 21.6, 32.8, 37.5, 41.2, 126.5, 127.9 (2C), 128.5 (2C), 128.7 (2C), 129.6 (2C), 134.9, 137.0, 144.3 ppm.

2-ethenyl-1-[(4-methylphenyl)sulfonyl]aziridine[23]

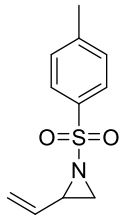

128

Colorless liquid.

Yield: 45%.

^{1}H NMR ($CDCl_3$, 500 MHz): δ = 2.24 (d, *J* = 7.1 Hz, 1H), 2.47 (s, 3H), 2.89 (d, *J* = 7.1 Hz, 1H), 3.28–3.31 (m, 1H), 5.25–5.27 (m, 1H), 5.43–5.46 (m, 1H), 5.51–5.57 (m, 1H), 7.36 (d, *J* = 8.1 Hz, 2H), 7.85 (d, *J* = 8.1 Hz, 2H) ppm.

^{13}C NMR ($CDCl_3$, 125 MHz): δ = 21.7, 34.2, 41.0, 120.3, 127.9 (2C), 129.8 (2C), 133.0, 135.2, 144.6 ppm.

2-methyl-1-[(4-methylphenyl)sulfonyl]-3-phenylaziridine[24]

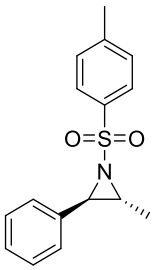

129

Colorless solid.

Yield: 40%.

^{1}H NMR ($CDCl_3$, 500 MHz): δ = 1.84 (d, *J* = 6.0 Hz, 3H), 2.39 (s, 3H), 2.94 (dq, *J* = 4.3, 6.0 Hz, 1H), 3.79 (d, *J* = 4.3 Hz, 1H), 7.11–7.18 (m, 2H), 7.23–7.26 (m, 5H), 7.82 (d, *J* = 8.3 Hz, 2H) ppm.

^{13}C NMR ($CDCl_3$, 125 MHz): δ = 14.2, 21.6, 49.1, 49.2, 126.3 (2C), 127.2 (2C), 128.1, 128.5 (2C), 129.5 (2C), 135.6, 138.0, 143.9 ppm.

1-[(4-methylphenyl)sulfonyl]-2,3-diphenylaziridine[20]

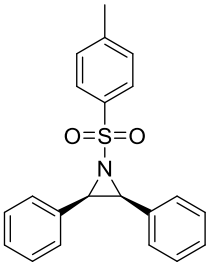

130

Yield: 33%.

Colorless solid.

^{1}H NMR ($CDCl_3$, 500 MHz): δ = 2.47 (s, 3H), 4.25 (s, 2H), 7.06–7.07 (m, 4H), 7.13–7.15 (m, 6H), 7.38 (d, *J* = 8.1 Hz, 2H), 7.98 (d, *J* = 8.1 Hz, 2H) ppm.

^{13}C NMR ($CDCl_3$, 125 MHz): δ = 21.7, 47.5 (2C), 127.7 (2C), 127.8 (4C), 128.0 (4C), 128.1 (2C), 129.9 (2C), 132.0 (2C), 134.9, 144.8 ppm.

6-[(4-methylphenyl)sulfonyl]-6-Azabicyclo[3.1.0]hexane[25]

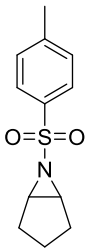

131

Colorless solid.

Yield: 67%.

^{1}H NMR (CDCl3, 500 MHz): δ = 1.33–1.41 (m, 1H), 1.53–1.61 (m, 3H), 1.95–1.99 (m, 2H), 2.42 (s, 3H), 3.31 (s, 2H), 7.30 (d, *J* = 8.1 Hz, 2H), 7.79 (d, *J* = 8.1 Hz, 2H) ppm.

^{13}C NMR ($CDCl_3$, 125 MHz): δ = 19.5, 21.6, 27.0 (2C), 46.7 (2C), 127.6 (2C), 129.6 (2C), 136.0, 144.1 ppm.

7-[(4-methylphenyl)sulfonyl]-7-Azabicyclo[4.1.0]heptane[26]

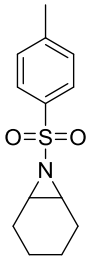

132

Colorless solid.

Yield: 82%.

^{1}H NMR ($CDCl_3$, 500 MHz): δ = 1.17–1.26 (m, 2H), 1.35–1.45 (m, 2H), 1.76–1.81 (m, 4H), 1.72 (s, 3H), 2.96–2.99 (m, 2H), 7.32 (d, *J* = 8.3 Hz, 2H), 7.82 (d, *J* = 8.3 Hz, 2H) ppm.

^{13}C NMR ($CDCl_3$, 125 MHz): δ = 19.5 (2C), 21.6, 27.0 (2C), 46.7 (2C), 127.6 (2C), 129.6 (2C), 136.0, 144.0 ppm.

2.5.2 Aziridine Ring Opening Products

Representative procedure for aziridine ring-opening using $TMSN_3$:

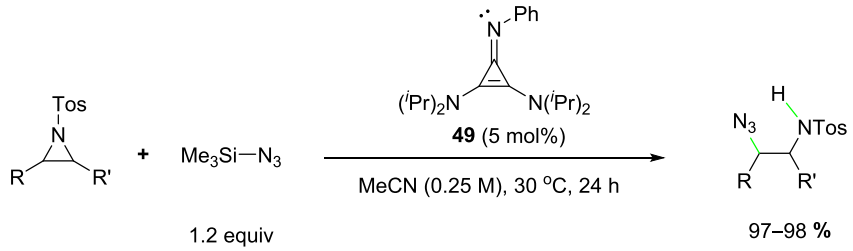

To an oven-dried reaction vessel with a magnetic stirring bar in a nitrogen glovebox were added **49** (3.2 mg, 10.0 μmol, 5.0 mol%), dioxane (400 μL), the corresponding aziridine (0.20 mmol, 1.00 equiv) and $TMS–N_3$ (27.7 mg, 0.24 mmol, 1.20 equiv). This mixture was stirred at 30 °C for 24 h. The mixture was concentrated *in vacuo*. The residue was purified by preparative thin-layer chromatography [PTLC; eluant: hexane/ethyl acetate = 9:1] to afford the corresponding β-functionalised sulfonamides.

***N*-(2-azido-2-phenylethyl)-4-methylbenzenesulfonamide** and ***N*-(2-azido-1-phe-nylethyl)-4-methyl-benzenesulfonamide.**[27]

Major Product: Minor Product:

122 **123**

Colorless solid.

Yield: 98% (6.5:1).

Major product:

^{1}H NMR ($CDCl_3$, 500 MHz): δ = 2.43 (s, 3H), 3.06–3.11 (m, 1H), 3.18–3.25 (m, 1H), 4.58–4.60 (m, 1H), 4.86 (br s, 1H), 7.22–7.23 (m, 2H), 7.31 (d, *J* = 7.8 Hz, 2H), 7.34–7.38 (m, 3H), 7.72 (d, *J* = 7.8 Hz, 2H) ppm.

^{13}C NMR ($CDCl_3$, 125 MHz): δ = 21.5, 48.1, 65.5, 127.0 (2C), 127.1 (2C), 129.0, 129.1 (2C), 129.9 (2C), 136.2, 136.9, 143.8 ppm.

Minor Product:

^{1}H NMR ($CDCl_3$, 500 MHz): δ = 2.38 (s, 3H), 3.56 (d, *J* = 6.0 Hz, 2H), 4.40 (q, *J* = 6.0 Hz, 1H), 5.28 (s br, 1H), 7.10–7.11 (m, 2H), 7.30–7.40 (m, 5 H), 7.61–7.62 (m, 2H) ppm.

^{13}C NMR ($CDCl_3$, 125 MHz): δ = 21.5, 56.0, 57.0, 126.8 (2C), 127.1 (2C), 128.3, 128.8 (2C), 129.6 (2C), 137.1, 137.5, 143.6 ppm.

***N*-[2-azido-2-(4-fluorophenyl)ethyl]-4-methyl-benzenesulfonamide** and ***N*-[2-azido-1-(4-fluorophenyl)ethyl]-4-methyl-benzenesulfonamide.**[20]

Major Product: Minor Product:

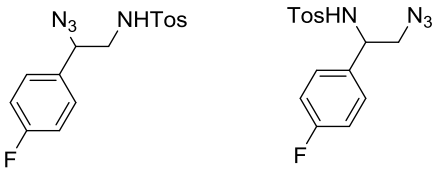

133 **134**

Colorless solid.

Yield: 97% (6.5:1).

Major product:

^{1}H NMR ($CDCl_3$, 500 MHz): δ = 2.43 (s, 3H), 3.04–3.08 (m, 1H), 3.18–3.22 (m, 1H), 4.59–4.61 (m, 1H), 4.93 (br s, 1H), 7.03–7.06 (m, 2H), 7.20–7.23 (m, 2H), 7.31 (d, *J* = 7.8 Hz, 2H), 7.72 (d, *J* = 7.8 Hz, 2H) ppm.

^{13}C NMR ($CDCl_3$, 125 MHz): δ = 21.5, 48.2, 64.8, 116.1 (d, J = 21.7 Hz, 2C), 127 (2C), 128.8 (d, J = 8.3 Hz, 2C), 130.0 (2C), 132.2 (d, *J* = 3.2 Hz), 136.9, 143.9, 162.9 (d, J = 248.4 Hz) ppm.

^{19}F NMR ($CDCl_3$, 470 MHz): δ = –112.1 ~ –112.3 (m) ppm.

Minor Product:

^{1}H NMR ($CDCl_3$, 500 MHz): δ = 2.39 (s, 3H), 3.51–3.53 (m, 2H), 4.45 (q, *J* = 6.4 Hz, 1H), 5.39 (br s, 1H), 6.89–6.91 (m, 2H), 7.07–7.10 (m, 2H), 7.18–7.20 (m, 2H), 7.60 (d, *J* = 7.8 Hz, 2H) ppm.

^{13}C NMR ($CDCl_3$, 125 MHz): δ = 29.8, 56.0, 56.4, 115.6 (d, J = 21.7, 2C), 127.1 (2C), 128.6 (d, J = 8.5 Hz, 2C), 129.6 (2C), 133.4, 137.0, 143.7, 162.5 (d, J = 247.6) ppm.

^{19}F NMR ($CDCl_3$, 470 MHz): δ = –113.4 ~ –113.5 (m) ppm.

***N*-(2-azidocyclohexyl)-4-methyl-benzenesulfonamide**[20]

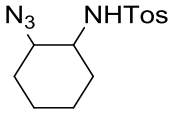

137

Colorless solid.

Yield: 97%.

^{1}H NMR ($CDCl_3$, 500 MHz): δ = 1.18–1.36 (m, 4H), 1.63–1.71 (m, 2H), 2.01–2.06 (m, 2H), 2.43 (s, 3H), 2.92–2.98 (m, 1H), 3.08 (td, *J* = 4.2, 10.1 Hz, 1H), 4.96 (br s, 1H), 7.30–7.32 (d, *J* = 8.0 Hz, 2H), 7.79–7.81 (d, *J* = 8.0 Hz, 2H) ppm.

^{13}C NMR ($CDCl_3$, 125 MHz): δ = 21.6, 23.6, 23.8, 30.2, 32.4, 56.8, 63.6, 127.1 (2C), 129.7 (2C), 137.6, 143.5 ppm.

Representative procedure for aziridine ring-opening using TMSCl:

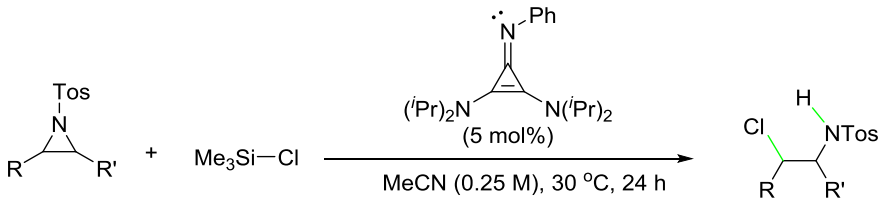

To an oven-dried reaction vessel with a magnetic stirring bar in a nitrogen glovebox were added **49** (3.2 mg, 10.0 μmol, 5.0 mol%), dioxane (400 μL), the corresponding aziridine (0.20 mmol, 1.00 equiv) and TMS–Cl (27.7 mg, 0.24 mmol, 1.20 equiv). This mixture was stirred at 30 °C for 24 h. The fmixture was concentrated *in vacuo*. The residue was purified by preparative thin-layer

chromatography [PTLC; eluant: hexane / ethyl acetate = 9:1] to afford the corresponding β-functionalised sulfonamides.

***N*-(2-chloro-2-phenylethyl)-4-methyl-benzenesulfonamide**[28]

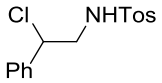

138

Colorless solid.

Yield: 96%.

^{1}H NMR ($CDCl_3$, 500 MHz): δ = 2.44 (s, 3H), 3.39–3.51 (m, 2H), 4.89–4.94 (m, 2H), 7.27–7.34 (m, 7H), 7.72 (d, *J* = 8.2 Hz, 2H) ppm.

^{13}C NMR ($CDCl_3$, 125 MHz): δ = 21.6, 50.4, 61.7, 127.1 (2C), 127.2 (2C), 129.0 (2C), 129.1, 129.9 (2C), 137.0, 137.8, 143.9 ppm.

***N*-(2-chlorocyclohexyl)-4-methyl-benzenesulfonamide**[27]

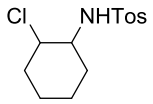

141

Colorless solid.

Yield: 97%.

^{1}H NMR ($CDCl_3$, 500 MHz): δ = 1.23–1.34 (m, 3H), 1.58–1.65 (m, 2H), 1.69–1.72 (m, 1H), 2.16–2.25 (m, 2H), 2.43 (s, 3H), 3.07–3.12 (m, 1H), 3.71 (td, *J* = 9.7, 4.1 Hz, 1H), 4.98 (br s, 1H), 7.30 (d, *J* = 8.2 Hz, 2H), 7.78 (d, *J* = 8.2 Hz, 2H) ppm.

^{13}C NMR ($CDCl_3$, 125 MHz): δ = 21.6, 23.4, 24.5, 32.6, 35.0, 58.8, 62.2, 127.3 (2C), 129.6 (2C), 137.2, 144.0 ppm.

2.6 Carbones or C(0)

2-(triphenylphosphoranylidene)ethenone (Bestmann Ketene)[29]

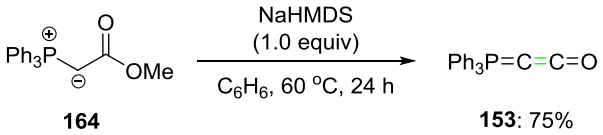

164 **153**: 75%

(Methoxycarbonylmethylene)-triphenylphosphorane (**164**; 4.00 g, 12.0 mmol, 1.00 equiv) was dissolved in toluene (14 mL) and NaHMDS (20.0 mL, 12.0 mmol, 0.6 M in toluene, 1.00 equiv) was added to the solution. After heating at 60 °C for 24 h, it was filtered over celite, while it was hot and volatiles were removed *in vacuo*. The brown solid was recrystallized in toluene (7 mL) to afford **153** as beige crystals (2.60 g, 72%).

^{1}H NMR ($CDCl_3$, 400 MHz): δ = 6.90–6.94 (m, 6H), 6.99–7.02 (m, 3H), 7.54–7.58 (m, 6H) ppm.

^{13}C NMR ($CDCl_3$, 100 MHz): δ = –10.7 (d, *J* = 193.4 Hz), 128.5 (d, *J* = 12.8, 6C), 130.5 (d, *J* = 98.9 Hz, 3C), 131.5 (d, *J* = 2.9 Hz, 3C), 132.2 (d, *J* = 11.2 Hz, 6C), 146.7 (d, *J* = 45.0 Hz) ppm.

(2,2-diethoxyethenyl)triphenylphosphonium tetrafluoroborate (170)[30]

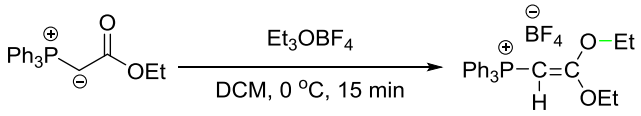

167: 3.0 equiv **168**: 68%

(2-triphenylphosphoranilydene)ethyl ester (**167**; 4.88 g, 14.0 mmol, 1.00 equiv) was dissolved in DCM (15 mL) and cooled down to 0 °C under inert atmosphere for 15 min. Triethyloxonium tetrafluoroborate (14.0 mL, 1.0 M in DCM, 14.0 mmol, 1.00 equiv) was added to the solution dropwise for over 30 min. The mixture was warmed up to room temperature, stirred for 2 hours, filtered and the volatiles were removed *in vacuo*. The gummy solid was dissolved in benzene (50 mL) and water (40 mL) was added. The mixture was stirred vigorously for 2 hours. The organic phase was extracted and the aqueous phase was washed with benzene (3 x 5 mL). The combined organic

solution was dried over $MgSO_4$ and filtered. The filtrate was concentrated *in vacuo*. The gummy solid was washed with EE (3 x 10 mL) and recrystallized from THF (8 mL) to afford product **168** as colorless crystals (2.38 g, 45%).

^{1}H NMR ($CDCl_3$, 500 MHz): δ = 0.74 (t, *J* = 7.0 Hz, 3H), 1.49 (t, *J* = 7.0 Hz, 3H), 4.01 (q, *J* = 7.0 Hz, 2H), 4.26 (d, *J* = 11.4 Hz, 1H), 4.48 (q, *J* = 7.0 Hz, 2H), 7.60–7.69 (m, 12H), 7.70–7.76 (m, 3H) ppm.

^{13}C NMR ($CDCl_3$, 125 MHz): δ = 13.8 (d, *J* = 12.4 Hz), 47.6 (d, *J* = 115.5 Hz), 64.9, 69.0, 121.7. 122.5, 129.9 (d, *J* = 13.0 Hz, 6C), 133.2, (d, *J* = 10.7 Hz, 6C), 134.0 (d, *J* = 2.7 Hz, 3C), 170.8 (d, *J* = 6.1 Hz, 3C) ppm.

^{31}P NMR ($CDCl_3$, 162 MHz): δ = 17.3 (s) ppm.

^{19}F NMR ($CDCl_3$, 470 MHz): δ = –153.6 ~ –153.7 (m) ppm.

^{11}B NMR ($CDCl_3$, 160 MHz): δ = –1.0 (s) ppm.

Preparation of pre-C(0) ***180***

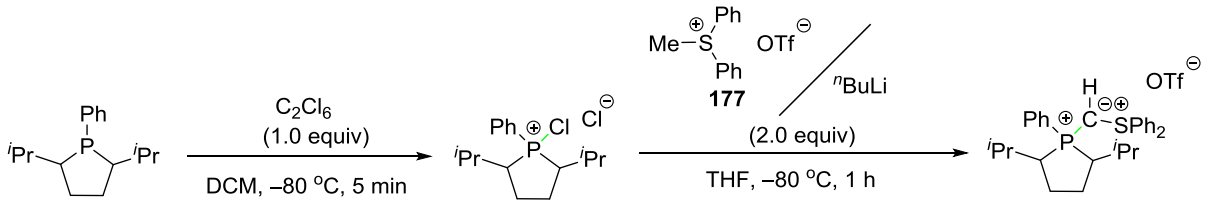

175 **176**: 76% **178**: 67%

Overall: 51%

Methyldiphenyl-1,1,1-sulfonium trifluoromethanesulfonate (179)[31]

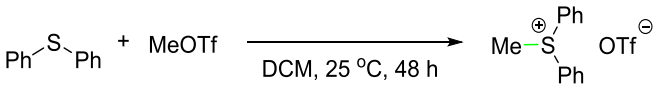

(1.0 equiv) **177**: 96%

Diphethyl sulfide (7.1 g, 3.80 mL, 76 mmol) was dissolved in DCM and methyl triflate (12.4 g, 76.0 mmol) was added dropwise under inert atmosphere. The mixture was stirred at 25 °C for 48 h. An aqueous solution of NaOH (1.25 M, 95 mL) was added and kept stirring for 12 h. The organic phase was extracted and the aqueous phase was washed with DCM (3 x 65 mL). The combined organic solution was dried over $MgSO_4$ and filtered at ambient pressure. The

solution was concentrated *in vacuo* to afford product **177** as a brown solid (12.8 g, 96.2%).

^{1}H NMR ($CDCl_3$, 500 MHz): δ = 3.66 (s, 3H), 7.58–7.61 (m, 4H), 7.64–7.67 (m, 2H), 7.90–7.92 (m, 4H) ppm.

^{13}C NMR ($CDCl_3$, 125 MHz): δ = 28.3, 120.8 (q, *J* = 320.6 Hz), 125.8 (2C), 129.9 (4C), 131.4 (4C), 134.4 (2C) ppm.

^{19}F NMR ($CDCl_3$, 470 MHz): δ = –78.3 (s) ppm.

2-Chloro-1,3-bis(1-methylethyl)-2-phenyl-1,3,2-diazaphospholidinium chloride (178)[31]

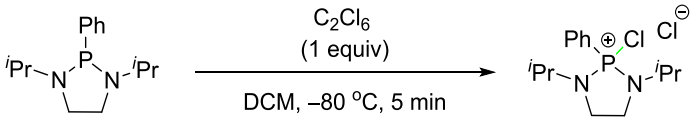

175 **176**: 76%

Hexachloroethane (5.40 g, 22.8 mmol, 1.00 equiv) was dissolved in EE (43 mL) and the mixture was cooled down to –78 °C under inert atmosphere. Solution of 1,3-bis(1-methylethyl)-2-phenyl-1,3,2 diazophospholidine **175** (5.70 g, 22.8 mmol) in diethyl ether (40 mL) was added dropwise. The mixture warmed slowly to the room temperature. The mixture was filtered and the volatiles were removed *in vacuo*. The residue was dissolved in DCE (20 mL) and EE (160 mL) was added to precipitate a brown solid. The suspension was filtered, the precipitate was washed with EE (3 x 10 mL) and dried *in vacuo* to afford product **176** as a brown solid (5.9 g, 80% yield).

^{1}H NMR ($CDCl_3$, 500 MHz): δ = 1.03–1.07 (m, 6H), 1.12–1.16 (m, 6H), 3.32–3.40 (m, 2H), 3.62–3.66 (m, 2H), 3.96–4.23 (m, 2H), 7.67–7.74 (m, 2H), 7.77–7.93 (m, 1H), 8.03–8.10 (m, 2H) ppm.

^{13}C NMR ($CDCl_3$, 125 MHz): δ = 20.46 (d, *J* = 2.3 Hz, 2C), 20.7 (d, *J* = 6.4 Hz, 2C), 42.3 (d, *J* = 9.3 Hz, 2C), 47.0 (d, *J* = 5.7 Hz, 2C), 121.5 (d, *J* = 154.0 Hz), 130.8 (d, *J* = 17.7 Hz, 2C), 134.0 (d, *J* = 14.4 Hz, 2C), 137.6 (d, *J* = 3.6 Hz) ppm.

^{31}P NMR ($CDCl_3$, 162 MHz): δ = 61.2 (s) ppm.

[1,3-bis(1-methylethyl)-2-phenyl-2λ5-1,3,2-diazaphospholidin-2-ylidene] methyl]diphenylsulfonium trifluoromethanesulfonate[31]

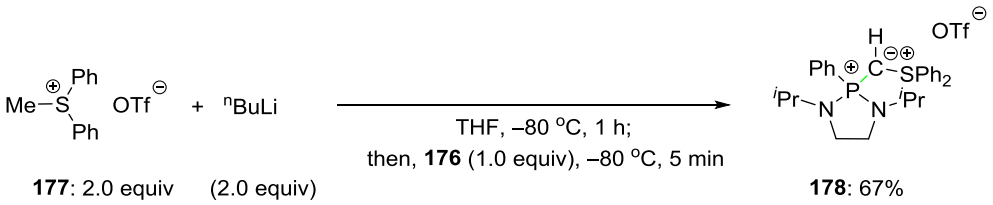

177: 2.0 equiv (2.0 equiv) **178**: 67%

Methyldiphenyl-1,1,1-sulfonium trifluoromethanesulfonate (**177**; 9.56 g, 27.3 mmol, 2.20 equiv) was dissolved in THF (83 mL) and the solution was cooled to –78 °C. *n*BuLi (17.1 mL, 27.3 mmol, 1.6 M in hexane, 2.20 equiv) was added dropwise and the mixture was stirred for 20 min at –78 °C. Solution of **176** (4.00 g, 12.4 mmol, 1.00 equiv) in THF (40 mL) was added dropwise and the solution was stirred at –78 °C for 5 min. The solvent was removed *in vacuo* to result in a brown gummy solid. The solid was washed with ether (2 x 75 mL), filtered, and the precipitate was dried *in vacuo* to afford product **178** as a colourless solid (5.90 g, 68.9 %).

^{1}H NMR ($CDCl_3$, 500 MHz): δ = 0.86 (d, *J* = 6.6 Hz, 6H), 0.92 (d, *J* = 6.6 Hz, 6H), 3.25–3.30 (m, 2H), 3.35–3.47 (m, 5H), 7.54–7.63 (m, 9H), 7.84–7.85 (m, 4H), 7.93–7.97 (m, 2H) ppm.

^{13}C NMR ($CDCl_3$, 125 MHz): δ = 14.2 (d, *J* = 158.4 Hz), 19.9 (d, *J* = 3.2 Hz), 20.9 (d, *J* = 4.5 Hz, 2C), 38.6 (d, *J* = 9.2 Hz, 2C), 44.3 (d, *J* = 6.5 Hz, 2C), 121.2 (q, *J* = 320 Hz), 127.5 (4C), 128.2 (d, *J* = 119.5 Hz), 129.6 (d, *J* = 13.1 Hz, 2C), 130.7 (4C), 132.1 (d, *J* = 10.7 Hz, 2C), 132.2 (2C), 133.7 (d, *J* = 2.9 Hz, 2C), 136.4 (d, *J* = 5.1 Hz, 2C) ppm.

^{31}P NMR ($CDCl_3$, 162 MHz): δ = 49.0 (s) ppm.

^{19}F NMR ($CDCl_3$, 470 MHz): δ = –78.0 ~ –78.1 (m) ppm.

Preparation of pre-C(0) ***172***

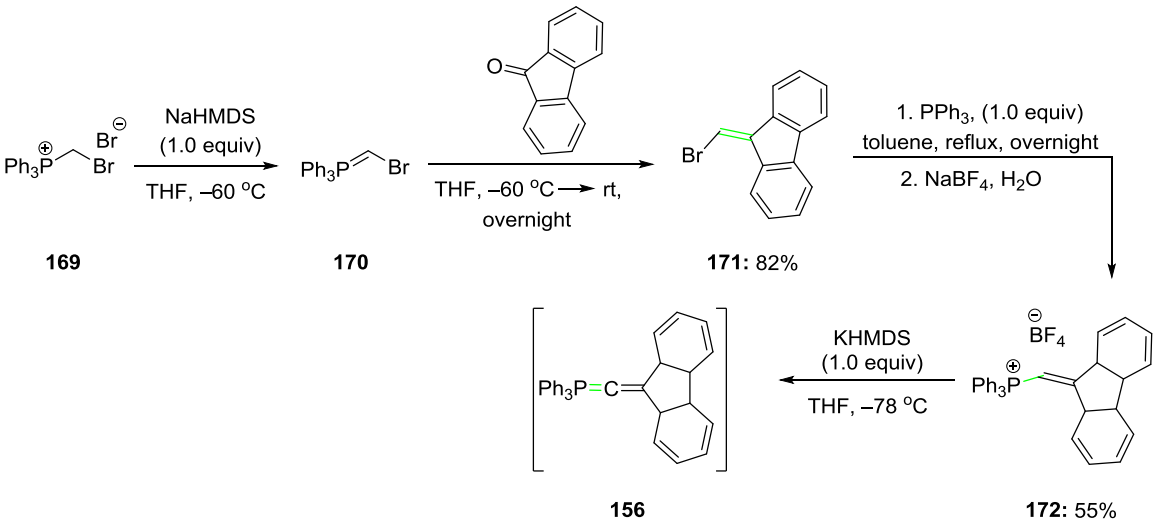

169 **170** **171:** 82% **156** **172:** 55%

(Bromomethyl)triphenylphosphonium bromide (170)[32]

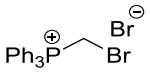

170

Triphenylphosphine (15.5 g, 59.0 mmol, 1.00 equiv) was dissolved in toluene (100 mL) and dibromomethane (133 mmol, 25.0 g, 2.25 equiv) was added dropwise in open air. The mixture was stirred and refluxed for 24 h. The formed suspension was filtered and the precipitate was washed with toluene (3 x 10 mL) to afford **170** as a colourless solid. The resulting solution was refluxed for other 24 h. Again, the suspension was filtered and the precipitate was washed with toluene (4 x 10 mL) to afford **170** as a colorless solid. The two batches were combined (7.70 g, 30% yield).

^{1}H NMR (400 MHz, $CDCl_3$): δ = 5.84 (d, *J* = 5.8 Hz, 2H), 7.74–7.87 (m, 9H) 7.97–8.02 (m, 6H) ppm.

^{31}P NMR (162 MHz, $CDCl_3$): δ = 24.0 (s) ppm.

9-Bromomethylene-9*H*-fluorene (171)[33]

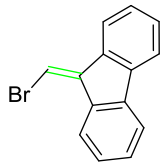

171

A suspension of **171** (10.2 g, 22.0 mmol, 1.00 equiv) in THF was prepared in a nitrogen glovebox. The suspension was cooled to –60° C under inert atmosphere and NaHMDS (23.4 mL, 1.0 M in THF, 23.4 mmol, 1.05 equiv) was added dropwise. After 40 min of stirring, a solution of fluorenone (3.8 g, 21.0 mmol) in THF (10 mL) was added to the yellow solution. The solution was warmed progressively to 25 °C and stirred overnight. After aqueous work-up and Et_2O extraction, the resulting organic solution was dried over $MgSO_4$, filtered at ambient pressure and the solvent was removed *in vacuo* to provide an orange solid. Filtration over silica gel using hexane as a solvent resulted in formation of a yellow solution. Volatiles were removed *in vacuo* to provide product **173** as a yellow solid (4.0 g, 75% yield).

^{1}H NMR ($CDCl_3$, 500 MHz): δ = 7.30 (td, *J* = 7.6, 0.9 Hz, 1H), 7.36–7.44 (m, 3H), 7.47 (td, *J* = 7.6, 0.9 Hz, 1H), 7.59 (d, *J* = 7.6 Hz, 1H), 7.70 (d, *J* = 7.6 Hz, 1H), 7.74 (d, *J* = 7.6 Hz, 1H), 8.61 (d, *J* = 7.6 Hz, 1H) ppm.

^{13}C NMR ($CDCl_3$, 125 MHz): δ = 105.8, 119.8, 119.9, 120.2, 125.7, 127.2, 127.3, 128.7, 129.5, 136.6, 138.4, 138.9, 139.2, 141.5 ppm.

(9*H*-fluoren-9-ylidenemethyl)triphenylphosphonium tetrafluroborate[34]

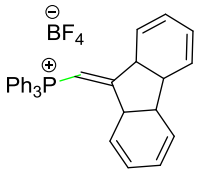

172

PPh_3 (0.82 g, 3.11 mmol, 1.00 equiv) was added to a solution of **171** (0.80 g, 3.11 mmol, 1.00 equiv) in toluene (40 mL) under nitrogen atmosphere and the resulting mixture was stirred at reflux temperature overnight. The precipitate was filtered off under nitrogen, washed with hexane and the volatiles were removed *in vacuo* to provide a bright yellow powder. A saturated aqueous solution of $NaBF_4$ (340 mg, 3.11 mmol, 1.00 equiv) was added to a solution of the salt in the minimum amount of H_2O/MeOH (10:1) to result in the immediate precipitation of a yellow solid. Then, the precipitate was extracted with DCM, dried over $MgSO_4$, filtered at ambient pressure and the solvent was removed *in vacuo* to provide product **172** as a yellow solid (0.55 g, 36%).

^{1}H NMR ($CDCl_3$, 500 MHz): δ = 6.59 (d, *J* = 7.6 Hz, 1H), 6.66 (td, *J* = 7.6, 1.0 Hz, 1H), 7.25–7.26 (m, 1H), 7.28–7.31 (m, 1H), 7.36 (td, *J* = 7.6, 1.0 Hz, 1H), 7.49–7.53 (m, 1H), 7.59–7.62 (m, 2H), 7.67–7.86 (m, 15H), 8.11 (d, *J* = 7.6 Hz, 1H) ppm.

^{13}C NMR ($CDCl_3$, 125 MHz): δ = 98.0 (d, *J* = 90.8 Hz), 118.2, 119.1, 120.3, 120.1, 124.1, 125.2, 127.3, 127.5, 128.2, 129.0, 131.0 (d, *J* = 13.1 Hz, 6C), 133.1 (d, *J* = 7.6 Hz, 3C), 137.6 (d, *J* = 10.8 Hz, 6C), 135.6 (d, *J* = 2.9 Hz, 3C), 137.5 (d, *J* = 18.2 Hz), 137.6 (d, J = 18.3 Hz), 140.7, 144.3, 161.4 ppm.

^{31}P NMR ($CDCl_3$, 162 MHz): δ = 14.2 (s) ppm.

^{19}F NMR ($CDCl_3$, 470 MHz): δ = –153.2 ~ –153.3 (m) ppm.

^{11}B NMR ($CDCl_3$, 160 MHz): δ = –1.0 (s) ppm.

*Preparation of the CDP **152**:*

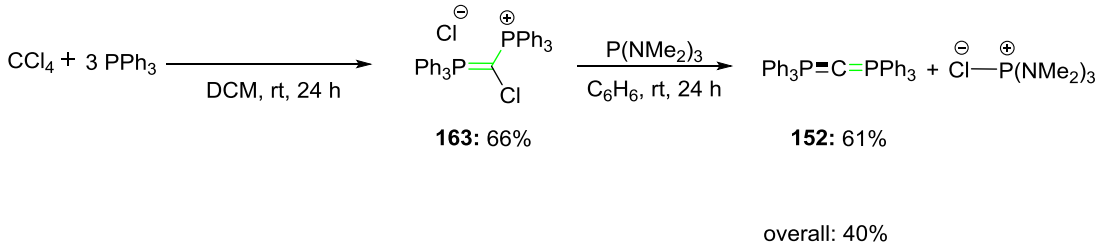

163: 66%

152: 61%

overall: 40%

[chloro(triphenylphosphoranylidene)methyl]triphenylphosphonium chloride[35]

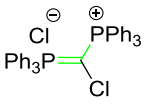

163

*The reaction was performed by Hanno Kossen

PPh_3 (26.3 g, 100 mmol, 1.50 equiv) was dissolved in DCM (50 mL) and carbon tetrachloride (6.43 mL, 66.7 mmol, 1.00 equiv) was added drop-wise at room temperature. The solution was stirred for 26 h where upon the solution changed colour from yellow to brown and colourless precipitate was formed. 1,2-epoxybutane (5.80 mL, 66.7 mmol, 1.00 equiv) was added slowly (temperature <20 °C) solubilizing colourless solid. EE (50 mL) was added drop-wise and the reaction mixture kept stirring for 20 min. The product was crystallized at 0 °C, filtered, washed with DCM (2 mL) and ether (2 mL). Finally, it was recrystallized from DCM (30 mL) and ether (10 mL) to generate light yellow crystals (13.3 g, 66%).

^{1}H NMR (C_6D_6): δ = 7.89–7.81 (m, 12H), 7.03–6.95 (m, 18H) ppm.
^{31}P NMR (C_6D_6): δ = 25.7 (s) ppm.

Carbodiphosphorane (CDP) [35]

$Ph_3P{=}C{=}PPh_3$

152

*The reaction was performed by Hanno Kossen

140 (1.6 g, 2.64 mmol, 1.00 equiv) was suspended to benzene (6 mL) and tris(dimethyl)aminophosphine (0.43 g, 2.64 mmol, 1.00 equiv) was added at ambient temperature. The reaction mixture left stirring for 1 h, and a bright yellow solution was formed. After 3 h, a colourless solid precipitated. The mixture was stirred for 24 h, and then it was refluxed. Then, while the mixture was hot, the colourless solid was filtered out, and the yellow solution was recrystallized to room temperature, washed with ether (2 mL) to give the bright yellow powder (1.32 g, 93%).

H NMR (C_6D_6): δ = 7.89–7.85 (m, 12H), 7.08–6.95 (m, 18H) ppm.
^{31}P NMR (C_6D_6): δ = –4.12 (s) ppm.

Preparation of the pre-C(0) ***159****:*

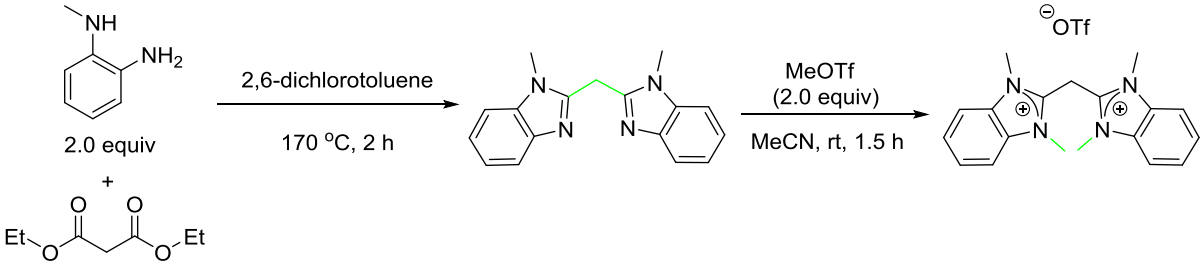

2,2'-methylenebis[1-methyl-1*H*-Benzimidazole[35]

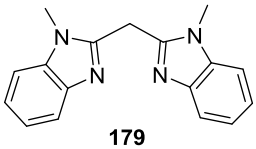

179

* The reaction was performed by Xun Lu.

To a 50-mL two-neck, round-bottomed flask fitted with Dean-Sttark apparatus and additional funnel was placed the *N*-methyl-1,2-phenylenediamine (1.20 g,

9.30 mmol, 2.00 equiv) in 2,6-dichlorotoluene (5 mL). The solution was heated to 170 °C, and then diethyl malonate (1.00 g, 4.60 mmol, 1.00 equiv) was added drop-wise to the reaction flask over 90 min. The temperature gradually increased to 185 °C during the addition process and maintained around 185 °C to 190 °C for 2 hours. The ending point of the reaction was monitored by ^{1}H NMR spectroscopy. The resulting mixture was cooled to ambient temperature. After filtration, the solid was washed with benzene (3 x 5 mL) and methanol (5 mL), and then dried *in vacuo* to afford product **179** as a pale beige solid (8.05 g, 70% yield).

^{1}H NMR ($CDCl_3$, 400 MHz): δ = 7.76–7.71 (m, 2H), 7.33–7.22 (m, 6H), 4.69 (s, 2H), 3.90 (s, 6H) ppm.

^{13}C NMR ($CDCl_3$, 100 MHz) δ = 149.8 (2C), 142.9 (2C), 136.7 (2C), 123.3 (2C), 122.7 (2C), 120.0 (2C), 109.9 (2C), 31.0, 29.1 (2C) ppm.

2,2'-methylenebis(1,3-methyl-benzimidazolium)trifluoromethanesulfonate[35]

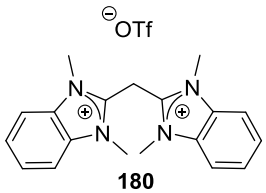

180

* The reaction was performed by Xun Lu.

In a 50-mL, two-necked, round-bottomed flask was placed **179** (3.00 g, 10.9 mmol, 1.00 equiv) in anhydrous acetonitrile (10.0 mL). Methyl trifluoromethansulfonate (4.00 mL, 35.3 mmol, 3.50 equiv) was added dropwise to the reaction flask. The resulting mixture was then stirred at room temperature for one hour and then EE (60.0 mL) was added to provide a white precipitate. The white precipitate was then washed with DCM (2 x 15 mL), and dried *in vacuo* to afford the product **180** as a colourless solid (1.22 g, 65% yield).

^{1}H NMR (CD_3CN, 400 MHz) δ = 7.85–7.80 (m, 8H), 5.44 (s, 2H), 3.97 (s, 12H) ppm.

^{13}C NMR (CD_3CN, 400 MHz): δ = 144.7 (2C), 133.5 (4C), 129.1 (4C), 126.5 (4C), 114.8 (q, *J* = 264.6 Hz), 34.2, 22.9 (4C) ppm.

2-[(1,3-dihydro-1,3-dimethyl-2*H*-benzimidazol-2-ylidene)methyl]-1,3-dimethyl-1*H*-Benzimidazolium trifluoromethanesulfonate[35]

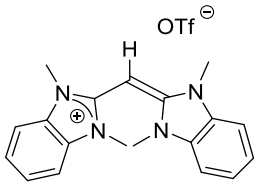

205

* The reaction was performed by Xun Lu.

In a 20-mL vial was placed Ag_2O (or KHMDS, or NaOMe, 1.00 equiv), **180** (0.50 g, 0.60 mmol, 1.00 equiv), and anhydrous dichloroethane (5 mL). The reaction mixture was stirred at room temperature for 6 hours. The reaction mixture was subsequently filtered and concentrated *in vacuo* to give product **205** as a colorless solid.

^{1}H NMR (CD_2Cl_2, 400 MHz): δ = 7.58–7.54 (m, 2H), 7.44–7.40 (m, 2H), 7.39–7.34 (m, 2H), 6.85–6.74 (m, 2H), 4.59 (s, 1H), 3.61 (s, 12H) ppm.

^{13}C NMR (CD_2Cl_2, 100 MHz): δ = 153.1, 140.2, 137.6 (2C), 134.2 (2C), 132.9 (2C), 130.1 (2C), 128.7 (2C), 126.4 (2C), 124.3, 112.5 (q, *J* = 262.8 Hz), 32.2 (4C) ppm.

Ag_2O, rt, 6 h, 20% yield; **KHMDS**, rt, 6 h, 60% yield; **NaOMe**, rt, 6 h, 90% yield.

Bis(1,3-methyl-benzimidazol-2-ylidene)methane[35]

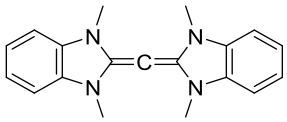

159

* The reaction was performed by Xun Lu.

In a 25-mL, round-bottomed flask was placed **205** (1.00 g, 1.50 mmol, 1.00 equiv) in anhydrous THF (5.00 mL). A solution of KHMDS (0.37 g, 1.82 mmol, 1.10 equiv) in THF (6.70 mL) was added dropwise to the reaction flask. The

reaction mixture was stirred at ambient temperature for 3 h and then filtered through celite. The filtrate was concentrated *in vacuo* and the residue was washed with EE, and then dried again *in vacuo* to provide product **205** as a yellow solid (0.64 g, 80% yield). *The obtained analytical data fit accurately with the reported data*.[35]

Mp: 150–152 °C.

^{1}H NMR (C_6D_6, 400 MHz): δ = 6.93–6.89 (m, 4H), 6.47–6.43 (m, 4H), 2.89 (s, 12H) ppm.

^{13}C NMR (C_6D_6, 100 MHz): δ = 144.8 (2C), 135.9 (4C), 132.4 (4C), 130.5 (4C), 110.2, 29.7 (4C) ppm.

2.7 Silylones or Si(0)

DIPP carbene has been prepared following a literature-reported method.[36]

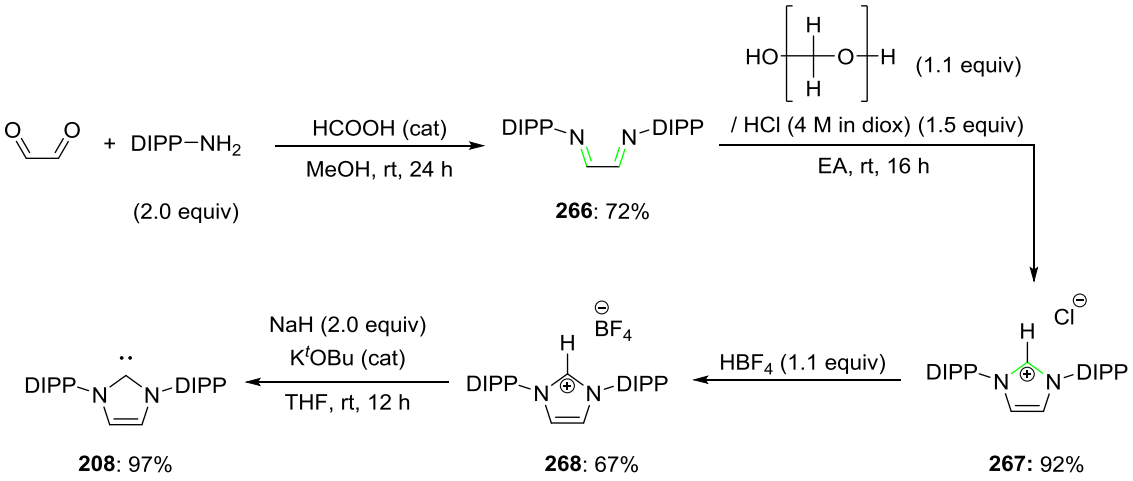

N,*N*'-1,2-ethanediylidenebis[2,6-bis(1-methylethyl)benzenamine]

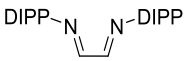

266

In a 250 mL round-bottomed flask, 1,3–diisopropylaniline (31.9 mL, 169.2 mmol, 2.00 equiv) was dissolved in methanol (85 mL) and the solution was stirred for 5 min. Then, glyoxal was added (9.7 mL, 84.6 mmol, 40% in water, 1.00 equiv) and a few drops of formic acid. After 10 min, yellow solid was precipitated. Additional methanol was added (85 mL) to facilitate stirring. The mixture was left stirring for 24 hours at room temperature. The suspension was filtered under pressure and the precipitate was washed with methanol (3 x 20 mL). The volatiles were removed *in vacuo* to afford product **266** as a yellow solid (23.0 g, 72%).

^{1}H NMR ($CDCl_3$, 500 MHz): δ = 1.25 (d, *J* = 6.8 Hz, 24H), 2.98 (sept, *J* = 6.8 Hz, 4H), 7.16–27 (m, 6H), 8.14 (s, 2H) ppm.

^{13}C NMR ($CDCl_3$, 100 MHz): δ = 23.4 (8C), 28.1 (4C), 123.2 (4C), 125.1 (2C), 136.7 (4C), 148.1 (2C), 163.1 (2C) ppm.

1,3-bis[2,6-bis(1-methylethyl)phenyl]-1*H*-Imidazolium chloride

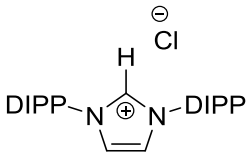

267

In a 100 mL round-bottomed flask, paraformaldehyde (2.1 g, 67.0 mmol, 1.10 equiv) and hydrogen chloride in dioxane (23 mL, 91.4 mmol, 4 M, 1.50 equiv) were added. The solution was stirred to fully dissolve the paraformaldehyde. Then, it was transferred to 150 mL addition funnel and added dropwise over an hour to 250 mL 3-necked round-bottomed flask, which contained **266** (23.0 g, 61.0 mmol, 1.00 equiv) dissolved in EA (122 mL). The solution turned brown and a precipitate appeared. The mixture was left stirring for 16 h. Then, it was filtered under ambient pressure and the precipitate was washed with EA (4 x 30 mL) and the volatiles were removed under reduced pressure to afford product **267** as a pink solid (23.9 g, 92% yield).

^{1}H NMR ($CDCl_3$, 500 MHz): δ = 1.24 (d, *J* = 6.8 Hz, 12H), 1.30 (d, *J* = 6.8 Hz, 12H), 2.43 (sept, *J* = 6.8 Hz, 4H), 7.37 (d, *J* = 7.8 Hz, 4H), 7.58–7.61 (m, 2H), 7.83 (d, *J* = 1.6 Hz, 2H), 8.72 (s, 1H).

1,3-bis[2,6-bis(1-methylethyl)phenyl]-1*H*-Imidazolium tetrafluoroborate

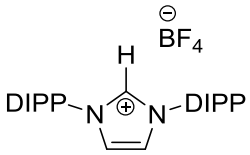

268

In a 2 L round-bottomed flask, **267** (23.9 g, 56.1 mmol, 1.00 equiv) was dissolved in water (700 mL). HBF_4 (8.06 mL, 61.7 mmol, 48% in water, 1.10 equiv) was added and the solution was stirred for 5 min. **268** was extracted with dichloromethane (3 x 20 mL) and the combined extracts were dried over $MgSO_4$. The solution was filtered at ambient pressure and the volatiles were removed *in vacuo*. The residue was purified by dissolution in DCM (150 mL) and precipitation by EE (70 mL). The precipitate was washed with EE (3 x 30

mL), filtered out and dried *in vacuo* to afford product **268** as a colourless powder (18.0 g, 67% yield).

^{1}H NMR ($CDCl_3$, 400 MHz): δ = 1.25 (d, *J* = 6.8 Hz, 12H), 1.32 (d, *J* = 6.8 Hz, 12H), 2.46 (sept, *J* = 6.8 Hz, 4H), 7.40 (d, *J* = 7.9 Hz, 2H), 7.61–7.64 (m, 2H) 7.85 (d, *J* = 1.6 Hz, 2H), 8.73 (s, 1H).

^{13}C NMR ($CDCl_3$, 100 MHz): δ = 23.9 (4C), 24.4 (4C), 29.2 (4C), 124.9 (2C), 126.6 (4C), 122.6 (2C), 132.4 (4C), 137.1 (2C), 145.1 ppm.

^{19}F NMR (CD_2Cl_2, 470 MHz): δ = –153.1 ~ –153.2 (m) ppm.

^{11}B NMR (CD_2Cl_2, 160 MHz): δ = –1.0 (s) ppm.

1,3-bis[2,6-bis(1-methylethyl)phenyl]-1*H*-Imidazolium

In a nitrogen glovebox, **268** (3.1 g, 6.5 mmol, 1.00 equiv) and THF (26 mL) were added in a 100 mL round-bottomed flask. Then, NaH (0.31 g, 13.0 mmol, 2.00 equiv) and KO^{t}Bu (using the tip of the spatula) were added and an empty balloon was attached immediately to the sealed system. The mixture was left stirring overnight at room temperature under inert atmosphere. The suspension was filtered under pressure and the volatiles were removed *in vacuo* to afford the product **208** as an off-white solid (2.38 g, 99% yield).

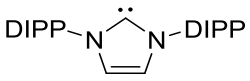

208

^{1}H NMR (C_6D_6, 600 MHz): δ = 1.30 (d, *J* = 6.9 Hz, 12H), 1.40 (d, *J* = 6.9 Hz, 12H), 3.08 (sept, *J* = 6.9 Hz, 4H), 6.74 (s, 2H), 7.30 (d, *J* = 7.7 Hz, 2H), 7.39–7.41 (m, 4H).

^{13}C NMR (C_6D_6, 150 MHz): δ = 26.0 (4C), 27.3 (4C), 31.2 (4C), 124.0 (2C), 126.1 (4C), 131.4 (2C), 141.4 (4C), 148.7 (2C), 223.1 ppm.

1,3-Bis[2,6-bis(1-methylethyl)phenyl]-1*H*-imidazolium-2-yl] dichlorosilylene[37]

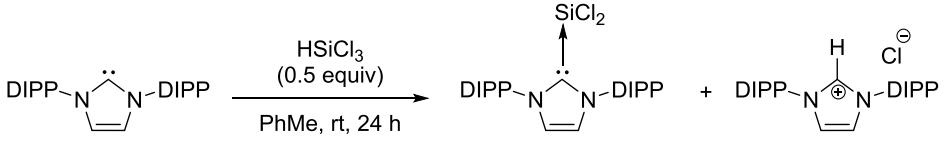

208 **251:** 79% **267**

208 (8.4 g, 21.6 mmol, 1.00 equiv) was dissolved in toluene (250 mL) and $HSiCl_3$ (1.46 g, 10.8 mmol, 0.50 equiv) was added at room temperature under inert atmosphere. The resulting light yellow suspension was left stirring at room temperature for 20 h. In a nitrogen atmosphere glovebox, the mixture was filtered, the precipitate washed with toluene (40 mL) and IPr•HCl regenerated (**267**). The yellow solution was concentrated *in vacuo* to afford **251** as a yellow powder (4.0 g, 76%).

^{1}H NMR (C_6D_6, 600 MHz): δ = 1.12 (d, *J* = 6.8 Hz, 12H), 1.54 (d, *J* = 6.8 Hz, 12H), 2.91 (sept, *J* = 6.8 Hz, 4H), 6.47 (s, 2H), 7.18 (d, *J* = 7.8 Hz, 2H), 7.32–7.34 (m, 4H) ppm.

Preparation of bis(NHC) ligand **256**[38]

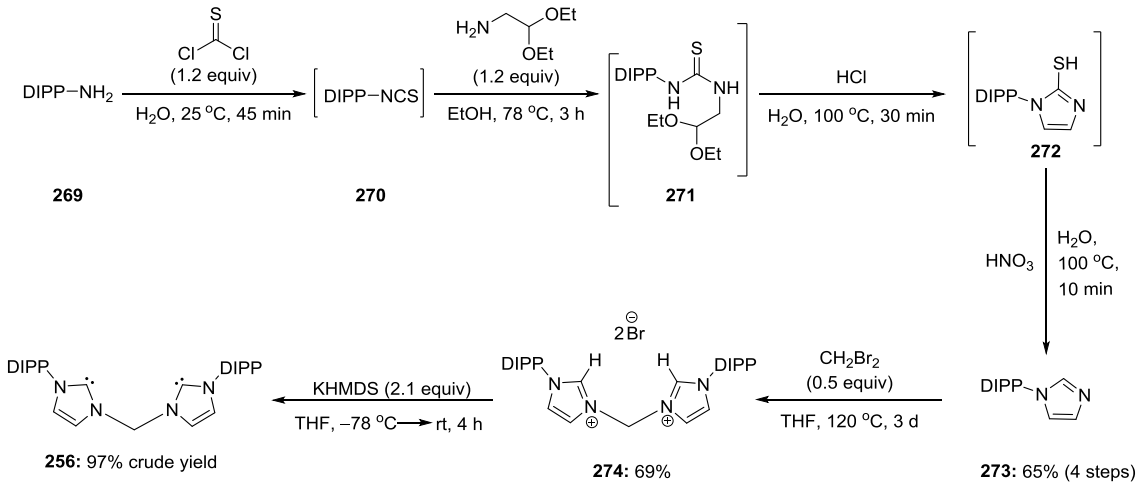

1-[2,6-bis(1-methylethyl)phenyl]-1*H*-imidazole[39]

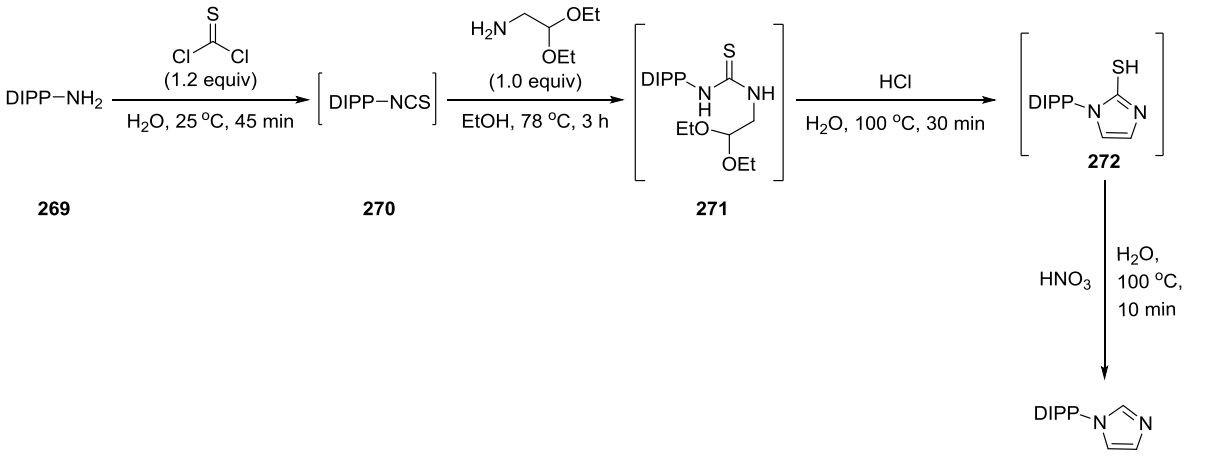

269 **270** **271** **272**

273: 65% (4 steps)

* The reaction was performed by Arseni Borisov under my direct supervision.

2,6-diisopropylaniline (**269**; 15.0 g, 89.6 mmol, 1.00 equiv) was added slowly over 30 min to a solution of thiophosgene (11.7 g, 101.5 mmol, 1.20 equiv) in H_2O (500 mL). After stirring for 45 min, 170 mL of EE were added and the organic layer was extracted. The volatiles were removed in *vacuo* and the crude isothiocyanate (**270**) was used for the next step without further purification. **270** (11.3 g, 89.6 mmol, 1.00 equiv) was added dropwise over 30 min to a solution of aminoacetaldehyde diethyl acetal dissolved in ethanol (170 mL). The mixture was refluxed and the progress of the reaction was monitored by TLC. The volatiles were removed in *vacuo* to give **271**. Aqueous solution of HCl (10%; 170 mL) was added and the mixture was refluxed for 30 min, filtered under ambient pressure to afford the crude mercaptoimidazole (**272**). Aqueous HNO_3 (20%) was added and the mixture was heated at 100 °C for 10 min. The organic phase was extracted with DCM (60 mL), dried over $MgSO_4$, filtered under ambient pressure and the volatiles were removed *in vacuo* to afford **273** as a colourless solid (12.6 g, 65%).

*Preparation of Si(0) compound **244:***[40]

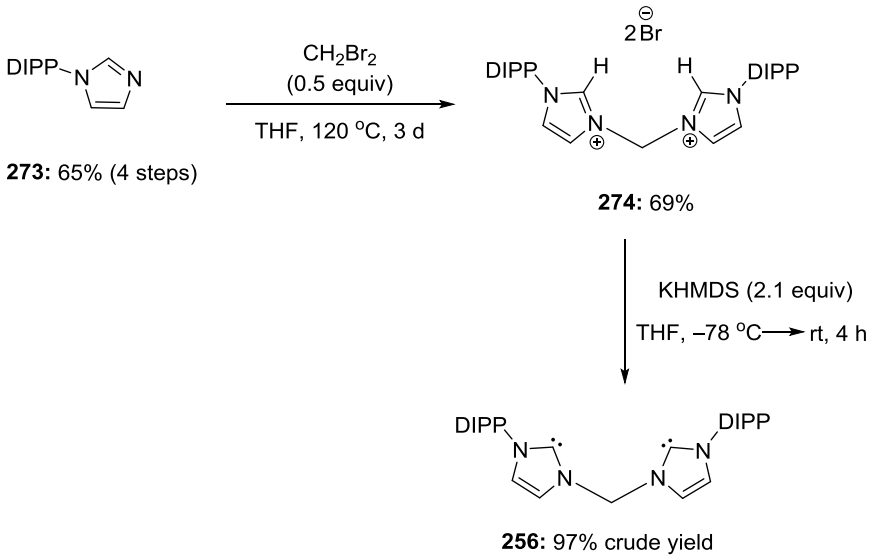

1,1´-methylene-3,3´-di-2,6-diisopropylphenylimidazolium dibromide[38]

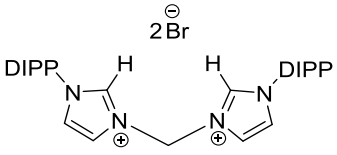

274

* The reaction was performed by Arseni Borisov under my direct supervision.

1-(2,6-Diisopropylphenyl)-*1H*-imidazole (**273**; 12.6 g, 55.0 mmol, 2.00 equiv) was suspended in THF (100 mL) in a steel bomb and dibromomethane (4.80 g, 27.5 mmol, 1.00 equiv) was added at room temperature. The solution was stirred at 120 °C for 3 days. The white precipitate was filtered out and washed with THF (3 x 15 mL). The volatiles were removed *in vacuo* to afford product **274** as a white powder (12.0 g, 69%).

^{1}H NMR ($CDCl_3$, 600 MHz): δ = 1.18 (d, *J* = 6.8 Hz, 12H), 1.24 (d, *J* = 6.8 Hz, 12H), 2.20 (sept, *J* = 6.8 Hz, 4H), 7.26 (br s, 2H), 7.35 (d, *J* = 7.9 Hz, 4H), 7.58–7.60 (m, 2H), 8.1 (s, 2H), 10.1 (t, *J* = 1.5 Hz, 2H), 11.5 (t, *J* = 1.5 Hz, 2H) ppm.

^{13}C NMR ($CDCl_3$, 125 MHz): δ = 24.0 (4C), 25.0 (4C), 29.0, 56.2 (4C), 124.7 (2C), 124.8 (2C), 125.0 (2C), 129.7 (2C), 132.5 (4C), 139.1 (2C), 144.8 (4C) ppm.

1,1´-methylene-3,3´-di-2,6-diisopropylphenylimidazole-2,2´-diylidene[38]

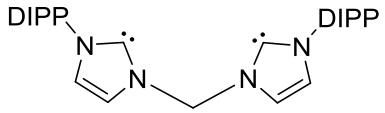

276

* The reaction was performed by Arseni Borisov under my direct supervision.

1,1´-methylene-3,3´-di-2,6-diisopropylphenylimidazolium dibromide (150 mg, 0.24 mmol, 1.00 equiv) was suspended in THF (1.5 mL) and cooled at –78 °C. A solution of KHMDS (104 mg, 0.52 mmol, 2.00 equiv) in THF (1.5 mL) was cannulated dropwise under inert atmosphere. The reaction mixture was stirred at –78 °C for 1 h, and progressively warmed to –30 °C. This temperature was maintained for 2 h and then, the mixture was warmed up slowly to room temperature. It was filtered over celite and the volatiles were removed *in vacuo* to afford product **276** as a colourless solid (108 mg, 97%).

^{1}H NMR (C_6D_6, 600 MHz): δ = 1.18 (d, *J* = 6.8 Hz, 12H), 1.35 (d, *J* = 6.8 Hz, 12H), 2.8 (sept, *J* = 6.8 Hz, 4H), 6.34 (s, 2H), 7.25 (s, 2H), 7.26–7.27 (m, 6H), 7.28 (d, *J* = 1.6 Hz, 2H), 7.38 (t, *J* = 7.7 Hz, 2H) ppm.

Preparation of Si(0) **244**:

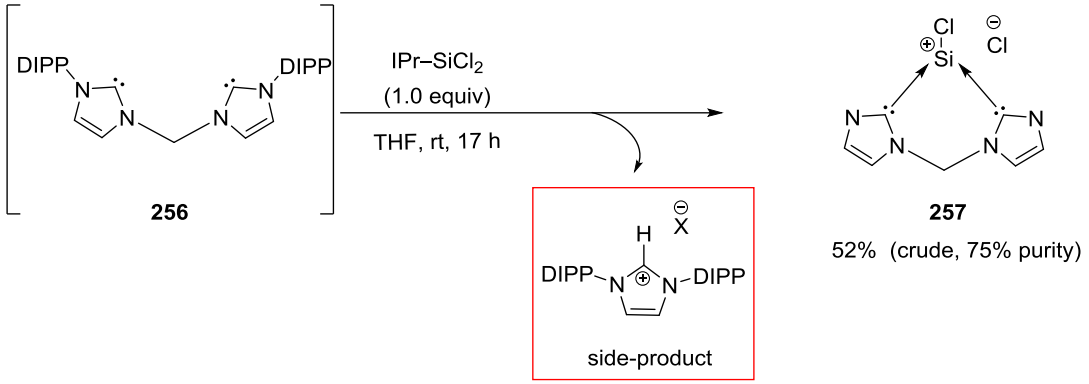

Chlorosilyliumylidene precursor **257**[40]

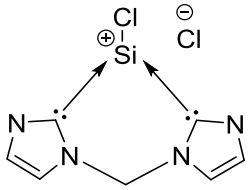

257

* The reaction was performed by Arseni Borisov under my direct supervision.

1,1´-methylene-3,3´-di-2,6-diisopropylphenylimidazolium dibromide (3.63 g, 5.7 mmol, 2.10 equiv) was suspended in THF (35 ml) and cooled down to −78 °C. A solution of KHMDS (2.39 g, 12.0 mmol, 2.10 equiv) in THF (33.0 mL) was cannulated to the mixture and the reaction mixture was stirred at –78 °C for 1 h, warmed up slowly to –30 °C, stirred for 30 min and warmed slowly to room temperature. This temperature was maintained for 2 h, and then the mixture was filtered over celite and the volume of the liquor was reduced to half. IPr·$SiCl_2$ (2.77 g, 5.7 mmol) was added and the mixture was stirred overnight at room temperature. The solution was filtered, the volatiles were removed *in vacuo* and **257** was obtained as a yellow solid (1.7 g, 52%, 75% purity based on ^{1}H NMR).

^{1}H NMR (C_6D_6, 600 MHz): δ = 1.09 (d, *J* = 6.8 Hz, 12H), 1.15 (d, *J* = 6.8 Hz, 12H), 2.42 (sept, *J* = 6.8 Hz, 4H), 7.07 (s, 2H), 7.28 (d, *J* = 7.9 Hz, 2H), 7.54–7.56 (m, 2H), 7.58 (d, *J* = 1.9 Hz, 2H), 8.25 (d, *J* = 1.9 Hz, 2H) ppm.

Preparation of Si(0) compound 244:

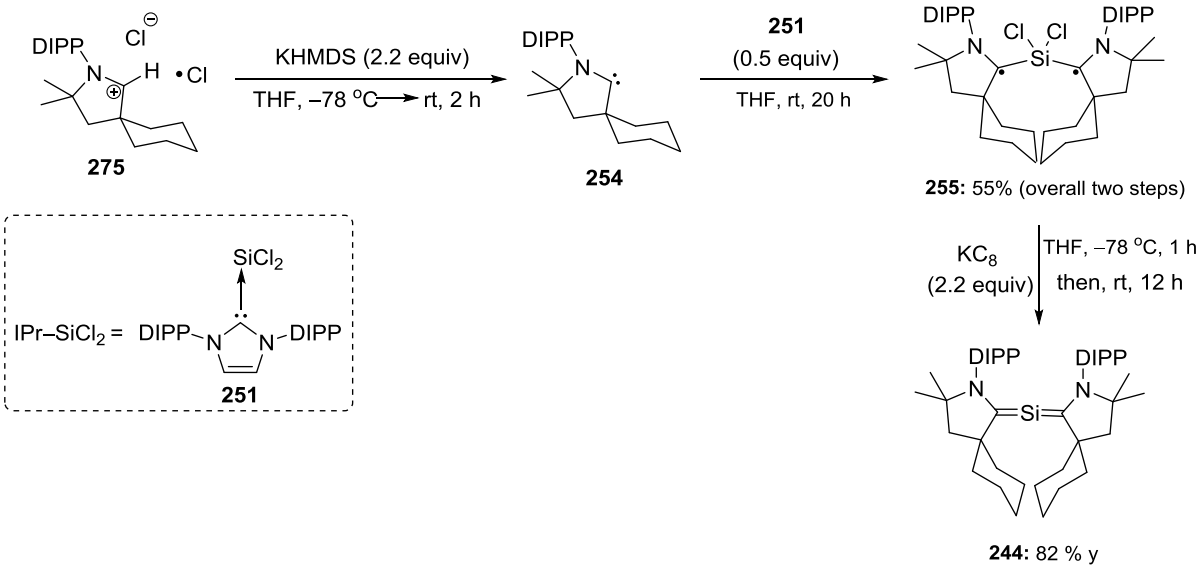

2-[2,6-bis(1-methylethyl)phenyl]-3,3-dimethyl-2-azoniaspiro[4.5]dec-1-ene chloride hydrogen chloride (275):

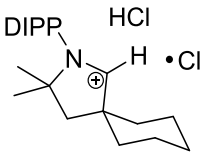

275

^{1}H NMR ($CDCl_3$, 400 MHz): δ = 1.26 (d, *J* = 6.8 Hz, 6H), 1.36 (d, *J* = 6.8 Hz, 6H), 1.41–1.50 (m, 3H), 1.52–1.70 (m, 7H), 1.72–1.75 (m, 3H), 1.90–1.94 (m, 2H), 2.46 (s, 2H), 2.49–2.55 (m, 2H), 2.67 (sept, *J* = 6.5 Hz, 2H), 7.35 (d, *J* = 7.8 Hz, 2H), 7.51–7.54 (m, 1H), 10.28 (br s, 1H), 10.47 (s, 1H) ppm.

^{13}C NMR ($CDCl_3$, 100 MHz): δ = 21.2, 22.1 (4C), 24.1, 26.7 (2C), 28.9 (2C), 29.9 (2C), 33.6, 45.5, 53.4, 82.7, 125.3 (2C), 128.8, 131.8 (2C), 144.4, 192.8 ppm.

1,1'-(dichlorosilylene)bis[2-[2,6-bis(1-methylethyl)phenyl]-3,3-dimethyl-2-azaspiro[4.5]dec-1-yl[41]

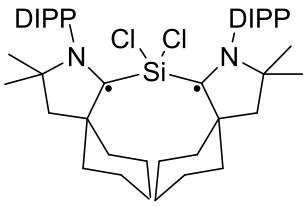

255

CAAC·2HCl (2.3 g, 5.75 mmol, 1.00 equiv) was suspended in THF (28 mL) and cooled to –78 °C. KHMDS (2.3 g, 11.5 mmol, 2.00 equiv) in THF (10 mL) cooled to –78 °C was cannulated slowly under inert atmosphere to the suspension. The mixture was left stirring for 10 min at –78 °C, warmed up to room temperature over 30 min and kept stirring at room temperature for 1 h. The mixture was filtered over celite, concentrated *in vacuo* and dissolved again in THF (5 mL). IPr•$SiCl_2$ (1.13 g, 11.5 mmol) in THF (4.5 mL) was added to the solution causing an instant colour change to royal blue suspension. The suspension was left stirring for 20 h, filtered and dried under vacuum affording a royal blue solid (800 mg, 54% y).

^{1}H NMR (C_6D_6, 500 MHz): δ = 0.78 (s, 6H), 1.17 (d, *J* = 6.6 Hz, 6H), 1.35–1.39 (m, 24H), 1.40 (d, *J* = 6.6 Hz, 6H), 1.62–1.89 (m, 10H), 2.00–2.02 (m, 2H), 2.07–2.11 (m, 2H), 2.41–2.47 (m, 2H), 2.50–2.53 (m, 2H), 3.56 (sept, *J* = 6.6 Hz, 2H), 3.75 (sept, *J* = 6.6 Hz, 2H), 7.05–7.11 (m, 6H) ppm.

1,1'-Silanetetraylbis[2-[2,6-bis(1-methylethyl)phenyl]-3,3-dimethyl-2-aza-spiro[4.5]decane[42]

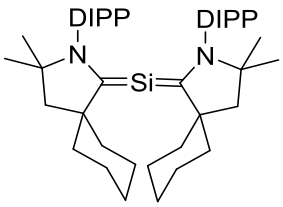

243

A mixture of **255** (760 mg, 0.93 mmol, 1.00 equiv) and KC_8 (325 mg, 2.33 mmol, 2.50 equiv) was cooled to –78 °C under inert atmosphere. THF (10 mL) cooled to –78 °C was cannulated into the mixture. The mixture was left stirring initially at –78 °C for 15 min, warmed up to room temperature and kept stirring overnight, filtered and the solution was concentrated *in vacuo* to afford **243** as a royal blue solid (520 mg, 82% y).

^{1}H NMR (C_6D_6, 500 MHz): δ = 1.01–1.02 (m, 12H), 1.17 (s, 6H), 1.23 (d, *J* = 6.6 Hz, 6H), 1.32 (d, *J* = 6.6 Hz, 8H), 1.49–1.57 (m, 12H), 1.69–1.78 (m, 6H), 1.82–1.90 (m, 4H), 2.19 (d, *J* = 12.9 Hz, 2H), 2.54 (td, *J* = 13.8, 13.2, 4.0 Hz, 2H), 2.68 (sept, *J* = 6.8 Hz, 2H), 2.90–2.93 (m, 2H), 3.18 (sept, *J* = 6.8 Hz, 2H), 7.09–7.10 (m, 2H), 7.17–7.21 (m, 4H).

^{13}C NMR (C_6D_6, 125 MHz): δ = 23.6, 24.4, 24.5, 25.2, 25.3, 27.6, 28.0, 28.4, 29.6, 30.2, 30.3, 35.6, 44.0, 50.2, 53.5, 68.8, 125.0, 126.0, 136.5, 148.5, 148.8, 210.0 ppm.

^{29}Si NMR (C_6D_6, 100 MHz): δ = 71.4 (s) ppm.

Allyl-9-BBN[43]

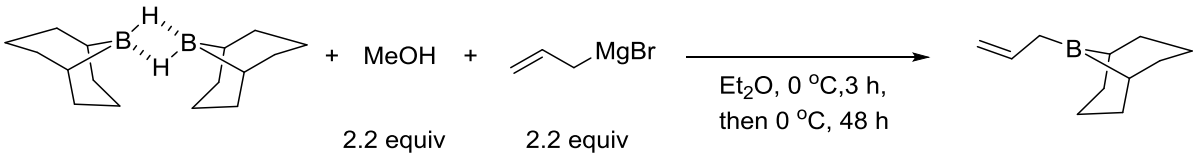

* The reaction was performed by Arseni Borisov under direct my supervision.

$[H–B(9\text{-bbn})]_2$ (732 mg, 3.00 mmol, 1.00 equiv) was suspended in EE (6.0 mL) and cooled to 0 °C. Dry methanol (267 µL, 6.60 mmol, 2.20 equiv) was added slowly and the solution was stirred firstly for 3 h at 0 °C and then warmed slowly to room temperature and stirred for 48 h. Allylmagnesium bromide (6.60 mmol, 1.0 M in Et_2O, 2.20 equiv) was added at 0 °C. After stirring for 1 h at 0 °C, the solvent was removed *in vacuo*. The residue was extracted with hexane to afford allyl-9-BBN confirmed by treatment with acetophenone (32%, 0.32 M).

^{1}H NMR (C_6D_6, 600 MHz): δ = 1.60–2.10 (m, 16H), 4.30–5.40 (m, 2H), 6.00 (m, 1H) ppm.

^{11}B NMR (C_6D_6, 160 MHz): δ = 86.0 ppm.

Reactivity Studies

1,4-Conjugate Addition

Benzoin Condensation

To a Young tube in a nitrogen atmosphere glovebox were added silylone **243** (13.6 mg, 20 μmol) dissolved in C_6D_6 (0.5 mL) and benzaldehyde (10.6 mg, 100 μmol). ^1H NMR spectroscopy of the reaction mixture disclosed no product formation.

* The reaction was performed by Arseni Borisov under my direct supervision.

Stetter Reaction

To a Young tube in a nitrogen atmosphere glovebox were added silylone **243** (13.6 mg, 20 μmol) dissolved in C_6D_6 (0.5 ml), benzaldehyde (10.6 mg, 100 μmol) and methyl vinyl ketone (7.0 mg, 100 μmol). ^1H NMR spectroscopy of the reaction mixture disclosed no product formation.

* The reaction was performed by Arseni Borisov under my direct supervision.

Interaction of (CAAC)Si with BH_3 SMe_2

To a Young tube in a nitrogen atmosphere glovebox were added silylone **243** (13.6 mg, 0.02 mmol, 1.00 equiv) and BH_3•SMe_2 (1.8 mg, 0.02 mmol, 1.00 equiv) in C_6D_6 (600 μL). The reaction mixture left stirring at 40 ^oC for 72 h and ^{11}B NMR spectroscopic analysis was obtained. An additional equivalent of BH_3•SMe_2 was added and the reaction mixture was heated at 60 ^oC for 24 h and ^{11}B NMR spectroscopic analysis was obtained again.

* The reaction was performed by Arseni Borisov under my direct supervision.

Interaction with Benzyl–B(9-bbn) and benzylation attempts of electrophiles.

To a Young tube in a nitrogen atmosphere glovebox were added silylone **243** (13.6 mg, 0.02 mmol) and benzyl–B(9-bbn) (0.024 mmol, 0.5 M in THF) in C_6D_6. The reaction mixture was stirred for 5 min and ^1H, ^{11}B NMR spectroscopic analysis were obtained.

* The reaction was performed by Arseni Borisov under my direct supervision.

Benzyl group transfer onto benzaldehyde

To a Young tube with a magnetic stirring bar in a nitrogen atmosphere glovebox were added silylone **243** (13.6 mg, 0.02 mmol), benzyl-B(9-bbn) (0.1 mmol, 0.5 M in THF) and benzaldehyde (10.6 mg, 0.1 mmol). The reaction mixture left stirring for 24 h and ^{1}H, ^{11}B NMR spectroscopic analyses were obtained. Then, it was heated to 40 ^{o}C for 5 h and ^{1}H, ^{11}B NMR spectroscopic analysis were obtained.

* The reaction was performed by Arseni Borisov under my direct supervision.

Benzyl group transfer onto chlorosuccinimide

To a Young tube with a magnetic stirring bar in a nitrogen atmosphere glovebox were added silylone **243** (13.6 mg, 0.02 mmol), benzyl–B(9-bbn) (0.1 mmol, 0.5 M in THF) and *N*-chlorosuccinimide (13.4 mg, 0.1 mmol). The reaction mixture left stirring for 22 h at 25 ^{o}C and ^{1}H, ^{11}B NMR spectroscopic analysis were obtained.

* The reaction was performed by Arseni Borisov under my direct supervision.

Allyl group transfer onto various electrophiles

To a Young tube in a nitrogen atmosphere glovebox were added silylone **243** (6.8 mg, 0.01 mmol), allyl-B(9-bbn) (0.01 mmol, 0.32 M in hexane) and an electrophile (0.01 mmol) in C_6D_6. The reaction mixture left stirring for 72 h at 25 ^{o}C. ^{1}H, ^{11}B NMR spectroscopic analysis were obtained.

* The reaction was performed by Arseni Borisov under my direct supervision.

Hydrosilylation

To a Young tube with a magnetic stirring bar in a nitrogen atmosphere glovebox were added silylone **243** (6.8 mg, 0.01 mmol), TfO-9BBN (0.01 mmol, 0.5 M in hexane) in C_6D_6. After stirring for 5 min, a ketone (0.1 mmol) and trichlorosilane (11.6 mg, 0.1 mmol) were added consecutively. The reaction mixture left stirring for 72 h at 25 ^oC. ^1H, ^{11}B NMR spectroscopic analysis were obtained.

* The reaction was performed by Arseni Borisov under my direct supervision.

Diels-Alder

To a Young tube with a magnetic stirring bar in a nitrogen atmosphere glovebox were added silylone **243** (3.4 mg, 5.0 μmol), TfO-9BBN (5.0 μmol mmol, 0.5 M in hexane) in C_6D_6. After stirring for 5 min, 1,3-cyclohexadiene (4 mg, 0.05 mmol) and methyl vinyl ketone (3.5 mg, 0. 05 mmol) were added consecutively. The reaction mixture left stirring for 4 h at 25 ^oC. ^1H, ^{11}B NMR spectroscopic analysis were obtained.

* The reaction was performed by Arseni Borisov under my direct supervision.

Frustrated Lewis Pair

To a Young tube with a magnetic stirring bar in a nitrogen atmosphere glovebox were added silylone **243** (6.8 mg, 0.01 mmol) and tris(pentafluorophenyl)borane (5.1 mg, 0.01 mmol) at –78 ^oC. After stirring for 5 min, either isobutylene oxide (1.1 μL, 0.012 mmol, 1.20 equiv) was added in toluene (0.5 mL); or THF (0.5 mL) was added; or toluene was added (0.5 mL) and hydrogen (1 atm) was flushed. The reaction mixture was warmed up to room temperature progressively and left stirring overnight. ^1H, ^{11}B NMR spectroscopic analysis were obtained.

* The reaction was performed by Arseni Borisov under my direct supervision.

Crystal Structure of 243

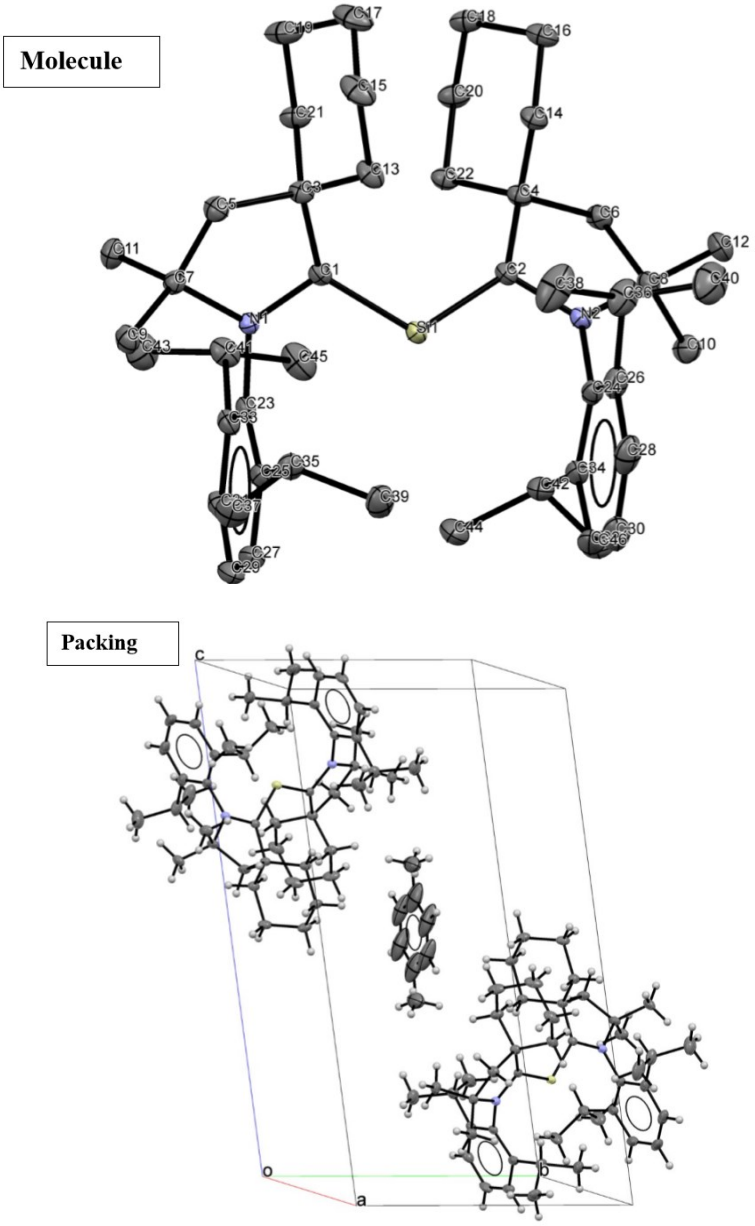

Figure 1. The molecular structure of us4001. Displacement ellipsoids are at the 50% probability level and H atoms are omitted.

Table 1. Crystal data and structure refinement for us4001.

Identification code	us4001
Empirical formula	C99 H148 N4 Si2
Formula weight	1450.39

Temperature	120 K	
Wavelength	0.71073 Å	
Crystal system	Triclinic	
Space group	P -1	
Unit cell dimensions	a = 9.41196(13) Å	α= 96.6331(13)°.
	b = 11.96367(18) Å	β= 99.1542(12)°.
	c = 19.8479(3) Å	γ = 96.0946(12)°.
Volume	2173.92(6) $Å^3$	
Z	1	
Density (calculated)	1.108 Mg/m^3	
Absorption coefficient	0.089 mm^{-1}	
F(000)	798	
Crystal size	0.4817 x 0.2852 x 0.1672 mm^3	
Theta range for data collection	2.884 to 31.216°.	
Index ranges	-13<=h<=13, -17<=k<=17, -28<=l<=28	
Reflections collected	186376	
Independent reflections	13498 [R(int) = 0.0655]	
Completeness to theta = 26.000°	99.8 %	
Absorption correction	Semi-empirical from equivalents	
Max. and min. transmission	1.00000 and 0.64320	
Refinement method	Full-matrix least-squares on F^2	
Data / restraints / parameters	13498 / 11 / 491	
Goodness-of-fit on F^2	1.093	
Final R indices [I>2sigma(I)]	R1 = 0.0576, wR2 = 0.1257	

R indices (all data)	R1 = 0.0691, wR2 = 0.1309
Extinction coefficient	n/a
Largest diff. peak and hole	0.889 and -0.546 e.Å^{-3}

Table 2. Atomic coordinates (x 10^4) and equivalent isotropic displacement parameters ($Å^2$x 10^3) for us4001. U(eq) is defined as one third of the trace of the orthogonalized U^{ij} tensor.

	x	y	z	U(eq)
Si(1)	7361(1)	8494(1)	2277(1)	14(1)
N(1)	7683(1)	6288(1)	1887(1)	13(1)
N(2)	7018(1)	10604(1)	2852(1)	14(1)
C(1)	7999(1)	7124(1)	2444(1)	13(1)
C(2)	7154(1)	9522(1)	3011(1)	13(1)
C(3)	9184(1)	6753(1)	2968(1)	14(1)
C(4)	6716(1)	9471(1)	3720(1)	14(1)
C(5)	9647(1)	5703(1)	2568(1)	18(1)
C(6)	5917(2)	10528(1)	3822(1)	18(1)
C(7)	8417(1)	5251(1)	1965(1)	15(1)
C(8)	6444(1)	11373(1)	3362(1)	17(1)
C(9)	9016(2)	4815(1)	1327(1)	19(1)
C(10)	5198(2)	11960(1)	3035(1)	22(1)
C(11)	7362(2)	4291(1)	2127(1)	21(1)
C(12)	7632(2)	12311(1)	3749(1)	24(1)
C(13)	10464(1)	7704(1)	3186(1)	19(1)
C(14)	8100(1)	9562(1)	4274(1)	17(1)
C(15)	11641(2)	7412(1)	3736(1)	27(1)
C(16)	7775(2)	9443(1)	4998(1)	21(1)

C(17)	11029(2)	7127(2)	4368(1)	31(1)
C(18)	6790(2)	8343(1)	4999(1)	21(1)
C(19)	9774(2)	6167(2)	4174(1)	29(1)
C(20)	5397(1)	8272(1)	4473(1)	19(1)
C(21)	8592(1)	6449(1)	3614(1)	19(1)
C(22)	5713(1)	8379(1)	3747(1)	15(1)
C(23)	6677(1)	6388(1)	1272(1)	14(1)
C(24)	7462(1)	10972(1)	2243(1)	16(1)
C(25)	7226(2)	6793(1)	710(1)	17(1)
C(26)	8941(2)	11357(1)	2257(1)	21(1)
C(27)	6244(2)	6809(1)	105(1)	22(1)
C(28)	9352(2)	11719(1)	1662(1)	29(1)
C(29)	4778(2)	6474(1)	55(1)	25(1)
C(30)	8351(2)	11697(1)	1073(1)	32(1)
C(31)	4248(2)	6135(1)	619(1)	22(1)
C(32)	6917(2)	11293(1)	1059(1)	28(1)
C(33)	5174(1)	6096(1)	1240(1)	17(1)
C(34)	6436(2)	10901(1)	1631(1)	20(1)
C(35)	8798(2)	7270(1)	733(1)	20(1)
C(36)	10124(2)	11322(1)	2869(1)	27(1)
C(37)	9474(2)	6653(1)	161(1)	30(1)
C(38)	11147(2)	10470(2)	2680(1)	40(1)
C(39)	8942(2)	8545(1)	670(1)	28(1)
C(40)	10995(2)	12493(2)	3140(1)	40(1)

C(41)	4497(1)	5827(1)	1859(1)	20(1)
C(42)	4867(2)	10355(1)	1539(1)	23(1)
C(43)	3565(2)	4662(1)	1730(1)	30(1)
C(44)	4581(2)	9306(1)	985(1)	32(1)
C(45)	3573(2)	6759(1)	2055(1)	28(1)
C(46)	3783(2)	11180(1)	1326(1)	33(1)
C(50)	6447(3)	5078(2)	5313(2)	92(1)
C(51)	6089(3)	5011(2)	4631(2)	80(1)
C(52)	4658(4)	4926(2)	4306(2)	86(1)
C(53)	4372(7)	4948(4)	3645(2)	60(1)
C(50')	6447(3)	5078(2)	5313(2)	92(1)
C(51')	6089(3)	5011(2)	4631(2)	80(1)
C(52')	4658(4)	4926(2)	4306(2)	86(1)

Table 3. Bond lengths [Å] and angles [°] for us4001.

Si(1)-C(1)	1.8519(12)
Si(1)-C(2)	1.8439(12)
N(1)-C(1)	1.3743(15)
N(1)-C(7)	1.4941(15)
N(1)-C(23)	1.4453(15)
N(2)-C(2)	1.3809(15)
N(2)-C(8)	1.4926(15)
N(2)-C(24)	1.4418(15)
C(1)-C(3)	1.5370(17)
C(2)-C(4)	1.5351(16)
C(3)-C(5)	1.5467(17)
C(3)-C(13)	1.5378(17)
C(3)-C(21)	1.5437(17)
C(4)-C(6)	1.5479(17)
C(4)-C(14)	1.5495(17)
C(4)-C(22)	1.5395(17)
C(5)-C(7)	1.5304(18)
C(6)-C(8)	1.5340(18)
C(7)-C(9)	1.5266(17)
C(7)-C(11)	1.5346(18)
C(8)-C(10)	1.5256(18)
C(8)-C(12)	1.5362(19)

C(13)-C(15)	1.5260(19)
C(14)-C(16)	1.5353(17)
C(15)-C(17)	1.520(2)
C(16)-C(18)	1.527(2)
C(17)-C(19)	1.525(2)
C(18)-C(20)	1.5283(18)
C(19)-C(21)	1.5359(19)
C(20)-C(22)	1.5330(17)
C(23)-C(25)	1.4152(17)
C(23)-C(33)	1.4092(17)
C(24)-C(26)	1.4131(19)
C(24)-C(34)	1.4129(18)
C(25)-C(27)	1.3969(18)
C(25)-C(35)	1.5203(19)
C(26)-C(28)	1.3992(19)
C(26)-C(36)	1.520(2)
C(27)-C(29)	1.380(2)
C(28)-C(30)	1.375(3)
C(29)-C(31)	1.381(2)
C(30)-C(32)	1.379(2)
C(31)-C(33)	1.3993(18)
C(32)-C(34)	1.3999(19)
C(33)-C(41)	1.5228(18)
C(34)-C(42)	1.524(2)

C(35)-C(37)	1.5412(19)
C(35)-C(39)	1.5389(19)
C(36)-C(38)	1.531(2)
C(36)-C(40)	1.537(2)
C(41)-C(43)	1.537(2)
C(41)-C(45)	1.538(2)
C(42)-C(44)	1.540(2)
C(42)-C(46)	1.539(2)
C(50)-C(51)	1.332(5)
C(50)-C(52)#1	1.380(4)
C(51)-C(52)	1.385(4)
C(52)-C(50)#1	1.380(4)
C(52)-C(53)	1.302(5)

C(2)-Si(1)-C(1)	119.17(5)
C(1)-N(1)-C(7)	115.54(10)
C(1)-N(1)-C(23)	122.44(10)
C(23)-N(1)-C(7)	122.00(9)
C(2)-N(2)-C(8)	116.02(10)
C(2)-N(2)-C(24)	121.47(10)
C(24)-N(2)-C(8)	122.47(10)
N(1)-C(1)-Si(1)	114.50(8)
N(1)-C(1)-C(3)	107.20(10)
C(3)-C(1)-Si(1)	135.20(9)

N(2)-C(2)-Si(1)	114.34(8)
N(2)-C(2)-C(4)	106.99(9)
C(4)-C(2)-Si(1)	136.60(9)
C(1)-C(3)-C(5)	103.80(9)
C(1)-C(3)-C(13)	110.30(10)
C(1)-C(3)-C(21)	111.36(10)
C(13)-C(3)-C(5)	110.96(10)
C(13)-C(3)-C(21)	109.01(10)
C(21)-C(3)-C(5)	111.36(11)
C(2)-C(4)-C(6)	103.22(9)
C(2)-C(4)-C(14)	109.32(10)
C(2)-C(4)-C(22)	112.64(10)
C(6)-C(4)-C(14)	111.01(10)
C(22)-C(4)-C(6)	110.85(10)
C(22)-C(4)-C(14)	109.67(10)
C(7)-C(5)-C(3)	107.41(10)
C(8)-C(6)-C(4)	107.69(10)
N(1)-C(7)-C(5)	100.82(9)
N(1)-C(7)-C(9)	113.40(10)
N(1)-C(7)-C(11)	110.35(10)
C(5)-C(7)-C(11)	113.05(11)
C(9)-C(7)-C(5)	111.01(10)
C(9)-C(7)-C(11)	108.17(10)
N(2)-C(8)-C(6)	100.83(10)

N(2)-C(8)-C(10)	113.21(10)
N(2)-C(8)-C(12)	111.33(11)
C(6)-C(8)-C(12)	113.50(11)
C(10)-C(8)-C(6)	111.07(11)
C(10)-C(8)-C(12)	107.00(11)
C(15)-C(13)-C(3)	112.78(12)
C(16)-C(14)-C(4)	113.38(10)
C(17)-C(15)-C(13)	111.32(12)
C(18)-C(16)-C(14)	111.20(11)
C(15)-C(17)-C(19)	110.92(12)
C(16)-C(18)-C(20)	110.61(11)
C(17)-C(19)-C(21)	111.31(13)
C(18)-C(20)-C(22)	111.92(10)
C(19)-C(21)-C(3)	112.84(11)
C(20)-C(22)-C(4)	112.64(10)
C(25)-C(23)-N(1)	118.87(11)
C(33)-C(23)-N(1)	120.30(11)
C(33)-C(23)-C(25)	120.83(11)
C(26)-C(24)-N(2)	119.20(12)
C(34)-C(24)-N(2)	120.02(12)
C(34)-C(24)-C(26)	120.73(12)
C(23)-C(25)-C(35)	124.28(11)
C(27)-C(25)-C(23)	117.82(12)
C(27)-C(25)-C(35)	117.82(12)

C(24)-C(26)-C(36)	123.27(12)
C(28)-C(26)-C(24)	118.47(14)
C(28)-C(26)-C(36)	118.12(13)
C(29)-C(27)-C(25)	121.83(13)
C(30)-C(28)-C(26)	121.20(15)
C(27)-C(29)-C(31)	119.68(12)
C(28)-C(30)-C(32)	119.93(13)
C(29)-C(31)-C(33)	121.29(13)
C(30)-C(32)-C(34)	121.80(15)
C(23)-C(33)-C(41)	123.33(11)
C(31)-C(33)-C(23)	118.35(12)
C(31)-C(33)-C(41)	118.16(12)
C(24)-C(34)-C(42)	124.44(12)
C(32)-C(34)-C(24)	117.75(13)
C(32)-C(34)-C(42)	117.68(13)
C(25)-C(35)-C(37)	112.27(12)
C(25)-C(35)-C(39)	111.17(12)
C(39)-C(35)-C(37)	108.71(11)
C(26)-C(36)-C(38)	110.22(14)
C(26)-C(36)-C(40)	112.60(13)
C(38)-C(36)-C(40)	109.99(13)
C(33)-C(41)-C(43)	112.73(11)
C(33)-C(41)-C(45)	109.59(12)
C(43)-C(41)-C(45)	109.79(12)

C(34)-C(42)-C(44)	110.65(13)
C(34)-C(42)-C(46)	112.15(12)
C(46)-C(42)-C(44)	108.17(12)
C(51)-C(50)-C(52)#1	117.8(3)
C(50)-C(51)-C(52)	121.8(3)
C(50)#1-C(52)-C(51)	120.3(3)
C(53)-C(52)-C(50)#1	120.0(4)
C(53)-C(52)-C(51)	119.4(4)

Symmetry transformations used to generate equivalent atoms:

#1 -x+1,-y+1,-z+1

Table 4. Anisotropic displacement parameters ($Å^2 x\ 10^3$) for us4001. The anisotropic displacement factor exponent takes the form: $-2\pi^2[\ h^2\ a^{*2}U^{11} + ...\ + 2\ h\ k\ a^*\ b^*\ U^{12}\ ]$

	U^{11}	U^{22}	U^{33}	U^{23}	U^{13}	U^{12}
Si(1)	19(1)	13(1)	11(1)	0(1)	3(1)	4(1)
N(1)	14(1)	12(1)	12(1)	1(1)	2(1)	3(1)
N(2)	17(1)	13(1)	11(1)	0(1)	4(1)	3(1)
C(1)	12(1)	14(1)	12(1)	1(1)	4(1)	0(1)
C(2)	12(1)	14(1)	12(1)	0(1)	2(1)	1(1)
C(3)	12(1)	18(1)	13(1)	1(1)	2(1)	4(1)
C(4)	13(1)	17(1)	12(1)	1(1)	3(1)	3(1)
C(5)	16(1)	19(1)	18(1)	1(1)	2(1)	6(1)
C(6)	21(1)	21(1)	14(1)	2(1)	6(1)	8(1)
C(7)	17(1)	13(1)	16(1)	2(1)	4(1)	4(1)
C(8)	21(1)	17(1)	13(1)	-1(1)	3(1)	6(1)
C(9)	22(1)	17(1)	20(1)	-1(1)	7(1)	5(1)
C(10)	26(1)	23(1)	20(1)	3(1)	5(1)	11(1)
C(11)	23(1)	15(1)	25(1)	4(1)	7(1)	2(1)
C(12)	33(1)	18(1)	18(1)	-4(1)	1(1)	2(1)
C(13)	14(1)	22(1)	19(1)	-3(1)	2(1)	1(1)
C(14)	14(1)	21(1)	14(1)	1(1)	1(1)	2(1)
C(15)	16(1)	38(1)	24(1)	-6(1)	-3(1)	6(1)
C(16)	19(1)	30(1)	12(1)	1(1)	0(1)	5(1)

C(17)	27(1)	48(1)	17(1)	-2(1)	-5(1)	16(1)
C(18)	21(1)	30(1)	14(1)	7(1)	4(1)	7(1)
C(19)	31(1)	42(1)	17(1)	10(1)	3(1)	16(1)
C(20)	17(1)	27(1)	16(1)	6(1)	6(1)	4(1)
C(21)	19(1)	26(1)	14(1)	5(1)	4(1)	5(1)
C(22)	13(1)	20(1)	13(1)	2(1)	3(1)	2(1)
C(23)	17(1)	12(1)	12(1)	-1(1)	1(1)	2(1)
C(24)	24(1)	12(1)	15(1)	1(1)	7(1)	3(1)
C(25)	24(1)	14(1)	13(1)	0(1)	5(1)	4(1)
C(26)	25(1)	15(1)	27(1)	4(1)	11(1)	3(1)
C(27)	35(1)	19(1)	13(1)	2(1)	3(1)	5(1)
C(28)	37(1)	18(1)	38(1)	7(1)	22(1)	2(1)
C(29)	34(1)	21(1)	16(1)	-2(1)	-7(1)	7(1)
C(30)	57(1)	20(1)	25(1)	5(1)	22(1)	1(1)
C(31)	20(1)	21(1)	22(1)	-4(1)	-4(1)	3(1)
C(32)	51(1)	19(1)	15(1)	2(1)	7(1)	2(1)
C(33)	17(1)	16(1)	16(1)	-2(1)	1(1)	2(1)
C(34)	31(1)	13(1)	14(1)	1(1)	4(1)	2(1)
C(35)	26(1)	19(1)	18(1)	4(1)	10(1)	2(1)
C(36)	18(1)	25(1)	41(1)	10(1)	7(1)	0(1)
C(37)	37(1)	30(1)	26(1)	6(1)	18(1)	6(1)
C(38)	22(1)	33(1)	71(1)	19(1)	17(1)	6(1)
C(39)	39(1)	20(1)	27(1)	4(1)	13(1)	-2(1)
C(40)	29(1)	32(1)	53(1)	8(1)	-1(1)	-7(1)

C(41)	14(1)	25(1)	20(1)	0(1)	4(1)	-1(1)
C(42)	31(1)	19(1)	16(1)	3(1)	-3(1)	2(1)
C(43)	24(1)	30(1)	35(1)	2(1)	8(1)	-6(1)
C(44)	45(1)	23(1)	20(1)	0(1)	-9(1)	-1(1)
C(45)	18(1)	36(1)	30(1)	-6(1)	7(1)	2(1)
C(46)	39(1)	30(1)	28(1)	7(1)	-8(1)	8(1)
C(50)	73(2)	51(2)	181(4)	60(2)	65(2)	30(1)
C(51)	56(2)	51(1)	160(3)	54(2)	62(2)	25(1)
C(52)	98(2)	36(1)	148(3)	44(2)	56(2)	27(1)
C(53)	102(4)	36(2)	39(2)	7(2)	6(2)	10(2)
C(50')	73(2)	51(2)	181(4)	60(2)	65(2)	30(1)
C(51')	56(2)	51(1)	160(3)	54(2)	62(2)	25(1)
C(52')	98(2)	36(1)	148(3)	44(2)	56(2)	27(1)

Table 5. Hydrogen coordinates (x 10^4) and isotropic displacement parameters ($Å^2$x 10^3) for us4001.

	x	y	z	U(eq)
H(5A)	10537	5913	2399	21
H(5B)	9814	5126	2867	21
H(6A)	4877	10314	3694	22
H(6B)	6131	10867	4301	22
H(9A)	8237	4631	940	29
H(9B)	9467	4148	1407	29
H(9C)	9719	5390	1231	29
H(10A)	5531	12424	2714	34
H(10B)	4859	12427	3388	34
H(10C)	4420	11399	2798	34
H(11A)	6965	4551	2524	31
H(11B)	7870	3654	2217	31
H(11C)	6590	4066	1740	31
H(12A)	8426	11973	3974	36
H(12B)	7243	12772	4087	36
H(12C)	7969	12774	3428	36
H(13A)	10886	7854	2785	23
H(13B)	10107	8392	3361	23

H(14A)	8678	8976	4142	20
H(14B)	8672	10290	4286	20
H(15A)	12070	6769	3548	32
H(15B)	12400	8051	3868	32
H(16A)	8678	9450	5313	25
H(16B)	7309	10084	5158	25
H(17A)	10692	7795	4585	38
H(17B)	11787	6904	4698	38
H(18A)	6549	8313	5455	25
H(18B)	7297	7700	4889	25
H(19A)	9359	6037	4580	34
H(19B)	10136	5476	4009	34
H(20A)	4845	8872	4612	23
H(20B)	4811	7552	4466	23
H(21A)	8148	7083	3803	23
H(21B)	7845	5802	3483	23
H(22A)	4804	8372	3437	18
H(22B)	6162	7728	3588	18
H(27)	6588	7052	-274	27
H(28)	10321	11979	1665	35
H(29)	4149	6478	-357	30
H(30)	8641	11953	686	39
H(31)	3256	5927	586	27
H(32)	6251	11281	657	34

H(35)	9354	7171	1179	24
H(36)	9660	11062	3241	33
H(37A)	9290	5849	161	44
H(37B)	10502	6884	243	44
H(37C)	9052	6844	-277	44
H(38A)	10589	9757	2478	60
H(38B)	11793	10364	3087	60
H(38C)	11701	10752	2355	60
H(39A)	8433	8657	229	42
H(39B)	9948	8834	713	42
H(39C)	8534	8939	1027	42
H(40A)	11495	12751	2790	59
H(40B)	11688	12436	3542	59
H(40C)	10347	13022	3257	59
H(41)	5282	5825	2248	24
H(42)	4690	10113	1977	27
H(43A)	2773	4654	1359	46
H(43B)	3191	4522	2140	46
H(43C)	4148	4083	1612	46
H(44A)	4685	9537	547	47
H(44B)	3613	8937	961	47
H(44C)	5265	8789	1103	47
H(45A)	4146	7487	2112	42
H(45B)	3247	6640	2479	42

H(45C)	2749	6731	1697	42
H(46A)	3947	11843	1664	50
H(46B)	2811	10815	1293	50
H(46C)	3915	11396	886	50
H(50)	7410	5126	5525	111
H(51)	6820	5022	4366	96
H(53A)	4516	5718	3552	72
H(53B)	3382	4632	3472	72
H(53C)	5006	4511	3422	72
H(50')	7410	5126	5525	111
H(51')	6820	5022	4366	96
H(52')	4442	4872	3829	103

Table 6. Torsion angles [°] for us4001.

Si(1)-C(1)-C(3)-C(5)	-148.97(10)
Si(1)-C(1)-C(3)-C(13)	-30.05(16)
Si(1)-C(1)-C(3)-C(21)	91.11(14)
Si(1)-C(2)-C(4)-C(6)	-146.10(11)
Si(1)-C(2)-C(4)-C(14)	95.70(13)
Si(1)-C(2)-C(4)-C(22)	-26.49(17)
N(1)-C(1)-C(3)-C(5)	9.14(12)
N(1)-C(1)-C(3)-C(13)	128.05(10)
N(1)-C(1)-C(3)-C(21)	-110.78(11)
N(1)-C(23)-C(25)-C(27)	175.72(11)
N(1)-C(23)-C(25)-C(35)	-7.62(18)
N(1)-C(23)-C(33)-C(31)	-175.88(11)
N(1)-C(23)-C(33)-C(41)	8.82(18)
N(2)-C(2)-C(4)-C(6)	15.78(12)
N(2)-C(2)-C(4)-C(14)	-102.42(11)
N(2)-C(2)-C(4)-C(22)	135.39(10)
N(2)-C(24)-C(26)-C(28)	-179.58(12)
N(2)-C(24)-C(26)-C(36)	4.81(19)
N(2)-C(24)-C(34)-C(32)	178.59(12)
N(2)-C(24)-C(34)-C(42)	-5.61(19)
C(1)-Si(1)-C(2)-N(2)	165.13(8)
C(1)-Si(1)-C(2)-C(4)	-33.92(14)

C(1)-N(1)-C(7)-C(5)	-18.06(13)
C(1)-N(1)-C(7)-C(9)	-136.78(11)
C(1)-N(1)-C(7)-C(11)	101.68(12)
C(1)-N(1)-C(23)-C(25)	95.33(14)
C(1)-N(1)-C(23)-C(33)	-83.98(15)
C(1)-C(3)-C(5)-C(7)	-20.19(13)
C(1)-C(3)-C(13)-C(15)	176.79(10)
C(1)-C(3)-C(21)-C(19)	-175.36(11)
C(2)-Si(1)-C(1)-N(1)	160.10(8)
C(2)-Si(1)-C(1)-C(3)	-42.95(14)
C(2)-N(2)-C(8)-C(6)	-11.40(13)
C(2)-N(2)-C(8)-C(10)	-130.11(12)
C(2)-N(2)-C(8)-C(12)	109.30(12)
C(2)-N(2)-C(24)-C(26)	-82.45(15)
C(2)-N(2)-C(24)-C(34)	94.86(14)
C(2)-C(4)-C(6)-C(8)	-23.02(12)
C(2)-C(4)-C(14)-C(16)	-176.35(10)
C(2)-C(4)-C(22)-C(20)	174.31(10)
C(3)-C(5)-C(7)-N(1)	22.53(12)
C(3)-C(5)-C(7)-C(9)	142.97(11)
C(3)-C(5)-C(7)-C(11)	-95.26(12)
C(3)-C(13)-C(15)-C(17)	-56.64(16)
C(4)-C(6)-C(8)-N(2)	20.82(12)
C(4)-C(6)-C(8)-C(10)	141.06(11)

C(4)-C(6)-C(8)-C(12)	-98.33(12)
C(4)-C(14)-C(16)-C(18)	54.82(15)
C(5)-C(3)-C(13)-C(15)	-68.75(13)
C(5)-C(3)-C(21)-C(19)	69.30(14)
C(6)-C(4)-C(14)-C(16)	70.43(14)
C(6)-C(4)-C(22)-C(20)	-70.60(13)
C(7)-N(1)-C(1)-Si(1)	169.03(8)
C(7)-N(1)-C(1)-C(3)	5.81(13)
C(7)-N(1)-C(23)-C(25)	-86.46(14)
C(7)-N(1)-C(23)-C(33)	94.23(14)
C(8)-N(2)-C(2)-Si(1)	163.57(8)
C(8)-N(2)-C(2)-C(4)	-2.86(14)
C(8)-N(2)-C(24)-C(26)	94.97(14)
C(8)-N(2)-C(24)-C(34)	-87.73(15)
C(13)-C(3)-C(5)-C(7)	-138.65(11)
C(13)-C(3)-C(21)-C(19)	-53.44(15)
C(13)-C(15)-C(17)-C(19)	55.90(17)
C(14)-C(4)-C(6)-C(8)	94.00(12)
C(14)-C(4)-C(22)-C(20)	52.32(13)
C(14)-C(16)-C(18)-C(20)	-55.38(14)
C(15)-C(17)-C(19)-C(21)	-55.08(16)
C(16)-C(18)-C(20)-C(22)	56.13(15)
C(17)-C(19)-C(21)-C(3)	54.98(16)
C(18)-C(20)-C(22)-C(4)	-55.58(15)

C(21)-C(3)-C(5)-C(7)	99.73(12)
C(21)-C(3)-C(13)-C(15)	54.23(14)
C(22)-C(4)-C(6)-C(8)	-143.86(10)
C(22)-C(4)-C(14)-C(16)	-52.39(14)
C(23)-N(1)-C(1)-Si(1)	-12.66(14)
C(23)-N(1)-C(1)-C(3)	-175.88(10)
C(23)-N(1)-C(7)-C(5)	163.62(10)
C(23)-N(1)-C(7)-C(9)	44.90(15)
C(23)-N(1)-C(7)-C(11)	-76.64(13)
C(23)-C(25)-C(27)-C(29)	1.85(19)
C(23)-C(25)-C(35)-C(37)	124.97(13)
C(23)-C(25)-C(35)-C(39)	-113.00(14)
C(23)-C(33)-C(41)-C(43)	-124.85(14)
C(23)-C(33)-C(41)-C(45)	112.55(14)
C(24)-N(2)-C(2)-Si(1)	-18.85(15)
C(24)-N(2)-C(2)-C(4)	174.71(10)
C(24)-N(2)-C(8)-C(6)	171.05(11)
C(24)-N(2)-C(8)-C(10)	52.35(16)
C(24)-N(2)-C(8)-C(12)	-68.25(15)
C(24)-C(26)-C(28)-C(30)	-0.4(2)
C(24)-C(26)-C(36)-C(38)	112.69(15)
C(24)-C(26)-C(36)-C(40)	-124.09(15)
C(24)-C(34)-C(42)-C(44)	-115.70(14)
C(24)-C(34)-C(42)-C(46)	123.43(14)

C(25)-C(23)-C(33)-C(31)	4.82(18)
C(25)-C(23)-C(33)-C(41)	-170.47(12)
C(25)-C(27)-C(29)-C(31)	1.4(2)
C(26)-C(24)-C(34)-C(32)	-4.14(19)
C(26)-C(24)-C(34)-C(42)	171.65(12)
C(26)-C(28)-C(30)-C(32)	-1.2(2)
C(27)-C(25)-C(35)-C(37)	-58.36(16)
C(27)-C(25)-C(35)-C(39)	63.66(15)
C(27)-C(29)-C(31)-C(33)	-1.5(2)
C(28)-C(26)-C(36)-C(38)	-62.94(17)
C(28)-C(26)-C(36)-C(40)	60.28(18)
C(28)-C(30)-C(32)-C(34)	0.1(2)
C(29)-C(31)-C(33)-C(23)	-1.52(19)
C(29)-C(31)-C(33)-C(41)	174.03(12)
C(30)-C(32)-C(34)-C(24)	2.5(2)
C(30)-C(32)-C(34)-C(42)	-173.55(13)
C(31)-C(33)-C(41)-C(43)	59.85(17)
C(31)-C(33)-C(41)-C(45)	-62.75(15)
C(32)-C(34)-C(42)-C(44)	60.10(16)
C(32)-C(34)-C(42)-C(46)	-60.77(17)
C(33)-C(23)-C(25)-C(27)	-4.98(18)
C(33)-C(23)-C(25)-C(35)	171.69(12)
C(34)-C(24)-C(26)-C(28)	3.14(19)
C(34)-C(24)-C(26)-C(36)	-172.48(12)

C(35)-C(25)-C(27)-C(29)	-175.03(12)
C(36)-C(26)-C(28)-C(30)	175.42(14)
C(50)-C(51)-C(52)-C(50)#1	0.7(4)
C(50)-C(51)-C(52)-C(53)	174.9(3)
C(52)#1-C(50)-C(51)-C(52)	-0.7(4)

Symmetry transformations used to generate equivalent atoms:

#1 -x+1,-y+1,-z+1

Table 7. Hydrogen bonds for us4001 [Å and °].

D-H...A	d(D-H)	d(H...A)	d(D...A)	<(DHA)

3. Bibliography

(1) Bruns, H.; Patil, M.; Carreras, J.; Vázquez, A.; Thiel, W.; Goddard, R.; Alcarazo, M. *Angew. Chemie - Int. Ed.* 2010, *49* (21), 3680–3683.

(2) Bandar, J. S.; Lambert, T. H. *J. Am. Chem. Soc.* 2012, *134* (12), 5552–5555.

(3) Nacsa, E. D.; Lambert, T. H. *J. Am. Chem. Soc.* 2015, *137* (32), 10246–10253.

(4) Kozma, Á.; Gopakumar, G.; Farès, C.; Thiel, W.; Alcarazo, M. *Chem. - A Eur. J.* 2013, *19* (11), 3542–3546.

(5) Stukenbroeker, T. S.; Bandar, J. S.; Zhang, X.; Lambert, T. H.; Waymouth, R. M. *ACS Macro Lett.* 2015, *4* (8), 853–856.

(6) Theophil Eicher, Richard Grof, Heinz Kunzmann, R. P. *Synthesis (Stuttg).* 1987, *10*, 887–892.

(7) Singh, P.; Bhargava, G.; Mahajan, M. P. *Tetrahedron* 2006, *62*, 11267–11273.

(8) Franchi, P.; Casati, C.; Mezzina, E.; Lucarini, M. *Org. Biomol. Chem.* 2011, *9*, 6396–6401.

(9) Kuster, G. J. T.; Berkom, L. W. a Van; Kalmoua, M.; Loevezijn, A. Van; Sliedregt, L. a J. M.; Steen, B. J. Van; Kruse, C. G.; Rutjes, F. P. J. T.; Scheeren, H. W. *J. Comb. Chem.* 2006, *8*, 85–94.

(10) Vatmurge, N. S.; Hazra, B. G.; Pore, V. S.; Shirazi, F.; Chavan, P. S.; Deshpande, M. V. *Bioorganic Med. Chem. Lett.* 2008, *18*, 2043–2047.

(11) Xu, J.; Zhuang, R.; Bao, L.; Tang, G.; Zhao, Y. *Green Chem.* 2012, *14* (9), 2384.

(12) Shen, Z.-L.; Ji, S.-J. *Synth. Commun.* 2009, *39* (5), 808–818.

(13) Zhang, Z.; Lippert, K. M.; Hausmann, H.; Kotke, M.; Schreiner, P. R. *J. Org. Chem.* 2011, *76* (23), 9764–9776.

(14) Zhang, J.; Du, G.; Xu, Y.; He, L.; Dai, B. *Tetrahedron Lett.* 2011, *52* (52), 7153–7156.

(15) Kadam, S. T.; Kim, S. S. *Tetrahedron* 2009, *65* (32), 6330–6334.

(16) Iwanami, K.; Aoyagi, M.; Oriyama, T. *Tetrahedron Lett.* 2005, *46* (44), 7487–7490.

(17) Mizuta, S.; Shibata, N.; Hibino, M.; Nagano, S.; Nakamura, S.; Toru, T. *Tetrahedron* 2007, *63* (35), 8521–8528.

(18) Prakash, G. K. S.; Panja, C.; Vaghoo, H.; Surampudi, V.; Kultyshev, R.; Mandal, M.; Rasul, G.; Mathew, T.; Olah, G. A. *J. Org. Chem.* 2006, *71* (18), 6806–6813.

(19) Kozaburo Nishiyama, T. Y. *Synthesis (Stuttg).* 1988, *2*, 106–108.

(20) Sun, H.; Yang, C.; Lin, R.; Xia, W. *Adv. Synth. Catal.* 2014, *356* (13), 2775–2780.

(21) Jensen, K. L.; Standley, E. A.; Jamison, T. F. *J. Am. Chem. Soc.* 2014, *136* (31), 11145–11152.

(22) Tasker, S. Z.; Jamison, T. F. *J. Am. Chem. Soc.* 2015, *137* (30), 9531–9534.

(23) Yin, J.; Mekelburg, T.; Hyland, C. *Org. Biomol. Chem.* 2014, *12* (45), 9113–9115.

(24) Minakata, S.; Morino, Y.; Oderaotoshi, Y.; Komatsu, M. *Chem. Commun. (Camb).* 2006, 3337–3339.

(25) Chouhan, G.; Alper, H. *Org. Lett.* 2009, *12*, 192–195.

(26) Sun, H.; Huang, B.; Lin, R.; Yang, C.; Xia, W. *Beilstein J. Org. Chem.* 2015, *11*, 524–529.

(27) Matsukawa, S.; Tsukamoto, K. *Org. Biomol. Chem.* 2009, *7* (18), 3792–3796.

(28) Martinez, C.; Muniz, K. *Adv. Synth. Catal.* 2014, *356* (1), 205–211.

(29) Boeckman, R. K.; Pero, J. E.; Boehmler, D. J. *J. Am. Chem. Soc.* 2006, *128* (34), 11032–11033.

(30) Bestmann, Jurgen and Roth, K. *Synthesis (Stuttg).* 1981, *12*, 998–999.

(31) Dellus, N.; Kato, T.; Bagán, X.; Saffon-Merceron, N.; Branchadell, V.; Baceiredo, A. *Angew. Chemie - Int. Ed.* 2010, *49* (38), 6798–6801.

(32) Hrobáriková, V.; Hrobárik, P.; Gajdoš, P.; Fitilis, I.; Fakis, M.;

Persephonis, P.; Zahradník, P. *J. Org. Chem.* 2010, *75* (9), 3053–3068.

(33) Gitendra C. Paul, J. G. *Synthesis (Stuttg).* 1996, 524–526.

(34) Alcarazo, M.; Suárez, R. M.; Goddard, R.; Fürstner, A. *Chem. - A Eur. J.* 2010, *16* (32), 9746–9749.

(35) Dyker, C. A.; Lavallo, V.; Donnadieu, B.; Bertrand, G. *Angew. Chemie - Int. Ed.* 2008, *47* (17), 3206–3209.

(36) Bantreil, X.; Nolan, S. P. *Nat. Protoc.* 2011, *6* (1), 69–77.

(37) Ghadwal, R. S.; Roesky, H. W.; Merkel, S.; Henn, J.; Stalke, D. *Angew. Chemie - Int. Ed.* 2009, *48* (31), 5683–5686.

(38) Perry, M. C.; Cui, X.; Powell, M. T.; Hou, D.; Reibenspies, J. H. *J. Am. Chem. Soc.* 2003, *125* (16), 1–27.

(39) Kumar, M. R.; Park, K.; Lee, S. *Adv. Synth. Catal.* 2010, *352* (18), 3255–3266.

(40) Xiong, Y.; Yao, S.; Inoue, S.; Epping, J. D.; Driess, M. *Angew. Chemie - Int. Ed.* 2013, *52* (28), 7147–7150.

(41) Mondal, K. C.; Roesky, H. W.; Schwarzer, M. C.; Frenking, G.; Tkach, I.; Wolf, H.; Kratzert, D.; Herbst-Irmer, R.; Niepötter, B.; Stalke, D. *Angew. Chemie - Int. Ed.* 2013, *52* (6), 1801–1805.

(42) Mondal, K. C.; Roesky, H. W.; Schwarzer, M. C.; Frenking, G.; Niepötter, B.; Wolf, H.; Herbst-Irmer, R.; Stalke, D. *Angew. Chemie - Int. Ed.* 2013, *52* (10), 2963–2967.

(43) Bailey, C. L.; Joh, A. Y.; Hurley, Z. Q.; Anderson, C. L.; Singaram, B. *J. Org. Chem.* 2016, *81*, 3619–3628.